SESSION

GRAPH BASED AND TREE METHODS + RELATED ISSUES

Chair(s)

TBA

Algorithms for Finding Magic Labelings of Triangles

James M. McQuillan[1] **and Dan McQuillan**[2]
[1]School of Computer Sciences, Western Illinois University, Macomb, IL, USA
[2]Department of Mathematics, Norwich University, Northfield, Vermont, USA

Abstract— *We present a new algorithm for finding vertex-magic total labelings of disjoint unions of triangles. Since exaustive searches are infeasible for large graphs, we use a specialized algorithm designed to find labelings with very restrictive properties, and then attempt to generate other labelings from these. We show constructively that there exists a vertex-magic total labeling, VMTL, for each of the feasible values of* $7C_3$, $9C_3$ *and* $11C_3$.

Keywords: graph labeling, algorithm, vertex-magic

1. Introduction

Let G be a simple graph with vertex set V and edge set E. A *total labeling* of a graph is a bijective map $f : V \cup E \longrightarrow \{1, 2, \ldots, |V|+|E|\}$. The *weight* of a vertex v incident with edges $e_1, \ldots, e_t$ is $wt_f(v) = f(v)+f(e_1)+\cdots+f(e_t)$. The total labeling f is a *vertex-magic total labeling*, or *VMTL*, if the weight of each vertex is a constant. In this case, the constant is called the *magic constant* of the VMTL. If a graph G has a VMTL, then G is called a *vertex-magic* graph.

Given a VMTL f of a graph G with degree Δ, there is a *dual* VMTL f^* of G in which $f^*(x) = |V|+|E|+1-f(x)$ for each $x \in V \cup E$. If the magic constant of f is h, then the magic constant of f^* is $(\Delta + 1)(|V| + |E| + 1) - h$.

The range of possible magic constants for a graph is called the *spectrum* of the graph. Assume that G is a 2-regular graph. Suppose further that G has a VMTL with magic constant h and with $n = |V| = |E|$. Then

$$\frac{5n+3}{2} \leq h \leq \frac{7n+3}{2}. \qquad (1)$$

The integral values in this range are the *feasible values* for the 2-regular graph G. (See [24] and [34] for a more general discussion.) For a 2-regular graph, the dual of a VMTL with magic constant h is a VMTL with magic constant $6n+3-h$.

Problem 1.1: The VMTL problem: given a feasible magic constant h, does there exist a VMTL with magic constant h?

There have been many exciting general VMTL constructions in recent years, such as [15], [11], and [22]. Some other important papers for labeling regular graphs include [21], [5], [13], [31], [2], [3] and [23]. For 2-regular graphs, Wallis proved in [33] that, for a vertex-magic regular graph G, the multiple graph sG is also vertex-magic provided that s is odd or the degree of G is odd. Gray gave VMTLs of $C_3 \cup C_{2n}$, $n \geq 3$ and $C_4 \cup C_{2n-1}$, $n \geq 3$ in [14]. In [27], it was shown that, for every $s \geq 4$ even, sC_3 is vertex-magic. For every $s \geq 6$ even, sC_3 has VMTLs with at least $2s-2$ different magic constants. For every s odd, VMTLs for sC_3 with $s+1$ different magic constants were also provided. In this paper, we are interested in algorithms that can be used to construct VMTLs in sC_3.

One approach to Problem 1.1 is to design an algorithm to construct VMTLs for certain special types of graphs. This is a part of our strategy as our algorithm is specifically designed for sC_3. An algorithm could be designed in an efficient way using properties of those graph types. For example, in [4], algorithms were designed specifically for finding all VMTLs on cycles and wheels. They provide a table giving the total number of VMTLs on cycles C_3 through C_{18}. Moreover, they give the number of VMTLs for these for a given magic constant. They give a table giving the number of VMTLs for wheel graphs $W_3, \ldots, W_{10}$. Moreover, they give the number of VMTLs for these for given magic constants. (They also give the number of VMTLs for some of the feasible magic constants for W_{11}.)

A second strategy for approaching this problem is to convert it into another well-studied problem. This approach is taken in [20], where they convert an instance of the VMTL problem into an instance of the satisfiability of boolean expressions problem. The SAT problem was the first NP-complete problem ([7]) and is fundamental to computer science. Variants of the Davis-Putnam algorithm ([9]), BDD's ([6]), and BED's ([1]) are the three main complete algorithms for the SAT problem. There are also many incomplete local search algorithms. GSAT, WalkSAT ([32]), and UnitWalk ([17]) were three of the early local search algorithms. There is a yearly competition to find an efficient SAT solver as part of the annual SAT conference [19]. Given the amount of research that has been done on this problem, it is natural to consider converting an instance of a problem into an instance of the SAT problem.

A third strategy, which is the approach taken here, is to combine mathematical intuition for finding new VMTLs in certain graphs with very focused, specific algorithms to generate labelings with certain properties. With this strategy, labelings might be found that other more general algorithms could not find in a reasonable amount of time. Such labelings might then be used to construct other labelings. This strategy was used in [27] and [18].

As mentioned above, tables are provided in [4] that give the number of VMTLs for C_3 through C_{18}. (They note

that of those, C_{11} through C_{18} had not previously been enumerated.) For sC_3, there appears to be fewer magic labelings than cycles of the same size. There are only 32 non-isomorphic magic labelings in $3C_3$ ([27]) even though C_9 has 1540 non-isomorphic magic labelings ([13]). This suggests that it will be difficult to write computer programs to generate VMTLs (in a reasonable amount of time) for sC_3 when s is big.

In the very important paper [16], a computer search was done in an attempt to find a VMTL with the biggest labels on the vertices (strong VMTL) for each 2-regular graph of order 7, 11, 13, 15. Based on their observations, they made the following conjecture:

Conjecture 1.1 ([16] Conjecture 1): A 2-regular graph of odd order possesses a strong VMTL if and only if it is not of the form $(2t-1)C_3 \cup C_4$ or $(2t)C_3 \cup C_5$.

They also found by computer search, strong VMTLs for all 2-regular graphs of order 17 except $C_5 \cup 4C_3$. It turns out that $C_5 \cup 4C_3$ does possess a strong VMTL [18], disproving part of the conjecture. This suggests that 2-regular graphs with many triangles require special attention, and special algorithms for efficient computer searches.

MacDougall's conjecture states that every regular graph of degree at least 2 is vertex-magic except for $2C_3$. This remains an open problem.

The rest of this paper is organized as follows. In Section 2, we explain the importance of common differences of components and as well as searching for specialized labelings in the design of efficient algorithms for solving Problem 1.1. In Section 3, we give a new algorithm for generating VMTLs for sC_3. In Section 4, we answer Problem 1.1 in the affirmative for each feasible magic constant in each of $7C_3$, $9C_3$ and $11C_3$. These three graphs have 21, 27 and 33 vertices respectively; we give a VMTL for each feasible value for each of these graphs.

2. The common difference of a component of sC_3

For the remainder of this paper, we restrict ourselves to the problem of finding VMTLs in sC_3.

Notation 2.1: Denote by $[x_1, x_2, x_3, x_4, x_5, x_6]$ the labels of one component of sC_3 written in the order vertex-edge-vertex-edge-vertex-edge. (So, x_1 is the vertex label of a vertex with weight $x_1 + x_2 + x_6$.)

Lemma 2.1 ([27] Lemma 2): Given a VMTL of sC_3 with a component labeled $[a_1, b_3, a_2, b_1, a_3, b_2]$, then $b_1 - a_1 = b_2 - a_2 = b_3 - a_3$.

Consider a VMTL of sC_3. Suppose that one of its components is labeled $[a_1, b_3, a_2, b_1, a_3, b_2]$. The *common difference* of this component is defined to be $d = b_1 - a_1 = b_2 - a_2 = b_3 - a_3$ ([27]). This concept is a key ingredient in our algorithm. Lemma 2.2 follows immediately from Lemma 2.1. We use it to make our algorithm more efficient.

Lemma 2.2: Suppose that we have a VMTL of sC_3 with magic constant h, and that a component has common difference d and labels $[a_1, b_3, a_2, b_1, a_3, b_2]$. Then

(i) $b_i = a_i + d$, $i = 1, 2, 3$;
(ii) the weight of each vertex in that component is $h = a_1 + (a_2 + d) + (a_3 + d) = a_1 + a_2 + a_3 + 2d$;
(iii) the vertex sum of that component is $h - 2d$;
(iv) $d = (h - (a_1 + a_2 + a_3))/2$; and
(v) $h - (a_1 + a_2 + a_3)$ is an even integer.

Proof: All of these follow immediately from Lemma 2.1. ∎

While it is trivial to rearrange any of (ii)-(iv) to obtain the others in Lemma 2.2, we prefer to state all of (i)-(v) so that we can refer to them individually. In an algorithm, when presented with three integers as possible labels for the vertices of one component, we can remove that triple from any further consideration if h minus the sum of the three numbers is not even by Lemma 2.2 part (v). If we wanted a component to have a specific common difference, we could also remove a triple from contention for vertex labels of a component if any of $a_1 + d$, $a_2 + d$, $a_3 + d$ had already been assigned to other components by Lemma 2.2 part (i). We use techniques such as these in our algorithm.

Because exhaustive computer searches are only feasible for small s, we chose to write computer programs that are specifically designed to look for VMTLs with very restrictive properties. Such a strategy might not lead to any examples of VMTLs, or perhaps it might lead to just a few sporadic examples. On the other hand, it might lead to some important examples that could be used to generate others. For example, consider the following special case of Problem 1.1.

Problem 2.1: Given a feasible magic constant h of sC_3, does there exist a VMTL with magic constant h such that the labels $1, 2, \ldots, s_0$ are on vertices of different compents, $s_0 \leq s$, and such that the common difference on each of these s_0 components is $3s$?

This seems like quite a restictive problem, but an efficient algorithm can be tailor-made for this problem, and any solution is very valuable when combined with the following lemma, as it could be used to generate many solutions to Problem 1.1, especially if s_0 is close to s.

Lemma 2.3 ([27] Lemma 3): Let s be a positive integer and let λ_0 be a VMTL of sC_3 with a magic constant of h. Assume that one of the components has a vertex labeled 1 and a common difference of $3s$. Then there exists another VMTL λ_1 of sC_3 with a magic constant of $h - 3$.

We gave some solutions to Problem 2.1 in [27, Theorem 4] for s odd, $s_0 = s$, and [27, Theorem 6] for $s \geq 6$ even, $s_0 = s - 2$.

3. A magic labeling algorithm for sC_3.

In this section, we present an algorithm for generating VMTLs in sC_3. We will use the following proposition to make our algorithm more efficient.

Proposition 3.1: A VMTL of sC_3 with a magic constant of h has sum of all vertex labels equal to $3s[2(6s+1)-h]$.

Proof: Let S_V denote the sum of all the vertex labels, and let S_E denote the sum of all the edge labels. Let $n = |V|$ and let $m = |E|$. It is easy to check that $S_V + S_E = 1+2+\cdots+(n+m) = (n+m)(n+m+1)/2$ and $S_V + 2S_E = nh$. (For proofs of these, see [27].) Here, $n = m = 3s$. Solving for S_V yields the desired equality. ■

In Algorithm 3.1 below, we assign labels to some components and then attempt to extend that to a VMTL. Our algorithm has a heavy emphasis on finding labels of vertices in individual components. We make sure that the appropriate and necessary edge labels are available at the same time. Here, we use Lemmas 2.1 and 2.2. If we know the vertex labels and the common differences of some components of a VMTL, we know the edge labels of those components.

For convenience, we use the following term in this situation to refer to the labels assigned to some but not necessarily all of the components. An *injective vertex magic labeling*, *IVML*, of sC_3 is an injective map f from a subset A of $V \cup E$ into $\{1, 2, \ldots, |V|+|E|\}$ such that A consists of zero or more components of sC_3, and the weight of each vertex in A is a constant. Given a VMTL, erasing the vertex and edge labels from one or more components gives an IVML. We are hoping to go in the other direction. We are hoping to extend some IVMLs to VMTLs. Note that Lemma 2.1 applies to IVMLs as well as VMTLs.

Algorithm 3.1: A VMTL algorithm for sC_3:

Input:

(a) the value of s that you want to find VMTLs for.
(b) if you are only interested in VMTLs for a particular magic constant h, then that value of h is taken as input as well.
(c) any information about restrictions there are on any of the labels that can be used to make the program run faster.

Output: all VMTLs that satisfy the given restrictions.

Our algorithm uses the following procedures:

1. $main(\,)$
   If a particular value for the magic constant h was not given as input, then we can use a loop to look for VMTLs for all feasible values of h. Equation (1) gives the range of feasible values. If we denote by h_{max} and h_{min} the upper and lower bounds in this inequality respectively, then let $h_{mid} = \lceil (h_{min}+h_{max})/2 \rceil$. Then the loop could go from h_{max} down to h_{mid}. By duality, the VMTLs for the other values of h can be generated later from those. (Note that the algorithm could look for VMTLs for different values of h in parallel.)
   For each value of h, calculate the sum k that the vertex labels of any VMTL must have according to Proposition 3.1. The $main$ should then call the procedure $whichLabelsAreForVertices$ by a call such as $whichLabelsAreForVertices(s, h, \{1, \ldots, 6s\}, 3s, k, 0, 0, 0, null)$; described below.
   Note: Three of the arguments for this call are s, h and k. The argument $\{1, \ldots, 6s\}$ represents the set of all possible labels, and the argument $3s$ represents the size of a set of labels for the vertices. Other arguments are used for the recursive nature of that procedure. They are described in that procedure.
2. procedure $whichLabelsAreForVertices$(int s, int h, int[ ] $theNumbersForLabels$, int $desiredSize$, int $desiredSum$, int $sizeSoFar$, int $sumSoFar$, int $currentIndexOfNumbersForLabels$, int[ ] $soFarForVertices$);
   This recursive procedure attempts to grow the empty set to sets each having size $desiredSize$ and sum $desiredSum$. For each such set that is found, the procedure $lookForVMTLsUsingIt$ is called in the hope that it can be used to label the vertices of sC_3 as part of VMTLs with magic constant h and vertex sum $desiredSum$.
   To grow the empty set to such a set of size $desiredSize$ and sum $desiredSum$, we have parameters to keep track of the set of elements we have chosen so far, $soFarForVertices$ (initially $null$), as well as its size, $sizeSoFar$ (initially 0), and its sum, $sumSoFar$ (initially 0). The parameter $currentIndexOfNumbersForLabels$ (initially 0) keeps track of what element of $theNumbersForLabels$ that we are currently considering to include from $soFarForVertices$.
   This recursive procedure could have multiple base cases. To make this procedure more efficient, one base case could simply $return$ if

$$\begin{aligned} &length(theNumbersForLabels) \\ &\quad - currentIndexOfNumbersForLabels \\ &< (desiredSize - sizeSoFar). \end{aligned}$$

   In such a case, there is no hope of extending $soFarForVertices$ to a desired set because there aren't enough numbers left to consider in $theNumbersForLabels$ to extend $soFarForVertices$ to a set of size $desiredSize$.
   Another base case could simply $return$ if $sumSoFar > desiredSum$, as there is no hope of extending $soFarForVertices$ to a desired set because we've already exceeded the desired sum.
   Another base case could simply $return$ if

$$\begin{aligned} &currentIndexOfNumbersForLabels \\ &\geq length(theNumbersForLabels) \end{aligned}$$

   as we've reached the end of the elements being considered in $numbersForLabels$ in this case.
   This recursive procedure should have a base case corresponding to the successful generation of a set with the

properties mentioned. In this case it calls the procedure $lookForVMTLsUsingIt$,

$lookForVMTLsUsingIt(s, h, theNumbersForLabels, soFarForVertices)$;

To complete this procedure, we need two recursive calls, one of which attempts to use the current element of $theNumbersForLabels$ to make a desired set of vertex labels, and the other of which attempts to make a desired set of vertex labels without the current element. The first corresponds to using the current element of $theNumbersForLabels$,

$$theNumbersForLabels[currentIndexOfChoices].$$

We recurse with that together with the information in the parameter $soFarForVertices$ for the last argument. (We also have to use the appropriate updated values for the sixth and seventh arguments corresponding to size and sum and the eighth argument corresponding to the element of $theNumbersForLabels$ that should be considered next.)

The second recursive call corresponds to us not selecting the current element of $theNumbersForLabels$. For this recursive call, no new information is being added to the information in $soFarForVertices$. The eighth argument corresponding to the element of $theNumbersForLabels$ needs to be updated.

3. procedure $lookForVMTLsUsingIt$(int s, int h, int[ ] $theNumbersForLabels$, int[ ] $theNumbersForVertices$);
   Since we have a specific subset of all possible labels to use for the vertices, the remaining labels must be for the edges. Store these in int[ ] $theNumbersForEdges$. Next, call the recursive procedure $generateVMTLs$, with a call such as
   $generateVMTLs(theNumbersForVertices, theNumbersForEdges, h, s, \{false, \ldots, false\}, null, -1)$;
   This procedure will attempt to generate VMTLs using these.
4. procedure $generateVMTLs$(int[ ] $theNumbersForVertices$, int[ ] $remainingNumbersForEdges$, int h, int s, boolean[ ] $usedVertexIndex$, int[ ][ ] $ivmlIndices$, int[ ] commonDifferences, int $currentIndexOfIVML$);
   This procedure tries to find VMTLs by labeling one component at a time. The first parameter, $theNumbersForVerices$, gives the set of numbers that is to be used for labeling all the vertices. The parameters $ivmlIndices$ and $commonDifferences$ keep track of an IVML that we are trying to grow. The parameter $ivmlIndices$ keeps track of triples of indices in $theNumbersForVertices$. One triple corresponds to one component, so if we ever get s triples we have our vertex labels. From such a triple, the corresponding three elements in $theNumbersForVertices$ are currently being used as the vertex labels for one component. The common difference for that component can be found in the appropriate element in $commonDifferences$. From these pieces of information, we have the edge labels for that component.
   As we grow an IVML, some labels are used for edges. The second parameter keeps track of the edge labels that have not as yet been used. The first parameter, $theNumbersForVertices$, is the set of all of the labels for the vertices, and the $usedVertexIndex$ parameter keeps track of those that have been used so far.
   This procedure has a base case corresponding to finding a solution. If the parameter $ivmlIndices$ has length s, then it corresponds to a VMTL, in which case that information is outputted, and the procedure $return$s.
   This procedure has a loop to continually look for all possible labelings of one component that could be used to augment the information in $ivmlIndices$ and $commonDifferences$, to give a bigger IVML. The corresponding edge labels need to be available. (Recall that Lemma 2.2 part (i) gives us these values.) If they are, then we can recurse on this bigger IVML with all parameters except the first updated. When the loop is finished, this procedure returns.
   It is important to note that we have several filters in place in the loop above so that (a) we ignore labels of a component that won't lead to a solution, and (b) so that we ignore labels of a component that won't lead to a specific type of solution that we are after. Filters of type (a) are used for the purposes of making the algorithm faster. If we exclude filters of the type (b), then our algorithm will find all possible VMTLs for the specified values of s and h. If we include filter of type (b), we will only be looking for VMTLs with certain properties. We often use filters of both types in order to find certain solutions quickly. We will discuss the use of filters further shortly.

Finally, we can generate other VMTLs from the output of $generateVMTLs$ using Lemma 2.3. This can be done by hand (or by another procedure).

Algorithm 3.1 uses several tools so that it is efficient:

(i) In the $main$, our loop considered roughly half of the feasible magic constants. Duality can be used for the others. Parallelism can also be used here.
(ii) In the second procedure, $whichLabelsAreForVertices$, we used the results of Proposition 3.1 to restrict the possibilities for sets of numbers to be considered as vertex labels.
(iii) In $generateVMTLs(\,)$, when we looked for a triple to label the vertices of one component, we eliminated possibilities that did not satisfy Lemma 2.2 part (v).

(iv) We were able to focus on labeling the vertices because of Lemma 2.2 part (iv). We just needed to make sure that the corresponding edge labels were available when we had labels that we liked for the vertices of a component.
Sometimes, we are interested in finding only labellings in which some components have specific common differences. In this case, Lemma 2.2 part (iv) helps us reduce the number of triples that we need to consider as possible labels for the vertices of a component. In $generateVMTLs(\,)$, when we looked for a triple to label the vertices of one component, we eliminated possibilities that did not satisfy Lemma 2.2 part (iv) in this situation.

(v) Use Lemma 2.3 to generate many other VMTLs.

In Algorithm 3.1, we use several filters.

In $generateVMTLs$, when we have an IVML with some components labeled, we try to extend it to VMTLs by labeling an additional component (recursively). Sometimes, a potential labeling of a "next" component can be removed from consideration ("filtered") because we can tell that it will never lead to a VMTL, or because it will not lead to a specific type of VMTL that we are interested in finding.

If we are given the common differences of any of the components as input, then some triples can be immediately eliminated from consideration as possible vertex labels for a component because of Lemma 2.2 part (iv). If restrictions are given, such as the common difference restiction of Problem 2.1, we might be able to eliminate triples here or at some other point in the algorithm.

4. VMTLs for $7C_3$, $9C_3$, and $11C_3$.

Using Algorithm 3.1, we now answer Problem 1.1 in the affirmative for $7C_3$, $9C_3$, and $11C_3$ for each of their respective feasible magic constants. In order to do so, we answer Problem 2.1 in the affirmative for certain values of h and s_0 for $7C_3$, $9C_3$, and $11C_3$. Then, we use Lemma 2.3.

Theorem 4.1: There exists VMTLs for all of the feasible values of $7C_3$.

Proof: Consider the VMTL with components labeled

$$[1, 37, 15, 22, 16, 36],\ [2, 39, 12, 23, 18, 33],$$
$$[3, 42, 8, 24, 21, 29],\ [4, 40, 9, 25, 19, 30],$$
$$[5, 38, 10, 26, 17, 31],\ [6, 41, 20, 13, 34, 27],$$
$$\text{and } [7, 35, 11, 28, 14, 32].$$

This VMTL has a magic constant of 74. The first three components have common differences of $3s$. Therefore, by using Lemma 2.3 three times, we have VMTLs of $7C_3$ with magic constants $71, 68, 65$. By duality, there exist VMTLs with magic constants of $55, 58, 61$ and 64.

Next, consider the VMTL with components labeled

$$[1, 37, 14, 22, 16, 35],\ [2, 38, 12, 23, 17, 33],$$
$$[3, 42, 20, 11, 34, 28],\ [4, 40, 15, 18, 26, 29],$$
$$[5, 36, 6, 31, 10, 32],\ [7, 39, 9, 25, 21, 27],$$
$$\text{and } [8, 41, 13, 19, 30, 24].$$

This VMTL has a magic constant of 73. The first two components have common differences of $3s$. By using Lemma 2.3 twice, there exist VMTLs of $7C_3$ with magic constants 70 and 67. By duality, there exist VMTLs with magic constants of $56, 59$ and 62.

Finally, in [27] it was shown that there exist VMTLs of $7C_3$ with magic constants with values $75, 72, 69, 66, 63, 60, 57, 54$. ■

Theorem 4.2: There exists VMTLs for all of the feasible values of $9C_3$.

Proof: Consider the VMTL with components labeled

$$[1, 46, 18, 28, 19, 45],\ [2, 52, 11, 29, 25, 38],$$
$$[3, 49, 13, 30, 22, 40],\ [4, 54, 12, 26, 32, 34],$$
$$[5, 44, 9, 39, 10, 43],\ [6, 53, 16, 23, 36, 33],$$
$$[7, 50, 27, 15, 42, 35],\ [8, 47, 31, 14, 41, 37],$$
$$\text{and } [17, 51, 21, 20, 48, 24].$$

This VMTL has a magic constant of 92. The first three components have common differences of $3s$. Therefore, by using Lemma 2.3 three times, we have VMTLs of $9C_3$ with magic constants $89, 86$, and 83. By duality, there exist VMTLs with magic constants of $73, 76, 79$, and 82.

Next, consider the VMTL with components labeled

$$[1, 47, 19, 28, 20, 46],\ [2, 50, 15, 29, 23, 42],$$
$$[3, 51, 13, 30, 24, 40],\ [4, 49, 9, 36, 17, 41],$$
$$[5, 52, 16, 26, 31, 37],\ [6, 45, 10, 39, 12, 43],$$
$$[7, 53, 14, 27, 33, 34],\ [8, 54, 22, 18, 44, 32],$$
$$\text{and } [11, 48, 25, 21, 38, 35].$$

This VMTL has a magic constant of 94. The first three components have common differences of $3s$. By using Lemma 2.3 thrice, there exist VMTLs of $9C_3$ with magic constants of $91, 88$ and 85. By duality, there exist VMTLs with magic constants of $71, 74, 77$, and 80.

Next, consider the VMTL with components labeled

$$[1, 50, 17, 28, 23, 44],\ [2, 47, 19, 29, 20, 46],$$
$$[3, 51, 14, 30, 24, 41],\ [4, 54, 16, 25, 33, 37],$$
$$[5, 48, 12, 35, 18, 42],\ [6, 53, 10, 32, 27, 36],$$
$$[7, 45, 11, 39, 13, 43],\ [8, 49, 15, 31, 26, 38],$$
$$\text{and } [9, 52, 22, 21, 40, 34].$$

This VMTL has a magic constant of 95. By duality, there exists a VMTL with a magic constant of 70.

Finally, in [27] it was shown that there exist VMTLs of $9C_3$ with magic constants with values $96, 93, 90, 87, 84, 81, 78, 75, 72$ and 69. ■

Theorem 4.3: There exists VMTLs for all of the feasible values of $11C_3$.

Proof: Consider the VMTL with components labeled

$$[1, 62, 20, 34, 29, 53],\ [2, 65, 16, 35, 32, 49],$$
$$[3, 61, 19, 36, 28, 52],\ [4, 57, 22, 37, 24, 55],$$
$$[5, 60, 18, 38, 27, 51],\ [6, 56, 10, 50, 12, 54],$$
$$[7, 66, 17, 33, 40, 43],\ [8, 63, 23, 30, 41, 45],$$
$$[9, 59, 15, 42, 26, 48],\ [11, 58, 14, 44, 25, 47],$$
and $[13, 64, 21, 31, 46, 39]$.

This VMTL has a magic constant of 116. The first five components have common differences of $3s$. Therefore, by using Lemma 2.3 five times, we have VMTLs of $119C_3$ with magic constants $113, 110, 107, 104$ and 101. By duality, there exist VMTLs with magic constants of $85, 88, 91, 94, 97$, and 100.

Next, consider the VMTL with components labeled

$$[1, 59, 22, 34, 26, 55],\ [2, 60, 20, 35, 27, 53],$$
$$[3, 66, 13, 36, 33, 46],\ [4, 63, 15, 37, 30, 48],$$
$$[5, 56, 10, 49, 12, 54],\ [6, 58, 17, 40, 24, 51],$$
$$[7, 65, 19, 31, 41, 43],\ [8, 57, 11, 47, 18, 50],$$
$$[9, 64, 23, 28, 45, 42],\ [14, 62, 21, 32, 44, 39],$$
and $[16, 61, 29, 25, 52, 38]$.

This VMTL has a magic constant of 115. The first four components have common differences of $3s$. By using Lemma 2.3 four times, there exist VMTLs of $11C_3$ with magic constants of $112, 109, 106$ and 103. By duality, there exist VMTLs with magic constants of $86, 89, 92, 95$, and 98.

Finally, in [27] it was shown that there exist VMTLs of $11C_3$ with magic constants with values $117, 114, 111, 108, 105, 102, 99, 96, 93, 90, 87$ and 84. ■

References

[1] H.R. Andersen and H. Hulgaard, "Boolean Expression Diagrams," *Information and Computation*, vol. 179, pp. 194-212, 2002.

[2] M. Baca, M. Miller and J.A. MacDougall, "Vertex-magic total labelings of generalized Peterson graphs and convex polytopes," J. Combin. *Math. Combin. Comput.*, vol. 59, pp. 89-99, 2006.

[3] M. Baca, M. Miller and Slamin, "Every generalized Peterson graph has a vertex-magic total labeling," *Int. J. Comp. Math.*, vol. 79, pp. 1259-1263, 2002.

[4] A. Baker and J. Sawada, "Magic Labelings on Cycles and Wheels," in *2nd Annual International Conference on Combinatorial Optimization and Applications (COCOA '08)*, Lecture Notes in Mathematics, vol. 5165, pp. 361-373, 2008.

[5] O. Berkman, M. Parnas and Y. Roditty, "All cycles are edge-magic," *Ars Combin.*, vol. 59, pp. 145-151, 2001.

[6] R.E. Bryant, "Symbolic Boolean Expression Manipulation with Ordered Binary Decision Diagrams," *ACM Computing Surveys,* Vol. 24, No. 3, pp. 294-318, 1992.

[7] S.A. Cook, "The complexity of theorem-proving procedures," in *Proceedings of the third annual ACM symposium on the Theory of computing*, ACM, NY, 1971, pp. 151-158.

[8] T.H. Cormen, C.E. Leiserson, R.L. Rivest, and C. Stein, *Introduction to Algorithms*, 3rd ed. MIT Press, 2009.

[9] M. Davis, G. Logemann, and D. Loveland, "A Machine Program for Theorem Proving," *Communications of the ACM*, vol. 3, pp. 394-397, 1962.

[10] G. Exoo, A.C.H. Ling, J.P. McSorley, N.C.K. Phillips, W.D. Wallis, "Totally magic graphs," *Discrete Math.*, vol. 254, pp. 103-113, 2002.

[11] D. Froncek, P. Kovar and T. Kovarova, "Vertex magic total labeling of products of cycles," *Australas J. Combin.*, vol. 33, pp. 169-181, 2005.

[12] J.A. Gallian, "A dynamic survey of graph labeling," *Electronic J. Combin.*, vol. 17, #DS6, 2010.

[13] R.D. Godbold and P.J. Slater, "All cycles are edge-magic," *Bull. Inst. Combin. Appl.*, vol. 22, pp. 93-97, 1998.

[14] I. Gray, "New construction methods for vertex-magic total labelings of graphs," Ph.D. thesis, University of Newcastle, 2006.

[15] I. Gray, "Vertex-magic total labellings of regular graphs," *SIAM J. Discrete Math.*, vol. 21, Issue 1, pp. 170-177, 2007.

[16] I.D. Gray and J.A. MacDougall, "Vertex-magic labelings of regular graphs II.," *Discrete Math.*, vol. 309, pp. 5986-5999, 2009.

[17] E.A. Hirsch, and A. Kojevnikov, "UnitWalk: A new SAT solver that uses local search guided by unit clause elimination," *Annals of Mathematics and Artificial Intelligence*, vol. 43, pp. 91-111, 2005.

[18] J. Holden, D. McQuillan, and J.M. McQuillan, "A conjecture on strong magic labelings of 2-regular graphs," *Discrete Mathematics*, vol. 309, pp. 4130-4136, 2009.

[19] The International Conferences on Theory and Applications of Satisfiability Testing (SAT). [Online]. Available: http://www.satisfiability.org

[20] G. Jäger, "An effective SAT encoding for magic labeling," in *Proceedings of the 9th Cologne Twente Workshop on Graphs and Combinatorial Optimization (CTW 2010)*, 2010, pp. 97-100.

[21] A. Kotzig and A. Rosa, "Magic valuations of finite graphs," *Canad. Math. Bull.*, vol. 13, pp. 451-461, 1970.

[22] P. Kovar, "Vertex magic total labeling of products of regular VMT graphs and regular supermagic graphs," *J. Combin. Math. Combin. Comput.*, vol. 54, pp. 21-31, 2005.

[23] Y. Lin and M. Miller, "Vertex-magic total labelings of complete graphs," *Bull. Inst. Combin. Appl.*, vol. 33, pp. 68-76, 2001.

[24] J.A. MacDougall, M. Miller, Slamin, and W.D. Wallis, "Vertex-magic total labelings of graphs," *Utilitas Mathematica*, vol. 61, pp. 3-21, 2002.

[25] D. McQuillan, "Edge-magic and vertex-magic total labelings of certain cycles," *Ars Combin.*, vol. 91, pp. 257-266, 2009.

[26] D. McQuillan, "A technique for constructing magic labelings of $2-$regular graphs," *JCMCC*, vol. 75, pp. 129-135, 2010.

[27] D. McQuillan and J.M. McQuillan, "Magic Labelings of Triangles," *Discrete Mathematics*, vol. 309, pp. 2755-2762, 2009.

[28] D. McQuillan and K. Smith, "Vertex-magic total labeling of multiple complete graphs," *Congr. Numer.*, vol. 180, pp. 201-205, 2006.

[29] D. McQuillan and K. Smith, "Vertex-magic total labeling of odd complete graphs," *Discrete Math.*, vol. 305, pp. 240-249, 2005.

[30] J.P. McSorley and W.D. Wallis, "On the spectra of totally magic labelings," *Bull. Inst. Combin. Appl.*, vol. 37, pp. 58-62, 2003.

[31] Y. Roditty and T. Bachar, "A note on edge-magic cycles," *Bull. Inst. Combin. Appl.* vol. 29, pp. 94-96, 2000.

[32] B. Selman, H. Kautz, and B. Cohen, "Local Search Strategies for Satisfiability Testing," in *Cliques, Coloring, and Satisfiability: Second DIMACS Implementation Challenge*, October 11-13, 1993.

[33] W.D. Wallis, "Vertex magic labelings of multiple graphs," *Congr. Numer.*, vol. 152, pp. 81-83, 2001.

[34] W.D. Wallis, *Magic Graphs*. Boston, MA: Birkhauser, 2001.

[35] W.D. Wallis, "Two results of Kotzig on magic labelings," *Bull. Inst. Combin. Appl.*, vol. 36, pp. 23-28, 2002.

Assortativity of links in directed networks

Mahendra Piraveenan[1], **Kon Shing Kenneth Chung**[1], **and Shahadat Uddin**[1]
[1]Centre for Complex Systems Research, Faculty of Engineering and IT,
The University of Sydney, NSW 2006, Australia

Abstract— *Assortativity is the tendency in networks where nodes connect with other nodes similar to themselves. Degree assortativity can be quantified as a Pearson correlation. However, it is insufficient to explain assortative or disassortative tendencies of individual links, which may be contrary to the overall tendency in the network. In this paper we define and analyse link assortativity in the context of directed networks. Using synthesised and real world networks, we show that the overall assortativity of a network may be due to the number of assortative or disassortative links it has, the strength of such links, or a combination of both factors, which may be reinforcing or opposing each other. We also show that in some directed networks, link assortativity can be used to highlight subnetworks which have vastly different topological structures. The quantity we propose is limited to directed networks and complements the earlier proposed metric of node assortativity.*

Keywords: Complex networks, graph theory, assortativity, social networks, biological networks

1. Introduction

In the last few decades, network approaches have been widely used to analyze complex systems in a number of domains, including technical, biological, social and physical domains [1], [2]. Assortativity is a much studied concept in the topological analysis of complex networks [3], [4], [5], [6]. Assortativity has been defined to quantify the tendency in networks where individual nodes connect with other nodes which are similar to themselves [3]. Thus, a social network of people tends to be assortative, since people often prefer to be friends with, or have links to, other people who are like them. A food web could be argued as disassortative, because predator and prey are unlikely to be similar in many respects. However, it is clear that the assortativity of a network needs to be defined in terms of a particular attribute of nodes in that network. A social network could be assortative when the considered attribute is the age of people, because people tend to be friends with other people similar to their age: however, the same network could be disassortative, when the gender of individuals is the considered attribute. Degree assortativity is the most common form of assortativity used in network analysis, whereby similarity between nodes is defined in terms of the number of connections the nodes have. Degree assortativity can be defined and quantified as a Pearson correlation [3], [7]. It has been shown that many technological and biological networks are slightly disassortative, while most social networks, predictably, tend to be assortative in terms of degrees [3], [5]. Recent work defined degree assortativity for directed networks in terms of in-degrees and out-degrees, and showed that an ensemble of definitions are possible in this case [6], [7].

It could be argued, however, that the overall assortativity tendency of a network may not be reflected by individual links of the network. For example, it is possible that in a social network, which is overall assortative, some people may maintain their 'fan-clubs'. In this situation, people who have a great number of friends may be connected to people who are less famous, or even loners. If there is a link which connects such a popular person with a loner, that link cannot be called an assortative link, even though the network is overall assortative. Similarly, in a network which is overall disassortative many links could arguably be assortative. A good example for this is the so-called rich club scenario in internet AS networks [8]. Even though these networks display overall disassortativity, it has been shown that the hubs among them are strongly connected to each other, forming a 'rich-club'. The links that connect these hubs, therefore should be considered assortative in nature. These examples highlight that the 'local assortativity' of links is a quantity, which, if defined, can throw light on the topological structure of networks. In directed networks, this can be defined separately for out-degree based mixing patterns and in-degree based mixing patterns.

Indeed, decomposing the assortativity coefficient of a network into values for network components has already been attempted, and the metric of 'local assortativity' has been defined and analysed in detail [4], [6]. However, this decomposition has been done in terms of network nodes, rather than network links. In this work however, we propose to analyze the 'local assortativity' of individual links, and will demonstrate that this approach has its advantages, particularly for defining the assortativity of sub networks or regions. We limit our analysis to directed networks.

Analyzing the 'local assortativity' of links can give us a number of insights about networks. We will be able to identify 'positive' and 'negative' links in the network in terms of assortativity, and based on these we can see which links help, or hinder, the overall assortative tendency in networks. We can identify if assortativity of a network is primarily determined by the number of a particular type of links, or rather by the strength of such links. If the

'strength' of a minority of links is the primary reason for a network's assortativity, then we could predict that, if the network evolves, its assortativity may change rapidly. Link assortativity can be an indicator of the importance of links in the network, particularly if the links are highly assortative. Furthermore, profiles of link assortativity will provide us with yet another tool to classify networks.

Our paper is structured as follows: in the next section, we will introduce the concept of link assortativity for directed networks. We will use the definition of assortativity described in [7] to establish this concept, since this form of definition is most conducive for link-based decomposition. Then we will analyze the link-based assortativity profiles of a number of synthesized and real world directed networks. These include citation networks, Gene regulatory networks, transcription networks, foodwebs and neural networks. We will draw observations from this analysis, showing that a network could be either assortative, disassortative or non-assortative, due to a number of combinations between the ratio of 'positive' and 'negative' links, and the average strength of such links. We will also look at link-assortativity distributions of a number of networks, and discuss what insights can be gained from these about the evolution and functionality of these networks. Finally we will present our summary and conclusions.

2. Link assortativity of directed networks

Degree assortativity has been defined by Newman, as a Pearson correlation between the 'expected degree' distribution q_k, and the 'joint degree' distribution $e_{j,k}$ [3]. The expected degree distribution is the probability distribution of traversing the links of the network, and finding nodes with degree k at the end of the links. Similarly, the 'joint degree' distribution is the probability distribution of an link having degree j on one end and degree k on the other end. In the undirected case, the normalized Pearson coefficient of $e_{j,k}$ and q_k gives us the assortativity coefficient of the network, r.

If a network has perfect assortativity ($r = 1$), then all nodes connect only with nodes with the same degree. For example, the joint distribution $e_{j,k} = q_k\delta_{j,k}$ where $\delta_{j,k}$ is the Kronecker delta function, produces a perfectly assortative network. If the network has no assortativity ($r = 0$), then any node can randomly connect to any other node. A sufficiency condition for a non-assortative network is $e_{j,k} = q_j q_k$. If a network is perfectly disassortative ($r = -1$), all nodes will have to connect to nodes with different degrees. A star network is an example of a perfectly disassortative network, and complex networks with star 'motifs' in them tend to be disassortative.

In the case of directed networks, the definition is a bit more involved due to the existence of in-degrees and out-degrees. Therefore, we must consider the probability distribution of links going *out* of source nodes with j *out*-degrees, denoted as q_j^{out}, and the probability distribution of links going *into* target nodes with k *in*-degrees, denoted q_k^{in}. In addition, we may consider the probability distribution of links going *into* target nodes with k *out*-degrees, denoted $\breve{q}_k^{out}$, and the probability distribution of links going *out* of source nodes with j *in*-degrees, denoted $\breve{q}_j^{in}$. In general, $q_k^{out} \neq \breve{q}_k^{out}$ and $q_j^{in} \neq \breve{q}_j^{in}$ [6].

We can also consider distribution $e_{j,k}^{out,out}$, abbreviated as $e_{j,k}^{out}$, as the joint probability distribution of links going into target nodes with k *out*-degrees, and out of source nodes of j *out*-degrees (i.e., the joint distribution in terms of out-degrees). Similarly, $e_{j,k}^{in} = e_{j,k}^{in,in}$ is the joint probability distribution of links going into target nodes of k *in*-degrees, and out of source nodes of j *in*-degrees (i.e., the joint distribution of in-degrees).

we can therefore define the out-assortativity of directed networks, as the tendency of nodes with similar out-degrees to connect to each other. Using the above distributions, out-assortativity is formally defined, for out-degrees j and k, by Piraveenan et al [6] as

$$r_{out} = \frac{1}{\sigma_q^{out}\sigma_{\breve{q}}^{out}}\left[\left(\sum_{jk} jke_{j,k}^{out}\right) - \mu_q^{out}\mu_{\breve{q}}^{out}\right] \quad (1)$$

where μ_q^{out} is the mean of q_k^{out}, $\mu_{\breve{q}}$ is the mean of $\breve{q}_k^{out}$, σ_q^{out} is the standard deviation of q_k^{out}, and $\sigma_{\breve{q}}^{out}$ is the standard deviation of $\breve{q}_k^{out}$.

Similarly, Piraveenan et al. [6] defined in-assortativity as the tendency in a network for nodes with similar in-degrees to connect to each other, and this was formally specified as:

$$r_{in} = \frac{1}{\sigma_q^{in}\sigma_{\breve{q}}^{in}}\left[\left(\sum_{jk} jke_{j,k}^{in}\right) - \mu_q^{in}\mu_{\breve{q}}^{in}\right] \quad (2)$$

where μ_q^{in} is the mean of q_k^{in}, $\mu_{\breve{q}}^{in}$ is the mean of $\breve{q}_k^{in}$, σ_q^{in} is the standard deviation of q_k^{in}, $\sigma_{\breve{q}}^{in}$ is the standard deviation of $\breve{q}_k^{in}$.

Meanwhile, Foster et al. [7] also defined assortativity of directed networks in terms of the above distributions. While they used a different set of notations, using our notation their definition for out-assortativity can be written as

$$r_{out} = \frac{M^{-1}}{\sigma_q^{out}\sigma_{\breve{q}}^{out}}\left[\sum_i (j_i^{out} - \mu_q^{out})(k_i^{out} - \mu_{\breve{q}}^{out})\right] \quad (3)$$

where M is the number of links. Similarly, the definition of Foster et al. for in-assortativity can be written as

$$r_{in} = \frac{M^{-1}}{\sigma_q^{in}\sigma_{\breve{q}}^{in}}\left[\sum_i (j_i^{in} - \mu_q^{in})(k_i^{in} - \mu_{\breve{q}}^{in})\right] \quad (4)$$

It can be analytically proven that the definitions of Foster et al. for out-assortativity and in-assortativity are equivalent to the definitions of Piraveenan et al. for the same quantities respectively. That is, R.H.S of Eq. 1 = R.H.S of Eq. 3 and R.H.S of Eq. 2 = R.H.S of Eq. 4. Such a proof is given in our recent work [9] and it is beyond the scope of this paper to repeat it here. However, the key difference of the equivalent definitions is in the way the sums are obtained. While in the definitions of Piraveenan et al. the summations are obtained by traversing over degrees, in Foster et al. the summations are obtained by traversing over links.

Indeed, from Eq. 3 it is apparent that the out-assortativity of a network can be decomposed into individual contributions of links in that network. the summation of the contribution, in turn, gives the overall network out-assortativity. Therefore, we can write that

$$r_{out} = \sum_i \rho_e^{out} \tag{5}$$

where ρ_e^{out} is the individual contribution of a given link i to the out-assortativity of the network, and is given by

$$\rho_e^{out} = \frac{M^{-1}}{\sigma_q^{out}\sigma_{\breve{q}}^{out}}\left[(j_i^{out} - \mu_q^{out})(k_i^{out} - \mu_{\breve{q}}^{out})\right] \tag{6}$$

Similarly, the contribution of an individual link to the overall in-assortativity of a network is given by

$$\rho_e^{in} = \frac{M^{-1}}{\sigma_q^{in}\sigma_{\breve{q}}^{in}}\left[(j_i^{in} - \mu_q^{in})(k_i^{in} - \mu_{\breve{q}}^{in})\right] \tag{7}$$

The definitions ρ_e^{out} and ρ_e^{in} indicate that, individual links can be classified as 'assortative' or 'disassortative' in the context of out-degree and in-degree mixing respectively, by considering the sign of these quantities.

We also observe that in most networks, there will be a correlation between the sign of link assortativity of a link, and the degrees of nodes it connects. Intuitively, a link that connects a smaller-degreed node with a larger-degreed node will be disassortative, while an link which connects two similar degreed nodes will be assortative. We found evidence of this in both synthetic and real world networks. For example, in Fig. 1 we show the average link-assortativity against the differences in degrees at either end of links, for a simulated Erdos - Renyi random network. On the x-axis is shown the absolute difference between degrees of two nodes that are at the ends of an link. On y-axis, we calculate and show the average of link assortativity values for all links that have such a degree-difference. The figure clearly shows that, as the difference between the degrees increase, the links become more and more disassortative, as expected. We obtained similar results for a range of simulated scale-free networks.

Fig. 2 demonstrates the same concept in a different manner. In this figure, the *sum* of degrees at either end of an link are shown, rather than the difference. If the sum is very high, it means that both ends of a link have high-valued degrees, where as if the sum is low, it means that both ends of a link have low-valued degrees. In both cases, we see that, on average, the links are assortative. If the sum is in the middle ranges however, it typically may mean that one end of the link has a high degree and the other end has a lower degree. Only a minority of links will have exactly the same middle-valued degrees on both ends. Here, predictably, most links are disassortative.

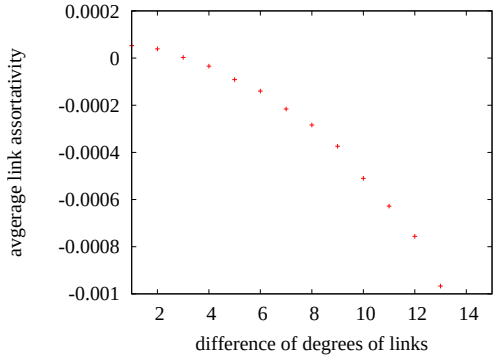

Fig. 1: Average link assortativity vs degree. The x-axis shows the difference between degrees at either end for a given link. The y-axis shows the average link assortativity of all links corresponding to the given x-value. As the difference between degrees increases, links on average become more disassortative.

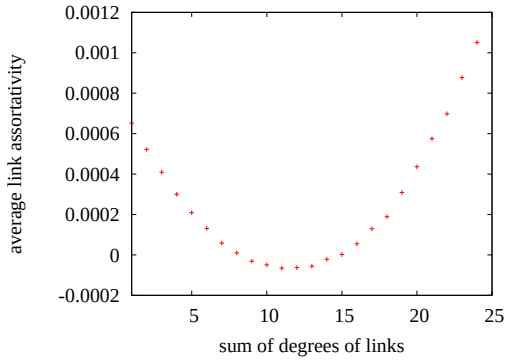

Fig. 2: Average link assortativity vs degree. The x-axis shows the sum of degrees at either end for a given link. The y-axis shows the average link assortativity of all links corresponding to the given x-value. It could be seen that, as the sum of degrees increases, links on average first become more disassortative and then more assortative.

3. Link assortativity of real world networks

We analyzed link assortativity patterns of a number of real world networks, including Gene regulatory networks, transcription networks, cortical networks, neural networks, food webs, and citation networks. An explanation is necessary to some of these types of networks, since the usage of names can be ambiguous. In our transcription networks, nodes are regulatory genes and regulated proteins, and the links are the interactions between them [1]. These are bipartite and directed networks. On the other hand, by gene regulatory networks we mean networks where nodes are genes, and the links are the inhibitory or inducing effects of one gene on the expression of another gene [10]. Note the subtlety that unlike transcription networks, only genes are considered as nodes in these directed networks. Similarly, by *cortical networks* we denote the networks of dependencies between various regions of the cerebral cortical (in a set of primates)[11]. The nodes are regions in the cortical, and the links are functional dependencies. Note that the nodes are *not* individual neurons. On the other hand, neural networks are networks where nodes are individual neurons belonging to an organism's neural system and links are anatomical connections between neurons [1]. In citation networks, nodes are research papers (or other citable documents) and links denote citations between these documents. In food webs, nodes are organisms in an ecosystem and the links represent predator-prey relationships between them [5]. These networks can be considered undirected or directed (prey to predator). A list of real world networks that we have studied is shown in Table 1, along with their out-assortativity and in-assortativity values. This is the same set studied in [6].

Table 2 shows the number of assortative and disassortative links in each network (M_{al} and M_{dl}), as well as the average strength of assortative and disassortative links in these networks ($< S >_{al}$ and $< S >_{dl}$). The average strength is calculated by summing the local link assortativity values of all links which are assortative or disassortative, and dividing it by their count. This is done for both out-assortativity and in-assortativity. It is apparent from the table that the assortativity coefficient of a network can be determined by (a) the numerical superiority of one type of links over the other (b) the strength superiority, on average, of one type of links over the other (c) a combination of these two factors, mutually reinforcing or otherwise. Specifically, we can observe the following scenarios.

In terms of out-assortatativity:

1) A Network can be assortative because a) it has more assortative links than disassortative links [such as C. elegans neural network, Human GRN, Chesapeake lower foodweb, E. coli and C. glutamicum transcription, Sci met, small World and Zewail citation networks, and human cortical]) The assortative links are, on average, stronger than disassortative links [No real world example] c) a combination of these two reasons [The GRNs of C. elegans, A. thaliana, R. norvegicus and M. musculus]
2) A network can be disassortative because a) it has more disassortative links than assortative links [transcription networks of C. jeikeium and C. efficiens] b) disassortative links are, on average, stronger than assortative links [No real world example] c) a combination of these two reasons [no real world example]
3) A network can be nearly non-assortative because a) It has almost equal assortative and disassortative links with equal strength on average [The food webs of Bay dry, chrystal D, chrystal C, Chessapeake upper, Bay wet, and the cortical networks of cat and macaque] b) It has more assortative links, but disassortative links are on average stronger [Lederburg, self organizing maps, and smart Grid citation networks] c) It has more disassortative links, but assortative links are on average stronger [No real world example]

The statement 'no real world example' is of course limited to the directed networks we have studied. As more directed networks are analysed, it is our hope that real world examples will turn up to illustrate the relevant scenarios.

A number of interesting contrasts can be made from these observations. For example, most foodwebs are non-assortative simply because there are equal number of assortative and disassortative links, with equal strength on average. However, many citation networks are also nearly non-assortative, for a very different reason. They all have more assortative links, but their disassortative links are much stronger! For example, the Lederburg citation network has 26730 assortative links to 14872 disassortative links, but its disassortative links are almost doubly stronger on average, making it overall rather non-assortative ($r = 0.06$). Similarly, while most assortative networks are assortative simply because they have more assortative links, and the average link strength is more or less equal for both types of links, this is not the case for most Gene Regulatory networks. They achieve such high assortativity values because not only they have a majority of assortative links, but also because some of these links are really strong. For example, the rat GRN has 12509 assortative links and 4147 disassortative links, but its assortative links are, one average, three times stronger compared to its disassortative links. These examples demonstrate that networks which appear to have similar assortativity values overall still may have very different topological designs. This was also highlighted by [4] in their derivation of node-based local assortativity.

We may do a similar analysis for in-assortativity of networks. Again, we may state that, In terms of in-assortatativity:

1) A Network can be assortative because a) it has more assortative links than disassortative links [such as

Network	Size N	r_{out}	r_{in}
Neural networks			
C. elegans	297	0.1	-0.09
GRNs			
rat (R. norvegicus)	819	0.64	0.59
human (H. sapiens)	1452	0.2	-0.01
mouse (M. musculus)	981	0.53	0.49
C. elegans	581	0.36	0.01
A. thaliana	395	0.16	0.03
Transcription networks			
E. coli	1147	0.17	0.03
C. glutamicum	539	0.09	-0.01
C. jeikeium	52	-1	-1
C. efficiens	50	-1	-1
Cortical networks			
human	994	0.17	0.17
Macaque monkey	71	0.06	-0.01
Cat cortical	65	-0.03	0.09
Food webs			
Chesapeake Lower	37	0.21	-0.06
Chesapeake Upper	37	0.1	-0.12
Crystal river C	24	0.08	-0.14
Crystal river D	24	0.06	-0.18
Bay wet	128	0.02	0.24
Bay dry	128	0.03	0.25
Citation networks			
Self organizing Maps	3772	0.21	-0.06
Small world	233	0.1	-0.12
Smart Grids	1024	0.08	-0.14
Lederberg	8324	0.06	-0.18
Zewail	6651	0.02	0.24
Sci met	2729	0.03	0.25

Table 1: Assortativity in real world directed networks. The table shows out-assortativity and in-assortativity coefficients. The source data for the networks is obtained from [12],[13],[14],[15],[16].

human cortical, baywet and baydry foodweb, Lderberg and Zewail citation networks] b) The assortative links are, on average, stronger than disassortative links [No real world example] c) a combination of these two reasons [The GRNs of R. norvegicus and M. musculus, and small world citation network]

2) A network can be disassortative because a) it has more disassortative links than assortative links [transcription network of C. jeikeium] b) disassortative links are, on average, stronger than assortative links [C. elegans neural network where this is the case even though there are more assortative links, and foodwebs of chrystal C and Chessapeake upper] c) a combination of these two reasons [Chrystal D foodweb]
3) A network can be nearly non-assortative because a) It has almost equal assortative and disassortative links with equal strength on average [cat cortical, macaque cortical and Chessapeake lower foodweb] b) It has more assortative links, but disassortative links are on average stronger [GRNs of A. Thaliana H. sapiens, C. elegans, transcription networks of E. coli and C. glutamicum, smart grid, sci met and self organising map citation networks] c) It has more disassortative links, but assortative links are on average stronger [No real world example]

Again, we may observe a number of interesting scenarios. For example, some disassortative networks can be disassortative on the strength of disassortative links, even while most links are in fact assortative, such as C. elegans neural network. Similarly, many networks are nearly non-assortative, because a majority of links are assortative while the disassortative links are on average stronger. These two

	In-In Distributions				Out-Out Distributions			
Network	$\mathbf{M_{al}}$	$\mathbf{M_{dl}}$	$< \mathbf{S} >_{\mathbf{al}}$	$< \mathbf{S} >_{\mathbf{dl}}$	$\mathbf{M_{al}}$	$\mathbf{M_{dl}}$	$< \mathbf{S} >_{\mathbf{al}}$	$< \mathbf{S} >_{\mathbf{dl}}$
Neural networks								
C. elegans	1251	877	1.69E-04	1.69E-04	1317	1028	0.00027	-2.55E-04
GRNS								
rat (R. norvegicus)	12169	4487	5.66E-05	-2.29E-05	12509	4147	5.85E-05	-2.13E-05
human (H. sapiens)	10037	6150	1.77E-05	-3.04E-05	10969	5218	3.69E-05	-3.95E-05
mouse (M. musculus)	10937	5200	5.71E-05	-2.54E-05	11386	4751	5.65E-05	-2.34E-05
C. elegans	1341	1004	1.14E-04	-2.44E-04	1436	692	0.000369	-2.40E-04
A. thaliana	1096	542	1.97E-04	-3.34E-04	1089	549	0.000215	-0.0001
Transcription nets								
E. coli	1430	733	7.38E-05	-1.08E-04	1269	894	0.00031	-0.00025
C. glutamicum	372	310	2.98E-04	-4.04E-04	376	306	0.00110	-0.00104
C. jeikeium	0	51	N.A	-0.01961	0	51	N.A	-0.01961
C. efficiens	45	0	0	N.A	0	45	N.A	-0.02222
Cortex networks								
human	15764	11276	2.64E-05	-2.15E-05	15764	11276	2.63E-05	-2.15E-05
Macaque monkey	375	371	8.35E-04	-8.63E-04	381	365	0.00097	-0.0008
Cat cortical	622	516	6.47E-04	-5.99E-04	579	559	0.00048	-0.00055
Food webs								
Chesapeake Lower	85	92	0.0028	-0.00325	107	70	0.00421	-0.00342
Chesapeake Upper	116	98	0.00185	-0.00339	124	90	0.00327	-0.00334
Crystal river C	66	59	0.0044	-0.00739	77	48	0.00492	-0.00617
Crystal river D	41	58	0.0056	-0.00700	57	42	0.00563	-0.00622
Bay wet	1398	708	2.75E-04	-2.07E-04	1041	1065	3.07E-04	-2.79E-04
Bay dry	1415	722	2.81E-04	-2.02E-04	1087	1050	0.00030	-0.00028
Citation networks								
Self organizing Maps	7065	5664	3.78E-05	-4.25E-05	9042	3687	9.48E-06	-1.95E-05
Small world	1324	664	2.96E-04	-1.49E-04	1246	742	0.00025	-0.00026
Smart Grids	3088	1833	4.63E-05	-6.36E-05	3090	1831	8.02E-05	-0.00010
Lederberg	25316	16286	9.25E-06	-7.74E-06	26730	14872	3.60E-06	-6.73E-06
Zewail	33314	20938	6.42E-06	-6.95E-06	34548	19704	9.11E-06	-7.72E-06
Sci met	6485	3930	1.72E-05	-2.77E-05	6522	3893	4.07E-05	-4.04E-05

Table 2: The table shows the number of assortative links M_{al}, and disassortative links M_{dl}, as well as the average strength of assortative links $< S >_{al}$ and disassortative links $< S >_{dl}$ respectively, for a number of real world networks, in the context of in-degree and out-degree mixing.

effects cancel each other out. Therefore, the interplay between the count of assortative and disassortative links, and the strength of such links, can give rise to a vast array of topologies, whose intricacies cannot be explained by a single Pearson coefficient.

4. Using link assortativity to calculate assortativity coefficient of subnetworks

Since link assortativity is a measure of individual links, it can be summed over a subset of links in a network. This could be used as a measure of assortativity for individual sub networks, where sub graphs show marked topological differences. While this would not be case in scale-free networks, which by definition show similar topological characteristics at all levels, there are many real world networks whose topological characteristics do not scale. This is particularly the case for man-made networks which have not evolved much.

One well known example is in the case of software networks, where individual classes or modules of software form nodes, and links are inter dependencies of such modules. An example of such a network is shown in Fig. 8 of [5], where it could be seen that the network consists of a distinct star and a chain-like structure. Here we analyse another such network of a Java software package, described in [17], where nodes are classes and links are strong dependencies (such as inheritance). As such, the network is directed. The considered network is shown in Fig. 3. It could be seen

that the network has a dominant star structure and a chain structure.

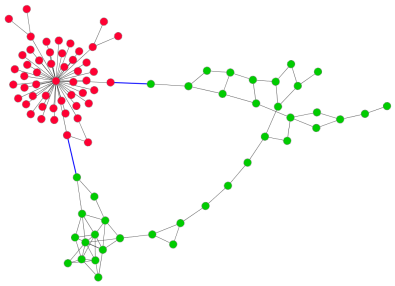

Fig. 3: Software network with classes as nodes and strong dependencies as links. It could be observed that two sub-networks are visible, where the topological patterns are very different to each other. These sub networks are shown by green and red nodes, respectively. The links which do not belong to either network are highlighted in blue.

The overall in-assortativity of this network is $r_{in} = -0.557$. However, it could be seen that the network is disassortative mainly because of the star structure. If the network is considered as the union of two sub networks (shown by the red nodes and the green nodes in Fig. 3) then we may see that the assortativity tendencies of each sub network are different. The sum of link assortativity values (for in-degrees) for the subnetwork in red are -0.314, while the same of link assortativities for the subnetwork in green are -0.235. Furthermore, if we look at the average strength of links, the subnetwork in red has an average strength of -0.0078, while the subnetwork in green has the average strength of -0.0039. The strength of the disassortative links in the red subgraph is double of those in the green subgraph. Therefore, it could be seen that the primary disassortative character from the overall network comes from the red subgraph. This is because of the presence of the star motif in the red subgraph, which by itself is perfectly disassortative. Analysing the out-assortativity of this network, we obtained similar results. This example demonstrates that the quantity of link-assortativity can be used to analyze, in a principled manner, assortative tendencies of subgraphs without breaking a network into components, which may itself change the assortative tendencies.

5. Conclusions

In this paper, we analyzed the local assortativity of links in directed networks. After establishing the expressions for link assortativity, we applied them to a number of synthetic and real world networks. We showed that the overall assortative tendency of a network is influenced by two factors (i) the relative number of assortative / disassortative links (ii) the relative strength of assortative / disassortative links - or a combination of these factors. we demonstrated, using a number of real world examples, that two directed networks may have the same level of assortativity for different reasons, influenced by the factors above. We also demonstrated that link assortativity in directed networks can be a useful measure to analyse assortative tendencies of subgraphs without breaking the original networks. Using a software network, we showed that portions of network may have very different assortative tendencies and link strengths. We also pointed out that link assortativity distributions could be constructed and used as a useful tool to understand network topology.

In conclusion, we believe that link-based local assortativity analysis demonstrates the duality of local assortativity analysis, initially proposed as a node-based metric, and together these measures will be used to understand the structure and function of complex directed networks.

References

[1] F. Kepes (Ed), *Biological Networks*. Singapore: World Scientific, 2007.

[2] S. N. Dorogovtsev and J. F. F. Mendes, *Evolution of Networks: From Biological Nets to the Internet and WWW*. Oxford: Oxford University Press, January 2003.

[3] M. E. J. Newman, "Assortative mixing in networks," *Physical Review Letters*, vol. 89, no. 20, p. 208701, 2002.

[4] M. Piraveenan, M. Prokopenko, and A. Y. Zomaya, "Local assortativeness in scale-free networks," *Europhysics Letters*, vol. 84, no. 2, p. 28002, 2008.

[5] R. V. Solé and S. Valverde, "Information theory of complex networks: on evolution and architectural constraints," in *Complex Networks*, ser. Lecture Notes in Physics, E. Ben-Naim, H. Frauenfelder, and Z. Toroczkai, Eds. Springer, 2004, vol. 650.

[6] M. Piraveenan, M. Prokopenko, and A. Y. Zomaya, "Assortative mixing in directed biological networks," *IEEE/ACM Transactions on computational biology and bioinformatics*, vol. 9(1), pp. 66–78, 2012.

[7] J. G. Foster, D. V. Foster, P. Grassberger, and M. Paczuski, "Edge direction and the structure of networks," *Proceedings of the National Academy of Sciences*, vol. 107, no. 24, pp. 10 815–10 820, June 2010. [Online]. Available: http://dx.doi.org/10.1073/pnas.0912671107

[8] V. Colizza, A. Flammini, M. A. Serrano, and A. Vespignani, "Detecting rich-club ordering in complex networks," *Nature Physics*, vol. 2, pp. 110–115, 2006.

[9] M. Piraveenan, M. Prokopenko, and A. Y. Zomaya, "On the equivalence of two definitions for directed assortativity in networks," *Under review*, 2012.

[10] P. Fernández and R. V. Solé, "The role of computation in complex regulatory networks," in *Scale-free Networks and Genome Biology*, E. V. Koonin, Y. I. Wolf, and G. P. Karev, Eds. Georgetown, TX: Landes Bioscience, 2006, pp. 206–225.

[11] A. Tang, C. Honey, J. Hobbs, A. Sher, A. Litke, O. Sporns, and J. Beggs, "Information flow in local cortical networks is not democratic," *BMC Neuroscience*, vol. 9, no. Suppl 1, p. O3, 2008.

[12] (2009) Collations of connectivity data on the Macaque brain. [Online]. Available: www.cocomac.org/

[13] J. Baumbach, "Coryneregnet 4.0 - a reference database for corynebacterial gene regulatory networks," *BMC Bioinformatics*, vol. 8, 2007.

[14] (2008) Michigan Molecular Interaction Database, University of Michigan. [Online]. Available: http://mimi.ncibi.org/MimiWeb/mainpage.jsp

[15] D. J. Watts and S. H. Strogatz, "Collective dynamics of small-world networks," *Nature*, vol. 393, no. 6684, pp. 440–442, June 1998. [Online]. Available: http://dx.doi.org/10.1038/30918

[16] (2007) Pajek datasets. [Online]. Available: http://vlado.fmf.uni-lj.si/pub/networks/data

[17] M. Piraveenan, "A software network based on network analysis software," *Under review*, 2012.

On the Optimality of a Family of Binary Trees

Dana Vrajitoru
Computer and Information Sciences Department
Indiana University South Bend
South Bend, IN 46645
Email: danav@cs.iusb.edu

William Knight
Computer and Information Sciences Department
Indiana University South Bend
South Bend, IN 46645
Email: wknight@iusb.edu

***Abstract*—In this paper we present an analysis of the complexity of a class of algorithms. These algorithms recursively explore a binary tree and need to make two recursive calls for one of the subtrees and only one for the other. We derive the complexity of these algorithms in the worst and in the best case and show the tree structures for which these cases happen.**

I. Introduction

Let us consider a traversal function for an arbitrary binary tree. Most of these functions are recursive, although an iterative version is not too difficult to implement with the use of a stack [1]. The object of this paper, though, is those functions that are recursive.

For the remainder of the paper we'll consider the classic C++ implementation of a tree node as follows:

```
template <class otype>
struct node {
  otype datum;
  node *left, *right;
};
```

When a recursive function makes a *simple traversal* of a binary tree with *n* nodes, in which the body of the traversal function contains exactly two recursive calls, one on the left subtree and one on the right, and all other parts of each call require $\Theta(1)$ time, then the execution time is roughly proportional to the total number of calls (initial and recursive) that are made. In this case that will be $1 + 2n$ (the call on the pointer to the root of the tree and one call on each of the $2n$ pointers in the tree), so the execution time is $\Theta(n)$. The analysis would apply, for example, to the function below that traverses the tree to calculate its height [2].

```
int height (node_ptr p) {
  if (p == NULL)
    return -1;
  int left_height  = height (p->left);
  int right_height = height (p->right);
  if (left_height <= right_height)
    return 1 + right_height;
  else
    return 1 + left_height;
}
```

The next function, `height1`, is a differently coded version of the function `height`. Note that this function looks simpler than the first one. The code of `height1`, though, is *not* a "simple traversal" of the kind described above. Here is the reason: when recursive calls are made, exactly one of the recursive calls is *repeated*. Clearly, then the total number of calls is not just $2n + 1$. We shall try to figure out the total number of calls that could be made when the function `height1` is called on a tree T with n nodes.

```
int height1 (node_ptr p) {
  if (p == NULL)
    return -1;
  if (height(p->left) <= height(p->right))
    return 1 + height(p->right);
  else
    return 1 + height(p->left);
}
```

At first sight it would seem that this is not a very useful problem to study because we can easily correct the fact that this function performs two recursive calls on one of the subtrees. We can store the result of the function in a local variable and use it instead of the second recursive call, as implemented in the first version of the function. Even if this is the case indeed, it would still be useful to know just "how bad" the complexity of the function can get from a simple change. Although the problem might sound simple, the complexity calculation requires a careful analysis of the tree structure and reveals interesting tree properties related to the height of the larger subtree.

The second motivation is that just as the function `height` is representative of a whole class of traversal functions for binary trees, the analysis for the function `height1` can also be applied to a whole class of functions. Some of these can be optimized with the method used for the function `height`, but some of them might require operations making the second recursive call on the same subtree necessary.

An example of such a problem would be modifying the `datum` in each of the nodes situated in the taller subtree of any node. One traversal is necessary to determine the height of the subtrees. A second traversal is necessary for the subtree of larger height to increment its datum values.

The trees that we are studying here are somewhat related to increasing trees that are also related to recursion [3]. Theorems providing limits to sum of weights and the path length of such trees can be found [4]. The problem is also related to binary trees with choosable edge length and cryptography [5].

The idea of balancing the weights in a tree to optimize a particular function is of a more general nature and is also

related to binary search trees [6], B-trees [7], priority queues [8], and mergeable trees [9]. These techniques have numerous applications, as for example, cryptography [10].

II. Complexity Function

Let $K(T)$ denote the total number of calls (initial and recursive) made when the second height function is called on a binary tree T, and let L_T and R_T denote the left and right subtrees of T. Then we can write

$$K(T) \quad = \begin{cases} 1 \quad \text{if } T \text{ is empty} \\ 1 + K(L_T) + 2\,K(R_T) \quad \text{if } R_T \\ \qquad \text{is at least as tall as } L_T \text{ and } T \neq \phi \\ 1 + 2\,K(L_T) + K(R_T) \quad \text{otherwise} \end{cases}$$

Theorem 2.1: For a tree with *n* nodes, the function *K* has complexity $\Theta(2^n)$ in the worst case.

Proof. For non-empty trees with *n* nodes, we can maximize the value of $K(T)$ by making every node (except the root) the right child of its parent. This results in a tree that has the maximum possible height $n-1$. Let $F(n)$ denote $K(T)$ for this kind of tree *T* with *n* nodes. Then we can write

$$F(0) = 1,\ F(n) = 1 + F(0) + 2F(n-1) = 2F(n-1) + 2. \quad (1)$$

This problem is easy to solve for $F(n)$, and the solution is $\Theta(2^n)$. That is, the function `height1` is exponential on degenerate binary trees of maximal height. This is the worst possible case for that algorithm. ■

Having identified the worst case for $K(T)$, let's now try to find the best case.

Definition 2.2: A K-*optimal tree* of size *n* is a binary tree *T* with *n* nodes that minimizes the value of *K* among all trees with *n* nodes.

Based on what we have just seen with trees that maximize $K(T)$, it is reasonable to conjecture that the way to build a *K*-optimal tree of size is to make it as short as possible.

Perhaps, one might guess, a binary tree is *K*-optimal if and only if it is *compact*, meaning that all of its levels except for the last one contain all the nodes that they can contain. As it turns out, however, many compact trees are not *K*-optimal, and many *K*-optimal trees are not compact.

Definition 2.3: A *right-heavy* tree is one in which every node has a left subtree of height less than or equal to the height of its right subtree.

Lemma 2.4: Let *T* be a binary tree. For any node in *T*, if the left subtree is taller than the right subtree, then the two subtrees can be interchanged without changing the value of the function *K*.

Proof. This is easy to see by examining the code in the second height function. ■

Lemma 2.4 allows us to simplify our search for *K*-optimal binary trees by restricting it to right-heavy trees.

For convenience, let's label each node *N* in a tree with the number of calls to the function `height1` that will be made on the pointer to *N*, and label each empty subtree E with the number of calls on the corresponding null pointer. Note that these labels will always be powers of 2. Figure 1 shows a tree labeled using this system. The *K* value of this tree is obtained by adding up all the numeric labels in the tree (118 in this example). We will also refer to the sum of the labels in a subtree as the *weight* of the subtree. Because the tree in Figure 1 is right heavy, for each node *N* in the tree, the left child of *N* always has the same label as *N*, while the right child always has a label that's twice the label on *N*.

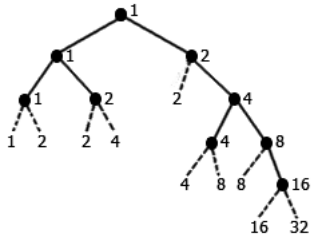

Fig. 1. An example of right-heavy tree with labeled nodes. The dashed lines indicate null pointers.

Suppose *A* and *n* are nodes in a binary tree; if *A* is an ancestor of *n*, and if *n* is reached from *A* by following only right pointers, then *n* is a "right descendant" of *A*, and *A* is a "right ancestor" of *n*.

Lemma 2.5: Let *T* be a right-heavy binary tree, and let *L* be a leaf of *T*. Then *L* can be removed without changing the label of any other node if and only if *L* satisfies one of the following conditions:

a) *L* is the only node in *T*;

b) *L* is a left child of its parent;

c) *L* is a right child of its parent, and for each right ancestor *A* of *L*, the left subtree of *A* is strictly shorter than its right subtree. (Figure 2 shows an example of a right leaf, in solid black color, that can be removed without changing the label on any other node in the tree.)

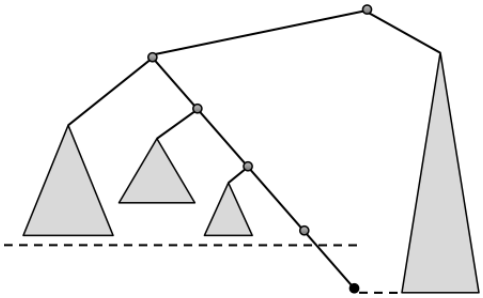

Fig. 2. A right leaf that can be removed without changing the labels in the tree

Proof. A simple observation tells us that the leaf *L* can be removed from *T* without changing the label of any other node in *T* if and only if the remaining tree is right-heavy after *L* is removed. Thus, to prove the Lemma, we'll prove that each of the three conditions (a), (b), and (c) separately implies that when *L* is removed from *T* the remaining tree is right-heavy; then we'll prove that if all three conditions are false, the remaining tree is not right-heavy after *T* is removed from *T*.

First, suppose the leaf L is the only node in T. Then removing L from T leaves the empty tree, which is vacuously right-heavy.

Second, suppose the leaf L is the left child of some node P. Since T is right-heavy, P must have a non-empty right subtree. It is now easy to see that if L is removed from T the remaining tree is right-heavy.

Now suppose the leaf L is the right child of some node P, and that for each right ancestor A of L, the left subtree of A is strictly shorter than its right subtree. Thus, by removing this node, each of these left subtrees will now have a height at most equal to their right counterparts. Then after the first left ancestor of L, if there is one, by removing L we reduce the height of a left subtree, and thus the tree remains right-heavy.

Finally, suppose that all three conditions (a), (b), and (c) of the Lemma are false, which means that the leaf L is the right child of some node in T and at least one right ancestor of L has left and right subtrees of equal height (the left can't be strictly taller because T is right-heavy). In this case, by removing L, we make the left subtree that had a height equal to its right sibling, now higher than it, so the tree would not be right-heavy anymore. ■

This proof is provided in more detail in [11].

Corollary 2.6: Let T be a right-heavy binary tree. We can add a new leaf L to the tree without changing the label of any other node if and only if L and T satisfy one of the following conditions:

a) T is empty before inserting L;
b) L is added as a left child of any node that has a right child;
c) L is added as the right-most leaf in the tree or in a place such that the first ancestor of L that is not a right ancestor has a right subtree of height strictly greater than the height of the left subtree before adding L.

Proof. This is a direct consequence of Lemma 2.5. ■

Theorem 2.7: The K function is strictly monotone over the number of nodes on the set of *K*-optimal trees. In other words, if T_m and T_n are two *K*-optimal trees with number of nodes equal to m and n respectively, where $m < n$, then $K(T_m) < K(T_n)$.

Proof. It suffices to prove the statement in the theorem for $m = n - 1$. Let T_n be a *K*-optimal tree with n nodes. Without loss of generality, we can assume that T_n is right-heavy.

Let us locate the left-most leaf, call it L. There are 3 possible situations that we need to consider, as shown in Figure 3 (shown without the labels of the empty subtrees for better clarity).

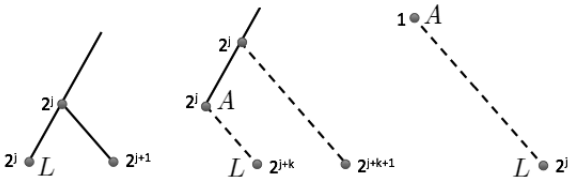

Fig. 3. Possible placement of the left-most leaf, denoted by L

Suppose L, is at the end of a left branch (left-most case in Figure 3). Since T_n is right-heavy, Lemma 2.5, case (b), tells us that we can remove L from T_n without changing any of the labels on the other internal nodes of the tree. This produces a right-heavy tree with $n-1$ nodes and strictly smaller *K* value. This smaller tree may not be optimal among all binary trees with $n-1$ nodes, in which case there is some *K*-optimal tree T_{n-1} with even smaller *K* value. Thus a *K*-optimal tree with $n-1$ nodes has a smaller *K*-value than $K(T_n)$.

Now suppose the leaf L is a right child. Let A be its highest right ancestor in T_n. In the most extreme case, A is the root of T_n and L is the only leaf in T_n, as shown in the right-most case in Figure 3. Then each of the right ancestors of L must have an empty left subtree, otherwise L would not be the left-most leaf. By Lemma 2.5 we can remove L without changing any of the other labels in T_n, leaving a right-heavy tree with smaller *K*-value. As in the preceding paragraph, this proves that *K*-optimal trees with $n-1$ nodes have smaller *K*-value than $K(T_n)$. ■

III. Two Special Cases

Definition 3.1: A *perfect binary tree* is one where all the levels contain all the nodes that they can hold.

A perfect tree of height h has a number of nodes $n = 2^{h+1} - 1$. We can reverse this to express $h = \lg(n+1) - 1 = \Theta(\lg(n))$.

Theorem 3.2: The function *K* has a complexity of $\Theta(n^{\lg(3)})$ on perfect trees, where *n* is the number of nodes in the tree.

Proof. For a perfect tree of height $h \geq 0$, the two subtrees are perfect trees of height $h-1$. If we denote by κ the value of the function *K* on a perfect tree of height h, we can write the sum of labels on these trees as

$$\kappa(h) = 1 + 3\kappa(h-1), \quad \kappa(0) = 4.$$

We can solve this recurrence relation by following the standard procedure and obtain the solution

$$\kappa(h) = \frac{9}{2}3^h - \frac{1}{2} = \Theta(3^h).$$

Let us denote by P_n a perfect binary tree with *n* nodes. Using the relationship between *n* and h, we can now express the same sum of labels as a function of the number of nodes, getting us back to the function *K* itself:

$$K(P_n) = \Theta(3^{\lg(n)}) = \Theta(n^{\lg(3)}).$$

Even though most perfect trees turn out not to be *K*-optimal, knowing what their sum of labels is and knowing that the *K*-optimal function is monotone gives us an upper bound for the minimal complexity for a given number of nodes. ■

Corollary 3.3: The height of a *K*-optimal tree with *n* nodes cannot be larger than $c + \lg(3)\lg(n)$, where c is a constant.

Proof. A *K*-optimal tree with *n* nodes and height h must have one longest path where the label of every node is an increasing power of 2, going from 1 for the root to 2^h for the leaf, plus the empty subtrees of the leaf, of labels 2^h and 2^{h+1}. The sum of the labels is $2^{h+2} - 1 + 2^h$. This sum is less than or equal to the *K*-value of this *K*-optimal tree with *n* nodes,

which, by monotonicity, is less than or equal to the *K*-value of the smallest perfect tree of a number of nodes $m \geq n$. If g is the height of this perfect tree, then its number of nodes is $m = 2^{g+1} - 1$. If we choose the smallest of these trees, then $2^g - 1 < n \leq 2^{g+1} - 1$, which implies $g = \lfloor \lg(n) \rfloor$.

Thus, the height of this perfect tree is equal to $\lfloor \lg(n) \rfloor$ and its number of nodes is $m = 2^{\lfloor \lg(n) \rfloor + 1} - 1 \leq 2n - 1$. By Theorem 3.2, this implies that,

$$2^{h+2} - 1 + 2^h \leq a\, m^{\lg(3)} \leq a(2n-1)^{\lg(3)} < a(2n)^{\lg(3)} = 3\, a\, n^{\lg(3)}$$

for some constant a. From this we can write

$$5\, 2^h \leq 3an^{\lg(3)} \quad \Rightarrow \quad h \leq \lg(3a/5) + \lg(3)\lg(n)$$

and the quantity $\lg(3a/5)$ is the constant c in the corollary. ■

Lemma 3.4: The sum of labels on level k of a perfect binary tree is equal to 3^k.

Proof. This Lemma is easily proved by induction, using the fact that every non-leaf node has two children nodes with a sum of labels equal to 3 times its own label. ■

Lemma 3.5: The number of nodes on level k of a perfect binary tree that have labels equal to 2^j, where $0 \leq j \leq k$, is equal to $C(k, j)$, where C(k,j) denotes the number of combinations of k things taken j at a time.

Proof. We will prove this lemma by induction over k using the following property of the combinations function:

$$C(m, p) = C(m-1, p) + C(m-1, p-1).$$

Let us denote by $C_t(k, j)$ the count of nodes with label equal to 2^j on level k. We'll prove that C_t is identical with the function C.

Base case. For $k = 0$ we only have one node, so $C_t(0, 0) = 1 = C(0, 0)$.

Inductive step. For an arbitrary k and j, there are two types of nodes with label 2^j on level k. The first type are left children of their parents and their labels are identical to those of their parents. The count of such nodes is $C_t(k-1, j) = C(k-1, j)$ by the inductive step. The second type of nodes are right children of their parents. These nodes have labels that are the double of the labels of their parents, so they come from nodes of label 2^{j-1} on level $k-1$. Thus, the count of such nodes on level k is equal to $C_t(k-1, j-1) = C(k-1, j-1)$ (by the inductive step).

By summing up the count of nodes that are left children and those that are right children, we have that

$$C_t(k, j) = C(k-1, j) + C(k-1, j-1) = C(k, j). \quad ■$$

Theorem 3.6: A perfect binary tree of height $h \geq 16$ is not *K*-optimal.

Proof. Let *T* be a perfect binary tree of height $h \geq 16$. Our strategy will be to show that we can find another binary tree, say T', with the same number of nodes as *T* but a smaller *K*-value. This will prove that *T* is not *K*-optimal. T' will be constructed by removing $h + 2$ of the leaves of *T* and re-attaching them elsewhere, as shown in Figure 4. Now let's look at how to do the removals.

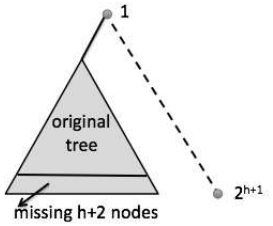

Fig. 4. Tree of smaller weight built from a perfect tree

The next-to-last level (level $h-1$) of our perfect tree *T* contains 2^{h-1} nodes, each with a label that's a power of 2. By Lemma 3.5, there are $C(h-1, h-2)$ labels of the form 2^{h-2}. Note that $C(h-1, h-2) = h-1$. By Lemma 2.5, the left child of each of these $h-1$ nodes can be removed from *T* without changing any of the labels on the remaining nodes. For each of these nodes, we remove two empty subtrees of labels 2^{h-2} and 2^{h-1}, and replace the leaf with an empty subtree of the same label. The net effect, then, is to decrease the sum of labels in *T* by $2^{h-2} + 2^{h-1} = 3 * 2^{h-2}$. When we do this for all $h-1$ of these left leaves with label 2^{h-2}, we have decreased the total weight (i.e., sum of labels) of *T* by $3(h-1)2^{h-2}$.

Then we are going to select 3 out of the $C(h-1, h-3)$ (> 3 for $h \geq 6$) leaves on level $h-1$ of label 2^{h-3} and remove their left children. Each child removed reduces the weight of the tree by $3 * 2^{h-3}$ by the same reasoning as we used in the preceding paragraph. Thus the total decrease in the weight of the tree is $9 * 2^{h-3}$ when these 3 nodes are removed. Thus, we've removed $h+2$ nodes from *T* with a total decrease in weight of $3 * (h-2)2^{h-2} + 9 * 2^{h-3}$.

We are going to re-attach them as shown in Figure 5: one of them will become the root of a new tree T', and all the others will be placed on a path going straight to the right. The labels in the original tree do not change. The nodes on the new path have labels 1, 2, 2^2, ..., 2^{h+1}, while their empty subtrees have labels 2, 2^2, 2^3, ..., 2^{h+2}. The total weight that has been added by the re-attachment of the nodes is therefore $3(2^{h+2} - 1)$.

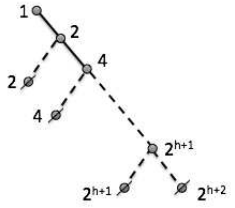

Fig. 5. Labels on the added path

Now we need to prove that the weight we subtracted is greater than the weight we added. That is, we need to verify

that

$$3(h-1)2^{h-2} + 9 * 2^{h-3} > 3(2^{h+2} - 1).$$

Solving this inequation results in

$$2(h-1) + 3 \geq 32,$$

which, since h is an integer, simplifies to $h \geq 16$. ■

Note. A slightly more complex proof allows us to lower the threshold in Theorem 3.6 to 12.

Definition 3.7: A binary tree *T* with *n* nodes is a **size-balanced** tree if and only if its left and right subtrees contain exactly $\lfloor (n-1)/2 \rfloor$ and $\lceil (n-1)/2 \rceil$ nodes respectively, and a similar partition of the descendents occurs at every node in the tree.

Theorem 3.8: The function *K* on a size-balanced tree with *n* nodes has a complexity that is $\Theta(n^{\lg(3)})$.

Proof. Let $S(n)$ denote the value of $K(T)$ when *T* is the size-balanced tree containing *n* nodes.

It is easy to prove by induction that size-balanced trees are right-heavy. The `height1` function will then make one call on the pointer to the left subtree and two calls on the pointer to the right subtree. Thus, we can write the following recurrence relation for $S(n)$:

$$S(n) = 1 + S\left(\left\lfloor \frac{n-1}{2} \right\rfloor\right) + 2S\left(\left\lceil \frac{n-1}{2} \right\rceil\right),$$

which is valid for all $n \geq 1$, with the initial value is $S(0) = 1$. This is a difficult recurrence relation to solve exactly, but instead, we can use the recurrence relation and induction to prove the inequalities

$$S(n) \leq \frac{3^{\lfloor \lg(n) \rfloor + 2} - 1}{2} \quad \text{and } S(n) \geq \frac{3^{\lfloor \lg(n+1) \rfloor + 1} - 1}{2},$$

which imply that $S(n) = \Theta(n^{\lg(3)})$. Since $\lg(3) \approx 1.585$, it follows that the growth rate of $S(n)$ is only a little greater than $\Theta(n\sqrt{n})$. Finally, remember that size-balanced trees are not necessarily *K*-optimal trees, and thus a *K*-optimal tree *T* with *n* nodes will satisfy $K(T) \leq S(n)$. From this it follows that $K(T) = O(n^{\lg(3)})$, where *n* denotes the number of nodes in *T*. ■

Theorem 3.8 now gives us an example of a class of trees where the function *K* has a complexity that is $\Theta(n^{\lg(3)})$ for any arbitrary number of nodes *n*.

IV. Best Case Complexity

Theorem 4.1: For *K*-optimal binary trees T_n with *n* nodes, $K(T_n) = \Theta\left(n^{\lg(3)}\right)$.

Suppose we want to build a *K*-optimal binary tree with a prescribed number of nodes *n*. We shall show how the majority of the nodes must be inserted so as to minimize the sum of labels. This will allow us to show that the *K*-optimal *n*-node tree we are building must have a sum of labels that's at least $A(n^{\lg(3)})$ for some number *A* independent of *n*. Since Theorem 3.8 implies that the sum of labels in a *K*-optimal tree with *n* nodes can be at most $B(n^{\lg(3)})$ for some constant *B*, we will have proved Theorem 4.1.

So suppose we are given some positive integer *n*. In building a *K*-optimal *n*-node tree, we can without loss of generality require that it be right-heavy (see Lemma 2.4). Then the longest branch in the tree will be the one that extends along the right edge of the tree. Its lowest node will be at level h, where h is the height of the tree. By Corollary 3.3, h will have to satisfy $\lfloor \lg(n) \rfloor \leq h \leq c + \lg(3)\lg(n)$ for a constant c. Thus h is $\Theta(\log(n))$. We can start with $h = \lfloor \lg(n) \rfloor$, then attach additional nodes to this longest branch if they are needed late in the construction. When *n* is large, we will have used only a small fraction of the prescribed *n* nodes during construction of this right-most branch. We will still have many nodes left over to insert into the optimal tree we are building. Finally, note that the longest branch will have $h+1$ nodes, with labels 2^0, 2^1, 2^2, …, 2^h. Their sum is $2^{h+1} - 1$.

Let us add nodes to this branch in the order of labels, following Corollary 2.6. Note that it is not always possible to add the node of lowest label, and oftentimes we need to add a right leaf of higher label before we can add a left one of lower label.

The first node that we can add is the left child of the root, of label 1, as shown in Figure 6 left. Then we can add all 3 nodes in the empty spots on level 2 of the tree, as shown in the second tree in Figure 6. At this point, there are 3 spots available for nodes of label 4, and that is the lowest label that can be added, as shown in the third tree in Figure 6. The left-most node of label 4 would allow us to add 3 nodes of labels lower than 4. The one to its right would allow only the addition of one node of label 2. The right-most node of label 4 does not open any other spots on the same level.

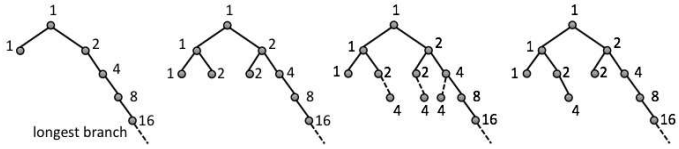

Fig. 6. Incremental level addition in a *K*-optimal tree

It stands to reason that we should insert the left-most label 4 first, as shown in the right-most tree in Figure 6. After this insertion there are two spots at which a label 2 can be added. The left-most one allows us to add a node of label 1, while the other one doesn't. Thus we would insert the left-most 2, followed by a 1. Then we can insert the other 2 into level 3, as shown in Figure 7.

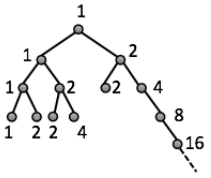

Fig. 7. Nodes that the addition of the one labeled 4 allows in the tree

Continuing a few more steps the same way, we notice that a structure emerges from the process, shown in Figure 8. We

shall call it the *skeleton structure*. At every step in a new level, these nodes represent the ones that would open the most spots of lower labels out of all available spots of optimal label. This figure does not show all the nodes added on a level before the next one is started, but rather the initial structure that the rest of the nodes are added on. In fact, the first few levels in the tree are filled up completely by the procedure. At some point it can become less expensive to start adding nodes on the next level down rather than continuing to complete all the upper levels. Theorem 3.6 indicates the level where this situation occurs.

The skeleton structure of the *K*-optimal tree we will construct will consist of the right-most branch of height h, the right-most branch of the left subtree, the right-most branch of the left subtree of the left subtree, and so on down the tree. Let's use g to denote the height of the left subtree, so that $g \leq h-1$. It follows that $g = O(log(n))$.

Note that the skeleton structure without the longest branch contains the first new nodes added to every new level. By trimming the whole tree at the level g, we only cut off $h-g$ number of nodes on the right-most branch, and their number is at most $h = \Theta(\log(n))$. Thus, this subtree of height g will contain at least $n-h+g$ nodes, and this number is asymptotic to *n*. Thus, $g \geq \lfloor \lg(n) \rfloor$ for *n* large enough. In general, $g = \Theta(\log(n))$. For the remaining of the proof, let us consider the skeleton structure to be trimmed at the level g.

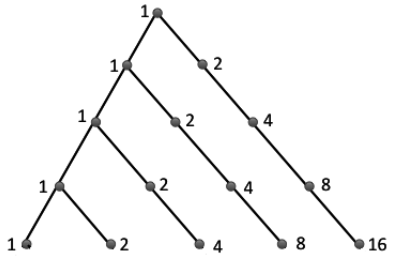

Fig. 8. The skeleton structure for a tree of height 4

Let us now examine the contribution of the skeleton structure trimmed to level g in terms of number of nodes and sum of labels. The *number of nodes* in this structure is calculated by noting that it is composed of $g+1$ paths, starting from one composed of $g+1$ nodes and decreasing by 1 every time. So we have

$$\sum_{i=0}^{g} i = \frac{(g+1)(g+2)}{2} = \Theta((\log(n))^2).$$

The sum of labels can be computed by observing that on each of these paths, we start with a label equal to 1, and then continue by incremental powers of 2 up to the length of the path. The sum of the labels on a path of length i is computed just like we did for the right-most branch, and is equal to $2^{i+1}-1$. Thus, we can compute the total *sum of labels* as

$$\sum_{i=0}^{g}(2^{i+1}-1) = 2^{g+2}-2-(g+1) = 2^{g+2}-g-3 = \Theta(n).$$

TABLE I
NODES OF LOWEST WEIGHT THAT CAN BE ADDED TO THE SKELETON STRUCTURE

Iteration	# Nodes	Weight
$i=1$	$g-1$	$2(g-1) = 2^1 \cdot 3^0(g-1)$
$i=2$	$g-2$	$4(g-2) = 2^2 \cdot 3^0(g-2)$
	$2(g-2)$	$6(g-2) = 2^1 \cdot 3^1(g-2)$
$i=3$	$2^0(g-3)$	$8(g-3) = 2^3 \cdot 3^0(g-3)$
	$2^1(g-3)$	$2^2 \cdot 3^1(g-3)$
	$2^2(g-3)$	$2^1 \cdot 3^2(g-3)$

We can see that this skeleton structure contributes only $\Theta(n)$ to the sum of labels in the tree, which will not change its overall complexity, but it also uses only $\Theta((\log(n))^2)$ of the *n* nodes.

Minimal Node Placement. For the next part of the proof, we shall place the remainder of the nodes in this structure in order starting from the empty places of lowest possible label going up. These nodes are naturally placed in the tree while the skeleton structure is being built up, but for the purpose of the calculation, it is easier to consider them separately.

A simple observation is that the empty spots of lowest labels available right now are the left children of all the nodes labeled 2. For all of them, a branch on the right side is present, so we can add them without any changes to the labels in the tree. There are $g-1$ such empty spots available, because the first of them is on level 2, as shown in Figure 9 left.

Next, by the same reasoning, we can add $g-2$ left children of label 4. At the same time, we can add a right child of label 4 to every node added at the previous step with label 2, except for the lowest one. That is, we can add $g-2$ right children, each having label 4, as shown in the $i=2$ column of Figure 9. In addition, we can also add the $g-2$ left children of the same parents. None of these additions causes any changes in the labels of the original nodes in Figure 8.

We can thus proceed in several steps, at each iteration adding nodes with labels going from 2 up to a power of 2 incrementing at every step. Let us examine one more step before we draw a general conclusion.

For the third step, we can add $g-3$ nodes of label $8 = 2^3$. Next to this, we can add a complete third level to $g-3$ perfect subtrees added at the very first step, that have a root labeled 2, and a second complete level to $g-3$ perfect subtrees of root labeled 4. This continues to grow the perfect subtrees started at the previous levels. The sum of labels on a level of a perfect tree is equal to a power of 3, but this quantity must also be multiplied by the label of the root in our case. Table I summarizes the nodes we have added and their total weight for the 3 steps we've examined so far. Figure 9 also illustrates this explanation.

From this table we can generalize that for the iteration number i we will have groups of nodes that can be added, with a count of $g-i$ groups in each category. For each category we will be adding the level k of a perfect tree that has a root labeled 2^{i-k}. The number of nodes in each such group is 2^k.

The weight of each group is $2^{i-k} \cdot 3^k$.

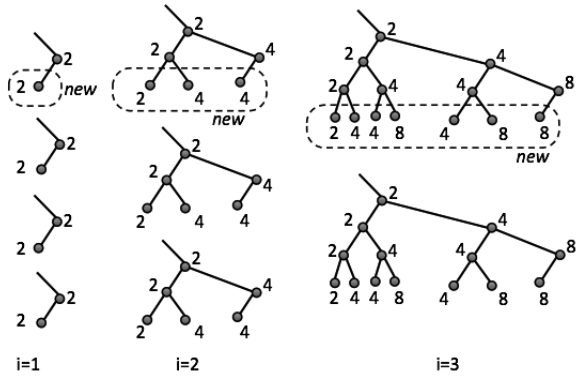

Fig. 9. Nodes added to the skeleton structure in 3 steps for a tree of height 5

Let us assume that to fill up the tree with the remainder of the nodes up to *n*, we need m such operations, and maybe another incomplete step after that. We can ignore that step for now, since it will not change the overall complexity. To find out what the total sum of labels is, we need to find a way to express m as a function of g or *n*.

The total number of nodes added at step i is $\sum_{k=0}^{i-1} 2^k(g-i) = (g-i)(2^i-1)$. If we add m such steps, then the total number of nodes that we've added is $\sum_{i=1}^{m}(g-i)(2^i-1)$. We need to find m such that this sum is approximately equal to $2^g-(g+1)(g+2)/2$, which is *n* from which we subtract the nodes in the skeleton structure. This is assuming that $g \approx \lg(n)$ and later we will address the case where g is approximately equal to a constant times $\lg(n)$, constant less than or equal to $\lg(3)$.

The total weight added in the step number i is

$$\sum_{k=0}^{i-1}(g-i)2^{i-k}3^k = 2(g-i)\sum_{k=0}^{i-1}2^{(i-1)-k}3^k =$$

$$2(g-i)2^{i-1}\sum_{k=0}^{i-1}\frac{3^k}{2^k} = 2^i(g-i)\sum_{k=0}^{i-1}\left(\frac{3}{2}\right)^k$$

We can use the formula $\sum_{k=0}^{i-1} x^k = \frac{x^i-1}{x-1}$ to compute the sum as

$$2^i(g-i)\frac{(3/2)^i-1}{(3/2)-1} = 2^i(g-i)\frac{3^i-2^i}{2^i}\frac{2}{3-2} = 2(g-i)(3^i-2^i)$$

To compute the number of nodes, we will need the following known sum, valid for all positive integers p and real numbers $t \neq 1$,

$$1+2t+3t^2+\ldots+pt^{p-1} = \sum_{i=1}^{p} it^{i-1} = \frac{1+pt^{p+1}-(p+1)t^p}{(t-1)^2}$$

We can rewrite our sum as

$$\sum_{i=1}^{m}(g-i)(2^i-1) = 2^g\sum_{i=1}^{m}(g-i)\frac{1}{2^{g-i+1}} - \sum_{i=1}^{m}(g-i) \quad .$$

By making the change of variable in both sums $j = g-i$, we have

$$2^g\sum_{j=g-m}^{g-1} j\frac{1}{2^{j+1}} - \sum_{j=g-m}^{g-1} j =$$

$$2^{g-2}\sum_{j=g-m}^{g-1} j\frac{1}{2^{j-1}} - \frac{(m-1)(2g-m-1)}{2}$$

Let us compute the sum in the last expression separately.

$$\sum_{j=g-m}^{g-1} j\frac{1}{2^{j-1}} = \sum_{j=1}^{g-1} j\frac{1}{2^{j-1}} - \sum_{j=1}^{g-m-1} j\frac{1}{2^{j-1}} =$$

$$\frac{1+(g-1)(1/2)^g - g(1/2)^{g-1}}{(1/2-1)^2} -$$

$$\frac{1+(g-m-1)(1/2)^{g-m} - (g-m)(1/2)^{g-m-1}}{(1/2-1)^2}$$

The two fractions have common denominator 1/4, so we combine the numerators. The leading 1s cancel each other. We can factor out $1/2^g$ from the remaining terms to obtain

$$\frac{4}{2^g}((g-1)-2g-(g-m-1)2^m+(g-m)2^{m+1})$$

$$\frac{1}{2^{g-2}}((g-1)-2g-(g-m-1)2^m+(g-m)2^{m+1})$$

$$= \frac{1}{2^{g-2}}(2^m(g-m+1)-g-1).$$

By replacing it back into the original formula, the number of nodes is equal to

$$2^m(g-m+1)-g-1-\frac{(m-1)(2g-m-1)}{2} = \Theta(2^m(g-m)).$$

Given the similarity between the two sums, we obtain that the total weight of the nodes in the tree is

$$\Theta((3^m-2^m)(g-m)) = \Theta(3^m(g-m)).$$

Coming back to the question of expressing m as a function of g, if we write

$$(g-m+1)2^m = 2^g \Leftrightarrow g-m+1 = 2^{g-m}$$

and then introduce $r = g-m$, we have the equation $r+1 = 2^r$ which has the solutions $r = 0$ and $r = 1$. Figure 10 shows the graph of the function $2^x - x$ in the interval $[-1, 3]$.

The first solution would mean that the tree is almost perfect, and we have proved before that perfect trees are not *K*-optimal. So we can conclude that $m = g-1$. Considering that the last level of the skeleton structure itself may be incomplete, this means that for g large enough, only 1 or 2 levels beyond the last may not be complete in the tree trimmed at the level g.

To examine the relationship between m and g further, let us assume that $g \approx d\lg(n)$, where $1 \leq d \leq \lg(3) \approx 1.585$. Then we can write $n \approx 2^{g/d}$. Going back to the formula computing the number of nodes in the tree, we have

$$2^m(g-m+1) \approx 2^{g/d}$$

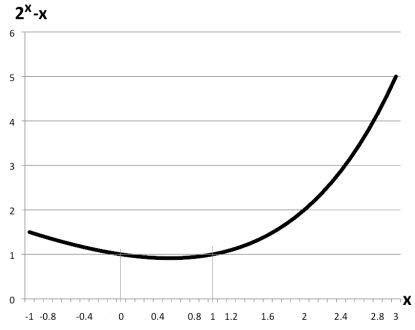

Fig. 10. The graph of the function $2^x - x$

from which we can write

$$g - m + 1 \approx 2^{g/d-m} = 2^{g-m+(g/d)-g} = \frac{2^{g-m}}{2^{g(d-1)/d}}.$$

Again, making the substitution $x = g - m$, we get

$$2^{g(d-1)/d} \approx \frac{2^x}{x+1}.$$

Remembering that $g \approx d\lg(n)$, we can write

$$n^{d(d-1)/d} = n^{d-1} \approx \frac{2^x}{x+1} \quad \text{or} \quad n \approx \left(\frac{2^x}{x+1}\right)^{1/(d-1)},$$

where $0 \leq d - 1 \leq 0.585$.

Let us write $f(y) = \frac{2^y}{y+1}$ and start with the observation that this function is monotone ascending for $y \geq 1$. Let us examine the hypothesis that $f(b\lg(n)) > f(x)$ for some constant b to be defined later. The hypothesis is true if and only if

$$f(b\lg(n)) = \frac{2^{b\lg(n)}}{b\lg(n)+1} = \frac{n^b}{b\lg(n)+1} > f(x) \approx n^{d-1}$$

which is equivalent to

$$\frac{n^b}{b\lg(n)+1} > n^{d-1} \Leftrightarrow n^{b-d+1} > b\lg(n) + 1.$$

Since a positive power of *n* grows faster than the logarithm in any base of *n*, we can say that the inequality above is true for any constant $b > d-1$. So we can choose a constant b, $d-1 < b < d$, such that $f(x) < f(b\lg(n))$. By the monotonicity of the function, this implies that $x < b\lg(n)$, which means that $g - m < b\lg(n)$, and considering that $g \approx d\lg(n)$, we can say that $(d-b)\lg(n) < m \leq \lg(3)\lg(n)$, from which we can conclude that $m = \Theta(log(n))$.

Coming back to the formula computing the weight as $\Theta(3^m(g-m))$, based on the result that $m = \Theta(log(n))$, we can conclude that the complexity of the function is minimal in the case where the value of $g - m$ is a constant, and that this complexity is indeed $\Theta(n^{\lg(3)})$ in this case. While this does not necessarily mean that $g - m = 1$, the difference between the two numbers must be a constant.

Now we can examine how many nodes we can have on the longest branch in the tree beyond the level of the skeleton structure. One node can be expected, for example in those cases where a perfect tree is *K*-optimal for small values of *n*, and a new node is added to it. If more nodes are present on the same branch, those node will have labels incrementing exponentially and larger than any empty spots still available on lower levels. They can easily be moved higher in the tree to decrease the total weight. Thus, we can deduce that $g = h$ or $g = h - 1$.

The weight of the tree, and thus the complexity of the *K* function, is the order of $\Theta(3^h) = \Theta(3^{\lg(n)}) = \Theta(n^{\lg(3)})$. ■

It is interesting to note that this is also the order of complexity of the function *K* on perfect trees and on size-balanced trees, even though neither of them is *K*-optimal in general.

V. Conclusion

In this paper we have studied the complexity of a special class of recursive functions traversing binary trees. We started with a recurrence relation describing this complexity in the general case. We continued with a simple analysis of the worst case complexity, which turned out to be exponential. Next, we showed two particular types of trees that give us a complexity of $\Theta(n^{\lg(3)})$.

Finally, after discussing a few more properties of the *K*-optimal trees that minimize the complexity function over the trees with a given number of nodes, we showed a constructive method to build these trees. In the process we have also shown that the complexity of the function on these trees is also $\Theta(n^{\lg(3)})$, which concludes the study of this function.

We can conclude from this analysis that any method that allows us to avoid repeating recursive calls will significantly improve the complexity of a function in all the cases.

References

[1] D. E. Knuth, *The Art Of Computer Programming, Volume 1: Fundamental Algorithms*, 3rd ed. Addison-Wesley, 1997.
[2] R. Sedgewick, *Algorithms in C++*, 3rd ed. Addison-Wesley, 2001.
[3] M. Kuba and A. Panholzer, "The left-right-imbalance of binary search trees," *Theoretical Computer Science*, vol. 370, no. 1-3, pp. 265–278, 2007, elsevier Science Publishers.
[4] R. Neininger and L. Rachendorf, "A general limit theorem for recursive algorithms and combinatorial structures," *The Annals of Applied Probability*, vol. 14, no. 1, pp. 378–418, 2004.
[5] J. Masberg and D. Rautenbach, "Binary trees with choosable edge lengths," *Infomation Processing Letters*, vol. 109, no. 18, pp. 1087–1092, 2009.
[6] N. Askitis and J. Zobel, "Redesigning the string hash table, burst trie, and bst to exploit cache," *ACM Journal of Experimental Algorithmics*, vol. 15, no. 1, p. 7, January 2011.
[7] M. Bender, M. F.-C. dand J. Fineman, Y. Fogel, B. Kuszmaul, and J. Nelson, "Cache-oblivious streaming b-trees," in *Proceedings of the ACM Symposium on Parallelism in Algorithms and Architectures*, San Diego, CA, June 9-11 2007, pp. 81–92.
[8] L. Arge, M. Bender, and E. Demaine, "Cache-oblivious priority queue and graph algorithm applications," in *Proceedings of the ACM Symposium on Theory of Computing*, Montreal, Quebec, Canada, May19-21 2002, pp. 268–276.
[9] L. Georgiadis, H. Kaplan, N. Shafrir, R. E. Tarjan, and R. F. Werneck, "Data structures for mergeable trees," *ACM Transactions on Algorithms*, vol. 7, no. 2, p. 14, 2011.
[10] N. Talukder and S. I. Ahamed, "Preventing multi-query attack in location-based services," in *Proceedings of the ACM Conference on Security and Privacy in Wireless and Mobile Networks*, Hoboken, New Jersey, March 22-24 2010, pp. 25–35.
[11] D. Vrajitoru and W. Knight, "On the k-optimality of a family of binary trees," Indiana University South Bend, Tech. Rep., 2011.

Improved Minimum Spanning Tree Heuristics for Steiner Tree problem in graph

Ali Nourollah[1,2] , Elnaz Pashaei[1], and Mohammad Reza Meybodi[3]
[1] Department of Electrical, Computer and IT Engineering, Qazvin Islamic Azad University, Qazvin, Iran
[2]Department of Electrical and Computer Engineering of Shahid Rajaee Teacher Training University, Tehran, Iran
[3]Department of Computer & IT Engineering, Amirkabir University of Technology, Tehran, Iran

Abstract - *The minimum Steiner tree problem, a classical combinatorial optimization problem with a long history, is a NP-complete problem. Due to its wide application, study of heuristic algorithm about Steiner tree problem has important practical and theoretical significance. In this paper we first review one of the existing algorithms for solving the Steiner problem in graphs, Minimum Spanning Tree Heuristic algorithm, then presenting a new heuristic algorithm IMSTH to improve it. We describe our algorithm and its computational results. It is shown that our algorithm can effectively improve the performance on MSTH.*

Keywords*:* Steiner Tree problem, Heuristic Algorithm, Minimum Spanning Tree Heuristic Algorithm

1 Introduction

A great number of the recent applications often require the underlying network to provide multicasting capabilities. Multicast refers to the delivery of packets from a single source to multiple destinations. At the routing level, a multicast routing scheme is responsible for determining the packet delivery path from the source to all destinations, typically a multicast tree [1]. Generation and minimization of the cost of such tree have been traditionally formulated as the Steiner Tree Problem. The Steiner Tree Problem involves constructing the least cost tree that spans a given set of points. In addition to multicast routing in communication networks, the Steiner tree problem has numerous applications especially in the area of telecommunication, distribution and transportation systems. The computation of phylogenetic trees in biology and the routing phase in VLSI design are real life problems that have been modeled as the Steiner tree problem [2]. Another interesting application is in the billing strategies of large telecommunications network service providers. The bill isn't based on the actual number of circuits provided, which may change over time, but on a simple formula calculated for an ideal network which will provide all the facilities at minimum cost. Several other network design problems can be formulated as generalizations of the Steiner tree problem. Steiner tree problem or so called Steiner Problem in Graphs (SPG) is a classic combinatorial optimization problem. Karp showed that its decision version is NP - complete [3], although some well known special cases of the SPG can be solved in polynomial time. When $|N| = 2$ the problem reduces to the shortest path problem while when $N= V$ the problem reduces to the minimum panning tree problem. Both these problems can be solved in polynomial time. On the other hand, the Steiner tree problem is NP-hard when the graph v is a chordal graph, a bipartite graph or a complete graph with edge weights either 1 or 2. Thus in the general case the problem is an NP-hard problem. In this paper, a novel solution based on MST to the construction of Steiner tree is presented. The rest of this paper is organized as follows: Section 2 review the definition of the problem and section 3 present a survey of proposed algorithms for the Steiner problem in graphs. Section 4 gives the description of MSTH algorithm. The proposed algorithm is presented in section 5. Section 6 describes experimental results and performance evaluation. Finally Section 7 draws a conclusion and makes suggestion for future works.

2 Basic definitions

Let $G = (V, E)$ be a connected undirected graph, where V is the set of nodes and E denote the set of edges. Given a non-negative weight function $w: E \rightarrow R+$ associated with graph edges and a subset $N \subseteq V$ of terminal nodes, the Steiner Problem in Graphs, SPG (V, E, w, N), consists of finding a minimum weighted connected sub tree of G spanning all terminal nodes in N. The solution of SPG (V, E, w, N) is Steiner minimum tree. The non-terminal nodes that end up in the Steiner minimum tree are called Steiner nodes. Terminal Steiner Tree Problem is a variation in which all the terminal nodes must appear at leaves of the tree. This problem that is also proved to be NP-complete has been matter of concern because it has direct application in VLSI design [5]. In Complete Steiner Problem the input graph is assumed to be complete. Another variation is the Complete Steiner (1, 2) in which the input is a complete graph with edge weights 1 or 2. All of these variations are NP-complete [6]. SPG – or its terminal version – are sometimes said to be metric, i.e. the triangle inequality holds for edge weights in the input graph. This imposes no limitation on the Steiner problem itself, since we can replace any edge with the shortest path connecting its

ends [7, 8]. The Steiner Network Problem generalizes the metric Steiner tree problem to higher connectivity requirements: Given a graph $G = (V, E)$, a cost function on edges, and a function r mapping unordered pairs of vertices to $Z+$, find a minimum cost graph that has $r(u, v)$ edge disjoint paths for each pair of vertices u and v [8]. The issue of multipoint routing for multimedia traffic has led to emergence of Constrained Steiner Tree Problem, in which the problem is to find a minimum cost tree such that the delay – delay variation or both between the source and each of the destinations is bounded. The Dynamic Steiner Tree Problem is another generalization of the problem, in which the set of destination nodes changes over time by receiving join or delete requests from nodes, and problem asks for a sequence of optimal trees [9].

3 Related Work

As SPG is NP-complete, there is little hope to find a polynomial time solution for it. All the work done to find a solution so far falls into three categories: Exact Algorithms, Approximation Algorithms and Meta heuristics. Two popular exact algorithms, the Spanning Tree Enumeration Algorithm (STEA) which enumerates all possible combinations of Steiner nodes, and the Dynamic Programming Algorithm (DPA), present time complexities of $O(p^2 2^{(n-p)} + n^3)$ and $O(3^p n + 2^p n^2 + n^3)$ respectively, where n is the number of nodes in the network and p is the number of multicast members [9]. These algorithms require long computation time or huge computational power for solving bigger problems, like the branch and bound algorithm proposed in [10], that makes use of computational grids. In [11], the author offers an approximation algorithm with performance ratio 5/3 based on finding a minimum spanning tree in 3-uniform hyper graphs that finds the solution with probability at least 1/2 and claims that the algorithm runs in O(lg2 n) time, using O(n3) processors. The best approximation algorithm known so far is due to Robins and Zelikovsky whose performance ratio is about 1.55 and even better for special cases such as quasi-bipartite and complete(1-2) graphs [7]. Among several heuristics proposed to find an Approximate solution, Traveling Salesman Problem Heuristic (TSPH), Average Distance Heuristic (ADH) have Performance ratio of 2. TSPH is a heuristic based on the traveling salesman problem (TSP) and involves finding a tour for the graph induced by the network followed by removing the most expensive link. Shortest path heuristic (SPH) computes the tree by connecting all the terminals to an arbitrary root through their shortest paths and then finding the minimum spanning tree of the graph induced by the union of these paths, repeatedly removing the non-terminal leaves. The algorithm presented in [10] is a distributed algorithm based on an improved version of the ADH heuristic, known as ADH with Full connection (ADHF). [9] Also provides an efficient approach that supports dynamic multicast membership, by means of periodic improvement of locally inefficient sub-trees. In [12] the author introduces a new algorithm using the Random Neural Networks to find potential Steiner vertices that are not already in the solution returned by the MSTH or ADH, starting with the solution of the MSTH or ADH. The first approximation algorithm for SPG having an approximation ratio constant lower than 2 was due to Zelikovsky [13] with performance ratio 11/6. Then he repeatedly improved this ratio to currently best known performance ratio: 1.55. The heuristics proposed to find the Steiner tree for routing applications are either centralized or distributed. In the centralized approach, a central node that is aware of the state of the whole network computes the tree. The computation is generally easy and fast. But impractical for large networks where the overhead of maintaining, in a single node, coherent information about the state of the entire network may be prohibitive. In a distributed approach, on the other hand, each node of the network actively contributes to the algorithm computation. Distributed routing algorithms can be slower and more complex than the centralized ones, but they become indispensable when the network nodes can't reach a complete knowledge of the topology and of the state of the network [9]. Some meta-heuristics are proposed as the solution for the Steiner problem in graphs too. Among the most efficient ones, it is found implementations of metaheuristics such as genetic algorithms, tabu search, Grasp and simulated annealing [14, 3]. Esbensen and Mazumder [15] proposed a genetic algorithm and discuss its application in global routing of VLSI layouts. The algorithm's encoding is based on the use of the Distance Network Heuristic (DNH) which is a deterministic heuristic for the SPG. The performance of algorithm is compared to that of two heuristics from the literature and it has been shown that the algorithm is superior. Di Fatta, Lo Presti, and Lo Re proposed a parallel genetic algorithm for the Steiner problem in networks. When solving Beasley's OR Library standard test problems, they obtain promising speedup values. Tabu Search was introduced by Glover in 1986. TS is an extension of classical local search methods typically used to find approximate solutions to difficult combinatorial optimization problems [16]. Ribeiro and Souza [14] proposed an improved tabu search for the Steiner problem in graphs. The important feature of the algorithm is that move estimations, elimination tests, and neighborhood reduction techniques are used to speed up the local search and lead to a much faster algorithm with similar performance in terms of solution quality. In the context of parallel tabu search for the Steiner problem in graphs, Bastos and Ribeiro [17] describe a two phase algorithm: in their approach, a parallel multi-thread reactive TS phase is followed by a distributed Path Relinking (PR) phase, i.e., all processes switch from TS to PR simultaneously. Martins, Ribeiro and Souza [14], proposed a parallel grasp for the Steiner problem in graphs. A Greedy Randomized Adaptive Search Procedure (GRASP) is a meta-heuristic for combinatorial optimization. A GRASP is an iterative process, where each of iteration consists of two phases: construction and local search. The construction phase of the algorithm is based on a version of distance network heuristic which is improved by Mehlhorn. Some heuristics are used in order to speed up the local search. For parallelization of GRASP, each

slave processor performs a fixed number of GRASP iterations. Once all processors have finished their computations, the best solution is collected by the master processor. The results of computational experiments illustrate the effectiveness of the proposed parallel GRASP procedure for the Steiner problem in graphs. Verhoeven and Severens proposed sequential and parallel local search methods for the Steiner tree problem based on a novel neighborhood. They claimed their approach is "better" than those known in the literature. Computational results indicated that good speedups could be obtained without loss in solution quality [18].

4 Minimum Spanning Tree Heuristic Algorithm

In the minimum spanning tree heuristic (MSTH) suggested by Takahashi and Matsuyama [19], the solution T_{MSTH} is obtained by deleting from the minimum spanning tree for G non-terminals of degree 1 (one at a time). The worst-case time complexity of the minimum spanning tree heuristic is $O(e + v \log v)$. The worst-case error ratio $|T_{MSTH}|/|T_G(N)|$ is tightly bounded by $v - n + 1$. Hence, the minimum spanning tree heuristic can be considered as inferior to the shortest paths heuristic in the worst-case sense. It also performs poorly on average. The proposed heuristic algorithm in this paper consists of eight steps. In the first step, after assuming that T_{IMSTH} is equal with null, we obtained T_{MSTH} by graph G.

5 Improve Minimum Spanning Tree Heuristic Algorithm

5.1 Description of the IMSTH Algorithm

The proposed heuristic algorithm in this paper consists of eight steps. In the first step, after assuming that T_{IMSTH} is equal with null, we obtained T_{MSTH} by graph G.

In the second step of algorithm, we assume two divisions of edges and paths between two terminals in T_{MSTH}:

- Existence direct edge in T_{MSTH}
- Not existence direct edge in T_{MSTH} and existence direct edge in graph.

In the third step, for the first category, select the direct edges of two terminals which obtained by T_{MSTH} and add into T_{IMSTH}. in the fourth step, for the second category, make compare between paths and direct edges of two terminals:

- If direct edge be shortest, add into T_{IMSTH}.
- If path be shortest, add into T_{IMSTH}.

In the next step, we study T_{IMSTH}, to determine all disjoin terminals. In the sixth step obtained the shortest paths between disjoin terminal and other terminals in the graph with Dijkstra algorithm. Select shortest path between reached paths and add into T_{IMSTH} .

In the next step, we study T_{IMSTH}, for connectivity. If we have forest, determine terminals with degree 1, then seek shortest path from this terminal to other terminals, and add it into T_{IMSTH} .

At the end, study T for cycle. If we have cycle, delete cycle. Fig. 1 shows our suggested algorithm.

Suggested algorithm: (INPUT: $G = (V, E)$ where $w: E \to R+$, $N \subseteq V$ set of Terminals, OUTPUT: T_{IMSTH} approximate optimal tree) {
Step 0: $T_{IMSTH} \to \emptyset$
Step 1: Compute T_{MSTH} of the graph G.
Step 2: Assume two divisions of edges and paths, between two terminals in T_{MSTH}:
a) Existence direct edge in T_{MSTH}
b) Not existence direct edge in T_{MSTH} and existence direct edge in graph
Step 3: For the first category, select the direct edges of two terminals which obtained by T_{MSTH} and add into T_{IMSTH}.
Step 4: For the second category, make compare between paths and direct edges of two terminals:
a) If direct edge be shortest, add into T_{IMSTH}.
b) If path be shortest, add into T_{IMSTH}.
Step 5: Study T_{IMSTH}, to determine all disjoin terminals.
Step 6: Determine the shortest paths between disjoin terminal and other terminals in the T_{IMSTH} with Dijkstra algorithm. Select shortest path between reached paths and add into T_{IMSTH} .
Step7: Study T_{IMSTH}, for connectivity. If we have forest, determine terminals with degree 1, seek shortest path from this terminal to other terminals, and add it into the T_{IMSTH} .
Step 8: Study T_{IMSTH} for cycle. If we have cycle, delete cycle.}

Fig. 1: Suggested algorithm for SPG in graph

5.2 Illustrative Example

In the example graph shown in Figure 2a, vertices $v0$, $v3$,$v4$, $v6$ and $v8$ are terminal vertices. We construct T_{MSTH} by this graph (Fig. 2b). The cost of T_{MSTH} is equal with 808. It can be observed that between two terminals $v3, v6$ and $v0, v8$ exists a direct edge in T_{MSTH}, so the direct edges< $v3, v6$> and < $v0, v8$> is selected and add into T_{IMSTH} . at the other hand, between two terminals $v3$ and $v4$ a direct edge in graph exists that is shortest than the paths between this two terminals, so in the fourth step the direct edge < $v3, v4$> is selected and add into the T_{IMSTH} (Fig. 2c). In the next step, we study T_{IMSTH} for disjoin terminals but don't find any disjoin terminal.

Now Study T_{IMSTH}, for connectivity. It is observed that we have forest. so determine terminals with degree 1, seek shortest path from this terminal to other terminals, and add it into the T_{IMSTH} (Fig. 2d). At the end, the cost of T_{IMSTH} is equal with 738(Fig. 2e). Fig. 2 illustrates steps of our algorithm.

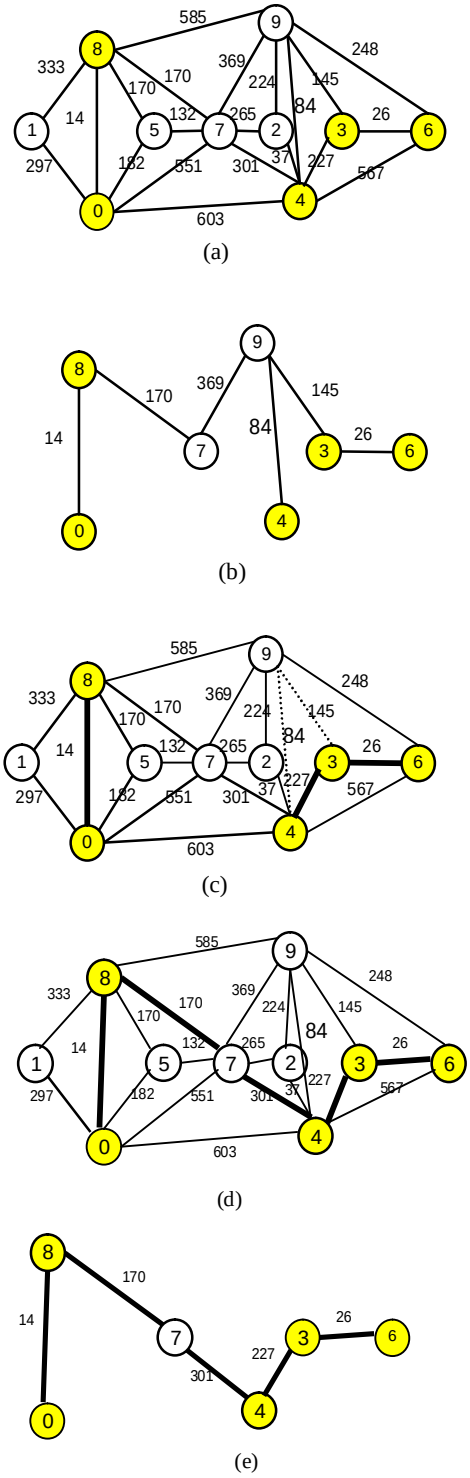

Fig. 2: Steiner tree that generated by our algorithm

6 Experimental Results

We have implemented our algorithms in C# programming language. The experiments are based on the STPs in graph from category B in the OR-library. In this paper, the experiments are made to test the performance of IMSTH with respect to Minimum Spanning Tree Heuristic (MSTH), Directed Convergence Heuristic (DCH), Optimal Shortest Paths Heuristic (OSPH) and Average Distance Heuristic (ADH). Table 1, show it. As illustrated in Table 1, our algorithms have achieved good results. Figure 3 show the performance of our suggested algorithm.

TABLE 1: Our Algorithm in Compare of B Problems

NO	$\|V_G\|$	$\|E_G\|$	$\|V_D\|$	OPT	DCH	ADH	MSTH	IMSTH
1	50	63	19	82	82	85	95	89
2	50	63	13	83	86	83	119	86
3	50	63	25	138	144	138	144	138
4	50	100	9	59	84	62	86	68
5	50	100	13	61	66	62	68	68
6	50	100	25	122	138	127	136	126
7	75	94	13	111	120	111	115	115
8	75	94	19	104	107	104	120	108
9	75	150	13	86	105	86	128	109
10	75	150	19	88	92	90	141	92
11	100	125	25	235	240	238	266	245
12	100	200	25	131	140	132	139	139

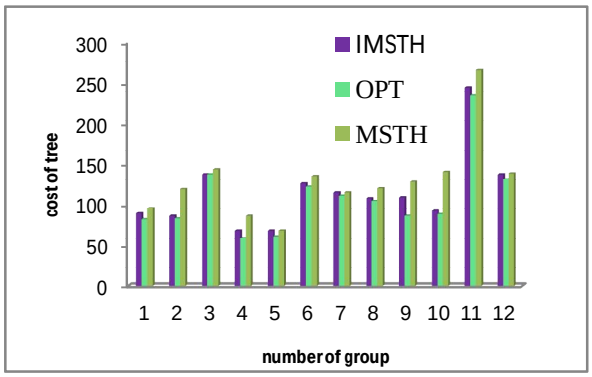

Fig. 3: Performance of our Algorithm

7 Conclusions

In this paper, we concern with the problem of finding minimum steiner tree in graph, which is a NP-complete problem. This paper presents a heuristic Steiner tree algorithm IMSTH. Experiment results show that IMSTH can effectively reduce the cost of Steiner tree by MSTH. This is a substantial improvement over previous improved works. The performance of our suggested algorithm was compared with Minimum Spanning Tree Heuristic (MSTH) Directed Convergence Heuristic (DCH), Optimal Shortest Paths Heuristic (OSPH) and Average Distance Heuristic (ADH). Experiment results show that our suggested algorithm produces good results and is comparable with other existing solutions.

8 References

[1] Z. Kun, W. Heng, and L. Feng-Yu, "Distributed multicast routing for delay and delay variation-bounded Steiner tree using simulated annealing", Computer Communications, vol.28, Issue 11, 5 July 2005, pp. 1356-1370.

[2] G. Kulkarni, "A Tabu Search Algorithm for the Steiner Tree Problem", M.Sc. Thesis, North Carolina State uiversity, 2000.

[3] C. C. Ribeiro and M. C. De Souza, "Improved Tabu Search for the Steiner Problem in Graphs", Working paper, Catholic University of Rio de Janeiro, Department of Computer Science, 1997.

[4] S.M. Wang, "A multiple source algorithm for suboptimum Steiner trees in graphs",Workshop on Graph-Theoretic Concepts, Depatment of Computer Science, 1985, pp. 387-396.

[5] D. E. Drake and S. Hougardy, On Approximation Algorithms for the Terminal Steiner Tree Problem", Information Processing Letters, vol. 89, Number 1, January 2004, pp. 15-18.

[6] M. Demange, J. Monnot, and V. Th. Paschos, "Differential Approximation Results for the Steiner Tree Problem", Applied Mathematics Letters, vol. 16, Issue 5, July 2003, pp. 733-739.

[7] G. Robins and A. Zelikovsky, "Improved Steiner Tree Approximation in Graphs", In Proceedings of the eleventh annual ACM-SIAM symposium on Discrete algorithms, San Francisco, California, United States, 2000, pp. 770-779.

[8] V. V. Vazirani, "Recent results on approximating the Steiner tree problem and its generalizations", Theoretical Computer Science, vol. 235, Issue 1, 17 March 2000, pp. 205- 216.

[9] L. Gatani, G. Lo Re, and S. Gaglio, "An efficient distributed algorithm for generating and updating multicast trees", Parallel Computing, vol. 32, Issues 11-12, December 2006, pp. 777-793.
URL:http://www.sciencedirect.com.

[10] L. M. A. Drummond, E. Uchoa, A. D. Goncalves, J. M.N.Silva, M. C.P. Santos, and M. C. S. de Castro, "A grid-enabled distributed branch-and-bound algorithm with application on the Steiner Problem in graphs", Parallel Computing, vol. 32, Issue 9, October 2006, pp. 629-642.
URL:http://www.sciencedirect.com/.

[11] H. J. Promel and A. Steger, "A New Approximation Algorithm for the Steiner Tree Problem with Performance Ratio 5/3", Journal of Algorithms, vol. 36, Issue 1, July 2000, pp. 89-101. URL:http://www.sciencedirect.com.

[12] A. Ghanwani, "Neural and delay based heuristics for the Steiner problem in networks", European Journal of Operational Research, vol. 108, Issue 2, 16 July 1998, pp. 241-265.
URL:http://www.sciencedirect.com/

[13] P. Guitart, "A Faster Implementation of Zelikovsky's 11/6-Approximation Algorithm for the Steiner Problem in Graphs", Electronic Notes in Discrete Mathematics, vol. 10, November 2001, pp. 133-136.
URL:http://www.sciencedirect.com.

[14] S. L. Martins, C. C. Ribeiro, and M. C. Souza, "A Parallel GRASP for the Steiner Problem in Graphs", Lecture Notes In Computer Science; vol. 1457, 1998, pp. 285-297.
URL:http://citeseer.ist.psu.edu/martins98parallel.html.

[15] H. Esbensen and P. Mazumder, "A Genetic Algorithm for the Steiner Problem in a graph", In Proceedings of the European Design and Test Conference, 1994, pp. 402-406.
URL:http://citeseer.ist.psu.edu/185181.html.

[16] T. G. Crainic, M. Gendreau, and J. Potvin, "Parallel Tabu Search", Parallel Metaheuristics, E. Alba (Ed.), John Wiley & Sons, 2005.
URL:http://www.iro.umontreal.ca/~gendron/Pisa/ReferenceMeta/Crainic05c.pdf.

[17] M. P. Bastos and C. C. Ribeiro, "Reactive Tabu Search with Path Relinking for the Steiner Problem in Graphs", In Proceedings of the Third Metaheuristics International Conference, 1999, pp. 31-36.
URL:http://citeseer.ist.psu.edu/bastos99reactive.html.

[18] T. G. Crainic and N. Hail, "Parallel Meta-heuristics Applications", Parallel Metaheuristics, E. Alba (Ed.), John Wiley \& Sons, 2005.
URL:http://www.iro.umontreal.ca/~gendron/Pisa/ReferenceMeta/Crainic05b.pdf.

[19] H. Takahashi and A.Matsuyama, "An approximate solution for the Steiner problem in Graphs", *Mach. Jap*. 24, 1980, pp. 573–577.

A Heuristic Algorithm for Solving Steiner Tree Problem on the Graph

F. Ghadimi[1], **A. Nourollah**[2], **M. Keyvanpour**[3]
[1]Department of Electrical & Computer Engineering, Qazvin Branch, Islamic Azad University, Qazvin, Iran
[2] Department of Electrical & Computer Engineering, Qazvin Branch, Islamic Azad University, Qazvin, Iran and Department of Electrical & Computer Engineering, Shahid Rajaee Teacher Training University, Tehran, Iran
[3]Department of Computer Engineering, Alzahra University, Tehran, Iran

Abstract - *Steiner tree problem on the graph is an NP-Complete problem and has no exact solution in polynomial time. Since this problem is practically useful, there are more attentions to heuristic and approximation approaches rather than exact ones. By using heuristic algorithms, the near optimum answers are obtained in polynomial time that this is faster than exact approaches. The goal of Steiner Tree problem is to find a minimum cost tree from the main graph that connects a subset of nodes called terminals. In this article, we have proposed a heuristic algorithm that solves Steiner Tree Problem. It has time complexity of* $O(n(m + n \log n))$ *that* n *is the number of nodes and* m *is the number of edges. This algorithm finds the near optimum answer and according to the experimental results and the comparisons, it has an appropriate rate in a reasonable time.*

Keywords: Steiner Tree on the Graph, NP-Complete problems, Heuristic Algorithms.

1 Introduction

The Steiner tree problem (STP) is a well-known issue that is used in many fields, like cabling design, canalization, VLSI design, routing, urban road design and also multicasting in computer networks. According to the different usages of this problem, some various definitions are exist for it: Euclidean STP which finds Steiner tree on the set of points in the plane; Rectilinear STP which finds Steiner tree in Manhattan space; Generalized STP which finds Steiner tree on an undirected, weighted graph; and Directed STP which finds Steiner tree on a directed, weighted graph.

In this article, the Steiner tree has been considered on an undirected, weighted graph $G = (V, E, W)$, which includes of a set of vertices (V), a set of edges (E) and a set of weights of edges (W). The graph G is one of the inputs of STP and it has no negative weight. The other input of this problem is a subset of nodes in V, which called Terminals (T). Steiner tree problem must find a sub graph of G that has the minimum summation of weights and connects all terminals. According to the following proof [1], the Steiner sub graph (S) must be a tree, because there is no negative weight. The proof says that if S isn't a tree, then it should have at least one cycle. Hence, there are two different paths that connect some terminal nodes to the other. So it is feasible to omit some edges from one of these paths, without losing the connectivity of S. This omission causes a reduction of cost of S and shows that S isn't the minimum possible answer.

In 1972 it was proved that STP is an NP-Complete problem [2], therefore there is no polynomial time approach to compute the exact answer. So far some exponential time approaches have been proposed for this problem that they find the optimum answer and called Exact Algorithms. But these algorithms aren't suitable for large networks with lots of nodes and edges, because of their low-speed execution. In this reason Heuristic and Approximation algorithms are widely used for solving STP, despite their near optimum answers. These approaches have near optimum answers in polynomial time and their evaluation measure is the ratio between their answer and the optimum answer.

In this article, a heuristic algorithm with polynomial time complexity is proposed that can compute Steiner tree on large graphs. This article is organized as follows: In the next Section, pervious works are reviewed. In Section3, our new algorithm and its time complexity are explained. In Section4, the experimental results are presented and finally in Section5 there are the conclusions.

2 Pervious Works

All the searching problems that have polynomial time solutions are in the P category, and all the other problems are NP. Because there are some problems that have no polynomial time solutions therefore P ≠ NP [3]. Since STP

is in the NP category, it has no polynomial time solution, until it will be proved that P = NP.

For solving STP on the graph, there are some exact approaches that one of them is Hakimi's algorithm with time complexity of $O(n^2 2^k)$ [4]. This algorithm for any subset S of $n-2$ terminals or less finds the Minimum Spanning Tree (MST) of $T \cup S$ and then it selects the minimum result as Steiner tree. The other famous exact algorithm for finding Steiner tree on the graph is Dreyfus and Wagner's algorithm that has $O(n3^k + n^2 2^k + n^3)$ time complexity and it has used dynamic programming [1].

Because of low-speed of exact approaches, they are not practically useful, therefore a lot of heuristic algorithms have been suggested for solving this problem. Those heuristic algorithms that have higher speeds and lower error percentages are better used. Some of these approaches are as follows: MST based algorithms like algorithms of Takahashi et al. [5] and Wong et al. [6] that for finding Steiner tree, they add an edge at each time until all terminals connect together; Node-based local search algorithms like Dolagh et al. [7] that find Steiner tree with using local search and identifying proper neighbors; Greedy Randomized Search algorithms [8] that have three phases: a construction phase, a local search phase and if necessary an updating phase. In each iteration of construction phase, a probable answer is created by selecting an element from a sorted list of candidate elements. This list is sorted based on greedy function, but the first element of the list is not always the best one, hence at the end of construction phase a local search is used for improving the answer and if necessary an updating phase is applied. There are also a lot of Meta heuristic algorithms for finding Steiner tree, like Ant colony approach [9, 10] and PSO [11]. Furthermore still the researches are done for finding algorithms for solving STP in better rates and shorter times.

3 The Proposed Algorithm

The algorithm that is suggested in this article that called MSTG, finds Steiner tree on an undirected and weighted graph $G = (V, E, W)$. In this graph n is the number of vertices in V, m is the number of edges in E and r is the number of terminal nodes in T. The set S that is defined as $S = V \backslash T$, contains Steiner nodes.

The inputs of this algorithm are the graph G and the set T and also there is an assumption that says there is no isolated terminal in G .This means that from each terminal, there are some edges to the other terminals. This algorithm consists of three phases: the preprocessing phase, the first phase and the second phase. Finally, the outputs of this algorithm are the Steiner tree and its cost.

3.1 Preprocessing Phase

The goal of this phase is the reduction of the counts of nodes and edges in the given graph. The Steiner nodes that have less than two edges ($\mathrm{Deg} < 2$) and their connected edges are those ones that aren't necessary in Steiner tree computation; therefore, in this phase, they are omitted. The resulted graph of this phase is called G' and the related pseudo code is Fig. 1.

Algorithm MSTG// Preprocessing Phase

Input: $T, G = (V, E, w)$
Output: $G' = (V', E', w)$
// $S = V \backslash T$
1 **for each** $s_i \in S$ **do**
2 **if** $\mathrm{Deg}(s_i) < 2$ **then**
3 Remove s_i from V and its edge from E;
4 **end if**
5 **end for**

Fig.1: Pseudo code of Preprocessing Phase

3.2 First Phase

In this phase of the algorithm, the shortest path between each terminal to one of the other terminals, which is the closest, is computed. The inputs of this phase are graph G' and the set T and the outputs are the set of edges (P) and the set of nodes (N) from the obtained paths. Fig. 2 is the pseudo code of this phase.

Definition: "ShrtTree (x, A)" is a procedure that its output is a set of shortest paths from node x to each node in the set A. These paths are obtained by computing the shortest tree that rooted in x and its leaves are the nodes in the set A. This procedure uses Dijkstra's algorithm.

The first loop (lines 1-5) of this pseudo code is executed for each terminal (t_i), and it obtains a shortest path tree from t_i to other terminals by using Dijkstra's algorithm. Afterward, among all these paths in the tree, the shortest path from t_i to another terminal is selected and added to the i^{th} cell in the array D. Then its edges are added to P, and its nodes are added to N.

The second loop (lines 6-20) is repeated for J times or until no changes occur in the P. This loop is exactly like the previous loop, but it obtains a shortest path tree from t_i to other nodes in N. If the weight of this shortest path is less than the weight of the previous path for t_i in D and it has no repeated edge with the previous path, then its edges and nodes are exchanged with the previous ones in P and N. The number of the variable J, according to the experimental results has been determined three, and it's sufficient. At the

end of this phase there is an omission of repeated nodes in N and repeated edges in P (lines 21, 22).

Algorithm MSTG// First Phase

Input: $T, G' = (V', E', w)$
Output: P, N
Initialization: $P = \phi, N = \phi, D = \phi,\ J$ =3.
//P is a set of edges; N is a set of nodes; D is an array of size r;
//J is a counter.

```
1  for each t_i ∈ T do
2     D_i ← Min{ShrtTree(t_i, T)};
3     P ← P + D_i.edges;
4     N ← N + D_i.nodes;
5  end for
6  repeat
7    flag ← true;
8     J←J-1;
9     for each t_i ∈ T do
10      Temp ← Min{ShrtTree(t_i, N)};
11      if Temp < D_i and Temp.edges ≠D_i.edges then
12          P ← P\D_i.edges;
13          N ← N\D_i.nodes;
14          D_i ← Temp;
15          P ← P + D_i.edges;
16          N ← N + D_i.nodes;
17        flag ← false;
18      end if
19    end for
20 until flag=true or J=0.
21 Remove all repeated edges in P;
22 Remove all repeated nodes in N;
```

Fig.2: Pseudo code of First Phase

3.3 Second Phase

In this phase after examination of the connectivity status of the terminals, if there are any isolated trees they should be connected. For this reason, all the edges in P that connected together are put in the same groups. Afterward if the number of groups be greater than one, three loops are executed. Fig. 3 is the pseudo code of this phase.

In the first loop (lines 3-6), the shortest paths from each node in N to other nodes of it that they are not in the same groups, are computed. Afterward, the resulted paths will be added to C.

In the second loop (lines 7-15), until all the separated trees are not joined together, a path with lowest-cost that connects two trees is selected from the C. The edges and nodes of the selected path are respectively added to P and N and also if there is any Steiner node in this path, it is added to set H. In this situation, the connectivity status of the groups and the number of isolated groups are updated.

Algorithm MSTG// Second Phase

Input: $T, G' = (V', E', w), P, N$
Output: Steiner tree path, Steiner tree Cost
Initialization: $C = \phi, H = \phi$.
//C is a set of founded paths; H is a set of selected Steiner //nodes.

```
1 Put all e_ij ∈ P which are connected together, in the
  same groups;
2  if groups number > 1 then
3   for each n_i ∈ N do
4    Temp ←all nodes in N with different groups from n_i
5    C ← C + ShrtTree(n_i, Temp);
6   end for
7  while groups number> 1 do
8    Temp← Min{C} which is not added yet;
9    if Temp connects two groups then
10        P ← P + Temp.edges;
11        N ← N + Temp.nodes;
12        H ← H + Temp.Steiner nodes;
13        Update groups number;
14    end if
15  end while
16  for each h_i ∈ H do
17     if h_i has a shorter path to any n_i ∈ N then
18       if this shorter path has the conditions then
19         Replace it with the previous one and update
           P and N;
20       end if
21     end if
22  end for
23  Delete all repeated edges in P;
24  Delete all repeated nodes in N;
25 end if
26 for each s_i ∈ N do
27   if Deg(s_i) < 2 then
28        Remove s_i from N and its edge from P;
29   end if
30 end for
31 Compute the summation of costs of all e_ij ∈ P.
```

Fig.3: Pseudo code of Second Phase

In the third loop (lines 16-22), if there are any Steiner nodes in the set H, for each of them, the shortest path is computed. If this path has lower cost than the previous one, and also it has the connection conditions, it is replaced with the previous path and the related edges and nodes in P and N are exchanged. In this algorithm, the path that has the connection condition doesn't make a cycle or it doesn't make terminals to be isolated.

At the end of this phase (lines 23- 30), there are omissions of repeated edges of P, and repeated nodes of N. Moreover, Steiner nodes with the deg less than 2 are also omitted from N, and their edges from P. Finally, all the edges in the set P are the edges of the Steiner tree, and the summation of their weights is the cost of the Steiner tree.

3.4 Time Complexity Analysis

In MSTG algorithm, the most time complexity belongs to the computations using Dijkstra's algorithm. By using Fibonacci-Heap for implementing Dijkstra's algorithm, it has $O(m + n \log n)$ time complexity [3].

In the preprocessing phase of the MSTG algorithm, Dijkstra's algorithm hasn't been used. In the first phase, Dijkstra's algorithm has been used for r times and in the second phase, at the worst condition it has been used for n times; therefore because $r \leq n$, the time complexity of our algorithm is $O(n(m + n \log n)$.

4 Experimental Results

The implementation of the proposed algorithm that called MSTG has been done by Visual C#, and it has been examined on some well-known data sets like the Beasley's data set [12]. The configuration of the system that has been used for this examination was a 2.50 GHz CPU and a 3 GB RAM. The results of running the MSTG algorithm on the sets B, C and D of Beasley's data set are respectively in tables 1, 2 and 3. The rate of this algorithm is computed from the ratio of the cost of MSTG to the optimum cost and also the time of execution has been shown in "hour: minute: second: mille second".

Table 1: The results of MSTG algorithm on the set B

Graph Number	Nodes Count	Edges Count	Terminals Count	Optimum Cost	MSTG Result	Rate (Opt/MSTG)	Time (h:m:s:ms)
1 B	50	63	9	82	82	1	0: 0: 0: 10
2 B	50	63	13	83	83	1	0: 0: 0: 16
3 B	50	63	25	138	138	1	0: 0: 0: 33
4 B	50	100	9	59	59	1	0: 0: 0: 15
5 B	50	100	13	61	61	1	0: 0: 0: 20
6 B	50	100	25	122	122	1	0: 0: 0: 50
7 B	75	94	13	111	111	1	0: 0: 0: 28
8 B	75	94	19	104	104	1	0: 0: 0: 37
9 B	75	94	38	220	220	1	0: 0: 0: 101
10 B	75	150	13	86	86	1	0: 0: 0: 54
11 B	75	150	19	88	92	1.045	0: 0: 0: 66
12 B	75	150	38	174	174	1	0: 0: 0: 131
13 B	100	125	17	165	170	1.03	0: 0: 0: 69
14 B	100	125	25	235	235	1	0: 0: 0: 123
15 B	100	125	50	318	321	1.009	0: 0: 0: 220
16 B	100	200	17	127	132	1.039	0: 0: 0: 125
17 B	100	200	25	131	131	1	0: 0: 0: 168
18 B	100	200	50	218	218	1	0: 0: 0:350

Table 2: The results of MSTG algorithm on the set C

Graph Number	Nodes Count	Edges Count	Terminals Count	Optimum Cost	MSTG Result	Rate (Opt/MSTG)	Time (h:m:s:ms)
1 C	500	625	5	85	85	1	0: 0: 0: 547
2 C	500	625	10	144	144	1	0: 0: 1: 306
3 C	500	625	83	754	760	1.008	0: 0: 4: 203
4 C	500	625	125	1079	1090	1.01	0: 0: 7: 578
5 C	500	625	250	1579	1581	1.001	0: 0: 17: 409
6 C	500	1000	5	55	55	1	0: 0: 0: 969
7 C	500	1000	10	102	102	1	0: 0: 1: 281
8 C	500	1000	83	509	519	1.019	0: 0: 7: 640
9 C	500	1000	125	707	720	1.018	0: 0: 10: 625
10 C	500	1000	250	1093	1100	1.006	0: 0: 22: 110
11 C	500	2500	5	32	33	1.031	0: 0: 1: 265
12 C	500	2500	10	46	49	1.065	0: 0: 1: 579
13 C	500	2500	83	258	262	1.015	0: 0: 7: 547
14 C	500	2500	125	323	330	1.021	0: 0: 11: 500
15 C	500	2500	250	556	561	1.009	0: 0: 25: 656
16 C	500	12500	5	11	12	1.09	0: 0: 1: 901
17 C	500	12500	10	18	20	1.111	0: 0: 2: 891
18 C	500	12500	83	113	119	1.0531	0: 0: 6: 937
19 C	500	12500	125	146	152	1.041	0: 0: 9: 312
20 C	500	12500	250	267	268	1.003	0: 0: 37: 16

Table 3: The results of MSTG algorithm on the set D

Graph Number	Nodes Count	Edges Count	Terminals Count	Optimum Cost	MSTG Result	Rate (Opt/MSTG)	Time (h:m:s:ms)
1 D	1000	1250	5	106	107	1.009	0: 0: 2: 890
2 D	1000	1250	10	220	220	1	0: 0: 4: 47
3 D	1000	1250	167	1565	1578	1.008	0: 0: 42: 515
4 D	1000	1250	250	1935	1951	1.008	0: 0: 52: 016
5 D	1000	1250	500	3250	3265	1.004	0: 4: 4: 484
6 D	1000	2000	5	67	73	1.09	0: 0: 5: 782
7 D	1000	2000	10	103	105	1.019	0: 0: 7: 719
8 D	1000	2000	167	1072	1097	1.023	0: 0: 50: 907
9 D	1000	2000	250	1448	1470	1.015	0: 1: 23: 578
10 D	1000	2000	500	2110	2120	1.005	0: 5: 9: 631
11 D	1000	5000	5	29	29	1	0: 0: 6: 734
12 D	1000	5000	10	42	42	1	0: 0: 7: 375
13 D	1000	5000	167	500	517	1.034	0: 0: 55: 94
14 D	1000	5000	250	667	676	1.013	0: 1: 24: 375
15 D	1000	5000	500	1116	1129	1.012	0: 5: 27: 762
16 D	1000	25000	5	13	15	1.154	0: 0: 28: 690
17 D	1000	25000	10	23	24	1.043	0: 0: 30: 336
18 D	1000	25000	167	223	237	1.063	0: 1: 47: 301
19 D	1000	25000	250	310	328	1.058	0: 2: 38: 931
20 D	1000	25000	500	537	542	1.009	0: 4: 56: 388

In Fig. 4, there are two samples of obtained Steiner trees from MSTG algorithm on graphs B1 and C15 that has been drawn with random vertices.

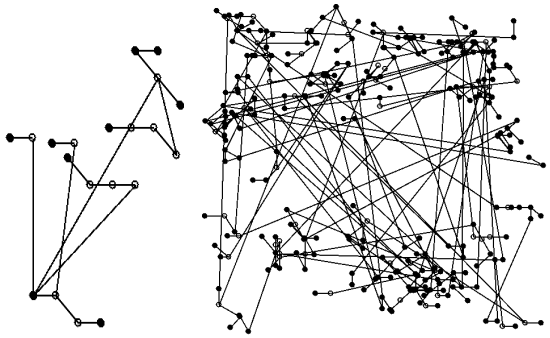

(a) (b)

Fig.4: Two samples of MSTG algorithm on graph B1 (a) and graph C15 (b)

According to the results of the MSTG algorithm that are shown in the tables, this algorithm can find near optimum answers of Steiner tree with a good rate in the polynomial time. Moreover, all the observed rates of this algorithm were below 1.5.

5 Conclusions

The Steiner tree problem is a well-known issue that is used in many fields. In this article, we proposed a heuristic algorithm to find Steiner tree on an undirected and weighted graph. This algorithm finds the near optimum answer in polynomial time, and the complexity of it is $O(n(m + n\log n))$. Since this algorithm had reasonable running times on the large graphs, it can be used for finding Steiner tree on the huge networks like Urban Transportation Network. Moreover, all the observed rates of this algorithm were below 1.5; So in the future works, we will try to proof the rate of this algorithm which it implies an approximation algorithm.

References

[1] Dreyfus S. E., Wagner R. A., "The Steiner Problem in Graphs", Networks, Vol. 1, pp. 195-207, 1972.

[2] Karp R.M., "Reducibility among combinatorial problems", Complexity of Computer Communications, Plenum Press, New York, pp. 85–103, 1972.

[3] Dasgupta S., Papadimitriou C. H., Vazirani U. V., "Algorithms", 2006.

[4] Hakimi S. L., "Steiner's problem in graphs and its implications", Networks, Vol. 1, pp. 113-133, 1972.

[5] Takahashi H., Matsuyama A., "An approximate solution for the Steiner problem in graphs", Math. Jpn., No. 24, pp. 573–577, 1980.

[6] Wu Y. F., Widmayer P., Wong C. K., "A faster approximation algorithm for the Steiner problem in graphs", Acta. Info. No. 23, pp. 223–229, 1986.

[7] Dolagh S. V., Moazzami D., "New Approximation Algorithm for Minimum Steiner Tree Problem", International Mathematical Forum, Vol. 6, No. 53, pp. 2625 - 2636, 2011.

[8] Martins S. L., Pardalos P. M., Resende M. G.C., Ribeiro C. C., "Greedy Randomized Adaptive Search Procedures For The Steiner Problem In Graphs", AT&T Labs Research Technical Report, 1998.

[9] Tashakkori M., Adibi P., Jahanian A., Nourollah A., "Ant colony solution dynamic Steiner tree problem", Proceedings of 9th Annual Computer Society of Iran Computer Conference, pp. 465-471, 2003.

[10] Luyet L., Varone S., Zuerey N., "An Ant Algorithm for the Steiner Tree Problem in Graphs", Springer EvoWorkshops, pp. 42–51, 2007.

[11] Consoli S., Moreno-Perez J. A., Darby-Dowman K., Mladenovic N., "Discrete Particle Swarm Optimization for the minimum labelling Steiner tree problem", Springer Nat Compute, pp. 29-46, 2010.

[12] Beasley J.E., "OR-Library: Distributing Test Problems by Electronic Mail", Operational Research. Soc., Vol. 41, No. 11, pp. 1069-1072, 1990.

The Parameterized Complexity of Perfect Code in Graphs without Small Cycles

Yong Zhang
Department of Computer Science, Kutztown University of Pennsylvania, Kutztown, PA 19530

Abstract— *We study the parameterized complexity of k-PERFECT CODE in graphs without small cycles. We show that k-PERFECT CODE is W[1]-hard in bipartite graphs and thus in graphs with girth 4. On the other hand, we show that k-PERFECT CODE admits a $k^2 + k$ kernel in graphs with girth ≥ 5.*

Keywords: parameterized complexity, perfect code

1. Introduction

Parameterized complexity is a powerful framework that deals with hard computational problems. A *parameterized problem* is a set of instances of the form (x, k), where x is the input instance and k is a nonnegative integer called the *parameter*. A parameterized problem is said to be *fixed parameter tractable* if there is an algorithm that solves the problem in time $f(k)|x|^{O(1)}$, where f is a computable function solely dependent on k, and $|x|$ is the size of the input instance. The *kernelization* of a parameterized problem is a reduction to a *problem kernel*, that is, to apply a polynomial-time algorithm to transform any input instance (x, k) to an equivalent reduced instance (x', k') with $k' \leq k$ and $|x'| \leq g(k)$ for some function g solely dependent on k . A parameterized problem is fixed parameter tractable if and only if it is kernelizable. On the other hand, many fixed parameter intractable problems can be classified in a hierarchy of complexity classes W[1] $\subseteq$ W[2] ... $\subseteq$ W[t]. For example, k-INDEPENDENT SET and k-CLIQUE are known to be W[1]-complete and k-DOMINATING SET is known to be W[2]-complete. We refer the readers to [1], [2] for more details.

Let $G = (V, E)$ be an undirected graph. For a vertex $v \in V$, let $N(v)$ and $N[v]$ be the open neighborhood and closed neighborhood of v, respectively. A *perfect code* in G is a subset of vertices $D \subseteq V$ such that for every vertex $v \in V$, there is exactly one vertex in $N[v] \cap D$.

Definition 1.1: Given an input graph G and a positive integer k, the k-PERFECT CODE problem is to determine whether G has a perfect code of size at most k.

In the literatures k-PERFECT CODE is also known as EFFICIENT DOMINATING SET, PERFECT DOMINATING SET, and INDEPENDENT PERFECT DOMINATING SET. It is a well-known NP-complete problem. Its computational complexity in various classes of graphs has been extensively studied. See Lu and Tang [3] for an overview. In terms of parameterized complexity, k-PERFECT CODE is known to be W[1]-complete [4], [5] in general graphs. Guo and Niedermeier [6] showed that k-PERFECT CODE is fixed parameter tractable in planar graphs by giving a $84k$ kernel. Dawar and Kreutzer [7] showed that it is fixed parameter tractable in effectively nowhere-dense classes of graphs.

The *girth* of a graph is the length of the shortest cycle contained in the graph. In this paper we study the parameterized complexity of k-PERFECT CODE in graphs with certain girths, i.e., graphs without small cycles. The parameterized complexity of several related problems, including k-DOMINATING SET and k-INDEPENDENT SET [8], and k-CONNECTED DOMINATING SET [9] in graphs without small cycles has been studied. In this paper we show that k-PERFECT CODE is W[1]-hard in bipartite graphs, and thus in triangle-free graphs or graphs with girth 4. Then we show that k-PERFECT CODE admits a k^2+k kernel in graphs with girth ≥ 5 and is therefore fixed parameter tractable.

2. Main results

2.1 Bipartite Graphs

To show the W[1]-hardness of k-PERFECT CODE in bipartite graphs, we give a reduction from the problem k-MULTICOLORED CLIQUE: Given a graph $G = (V, E)$ and a vertex-coloring $\kappa : V \to \{1, 2, \ldots, k\}$, decide whether G has a clique of k vertices containing exactly one vertex of each color. k-MULTICOLORED CLIQUE is shown to be W[1]-complete by Fellows et al. [10].

Theorem 2.1: k-PERFECT CODE is W[1]-complete in bipartite graphs.

Proof: Let $(G = (V, E), \kappa)$ be an input instance of k-MULTICOLORED CLIQUE. For each color i, $1 \leq i \leq k$, let V_i be the set of vertices in G with color i. Let n_i be the number of vertices in V_i. Without loss of generality, we assume that $n_i > 1$ for all i. We fixed an ordering of the vertices in each V_i. To simplify the presentation, we abuse notations here: for two vertices $u, v \in V_i$, $u > v$ means u is in front of v with respect to the fixed ordering. Without loss of generality, we also assume that no edge in G connects two vertices of the same color. For any two colors i and j, $1 \leq i < j \leq k$, let E_{ij} be the set of edges in G that connect

vertices in V_i and V_j. Let m_{ij} be the number of edges in E_{ij}.

We construct a graph $G' = (V', E')$. The vertex set V' is a union of the following sets of vertices:

$$\begin{aligned}
S_1 &= \{a[i,v], b[i,v] \mid 1 \le i \le k, v \in V_i\} \\
&\quad \cup \{x[i] \mid 1 \le i \le k\} \\
S_2 &= \{c[i,j,e], d[i,j,e] \mid 1 \le i < j \le k, e \in E_{ij}\} \\
&\quad \cup \{y[i,j] \mid 1 \le i < j \le k\} \\
S_3 &= \{f[i,j,v] \mid 1 \le i < j \le k, v \in V_i\} \\
S_4 &= \{g[i,j,v] \mid 1 \le i < j \le k, v \in V_j\}
\end{aligned}$$

The edge set E' is a union of the following set of edges:

$$\begin{aligned}
E_1 &= \{(a[i,v_1], b[i,v_2]) \mid 1 \le i \le k, v_1, v_2 \in V_i \\
&\quad \text{and } v_1 \ne v_2\} \\
E_2 &= \{(x[i], b[i,v]) \mid 1 \le i \le k, v \in V_i\} \\
E_3 &= \{(c[i,j,e_1], d[i,j,e_2]) \mid 1 \le i < j \le k, \\
&\quad e_1, e_2 \in E_{ij} \text{ and } e_1 \ne e_2\} \\
E_4 &= \{(y[i,j], c[i,j,e]) \mid 1 \le i < j \le k, e \in E_{ij}\} \\
E_5 &= \{(b[i,v_1], f[i,j,v_2]) \mid 1 \le i < j \le k, \\
&\quad v_1, v_2 \in V_i \text{ and } v_1 \ge v_2\} \\
E_5 &= \{(b[j,v_1], g[i,j,v_2]) \mid 1 \le i < j \le k, \\
&\quad v_1, v_2 \in V_j \text{ and } v_1 \ge v_2\} \\
E_6 &= \{(c[i,j,e], f[i,j,v]) \mid 1 \le i < j \le k, \\
&\quad e = (v_1, v_2) \in E_{ij}, v, v_1 \in V_i \text{ and } v_1 < v\} \\
E_7 &= \{(c[i,j,e], g[i,j,v]) \mid 1 \le i < j \le k, \\
&\quad e = (v_1, v_2) \in E_{ij}, v, v_2 \in V_j \text{ and } v_2 < v\}
\end{aligned}$$

Informally speaking, for each V_i, $1 \le i \le k$, we construct a vertex selection gadget that contains $2n_i + 1$ vertices. For each $v \in V_i$, there are two vertices $a[i,v]$ and $b[i,v]$. For two vertices $a[i,v_1]$ and $b[i,v_2]$, $v_1, v_2 \in V_i$, they are adjacent if and only if $v_1 \ne v_2$. There is a dummy vertex $x[i]$ which is adjacent to all vertices $\{b[i,v] \mid v \in V_i\}$ and none of the vertices $\{a[i,v] \mid v \in V_i\}$. Then, for each edge set E_{ij}, $1 \le i < j \le k$, we construct an edge selection gadget that contains $2m_{ij} + 1$. For each edge $e \in E_{ij}$, there are two vertices $c[i,j,e]$ and $d[i,j,e]$. There is also a dummy vertex $y[i,j]$. They are connected in a similar fashion as in the vertex selection gadget. Finally, for each pair of colors i and j with $1 \le i < j \le k$, we also construct a validation gadget that contains $n_i + n_j$ vertices, namely $\{f[i,j,v] \mid v \in V_i\}$ and $\{g[i,j,v] \mid v \in V_j\}$. The vertices in the validation gadget are not adjacent to each other, instead they are adjacent to vertices in the vertex selection gadgets for V_i and V_j, and the edge selection gadget for E_{ij}. For a vertex $v_1 \in V_i$, the corresponding vertex $b[i,v_1]$ is adjacent to $f[i,j,v_2]$ for all $v_2 \in V_i$ such that $v_1 \ge v_2$ with respect to the fixed vertex ordering of V_i. Similarly, for a vertex $v_1 \in V_j$, the corresponding vertex $b[j,v_1]$ is adjacent to $g[i,j,v_2]$ for all $v_2 \in V_j$ such that $v_1 \ge v_2$ with respect to the fixed vertex ordering of V_j. On the other hand, for an edge $e = (v_1, v_2) \in E_{ij}$ with $v_1 \in V_i$ and $v_2 \in V_j$, the corresponding vertex $c[i,j,e]$ in the edge selection gadget is adjacent to $f[i,j,v]$ for all $v \in V_j$ such that $v > v_1$, and to $g[i,j,v]$ for all $v \in V_j$ such that $v > v_2$. See Figure 1 for an illustration of the construction. Clearly G' is a bipartite graph.

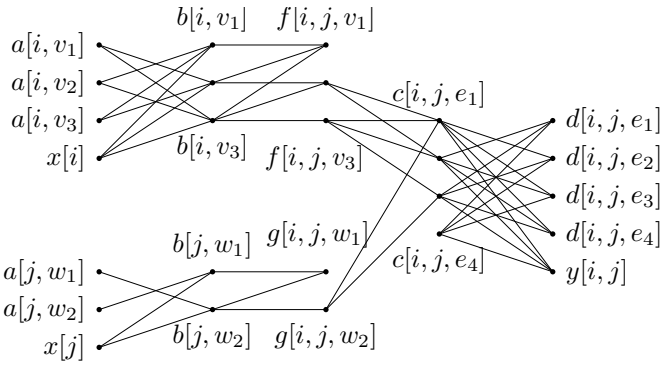

Fig. 1: A partial illustration of the construction of G'. Let $V_i = \{v_1, v_2, v_3\}$ and $V_j = \{w_1, w_2\}$. Let $E_{ij} = \{e_1, e_2, e_3, e_4\}$ where $e_1 = (v_1, w_1), e_2 = (v_1, w_2), e_3 = (v_2, w_1), e_4 = (v_3, w_2)$. The figure shows how the vertex selection gadgets for V_i and V_j (left), the edge selection gadget E_{ij} (right), and the validation gadgets (middle) are constructed.

Lemma 2.2: G has a k-multicolored clique if and only if G' has a perfect code of size $k' = 2k + 2\binom{k}{2}$.

Proof: For the direct implication, suppose $G = (V, E)$ has a k-multicolored clique $K \subseteq V$ such that $K = \{v_i \mid 1 \le i \le k, v_i \in V_i\}$, then it is easy to verify that the following set $\mathcal{D}$ of vertices in V' is a perfect code of size k' for G':

$$\begin{aligned}
\mathcal{D} &= \{a[i,v_i], b[i,v_i] \mid v_i \in K\} \cup \{c[i,j,e], d[i,j,e] \mid \\
&\quad 1 \le i < j \le k, e = (v_i, v_j) \text{ and } v_i, v_j \in K\}.
\end{aligned}$$

For the reverse implication, suppose $\mathcal{D}$ is a perfect code of size k' for G'. First observe that the dummy vertex $x[i]$ in the vertex selection gadget for V_i cannot be in $\mathcal{D}$ since otherwise vertices $\{a[i,v] \mid v \in V_i\}$ cannot be dominated. To dominate $x[i]$, $\mathcal{D}$ must contain exactly one vertex from the set $\{b[i,v] \mid v \in V_i\}$. Let $b[i,v_s]$ be such a vertex, $b[i,v_s]$ dominates all vertices $\{a[i,v] \mid v \in V_i\}$ except $a[i,v_s]$, this implies that $a[i,v_s]$ must also be in $\mathcal{D}$. By this argument, we see that $\mathcal{D}$ must contain exactly two vertices from each vertex selection gadget and each edge selection gadget. In another word, the following $2k + 2\binom{k}{2}$ vertices must be in $\mathcal{D}$:

$$\{a[i,v_i], b[i,v_i] \mid 1 \le i \le k, v_i \in V_i\} \cup$$
$$\{c[i,j,e_{ij}], d[i,j,e_{ij}] \mid 1 \le i < j \le k, e_{ij} \in E_{ij}\}.$$

So no vertex from the validation gadgets will be in $\mathcal{D}$.

Let $b[i, v_i]$ and $b[j, v_j]$ be the two vertices in $\mathcal{D}$. We see that $b[i, v_i]$ dominates vertices $f[i, j, v]$ for all $v \leq v_i$ in V_i and $b[j, v_j]$ dominates vertices $g[i, j, v]$ for all $v \leq v_j$ in V_j. By the construction of G', to perfectly dominate the rest of the validation vertices, $f[i, j, v]$ for all $v > v_i$ and $g[i, j, v]$ for all $v > v_j$, the vertex $c[i, j, e]$ must be in $\mathcal{D}$ where $e = (v_i, v_j) \in E_{ij}$. Conversely, if $c[i, j, e]$ with $e = (v_i, v_j) \in E_{ij}$ is a vertex in $\mathcal{D}$, $c[i, j, e]$ dominates $f[i, j, v]$ for all $v < v_i$ in V_i and $g[i, j, v]$ for all $v < v_j$ in V_j, to perfectly dominate the rest of validation vertices, $b[i, v_i]$ and $b[j, v_j]$ must be in $\mathcal{D}$. Therefore the set $\{v_i \mid b[i, v_i] \in \mathcal{D}\}$ is a k-multicolored clique in G.

■

■

2.2 Graphs with girth ≥ 5

Let $G = (V, E)$ be a graph with girth ≥ 5. To obtain a $k^2 + k$ kernel, we only need the following simple reduction rule.

Reduction Rule 1: If a vertex $v \in V$ has degree $> k$, then remove v and all vertices adjacent to v from G and decrease k by 1.

Lemma 2.3: Reduction Rule 1 is correct.

Proof: Let $v \in G$ be a vertex with degree $> k$. We claim that if G has a set S which is a perfect code of size at most k, then v must be in S. Suppose this is not true and $v \notin S$. Let $w_1, w_2, \ldots, w_l$ be the neighbors of v with $l > k$. Since v is not in S, exactly one of v's neighbors must be in S. Without loss of generality, let w_1 be the vertex that is in S. w_1 is not adjacent to any w_i for $1 < i \leq l$, since otherwise v, w_1, w_i forms a triangle in G. Therefore $w_2, \ldots, w_l$ have to be dominated by vertices in S other than w_1. We claim that any vertex $s \in S$ with $s \neq w_1$ can be adjacent to only one w_i. Suppose this is not true, i.e., there is a vertex $s \in S$ such that $(s, w_i), (s, w_j) \in E$ for $1 < i, j \leq l$, then v, w_i, s, w_j forms a 4-cycle, contradicting that G has girth ≥ 5. Therefore S contains w_1 and $l - 1$ more vertices, one for dominating each w_i ($1 < i \leq l$), this makes $|S| \geq l$, contradicting the assumption that $|S| \leq k$.

■

Let G' be the reduced graph after Reduction Rule 1. Clearly any vertex in G' has degree at most k. Suppose G' has a perfect code S of size k, any vertex in G' is either in S or dominated by a vertex in S. Since each vertex in S can dominate at most k other vertices in G', the size of $G' - S$ is at most k^2 and thus G' has at most $k^2 + k$ vertices.

Theorem 2.4: k-PERFECT CODE admits a $k^2 + k$ kernel in graphs with girth ≥ 5.

References

[1] R. G. Downey and M. R. Fellows, *Parameterized Complexity*. Springer-Verlag, 1999.

[2] J. Guo and R. Niedermeier, "Invitation to data reduction and problem kernelization," *SIGACT News*, vol. 38, no. 1, pp. 31–45, 2007.

[3] C. L. Lu and C. Y. Tang, "Weighted efficient domination problem on some perfect graphs," *Discrete Applied Mathematics*, vol. 117, no. 1-3, pp. 163–182, 2002.

[4] R. G. Downey and M. R. Fellows, "Fixed-parameter tractability and completeness II: on completeness for W[1]," *Theoretical Computer Science*, vol. 141, pp. 109–131, 1995.

[5] M. Cesati, "Perfect Code is W[1]-complete," *Information Processing Letters*, vol. 81, pp. 163–168, 2002.

[6] J. Guo and R. Niedermeier, "Linear problem kernels for NP-hard problems on planar graphs," in *Proceedings of the 34th International Colloquium on Automata, Languages and Programming*, 2007, pp. 375–386.

[7] A. Dawar and S. Kreutzer, "Domination problems in nowhere-dense classes," in *Proceedings of the IARCS Annual Conference on Foundations of Software Technology and Theoretical Computer Science*, 2009, pp. 157–168.

[8] V. Raman and S. Saurabh, "Short cycles make W-hard problems hard: FPT algorithms for W-hard problems in graphs with no short cycles," *Algorithmica*, vol. 52, no. 2, pp. 203–225, 2008.

[9] N. Misra, G. Philip, V. Raman, and S. Saurabh, "The effect of girth on the kernelization complexity of connected dominating set," in *Proceedings of the IARCS Annual Conference on Foundations of Software Technology and Theoretical Computer Science*, 2010, pp. 96–107.

[10] M. R. Fellows, D. Hermelin, F. Rosamond, and S. Vialette, "On the parameterized complexity of multiple-interval graph problems," *Theoretical Computer Science*, vol. 410, pp. 53–61, 2009.

A New Node Splitting Algorithm for R-Tree

Chandan Garai[1] **and Ranjan Dasgupta**[2]
[1] Student, Dept. of Computer Science & Engineering, National Institute of Technical Teachers' Training And Research, Kolkata, West Bengal, India
[2] Dept. of Computer Science & Engineering, National Institute of Technical Teachers' Training And Research, Kolkata, West Bengal, India

Abstract – *R-Tree being a multi-dimensional version of B-Tree is being used in various applications including geographic information systems, computer aided designing systems, spatial databases etc. Efficient searching of this tree is always a challenge to the research community and several methods have been proposed for this purpose. In this paper, we propose a new splitting algorithm to help efficient retrieval by reducing chances of overlap.*

Keywords: Spatial Database, Multi-Dimensional Indexing, R-Tree, Node Splitting Algorithm.

1 Introduction

An R-Tree [2] [4] [7-8] is a height-balanced tree. The index records in its leaf nodes contain pointers to data objects. It is the multidimensional extension of B-tree. Nodes correspond to disk pages. The structure is designed in such a manner that a spatial search requires visiting only a small number of nodes. The index is dynamic in nature. Insertions and deletions can be intermixed with searches and no periodic reorganization is required.

2 Spatial Database and R-Tree

A spatial database [1] [5-6] [9] [10] consists of a collection of tuples representing spatial objects, and each tuple has a unique identifier which can be used to retrieve it. Leaf nodes in an R-Tree contain index record entries of the form

(I, tuple_identifier)

Where, tuple_identifier refers to a tuple in the database and I is an n-dimensional rectangle which is the minimum bounding rectangle (MBR) of the spatial object indexed. Non-leaf nodes contain entries of the form

(I, child_pointer)

Where, child_pointer is the address of a lower node in the R-Tree and I covers all internal minimum bounding rectangles (iMBR) in the lower node's entries. Fig. 1 shows the index structure of R-Tree.

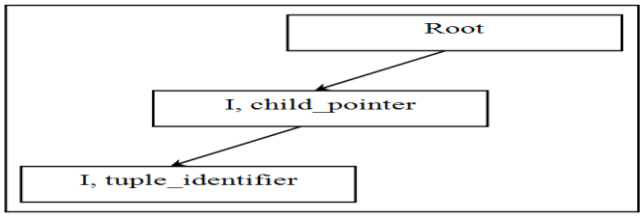

Fig. 1 Index Structure of R-Tree

Let, M is the maximum number of entries that will fit in one node and let $m \leq \frac{M}{2}$ be a parameter specifying the minimum number of entries in a node. An R-Tree [2] satisfies the following properties

(1) Every leaf node contains between m and M index records unless it is the root.
(2) For each index record (I, tuple_identifier) in a leaf node, I is the smallest rectangle that spatially contains the n-dimensional data object represented by the indicated tuple.
(3) Every non-leaf node has between m and M children unless it is the root.
(4) For each entry (I, child_pointer) in a non-leaf node, I is the smallest rectangle that spatially contains the rectangles in the child node.
(5) The root node has at least two children unless it is a leaf.
(6) All leaves appear on the same level.

3 Node Splitting Algorithms

In R-Tree, when we need to insert a data to any node and the node is full, then, we need to split that node to make room for the newly inserted records. There have been several R-Tree node splitting algorithms developed since R-Tree was introduced. Among them, Guttman's Quadratic-Cost Algorithm [2], the Optimal node splitting algorithm [11], the Linear node splitting algorithm [12] and Basic node splitting with bipartition [3] are most popular. One important area of concern is the overlapping area. As in region data types zero overlapping is not possible, so a good node splitting algorithm should confirm the minimum overlapping area among the minimum bounding rectangles.

3.1 Guttman's node splitting algorithms

These algorithms were proposed when R-Tree was introduced for the first time. In that work there were three node splitting algorithms, namely the Exhaustive algorithm, A Quadratic-Cost Algorithm and A Linear-Cost Algorithm.

3.1.1 Exhaustive algorithm

In this algorithm the author finds the most straight forward way to find the minimum area node split is to generate all possible groupings and choose the best grouping. However the number of possibilities is

approximately 2^{M-1} for M number of MBRs. So, the number of possible splits is very large.

3.1.2 Quadratic-Cost algorithm

The mostly used one among the three algorithms is the quadratic method. This node splitting algorithm first picks two records that may cause the worst split if put into the same node. These two records are used as seeds and the algorithm repetitively finds a record that may affect the splitting quality the most and assigns it to the appropriate node until all records are assigned. If there are just enough records left unassigned that can make one of the two newly generated nodes to satisfy the lower bound of the number of records, then, the rest of records will be assigned to that node directly.

3.1.3 Linear-Cost algorithm

This algorithm is identical to Quadratic Split but uses a different way to choose the seeds. It finds the iMBRs which have highest low side and the lowest high side along any dimension. According to that it finds the seeds for the splitting. The rest of the iMBRs are simply chosen at random.

3.3 The optimal node splitting algorithm

Here two algorithms were proposed. The first one is a basic node splitting algorithm which partitions a full node into two. It is like the exhaustive method but has a time complexity of O(Nd) instead of O(2N), where d is the dimension of data. The second algorithm is called SHIFT method. It first executes a pre-processing to get complementary MBRs with respect to all records. Then it tests each possible bipartition which is O(Nd), and find the one with the best metric. Here area and perimeter are two metrics used to gain a high occupancy of disk pages.

3.4 A linear node splitting algorithm

The algorithm partitions the records into two groups along each axis according to the distance between a record's MBR and the minimum and maximum coordinates on the axis. It then chooses a split axis by examining the number of records in each group. Then the partition along the selected axis will be the final splitting result. The algorithm's time complexity is O(N), where N is the number of records in a node. The algorithm does not consider the overlapping between the nodes.

3.5 Basic node splitting with bipartition

This algorithm first decides the splitting axis using some parameter. Taking the ratio of the two axis it decides the splitting dimension and if not possible then counting the maximum numbers of iMBR stretched along a particular axis. As this algorithm is not concerned about the internal organization of the iMBRs therefore, sometimes splitting from other dimension can give better result and less overlapping.

4 Scope of Work

There are three parameters for R-Tree node splitting. Area is one of them. Smaller node's area gives lower probability of the node being accessed. Some of the algorithms [2-3] [11-13] which are already available are only concerned about area increasing while choosing a leaf for new data and splitting a full node. Another parameter is the perimeter. Perimeter is responsible for the shape of the node's MBR. For a particular area, smaller perimeter conforms to more square shape of the MBR.

Overlap area is the third area of concern. Overlap between nodes causes multiple nodes to be accessed when a query object falls into that particular region. So it is one important parameter and needs to be dealt properly while designing R-Tree constructing algorithms. The algorithms which are already available [2] [11-13] are less concerned about the overlapping area during the time to decide the splitting axis. As attaining zero overlapping is practically impossible for region data types, so, a new node splitting algorithm, which can check the overlapping before deciding the splitting axis is proposed here. Two case study shows that, it can give a satisfactory performance by ensuring to minimize the total overlapping area.

5 Our Proposed Node Splitting Algorithms

Here in the algorithm, length-of-X is the length of the MBR along the X axis and length-of-Y is the length of the MBR along the Y axis. X-length-count is the summation of the lengths of all the iMBRs along the X axis and Y-length-count is the summation of the lengths of all the iMBRs along the Y axis. TOR-of-X is the total overlapping region if splitted along the X axis and TOR-of-Y is the total overlapping region if splitted along Y axis. If a node in a R-Tree can contain M number of data then the lower bound(m) is $\left\lceil \frac{M}{2} \right\rceil$. Overflown MBR is the MBR which contains more number of iMBRs than M.

Algorithm SplitNode:

Input: iMBR of a data
Output: two new nodes

Step 1: The algorithm '*SplitNode'* first invokes '*FindSplitDim'* to decide the splitting dimension for that particular node.

Step 2: When the splitting axis is determined, then, the algorithm divides the MBR in the middle of the axis.

Step 3: Now for each iMBR it checks which iMBR is

fully contained by which MBR. Then it assigns that iMBR to that new node.

Step 4: If any iMBR is not fully contained by any of the MBR alone then fitting it into which MBR gives less area increase gets the priority.

Step 5: Breaks ties by assigning it to the one which will produce less overlapping area.

Step 6: Now the two new nodes are checked for the lowerbound condition. If passes then these nodes are the final nodes.

Step 7: If any MBR fails then the splitting dimension is changed and the same procedure is applied again.

Step 8: If it is also not able to produce satisfactory rasult then for the underflowing MBR, the nearest iMBR, which produce less area increase, is inserted.

Step 9: Step 8 continues until the underflowing MBR gets sufficient iMBR to overcome the lowerbound criteria.

Algorithm FindSplitDim:

Input: Over flown MBR
Output: Splitting axis

Step 1: *'FindSplitDim'* first checks the length of the MBR in X & Y dimension and takes the longest axis as the initial splitting axis.

Step 2: If it is an square MBR then it checks the summation of the iMBRs in X & Y dimension. If the X-length-count is greater than Y-length-count then it takes Y as the initial splitting axis and vice-versa.

Step 3: If these two are equeal then it arbitrarily chooses the initial splitting axis.

Step 4: Now it checks which iMBRs are left aligned. There must be atleast one.

Step 5: After getting the iMBR then sets the value of the variable Z as the value of x2 of that iMBR.

Step 6: Now the algorithm finds the iMBR whose smaller value of x axis is lesser than variable Z and the bigger value x of that iMBR is greater than that of Z.

Step 7: If there is such an iMBR then the value of Z gets updated by the value of x2.

Step 8: When there is no such iMBR which has the same criteria and Z is equal to the bigger value of the minimum bounding rectangle then non-overlapping is not possible for that MBR along the X axis.

Step 9: So the algorithm checks the Y axis in the same manner. If a non-overlapping region is found then the final value of Z must be lesser than the bigger value of that axis.

Step 10: When non-overlapping split is not possible along any of the two dimensions then the algorithm invokes the '*FindTotalOverlappingRegion'*.

Step 11: After getting the values of the two variables (TOR-of-X & TOR-of-Y), now the '*FindSplitDim'* algorithm decides the final splitting dimension.

Step 12: Dimension with less overlapping area is the key criteria for selecting the splitting dimension. If a tie occurs then it arbitrarily decides the splitting axis and returns the value.

Algorithm FindTotalOverlappingRegion:

Input: Over flown MBR whose non overlapping splitting is not possible
Output: TOR-of-X & TOR-of-Y

Step 1: A new variable P is initialised with the length of that particular axis.

Step 2: The algorithm starts in the same manner as FindSplitDim and when there is an iMBR which passes that particular criteria then the algorithm finds the minimum length of small value of that iMBR along X axis to Z and Z to the larger value of that iMBR along X axis.

Step 3: If this minimum value is less than the present value of P then P gets updated with it.

Step 4: When Z = X2 then the value of P is taken into account and multiplied with the length of the MBR along the other axis and value is stored in TOR-of-X variable.

Step 5: In the same way the TOR-of-Y is also calculated and the values are returned.

6 Step-by-step Operations

We have taken two examples to check the step-by-step operations of our algorithm and compare the output of our node splitting algorithm with *basic node splitting with bipartition*. Here, 4 numbers of data can be put into one node at maximum i.e. an MBR can contain maximum 4 numbers of iMBRs. The MBRs which have more than 4 numbers of iMBRs are taken as over flown MBRs.

Case study I:

In Fig. 2.a we have taken an over flown MBR. For the MBR X1 = 0, X2 = 36, Y1 = 0, Y2 = 21. There are five iMBRs, r1, r2, r3, r4, r5. Table 1 shows the specifications of these iMBRs

Table 1: Specifications of the iMBRs

iMBR	x1	x2	y1	y2
r1	0	12	11	21
r2	24	36	11	21
r3	0	6	0	10
r4	30	36	0	10
r5	9	27	0	10

Step 1: The algorithm first checks for the length of the MBR along X & Y dimension.

Step 2: The larger one decides the initial splitting axis. Here X is the initial splitting axis.

Step 3: Now the algorithm checks whether in X dimension, there is any overlapping or not.

Step 4: For that it first checks which iMBR has x1 equals to X1. There must be at least one iMBR satisfying this criterion. Here is r1 & r3. Our algorithm takes r1 arbitrarily.

Step 5: Then for that iMBR (r1) it updates the value of Z variable with the value of x2(here it becomes Z = 12).

Step 6: Now the algorithm continues with for loop and checks which iMBR has (x1 < Z) & (x2 > Z). Here it finds that r5 satisfies that criterion. So the Z now becomes 27.

Step 7: Again in next step it gets r2 and the Z becomes 36. Now (Z = X2). So, in X dimension non-overlapping splitting is not possible.

Step 8: Now the algorithm changes the dimension and does the same. Here it finds that in Y dimension non-overlapping splitting is possible.

Step 9: It takes Y as the final splitting dimension and starts to split.

Step 10: The splitting is done in the middle of the splitting axis and the iMBRs which are fully contained by any of the two MBRs are assigned to them. Here r1 & r2 are fully contained by R1and r3, r5, r4 are fully contained by R2. So, these are assigned accordingly.

Fig. 2.c shows the result of splitting using our proposed algorithm. The corresponding R-Tree is shown in Fig. 2.e.

Fig. 2.b shows the result of splitting using the algorithm basic node splitting using bipartition. This algorithm first check whether the given rectangle is j-long or not; i.e. the ratio between the length of X & Y axis is greater than Θ or not (Where Θ > 0). If it is a square MBR then it checks whether the number of iMBRs whose length along X axis is greater than the same of Y axis. Thus it decides the splitting axis and assigns the iMBR accordingly. There is no way to check whether the splitting generates a huge overlapping area. Here the splitting produces an overlapping area whether non-overlapping splitting is possible. Fig. 2.d shows the R-Tree constructed form the result of that splitting.

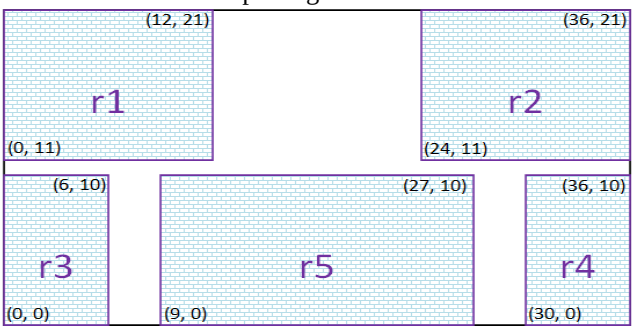

Fig. 2.a The Over flown MBR

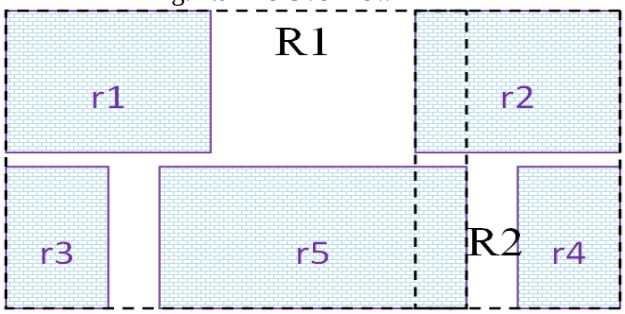

Fig. 2.b Result of the Basic Node Splitting with Bipartition

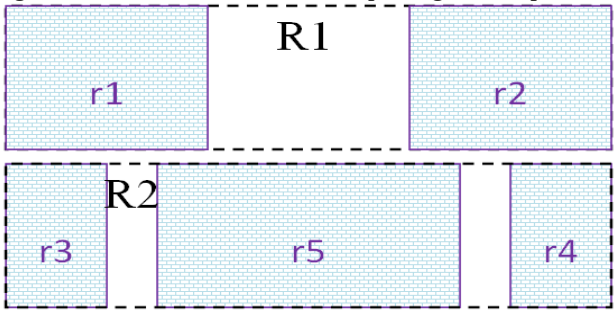

Fig. 2.c Result of our proposed Node Splitting

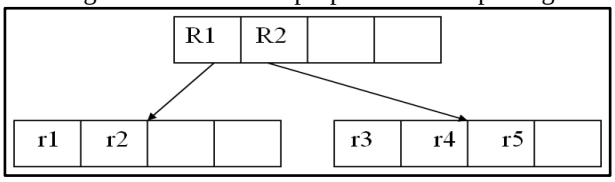

Fig. 2.d R-Tree constructed by basic node splitting with bipartition

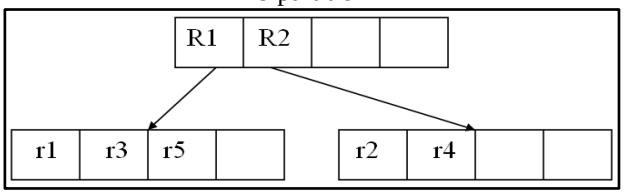

Fig. 2.e R-Tree constructed by our proposed node splitting algorithm

Case study II: Here we have taken another example. In Fig. 3.a we have taken an over flown MBR. For the MBR X1 = 0, X2 = 36, Y1 = 0, Y2 = 21. There are five iMBRs, r1, r2, r3, r4, r5. Table 1 shows the specifications of these iMBRs.

Table 2: Specifications of the iMBRs

iMBR	x1	x2	y1	y2
r1	0	18	11	21
r2	19	36	15	21
r3	0	6	0	10
r4	30	36	0	14
r5	10	28	0	10

Step 1: The algorithm starts by finding the iMBRs which have (x1 = X1). Here, r1 & r3.

Step 2: It continues by updating the value of Z after satisfying the criterion of (x1 < Z) & (x2 > Z).

Step 3: Finally for X dimension Z becomes X2 i.e. non-overlapping splitting is not possible in the X dimension.

Step 4: In the same way it checks in Y dimension and finds that in this case also non-overlapping splitting is not possible.

Step 5: Now, *'FindTotalOverlappingRegion'* is invoked**.**

Step 6: As the same way it first checks for the iMBR having (x1 = X1). When it finds one, it updates the value of Z.

Step 7: Now here a new variable P is introduced and initialized with the length of the MBR along that axis.

Step 8: For rest of the iMBRs it checks if, (x1 < Z) & (x2 > Z).Now it finds the minimum of (Z-x1) & (x2-Z).

Step 9: If P > MIN{(Z-x1), (x2-Z)} then it updates the value of P with MIN{(Z-x1), (x2-Z)}. Finally P becomes 8 for X dimension.

Step 10: Finally when (Z = X2) then it multiplies P with the length along the other axis and stores the area in a variable as the total overlapping region along X axis. TOR-of-X is now (8 * 21) i.e. 168 units.

Step 11: In the same way it finds the total overlapping area for Y axis and returns the values. TOR-of-Y = 4 * 36 = 144 units.

Step 12: Then algorithm *'FindSplitDim'* compares these values and decides the final splitting axis and returns the splitting dimension.

Step 13: Now the algorithm *'SplitNode'* splits the node in Y dimension.

Step 14: r2 is assigned to R1 and r3 & r5 are assigned to R2 as they are fully contained by these MBRs.

Step 15: Now, r1 is assigned to R1 and r4 is assigned to R2 as they give less increase in the area.

Here in Fig. 3.b we can see the total overlapping region for X axis. It is also the result of the node splitting by the basic node splitting with bipartition. Fig. 3.d shows the R-Tree constructed by basic node splitting with bipartition.

The algorithm decides Y as the final splitting dimension for this MBR and Fig. 3.c shows total overlapping region along Y axis. It is the result of the node splitting using our proposed node splitting algorithm which significantly have less overlapping area. Fig. 3.e shows the R-Tree constructed by our proposed node splitting algorithm.

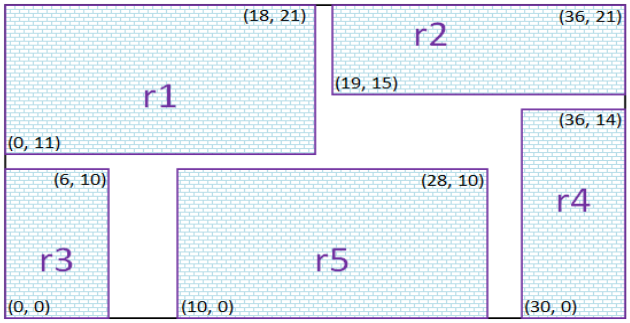

Fig. 3.a The Over flown MBR

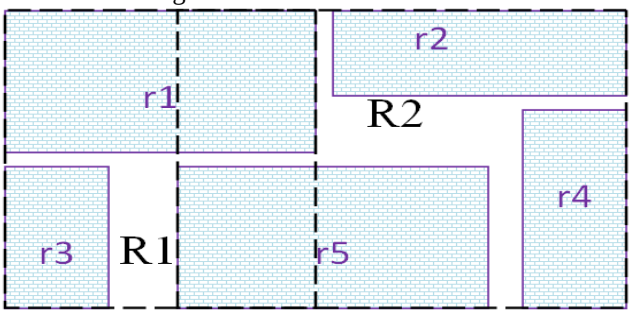

Fig. 3.b Result of the Basic Node Splitting with Bipartition

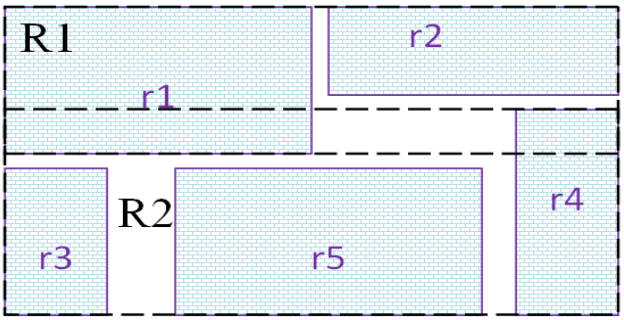

Fig.3.c Result of our proposed Node Splitting

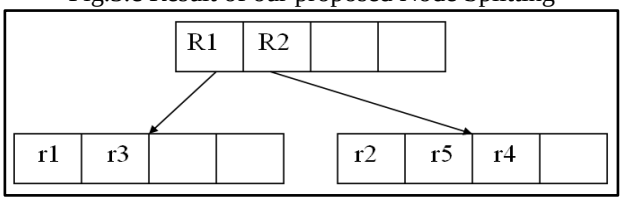

Fig. 3.d R-Tree constructed by basic node splitting with bipartition

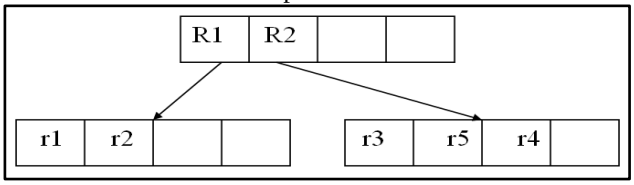

Fig. 3.e R-Tree constructed by our proposed node splitting algorithm

After splitting the MBR using our proposed algorithm, if any underflow condition occurs then the

algorithm changes its splitting dimension and splits again. If it can't satisfy the result then the under flown node includes the iMBR from the other which calls for a less area increase. This process continues until both the nodes passes the underflow condition.

7 Conclusions

In this paper, we have proposed a new algorithm to identify the best possible splitting axis to minimize overlapping. Minimization of overlapping in turn yields better result of searching. It goes without say, that in some cases, overlapping cannot be avoided, however our algorithm ensures minimum overlapping in such cases. We also compared our output with *basic node splitting with bipartition* and it has been shown that our splitting algorithm produces better result.

8 References

[1] Ralf Hartmut Güting, "An Introduction to Spatial Database Systems", Invited Contribution to a Special Issue on Spatial Database Systems of the VLDB Journal (Vol. 3, No. 4, October 1994), September 1994.

[2] A. Guttman, "R-Trees: a dynamic index structure for spatial searching," in SIGMOD '84: Proceedings of the 1984 ACM SIGMOD international conference on Management of data. New York, NY, USA: ACM, 1984, pp. 47–57.

[3] Yan Liu, Jinyun Fang, Chengde Han, "A New R-Tree Node Splitting Algorithm Using MBR Partition Policy," in IEEE 2009.

[4] Hui Li, Shiguang Ju, Weihe Chen," Design and Implementation of Generalized R-Tree", in 2008 IEEE DOI 10.1109/ISCSCT.2008.317

[5] Jia Bei, Wang Changming, Liu Chen and Sun Wei wei, "Design and Implementation of Object-Oriented Spatial Database of Coalfield Geological Hazards -Based on object-oriented data model", 2010 International Conference on Computer Application and System Modeling (ICCASM 2010).

[6] Kian-Lee Tan, Beng Chin Ooi, and David J. Abel, "Exploiting Spatial Indexes for Semijoin-Based Join Processing in Distributed Spatial Databases", IEEE TRANSACTIONS ON KNOWLEDGE AND DATA ENGINEERING, VOL. 12, NO. 6, NOVEMBER/DECEMBER 2000.

[7] I. Kamel, C. Faloutsos, "On Packing R-Trees", In Proceedings of the 2nd International Conference on Information and Knowledge Management (CIKM), November 1993.

[8] I. Kamel, C. Faloutsos, "Hilbert R-Tree: An Improved R-Tree Using Fractals", In Proceedings of the 20th International Conference on Very Large Data Bases (VLDB), September 1994.

[9] Shashi Shekhar, Siva Ravada, and Xuan Liu, "Spatial Databases- Acomplishments and Research needs", IEEE TRANSACTIONS ON KNOWLEDGE AND DATA ENGINEERING, VOL. 11, NO. 1, JANUARY/FEBRUARY 1999.

[10] Gang Liu, Qing Zhu, Zhenwen He, Yeting Zhang, Chonglong Wu, Xiaoming Li, Zhengping Weng, "3D GIS Database Model for Efficient Management of Large Scale Underground Spatial Data".

[11] Y. J. Garc´ıa, M. A. Lopez, and S. T. Leutenegger, "On optimal node splitting for R-Trees," in VLDB '98: Proceedings of the 24rd International Conference on Very Large Data Bases. San Francisco, CA, USA: Morgan Kaufmann Publishers Inc., 1998, pp. 334–344.

[12] C.-H. Ang and T. C. Tan,"New linear node splitting algorithm for R-Trees", in SSD '97: Proceedings of the 5th International Symposium on Advances in Spatial Databases. London, UK: Springer-Verlag, 1997, pp. 339-349.

[13] Liang Wang; Songnian Yu; Feng Chen,"A new solution of node splitting to the R-Tree algorithm", International Conference on Intelligent Control and Information Processing (ICICIP), 13-15 August, 2010, pp. 611-614.

SESSION

ALGORITHMS AND APPLICATIONS + FORMAL VERIFICATION

Chair(s)

TBA

Formalization and Verification of Number Theoretic Algorithms Using the Mizar Proof Checker

Hiroyuki Okazaki†,Yoshiki Aoki† and Yasunari Shidama†
†Shinshu University
4-17-1 Wakasato Nagano-city, Nagano 380-8553 Japan
okazaki@cs.shinshu-u.ac.jp,11ta501a@shinshu-u.ac.jp, shidama@shinshu-u.ac.jp
Tel:+81(26)269-5503 Fax:+81(26)269-5503

Abstract: *In this paper, we introduce formalization of well-known number theoretic algorithms on the Mizar proof checking system. We formalized the Euclidean algorithm, the extended Euclidean algorithm and the algorithm computing the solution of the Chinese reminder theorem based on the source code of NZMATH which is a Python based number theory oriented calculation system. We prove the accuracy of our formalization using the Mizar proof checking system as a formal verification tool.*

Keywords: Formal Verification, Mizar, Number theoretic algorithm

1 Introduction

Mizar[1, 2] is a project that formalizes mathematics with a computer-aided proving technique. Number theoretic algorithms play an important role in information society. For example, number theoretic algorithms are essential to cryptology and code theory because they provide secure and high-speed communications. However, there is no evidence that the calculated value producted by an algorithm is accurate, although the algorithm has a processing nature. Therefore, when we propose an algorithm, we have to prove the accuracy of the algorithm.

On the other hand, a developed program for an algorithm is not necessary to calculate a precise value although the accuracy of the algorithm was proven. This is because it is difficult to develop a program which functions exactly like the algorithm. We have to verify that the algorithm is accurately encoded into a programing language.

The objective of this study is to prove the accuracy of the algorithms, encoded in a programing language, using the Mizar proof checker. To achieve this, first, we formalized algorithms in the Mizar language to confirm that the formalization agrees with our aim. This is because there are several methods how to formalize algorithms.

In this paper, we introduce formalization of well-known number theoretic algorithms on the Mizar proof checking system. We formalized the Euclidean algorithm, the extended Euclidean algorithm and the algorithm computing the solution of the Chinese reminder theorem based on the source code of NZMATH[3], which is a Python based number theory oriented calculation system. Then we verified the accuracy of the formalized algorithms using the Mizar proof checker.

The remainder of the study is organized as follows. We briefly introduce the Mizar project in Section 2 and NZMATH in Section 3. In Section 4, we discuss our strategy for formalizing algorithms in Mizar, followed by Section 5 where propose a formalization of the Euclidean algorithm. In Section 6, we propose the formalization of the extended Euclidean algorithm, and in Section 7, we propose a formalization of the algorithm, computing the solution of the Chinese reminder theorem. We conclude our discussions in Section 8. The definitions and theorems in this study have been verified for accuracy using the Mizar proof checker.

2 Mizar

Mizar [1, 2] is an advanced project of the Mizar Society led by Andrzej Trybulec. It formalizes mathematicals with a computer-aided proving technique. The Mizar project describes mathematical proofs in the Mizar-language, which is created to describe mathematics formally. The Mizar proof checker operates in both Windows and UNIX environments and registers proven definitions and theorems in the Mizar Mathematical Library (MML).

Furthermore, the objective of the Mizar project is to create a checking system for mathematical theses. An "article" formalizes and describes mathematical proofs by Mizar. When an article is newly described, it is possible to advance it by referring to articles registered in MML, which have already been inspected as proofs. Similarly, other articles can refer to an article after it is registered in MML. Although the Mizar language is based on the description method for general mathematical proofs, the reader should consult the references for grammatical details, because Mizar uses a specific, unique notation[1, 2].

3 NZMATH

NZMATH[3] is a number theory oriented calculation system mainly developed by the Nakamula laboratory at Tokyo Metropolitan University. Number theoretic algorithms are implemented as Python functions on NZMATH, which is freely available and distributed under the BSD license. NZMATH is at an early stage of development and is currently being developed.

4 Strategy of Formalizing Algorithms in Mizar

In Mizar, there are several methods to define computational routines, representing algorithms. One method is to define a routine as a program for SCM. SCM is a general model of a stack machine defined in the Mizar system. In principle, we may formalize arbitrary programs in SCM. However, this approach may not be suitable to prove the accuracy of algorithms encoded in a high level programing language, because we have to define an algorithm as the machine code of SCM. For example, the Euclidean Algorithm has been formalized in SCM[4] (Definition A.1).

Another method is to define a routine as a functor or a Function. A functor is a relation between input and output of the routine in Mizar. It is easy to write and understand the formalization of a routine as functor because the format of a functor in Mizar is similar to that of a function in programming languages. Thus, in this paper, we formalize an algorithm as a functor.

A Function is a map from the input space onto the output space. We can handle a Function as an element of the set of Functions. Note that both functor and Function can use a Function as their substitutable subroutine. For example, we formalized the algorithm of DES cipher as a functor, which uses substitution subroutines defined as Functions[5, 6].

4.1 Formalizing Loop Structure in Mizar

In this section, we propose an approach to describe programs with a loop structure. Particularly, we elucidate the method to formalize programs with a non-nested loop structure[1]. This suggests that it is possible to formalize a program with looped structures by nesting single loop structures recursively.

A loop is a sequence of statements. In a computer implementation, variables that are allocated memory segments, are assigned destructively according to the given recursion formula in each iteration.

To describe the loop structure in the Mizar language, we consider that there are sequences of variables to capture the repetition of operations. For example, let a be the sequence of variables such that a_i, the ith member of a, represents the temporary value assigned as a in the ith iteration of the loop structure. Note that we can describe the control condition of the iteration using the index number of the sequences of variables.

We can employ the inductive method to prove the property of the variables using such sequences. The Mizar system has a mechanism, called "scheme", which enables us to prove propositions using the inductive method. We will show an example of a proof using "scheme" in Section 5.

[1] Note that all algorithms, which were formalized in this paper, do not have nested loops.

5 Formalization of the Euclidean Algorithm

In this section we introduce our formalization of the Euclidean algorithm.

The Euclidean algorithm is a the method that computes the greatest common divisor of two given integers. This algorithm is implemented in NZMATH as follows:

Code 5.1 (Euclidean algorithm in NZMATH)

```
def gcd(a, b):
    a, b = abs(a), abs(b)
    while b:
        a, b = b, a % b
    return a
```

We formalize this algorithm as the following functor in the Mizar language:

Definition 5.1 (Euclidean Algorithm in Mizar)

```
let a,b be Element of INT;
func ALGO_GCD(a,b)
  -> Element of NAT
means
ex A,B be sequence of NAT
st
A.0 = abs(a) & B.0 = abs(b) &
(for i be Element of NAT holds
A.(i+1) = B.i &
B.(i+1) = A.i mod B.i) &
it = A.(min*{i where i is Nat: B.i = 0});
```

Here the symbol 'it' denotes the value returned by the functor. `min*` is the definition of the minimum member of a given set in Mizar (Definition A.2). `A` and `B` are infinite sequences of $\mathbb{N}$ such that

$$\begin{aligned} \mathrm{A} &= \{a_0, a_1, \ldots, a_i, a_{i+1}, \ldots\}, \\ \mathrm{B} &= \{b_0, b_1, \ldots, b_i, b_{i+1}, \ldots\}, \\ & \quad a_0 = a, b_0 = b, \\ & \quad a_{i+1} = b_i, b_{i+1} = a_i \bmod b_i. \end{aligned}$$

Note that a_i, b_i are the values of `a`, `b` in the ith iteration, respectively.

5.1 Accuracy of ALGO_GCD

In this section we prove the accuracy of our formalization that the functor ALGO_GCD returns the greatest common divisor of a given two integers.

We will prove the following theorem:

Theorem 5.1 (Accuracy of ALGO_GCD)

```
for a,b be Element of INT
holds
ALGO_GCD(a,b) = a gcd b
```

Here gcd is the conceptual definition of the greatest common divisor in Mizar as follows:

Definition 5.2 (gcd of Mizar)

```
let a,b be Integer;
func a gcd b -> Nat means
it divides a
& it divides b
& for m being Integer st m divides a
& m divides b holds m divides it;
```

We proved Theorem. 5.1 using the following lemma:

Lemma 5.1

```
for i be Element of NAT
st B.i <> 0
holds
A.0 gcd B.0 = A.i gcd B.i
```

In the rest of this section, we show a schematic proof for Lemma. 5.1. First, we defined the following predicate

```
defpred P[Nat] means
B.$1 <> 0 implies
A.0 gcd B.0 = A.$1 gcd B.$1;
```

Here, the symbol '$1' denotes the argument of P[2].

Therefore, P[0] is evidently *true*. Next, we prove that P[$i+1$] is *true* if P[i] is *true* as follows:

```
for i being Element of NAT
st P[i] holds P[i+1];
```

Finally, we can prove Lemma 5.1 with the following mathematical induction scheme that had been defined in the Mizar system:

Scheme 5.1 (Mathematical Induction scheme)

```
Ind{ P1[ Nat] } :
for k being Nat holds P1[k]
provided
P1[ 0 ] and
for k being Nat st P1[k] holds
P1[k + 1]
```

It should be noted that we are allowed to create new schemes.

[2] If the predicate P uses two natural numbers, we can define it as "defpred P[Nat,Nat] means,...," and the symbol '$n' denotes the nth argument of P.

6 Formalization of the Extended Euclidean Algorithm

In this section we formalize the extended Euclidean algorithm. The extended Euclidean algorithm can compute a, b and g for given integers x, y such that $ax + by = g$(g is the greatest common divisor of x, y). This algorithm is implemented in NZMATH as follows:

Code 6.1 (The extended Eucliean algorithm in NZMATH)

```
def extgcd(x,y):
    a,b,g,u,v,w = 1,0,x,0,1,y
    while w:
        q,t = divmod(g,w)
        a,b,g,u,v,w = u,v,w,a-q*u,b-q*v,t
    if g >= 0:
        return (a,b,g)
    else:
        return (-a,-b,-g)
```

We formalize this algorithm as the following functor in the Mizar language:

Definition 6.1 (The extended Euclidean algorithm in Mizar)

```
let x,y be Element of INT;
func ALGO_EXGCD(x,y)
  -> Element of [:INT,INT,INT:]
means
ex g,w,q,t be sequence of INT,
a,b,v,u be sequence of INT,
istop be Element of NAT
st
a.0 = 1 & b.0 = 0 & g.0 = x & q.0 =0
& u.0 = 0 & v.0 = 1 & w.0 = y & t.0 =0
&
(for i be Element of NAT
holds
q.(i+1) = g.i div w.i
& t.(i+1) = g.i mod w.i
& a.(i+1) = u.i & b.(i+1) = v.i
& g.(i+1) = w.i
& u.(i+1) = a.i - q.(i+1)*u.i
& v.(i+1) = b.i - q.(i+1)*v.i
& w.(i+1) = t.(i+1))
&
istop =
  min*{i where i is Nat: w.i = 0}
&
(0 <= g.istop implies
it =[a.istop,b.istop,g.istop])
&
(g.istop < 0 implies
it =[-(a.istop),-(b.istop),-(g.istop)]);
```

Note that ALGO_EXGCD(x,y) returns the 3-tuple (a, b, g) such that $ax + by = g$ and g is the greatest common divisor of x and y.

6.1 Accuracy of ALGO_EXGCD

In this section we prove the accuracy of our formalization that the functor ALGO_EXGCD returns a, b and g for given integers x and y such that $ax + by = g$(g is the greatest common divisor of x and y).

We can prove the following theorem in a similarly for proving Theorem 6.1:

Theorem 6.1 (Accuracy of ALGO_EXGCD)

```
for x,y be Element of INT
holds
ALGO_EXGCD(x,y)‘3 = x gcd y
&
ALGO_EXGCD(x,y)‘1 * x
+ ALGO_EXGCD(x,y)‘2 * y
= x gcd y,
```

where ALGO_EXGCD(x,y)‘n denotes the nth member of ALGO_EXGCD(x,y). Thus we proved the accuracy of our formalization of extended Euclidean algorithm.

6.2 Multiplicative Inverse

Then, we define the functor that computes the multiplicative inverse over a residue class ring using the ALGO_EXGCD as follows:

Definition 6.2 (Inverse)

```
let x,p be Element of INT;
func ALGO_INVERSE(x,p) -> Element of INT
means
for y be Element of INT
st y = (x mod p)
holds
(ALGO_EXGCD(p,y)‘3 = 1 implies
((ALGO_EXGCD(p,y)‘2 < 0) implies
(ex z be Element of INT
st z = ALGO_EXGCD(p,y)‘2
& it = p + z ))
& ( (0 <= ALGO_EXGCD(p,y)‘2)
    implies it = ALGO_EXGCD(p,y)‘2) )
&( ALGO_EXGCD(p,y)‘3 <> 1 implies it = {} );
```

We will define another algorithm with this functor in Section 7.

7 Formalization of the Algorithm Computing the Solution of the Chinese Reminder Theorem

In this section we formalize the algorithm computing the solution of the Chinese reminder theorem.

7.1 The Chinese Reminder Theorem

First, we review the Chinese reminder theorem briefly.

Theorem 7.1 (Chinese Reminder Theorem) *Let $m_1, m_2, \cdots, m_r$ be relatively prime. For any integer $a_1, a_2, \cdots, a_r$, there exists the unique solution $x \in \mathbb{Z}/(m_1 \cdot m_2 \cdots m_r)\mathbb{Z}$ such that*

$$\begin{aligned} x &\equiv a_1 \bmod m_1 \\ x &\equiv a_2 \bmod m_2 \\ &\vdots \\ x &\equiv a_r \bmod m_r. \end{aligned}$$

We can compute such a solution x by the following steps:
First, we solve

$$\begin{aligned} x \equiv a_1 \bmod m_1 \\ x \equiv a_2 \bmod m_2 \end{aligned} \tag{1}$$

by

$$x_0 = a_1 + (a_2 - a_1)(m_1^{-1} \bmod m_2)m_1. \tag{2}$$

Then:

$$\begin{aligned} x_0 \bmod m_1 &= a_1 \\ x_0 \bmod m_2 &= a_1 + (a_2 - a_1) \\ &= a_2 \end{aligned}$$

Thus, x_0 is the solution of (1).

Next, we solve the congruencies:

$$\begin{aligned} x \equiv x_0 \bmod m_1 m_2 \\ x \equiv a_3 \bmod m_3 \end{aligned} \tag{3}$$

Then we solve the next congruent expression and the solution of (3) sequentially. Finally, we can solve (1).

7.2 Formalization of the Algorithm Computing the Solution of the Chinese Reminder Theorem

In this paper, let us term the algorithm mentioned in Sec. 7.1 as "CRT algorithm". The CRT algorithm is implemented in NZMATH as follows:

Code 7.1 (CRT in NZMATH)

```
def CRT(nlist):
  r = len(nlist)
  if r == 1 :
    return nlist[0][0]

  product = []
  prodinv = []
  m = 1
  for i in range(1, r):
    m = m*nlist[i-1][1]
    c = inverse(m, nlist[i][1])
    product.append(m)
    prodinv.append(c)

  M = product[r-2]*nlist[r-1][1]
  n = nlist[0][0]
```

```
for i in range(1, r):
  u = ((nlist[i][0]-n)*prodinv[i-1])
      % nlist[i][1]
  n += u*product[i-1]
return n % M
```

Here `nlist` denotes the given congruencies. For example, if the given congruencies are

$$x \equiv 2 \bmod 3$$
$$x \equiv 3 \bmod 5$$
$$x \equiv 2 \bmod 7$$

then `nlist` is as follows:

```
nlist = [ (2,3), (3,5), (2,7) ]
```

We then formalize the algorithm as the following functor in the Mizar language:

Definition 7.1 (CRT in Mizar)

```
let nlist be
  non empty FinSequence
  of [:INT,INT:];
func ALGO_CRT(nlist)->Element of INT
means
(
  len nlist=1 implies it=(nlist.1)‘1
)
&
(
  len nlist <> 1 implies
  ex m,n,prodc,prodi
    be FinSequence of INT,
    M0,M be Element of INT
  st len m = len nlist
  & len n = len nlist
  & len prodc = len nlist - 1
  & len prodi = len nlist - 1
  & m.1 = 1
  &
  (
    for i be Nat
      st 1<=i & i<=(len m) - 1
    holds
    ex d,x,y be Element of INT
    st x = (nlist.i)‘2
    & m.(i+1) = m.i * x
    & y = m.(i+1)
    & d = (nlist.(i+1))‘2
    & prodi.i = ALGO_INVERSE(y,d)
    & prodc.i = y
  )

  & M0 = (nlist.(len m))‘2
  & M = (prodc.((len m)-1))*M0
  & n.1 = (nlist.1)‘1
  &
  (
    for i be Nat
      st 1<=i & i<=len m - 1
    holds
      ex u,u0,u1 be Element of INT
      st u0 = (nlist.(i+1))‘1
      & u1 = (nlist.(i+1))‘2
      & u = ((u0-n.i) * (prodi.i))
            mod u1
      & n.(i+1) = n.i + u*(prodc.i)
  )
  & it = n.(len m) mod M
);
```

Here, `m`, `prod`, `prodi`, `M` and `n` are finite sequences of $\mathbb{N}$ such that

$$\begin{aligned}
\text{prodc} &= \{prodc_1, prodc_2, \ldots, prodc_i, \\
&\quad prodc_{i+1}, \ldots, prodc_r\}, \\
\text{prodi} &= \{prodi_1, prodi_2, \ldots, prodi_i, \\
&\quad prodi_{i+1}, \ldots, prodi_r\}, \\
\text{m} &= \{m_1, m_1, \ldots, m_i, m_{i+1}, \ldots, m_r\}, \\
\text{n} &= \{n_1, n_2, \ldots, n_i, n_{i+1}, \ldots, n_r\}, \\
&\quad m_1 = 1,\ n_1 = nlist[1][1], \\
&\quad m_{i+1} = m_i * nlist[i][2], \\
&\quad prodc_i = m_{i+1}^{-1} \bmod nlist[i+1][2] \\
&\quad prodi_i = m_{i+1} \\
&\quad n_{i+1} = n_i + u * prodc_i,
\end{aligned}$$

Note that $prodc_i, prodi_i, m_i$ and n_i are the value of `product`, `prodinv`, `m` and `n` in the ith iteration respectively. Additionally, we do not use infinite sequences but finite sequences for this algorithm because the count of the iteration is predetermined.

We then prove the following theorem:

Theorem 7.2 (Accuracy of ALGO_CRT)

```
for nlist be non empty FinSequence
  of [:INT,INT:],
a,b be non empty FinSequence of INT,
x,y be Element of INT
st len a = len b
& len a = len nlist
& (for i be Nat
    st i in Seg (len nlist)
  holds
    b.i <> 0 )
& (for i be Nat
    st i in Seg (len nlist)
  holds
    (nlist.i)‘1 = a.i
    & (nlist.i)‘2 =b.i )
& (for i,j be Nat
    st i in Seg (len nlist)
    & j in Seg (len nlist)
    & i <> j
  holds
    b.i,b.j are_relative_prime )
& (for i be Nat
    st i in Seg (len nlist)
  holds
    x mod b.i = a.i mod b.i )
```

```
& y = Product b
holds
ALGO_CRT(nlist) mod y = x mod y
```

Here `are_relative_prime` and `Product` denote the definition in Mizar (Definitions A.3 and A.4). Thus, we proved the accuracy of our formalization of the CRT algorithm.

8 Conclusions

In this study, we introduced our formalization of the Euclidean algorithm, the extended Euclidean algorithm, and the CRT algorithm based on the source code of NZMATH. Moreover, we proved the accuracy of our formalization using the Mizar proof checking system as a formal verification tool. Therefore, we can conclude that our approach can formalize algorithms with a single loop structure precisely. Currently, we are attempting to develop methods to convert the encoded algorithms from NZMATH into Mizar automatically [3].

Acknowledgments

This work was supported by JSPS KAKENHI 21240001 and 22300285.

References

[1] *Mizar Proof Checker*, *Available at* `http://mizar.org/`.

[2] E.Bonarska, *An Introduction to PC Mizar*, Mizar Users Group, Fondation Philippe le Hodey, Brussels, 1990.

[3] *NZMATH*, *Available at* `http://tnt.math.se.tmu.ac.jp/nzmath/index.html`.

[4] J.-C.Chen, *'Recursive Euclide Algorithm*, Formalized Mathematics, Vol. 9, No. 1, pp. 1–4, 2001.

[5] H.Okazaki, K.Arai, and Y.Shidama, *Formal Verification of DES Using the Mizar Proof Checker*, in *Proc. FCS'11*, pp. 63–68, 2011.

[6] H.Okazaki, K.Arai, and Y.Shidama, *Formalization of the Data Encryption Standard*, *Available at* `http://www.mizar.org/version/current/abstr/descip_1.abs`.

[7] R.Kwiatek and G.Zwara, *The Divisibility of Integers and Integer Relative Primes*, Formalized Mathematics, Vol. 1, No. 5, pp. 829–832, 1990.

[8] G.Bancerek, *The Fundamental Properties of Natural Numbers*, Formalized Mathematics, Vol. 1, No. 1, pp. 41–46, 1990.

[9] G.Bancerek, *Arithmetic of Non-Negative Rational Numbers*, Journal of Formalized Mathematics, Addenda, 1998.

[10] G.Bancerek, *König's Theorem*, Formalized Mathematics, Vol. 1, No. 3, pp. 589–593, 1990.

[3] We have already been able to convert Python programs with a single loop structure.

A Related Definitions of Functors in Mizar

Definition A.1 (Euclidean Algorithm in SCM)

```
func GCD-Algorithm -> Program of SCMPDS
equals
(((GBP:=0) ';' (SBP := 7) ';'
saveIC(SBP,RetIC) ';' goto 2 ';'
halt SCMPDS ) ';' (SBP,3)<=0_goto 9 ';'
((SBP,6):=(SBP,3)) ';'
Divide(SBP,2,SBP,3) ';'
((SBP,7):=(SBP,3)) ';'
((SBP,4+RetSP):=(GBP,1))) ';'
AddTo(GBP,1,4) ';' saveIC(SBP,RetIC) ';'
(goto -7) ';' ((SBP,2):=(SBP,6)) ';'
return SBP;
```

Definition A.2 (Minimum Member)

```
let A be set ;
func min* A -> Element of NAT means
(
  it in A
  & ( for k being Nat
      st k in A holds it <= k )
)
if A is non empty Subset of NAT
otherwise it = 0 ;
```

Definition A.3 (Relatively Prime)

```
let a, b be Ordinal;
pred a,b are_relative_prime means
for c, d1, d2 being Ordinal
st a = c *^ d1 & b = c *^ d2
holds c = 1;
```

Definition A.4 (Product)

```
func product f -> set means
for x being set
holds
( x in it iff ex g being Function
st
( x = g & dom g = dom f
& ( for y being set st y in dom f
holds g . y in f . y ) ) );
```

Static and Dynamical Equilibrium Properties to Categorise Generalised Game-of-Life Related Cellular Automata

K.A. Hawick
Computer Science, Institute for Information and Mathematical Sciences,
Massey University, North Shore 102-904, Auckland, New Zealand
email: k.a.hawick@massey.ac.nz
Tel: +64 9 414 0800 Fax: +64 9 441 8181

April 2012

ABSTRACT
Conways's Game-of-Life (GoL) is one of a family of spatial cellular automata rule sets that employ the Moore neighbourhood on a rectilinear lattice of cells. GoL generalises to set of other automata using different neighbour-numbers that lead to birth and survival. These models exhibit different static properties and also different long term dynamical equilibrium points. We define some quantifiable metrics and explore how some well known GoL variants can be categorised into groupings, categorised by their static properties and dynamical equilibria. We also explore effects due to differing initial crowding levels of the live seed cell population, and how this affects the categories.

KEY WORDS
statistical mechanics; Game of Life; generalised rules; cellular automata; complex system.

1 Introduction

Cellular Automata (CA) models [1, 13, 28] have long played an important role in exploring and understanding of the fundamentals of complex systems [17, 33, 34].

Studies of many CA systems are reported in the literature and for many complex systems applications including: damage spreading [21]; network analysis [38]; food chain systems [16]; lattice gases [37]; and fluid flow [7]. Two fundamental and classic CAs that provide a basis for much other work are the Wolfram's one dimensional automaton [36], and Conway's Game of Life [14]. The Wolfram system is especially useful because of it conciseness and the fact that the whole automaton rule state space is easily described as a family of bit valued cell-wise truth tables and can be systematically explored. Two dimensional automata can be also be formulated using the Wolfram approach [26]. Conway's Game of Life (GoL) however, also has a concise specification, but it is formulated in terms of counts of live neighbouring cells rather than specific patterns.

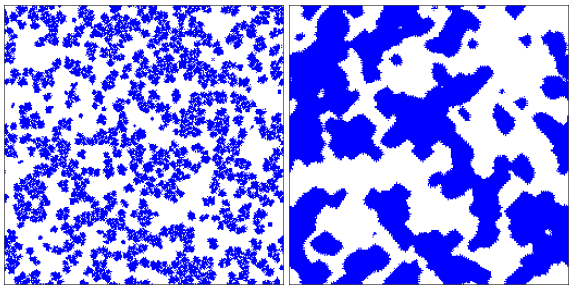

Figure 1: Coral and Diamoeba Automata.

There is a space of similarly formulated automaton rules [24] in the same family as GoL [22]. Like the Wolfram automata not all the rules in the GoL family are "interesting" or can be classified as complex. The Conway precise specification turns out to be special in the rule set space of the family, but there are some other related automata in the family that do have interesting properties and which have been given names. Figure 1 shows snapshots from two such GoL family members - known as "Coral" and "diamoeba."

There are a number of other variants of cellular automata including: the game of death [12], with an extra zombie state added; ratchet automata [15]; and other variants of GoL such as hyperbolic life [27]. GoL and its variants have also also been studied: on other non-square geometries [5]; on Penrose tilings [25]; on hexagonal lattices [4]; and on generalised networks [9]. Work has also been reported on three dimensional GoL variants [2, 3].

This present article reports work exploring some of the transient and long term dynamical properties of the GoL family of automata in two dimensions and on a square, periodic lattice. In particular a preliminary attempt is made

to see how this GoL family can be categorised according to some quantitative metrics that can be obtained from numerical experiments. Attempts to automatically classify automata by their behaviours have been reported [19], although here we discuss a set of manually carried out experiments.

Much work has been done on studying the coherent structures that occur in GoL and its variants [11]. It is possible to implant specific patterns such as gliders, glider guns and so forth to obtain specific sequences of GoL automata configurations. However, in this present paper we investigate GoL automata systems that have been randomly initialised with an initial fraction of live cells. Providing we simulate a large enough sample of large enough automata systems, many different individual patterns can occur by chance, will interact and the system will eventually arrive a static or dynamical equilibrium. This approach supports study of the statistical mechanical properties [31] of the automata systems and the identification of which automata have stable points [6] or not, as well as a framework to study universality properties [32] in cellular automata theory [35].

Although stochastic thermal or random effects [18, 20] have been introduced into cellular automata to study such properties, in this present work we restrict ourselves to entirely deterministic automata. We avoid asynchronous automaton [8, 23, 29, 30] effects by using a two phase synchronous update implementation of the automata reported here. The only randomness or ambiguity introduced is in the initial random pattern of live cells seeded.

The article is structured as follows: In Section 2 we describe the notation for the GoL family of automata and the statistical metrics that can be applied to study them numerically. In Section 3 we present some results for some of the automata in the family. We discuss the implications in Section 4 and summarise some conclusions and areas for further work in Section 5.

2 Automata Notation & Metrics

The game of Live and its family of variant automata are implemented using the Moore neighbourhood on a $d = 2$ dimensional array of cells, where the number of (Moore) Neighbouring sites $N_M = 8$, for $d = 2$ as shown in Figure 2. We define the (square) lattice Length as L and hence the number of sites N, typically $N = L^d$. We define the number of live sites N_L, and so the metric fraction $f_l = N_L/N$ and similarly the number of dead sites N_D, and fraction $f_D = N_D/N$.

The GoL community has developed various generalised notations for a GoL-like automata [1, 24]. We

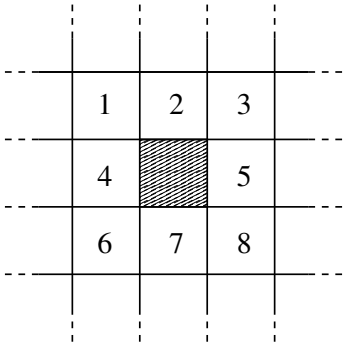

Figure 2: Moore neighbourhood of 8 sites in 2-D.

elaborate these and use the more verbose form of $\mathbf{Bn_1, n_2, .../Sm_1, m_2, ...}$ This notation specifies the rules that area applied to each site exactly once at each time step. The notation gives a comma-separated-list of the allowable numbers n_i of live neighbours which give rise to **B**irth of a live site from a dead site before the slash, and likewise another comma-separated list of the allowable number m_i of live neighbours that are necessary for a live site to survive.

Algorithm 1 Synchronous **automaton update cells** algorithm.

for all i, j in (L, L) **do**
  gather Moore Neighbour-hood $\mathcal{M}_{i,j}$
  apply rule $b[i][j] \leftarrow \{s[i][j], \mathcal{M}_{i,j}\}$
end for
for all i, j in (L, L) **do**
  copy $b[i][j] \rightarrow s[i][j]$
end for

Algorithm 2 CA Experimental procedure

declare $s[L][L]; b[L][L]$
for $r = 0$ to runs **do**
  initialise s, st $n_L = pN$ live, rest dead
  for $t = 0$ to t_e **do**
    automaton update cells
  end for
  for $t = t_e$ to t_m **do**
    automaton update cells
    make measurements
  end for
end for
normalise averages

The rules thus support death both from "overcrowding" and also from "lack of parents." The classic Conway game of life is thus specified by the notation **B3/S2,3**. We use this notation to specify explicitly the 26 GoL variants we experiment with below. Although GoL automata are well

studied, for completeness and to avoid ambiguity, we give the algorithm for implementing these e automata.

Algorithm 2 shows the experimental procedure we deploy, based upon the automata update rule procedure specified in Algorithm alg:synch-update. We use a two-phase update algorithm and so each rule is applied to change the site at time $t+1$ based on its state and that of its neighbouring sites at time t.

The following metrics are used to study the automata experimentally:

- the 1-step time correlation function $C_1 = \frac{1}{N}\sum_{i,j} s(i,j,t).s(i,j,t-1)$
- the fraction of neighbours that are the same as the site they surround. This is essentially a count of the like-like bonds, normalised by divining by $(N.N_M)$
- likewise, the fraction of neighbours that are different from the site they surround
- the number of monomers is the number of live sites that are completely surrounded by dead sites.
- the number of dimers is the number of connected-pairs of live sites that are each otherwise surrounded by dead sites.

The number of arbitrary sized cluster components of live sites is expensive to compute and we do not use it in this study.

3 Experimental Results

The GoL family of automata were investigated numerically. The reported experiments are based on averages over 100 independently randomly initialised runs of a periodic 256^2 cell system, equilibrated for 512 time steps and then run with measured metrics recorded and averaged over a subsequent 512 steps.

Table 1 shows 26 members of the GoL family of automata simulated for the specified times t on a 256^2 periodic lattice, with random initial fractions of live sites of the specified fractions p.

Figure 3 shows some of the metrics described in Section 2 applied to the family of automata. The plots are of the 1-step correlation function; the fraction of live and Vacant(=dead) cells and the fraction of neighbour links that have the same (live-live or dead-dead) cell on them. The plots are sorted according to rank and the labelled points indicate the automata model. Note that the plot lines naturally group onto plateaux with sharp cliffs separating them. Automata of similar properties thus group together.

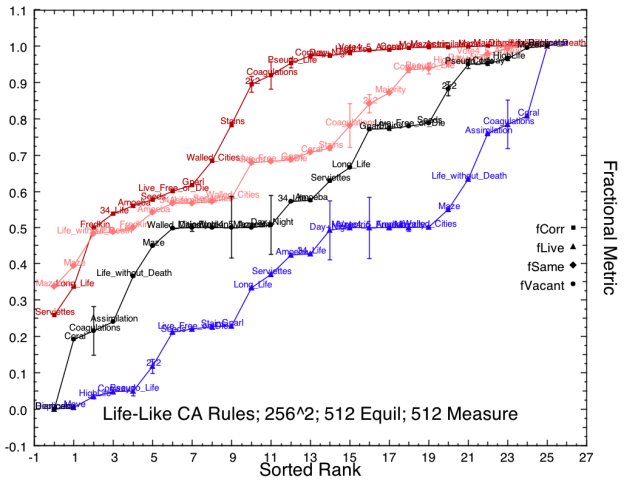

Figure 3: 1-Step Correlation and static fractional metrics.

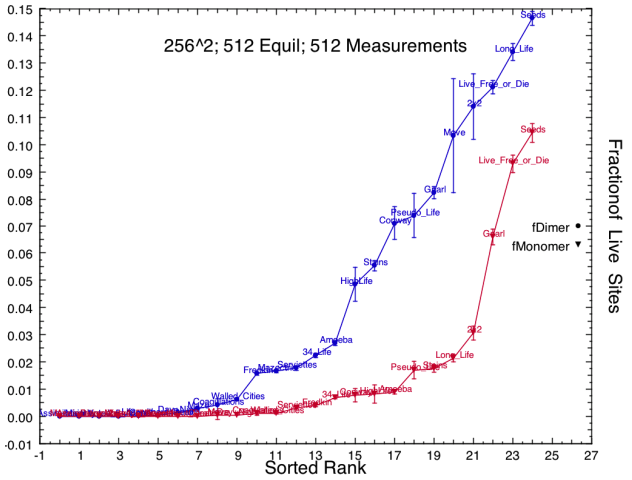

Figure 4: Monomer and Dimer counts.

Figure 4 shows the number of monomers and dimers of live cells for the different GoL automata with a starting initialisation fraction of $p = 0.5$. The curves are again ranked and points labelled by automata models. As can be seen most models do not lead to large numbers of dimers or monomers, but a small number do exhibit large numbers. The grouping is split by a relatively sharp shoulder in the curves.

Figure 5 shows a scatter-plot of the 1-step correlation metric plotted against the fraction of live sites. There are clear and obvious groupings with some annotations drawn (in red, online version) indicating which automata behave similarly.

The plotted metrics are shown with error bars based on the estimated experimental standard deviations. These themselves give some interesting insights into the behaviours

Rule (B/S) format	Common Name for Rule	t=128 p=0.5	t=256 p=0.5	t=128 p=0.3	t=256 p=0.3	t=128 p=0.1	t=256 p=0.1
B1/S1	Gnarl						
B1,3,5,7/S1,3,5,7	Replicator						
B1,3,5,7/S0,2,4,6,8	Fredkin						
B2/S	Seeds						
B2/S0	Live Free/Die						
B2,3,4/S	Serviettes						
B3/S0,1,2,3,4,5,6,7,8	Life w/o Death						
B3/S1,2,3,4	Mazectric						
B3/S1,2,3,4,5	Maze						
B3/S2,3	Conway						
B3/S4,5,6,7,8	Coral						
B3,4/S3,4	34 Life						
B3,4,5/S4,5,6,7	Assimilation						
B3,4,5/S5	Long Life						
B3,5,6,7,8/S5,6,7,8	Diamoeba						
B3,5,7/S1,3,5,8	Amoeba						
B3,5,7/S2,3,8	Pseudo Life						
B3,6/S1,2,5	2x2						
B3,6/S2,3	HighLife						
B3,6,8/S2,4,5	Move						
B3,6,7,8/S2,3,56,7,8	Stains						
B3,6,7,8/S3,4,6,7,8	Day & Night						
B3,7,8/S2,3,5,6,7,8	Coagulations						
B4,6,7,8/S2,3,4,5	Walled Cities						
B4,6,7,8/S3,5,6,7,8	Vote4/5/Annl						
B5,6,7,8/S4,5,6,7,8	Majority						

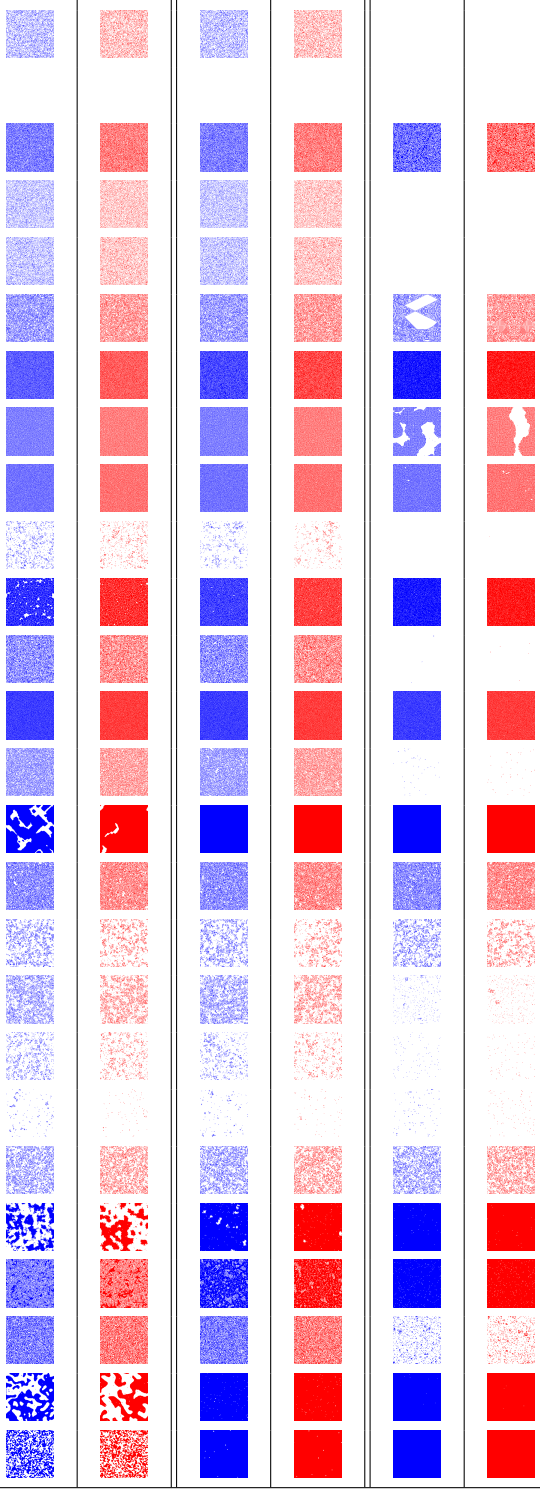

Table 1: 256^2 Automata for different rules at times 128 and 256, for $p = 0.5, 0.3, 0.1$.

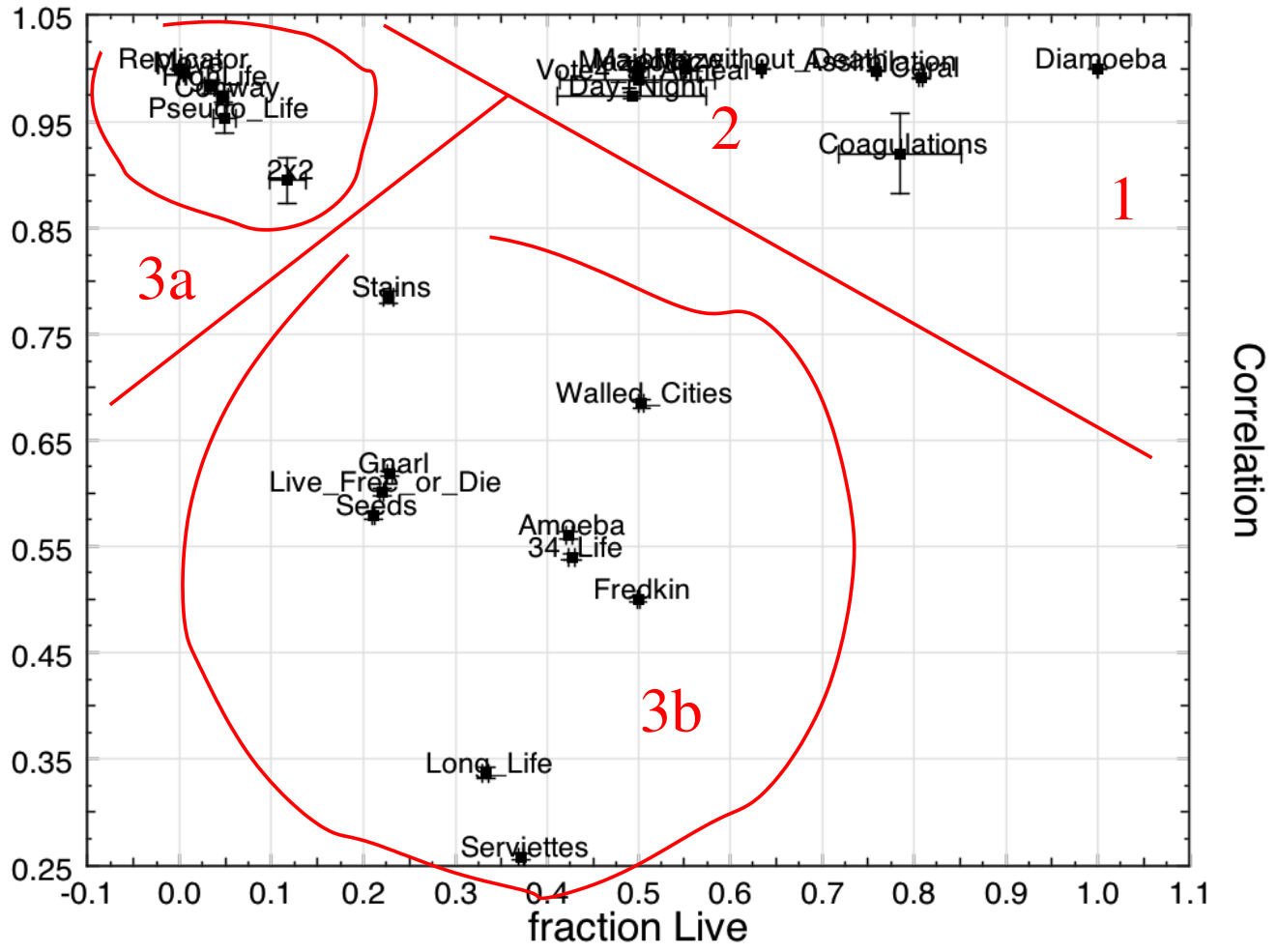

Figure 5: Scatter-plot of fCorr vs fLive, with annotated groupings in red (colour, online).

of the different automata. Models like "coagulation" and "anneal" have the highest fluctuations - due to the slowly but continually varying spatial pattern observed in those automata over the time frame of the measurements.

4 Discussion

One long term goal of this approach is to identify the dynamical growth and equilibria properties of the different automata [10]. To this end it is useful to attempt a grouping of classification based on temporal as well s spatial behaviour. The experimental data gathered indicates that the GoL automata studied fall into one of the following categories:

1. rapidly reach a single saturated state of almost all dead or live with at most minor fluctuations
2. steady growth in a complex structural pattern that then subsequently reaches a saturated state
3. a dynamic equilibrium of structures that fluctuate and gives rise to a permanently changing pattern - these refine into a) those with large scale structures and b) those that only exhibit short scale fluctuations

Table 2 was originally constructed somewhat subjectively after examination of the time sequences of patterns obtained from the 26 automata. The method involved eyeballing the models as movies trying to describe some common words from the observations. Somewhat amazingly, these however do appear to agree with the clusters found upon examination of Figure 5. The category 3a - "dynamic equilibrium with long and multi-scale structures" cluster together at the top left of the scatter plot.

The category 3b - " dynamic equilibrium but with short length scale structures" cluster in a larger area at the lower left. The other two groups are at the top right area with

Category	Game-of-Live Family Examples - Categorised by Subjective Observation
1	Assimilation; Diamoeba; Live w/o Death; Replicator
2	Coagulations; Coral; Day+Night; Majority; Maze; Mazectric; Move; Anneal
3 a	2x2; Conway; Highlife; Pseudo Life
3 b	34-Life; Amoeba; Fredkin; Gnarl; Live Free or Die; Long Life; Seeds; Serviettes; Stains; Walled Cities

Table 2: Categorisation of GoL Automata for $p = 0.5$

some differentiation between fast and slow equilibration at the far right and middle right respectively.

The single exception to this grouping is the "replicator" automata. It exhibits the strange behaviour of remaining in fluctuation for a long time then suddenly saturating to a single dead state, and this may be due to finite size effects of the simulations.

In Figure 4 the monomers and dimer curves are less obvious discriminators by themselves. The category 3a automata do however group closely on the mid or upper shoulder of the monomer and dimer curves, respectively.

Similarly, in Figure 3 the single metric averages do not provide good discriminators individually, although there are obvious groupings of the 3a automata appearing together, and the category 1 also tend to be close together.

We might expect that a caveat of this analysis is that when the system is not sufficiently "thermodynamically large enough" then:

- the pattern might otherwise continue to grow if it did not reach the periodic boundaries
- the particular set of structural patterns that might lead to categories 3a or 3b cannot arise simply by chance on a finite sized system.

Nevertheless the classification clustering pattern from examining the 1-step time correlation function scatter-plotted against the fraction of live cells does seem to give a good combined discriminator and grouping that matches observation.

The fraction of initial live cells can be varied and a variant of figure 5 interpreted. We do not include these due to lack of space, but the effect is that if p is too low many of the automata patterns do not have enough material to form and so they die out with no live cells and 100% correlation forever.

Likewise if p is too large then overcrowding also prevents the complex patterns from forming. The structure shown in Figure 5 is largely stable and unchanged if the stability condition $0.3 < p <= 0.5$ is satisfied.

5 Conclusions

We have shown how a family of Game-of-Life-like Cellular Automata can be formulated in terms of a common and extensible notation and systematically studied. We have shown that some simple metrics help make preliminary attempts to categorise this family of automata into groups.

We have postulated four categories – originally conceived in terms of a mix of temporal and spatial structural observations. These map quite closely to the groupings that emerge from a scatter plot of the long term averaged values of the fraction of live cells and the 1-step time correlation function.

There are interesting features in all the GoL automata studied - this is no doubt why the community (See `http://www.conwaylife.com/wiki`) has troubled to give these models specific names. However, perhaps the "most interesting" ones are those that seem to exhibit the highest degree of complexity and not-coincidentally have been given the names with the word "life" in their names. These category 3a automata stabilise to a dynamic equilibria of a relatively low fraction of live cells, with a high degree of time correlation between their states.

There is scope for further work in examining time-correlations longer than a single time-step and also component sizes larger than dimers. It seems likely that some more discriminating combinations of static and temporal metric can further refine the behaviours observed in category 3b.

In this work we have limited the study to known named automata in the GoL family. There is scope to conduct a more systematic search using the metrics discussed here to look for other category 3a automata. These criteria might also be usefully applied to higher dimensional GoL type models where it is considerably harder to visualise the patterns and behaviours.

References

[1] Adamatzky, A. (ed.): Game of Life Cellular Automata. No. ISBN 978-1-84996-216-2, Springer (2010)
[2] Bays, C.: Candidates for the game of life in three dimen-

sions. Complex Systems 1, 373–400 (1987)
[3] Bays, C.: A new candidate rule for the game of three-dimensional life. Complex Sytems 6, 433–441 (1992)
[4] Bays, C.: A note on the game of life in hexagonal and pentagonal tesellations. Complex Systems 15, 245–252 (2005)
[5] Bays, C.: Game of Life Cellular Automata, chap. The Game of Life in Non-Square Environments, pp. 319–329. Springer (2010)
[6] Binder, P.M.: (anti-) stable points and the dynamics of extended systems. Physics Letters A 187, 167–170 (1994)
[7] Boghosian, B.M., Rothman, D.H., W.Taylor: A Cellular Automata Simulation of Two-Phase Flow on the CM-2 Connection Machine Computer (Mar 1988), private Communication
[8] Capcarrere, M.S.: Evolution of asynchronous cellular automata. In: Parallel Problem Solving from Nature Proc. PPSN VII. vol. 2439 (2002)
[9] Darabos, C., Giacobini, M., Tomassini, M.: Scale-free automata networks are not robust in a collective computational task. In: et al., E.Y.S. (ed.) Proc. Cellular Automata: 5th International Conference on Cellular Automata for Research and Industry. vol. LNCS 4173. Springer (2006)
[10] Eppstein, D.: Game of Life Cellular Automata, chap. Growth and Decay in Life-Like Cellular Automata, pp. 71–98. Springer (2010)
[11] Evans, K.M.: Larger than life: threshold-range scaling of life?s coherent structures. Physica D 183, 45–67 (2003)
[12] Evans, M.S.: Cellular Automata - Brian's Brain (2002), `http://www.msevans.com/automata/briansbrain.html`, department of Neurology, Southern Illinois University School of Medicine
[13] Ganguly, N., Sikdar, B.K., Deutsch, A., Canright, G., Chaudhuri, P.P.: A survey on cellular automata. Tech. rep., Dresden University of Technology (2003)
[14] Gardner, M.: Mathematical Games: The fantastic combinations of John Conway's new solitaire game "Life". Scientific American 223, 120–123 (October 1970)
[15] Hastings, M.B., Reichhardt, C.J.O., Reichhardt, C.: Ratchet cellular automata. Phys. Rev. Lett. 90, 247004 (2003)
[16] Hawick, K.A., Scogings, C.J.: A minimal spatial cellular automata for hierarchical predator-prey simulation of food chains. In: International Conference on Scientific Computing (CSC'10). pp. 75–80. WorldComp, Las Vegas, USA (July 2010), `www.massey.ac.nz/~kahawick/cstn/040`
[17] Hernandez-Montoya, A.R., Coronel-Brizio, H., Rodriguez-Achach, M.: Game of Life Cellular Automata, chap. Macroscopic Spatial Complexity of teh Game of Life Cellular Automaton: A sSimple Data Analysis, pp. 437–450. Springer (2010)
[18] Kaneko, K., Akutsu, Y.: Phase Transitions in two-dimensional stochastic cellular automata. J.Phys.A. Letters 19, 69–75 (1986)
[19] Kunkle, D.R.: Automatic Classification of One-Dimensional Cellular Automata. Master's thesis, Rochester Institute of Technology (2003)
[20] Lynch, J.F.: On the threshold of chaos in random boolean cellular automata. Random Structures & Algorithms 6(2-3), 239–260 (March-May 1995)
[21] Martin, B.: Damage spreading and mu-sensitivity on cellular automata. Ergod. Th. and Dynam. Sys. 27, 545–565 (2007)
[22] Martinez, G., Adamatzky, A., Morita, K., Margenstern, M.: Game of Life Cellular Automata, chap. Computation with Competing patterns in Life-Like Automaton, pp. 547–572. Springer (2010)
[23] Nehaniv, C.L.: Evolution in asynchronous cellular automata. In: Proc ICAL 2003 - Eighth Int. Conf. on Artificial Life. pp. 65–73. MIT Press (2003)
[24] de Oliveira, G.M.B., Siqueira, S.R.C.: Parameter characterization of two-dimensional cellular automata rule space. Physica D: Nonlinear Phenomena 217, 1–6 (2006)
[25] Owens, N., Stepney, S.: Investigations of game of life cellular automata rules on penrose tilings: lifetime and ash statistics. Journal of Cellular Automata 5, 207–225 (2010)
[26] Packard, N., Wolfram, S.: Two-dimensional cellular automata. J. Stat. Phys. 38, 901–946 (1985)
[27] Reiter, C.A.: The game of life on a hyperbolic domain. Comput. & Graphics 21(5), 673–683 (1997)
[28] Sarkar, P.: A brief history of cellular automata. ACM Computing Surveys 32, 80–107 (2000)
[29] Sipper, M., Tomassini, M., Capcarrere, M.S.: Evolving asynchronous and scalable non-uniform cellular automata. In: In Proceedings of International Conference on Artificial Neural Networks and Genetic Algorithms (ICANNGA97. pp. 67–71. Springer-Verlag (1997)
[30] Suzudo, T.: Spatial pattern formation in asynchronous cellular automata with mass conservation. Physica A: Stat. Mech. and Applications 343, 185–200 (November 2004)
[31] Wolfram, S.: Statistical Mechanics of Cellular Automata. Rev.Mod.Phys 55(3), 601–644 (1983)
[32] Wolfram, S.: Universality and complexity in cellular automata. Physica D 10, 1–35 (1985)
[33] Wolfram, S.: Cellular Automata as models of complexity. Nature 311, 419–424 (Oct 1984)
[34] Wolfram, S.: Complex systems theory. Tech. rep., Institute for Advanced Study, Princton, NJ 08540 (6-7 October 1984 1985), presented at Santa Fe Workshop on "A response to the challenge of emerging synthesis in science"
[35] Wolfram, S.: Twenty problems in the theory of cellular automata. Physica Scripta T9, 170–183 (1985)
[36] Wolfram, S.: Theory and Applications of Cellular Automata. World Scientific (1986)
[37] Wylie, B.J.: Application of Two-Dimensional Cellular Automaton Lattice-Gas Models to the Simulation of Hydrodynamics. Ph.D. thesis, Physics Department, Edinburgh University (1990)
[38] Yey, W.C., Lin, Y.C., Chung, Y.Y.: Performance analysis of cellular automata monte carlo simulation for estimating network reliability. Expert Systems with Applications 36(5), 3537–3544 (2009)

Asynchronous SN P systems for logical and arithmetic operations

Ryoma Hamabe and Akihiro Fujiwara
Graduate School of Computer Science and Systems Engineering, Kyushu Institute of Technology
Iizuka, Fukuoka, 820-8502, Japan

Abstract— *In the present pater, we consider the asynchronous parallelism on the SN P system, which is a representative of natural computing, and propose asynchronous SN P systems that perform logical and arithmetic operations.*

We first propose SN P systems that compute logical operations, which are NOT, OR, AND and EX-OR. The SN P systems work in $O(1)$ sequential and parallel steps using $O(1)$ neurons. We next propose a SN P system that computes addition of k binary numbers of m bits. The SN P system works in $O(km)$ sequential steps or $O(m)$ parallel steps using $O(m)$ neurons. Finally, we propose a SN P system that computes multiplication of two binary numbers of m bits, and show that the SN P system works in $O(m^2)$ sequential steps or $O(m)$ parallel steps using $O(m^2)$ neurons.

Keywords: asynchronous SN P system, logical and arithmetic operations

1. Introduction

The Spiking neural P system [3] (in short, SN P system) is a representative of natural computing, and is a computing device such that neurons communicate using electrical impulses (a.k.a. spikes). The SN P system is proved to be able to simulate Turing machines [2], [3], and the fact means the computation model has enough computational power.

The SN P system consists of a set of neurons and synapses that connect two neurons. The contents of each neuron consist of a number of copies of a single object type, called the *spike*. In addition, *firing rules* are assigned to each neuron, and the firing rules allow a neuron to send spikes to other neurons as messages. The application of the rules depends on the contents of the neuron; in the general case, applicability is determined by checking the contents of the neuron against a regular set associated with the rule.

Several SN P systems have been proposed for numerical NP problems [4], [5], [6], [7]. For example, Leporati et al. [1] proposed four SN P systems for the following arithmetic operations: addition, multiple addition, comparison, and multiplication with a fixed factor. All numbers given as inputs to the systems are expressed in encoded binary form using a spike train, in which the presence of a spike denotes 1, and the absence of a spike denotes 0. The outputs of the computation are also expressed in the same form, and are sent out to the environment. All of the four SN P systems work in $O(m)$ steps for binary numbers of m bits, because the systems output the result sequentially.

However, synchronous application of firing rules is assumed on the above SN P systems. The synchronous application means that all applicable firing rules in all neurons are applied synchronously.

On the other hand, there is obvious asynchronous parallelism on the biological background of neurons that send electrical impulses along axons to other neurons. The asynchronous parallelism means that all neurons may independently react on firing rules with different timing. Since all neurons basically works in asynchronous manner, the asynchronous parallelism must be considered to make SN P system more realistic computational model.

In the present paper, we propose SN P systems with fully asynchronous parallelism. The fully asynchronous parallelism means that any number of applicable firing rules may be applied in one steps on the SN P system. As complexity of the asynchronous SN P system, we consider two kinds of numbers, which are a number of sequential steps and a number of parallel steps. The number of sequential steps is a number of executed steps in case that firing rules are applied sequentially, and the number of parallel steps is a number of executed steps with synchronous application of firing rules.

Using the fully asynchronous parallelism, We propose SN P systems for logical and arithmetic operations. We first propose SN P systems that compute logical operations, which are NOT, 2-input logical operation, and k-input logical operation. We show all SN P systems for the logical operations work in $O(1)$ sequential and parallel steps using $O(1)$ neurons.

We next propose two asynchronous SN P systems that compute addition. The first SN P system computes addition for two binary numbers of m bits, and the second SN P system computes addition for k binary numbers of m bits. We show that both SN P systems work in $O(m)$ sequential and parallel steps using $O(m)$ neurons.

Finally, we propose a SN P system for multiplication of two binary numbers of m bits. The SN P system contains sub-systems that compute logical AND operation and addition for k binary numbers, which are given above. We show that the SN P system works in $O(m^2)$ sequential steps or $O(m)$ parallel steps using $O(m^2)$ neurons.

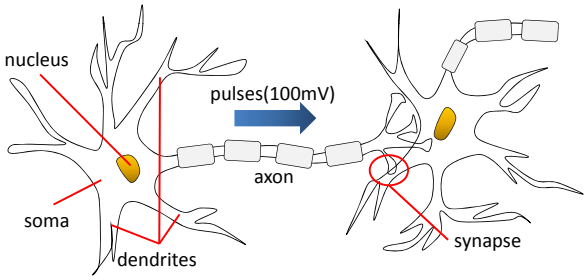

Figure 1: An example of neural circuits.

2. Preliminaries

2.1 Neural cells and spikes

We first describe neural cells and spikes, which are conceptual bases of the SN P system. The neural cells communicate by transmitting electric pulses between cells. The pulse is usually called a *spike*, or *action potential*.

Figure 1 shows an example such that a neural action potential is given altogether with the main parts of a neuron – the cell itself (soma), the axon, the dendrites.

The neuronal signals consist of short electrical pulses, and the signals are propagated along the axon. The contact of the axon of a neuron with the dendrites of another neuron is called a *synapse*. When an action potential arrives at a synapse, the arrival triggers an electrical response in a received neuron.

2.2 Standard SN P systems

Using the concept of the above neurons, spiking neural P systems (SN P systems, in short) were proposed in [3]. The basic idea of the SN P system is based on a concept of *cells* related by *synapses* and behavior according to the *states*.

Formally, a spiking neural P system is defined as follows.

$$\Pi = (O, \sigma_1, \sigma_2, \cdots, \sigma_m, syn, in, out)$$

- $O = \{a\}$ is the singleton alphabet (a is called *spike*).
- $\sigma_1, \sigma_2, \cdots, \sigma_m$ are neurons such that,

$$\sigma_i = (n_i, R_i), 1 \leq i \leq m$$

  - n_i (≥ 0) is an initial number of *spikes* contained in the neuron σ_i.
  - R_i is a finite set of *rules* of the following two forms:

    (1) $E/a^c \rightarrow a; d$
    E is a regular expression over a, and $c \geq 1$, $d \geq 0$ are integer numbers; if $E = a^c$, then it is usually written in the following simplified form: $a^c \rightarrow a; d$.

    (2) $a^s \rightarrow \lambda$
    $s \geq 1$ is an integer, and $a^s \notin L(E)$, where $L(E)$ denotes the regular language defined by E, and E is a regular expression defined in (1) in the same neuron.

- $syn \subseteq \{1, 2, \cdots, m\} \times \{1, 2, \cdots, m\}$, with $(i,i) \notin syn$ for $1 \leq i \leq m$. (The syn denotes synapses between neurons.)
- $in, out \in \{1, 2, \cdots, m\}$ indicate the *input* and *output* neurons of Π.

The rules of type (1) are called *firing rules*, and the rules are applied as follows. If neuron σ_i contains $k \geq c$ spikes, and $a^k \in L(E)$, then the rule can be applied. The execution of the rule removes c spikes from neuron σ_i (thus leaving $k - c$ spikes), and prepares one spike to be delivered to all neurons σ_j such that $(i, j) \in syn$. In case of $d = 0$, the spike is immediately emitted, otherwise the spike is emitted after d computation steps of the system. (As usually happens in membrane computing, a global clock is assumed, marking the time for the whole system, hence the functioning of the system is synchronized.) If the rule is used in step t and $d \geq 1$, then the neuron is *closed* in steps $t, t+1, t+2, \cdots, t+d-1$. The closed neuron cannot fire according to the rule, and cannot receive any spike. (All spikes that are sent to the closed neuron are lost.) In step $t + d$, the neuron becomes open, so that the neuron can receive spikes and select rules to be fired.

Rules of type (2) are called *forgetting rules*, and are applied as follows. In case that neuron σ_i contains exactly s spikes, the rule is applied, and all s spikes are removed from the neuron σ_i. Note that, by definition, if a firing rule is applicable to the neuron, no forgetting rule is applicable in the neuron.

In each time unit in computation on the SN P system, if at least one of the rules are applicable in a neuron σ_i, then a rule in R_i must be applied. Since two firing rules, $E_1 : a^{c_1} \rightarrow a; d_1$ and $E_2 : a^{c_2} \rightarrow a; d_2$, may be $L(E_1) \cup L(E_2) \neq \phi$, it is possible that two or more rules can be applied in a neuron. In such a case, only one of the rules is chosen non-deterministically.

The initial configuration of the system is described by the numbers $n_1, n_2, \cdots, n_m$ of spikes in neurons, with all neurons being open. During the computation, a configuration is defined by the numbers of spikes in neurons and states of the neurons, which can be expressed as the number of steps to count down until it becomes open. (The number is zero if the neuron is open). A *computation* in a SN P system starts in the initial configuration. In each step of computation, all spikes and neurons can be transformed in parallel according to applicable rules. If no rule is applicable for all neurons, the system ceases computation.

We now show an example of the standard SN P system in Figure 2. The SN P system in Figure 2 is given below.

$$\Pi = (O, \sigma_1, \sigma_2, syn, 2)$$

- $O = \{a\}$

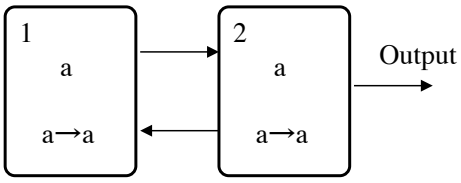

Figure 2: An example of a standard SN P system.

- $\sigma_1 = (1, \{a \to a\})$
- $\sigma_2 = (1, \{a \to a\})$
- $syn = \{(1,2), (2,1)\}$

The example has two neurons, σ_1 and σ_2; neuron σ_2 is the output neuron. Both neurons have one rule. In the first step, neuron σ_1 and neuron σ_2 send one spike to each neurons, and neuron σ_2 sends one spike to the environment. In the next step, the same rule is applied in both neurons as step 1. Therefore, the SN P system outputs a spike forever in synchronous manner.

2.3 Asynchronous SN P systems

In this section, we explain the difference between a standard SN P system and an asynchronous SN P system, which is considered in the present paper.

On the standard SN P system, all of the rules are applied in a non-deterministic maximally parallel manner (synchronous manner). In one step of the standard SN P system, one of applicable rules is applied in each neuron. (In case there are several possibilities, one of the applicable rules is non-deterministically chosen.) All neurons, for which no rule is applicable, remain unchanged to the next step. In other words, all applicable rules are applied in parallel in each step of computation.

On the other hand, we assume that rules are applied in fully asynchronous manner in the asynchronous SN P system, and any number of applicable rules is applied in each step of computation. In other words, the asynchronous SN P system can be executed sequentially, and also can be executed in maximal parallel manner.

Note that delay d and states of neurons, which are defined in a standard SN P system, cannot be defined in the asynchronous SN P system, because global clock cannot be assumed in the asynchronous computation. Therefore, each firing rule forms $E/a^c \to a$ in the asynchronous SN P system.

We consider an execution in case that SN P system Π in Figure 2 is executed in asynchronous manner. There are applicable firing rules in neuron σ_1 and neuron σ_2 in the initial state of the system. If these rules are applied in parallel, the system Π output a spike forever. However, if a firing rule is applied in one of neurons, the system stops computation because the other neuron contains two spikes and no rule can be applied in the system. The example implies that the asynchronous SN P system performs several computations.

We now describe complexity of the asynchronous SN P system. We consider two kinds of complexities on the asynchronous SN P system, which are *the number of sequential steps* and *the number of parallel steps*. The number of sequential steps is the number of executed steps in case that the SN P system is executed sequentially. Since various sequential executions can be considered on the asynchronous SN P system, we define that the worst number of sequentially executed steps is the number of sequential steps. On the other hand, The number of parallel steps is defined to be the number of executed steps in case that the SN P system is executed in maximal parallel manner.

3. Logical operation

In this section, we propose asynchronous SN P systems that compute logical operations. We first describe the input and output of the logical operations. Then, we next propose the asynchronous SN P systems that compute NOT, 2-input logical operations, and k-input logical operations. We finally show complexity of the proposed SN P systems.

3.1 Input and output

Boolean values, 0 and 1, are inputs and outputs of the logical function. We assume that the two values, 0 and 1, are denoted by spikes a and a^{k+1}, where k is a constant that is equal to the number of Boolean inputs of the logical operation. (In case of 2-input logical function, a^3 denotes Boolean value 1.)

3.2 NOT

The asynchronous SN P system that executes NOT is given as follows.

$$\Pi_{NOT} = (\{a\}, \sigma_1, \sigma_2, syn, 2)$$

- $\sigma_1 = (k+1, \{a^{k+2} \to a^{k+1}, a^{2(k+1)}/a^{2k+1} \to a\})$
- $\sigma_2 = (0, \{a \to a, a^{k+1} \to a^{k+1}\})$
- $syn = \{(1,2), (2,1)\}$

Figure 3 illustrates the SN P system Π_{NOT} for $k = 1$. First, an instance, a or a^2, is inputted in neuron σ_1. In case that the instance is 0, a firing rule $a^3 \to a^2$ is applied, and spike a^2 is sent to neuron σ_2. Since a firing rules $a^2 \to a^2$ is applied in neuron σ_2, a^2 is sent out as output. On the other hand, in case that the instance is 1, a firing rule $a^4/a^3 \to a^2$ is applied in neuron σ_1, spike a is sent to neuron σ_2, and spike a is sent out from neuron σ_2 as output. In both cases, spike a^2 is re-stored in neuron σ_1 for another computation.

3.3 2-input logical operations

In case of 2-input logical operations, two inputs are given in parallel to the SN P system. Since we assume that 0 and 1 are denoted a and a^{k+1} in the SN P system, instances 00,

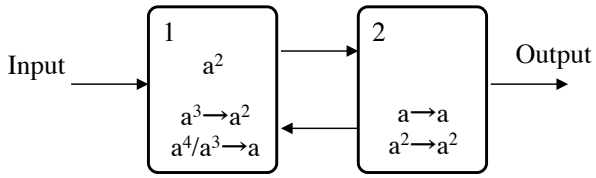

Figure 3: The asynchronous SN P system that executes NOT.

Table 1: A truth table for 2- input logical operation.

	instance	OR	AND	EX-OR
α	$00 = a^2$	$0 = a$	$0 = a$	$0 = a$
β	$01(10) = a^{k+2}$	$1 = a^{k+1}$	$0 = a$	$1 = a^{k+1}$
γ	$11 = a^{2(k+1)}$	$1 = a^{k+1}$	$1 = a^{k+1}$	$0 = a$

01, 10, and 11 are denoted using spikes a^2, a^{k+2}, a^{k+2} and $a^{2(k+1)}$, respectively. Then, we can define appropriate output values for the above spikes. Table 1 shows an example of output patterns for the inputs.

We must assume that one of the inputs is given to the SN P system because the SN P system is asynchronous. In such case, spikes in the system is a or a^{k+1}, and no firing rule can be applied. Then, we can distinguish the number of values given to the system.

The asynchronous SN P system $\Pi_{2\text{-}LO}$ that compute 2-input logical operation is given as follows. (α, β, and γ are Boolean values in Table 1.)

$$\Pi_{2\text{-}LO} = (\{a\}, \sigma_1, syn, 1)$$

- $\sigma_1 = (0, \{a^2 \rightarrow \alpha, a^{k+2} \rightarrow \beta, a^{2(k+1)} \rightarrow \gamma\})$
- $syn = \phi$

Figure 4 illustrates the SN P system $\Pi_{2\text{-}LO}$.

3.4 k-input logical operation

In this section, we propose the SN P system that computes k-input logical operation. Since the proposed SN P system is asynchronous, we must assume that some of the inputs are given to the SN P system. We first describe how to distinguish the number of given inputs using the number of spikes in the neuron.

Let $N(\sigma_i)$ be the number of spikes in neuron σ_i. Since the Boolean values, 0 and 1, are denoted using a and a^{k+1} for the k-input operation, $N(\sigma_i)$ satisfies the following condition in case that j_1 and j_2 are the numbers of 0 and 1 that are given to the neuron.

$$\begin{aligned} N(\sigma_i) &= j_1 + (k+1)j_2 \\ &= kj_2 + (j_1 + j_2) \end{aligned}$$

We now consider the above condition in two cases. If all inputs are given to σ_i, i.e. $j_1 + j_2 = k$, $N(\sigma_i)$ is a multiple of k. On the other hand, $N(\sigma_i)$ is not a multiple of k in case that some of input values are not given to the neuron because $j_1 + j_2 < k$.

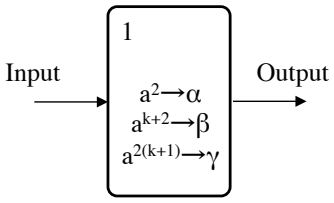

Figure 4: The asynchronous SN P system that executes 2-input logical operation.

Table 2: A truth table for k-input logical operation ($k = 4$).

	instance	OR	AND	EX-OR
α_0	a^4	$0 = a$	$0 = a$	$0 = a$
α_1	a^8	$1 = a^3$	$0 = a$	$1 = a^3$
α_2	a^{12}	$1 = a^3$	$0 = a$	$0 = a$
α_3	a^{16}	$1 = a^3$	$0 = a$	$1 = a^3$
α_4	a^{20}	$1 = a^3$	$1 = a^3$	$0 = a$

Therefore, we can distinguish the number of given inputs by the above condition, i.e, the number of spikes is a multiple of k if and only if all k input values are given to the neuron. Using the condition, we can proposed the asynchronous SN P system $\Pi_{k\text{-}LO}$ using firing rules defined only for cases that the number of spikes is a multiple of k.

$$\Pi_{k\text{-}LO} = (\{a\}, \sigma_1, syn, 1)$$

- $\sigma_1 = (0, \{a^{k(j+1)} \rightarrow \alpha_j \mid 0 \leq j \leq k\})$
- $syn = \phi$

Figure 5 illustrates the SN P system $\Pi_{k\text{-}LO}$, and Table 2 shows examples of the above α_j for k-input OR, AND, and EX-OR for $k = 4$.

3.5 Complexity

We consider complexity of proposed SN P systems Π_{NOT}, $\Pi_{2\text{-}LO}$, and , $\Pi_{k\text{-}LO}$. All of the SN P systems consist of 1 neuron, and work in 1 step if all input values are given to the system. Therefore, we obtain the following theorem.

Thorem 1: The asynchronous SN P systems, Π_{NOT}, $\Pi_{2\text{-}LO}$, and, $\Pi_{k\text{-}LO}$, work in $O(1)$ sequential and parallel steps using $O(1)$ neurons. □

4. Addition

In this section, we propose asynchronous SN P systems for addition. We first propose a SN P system that computes addition of two binary numbers of m bits. We next propose a SN P system that computes addition of k binary numbers of m bits.

4.1 Addition of two binary numbers

An idea of the SN P system for addition of two binary numbers is based on a logic circuit for addition. As described in Section III, we assume that the two Boolean values, 0 and 1, are denoted by spikes a and a^{k+1}.

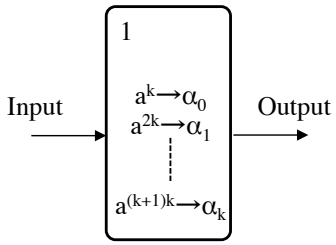

Figure 5: Asynchronous SN P system that executes k-input logical operation.

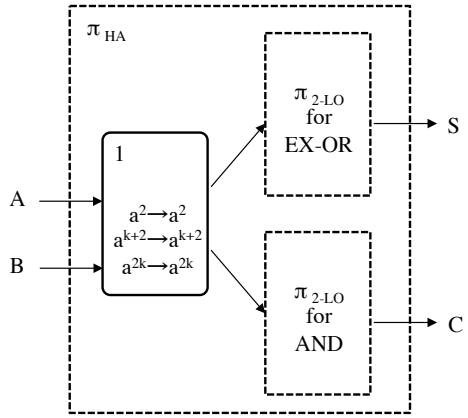

Figure 6: A SN P system Π_{HA} for the half adder.

We first introduce a half adder (HA), and propose a SN P system whose input and output is the same as the half adder. The half adder is a logic circuit that adds two Boolean values, A and B, and output two Boolean values, S and C such that the sum of A and B is $2C + S$. In other words, S and C are defined as $S = A \oplus B$ and $C = A \wedge B$. Since we can compute the logical operations using SN P systems described in Section III, we obtain an asynchronous SN P system Π_{HA}, which is illustrated in Figure 6, for the half adder.

We next introduce a full adder (FA), and propose a SN P system for the full adder. The full adder is a logic circuit that adds three Boolean values, A, B and C_{in}, and output two Boolean values, S and C_{out} such that the sum of A, B and C_{in} is $2C_{out} + S$. Since it is well known that the full adder can be constructed from two half adder and one OR gate, we can obtain an asynchronous SN P system Π_{FA}, which is illustrated in Figure 7, for the full adder.

Using the SN P system for the full adder, we can construct a SN P system for addition of two binary numbers of m bits. We assume that input of the addition is a pair of two binary numbers $A_0, A_1, \cdots, A_{m-1}$ and $B_0, B_1, \cdots, B_{m-1}$ that represent two numbers A and B such that $A = \sum_{j=0}^{m-1} A_j * 2^j$ and $B = \sum_{j=0}^{m-1} B_j * 2^j$, and also assume that a binary number $S_0, S_1, \cdots S_m$ denote a sum of A and B. Then, we obtain a SN P system $\Pi_{2\text{-}ADD}$, which computes

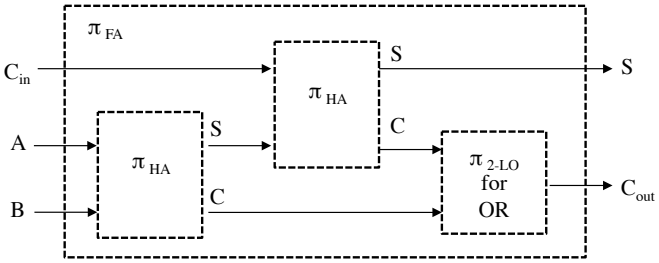

Figure 7: A SN P system Π_{FA} for the full adder.

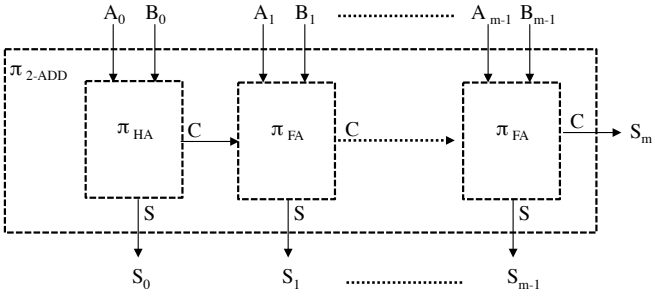

Figure 8: A SN P system for addition of two binary numbers.

addition of two binary numbers of m bits, in Figure 8.

Finally, we consider complexity of the proposed SN P systems. Since complexity of Π_{HA} or Π_{FA} is $O(1)$ parallel and sequential steps, we obtain the following theorem for Π_{ADD}.

Thorem 2: The asynchronous SN P system $\Pi_{2\text{-}ADD}$ works in $O(m)$ sequential and parallel steps using $O(m)$ neurons. □

4.2 Addition for k binary numbers

In this section, we propose an asynchronous SN P system that computes addition for k binary numbers for $k > 2$. Although we can easily obtain the SN P system that computes the addition using the SN P system proposed in the previous section, the SN P system needs $O(m^2)$ neurons and $O(km)$ parallel and sequential steps. In the following, we propose the SN P system that works in $O(m)$ sequential and parallel steps using $O(m)$ neurons.

We first consider input and output for the addition. We assume that the input of the addition is k binary numbers, $X_0, X_1, \cdots, X_{k-1}$, such that $X_i == \sum_{j=0}^{m-1} X_{i,j} * 2^j$ for m Boolean values, $X_{i,0}, X_{i,1}, \cdot X_{i,m-1}$. The output of the addition is a binary number $S_0, S_1, \cdots S_m$, which denote a sum of the binary numbers. (We assume the sum dose not overflow in $m+1$-th bit to simplify the description.)

We next proposed a multi-input full adder (MFA), which computes a sum and a carry for k inputs. The input and output of MFA are defined as follows.

Input: k Boolean values, $X_{0,j}, X_{1,j}, \cdots, X_{k-1,j}$, and an integer C_{in} such that $C_{in} \leq k$.

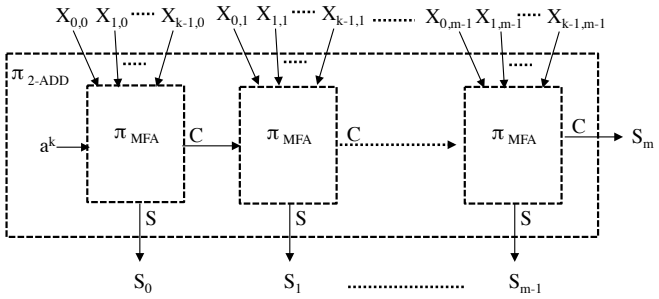

Figure 9: A SN P system for addition of k binary numbers.

Output: A sum S and a carry C_{out}, which are defined as follows. (S is a Boolean value, and C_{out} is an integer.)

$$S = \begin{cases} 0 & (\text{If } C_{in} + \sum_{i=0}^{k-1} X_{i,j} \text{ is even}) \\ 1 & (\text{Otherwise}) \end{cases}$$

$$C = \left\lfloor \frac{C_{in} + \sum_{i=0}^{k-1} X_{i,j}}{2} \right\rfloor$$

Since 0 and 1 are denoted by spikes a or a^{k+1} in the SN P systems, we assume that an integer c is denoted by a spike $a^{c(k+1)+(k-c)}$, which means $(k-c)$ 0s and c 1s. (As we discussed in Section III, the spikes are distinct for $0 \le c \le k$.)

If we obtain Π_{MFA}, which is a SN P system for the multi-input full adder, $\Pi_{k\text{-}ADD}$, which is a SN P system for addition of k binary numbers of m bits, can be easily constructed as shown in Figure 9.

We now describe details of a SN P system Π_{MFA}, which is illustrated in Figure 10. In Figure 10, σ_{CP} is a neuron that copies input spikes and output the spikes to two other neurons. One of the copied spikes are sent to $\Pi_{k\text{-}LO}$ for EX-OR, and then, the output is sent to $P_{2\text{-}LO}$, which are SN P systems described in Section III. EX-OR of the input values is computed in the SN P systems, and the result of EX-OR is outputted as S.

The other copied spikes are sent to a neuron CP_{-1}, in which the number of spikes is decremented by one for barrier synchronization in the next neuron σ_{CC}. Then, the number of spikes are halved in σ_{CC}, and the spikes are outputted as C_{out}.

Finally, we consider complexity of the proposed SN P system $\Pi_{k\text{-}ADD}$. Since Π_{MFA} works $O(1)$ parallel and sequential steps, we obtain the following theorem for $\Pi_{k\text{-}ADD}$.

Thorem 3: Asynchronous SN P system $\Pi_{k\text{-}ADD}$ works in $O(m)$ sequential and parallel steps using $O(m)$ neurons. □

5. Multiplication

In this section, we propose an asynchronous SN P system that computes multiplication of two binary numbers of m bits. We assume that input for the multiplication is the same as input for the addition of two binary numbers A and B, which are $A_0, A_1, \cdots, A_{m-1}$ and $B_0, B_1, \cdots, B_{m-1}$ such that $A = \sum_{i=0}^{m-1} A_i * 2^i$ and $B = \sum_{j=0}^{m-1} B_j * 2^j$, and also assume a binary number $P_0, P_1, \cdots P_{2m-1}$ is an output binary number of the multiplication $A \times B$. The two Boolean values, 0 and 1, are denoted by spikes a and a^{k+1} such that $k \ge m$, respectively.

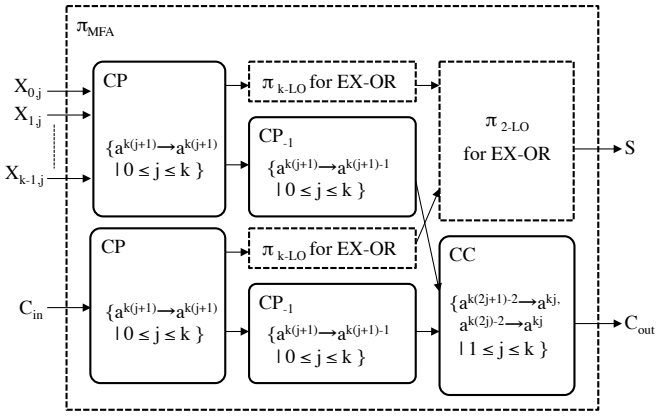

Figure 10: A SN P system for the multi-input full adder

$$\begin{array}{rr} & A_2A_1A_0 \\ \times) & B_2B_1B_0 \\ \hline 0 & 0\ A_2B_0\ A_1B_0\ A_0B_0 \\ 0 & A_2B_1\ A_1B_1\ A_0B_1\ 0 \\ +) & A_2B_2\ A_1B_2\ A_0B_2\ 0\ 0 \\ \hline & P_4\ P_3\ P_2\ P_1\ P_0 \end{array}$$

Figure 11: An example of the multiplication of the binary numbers for $m = 3$.

We now explain an outline of the proposed SN P system for the multiplication. (Due to space limitation, we omit details of the SN P system.) The SN P system computes the multiplication using the following 2 steps.

Step 1: Compute AND operation between $A_0, A_1, \cdots, A_{m-1}$ and each bit B_j for $0 \le j \le m-1$, then store the result in $X_{j,0}, X_{j,1}, \cdots, X_{j,2m-2}$ as a j-bit left-shifted binary number.

Step 2: Compute addition of $X_0, X_1, \cdots, X_{m-1}$, which are the results of Step 1, using the SN P system $\Pi_{k\text{-}ADD}$, which is described in Section III.

Figure 11 illustrates an idea of the multiplication in case of $m = 3$. The A_iB_j $(0 \le i \le 2, 0 \le j \le 2)$ represent the result of $A_i \wedge B_j$, and 0s are added to the value for j-bit shift. Then, the system executes addition of the values, and we obtain the the multiplication of A and B.

We now show a SN P system Π_{MUL} for the multiplication in Figure 12. A SN P system Π_{MUL} contains a set of

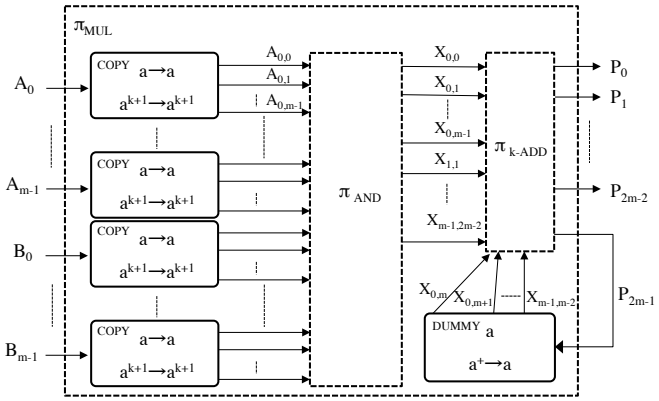

Figure 12: An SN P system Π_{MUL}

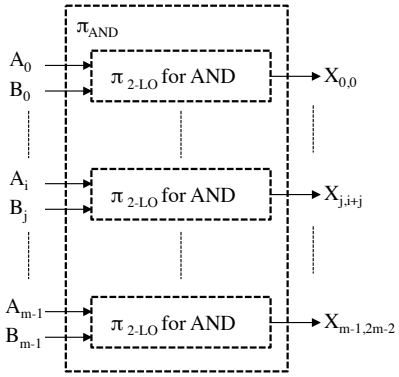

Figure 13: An SN P system Π_{AND}

membranes σ_{COPY}, Π_{AND}, $\Pi_{k\text{-}ADD}$, and a membrane σ_{DUMMY} as sub-systems. We explain each of the sub-systems in the following.

- σ_{COPY} is a membrane that copies each input value, and output m copies of the input value to Π_{AND}.
- Π_{AND} is a SN P system that consists of m^2 sub-systems, $\Pi_{2\text{-}LO}$. Each $\Pi_{2\text{-}LO}$ executes AND operation of A_i and B_j, and outputs the result to $\Pi_{k\text{-}ADD}$ as $X_{j,i+j}$. Figure 13 illustrates the SN P system Π_{AND}.
- σ_{DUMMY} is a membrane that send a dummy value 0 to $\Pi_{k\text{-}ADD}$. The dummy values is used for creating left-shifted values.
- $\Pi_{k\text{-}ADD}$ is a SN P system that executes addition for $X_0, X_1, \cdots, X_{m-1}$. As output of the system, we obtain $P_0, P_1, \cdots, P_{2m-2}$, which is the multiplication of A and B.

Finally, we consider complexity of proposed SN P system Π_{MUL}. Since Π_{AND} works in $O(m^2)$ sequential steps and $O(m)$ parallel steps in Π_{MUL}, we obtain the following theorem for Π_{MUL}.

Thorem 4: The asynchronous SN P system Π_{MUL} works in $O(m^2)$ sequential steps or $O(m)$ parallel steps using $O(m^2)$ neurons. □

6. Conclusion and Future Work

In the present paper, we have proposed asynchronous SN P systems that compute logical operations, addition and multiplication. We first proposed the SN P systems for logical operations works in $O(1)$ sequential and parallel steps using $O(1)$ neurons. We next proposed two SN P systems that computes addition of binary numbers of m bits, and show that the SN P systems work in $O(m)$ sequential and parallel steps using $O(m)$ neurons. We finally proposed a SN P system for multiplication of two binary numbers of m bits, and show that the SN P system works in $O(m)$ parallel steps or $O(m^2)$ sequential steps using $O(m^2)$ neurons.

In the future research, we will propose another asynchronous SN P systems that deal with computationally hard numerical problems, such as the subset sum problem or the knapsack problem.

References

[1] M. A. Gutiérrez-Naranjo and A. Leporati. First steps towards a CPU made of spiking neural P systems. *International Journal of Computers, Communications and Control*, IV:244–252, 2009.

[2] M. Ionescu, Gh. Păun, M. Cavaliere, O. H. Ibarra, O. Egecioglu, and S. Woodworth. Asynchronous spiking neural P systems. *Theoretical Computer Science, vol.410,No. 24-25*, pages 2352–2364, 2009.

[3] M. Ionescu, Gh. Păun, and T. Yokomori. Spiking neural P systems. *Fundamenta Informaticae*, 71:279–308, 2006.

[4] T.O. Ishdorj, A. Leporati, L. Pan, and J. Wang. Solving NP-Complete Problems by Spiking Neural P Systems with Budding Rules. *Workshop on Membrane Computing,(LNCS5957)*, pages 335–353, 2010.

[5] T.O. Ishdorj, A. Leporati, L. Pan, X. Zeng, and X. Zhang. Deterministic solutions to QSAT and Q3SAT by spiking neural P systems with pre-computed resources. *Theoretical Computer Science*, 411(25):2345–2358, 2010.

[6] A. Leporati, G. Mauri, C. Zandron, G. Păun, and M.J. Pérez-Jiménez. Uniform solutions to sat and subset sum by spiking neural p systems. *Natural Computing*, 8(4):681–702, 2009.

[7] A. Leporati, C. Zandron, C. Ferretti, and G. Mauri. Solving numerical NP-complete problems with spiking neural P systems. *Membrane Computing, International Workshop, WMC8, Selected and Invited Papers, LNCS 4860*, pages 336–352, 2007.

Cell Decomposition Algorithm Using Pseudo Triangulation

Ali Nourollah[1,2], Saeed Bazzaz[2], and Mohammad Reza Meybodi[2,3]
[1]Electrical and Computer Engineering Department,
Shahid Rajaee Teacher Training University, Tehran, Iran
[2] Electrical and Computer Engineering Department,
Qazvin Islamic Azad University, Qazvin, Iran
[3] Computer Engineering and Information Technology Department,
Amirkabir University of Technology, Tehran, Iran

Abstract - *This article reviews cell decomposition as a method of motion planning. To analyse test case algorithm, use a polygon with some holes as routing space and contain of some obstacles. In order the original polygon triangulation or pseudo-triangulation, use the sweep-line algorithm to divide the original polygon into multiple polygons without holes. Then each monotone polygons triangulates and using triangles center and the edges center, roadmap graph will be constructed.*
Origin and destination points is located within a separate triangle. Routing from origin triangle to destination triangle using Dijkstra algorithm will be done and the shortest path can be obtained without collision with obstacles. The new innovative algorithm pseudo triangulates the Monotone polygons instead of triangulation and center of the pseudo triangles are obtained with this method. Pseudo-triangulation makes shorter path from origin to destination. The sweep line algorithm order is O(nlogn) and the pseudo triangulation algorithm order is O(nlogn).

Keywords: Cell decomposition, Pseudo triangle, Sweep-line, Monotone polygon, Motion planning

1 Introduction

One of the major challenges in controlling the robot is motion planning. Motion planning problem is used to run the software in various environments, designing surgeon robotic arm, mapping unknown environments, controlling the variable environments and designing structure of the chemical material [2].

Motion planning algorithms include methods based on Sampling and Combinatorial. Methods based on sampling do the routing with getting a new random point from the movement environment at each stage. All combinatorial motion planning methods, jointly build a Roadmap [5]. Path is a graph which is located within the routing environment and crosses between obstacles. It can search the shortest path from origin to destination.

Cell decomposition is one of the combinatorial motion planning methods. Cell decomposition using different methods such as the trapezoidal, vertical, cylindrical, rectangular, polytopal, and triangular divides polygon including obstacles to number of cells [5, 7]. In this research using triangulation and pseudo triangulation methods, cell decomposition can be studied.

In section 2 will be familiar with the concepts of cell decomposition. In section 3, using the sweep line algorithm, original polygon divides into multiple monotone polygons. In section 4 with the help of triangulation and pseudo triangulation algorithms, each monotone polygon divides into number of cells. Also in section 5 roadmap graph is created using pseudo triangles and triangles, weighted graph search algorithm will search the roadmap to find the shortest path from origin to destination. In section 6 cell decomposition using triangulation and pseudo triangulation methods are compared and the research results are described.

2 Cell decomposition

Combinatorial motion planning methods search paths using continuous configuration space and unlike sampling methods don't use approximate methods. In fact, these methods use an exact algorithm. These methods are in contrary motion planning methods based on sampling.

Combinatorial method algorithm is Perfect, This means that finds the answer to the problem or correctly reports that there is no answer. In some cases the sampling algorithms are unable to determine whether problem has answer or not. Also in cell decomposition methods, algorithms can be found that solve the problem in time *O(n)*, but the probability that they can be implemented is very low. Consequently, all combinatorial method issues cannot be implemented.

2.1 Polygonal obstacles

In this method, we assume that robots are point and if robots were not point, Minkowski Difference should be calculated for them. In Fig. 1, you can see the two obstacles within the routing space. In fact we have a polygon with two holes. If there's a hole in the obstacle, be ignored.

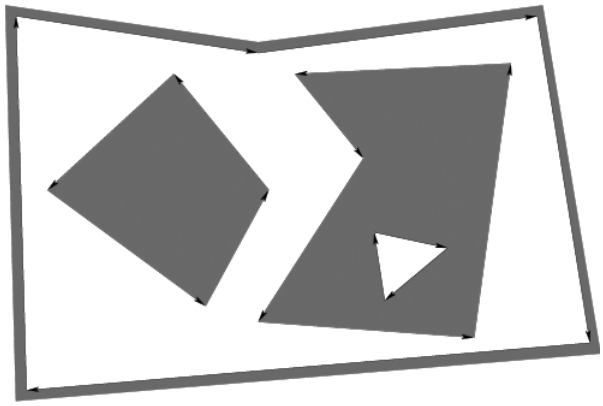

Fig. 1. Polygon with holes

The cell decomposition method includes three types of data structure: The first type is *Vertices*, Each vertex *v* contains a pointer to the point *(x, y)* $\in C = R2$ and contains another pointer to some half-edge that their source is *v*. The second type is *Area*; each area has some pointers to surrounding half-edges that they are on area borders. If the edge is out of the last border point, the pointer value is *null*. Area includes a list of pointers for each component (hole) that located within area.

The third type is *Edge*, edges are directed, usually as a circular chain are around an area. Each edge is stored as a pointer to its inner area, In Fig. 1; these three types are observed [5].

2.2 Cell decomposition method

For the original polygon triangulation or pseudo triangulation, primarily using a sweep line algorithm divide the original polygon into multiple polygons without holes and then these monotone polygons triangulate and pseudo triangulate, sweep line algorithm will be described in the next section.

3 Sweep line and monotone polygon

Primarily using a horizontal line the original polygon is swept along the y-axis. Using the sweep line, original polygon vertices and obstacles vertices are arranged in order of y. The vertices have identical y, are arranged based on x. A list of all the vertices is produced that are arranged respectively on y and then x.

3.1 Identify the type of vertices

Now vertices according to the order in the list are examined. Based on the position of the vertex v_i in adjacent of previous neighbor vertex v_{i-1} and next neighbor vertex v_{i+1}, type of vertex is specified.

1) If the vertex v_{i-1} and v_{i+1} in terms of height (y component) to be respectively the one above and one below the vertex vi, vi is a *Regular* vertex.
2) If any two vertices v_{i-1} and v_{i+1} to be the vertices of the lower altitude, this is a *Start* vertex or *Split*. To determine that being faced with what type of vertices must draw a horizontal line from this point on the entire original polygon. If the number of points on the original polygon and the obstacles, of dealing with this line, separately right and left this vertex was *odd*, vertex is *"Split*" and if it was *even*, vertex is *"Start"*.
   Only an issue that should be noted, Vertices that are located on the horizontal line and both neighbor vertices are above or below, these points are not counted. Because this is a tangent point and not intersection. This is the horizontal line method concept that if the top of the vertex was outside the original polygon, this is a *Start* vertex. If the top of the vertex was inside the original polygon, this is a *Split* vertex (Fig. 2).

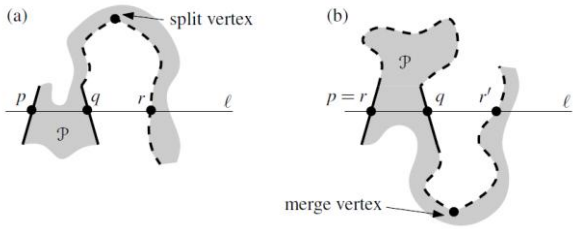

Fig. 2. Split and merge vertex

3) If any two vertices v_{i-1} and v_{i+1} to be the vertices of the higher altitude, this is an *End* vertex or *Merge*. To determine that being faced with what type of vertices must draw a horizontal line from this point on the entire original polygon. If the number of points on the original polygon and the obstacles, of dealing with this line, separately right and left this vertex was *odd*, vertex is *"Merge*" and if it was *even*, vertex is *"End"* [2].

After identifying the type of vertices, to derive the monotone polygons from within original polygons, do the below operations on "Split" and "Merge" vertices:

1) Each "split" vertex is connected to vertex that is located above it and the connected vertex must be closest vertex of height and visible.
2) Each "merge" vertex is connected to vertex that is located below it and the connected vertex must be closest vertex of height and visible.

In Fig. 3, a polygon with an obstacle is observed; Respectively "split" and "merge" vertices are connected to the nearest vertex of their top and bottom. Drawing diameters divide the original polygon into smaller monotone polygons. The sweep line algorithm order for obtain monotone polygons is *O(nlogn)*.

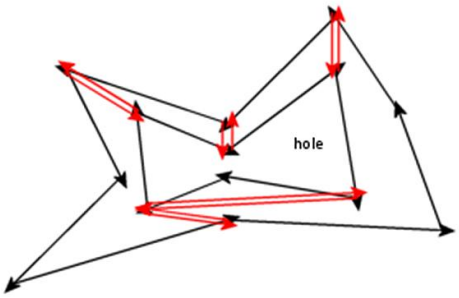

Fig. 3. The internal diameters between "Split" and "Merge" vertices

Monotone polygon is a simple polygon that is no obstacle in it and excluding the highest and lowest vertex of y, the rest are regular type. After drawing internal diameters should obtain a list of generated monotone polygons. To do this, as in Fig. 3 you can see, original polygon vertices in clockwise direction and obstacles polygons vertices in anti clockwise direction will be stored.

Make a list named "total" that includes all the vertices of the original polygon and obstacles. On one of the original polygon vertices, starting to move in order polygons were stored. Always must move on the original polygon in the clockwise order and on the obstacles polygons in the anti clockwise order. When we got to the vertex that it's degree was more than 2, means that it was attached to one or several internal diameter, CCW angle between previous surveyed vertex v_{i-1} and the current vertex v_i and the next vertices which were connected to vertex v_i by edges, is obtained.

The next vertex must make the least CCW angle with the vertex v_i and vertex v_{i-1}. Then, most likely the next vertex will be located on vertices of the obstacles polygons. This process continues until we reach the first traversed vertex, a monotone polygon is extracted. All these polygon vertices are removed from the "total" list and now again, start to traverse from a vertex on the original polygon, this is repeated until all monotone polygons are extracted and "total" list is empty [3].

In the next section using triangulation and pseudo triangulation algorithms, each monotone polygon will be divided into several cells.

4 Triangulation and pseudo triangulation

In this section, using monotone triangulation and incremental pseudo triangulation, the cells within each monotone polygon are obtained. Triangulation algorithm has linear time *O(n)* and pseudo triangulation algorithm order is *O(nlogn)*.

4.1 Triangulation algorithm

In Fig. 3 , created monotone polygons are triangulated using the monotone triangulation method and the triangulation result is observed in Fig. 4. Monotone triangulation algorithm is described in Fig. 5. This method arranges vertices in order of y. The vertices have identical y, are arranged based on x. Then compare the two consecutive edges on left and right chains of monotone polygon and draw the required diameters for the triangulation [2].

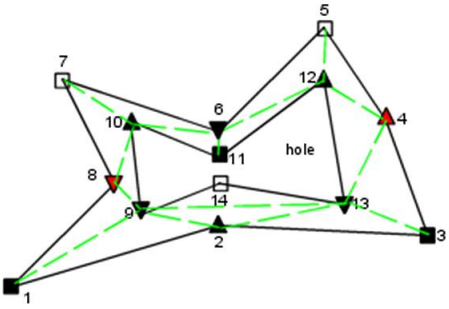

Fig. 4. Monotone polygon triangulation

Algorithm TRIANGULATEMONOTONE(P)
Input. A strictly y-monotone polygon P stored in a doubly-connected edge list D.
Output. A triangulation of P stored in the doubly-connected edge list D.
1. *Merge the vertices on the left chain and the vertices on the right chain of P into one sequence, sorted on decreasing y-coordinate. If two vertices have the same y-coordinate, then the leftmost one comes first. Let* $u_1, \ldots, u_n$ *denote the sorted sequence.*
2. *Initialize an empty stack S, and push* u_1 *and* u_2 *onto it.*
3. *for* $j \leftarrow 3$ *to* $n-1$
4. *do if* u_j *and the vertex on top of S are on different chains*
5. *then Pop all vertices from S.*
6. *Insert into D a diagonal from* u_j *to each popped vertex, except the last one.*
7. *Push* u_{j-1} *and* u_j *onto S.*
8. *else Pop one vertex from S.*
9. *Pop the other vertices from S as long as the diagonals from* u_j *to them are inside P Insert these diagonals into D Push the last vertex that has been popped back onto S.*
10. *Push* u_j *onto S.*
11. *Add diagonals from* u_n *to all stack vertices except the first and the last one.*

Fig. 5. Monotone triangulation algorithm

4.2 Pseudo triangulation algorithm

Pseudo triangle is said to polygon that exactly has three convex interior angles and the rest of the interior angles are concave. This polygon is shaped like a triangle. Pseudo triangulated polygon for n vertices has at least 2n-3 edges. Pointed pseudo triangulated polygon for n vertices exactly has 2n-3 edges [1].

Cell decomposition method using pseudo triangulation divides the area including obstacles into number of pseudo triangles. Incremental pseudo triangulation algorithm is

described in Fig. 6. In this method, traversing is started from a vertex on polygon convex hull and makes a triangle with two initial edges.

At each step a new vertex is added, as regards pointedness or planarity is violated, pseudo triangles creation begins. At some stage split the existing edges into two parts and use the new edge as a diameter [4, 6].

Algorithm INCREMENTAL PSEUDO-TRIANGULATION(P)
Input. A simple polygon P given by its point set, in ccw order around its boundary.
Output. A pointed pseudo-triangulation of P
***1**. Start from a vertex on the convex hull of the polygon and the first two edges to obtain a triangle.*

***2**. Add the vertices one at a time, together with a new polygon edge.*

***3**. If pointedness is violated, split the existing edges incident to the last vertex into two parts, using the new edge as a divider. Move half of them (the part containing only added edges, not the other polygon edge incident to the vertex) to the new endpoint. Recourse, to maintain planarity and pointedness.*

***4**. If planarity is violated, it is because the new edge is cutting through several added edges. Subdivide these crossed edges into two, and recourse to maintain planarity and pointedness on each half. Some of these new edges will coincide.*

Fig. 6. Pseudo monotone triangulation algorithm

For example, in Fig. 7 (d) there is a polygon with holes that is pseudo triangulated. Fig. 7 shows the output of implemented software with this research. In part (a) a polygon with holes is observed, Obstacles within the polygon was generated using an innovative technique that developed by the author and Its description is beyond the scope of this article.

In part (b) using sweep line method, the original polygon is divided into several monotone polygons. In part (c) Each monotone polygon is divided into the number of cells using triangulation method. In part (d) cells are obtained using incremental pseudo triangulation. In the next section, roadmap generation and searching algorithm will be described.

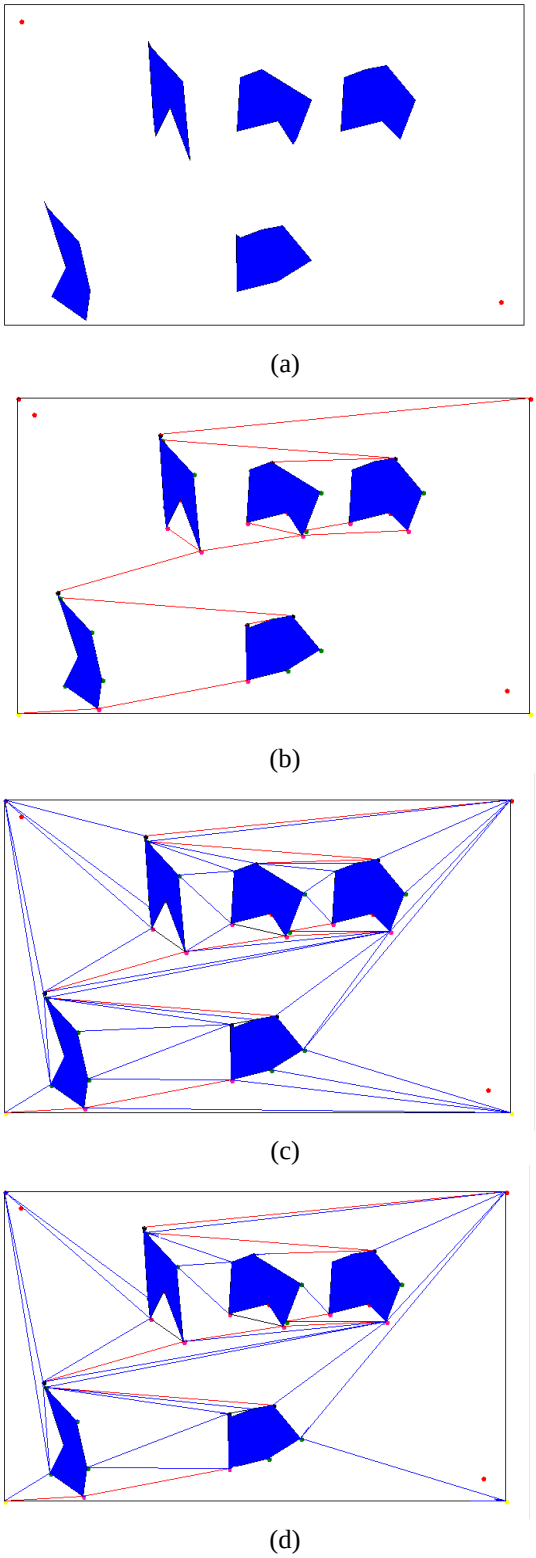

(a) (b) (c) (d)

Fig. 7. (a) Polygon with holes. (b) The original polygon is divided into monotone polygons. (c) Monotone polygons are triangulated. (d) Monotone polygons are pseudo triangulated.

5 Roadmap and searching weighted graph

5.1 Maximum-clearance roadmaps

In Fig. 8, when a roadmap is creating, maximum distance from obstacles must be kept. Moving in space while maintaining a maximum distance of obstacles is ensured that probability of collision reduces. In Fig. 8, part of the roadmap passes the inside corridor in an equal distance from obstacles [5].

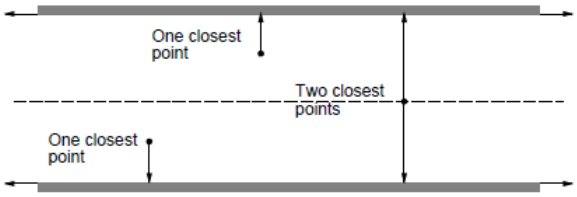

Fig. 8. Maximum-clearance roadmaps

To generate roadmap in triangulation and pseudo triangulation cell decomposition method, triangles and pseudo triangles centers must be achieved. Roadmap graph is generated through connecting the center of triangles, pseudo triangles and middle of edges. To find the triangle center obtains triangle gravity point, it means average coordinates of triangle is obtained. In the next section, innovative approach to find pseudo triangle center will be provided.

5.2 Pseudo triangle center

Pseudo triangle center is the point that all three convex vertices be able to see that. Three convex vertex of pseudo triangle are connected through a direct line L_i *(i=1,2,3)*. Middle point of each three lines find and is called M_i. A perpendicular line from M_i is drawn to the chain of the edges between two head of the line L_i and the collision place with chain of the edges is called T_i. Gravity center of the points T_i is pseudo triangle center. In Fig. 9, pseudo triangle center finding method is observed.

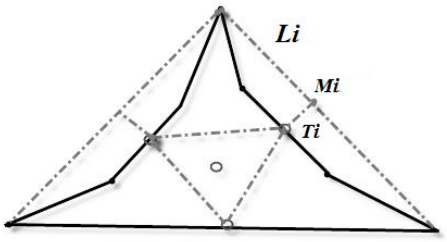

Fig. 9. Finding pseudo triangle center

5.3 Weighted search graph

Each of routing origin and destination points are located within one of the triangles or pseudo triangles. The origin point is connected to nearest vertex of the roadmap graph and this vertex is called Start V_s, the destination point is connected to nearest vertex of the roadmap graph and this vertex is called Start V_Q

If the above cases be adhered, motion planning problem can be reduced to a graph search problem. Constructed roadmap graph in cell decomposition method is observed in Fig. 10. This is a weighted graph, because the goal is finding the shortest path from origin to destination without collision with obstacles. The length of each edge is considered as its weight. Weighted graph searching algorithms is used for searching graph. For example, the Dijkstra basic algorithm is used for weighted graph searching, this algorithm acquires the shortest path from one vertex to all vertices of the graph. The shortest path from vertex V_s to vertex V_Q is acquired by this algorithm.

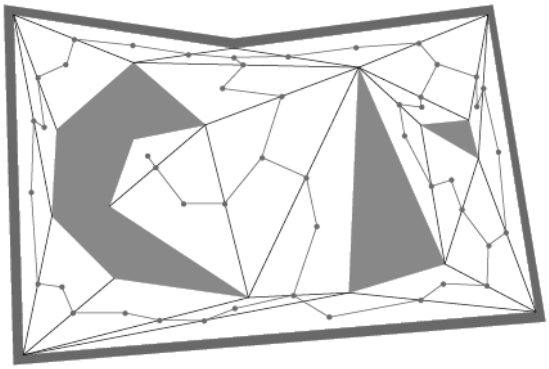

Fig. 10. The triangular cell decomposition roadmap

6 Conclusions

In this paper, the triangular cell decomposition algorithm was evaluated. Then a new idea of the pseudo triangulation was considered instead of triangulation. If the cell decomposition performs using a pseudo triangulation, the number of cells is smaller and more efficient than the number of cells that are created from the triangulation.

Sweep line algorithm was used to create monotone polygons, with the order *O(nlogn)*. Monotone triangulation has linear time *O(n)* and pseudo triangulation did with order *O(nlogn)*. The proposed new algorithm is an optimal algorithm. The cell decomposition method is a combinatorial method and it is used in offline robot motion planning.

References

[1] Joachim Gudmundsson, and Christos Levcopoulos. "*Minimum weight pseudo-triangulations*". 2007 Elsevier, Computational Geometry 38, 139–153.

[2] Mark de Berg, Otfried Cheong, Marc van Kreveld, and Mark Overmars. "*Computational Geometry - Algorithms and Applications*". Springer 2008.

[3] Wu Liang, "*Poly2Tri: Fast and Robust Simple Polygon Triangulation With/Without Holes by Sweep Line Algorithm*". Centre for Systems Engineering and Applied Mechanics (CESAME) 2005, University Catholique de Louvain , http://sites-final.uclouvain.be/mema/Poly2Tri/.

[4] Ileana Streinu. "*Pseudo-Triangulations, Rigidity and Motion Planning*". Department of Computer Science, Smith College, Northampton, MA 01063, USA.

[5] Steven M. Lavelle. "*Planning Algorithms*". Cambridge University 2006.

[6] Gunter Rote, Francisco Santos, and Ileana Streinu, "*Pseudo-Triangulations - a Survey*". 2007 Mathematics Subject Classification.

[7] Marius Kloetzer, and Narcis Ghita, "*Software Tool for Constructing Cell Decompositions*". 2011 IEEE International Conference on Automation Science and Engineering, Trieste, Italy.

A Case Study in Software Project Estimation

Michelle A. Willcox, Devon M. Simmonds, Thomas D. Lovette, Yuli Bonner
University of North Carolina Wilmington
601 South College Road, Wilmington, NC 28403
{ maw3067, simmondsd, tdl6020, myb7721 }@uncw.edu

Abstract

Software estimation is a pivotal activity in the software engineering lifecycle. Indeed, software project planning, including scheduling and resource management are all predicated on the computation of realistic estimates. This paper reports on a case study to evaluate the use of estimation in the model-based development of clipboard management software called ClipBits. Multiple techniques are available for performing software estimation. In this project, three estimation techniques were used: function point estimation, the COCOMO II model and a lines-of-code approach. Our analysis of the results revealed that estimation produced reasonable results. We provide some foresight as to larger variability from actual data for some estimates. In addition, the duration and scheduling predictions proved useful as an aid to help keep the team true to its deadlines. Overall, the results support the fact that software estimation can greatly improve the successful completion of software engineering projects.

Keywords: software engineering, software estimation, planning, scheduling, clipboard.

1. Introduction

Software engineering [1] is a task that requires a lot of preparation and planning. With proper planning, all stakeholders, including investors, project managers, and programmers can have a solid basis for project execution and greater assurance that the project will succeed. While it is hard to accurately predict the software duration, schedule and cost before starting a software project, proper early software project estimation [2, 3] provides goals and milestones for the development team, and enables the allocation and management of human and other resources in a systematic and predictable manner. Estimation is beneficial because it is essential that room be allowed in the development process, for the many unforeseen circumstances that typically accompany complex projects.

Some of the areas involved in software project planning include the schedule the software development team will follow; the project duration, the project size, required human resources, specialized skills and an assessment of risks. Schedule estimation includes such tasks as determining when a requirement of the software should be completed, and how long it is expected to take. Several techniques are available for software sizing including techniques based on the projected lines of code, techniques based on the functionality of the software, and empirical models [3]. Significant project anomalies are typically forecasted and addressed through systematic and continuous risk assessment. While some of the risks might never occur, it is good to plan for them regardless of the outcome. Lastly, the software development team needs to set forth an understanding of what each member's tasks are going to be throughout the project. This may be done using a tool such as a responsibility matrix. All of these areas need to be accounted for during the software project planning. Needless to say, that while software project planning begins at project inception, project planning is an ongoing activity throughout the life of the project.

This paper reports on a case study designed to assess the importance of effective software project planning for successful software development. By analyzing the estimates with actual data, we will be able to see how accurate our estimates were in the end, and what can be done to improve this process. The software that was developed in this case study improved upon the functionality of the system clipboard [4 – 8, 14 – 16] to allow users to increase their work efficiency and productivity [9]. The application, called ClipBits, enables users to store past clipboard data as ClipButtons, and save multiple ClipButtons in ButtonSets locally to be used at any time. This is all done using an unobtrusive user interface that is intuitive and easy to use. Our main

focus was on determining the facets of software project planning that were most helpful for developers, what areas were or were not estimated accurately, and the quality [10, 11] of the resulting application.

The rest of the paper is organized as follows: project planning and estimation is presented in Section 2, software design in Section 3, the results and lessons learned in Section 4, and lastly, Section 5 will present the discussion and conclusion.

2. Project Planning and Estimation

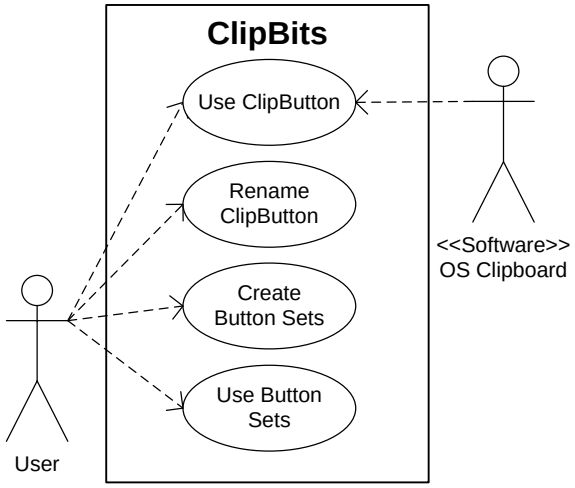

Figure 1. ClipBits Use Case Diagram

The above Use Case Diagram (Figure 1) demonstrates typical actor interaction with the ClipBits software. Actors include the end user and the operating system clipboard, both of which interact with the application. However, the methods through which they interact are slightly different. The end user interacts with ClipBits through the use of clip buttons and UI components, whereas the OS clipboard interacts with the application via Windows messaging. Figure 1 is a context model for the application, and therefore understanding this context model during the software planning phase will allow each of the developers to relate their specific development task to the actor(s) for whom the feature is required.

The many vital roles necessary to the completion of the ClipBits software were assigned as illustrated by the responsibility matrix shown in Table 1. The table shows the lead software engineer for each task. The tasks were well-distributed according to the various areas of expertise present within the group for the purposes of increasing efficiency while mitigating the risk associated with learning curves (see Table 3). Throughout the development process, each member will be able to refer back to this table if there is every any task in question regarding who is responsible.

	Thomas Lovette	Yuli Bonner	Michelle Willcox
Project Management	x		
Requirements Engineering		x	
Software Design	x	x	x
Quality Assurance			x
Data Storage/Retrieval Mechanism	x		
ButtonSet Design/Implementation	x		
Clipboard Management		x	
ClipButton Development		x	
UI Design/Development			x
Cross-Tier Integration	x	x	x
Product Testing			x
Project Proposal	x		
Requirements Engineering Document		x	
Software Design Document	x		
Implementation/ Testing Document			x

Table 1. ClipBits Responsibility Matrix

The overall estimation process for development of the ClipBits application began with the development of the work items in the work breakdown structure shown in Figure 2. Broad task categories include Planning and Research, Modeling and Design, Construction, and Deployment. Each category contains multiple sub-tasks, each with unique requirements and deadlines. However, the work items have been structured in such a way that the main categories can fall one after another, with Planning and Research directly preceding Modeling and Design, etc. Some tasks- such as research and integration- are carried out irrespective of hierarchical patterns, as their success impacts every area of the development process. It is evident that much is to be determined in the Planning and Research phases because these activities greatly influence the Modeling and Design, Construction, and Deployment phases.

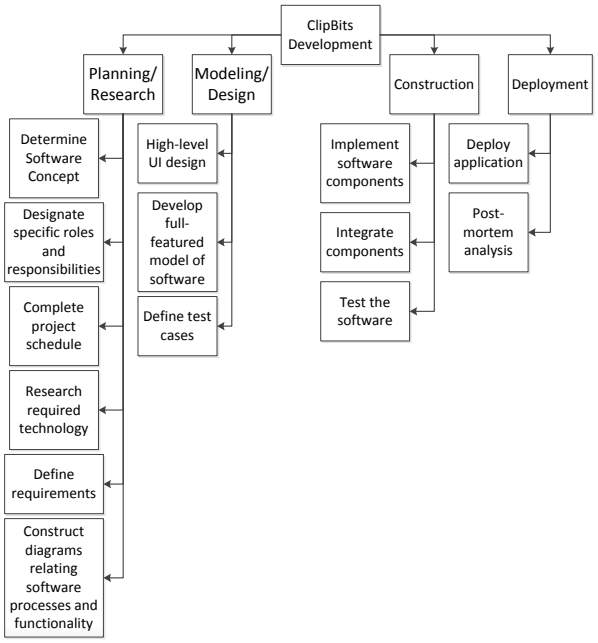

Figure 2. ClipBits Work Breakdown Structure (WBS)

Lines of Code Estimation

Table 1. ClipBits Cost Estimation using Lines of Code Model

Function	Optimistic LOC Estimate	Average LOC Estimate	Pessimistic LOC Estimate	Estimated LOC
User Interface	1,550	3,000	4,500	3,000
Clipboard Monitor	100	500	1,000	516
Clip Buttons	200	800	2,000	900
Data Read/ Write	250	600	1,500	691
Button Set	100	300	500	300
				5,407

Table 1 shows the basic data used to compute the software estimates using the lines of code (LOC) approach. The computation is done by finding the mean of the optimistic, likely, and pessimistic LOC estimates following a beta distribution [12], for the five broad categories of the application. Each item in The "Estimated LOC" column is calculated using the formula:

$$Estimated\ LOC = \frac{Optimistic + (4 \times Average) + Pessimistic}{6}$$

The total estimated Lines of Code for the application is then simply the sum of the entries in the "Estimated LOC" column. If an organizational average productivity rate of 620 LOC/person-month is assumed along with a burdened labor rate of $8,000.00/month [**pressman]**, then the average cost per line of code is approximately $12.90. Given this information, the total estimated cost of building this application is:

$$\$12.90/LOC \times 5{,}407\ LOC = \mathbf{\$69{,}750.30}$$

Likewise, the estimated effort required to build this application is:

$$\$69{,}750.30 \div \$8{,}000\ per\ mmonth = \mathbf{8.72\ person\ months}$$

These lines of code estimations allow the developers to visualize how much work each function will require, and can be used to further predict how long the implementation process will take.

Function Points Estimation

The Function Points estimate [13] for an application can be calculated using data as shown in Table 2. The computation consists of two components: an information domain value and a value adjustment factor. The information domain value (IDV) is computed in three steps. In the first step an estimate for five information domain factors such as "External Input" is computed. This is typically done following a beta distribution scheme as was outlined above, by computing the mean of optimistic, average and pessimistic values. In the second step the mean is multiplied by a weighting factor to get the total estimate for that information domain element. For example, in Table 2 the mean for "External Input", 10, is multiplied by the weighting factor, 4, to get a total of 40. Weighting is typically done based on the estimated complexity of the software as shown in Table 3 [17]. In the third step, a value adjustment factor (VAF) is computed by estimating the importance of fourteen factors to the overall project. These factors include such element as "backup and recovery", "distributed processing" and "code designed for reuse". In step 4, the number of function points for the project is computed using the formula:

$$Function\ Points = IDV * [0.65 + (.01 \times VAF)] = 102 \times [0.65 + (.01 \times 46)] = \mathbf{113.22}$$

Table 2. ClipBits Function Points IDV Computation

Function	Count	Weighting Factor	
External Input	10	4	40
External Output	5	5	25
External Inquiries	0	4	0
Internal Logical Files	3	10	30
External Interface Files	1	7	7
Count total			**102**

Table 3. Weighting Factors in IDV Computation

	Weighting Factor		
	Simple	**Average**	**Complex**
External Input	3	4	6
External Output	4	5	7
External Inquiries	3	4	6
Internal Logical Files	7	10	15
External Interface Files	5	7	10

The function points analysis has proven to be a reliable estimation method that helps express the software functionality more from the user's prospective than from the developers' perspective.

PERT Chart

The PERT Chart (Figure 3) demonstrates directed, parallel paths from the start of the project to deployment. Many of the preliminary items were simpler, whereas many of the later tasks are predicted to require several weeks. However, most tasks can occur concurrently, implying that, whereas there are many tasks to complete, the overall amount of time spent is well-distributed among various branches, and no one branch dominates the others in terms of effort and manpower. The time (in days) estimates are based upon how complex the developers predicted each task to be in the development phase.

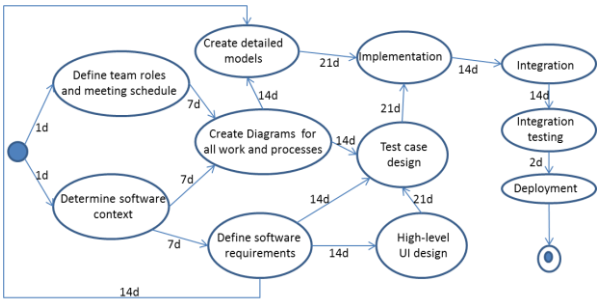

Figure 3. PERT Chart

Risk Plan

Table 3. ClipBits Risk Assessment and Mitigation Plan

Risks	Cat	Prob	Imp	RMMM
Unable to meet established deadlines	BU	40%	1	Set up meetings multiple times per week in order to monitor progress. Allow team member input in order to make realistic deadline decisions.
Compartmentalization overlaps and slows momentum down	PS	20%	2	Equally divide tasks among team members and increase the amount of communication.
Slower performance with larger data	TE	60%	3	Create a file size limit in order to prevent users from slowing down the software's execution time.
Performance impact of using a database versus serialization	TE	50%	3	Research each method in depth in order to decide which method is more efficient.
Standard library is not sufficient for our needs	TE	75%	2	Examine other libraries that have the functionality that will benefit our requirements.
Staff is unable to learn necessary skills/ technology	ST	30%	1	Assist team members in the learning process by pointing them to useful resources that will allow them to acquire the necessary skillset.

Key (Cat=Category, Imp=impact, Prob=probability)

Category	Impact
BU- Business Risk	1- Catastrophic
PS- Project Risk	2- Critical
TE- Technical Risk	3- Marginal
ST- Staff Risk	4- Negligible

There are numerous possible risks associated with the development of ClipBits. The table above (Table 3) lists several categories of risks, along with the development team's planned methods of mitigation. Through wise delegation of responsibility, proper research methods, and effective advance prototyping, many of the listed risks were effectively eliminated.

3. Software Design & Implementation

Figure 4 shows the state diagram for the ClipBits software. The application responds to the system clipboard events by creating ClipButtons and storing them in a stack. Of note are the starting and ending states: the application starts with an initialization of the ClipButton Stack and ends with its disposal. Since the application is largely UI-driven, it is to be expected that many of the states consist of windows opening and closing, with processing occurring within.

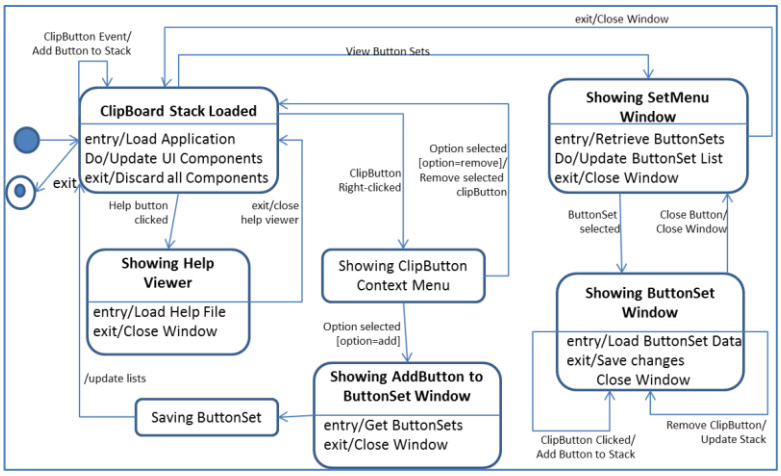

Figure 4. ClipBits State Diagram

A screen shot of the resulting UI for the ClipBits software is shown in Figure 5. The figure shows the Main Window, the Add-All-Buttons-t-ButtonSet Window, the Button Set Menu Window, and finally the individual Button Set window displaying the ClipButtons contained in the Button Set. This design went through multiple alterations in order to satisfy the requirements that were set forth in the planning phase.

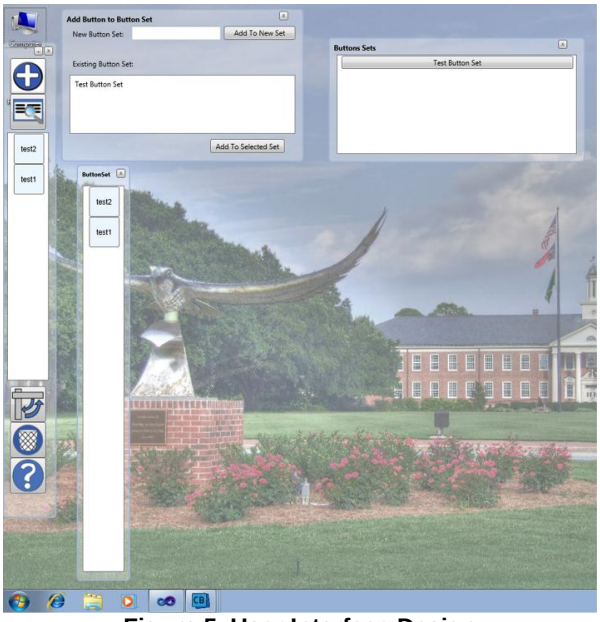

Figure 5. User Interface Design

4. Results and Lessons Learned

The original cost and effort estimates for ClipBits were misjudged. Original estimates called for 5,407 lines of code, but the final product contained far less: approximately 2,000. This is due largely to uncertainty about the extent to which Windows Presentation Foundation (WPF) would be used in development. With WPF's declarative syntax, it ended up being ideal for data-binding scenarios. Thus, operations that would have taken many lines of code to implement (such as UI updates) were relegated to the framework, drastically reducing the amount of necessary coding. In the future, more research on WPF's syntax, specifically for the UI, would allow us to predict our lines of code estimation better.

In the requirements phase of our work, we established a list of non-functional requirements that we strived to meet:

- Users have easy access to *Button Sets* in the current session and in later sessions because a Button Sets folder is stored locally on the user's hard drive.
- UI is user friendly and unobtrusive.
- UI docks to both the top and left sides of the screen.

- User documentation such as a manual or other help feature should are included when the user clicks the help button.
- The interface includes a significant level of customization options in terms of size, shape, and/or orientation.
- The program is lightweight in terms of performance so that it does not impede the performance of any other applications with which it is being used.

Overall, we drafted these requirements with the user's experience in mind, we wanted to minimize the learning curve for ClipBits so that anyone could easily use it for their benefit. The serialization of Button Sets is a key feature that enables users to refer back to data that they created or used in the past. This was made possible by serializing the ButtonSet data into a file that was automatically stored in the user's Documents folder. As such, any future time when a user browses their Button Sets, the file is read and the Button Set data is accessible and may be copied right back to the system clipboard.

The realization of non-functional requirements was a significant element of the user interface design. By creating simple icons for each button, and making the windows semi-transparent we were able to make the application easy to use and unobtrusive. In addition, the main window is easily positioned by the click of a button to either the top of the screen horizontally or to the left side vertically. Therefore, the windows would stay out of the way from other applications. The user also has the choice to hide the windows all together, and move it manually to another position on the screen.

Not only does the application not visually other applications, but performance-wise, the application doesn't slow down the computer's other processes because it is a lightweight design. The only thing the application is constantly monitoring is the system clipboard, and when it recognizes that something has been copied, it generates Clip Button data and displays it in the window.

Lastly, if the user is ever confused or in need of help while using the application, then they can easily access the user manual from the help button on the main window. The user manual features a description of each UI element and explains how each element is utilized.

In the end, our group was able to stay very close to our estimated schedule and designated tasks, even though we ran into multiple small issues. What really helped us stay on that schedule was our meetings twice a week where we would go over what we had been working on during our own time, reviewing what deadlines were coming up, discussing what needed to be done, and designating tasks. We also made it a point to communicate constantly via email or at meetings so that even if we were not designated a specific a task, we were involved to some degree that would allow us to understand where the project stood in relation to our overall schedule.

5. Discussion and Conclusion

Now that the project has come to completion, it is evident that an emphasis on comprehensive software estimation techniques can only be a benefit to the software developers throughout the whole project. Even if there are some inaccurate predictions, they will still assist in the goals and visualization of the software's end product. In addition, estimation is a learnt discipline predicated on the availability of historical data. As such this project has taught us not only valuable lessons, but given us some basic data to assist in the next estimation project. A lot of software estimation and planning diagrams and tables were used; and our team was able to supplement that data with frequently collaborations and reacting in an agile manner to issues as they arose. Without that, then our team would not be able to help each other out when these problems surfaced, and our estimated project schedule would have been thrown way off. Luckily, with the help of effective software estimation, we were able to keep on track all of our deadlines relatively well and successfully implement all of our non-functional, and functional requirements.

In the future, our team will most likely be involved in developing other projects. As a whole, we all learned a great deal about the significance of software planning and estimation and we will be able to take this knowledge and apply it to any future software projects we may come across.

References

[1] Pressman, Roger. *Software Engineering: A Practitioner's Approach.* New York: McGraw Hill., 2010. Print.

[2] [30] Roger S. Pressman. Estimating Software Projects, Chapter 26 of Software Engineering: A Practitioner's Approach, McGraw-Hill 2010.

[3] Violeta Bozhikova and Mariana Stoeva. 2010. An approach for software cost estimation. In *Proceedings of the 11th International Conference on Computer Systems and Technologies and Workshop*

for PhD Students in Computing on International Conference on Computer Systems and Technologies (CompSysTech '10), Boris Rachev and Angel Smrikarov (Eds.). ACM, New York, NY, USA, 119-124. DOI=10.1145/1839379.1839401 http://0-doi.acm.org.uncclc.coast.uncwil.edu/10.1145/1839379.1839401

[4] Frakes, Dan. "Clipboard Managers." *MacWorld* 7 Nov. 2010: 36-37. Print.

[5] Frakes, Dan. "Clipboard Managers." *Macworld* 27.7 (July 2010): 36-37. *Academic Search Premier*. Web.

[6] Stone, David "The Office Clipboard."*PC Magazine* 21, Dec. 2001: 83-86. Print.

[7] Zardetto, Sharon. "Two Quick Copy and Paste Tricks." *Macworld* 27.4 (April 2010): 53. *Academic Search Premier*. Web.

[8] *xNeat.com*. xNeat. 2011. Web. 5 Nov. 2011.

[9] Champy, James. "Productivity Promise." *Financial Executive.* Oct. 2003: 35. Print.

[10] D. Milicic, Software quality models and philosophies, in *Software quality attributes and trade-offs*, eds L. Lundberg, M. Mattson, C. Wohlin (2008), http://www.bth.se/tek/besq.nsf/%28WebFiles%29/CF1C3230DB425EDCC125706900317C44/$FILE/chapter_1.pdf

[11] B. Zeiss et al, Applying the ISO 9126 quality model to test specifications – exemplified for TTCN-3 Test Specifications (Bonn, 2007), Software Engineering Conference 2007, Lecture Notes in Informatics (LNI) 105.

[12] Roger S. Pressman. Software Engineering: A Practitioner's Approach 7th Ed. Page 700, McGraw-Hill 2010.

[13] Vipin Saxena and Manish Shrivastava. 2009. Performance of function point analysis through UML modeling. *SIGSOFT Softw. Eng. Notes* 34, 2 (February 2009).

[14] Li, Shaobo, Lv, Shulin, Jia, Xiaohui, and Shao, Zhisheng. "Application of Clipboard Monitoring Technology in Graphic and Document Information Security Protection System." *Intelligent Information Technology and Security Informatics* (April 2010):423-6. *IEEE*. Web.

[15] Pomeroy, Bryony and Wiseman, Simon. "Private Desktops and Shared Store." *Computer Security Applications Conference, Annual* (December 1998): 190-200. *IEEE*. Web.

[16] Birss, Edward W.. "The Integrated Software and User Interface of Apple's Lisa." *National Computer Conference* (1984):319-28. *IEEE*. Web.

[17] Roger S. Pressman. Figure 23.1: Computing Function Points *in* Software Engineering: A Practitioner's Approach, McGraw-Hill 2010, page 621.

Formal Verification of AES Using the Mizar Proof Checker

Hiroyuki Okazaki[1], **Kenichi Arai**[2], **and Yasunari Shidama**[1]
[1]Shinshu University, 4-17-1 Wakasato Nagano-city, Nagano 380-8553, Japan
[2]Tokyo University of Science, 2641 Yamazaki Noda-City, Chiba 278-8510, Japan

Abstract— *In this paper, we introduce our formalization of the Advanced Encryption Standard (AES) algorithm. AES, which is the most widely used symmetric cryptosystem in the world, is a block cipher that was selected by the National Institute of Standards and Technology (NIST) as an official Federal Information Processing Standard for the United States in 2001. We prove the correctness of our formalization using the Mizar proof checking system as a formal verification tool. Mizar is a project that formalizes mathematics with a computer-aided proving technique and is a universally accepted proof checking system. The main objective of this work is to prove the security of cryptographic systems using the Mizar proof checker.*

Keywords: Formal Verification, Mizar, Cryptology, Advanced Encryption Standard (AES)

1. Introduction

Mizar[1] is a project that formalizes mathematics with a computer-aided proving technique. The objective of this study is to prove the security of cryptographic systems using the Mizar proof checker. To achieve this study, we intend to formalize several topics concerning cryptology. As a part of this effort, we introduced our formalization of the Data Encryption Standard (DES)[2] at the FCS'11[3].

In this paper, we introduce our formalization of the Advanced Encryption Standard (AES). AES, which is the most widely used symmetric cryptosystem in the world, is a block cipher that was selected by the National Institute of Standards and Technology (NIST) as an official Federal Information Processing Standard for the United States in 2001[4]. AES is the successor to DES, which was formerly the most widely used symmetric cryptosystem in the world. However, DES is now considered insecure and has been replaced by AES[5]. We formalized the AES algorithm as shown in FIPS 197[4] in the Mizar language. We then verified the correctness of the formalized algorithm that the ciphertext encoded by the AES algorithm can be decoded uniquely by the same key using the Mizar proof checker.

The remainder of this paper is organized as follows. In Section 2, we briefly introduce the Mizar project. In Section 3, we briefly introduce the Advanced Encryption Standard (AES). In Section 4, we discuss our strategy for formalizing AES in Mizar. In Sections 5 and 6, we propose a formalization of AES. We conclude our discussion in Section 7. The definitions and theorems in this paper have been verified for correctness using the Mizar proof checker.

2. Mizar

Mizar[1] is an advanced project of the Mizar Society led by A.Trybulec which formalizes mathematics with a computer-aided proving technique. The Mizar project describes mathematical proofs in the Mizar language, which is created to formally describe mathematics. The Mizar proof checker operates in both Windows and UNIX environments, and registers the proven definitions and theorems in the Mizar Mathematical Library (MML).

What formalizes the proof of mathematics by Mizar and describes it is called "article". When an article is newly described, it is possible to advance it by referring to articles registered in the MML that have already been inspected as proof. Although the Mizar language is based on the description method for general mathematical proofs, the reader should consult the references for its grammatical details, because Mizar uses a specific, unique notation[6], [7], [8], [9].

3. Advanced Encryption Standard

In this section, we review the outline of the AES algorithm, which is a variant of Rijndael algorithm[10]. The AES algorithm can process 128–bit data blocks using secret keys of lengths 128, 192, or 256 bits. Decryption must be performed using the same key as that used for encryption. However, the decryption algorithm is different from the encryption algorithm. Depending on the key lengths, AES is referred to as AES–128, AES–192, or AES–256.

AES is a type of iterated block cipher that has a Substitution Permutation Network (SPN) structure. The SPN structure alternately performs substitution and permutation operations. The encryption and decryption of the SPN structure involve different processes. The AES algorithm is composed of the SPN structure and a key scheduling. In the SPN structure of AES, there are 10, 12, and 14 rounds of processing iterations. The number of rounds to be performed during the execution of the AES algorithm is dependent on the key lengths. In AES algorithm, the key length, block size, and number of rounds are represented by Nk, Nb, and Nr, respectively. The Nk–Nb–Nr combinations are shown in Figure 1.

	Key Length (*Nk* words)	Block Size (*Nb* words)	Number of Rounds(*Nr*)
AES-128	4	4	10
AES-192	6	4	12
AES-256	8	4	14

1 word = 4 bytes = 32 bits

Figure 1: Nk–Nb–Nr combinations

The AES algorithm is performed on a two-dimensional array of bytes called the "State". Before the main iterations, the plaintext block is copied into the State array. After an initial round key addition, the State array is transformed by performing a round process Nr times. However, only the final round is different. Finally, the final State is copied to the ciphertext block. The round process is composed of the "SubBytes", "ShiftRows", "MixColumns", and "AddRoundKey" transformations. The final round does not include the MixColumns transformation. The round key is yielded by the key scheduling from the given secret key and is added to the State array using the AddRoundKey transformation. Figure 2 shows the pseudo code for the encryption algorithm of AES.

```
AES-ENC(byte input[4*Nb], byte output[4*Nb], word w[Nb*(Nr+1)])
begin
  byte state[4, Nb]

  state = input

  AddRoundKey(state, w[0, Nb-1])

  for round = 1 step 1 to Nr-1
    SubBytes(state)
    ShiftRows(state)
    MixColumns(state)
    AddRoundKey(state, w[round*Nb, (round+1)*Nb-1])
  end for

  SubBytes(state)
  ShiftRows(state)
  AddRoundKey(state, w[Nr*Nb, (Nr+1)*Nb-1])

  output = state
end
```

w[0,3] = w[0] w[1] w[2] w[3] — Initial round key (4 words)

Final round

Figure 2: Pseudo code for the encryption algorithm

In decryption, the round process is composed of the "InvSubBytes", "InvShiftRows", "InvMixColumns", and AddRoundKey transformations. The InvSubBytes, InvShiftRows, and InvMixColumns are the inverse of the SubBytes, ShiftRows, and MixColumns transformations, respectively. In decryption, each transformation is performed in the reverse order of encryption and the round keys are used in the reverse order of encryption.

4. Strategy for Formalizing AES

In Mizar, there are two ways to define computational routines in an algorithmic sense. One way is by defining a routine as a "Function". A Function is a map from the space of the input onto that of the output. We can handle a Function as an element of the set of Functions.

The other way is by defining a routine as a "functor". A functor is a relation between the input and output of a routine in Mizar. It is easy to write and understand the formalization of a routine as a functor, because the format of a functor in Mizar is similar to that of a function in certain programming languages. Note that both functor and Function can take a Function as their substitutable subroutines.

In Section 5, we will formalize the subroutines, that is, the primitives of AES, according to FIPS 197[4]. In Section 6, we first formalize the algorithm of generalized AES as a functor that takes substitutional subroutines. This generalized definition of AES is easily reusable for the formalization of different key lengths of AES. We will then formalize the AES algorithm using the formalization of the primitives in Section 5 and the generalized definition in Section 6.1.

5. Formalization of AES Primitives

In this section, we formalize the AES primitives according to FIPS 197[4].

5.1 State array

Figure 3 shows a sketch of the State array.

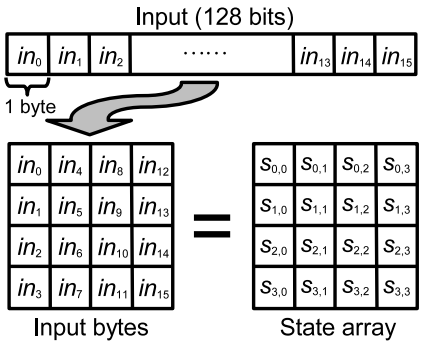

Figure 3: State array

The State array consists of 4 rows of bytes, each of which contains Nb bytes.

We formalize the State array as the following functor in the Mizar language:

Definition 5.1: (State array)

```
func AES-Statearray ->
  Function of 128-tuples_on BOOLEAN,
  4-tuples_on (4-tuples_on (8-tuples_on
  BOOLEAN))
means
for input be Element of 128-tuples_on
  BOOLEAN
for i,j be Nat st i in Seg 4 & j in Seg 4
holds
((it.input).i).j = mid(input,1+(i-'1)*8+
  (j-'1)*32,1+(i-'1)*8+(j-'1)*32+7);
```

□

Here, mid is a function that extracts a subsequence (finite sequence) and * is multiplication. For example,

mid(input,9,16) is a finite sequence (input.9,.....,input.16) of length 8. Note that the index of the finite sequence starts from 1 in the Mizar language.

We similarly defined the functor of the inverse of the State array as AES-Statearray".

5.2 SubBytes

Figure 4 shows a sketch of the SubBytes transformation.

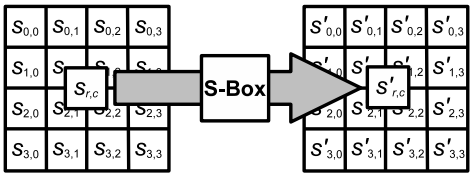

Figure 4: SubBytes

The SubBytes transformation is a nonlinear byte substitution that independently operates on each byte of the State array using a 1-byte substitution table. The substitution table is called the "S-Box". The S-Box, which is invertible, is constructed by composing two transformations. Two transformations are composed of the calculation of the multiplicative inverse in the finite field GF(2^8) and the affine transformation over GF(2). Figure 5 shows a sketch of the S-Box.

Most Significant 4 bits of $S_{r,c}$ \ Least Significant 4 bits of $S_{r,c}$	0	1	2	3	4	5	6	7	8	9	a	b	c	d	e	f
0	63	7c	77	7b	f2	6b	6f	c5	30	01	67	2b	fe	d7	ab	76
1	ca	82	c9	7d	fa	59	47	f0	ad	d4	a2	af	9c	a4	72	c0
2	b7	fd	93	26	36	3f	f7	cc	34	a5	e5	f1	71	d8	31	15
3	04	c7	23	c3	18	96	05	9a	07	12	80	e2	eb	27	b2	75
4	09	83	2c	1a	1b	6e	5a	a0	52	3b	d6	b3	29	e3	2f	84
5	53	d1	00	ed	20	fc	b1	5b	6a	cb	be	39	4a	4c	58	cf
6	d0	ef	aa	fb	43	4d	33	85	45	f9	02	7f	50	3c	9f	a8
7	51	a3	40	8f	92	9d	38	f5	bc	b6	da	21	10	ff	f3	d2
8	cd	0c	13	ec	5f	97	44	17	c4	a7	7e	3d	64	5d	19	73
9	60	81	4f	dc	22	2a	90	88	46	ee	b8	14	de	5e	0b	db
a	e0	32	3a	0a	49	06	24	5c	c2	d3	ac	62	91	95	e4	79
b	e7	c8	37	6d	8d	d5	4e	a9	6c	56	f4	ea	65	7a	ae	08
c	ba	78	25	2e	1c	a6	b4	c6	e8	dd	74	1f	4b	bd	8b	8a
d	70	3e	b5	66	48	03	f6	0e	61	35	57	b9	86	c1	1d	9e
e	e1	f8	98	11	69	d9	8e	94	9b	1e	87	e9	ce	55	28	df
f	8c	a1	89	0d	bf	e6	42	68	41	99	2d	0f	b0	54	bb	16

Figure 5: S-Box (in hexadecimal form)

We formalize the SubBytes transformation as the following functor in the Mizar language:

Definition 5.2: (SubBytes)

```
let SBT be Permutation of (8-tuples_on
  BOOLEAN);
func SubBytes(SBT) ->
  Function of 4-tuples_on (4-tuples_on
  (8-tuples_on BOOLEAN)),4-tuples_on
  (4-tuples_on (8-tuples_on BOOLEAN))
means
for input be Element of 4-tuples_on
  (4-tuples_on (8-tuples_on BOOLEAN))
holds
(for i,j be Nat st i in Seg 4 & j in Seg 4
holds
ex inputij be Element of 8-tuples_on
  BOOLEAN
st inputij = (input.i).j &
((it.input).i).j = SBT.(inputij));
```

□

Please note the following points about this formalization. This functor can specify an arbitrary Permutation of 8-tuples_on BOOLEAN because it takes SBT as an argument. In this formalization, so as not to lose generality, we describe this functor as the SubBytes transformation. The actual SubBytes transformation uses the S-Box, as shown in Figure 5. However, the formal description of this S-Box is not significant. Therefore, we described this functor as the SubBytes transformation.

We similarly defined the functor of the InvSubBytes transformation (Definition A. 1).

5.3 ShiftRows

Figure 6 shows a sketch of the ShiftRows transformation.

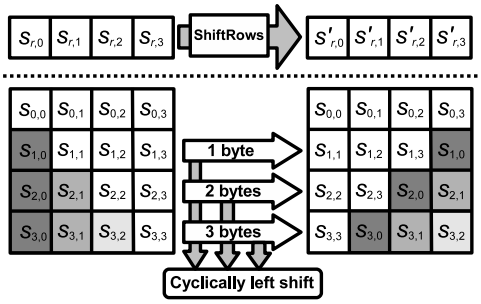

Figure 6: ShiftRows

The ShiftRows transformation operates the State array by cyclically shifting the last three rows of the State array by different offsets (numbers of bytes). Note that the first row is not shifted.

We formalize the ShiftRows transformation as the following functor in the Mizar language:

Definition 5.3: (ShiftRows)

```
func ShiftRows ->
  Function of 4-tuples_on (4-tuples_on
  (8-tuples_on BOOLEAN)),4-tuples_on
  (4-tuples_on (8-tuples_on BOOLEAN))
means
for input be Element of 4-tuples_on
  (4-tuples_on (8-tuples_on BOOLEAN))
holds
(for i be Nat st i in Seg 4
holds
ex xi be Element of 4-tuples_on
  (8-tuples_on BOOLEAN)
st xi = input.i &
(it.input).i = Op-Shift(xi,5-i));
```

□

Here, Op-Shift is a cyclically left shift function.

We similarly defined the functor of the InvShiftRows transformation (Definition A. 2).

5.4 MixColumns

Figure 7 shows a sketch of the MixColumns transformation.

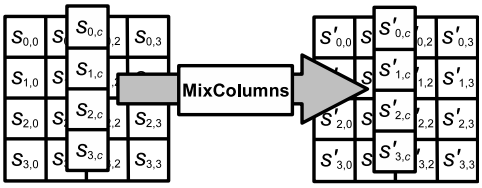

Figure 7: MixColumns

In the MixColumns transformation, the 4 bytes of each column of the State array are mixed using an invertible linear transformation. The columns are considered as polynomials over GF(2^8) and multiplied modulo x^4+1 with a fixed polynomial $a(x)$, given by $a(x) = \{03\}x^3 + \{01\}x^2 + \{01\}x + \{02\}$. As a result of the above mentioned multiplication, the 4 bytes in a column are replaced by the following:

$$s'_{0,c} = (\{02\} \bullet s_{0,c}) \oplus (\{03\} \bullet s_{1,c}) \oplus s_{2,c} \oplus s_{3,c},$$
$$s'_{1,c} = s_{0,c} \oplus (\{02\} \bullet s_{1,c}) \oplus (\{03\} \bullet s_{2,c}) \oplus s_{3,c},$$
$$s'_{2,c} = s_{0,c} \oplus s_{1,c} \oplus (\{02\} \bullet s_{2,c}) \oplus (\{03\} \bullet s_{3,c}),$$
$$s'_{3,c} = (\{03\} \bullet s_{0,c}) \oplus s_{1,c} \oplus s_{2,c} \oplus (\{02\} \bullet s_{3,c}).$$

Note that {01}, {02}, and {03} are hexadecimal notations and • is a multiplication in GF(2^8).

We formalize the MixColumns transformation as the following functor in the Mizar language:

Definition 5.4: (MixColumns)

```
func MixColumns ->
  Function of 4-tuples_on(4-tuples_on
   (8-tuples_on BOOLEAN)),4-tuples_on
   (4-tuples_on (8-tuples_on BOOLEAN))
means
for input be Element of 4-tuples_on
   (4-tuples_on (8-tuples_on BOOLEAN))
holds
ex x,y being Element of 4-tuples_on
   (4-tuples_on (8-tuples_on BOOLEAN))
st x = input & y = it.input &
for i be Element of NAT st i in Seg 4
holds
ex x1,x2,x3,x4 be Element of
  8-tuples_on BOOLEAN
st x1 = (x.i).1 & x2 = (x.i).2 &
x3 = (x.i).3 & x4 = (x.i).4 &
(y.1).i = Op-XOR(Op-XOR(Op-XOR(2 'gf' x1,
  3 'gf' x2),1 'gf' x3),1 'gf' x4) &
(y.2).i = Op-XOR(Op-XOR(Op-XOR(1 'gf' x1,
  2 'gf' x2),3 'gf' x3),1 'gf' x4) &
(y.3).i = Op-XOR(Op-XOR(Op-XOR(1 'gf' x1,
  1 'gf' x2),2 'gf' x3),3 'gf' x4) &
(y.4).i = Op-XOR(Op-XOR(Op-XOR(3 'gf' x1,
  1 'gf' x2),1 'gf' x3),2 'gf' x4);
```

□

Here, Op-XOR is a bitwise XOR (exclusive OR) function and 'gf' is a multiplication in GF(2^8).

We similarly defined the functor of the InvMixColumns transformation (Definition A. 3).

5.5 AddRoundKey

Figure 8 shows a sketch of the AddRoundKey transformation. Here, w_{l+c} are the key scheduling words and $round$

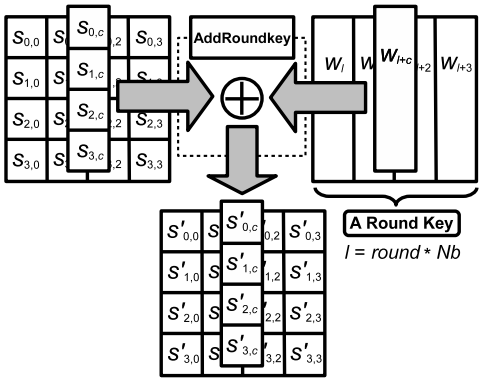

Figure 8: AddRoundKey

is a value in the range $0 \leq round \leq Nr$.

The AddRoundKey transformation adds a Round Key and the State array using a bitwise XOR.

We formalize the AddRoundKey transformation as the following functor in the Mizar language:

Definition 5.5: (AddRoundKey)

```
func AddRoundKey ->
  Function of [:4-tuples_on (4-tuples_on
   (8-tuples_on BOOLEAN)),4-tuples_on
   (4-tuples_on (8-tuples_on BOOLEAN)):],
   4-tuples_on (4-tuples_on (8-tuples_on
   BOOLEAN))
means
for text,key be Element of 4-tuples_on
   (4-tuples_on (8-tuples_on BOOLEAN))
holds
for i,j be Nat st i in Seg 4 & j in Seg 4
holds
ex textij,keyij be Element of
  8-tuples_on BOOLEAN
st textij = (text.i).j & keyij = (key.i).j
& ((it.(text,key)).i).j =
  Op-XOR(textij,keyij);
```

□

5.6 Key Expansion

The AES algorithm takes the secret key and performs a Key Expansion process to generate the key scheduling. The resulting key scheduling consists of a linear array of 4-byte words, denoted as w_i, with i being in the range $0 \leq i \leq$

$Nb(Nr+1)$. Figure 9 shows the pseudo code for the Key Expansion.

```
KeyExpansion(byte skey[4∗Nk], word w[Nb∗(Nr+1)], Nk)
begin
  word temp

  i = 0

  while(i < Nk)
    w[i] = word(skey[4∗i], skey[4∗i+1], skey[4∗i+2], skey[4∗i+3])
    i = i+1
  end while

  i = Nk

  while(i < Nb∗(Nr+1))
    temp = w[i-1]
    if(i mod Nk = 0)
      temp = SubWord(RotWord(temp)) xor Rcon[i/Nk]
    else if(Nk > 6 and i mod Nk = 4)
      temp = SubWord(temp)
    end if
    w[i] = w[i-Nk] xor temp
    i = i+1
  end while
end

Rcon[1] = [{01},{00},{00},{00}]
Rcon[2] = [{02},{00},{00},{00}]
Rcon[3] = [{04},{00},{00},{00}]
Rcon[8] = [{80},{00},{00},{00}]
Rcon[9] = [{1b},{00},{00},{00}]
Rcon[10] = [{36},{00},{00},{00}]
```

Figure 9: Pseudo code for the Key Expansion

SubWord is a function that takes an input word of 4 bytes and applies the S-Box to each of the 4 bytes to produce an output word.

We formalize SubWord as the following functor in the Mizar language:

Definition 5.6: (SubWord)

```
let SBT be Permutation of (8-tuples_on
  BOOLEAN);
let x be Element of 4-tuples_on
  (8-tuples_on BOOLEAN);
func SubWord(SBT,x) ->
  Element of 4-tuples_on (8-tuples_on
  BOOLEAN)
means
for i be Element of Seg 4
holds
it.i = SBT.(x.i);
```

□

RotWord is a function that takes a word $[b_0, b_1, b_2, b_3]$ as the input, performs a cyclically left shift, and returns the word $[b_1, b_2, b_3, b_0]$.

We formalize RotWord as the following functor:

Definition 5.7: (RotWord)

```
let x be Element of 4-tuples_on
  (8-tuples_on BOOLEAN);
func RotWord(x) ->
  Element of 4-tuples_on (8-tuples_on
  BOOLEAN)
equals
Op-LeftShift(x);
```

□

Here, Op-LeftShift is a cyclically 1 byte left shift function.

The round constant word array, Rcon, is a constant that is different for each round. Rcon[i] is defined as $x^{i-1}, \{00\}, \{00\}, \{00\}$. Here, x^{i-1} are powers of $x(= \{02\})$ in the field GF(2^8). Note that i starts from 1.

We formalize Rcon as the following functor:

Definition 5.8: (Rcon)

```
func Rcon ->
  Element of 10-tuples_on (4-tuples_on
  (8-tuples_on BOOLEAN))
means
it.1 = <* <*0,0,0,0*>^<*0,0,0,1*>,
  <*0,0,0,0*>^<*0,0,0,0*>,
  <*0,0,0,0*>^<*0,0,0,0*>,
  <*0,0,0,0*>^<*0,0,0,0*> *> &
                :
            (omitted)
                :
it.10 = <* <*0,0,1,1*>^<*0,1,1,0*>,
  <*0,0,0,0*>^<*0,0,0,0*>,
  <*0,0,0,0*>^<*0,0,0,0*>,
  <*0,0,0,0*>^<*0,0,0,0*> *>;
```

□

Here, ^ is concatenation. For example, $\langle *0,0,1,1* \rangle \hat{} \langle *0,1,1,0* \rangle = \{36\}$.

Next, to formalize the Key Expansion, we formalize the KeyExTemp and KeyExMain as the following functors.

Definition 5.9: (KeyExTemp)

```
let SBT be Permutation of (8-tuples_on
  BOOLEAN);
let m,i be Nat,
w be Element of (4-tuples_on (8-tuples_on
  BOOLEAN));
assume (m = 4 or m = 6 or m = 8) &
i < 4*(7+m) & m <= i;
func KeyExTemp(SBT,m,i,w) ->
  Element of (4-tuples_on (8-tuples_on
  BOOLEAN))
means
(ex T3 be Element of (4-tuples_on
  (8-tuples_on BOOLEAN))
st T3 = Rcon.(i/m) &
it = Op-WXOR(SubWord(SBT,RotWord(w)),T3))
if ((i mod m) = 0),(it = SubWord(SBT,w))
if (m = 8 & (i mod 8) = 4) otherwise
  it = w;
```

□

Definition 5.10: (KeyExMain)

```
let SBT be Permutation of (8-tuples_on
  BOOLEAN);
let m be Nat;
assume m = 4 or m = 6 or m = 8;
func KeyExMain(SBT,m) ->
  Function of m-tuples_on (4-tuples_on
  (8-tuples_on BOOLEAN)),(4*(7+m))-tuples_on
  (4-tuples_on (8-tuples_on BOOLEAN))
means
for Key be Element of m-tuples_on
  (4-tuples_on (8-tuples_on BOOLEAN))
holds
(for i be Element of NAT st i < m
  holds (it.Key).(i+1) = Key.(i+1)) &
(for i be Element of NAT st m <= i &
  i < 4*(7+m)
holds ex P be Element of (4-tuples_on
  (8-tuples_on BOOLEAN)),Q be Element of
  4-tuples_on (8-tuples_on BOOLEAN)
```

```
  st P = (it.Key).((i-m)+1) &
  Q = (it.Key).i & (it.Key).(i+1) =
    Op-WXOR(P,KeyExTemp(SBT,m,i,Q)));
```

□

Finally, we formalize the Key Expansion as the following functor.

Definition 5.11: (Key Expansion)

```
let SBT be Permutation of (8-tuples_on
  BOOLEAN);
let m be Nat;
assume m = 4 or m = 6 or m = 8;
func KeyExpansion(SBT,m) ->
  Function of m-tuples_on (4-tuples_on
  (8-tuples_on BOOLEAN)),(7+m)-tuples_on
  (4-tuples_on (4-tuples_on (8-tuples_on
  BOOLEAN)))
means
for Key be Element of m-tuples_on
  (4-tuples_on (8-tuples_on BOOLEAN))
holds
ex w be Element of (4*(7+m))-tuples_on
  (4-tuples_on (8-tuples_on BOOLEAN))
st w = (KeyExMain(SBT,m)).Key &
for i be Nat st i < 7+m
holds
(it.Key).(i+1) = <*w.(4*i+1),w.(4*i+2),
  w.(4*i+3),w.(4*i+4)*>;
```

□

6. Formalization of AES

In this section, we formalize the AES algorithm according to FIPS 197[4] in the Mizar language. First, we formalize and prove the correctness of the generalized AES algorithm. Next, we formalize and prove the correctness of the AES algorithm.

6.1 Formalization of Generalized AES

The generalized AES algorithm is easily reusable for the formalization of different key lengths of AES.

We formalize the encryption algorithm of generalized AES as a functor in the Mizar language as follows:

Definition 6.1: (Generalized AES encryption algorithm)

```
let SBT be Permutation of (8-tuples_on
  BOOLEAN);
let MCFunc be Permutation of 4-tuples_on
  (4-tuples_on (8-tuples_on BOOLEAN));
let m be Nat;
let text be Element of 4-tuples_on
  (4-tuples_on (8-tuples_on BOOLEAN));
let Key be Element of m-tuples_on
  (4-tuples_on (8-tuples_on BOOLEAN));
assume 4 <= m;
func AES-ENC(SBT,MCFunc,text,Key) ->
  Element of 4-tuples_on (4-tuples_on
  (8-tuples_on BOOLEAN))
means
ex seq be FinSequence of (4-tuples_on
  (4-tuples_on (8-tuples_on BOOLEAN)))
st len seq = 7+m-1 &
(ex Keyi1 be Element of 4-tuples_on
  (4-tuples_on (8-tuples_on BOOLEAN))
  st Keyi1 = ((KeyExpansion(SBT,m)).(Key)).1
  & seq.1 = AddRoundKey.(text,Keyi1)) &
(for i be Nat st 1 <= i & i < 7+m-1
  holds
  ex Keyi be Element of 4-tuples_on
    (4-tuples_on (8-tuples_on BOOLEAN))
  st Keyi = ((KeyExpansion(SBT,m)).(Key)).
    (i+1) & seq.(i+1) = AddRoundKey.
    ((MCFunc*ShiftRows*SubBytes(SBT)).
    (seq.i),Keyi)) &
ex KeyNr be Element of 4-tuples_on
  (4-tuples_on (8-tuples_on BOOLEAN))
st KeyNr = ((KeyExpansion(SBT,m)).(Key)).
  (7+m) & it = AddRoundKey.((ShiftRows*
  SubBytes(SBT)).(seq.(7+m-1)),KeyNr);
```

□

Here, * is composition. Note that the composition of the function is described in the reverse order of the actual processing.

We similarly defined the functor of the decryption algorithm of generalized AES as AES-DEC (Definition A. 4).

We then prove the following theorem:

Theorem 6.1: (Correctness of generalized AES)

```
for SBT be Permutation of (8-tuples_on
  BOOLEAN),
MCFunc be Permutation of 4-tuples_on
  (4-tuples_on (8-tuples_on BOOLEAN)),
m be Nat,
text be Element of 4-tuples_on (4-tuples_on
  (8-tuples_on BOOLEAN)),
Key be Element of m-tuples_on (4-tuples_on
  (8-tuples_on BOOLEAN))
st 4 <= m
holds
AES-DEC(SBT,MCFunc,AES-ENC(SBT,MCFunc,text,
  Key),Key) = text
```

□

Thus, we proved in the Mizar system that the ciphertext encoded by the generalized AES algorithm can be decoded uniquely with the same secret key that was used in encryption.

6.2 AES Algorithm

In this section, we formalize the AES algorithm in the Mizar language using our formalization of the AES primitives in Section 5 and the generalized AES algorithm in Section 6.1.

First, we formalize the encryption algorithm of AES–128 as a functor in the Mizar language as follows:

Definition 6.2: (AES–128 encryption algorithm)

```
let SBT be Permutation of (8-tuples_on
  BOOLEAN);
let message be Element of 128-tuples_on
  BOOLEAN;
let Key be Element of 128-tuples_on
  BOOLEAN;
func AES128-ENC(SBT,message,Key) ->
  Element of 128-tuples_on BOOLEAN
```

```
equals
(AES-Statearray").(AES-ENC(SBT,MixColumns,
  AES-Statearray.message,AES-Statearray.
  Key));
```

□

Here, AES-Statearray" is the inverse of AES-Statearray.

Next, we formalize the decryption algorithm of AES–128 as a functor in the Mizar language as follows:

Definition 6.3: (AES–128 decryption algorithm)

```
let SBT be Permutation of (8-tuples_on
  BOOLEAN);
let cipher be Element of 128-tuples_on
  BOOLEAN;
let Key be Element of 128-tuples_on
  BOOLEAN;
func AES128-DEC(SBT,cipher,Key) ->
  Element of 128-tuples_on BOOLEAN
equals
(AES-Statearray").(AES-DEC(SBT,MixColumns,
  AES-Statearray.cipher,AES-Statearray.
  Key));
```

□

Finally, we then prove the following theorem:

Theorem 6.2: (Correctness of AES–128)

```
for SBT be Permutation of (8-tuples_on
  BOOLEAN),
message,Key be Element of 128-tuples_on
  BOOLEAN
holds
AES128-DEC(SBT,AES128-ENC(SBT,message,Key),
  Key) = message
```

□

We similarly formalized AES–192 and AES–256 using our formalization of the AES primitives and the generalized AES algorithm.

Thus, we proved using the Mizar system that the ciphertext encoded by the AES algorithm can be decoded uniquely with the same secret key that was used in encryption.

7. Conclusion

In this paper, we introduced our formalization of the AES algorithm in Mizar. We also proved the correctness of the AES algorithm using the Mizar proof checking system as a formal verification tool. Currently, we are analyzing the cryptographic systems using our formalization in order to achieve the security proof of cryptographic systems.

Acknowledgments

This work was supported by JSPS KAKENHI 21240001 and 22300285. We sincerely thank Prof. Kaneko at the Tokyo University of Science for his helpful discussions about AES.

References

[1] *Mizar Proof Checker*. *Available at* http://mizar.org/.

[2] U.S. Department of Commerce/National Institute of Standards and Technology, *FIPS PUB 46-3, DATA ENCRYPTION STANDARD (DES)*, Federal Information Processing Standars Publication, 1999. *Available at* http://csrc.nist.gov/publications/fips/fips46-3/fips46-3.pdf.

[3] H.Okazaki, K.Arai, and Y.Shidama, *Formal Verification of DES Using the Mizar Proof Checker*, Proceedings of the 2011 International Conference on Foundations of Computer Science (FCS'11), pp.63–68, 2011.

[4] U.S. Department of Commerce/National Institute of Standards and Technology, *FIPS PUB 197, Advanced Encryption Standard (AES)*, Federal Information Processing Standars Publication, 2001. *Available at* http://csrc.nist.gov/publications/fips/fips197/fips-197.pdf.

[5] NIST Special Publication 800-67 Version 1.1, *Recommendation for the Triple Data Encryption Algorithm (TDEA) Block Cipher*, National Institute of Standards and Technology, 2008. *Available at* http://csrc.nist.gov/publications/nistpubs/800-67/SP800-67.pdf.

[6] E.Bonarska, *An Introduction to PC Mizar*, Mizar Users Group, Fondation Philippe le Hodey, Brussels, 1990.

[7] M.Muzalewski, *An Outline of PC Mizar*, Fondation Philippe le Hodey, Brussels, 1993.

[8] Y.Nakamura, T.Watanabe, Y.Tanaka, and P.Kawamoto, *Mizar Lecture Notes (4th Edition)*, Shinshu University, Nagano, 2001. *Available at* http://markun.cs.shinshu-u.ac.jp/kiso/projects/proofchecker/mizar/index-e.html.

[9] A.Grabowski, A.Kornilowicz, and A.Naumowicz, *Mizar in a Nutshell*, Journal of Formalized Reasoning 3(2), pp.153–245, 2010.

[10] J.Daemen and V. Rijmen, *The block cipher Rijndael*, Smart Card research and Applications, LNCS 1820, Springer-Verlag, pp.288–296, 2000.

Appendix

Definition A. 1: (InvSubBytes)

```
let SBT be Permutation of (8-tuples_on BOOLEAN);
func InvSubBytes(SBT) ->
  Function of 4-tuples_on (4-tuples_on (8-tuples_on BOOLEAN)),
  4-tuples_on (4-tuples_on (8-tuples_on BOOLEAN))
means
for input be Element of 4-tuples_on (4-tuples_on (8-tuples_on BOOLEAN))
holds
for i,j be Nat st i in Seg 4 & j in Seg 4
holds
ex inputij be Element of 8-tuples_on BOOLEAN
st inputij = (input.i).j & ((it.input).i).j = (SBT").(inputij);
```

□

Definition A. 2: (InvShiftRows)

```
func InvShiftRows ->
  Function of 4-tuples_on (4-tuples_on (8-tuples_on BOOLEAN)),
  4-tuples_on (4-tuples_on (8-tuples_on BOOLEAN))
means
for input be Element of 4-tuples_on (4-tuples_on (8-tuples_on BOOLEAN))
holds
(for i be Nat st i in Seg 4 holds ex xi be Element of 4-tuples_on
  (8-tuples_on BOOLEAN) st xi = input.i & (it.input).i = Op-Shift(xi,i-1));
```

□

Definition A. 3: (InvMixColumns)

```
func InvMixColumns ->
  Function of 4-tuples_on(4-tuples_on (8-tuples_on BOOLEAN)),
  4-tuples_on (4-tuples_on (8-tuples_on BOOLEAN))
means
for input be Element of 4-tuples_on (4-tuples_on (8-tuples_on BOOLEAN))
holds
ex x,y being Element of 4-tuples_on (4-tuples_on (8-tuples_on BOOLEAN))
st x = input & y = it.input & for i be Element of NAT st i in Seg 4
holds
ex x1,x2,x3,x4 be Element of 8-tuples_on BOOLEAN
st x1 = (x.i).1 & x2 = (x.i).2 & x3 = (x.i).3 & x4 = (x.i).4 &
(y.1).i = Op-XOR(Op-XOR(Op-XOR(14 'gf' x1,11 'gf' x2),13 'gf' x3),9 'gf' x4) &
(y.2).i = Op-XOR(Op-XOR(Op-XOR(9 'gf' x1,14 'gf' x2),11 'gf' x3),13 'gf' x4) &
(y.3).i = Op-XOR(Op-XOR(Op-XOR(13 'gf' x1,9 'gf' x2),14 'gf' x3),11 'gf' x4) &
(y.4).i = Op-XOR(Op-XOR(Op-XOR(11 'gf' x1,13 'gf' x2),9 'gf' x3),14 'gf' x4);
```

□

Definition A. 4: (AES-DEC)

```
let SBT be Permutation of (8-tuples_on BOOLEAN);
let MCFunc be Permutation of 4-tuples_on (4-tuples_on (8-tuples_on BOOLEAN));
let m be Nat;
let text be Element of 4-tuples_on (4-tuples_on (8-tuples_on BOOLEAN));
let Key be Element of m-tuples_on (4-tuples_on (8-tuples_on BOOLEAN));
assume 4 <= m;
func AES-DEC(SBT,MCFunc,text,Key) ->
  Element of 4-tuples_on (4-tuples_on (8-tuples_on BOOLEAN))
means
ex seq be FinSequence of (4-tuples_on (4-tuples_on (8-tuples_on BOOLEAN)))
st len seq = 7+m-1 & (ex Keyil be Element of 4-tuples_on (4-tuples_on
  (8-tuples_on BOOLEAN)) st Keyil = (Rev((KeyExpansion(SBT,m)).(Key))).1 &
  seq.1 = (InvSubBytes(SBT)*InvShiftRows).(AddRoundKey.(text,Keyil))) &
(for i be Nat st 1 <= i & i < 7+m-1 holds
  ex Keyi be Element of 4-tuples_on (4-tuples_on (8-tuples_on BOOLEAN))
  st Keyi = (Rev((KeyExpansion(SBT,m)).(Key))).(i+1) &
  seq.(i+1) = (InvSubBytes(SBT)*InvShiftRows*(MCFunc")).(AddRoundKey.
  (seq.i,Keyi))) &
ex KeyNr be Element of 4-tuples_on (4-tuples_on (8-tuples_on BOOLEAN))
st KeyNr = (Rev((KeyExpansion(SBT,m)).(Key))).(7+m) &
it = AddRoundKey.(seq.(7+m-1),KeyNr);
```

□

Mathematical Approaches for Collision Detection in Fundamental Game Objects

Weihu Hong[1] , Junfeng Qu[2], Mingshen Wu[3]
[1] Department of Mathematics, Clayton State University, Morrow, GA, 30260
[2] Department of Information Technology, Clayton State University, Morrow, GA, 30260
[3]Department of Mathematics, Statistics, and Computer Science, University of Wisconsin-Stout, Menomonie, WI 54751

Abstract – *This paper presents mathematical solutions for computing whether or not fundamental objects in game development collide with each other. In game development, detection of collision of two or more objects is often brought up. By categorizing most fundamental boundaries in game object, this paper will provide some mathematical fundamental methods for detection of collisions between objects identified. The approached methods provide more precise and efficient solutions to detect collisions between most game objects with mathematical formula proposed.*

Keywords: *Collision detection, algorithm, sprite, game object, game development.*

1 Introduction

The goal of collision detection is to automatically report a geometric contact when it is about to occur or has actually occurred. It is very common in game development that objects in the game science controlled by game player might collide each other. Collision detection is an essential component in video game implementation because it delivers events in the game world and drives game moving though game paths designed.

In most game developing environment, game developers relies on written APIs to detect collisions in the game, for example, XNA Game Studio from Microsoft, Cocoa from Apple, and some other software packages developed by other parties. Most open source or proprietary game engines supports collision detection, such Unreal, C4, Havok, Unity etc. However, a primary limitation of game development kits or game engines is the precision is too low, and the collision detection approaches are limited in the package.

Since the advent of computer games, programmers have continually devised ways to simulate the world more precisely. It's very often that programmers need to develop their own collision detection algorithms for a higher precision and performance.

The most basic approach is collision detection of the sprite or boundary class which represents an object in the game scenes and is often rectangle, sphere, or cube. This approach works well if the object that is represented by is a simple shape and there is almost no blank space between object and the image. Otherwise, a lot of false alarm will be introduced in collision detection as show in Figure 1, where two objects, one circle and one pentagon, are not collided at all even the represented sprites collide each other.

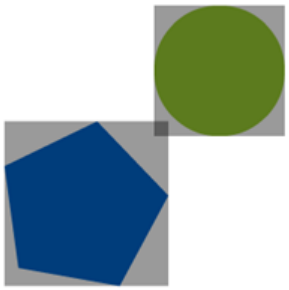

Figure 1. Collision detection based on Boundary

(a) (b)

Figure 2. Per-Pixel based collision detection

Per-pixel collision detection is a relic from the past. It uses bit-masks to determine whether two objects collide. The biggest advantages of using this detection method are that it also checks the empty space within the objects boundaries, and collision is detected with high precision as pixel-perfect and fair, there are no false positives nor false negatives as shown in Figure 2, where (a) shows the improved per-pixel detection, and (b) shows correct collision happed when two object contacting each other. The main disadvantage is that it's expensive to compute, and is extremely slow compared to bounding boxes and it won't work if you do any transformations on the target objects such as rotating, or resizing. For example, if viewable sprites are 32x32 pixels. In order to check collision, the program needs to check 32X32x32x32 pixels with each pass to find out if a single pixel of a 32x32 frame of the sprite sheet has collided with

another image. Therefore per-pixel collision checks are rarely used, especially because object visible shape and collision shape are usually different.

In computational geometry, there is a point-in-polygon (PIP) problem that asks whether a given point in the plane lies inside, outside, or on the boundary of a polygon. It is a special case of point location problems and finds applications in areas that deal with processing geometrical data, such as computer graphics, computer vision, geographical information systems (GIS), motion planning, and CAD. The Ray Casting method is one simple way of finding whether the point is inside or outside a simple polygon by testing how many times a ray, starting from the point and going any fixed direction, intersects the edges of the polygon. If the point in question is not on the boundary of the polygon, the number of intersections is an even number; if the point is outside, and it is odd if inside (see [1] to [12]).

However, the detection of collision problem is different from the PIP problem. We are not interested in whether a point inside or outside of a polygon. We are just interested in a collision occurs or not. Therefore, it is not good idea to use the Ray Casting method in our collision detection problem.

There are a lot of work have been done to improve collision detection For example to solve the performance issues with per-pixel algorithm, space partition algorithms has been used, such as Quadtree or Octree. Reference [13] to [23] has listed a spectrum of researches in collision detection.

In this paper, we proposed mathematic solutions for collision of each fundamental game object shape identified. The approach is not based on the bounding of the sprite, but the collision detection is based on the bounding shape which represents the game object with minimum empty space between the object and bounding shape. The approach works as follows. For each object that in the game scene, define a fundamental geometric shape or combination of fundamental geometric shaped that encloses its texture. The fundamental shapes that are identified in the research including: point, segment, squares, rectangles, triangles or circles. The following figure shows some example of bounding shapes for some sprites for example.

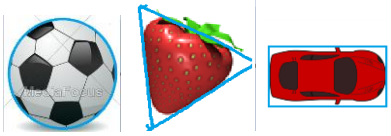

Figure 3. Bounding Shape of Circle, Triangle, and Rectangle in Game.

By defining the bounding shape for a game object, once we have mathematical solution for collision detection of bounding shape, it should be easily accommodate sizing and rotating, it also provides better accuracy of collision detection without performance sacrificing of check each pixel. We believe that our method for detection of collision between two triangles is easier to implement than some of existing methods. To represent a complicated visual object, a different combination of fundamental bounding shapes can be used together.

2 Collision detection of bounding shapes

Here upon, we will refer our defined bounding shape of a visible object as an object. Let us consider collision between an object in motion and another object in still.

2.1 Between two points

Let P be fixed with coordinates (x, y, z) and Q be point in motion. If the motion of Q is given in $u = u(t)$, $v = v(t)$, and $w = w(t)$, then P and Q will be collided if and only if there exists a real number t such that

$$u(t) = x, v(t) = y, and\ w(t) = z.$$

2.2 Between a line segment and a point in a plane

Let L be a fixed line segment with end points A and B and Q be the point in motion as shown in Figure 4. Let $(x_0, y_0)\ and\ (x_1, y_1)$ be coordinates of A and B, respectively. If the motion of Q is given by $u = u(t)$, $v = v(t)$, and the line segment L is given by $px + qy + c = 0$, then Q will collide with L if and only if there exists a real number t such that

$$pu(t) + qv(t) + c = 0$$

And

$$= \sum_{k=0}^{1} \frac{\sqrt{(x_1 - x_0)^2 + (y_1 - y_0)^2}}{\sqrt{(u(t) - x_k)^2 + (v(t) - y_k)^2}}$$

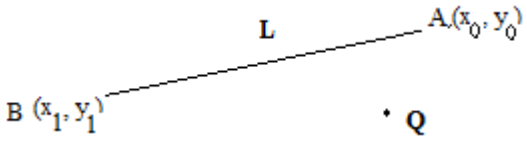

Figure 4

2.3 Between a circle and a point in a plane

As indicated in Figure 5, let's consider a circle ʘC with center $C(a, b)$ and radius of r. Let Q be the point in motion. Then Q will collide with the circle if and only if there exists a real number t, such that

$$(u(t) - a)^2 + (v(t) - b)^2 = r^2$$

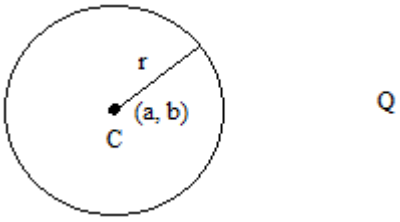

Figure 5

We can generalize it to three dimensional case: if Q is the point in motion in space, let Q be given by (*u(t), v(t), w(t)*) and a sphere with center at (a, b, c) and radius of r as shown in Figure 6. Then Q will collide with the sphere if and only if there exists a real number t such that

$$(u(t)-a)^2+(v(t)-b)^2+(w(t)-c)^2=r^2$$

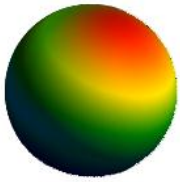

Figure 6

2.4 Between a triangle and a point

Let us consider a triangle with the set of vertices $\{(x_k, y_k): k = 1,2,3\}$ as shown in Figure 7.

Assume Q is the point in motion with coordinates $(u(t), v(t))$ Then point Q will collide with the triangle if and only if

$$\sum_{k=1}^{3}\left|(x_{h(k)}-x_k)(v(t)-y_k)-(y_{h(k)}-y_k)(u(t)-x_k)\right| = \left|\begin{vmatrix} x_1 & y_1 & 1 \\ x_2 & y_2 & 1 \\ x_3 & y_3 & 1 \end{vmatrix}\right|$$

Where h(k) = k+1 if k =1, 2; 1 if k=3.

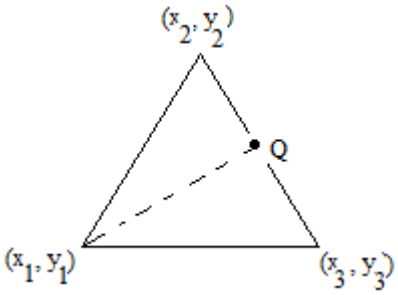

Figure 7

2.5 Between a polygon and a point

Let us consider a rectangle $\{(x,y): a \le x \le b, c \le y \le d\}$ and Q as point in motion. Then point Q(u, v) will collide with the rectangle if and only if there exists a real number t such that

$$a \le u(t) \le b \; and \; c \le v(t) \le d.$$

If the rectangle does not have sides that are parallel to the axes, then the above detection will not work. In this case, we can use the following criteria. Assume the rectangle has area T with consecutive vertices $(x_k, y_k), k = 1,2,3,4$. Then Q will collide with the rectangle if and only if there exists a real number t such that

$$\sum_{k=1}^{4}\left|\begin{vmatrix} u(t) & v(t) & 1 \\ x_k & y_k & 1 \\ x_{h(k)} & y_{h(k)} & 1 \end{vmatrix}\right| = 2T$$

This is based on the fact that the total area formed by Q with any two consecutive vertices of the rectangle equals to the area of the rectangle. Where h(k) = k + 1 if k =1, 2, 3; 1 if k=4.

As we can see that the problem of detection of collision is different from the PIP that is to determine whether a point is inside a polygon (PIP). Therefore, it is not a good idea to use the method of Ray Casting (see [1] and [2], [12]) because it needs to find number of intersections with the boundary of the polygon, which will be time-consuming.

2.6 Between a set of polygon and a point

If an object is consisting of a set of non-overlapping polygons as shown in Figure 8, then we can use the method given in previous section to check each of polygons involved. If an object is consisting of a large polygon and some small polygons that are contained in the large polygon as shown in Figure 9, then we can use the above method to check the large polygon if we just need to determine whether the point Q will collide the object. If we need determine whether the point will collide with small polygons, then we can apply the method to check the small polygons.

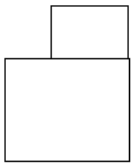

Figure 8

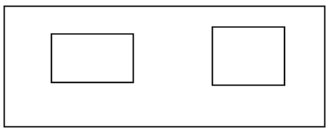

Figure 9

2.7 Between two line segments

Let us consider two line segments $L_k, k = 1,2$ as shown in Figure 10. It is easy to verify that these two segments intersect if and only if $d = \begin{vmatrix} x_1 - x_0 & y_0 - y_1 \\ x_1' - x_0' & y_0' - y_1' \end{vmatrix} \neq 0$ and $\min\{x_0, x_1\} \le \bar{x} \le \max\{x_0, x_1\}$ and $\min\{x_0', x_1'\} \le \bar{x} \le \max\{x_0', x_1'\}$ *and* $\min\{y_0, y\} \le \bar{y} \le \max\{y_0, y_1\}$ *and* $\min\{y_0', y_1'\} \le \bar{y} \le \max\{y_0', y_1'\}$.Where the intersection point $(\bar{x}, \bar{y})$ can be found by Cramer's rule, in fact, $\bar{x} = \frac{\begin{vmatrix} x_1-x_0 & y_0x_1-y_1x_0 \\ x_1'-x_0' & y_0'x_1'-y_1'x_0' \end{vmatrix}}{d}$, and $\bar{y} = \frac{\begin{vmatrix} y_0x_1-y_1x_0 & y_0-y_1 \\ y_0'x_1'-y_1'x_0' & y_0'-y_1' \end{vmatrix}}{d}$.

If $d = 0$, it means these two line segments are parallel. If any three end points of them form a triangle with non-zero area, then they don't collide. Otherwise, they collide. That is, if $d = 0$ *and*

$$\begin{vmatrix} x_0 & y_0 & 1 \\ x_0' & y_0' & 1 \\ x_1 & y_1 & 1 \end{vmatrix} = 0$$

Then they collide.

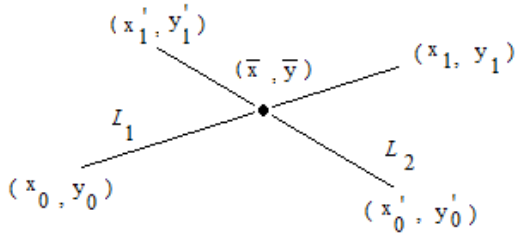

Figure 10

2.8 Between one triangle and a line segment

Consider a triangle with the set of vertices $\{(x_k, y_k): 1 \le k \le 3\}$ and a line segment L with end points A and B as shown in Figure 11. To check for any collision between the line segment and the triangle, we can perform a loop for each side of the triangle and the segment L by applying the method given in section 2.7. If the line segment does not intersect any side of the triangle, we just need check whether it lies entirely inside the triangle by checking one of the end points of L by using the method given in section 2.4 above.

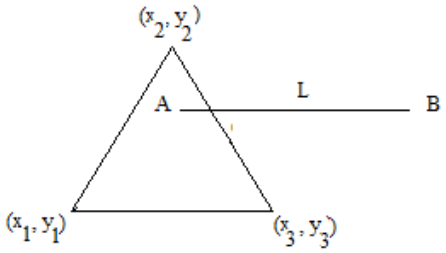

Figure 11

2.9 Between two triangles both in motion

Consider triangles $T_k\ (k = 1,2)$ with the sets of vertices $S_k = \{(x_j^k, y_j^k): 1 \le j \le 3\}, (k = 1,2)$ as shown in Figure 12. To check for any collision between these two triangles, we can perform a loop for each side of $T_1$and consider that side and the triangle T_2 by applying the method given in section 2.8.

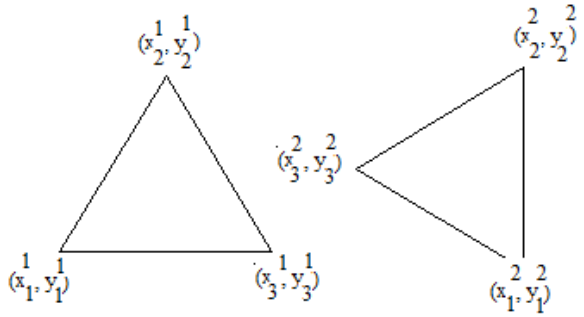

Figure 12

2.10 Between two line segments in space

Consider two line segments in space as shown in Figure 10.

$L_k(t) = (x_k, y_k, z_k) + t < p_k, q_k, r_k >, t \in [0,1]; k = 1,2.$

It is well known that

$$L_1 || L_2 \ if \ and \ only \ if \ \frac{p_1}{p_2} = \frac{q_1}{q_2} = \frac{r_1}{r_2}$$

And

$$If\ L_1\ and\ L_2\ are\ not\ parallel, then$$
$$they\ intersect\ if\ and\ only\ if$$
$$\begin{vmatrix} x_2 - x_1 & y_2 - y_1 & z_2 - z_1 \\ p_1 & q_1 & r_1 \\ p_2 & q_2 & r_2 \end{vmatrix} = 0\ and\ \exists t \in [0,1] \text{ such that}$$
$$(p_2 - p_1)t = x_1 - x_2$$
$$(q_2 - q_1)t = y_1 - y_2$$
$$(r_2 - r_1)t = z_1 - z_2$$

Therefore, we can detect whether two line segments collide as follows.

(1) Check to see if two line segments are parallel. If they are parallel, then check $\vec{u} \times \vec{v}$, where $\vec{u} =< p_1, q_1, r_1 >$, and $\vec{v} =< x_2 - x_1, y_2 - y_1, z_2 - z_1 >$. If $\vec{u} \times \vec{v} = \vec{0}$, then the line segments collide. Otherwise, they don't collide.

(2) If they are not parallel, then check the determinant If $\begin{vmatrix} x_2 - x_1 & y_2 - y_1 & z_2 - z_1 \\ p_1 & q_1 & r_1 \\ p_2 & q_2 & r_2 \end{vmatrix} = 0$, then find the value of t. If $t \in [0,1]$, then they intersect. Otherwise, they don't intersect.

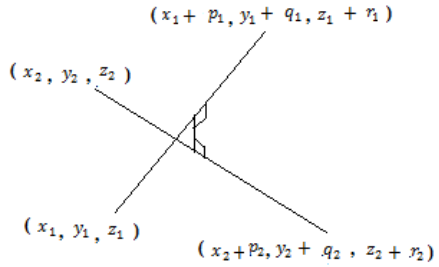

Figure 13

2.11 Between a triangle and a line segment in space

Consider a triangle and a line segment L. To check for any collision between the line segment and the triangle, we can perform a loop for each side of the triangle and the segment L by applying the method given in section 2.10. If L does not collide with any side of the triangle, we need check whether it lies entirely inside triangle by applying the method given in section 2.4 or it might penetrate the surface of the triangle by checking the signs of $\vec{n} \cdot \overrightarrow{u_1}$ *and* $\vec{n} \cdot \overrightarrow{u_2}$, where $\vec{n}$ is the normal vector of the triangle surface, $\overrightarrow{u_k}\ (k = 1,2)$ are vectors with one of the end points of L as an initial point and the point P as the terminal point, where the point P is defined as $P = \left(\frac{1}{3}\sum_{k=1}^{3} x_k, \frac{1}{3}\sum_{k=1}^{3} y_k, \frac{1}{3}\sum_{k=1}^{3} z_k\right)$, which lies on the surface of the triangle with vertices $V_k\ (k = 1,2,3)$. If the signs of $\vec{n} \cdot \overrightarrow{u_1}$ *and* $\vec{n} \cdot \overrightarrow{u_2}$ are different, then we need check to see if the distance from the point P to L is less than the $\min\{d(P, V_k): k = 1,2,3\}$. If it is true, then L penetrates the surface of the triangle, otherwise, it does not penetrate.

2.12 Between two triangles in space

Consider triangles $T_k\ (k = 1,2)$. To check for any collision between these two triangles, we can perform a loop for each side of T_1 and consider that side and the triangle T_2 by applying the method given in section 2.11.

3 Conclusions and Future Work

This paper has presented some mathematical solution for some fundamental bounding shape in game collision detection in 2D and 3D. Our method is easy to implement without a lot of performance issues in per-pixel based algorithm, but the accuracy and precision improved greatly compared with pixel based collision detection mechanism.

In the future, collision between combination of different fundamental bounding shape and their represented visual object will be studied.

4 References

[1] Ivan Sutherland et al.,"A Characterization of Ten Hidden-Surface Algorithms" 1974, *ACM Computing Surveys* vol. 6 no. 1.

[2] "Point in Polygon, One More Time..." (http://jedi.ks.uiuc.edu/~johns/raytracer/rtn /rtnv3n4.html#art22), *Ray Tracing News*, vol. 3 no. 4, October 1, 1990.

[3] C code to determine if a point is in a polygon http://www.ecse.rpi.edu/Homepages/wrf /research/geom/pnpoly.html)

[4] C code for an algorithm using integers and no divides (http://www.visibone.com/inpoly/)

[5] Google Maps Point in Polygon JavaScript extension (http://appdelegateinc.com/blog/2010/05/16/point-in-polygon-checking)

[6] Geometry Engine Open Source (GEOS) (http://trac.osgeo.org/geos/) based on Java Topology Suite (JTS)

[7] Python Shapely package (http://pypi.python.org/pypi/Shapely) based on GEOS

[8] GeoDjango geographic web framework plugin (http://geodjango.org/) for the Django web framework

[9] SQL code to determine if a point is in a polygon (http://www.sql-statements.com/point-inpolygon.html)

[10] Pascal code to verify if a point is inside a polygon (http://wiki.lazarus.freepascal.org/Geometry_in_Pascal #Checking_if_a_point_is_inside_a_poly

[11] Fortran implementation of an improved version of the Nordbeck and Rystedt algorithm (http://www.newcastle.edu.au/Resources /Research%20Centres/CGMM/Publications/Scott% 20Sloan/A%20point%20in%20polygon %20program.pdf)

[12] Point in polygon - Wikipedia, the free encyclopedia Page 1 of 3, http://en.wikipedia.org/wiki/

[13]. Barequet G, Chazelle B, Guibas LJ, Mitchell J, Tal A. BOXTREE: a hierarchical representation for surfaces in 3D. In Proceedings of Eurographics, 1996; pp. 387–396.

[14]. Cohen J, Lin M, Manocha D, Ponamgi K. I-COLLIDE: An interactive and exact collision detection system for Largescaled environments. In Proceedings of the 1995 Symposium on Interactive 3D graphics; pp. 189–196.

[15]. Dobkin DP, Kirkpatrick DG. Fast detection of Polyhedral intersection. Theoretical Computer Science, 1983; 27: 241–253.

[16]. Gottschalk S, Lin MC, Manocha D. OBBTree: a Hierarchical structure for rapid interference detection. SIGGRAPH'96: Proceedings of the 23rd annual conference on Computer graphics and interactive techniques ACM SIGGRAPH 1996; 30: 171–180.

[17]. Klosowski JT, Held M, Mitchell JSB. Evaluation of Collision detection methods for virtual reality fly-throughs. The 7th Canad. Conf. Computat. Geometry 1995; 14: 36–43(2): 205–210.

[18]. Gottschalk S, Lin M. Collision detection between Geometric models: a survey. In Proceedings of IMA Conference on Mathematics of Surfaces 1998; pp. 3–15.

[19]. Floriani De L, Puppo E, Magillo P. Applications of Computational Geometry to Geographic Information Systems, chapter 7, Elsevier Science & Technology: 1999; 333–388.

[20]. Mo¨ ller T. A fast triangle-triangle intersection test. Journal of Graphics Tools, 1997; 2(2): 25–30.

[21]. Held M. ERIT a collection of efficient and reliable Intersection tests. Journal of Graphics Tools 1997; 2(4): 25–44.

[22]. Guigue P, Devillers O. Fast and robust triangle-triangle overlap test using orientation predicates. Journal of Graphics Tools 2003; 8(1): 25–42.

[23]. Devillers O, Guigue P. Faster triangle-triangle Intersection tests. Technical Report 4488, INRIA, 2002.

[24]. Shen H, Heng PA, Tang Z. A fast triangle-triangle Overlap test using signed distances. Journal of Graphics Tools 2003; 8(1): 3–15.

[25]. http://www.cs.unc.edu/?geom/obb/obbt.html.

Kopenograms – Graphical Language for Structured Algorithms

Jiří Kofránek[1], Rudolf Pecinovský[2], Petr Novák[3]
[1]Charles University in Prague, Laboratory of Biocybernetics, Prague, Czech Republic
[2]University of Economics, Dept. of Information Technologies, Prague, Czech Republic
[3]HID Global, Prague, Czech Republic

Abstract - *In the OOP era of the present times, it tends to be forgotten sometimes that the design of rather complex algorithms may be ahead of us at the end of object analysis. Several graphical languages are available for their representation. Kopenograms are one of the clearest ways how to represent structured algorithms. They are an apt supplement of UML diagrams used to show algorithmic structures, and they have proven themselves as a very effective tool in programming classes.*

Keywords: Education, Graphical language, Algorithms, Programmiong methodology, UML

1 Introduction

Kopenograms are one of graphical ways of representing algorithms and data. The acronym ***KOPENOGRAM*** expresses the fundamental idea of this graphical representation: ***K**eep **O**ur **P**rogram in **E**mbedded **N**oted **O**blongs for **G**raphical **R**epresentation of **A**lgorithmic **M**odules.*

The original idea of graphical representation of algorithms emerged in the 80ies of the past century, in a discussion of three programmers (Kofránek, Novák, Pecinovský), as a reaction to the defects of existing ways of structured representation of algorithms and data structures (such as flowcharts [1], Jackson diagrams [2, 3], Nassi-Schneiderman diagrams [4] etc.). However, it became apparent soon that the chosen notation can also be used for visually clear demonstration of algorithm and data structuring in teaching. Named kopenograms (originally a temporary name composed of the surnames of the authors) [5] in the then Czechoslovakia and later in the Czech and Slovak Republics, these diagrams started to be used as a teaching aid both for the teaching of programming essentials, e.g. using the programming language Karel [6, 8], and also for the teaching of more advanced programming methods (8-15).

Block is a basic term in any kopenogram, and it means a certain part of the program. A block may be data declaration, class, procedure, function, statement, etc. Every block is shown as a rectangle.

The graphical language of kopenograms includes expression means for writing algorithmic structures as well as data structures. However, UML is now used as standard for writing data structures. Therefore in our contribution, we shall focus only on describing how those algorithmic structures are written for which no diagram is offered by UML that could display them, without "seducing" the developer to using non-structured statements.

2 Algorithmic Structure Blocks

Some blocks exhibit more complex inner structure.:

- **Header** is the upper part of the block divided from the rest of the block using a single or double line. If divided using a double line, it contains the name of the block; if divided using a single line, it contains the input condition of the block.
- **Footer** is the lower part of the block divided using a single line in algorithmic blocks. The footer denotes the end of the body of the cycle and contains the so called output condition of the cycle.
- **Qualification** is the left part of the block, separated using a single vertical line in algorithmic blocks; this part contains access operation for the components of a structured constant or variable.
- **Body** of the block is the remaining part of the block between any header and footer, right of any qualification.
- **Dividing bar** is a special part within the body of the block; this part may contain a condition causing leaving the body of the block prematurely.
- **Compound block** has a body with embedded blocks.
- **Block with several bodies** is a compound block that incorporates several bodies, immediately adjacent horizontally, and separated by single vertical lines.

2.1 Colors

Initially, kopenograms were designed so that the color provides additional information, similarly as colored highlighting of the syntax started to be used later. Colors were assigned to individual types of the blocks and their parts as follows:

- Yellow color is used to fill headers of procedures,

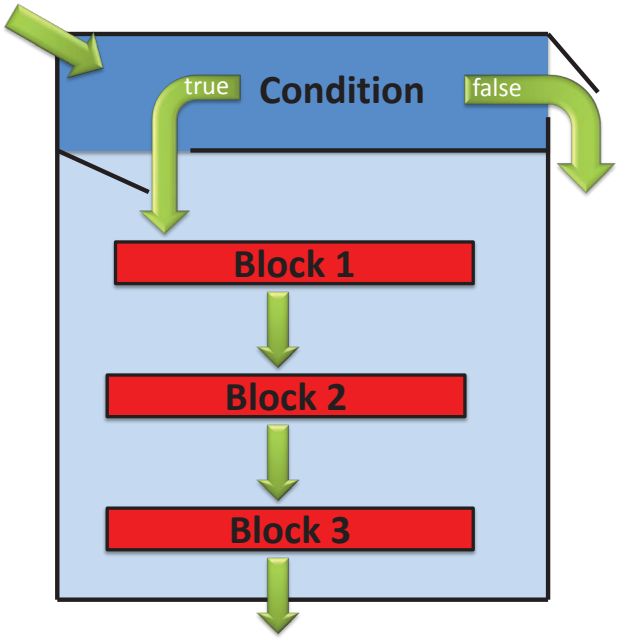

Figure 1: Evaluation flow in kopenogram. Evaluation is started from the upper left corner of the block. If the condition is true, the program continues downward; if false, the program continues to the right.

functions and methods. Yellow is also used to highlight recursive calls.

- Red color is used to fill blocks with actions with the exception of recursive calls, in which case yellow is used as mentioned above.
- Green color is used to fill headers, footers and dividing bars of cycles.
- Blue color is used to fill headers with conditions in conditional statements and switches. It is also used in dividing bars of blocks not used to represent cycles.
- Block qualifications are filled identically as statements, i.e. using red color.

In order to enhance clear arrangement, a lighter shade of the header color is used to fill also the inner area of the given block.

2.2 Comments

Any text written outside a simple block or outside the header, footer and qualification of compound blocks, respectively, is a **comment**. Connecting dashed lines may be used to express relationships of comments to appropriate blocks.

Arrows are a special type of comments; they represent input and output statements. The fact that any data should be input or output, respectively, can be represented by adding an arrow to the right side of a simple block, oriented to the right for the output or to the left for the input, respectively. Then it only remains to write in the block the list of data to be transferred. If the type of the used input/output device or file is to be emphasized, an appropriate schematic mark or name of the file can be drawn to the

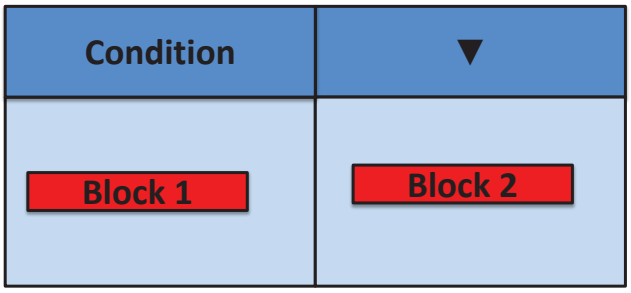

Figure 2: Block of simple alternative "if..then..else".

right of the arrow.

2.3 Compound Blocks

Embedded blocks in the body of a compound block are ordered from the top downward, which illustrates their sequential execution (see Fig. 1).

In compound blocks, the program "grows" toward the inside, thereby naturally limiting the size of defined subprograms. This urges the developer to design simple subprograms.

If any developer feels limited by this characteristic, an analogue of a connector in flowcharts may be used. An empty block can be used as such a connector, with its name put inside. The contents of such a block may be expanded on in another picture. However, in interactive electronic charts, the structure of such an empty block is expanded automatically upon clicking the empty block.

Attaching a qualification from the left to the block and inserting an identifier of any structured variable in the qualification, access operation to appropriate components of the variable can be expressed. These components then become immediately accessible from within the body of the block and all embedded blocks with no need of explicit qualification (analogue of the structure with in Algol, Pascal, Visual Basic, …).

Conditions that affect the run of the program are entered in the header, footer and dividing bars.

Compound conditional block of the type if … then … else can be expressed using a block with one header and two bodies where the condition in the header of the right body will always be true – see Fig. 2. Analogically, a general conditional statement can be represented using a block with several bodies – see Fig. 3.

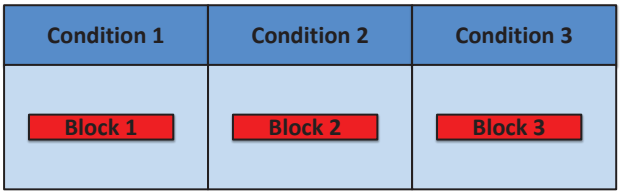

Figure 3: Block of general conditional statement.

Switch or case is a special case of the general conditional statement. Reduced notation according to Fig. 4 is established to eliminate the necessity of writing all condi-

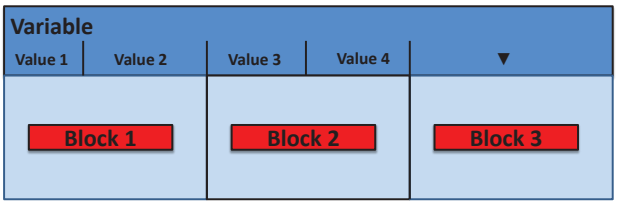

Figure 4: Block of switch statement.

tions in the header as "variable=value".

In some cases, all parts of a block with several bodies may not fit next to each other. If this is the case, individual parts of the block may be placed below each other and connected – see Fig. 5.

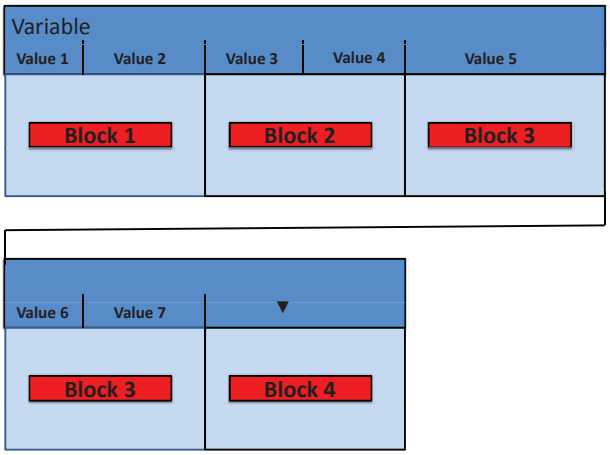

Figure 5: Order individual parts of the block when lack of space.

2.4 Evaluating Conditions

Headers, footers and dividing bars contain conditions that affect further evaluation procedure of the algorithm. The following general rule applies to evaluation of conditions: If the condition is true, the program continues downward; if false, the program continues to the right.

The header contains a condition that determines whether the body of the block will be entered. If true, the program continues downward to the body; if false, the program continues to the right by evaluating the next condition, and in the last condition on the right, by leaving the block and continuing with the subsequent block.

If the body of the block is divided using a dividing bar (see Fig. 6), its condition is evaluated identically. If true,

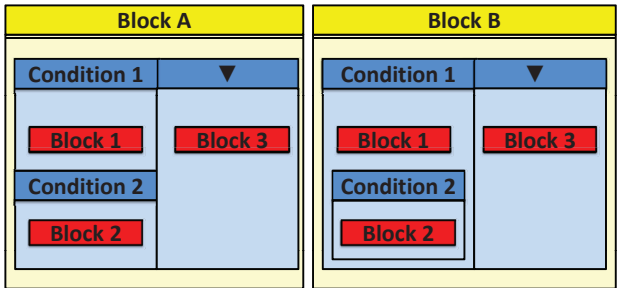

Figure 6: Dividing bar in the block. Algorithms written in blocks A and B are equivalent.

the program continues downward and executes the body of the block; if false, the program continues to the right and if it is the last condition, the block is left.

Blocks representing a cycle contain, besides a header, also a footer. In order to evaluate a condition in the footer, the cycle block can be understood as wound up on a roller. When the footer condition is true, the program does continue downward; however, continuing downward on a roller means evaluating the header again. If the condition is false, the program continues to the right, and if the last condition on the right is false, the cycle block is left (see Fig. 7).

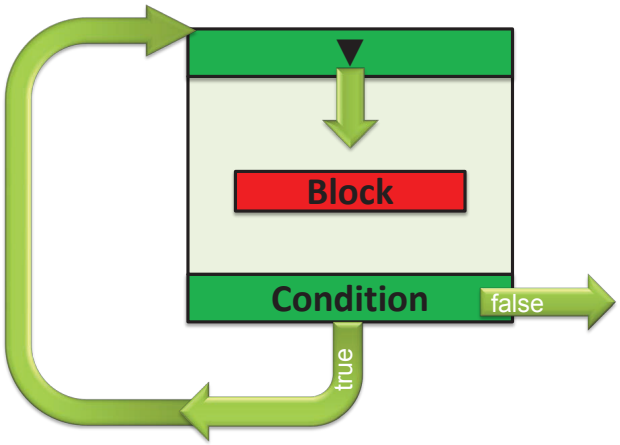

Figure 7: Evaluation flow in the cycle with condition in the footer.

Any condition that is always true should be marked using an arrow oriented downward. However, in the footer such a condition may also be marked using an upward arrow to make the arrangement clearer, given that it returns the program to the beginning of the cycle, thus to the point of header evaluation (see Fig. 8).

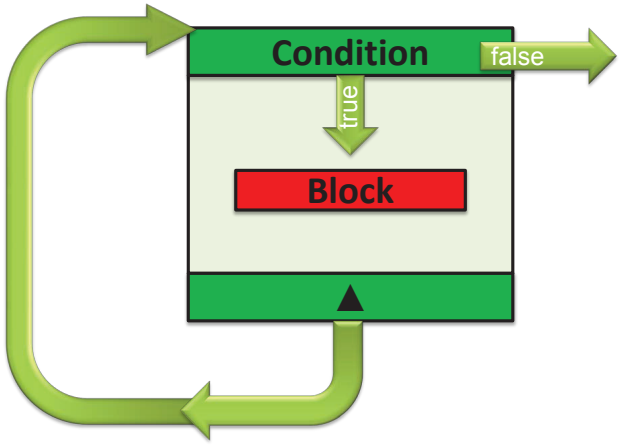

Figure 8: Evaluation flow in the cycle with condition in the header.

This simple way can be used to clearly express how various types of cycles are executed – see Fig. 9.

By dividing the block in several bodies, cycles with several bodies can be easily expressed, which are known from some programming languages. (see Fig. 10)

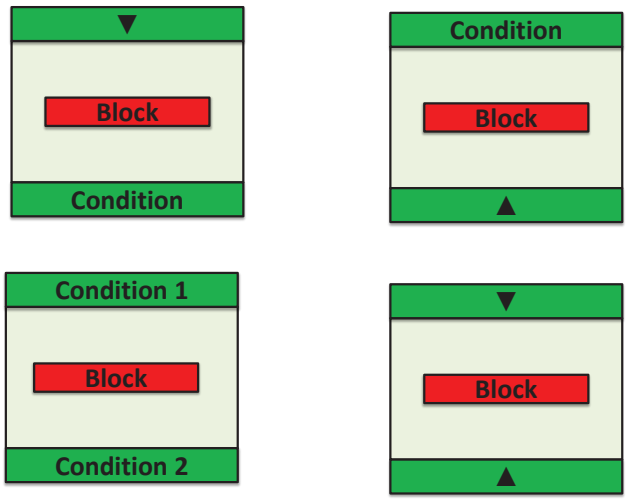

Figure 9: Basic types of cycles.

Input conditions in the header are evaluated identically as in a single-body cycle, i.e. the header is always evaluated from the upper left corner, irrespective of which of the bodies was gone through before. However, output conditions in the footer are evaluated only in the part adjacent to the given body (see Fig. 10). If several bodies share one output condition, such a condition can be represented as their shared footer – see Fig. 11.

In addition, upon adding embedded headers to a multiple-body block, a powerful algorithmic structure is achieved, which makes it possible to arrive at a simple and well-arranged representation of a number of algorithms structured only with difficulty before – see Fig. 21.

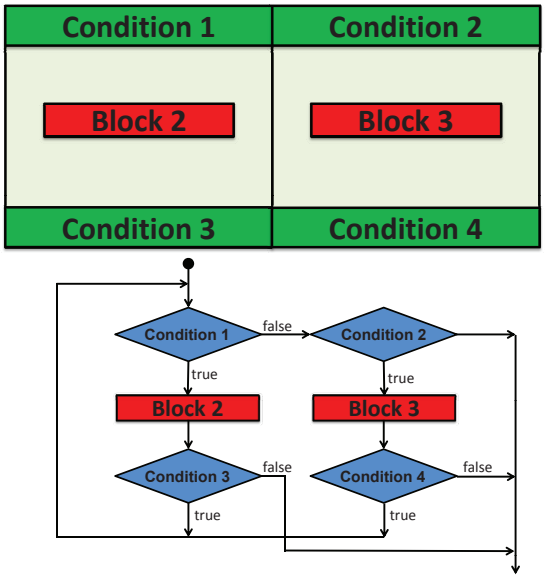

Figure 10: Cycle with several bodies.

2.5 Compound Conditions

Conditions expressed in the header, footer and dividing bar can also exhibit complex structures. A structured condition can be represented as a table whose cells include the tested conditions (see Figs. 12 – 14). These conditions are evaluated based on the following rules:

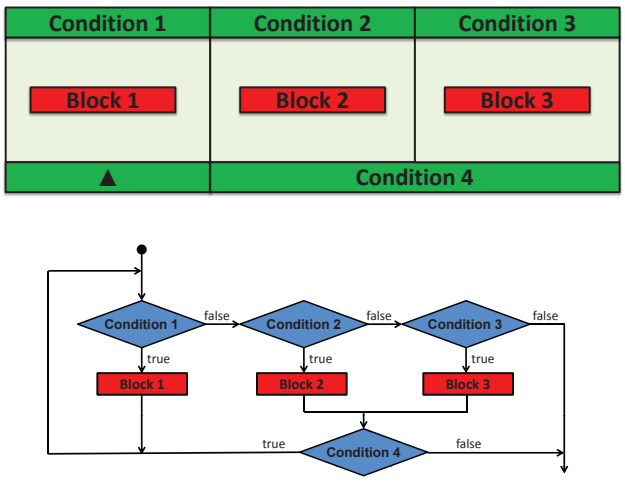

Figure 11: Cycle with several bodies with shared output footer

- Evaluation is started from the upper left corner.
- If the condition is true, the program continues downward.
- If the condition is false, the program continues to the right.
- An empty condition (empty rectangle) is run in the direction in which it was entered (if entered from the left, the rectangle will be left to the left; if entered from above, the rectangle will be left in the downward direction).
- A condition always true is represented using a downward arrow; in the footer, it may also be represented using an upward arrow to enhance the clarity of visual arrangement.
- A condition always false is represented using an arrow to the right.
- If any header or footer is left to the right due to evaluation of the conditions, it means that the whole block is left, as well, and program control is passed on to the next part of the program.
- If a header is left in the downward direction, the body is executed. If a footer is left in the downward direction, evaluation of the header will be the next step (see the analogy with a roller cycle described above).
- If the cycle block is divided in several parts, this division logically continues also in the footer, and evaluation of the footer starts from the upper left corner below the appropriate body. The program returns to the start of the block if the footer is left in the downward direction. The cycle is left if the footer is left to the right or if a bar is encountered while evaluating the conditions, which divides the cycle to individual parts corresponding to different bodies – see Figures 10 and 20.
- Evaluation of the footer in cycles with several bodies is started in the upper left corner again.

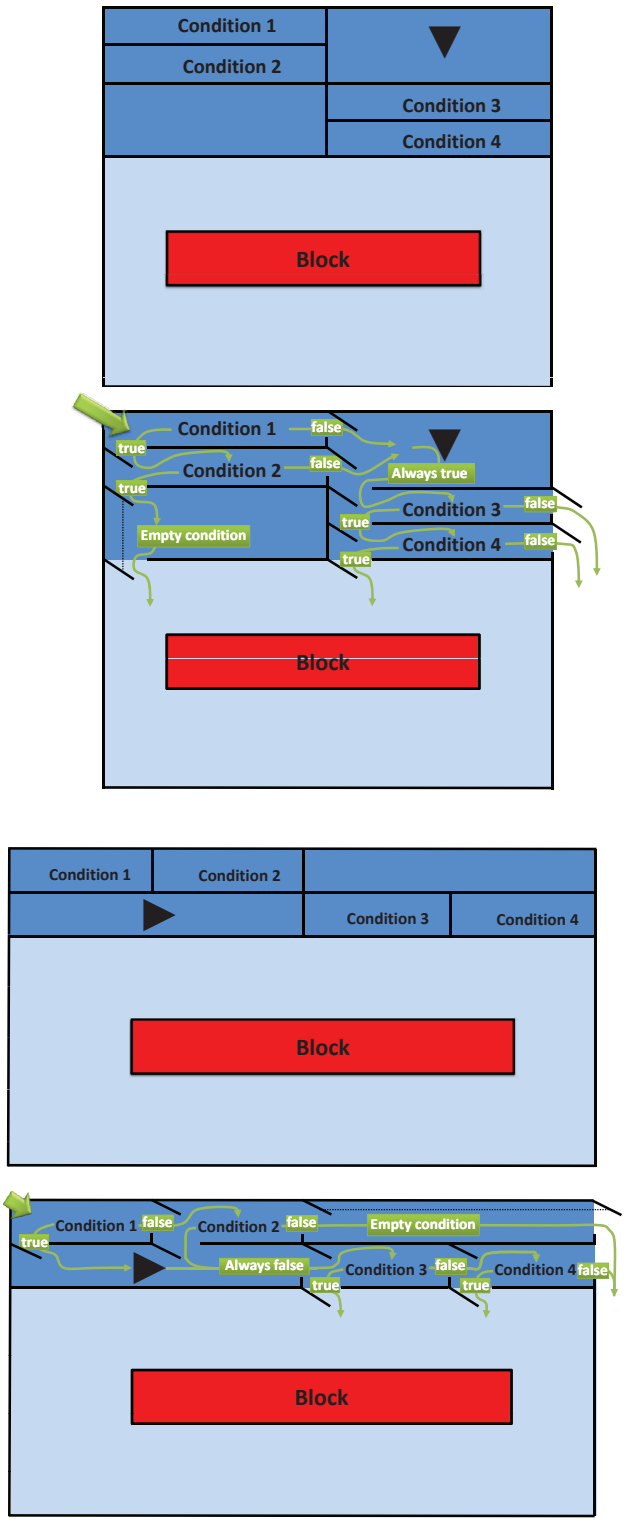

Figure 12: Evaluation flow in structured conditional blocks. Evaluation is started from the upper left corner of the blocks. If the condition is true, the program continues downward; if false, the program continues to the right. A condition always true is represented using a downward arrow; a condition always false is represented using an arrow to the right. An empty condition (empty rectangle) is run in the direction in which it was entered - if empty rectangle entered from the left, the rectangle will be left to the left; if entered from above, the rectangle will be left in the downward direction.

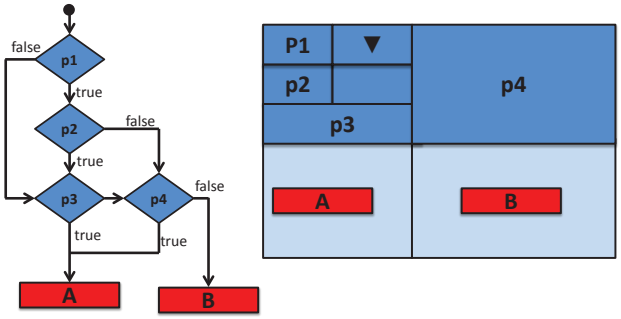

Figure 13: Intricately structured condition in header.

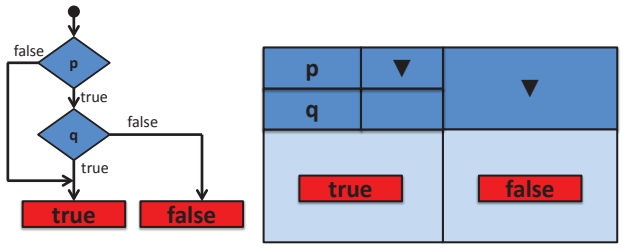

Figure 14: The algorithm evaluation of implication p → q using compound structured conditions.

The cycle is left only if, upon evaluating the conditions, the footer (and thus the whole cycle) is left to the right. If the program falls through the footer in the downward direction, the cycle is not left, and thus the cycle keeps running and the program continues by evaluating the conditions in the header (see Figures 10 and 21).

2.6 Non-Structured Statements

In theory, a structured algorithm is defined as one that observes the following rules:

- Algorithm is formed by a linear sequence of blocks where each has only one input and one output.
- Where a decision is to be made in the program, an equivalent of the block *if ... then ... else* is used.
- Where a part of the code is to be repeated, one of the cycles while or *repeat ... until* is used.

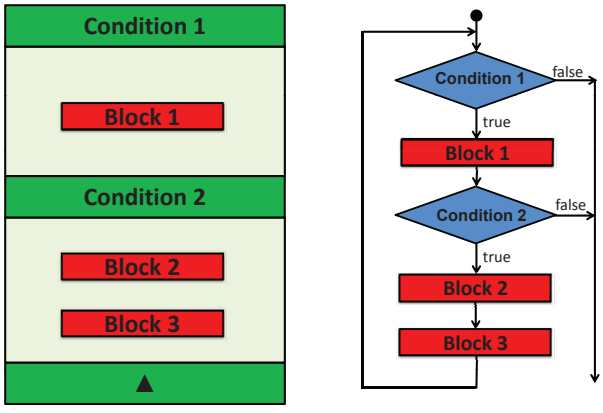

Figure 15: Dividing bar in the cycle.

While it can be proven that every algorithm can be written observing the rules above, in some cases its structure may be easier to understand if some of the rules is violated. Therefore the majority of programming languages offer syntactic structures for such operations.

That is why kopenograms allow for representing typical statements that violate the purity of its structure for the sake of its clear arrangement.

2.6.1 Break

Premature leaving of a block can be represented using a dividing bar (Fig. 6 and 15). However, if multiple blocks are to be left at the same time, the graphical representation in Figs. 16 and 17 can be used.

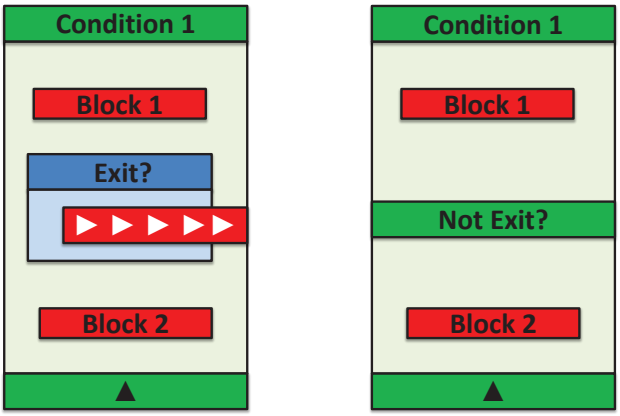

Figure 16: Early exit cycle (using the "break"). However, the use of dividing bar and inversion condition is clearer.

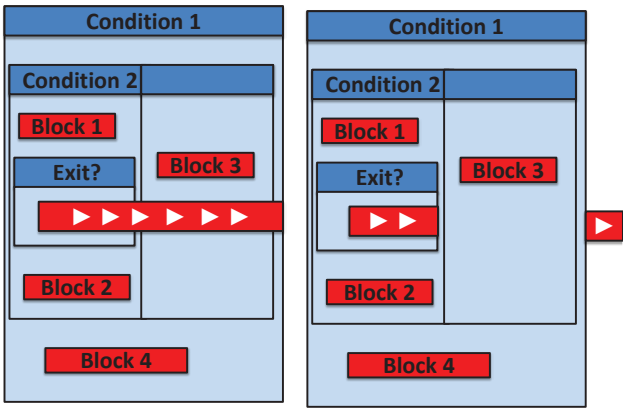

Figure 17: Two equivalent forms of graphical representation of leaving inner block.

2.6.2 Continue

Continue is shown as a classic statement whose name is represented by an upward arrow (Fig. 18). The program then continues by evaluating the header of the innermost cycle.

2.6.2 Return

The statement of premature termination of a subprogram can be represented similarly as break, and/or as a classic statement named return.

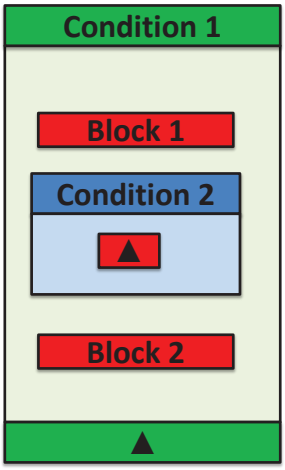

Figure 18: The "Continue" statement in the cycle.

2.6.2 Exceptions

In order to represent a block with an expected exception and also a block that is used to handle such a raised exception, only color is used (see Fig. 19):

- The header of the block with an expected exception and also of the subsequent block to handle the exception is filled using white color.
- The body of the block with an expected exception is filled using violet color.
- The body of the block where such a raised exception is handled is filled using orange color, similarly as any body of a block executed irrespective of whether an exception was or was not raised (the block finally).

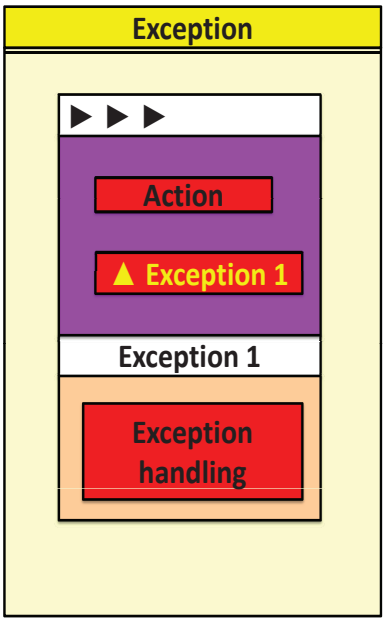

Figure 19: Throwing an handling the exceptions.

2.6.2 Goto

The general statement goto represents considerable violation of the structure, and therefore it is also strongly

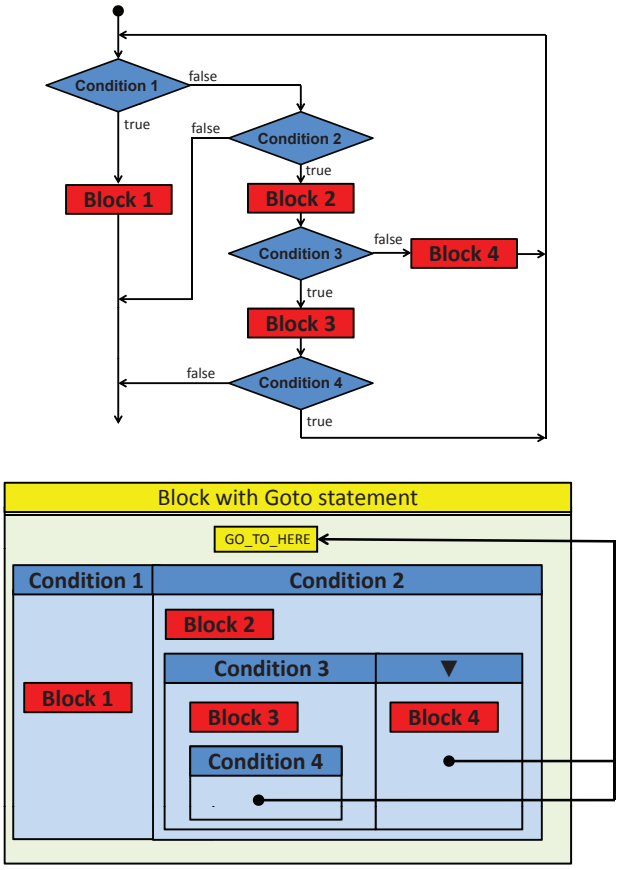

Figure 20: Goto statement in kopenogram.

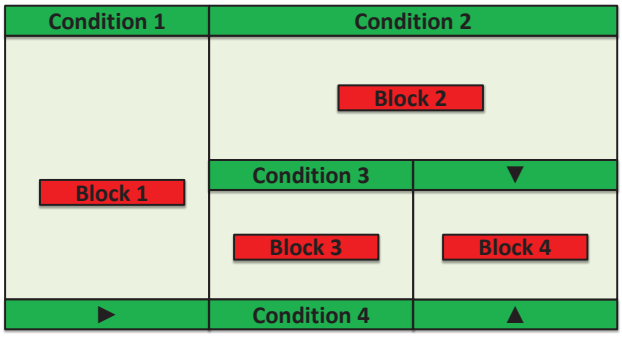

Figure 21: The general algorithmic block with embedded headers and multiple bodies. This block performs the same algorithm as a block in Figure 20.

highlighted. This statement is shown as an arrow oriented from the point of the jump to the right, outside of the block, and then up or down and finally to the left of the block with the target label (Fig. 20).

3 Conclusion

Kopenograms are a handy tool for clear graphical representation of the structure of algorithms, and they have found long-term application particularly in teaching programming classes.

These are a convenient supplement of UML diagrams used to represent algorithmic structures.

Kopenogram specification is published on [16].

4 Acknowledgement

This paper describes the outcome of research that has been accomplished as part of research program funded by GrantAgency of the Czech Republic Grant No. GACR P403-10-0092 and by the grant FR—TI3/869.

5 References

[1] ISO (1985). Information processing -- Documentation symbols and conventions for data, program and system flowcharts, program network charts and system resources charts. International Organization for Standardization. ISO 5807:1985.

[2] Jackson, M. A.: Principles of Program design. Academic Press, 197

[3] (Jackson, M. A.: System Development. Prentince Hall, 1983

[4] Nassi, I., Schneiderman, B.: Flowchart techniques for structured programming, ACM SIGPLAN Notices, Vol. 8 Issue 8, August 1973. ACM, ISSN: 0362 1340

[5] Kofránek, J.; Novák, P.: Kopenograms - graphical method of representation of programs (in Czech) Kopenogramy – způsob grafické reprezentace programů. In Moderní programování – Vinné 1987, Dům techniky ČSVTS, díl 4, Žilina, str. 11–161. 1987.

[6] Pattis, R. E., Karel The Robot: A Gentle Introduction to the Art of Programming.John Wiley & Sons, 1981. ISBN 0471597252

[7] PC-Karel : interpret of KAREL language for PC [online]. c2004 [cit. 2012-04-12]. Available from: <http://pckarel.sweb.cz/pckarel.html>.

[8] Pecinovský, R.: Fundamentals of Algorithmics I (in Czech) 602 ZO Svazarmu, 1985.

[9] Pecinovský, R.: Fundamentals of Algorithmics II (in Czech) 602 ZO Svazarmu, 1985.

[10] Pecinovský, R., Kofránek, J.: Simple data types (in Czech) 602 ZO Svazarmu, 1985.

[11] Pecinovský, R., Kofránek, J..: Structured data types (in Czech) 602 ZO Svazarmu, 1986.

[12] Pecinovský, R., Kofránek, J..: Searching and sorting (in Czech), 602 ZO Svazarmu, 1986.

[13] Pecinovský, R., Kofránek, J.: Dynamic data structures (in Czech), 602 ZO Svazarmu, 1986.

[14] Pecinovský, R., Kofránek, J.: Modular programming (in Czech) Modulární programování, 602 ZO Svazarmu, 1987.

[15] Pecinovský R., Ryant I.: Programming of of parallel processes (in Czech) 602 ZO Svazarmu, 1987.

[16] www.kopenogram.org

Email to corresponding author: kofranek@gmail.com

Ultra Encryption Standard (UES) Version-II: Symmetric key Cryptosystem using generalized modified Vernam Cipher method, Permutation method, Columnar Transposition method and TTJSA method.

A. Satyaki Roy[1], B. Navajit Maitra[2], C. Joyshree Nath[3], D. Shalabh Agarwal[4] and E. Asoke Nath[5]

Department of Computer Science, St. Xavier's College (Autonomous), Kolkata, India[1, 2, 4, 5]

A.K.Chaudhuri School of IT, Raja Bazar Science College, Calcutta University, Kolkata, India[3]

Abstract- *Nath et al recently developed encryption method called UES version-I where they have 3 distinct encryption methods such as Modified generalized Vernam Cipher method using feedback, multiple round transposition method and permutation method have been amalgamated. A new combined cryptographic method called UES Version-II has been introduced here as the extension of UES version-I. Nath et al. have already developed several symmetric key methods such as MSA, DJSA, NJJSAA, TTJSA, TTSJA, DJMNA, DJJSA, UES-I etc. In the present work multiple methods such as generalized modified vernam Cipher method Permutation method, Columnar transposition method and TTJSA have been implemented. UES-I has been extended to UES-II by adding one encryption module called TTJSA to make the encryption standard harder than UES-I. An encryption key pad in Vernam Cipher Method and also the feedback used in this method is considered to make the encryption process stronger. UES-II incorporates multiple encryption and decryption to defeat common cryptography attack such as differential attack or simple plain text attack.*

Keywords: encryption, decryption, feedback, cycling, randomized Vernam key, TTJSA.

I. INTRODUCTION

In the current communication network it is a real challenge us to send confidential data/information from one computer to another computer. When a sender is sending some confidential data, there may be a middle man attack and the data may be intercepted and diverted to different places. The confidentiality and security of data has now become a big challenge in data communication network. Due to network facility the access of data is now very easy and the hackers are always try to hack data from the network. The trainers and the teachers must be careful to send question papers or marks sheet through e-mail as there is no guarantee that it will not be intercepted by someone. In banking and corporate sectors the finance or management data must be secured if by chance the data goes to the hacker then the entire service will be collapsed. Password breaking is now not a problem. Many public software are available to decode password of some unknown e-mail. Under no circumstances the confidential data should be intercepted by any intruder while transmitting from client machine to server or to another client machine. Due this intrusion problem now the network security and cryptography is an emerging research area where the people are trying to develop some good encryption algorithm so that no intruder can intercept the encrypted message. Nath et al. had developed some advanced symmetric key algorithm [1-8]. In the present work we are proposing a symmetric key method called UES version-II which is a combination of 4 distinct cryptographic methods, namely, (i) Generalized Modified Vernam Cipher Method, (ii) Permutation method (iii)Columnar transposition method and (iv) TTJSA modules. We have tested this method on various types of known text files and we have found that, even if there is repetition in the input file, the encrypted file contains no repetition of patterns. The real challenge in the UES version-II algorithm was to ensure the effective integration of the four levels of encryption to produce strong encryption with the features such a multiple encryption, randomized key generation and a new method i.e. TTJSA.

II. UES VERSION-II ALGORITHM

ENCRYPTION PROCESS

In UES-II we have four distinct levels of encryption such as Modified Vernam Cipher with feedback, Columnar Transposition, Randomization Encryption Process and finally TTJSA[ref-no]. The first three levels of encryption are performed in blocks of 900 bytes. The residual bytes (of size less than 900 bytes) are encrypted with the Modified Vernam Cipher Encryption Method. The output is encrypted further by TTJSA method. TTJSA method comprises of 3 distinct encryption methods namely (i) MSA method[Ref-no], (ii) NJJSAA methd [Ref-no], (iii)Generalized modified vernam cipher method with feedback. The randomized vernam key is generated in

every iteration from a mathematical calculation from the user given password which can be 64-byte long. While doing columnar transposition method the sequence of the column extraction is also decided internally from the password entered by the user. The password will also decide the number of times encryption is to be performed.

Integration and key generation algorithm

Step 1: Start
Step 2: Input the plain text file name in 'plain[]' (The plain file may be of any format).
Step 3: Input the cipher text file name in 'cipher[]'
Step4: The extracts the first byte in the file and stores it in 'ch' and it extracts the last byte of the file and stores in 'cha'. It replaces the first byte of the file with character with ASCII (ch+cha)%256.
Step 5: The user enters a 64 byte encryption-key that is stored in 'key[]'.
Step 6: Now the algorithm computes the 'cod' value equal to Σ key[i]*(i+1) where i represents the position of every character in the key.

Step 7: The encryption number (enc) is computed by calculating the cod modulus 17. If enc <0 then enc=7

Step 8: Take the input file pointer to the end of the input file, such that the size of the input file can be computed. (The size of the input file is stored in long integer variable 'n'.)

Step 9: Declare a variable 'n1' of long int datatype where n1 will store the number of iterations. Each iteration will process a 30 X 30 bytes block in every iteration of encryption.
Step 10: Introduce a variable p=0.
Step 11: Compute cod=cod modulus 256
Step 12: If p is greater than or equal to enc then GOTO step 29.
Step 13: Increment cod and perform cod=cod%256;
Step 14: Now create a key file by printing the characters with ASCII values of 0-255 in rotation. The first character is however the character with ASCII 'cod'. This key file serves as the input for the Modified Vernam Cipher with feedback.
Step 15: This key is further randomized using randomization module and stored in the file 'file1.c'.
Step 16: Initialize integer variable count to 0.
Step 17: If count greater than or equal to n1 then Goto 25
Step 18: Define the intermediate file which will open, extract and process the first 900 bytes of the plain file.
Step 19: The 900 bytes that have been extracted now is encrypted with the Modified Vernam Encryption process with Feedback
Step 20: The output from the modified vernam cipher encryption process is fed as input to the columnar transposition encryption process.
Step 21: The output from the columnar encryption method will now undergo randomization/permutation encryption method.
Step 22: The output file from the randomization process holds the encrypted 900 bytes.
Step 23: The 900 bytes is written to the cipher file name provided by the user.
Step 24: The value of 'count' is incremented by 1. Goto 17.
Step 25: Once the control breaks from the loop, the program is left to process the residual bytes from the input file.
Step 26: The residual bytes are processed by the modified vernam cipher encryption technique. The encrypted bits are again written into the cipher file which serves as the input for the next iterations of encryption.
Step 27: Increment p
Step 28: Goto step-12
Step 29: When the control reaches this encryption the Modified Vernam Cipher, Columnar Transposition, and Randomization modules are complete. The file is further fed as input to the TTJSA module.
Step 30: The output is again written back to the cipher file whose name is provided by the user.
Step 31: End

Algorithm for the first level of encryption – modified vernam cipher encryption method with feedback.

Step 1: Start
Step 2: The plain text serves as the input file for the program.
Step 3: Create a dictionary of characters in the character array where position i will be the ASCII value for the character placed in the i-th location of the array.
Step 4: Define the encryption key which must be same as the key provided during decryption.
Step 5: Start processing the characters in the input file. Define a integer variable 'feed' and initialize it with 0.
Step 6: Extract a character in the input file and store in ch1. If ch1is NULL, goto 12
Step 7: Extract a single character from the key file.
Step 8: Compute m,n from the arrays arr[] where m and n are the ASCII values for the first characters of the input file and key files.
Step 9: Perform addition m=m+n+feed. Then calculate n=m modulus 256.The value of n is called the **'Feedback'** which allows the program to encrypt the characters in the plain file.

Table 1: Modified Vernam Cipher
Key: abc
aaa → ┬àI

Plain text:	A	A	A
Plain Index(m):	97	97	97
Key text:	a	B	C
Key Index(n):	97	98	99
Feedback (feed):	0	194	133
m=m+n+feed	194	389	329
n=m%256	194	133	73
Cipher text:	┬	À	I

Step 10: Write the contents of the array in the intermediate output file one by one, where the array in the n-th place of the array is the encrypted character.
Step 11: Goto 7.
Step 12: Once the control comes out of the loop, the encryption process is complete.
Step 13: END

Algorithm for the second level of encryption- Columnar Transposition Method

Step 1: Start
Step 2: Now the algorithm extracts the first character of the 'file1.c' in 'cha' and computes 'od'=cha modulus 6. The value of od determines the sequence of columns everytime the columnar module is invoked.
Step 3: Now we compute the array 'arra[]' where the first entry is od. Then 'od' is subsequentely decremented. If the value of od becomes 0 then it is replaced by 5. This array decided the definite order of the sequence of columns extracted.
Step 4: The 900 bytes of output from the Modified Vernam Method serves as the input file for Columnar Transposition Method.
Step 5: Initialize the variable n to an arbitrary integer value which represents the number of columns of the columnar transposition array in which the plain file characters will be stored. Typically n may have any value.
Step 6 : Initialize both integer variables 'row' and 'col' to 0
Step 7 : Initialize all the elements in the specified array arr[][] to NULL('\0')
Step 8 : Store the plain text file byte by byte in the array arr[][] where the row and column positions are determined by 'row' and 'col'.
Step 9: Increment column index by 1 once a byte is read and placed in the array
Step 10: If col is equal to n then increment row by 1 and intialize col variable to 0 to keep a check on the row and column parameters.
Step 11: Goto 9 until the storing of the intermediate plain text in the array is complete.
Step 12. If col==0 then we decrement the row index by 1 to ensure that the character array arr[] does not produce an extra row.This happens when a character is placed at the last column of a particular row.
Step 13: Initialize both variables 'count' and 'index' to 0.
Step 14: If(count>=n) goto 17

Table 2(a), (b): Columnar Transposition

Table 2(a): Plain text: letsallgonow
The plain text is placed in array 'arr'.

0	**1**	**2**	**3**	**4**	**5**
L	**E**	**T**	**s**	**a**	**L**
L	**G**	**O**	**n**	**o**	**w**

Table-2(b): **Cipher Text:lwaosntoegll**

0	**1**	**2**	**3**	**4**	**5**
l	**w**	**A**	**o**	**S**	**n**
t	**o**	**E**	**g**	**L**	**l**

arra[]={5,4,3,2,1,0} (assume)

p=arra[index](where index=0 and subsequently index=index+1)

p=5, 4, 3,2,1,0 respectively where p stands for the extracted column.

Step 15 : Count is incremented by 1
Step 16 : Initialize variable p to arra[index]. Here the 'arra[]' stores the order in which the columns will be transported to the same columnar transposition array arr[] to implement the columnar transposition encryption method. The variable 'index' is subsequently incremented to transport the rest of the columns of the columnar transposition array
Step 17: End

Algorithm for Randomization/Permutation Encryption Method

Step 1: Start
Step 2: The output from the columnar transpositionmethod serves as the input for the randomization/permutation process.
Step 3: Define integer arrays 'arr' that will store the randomization key. Define 2-d character arrays 'chararr[][]to store all the 900 bytes in the file and chararr2[][] to store the randomized characters.
Step 4: Initialize all the elements in the character arrayschararr[][] and chararr2[][] to 'null'.
Step 5: Initialize m to 30 and n to 1. 'm' holds the numberof rows and columns in the square matrix of chararr[][],chararr2[][], arr[][].
Step 6: Input the numbers 1,2,3...,900 to the integer array arr[][] by incrementing the value of n. The characters in the input file are copied to the character array 'chararr[]'.
Step 7: Now randomize the numbers in the integer array with the help of the functions defined in the program.
Step 8: The program invokes function 'leftshift()' which shifts every column in the integer array to one place left thus the first column is displaced to the position of the last column.
Step 9: Invoke function 'topshift() which shifts very row to the row above. Therefore the elements in first row is displaced in the corresponding position of the last row.
Step 10: Subsequently perform cycling operation on the integer array 'arr[][]' . Intialize i to 1.
Step 11: If i is greater than m/2 goto 15.
Step 12: If i is odd, perform clockwise cycling of the i-th cycle of the character array. Invoke functions rights(),downs(), lefts(),tops() to implement the clockwise displacement of the elements in arr[][].
Step 13: If i is even, perform anti-clockwise cycling of the i-th cycle of the character array.
Invoke functions ac_rights(),ac_downs(), ac_lefts(),ac_tops() to implement the anti-clockwise displacement of the elements in arr[][]. Therefore the integer array arr[][] is alternately randomized in clockwise and anit-clockwise cycles.
Step 14: Increment i. Goto 11.
Step 15: The program invokes function 'rightshift()' which shifts every column in the integer array to one place right thus the last column is displaced to the position of the first column.
Step 16: Invoke function 'downshift() which shifts very row to the row below. Therefore the elements last row is displaced in the corresponding position of the first row.
Step 17: Invoke the function 'leftdiagonal()' that performs downshift on the elements in the left diagonal such that the lowermost element is displaced to the position of the topmost element in the left diagonal.
Step 18: Invoke the function 'rightdiagonal()' that performs downshift on the elements in the right diagonal such that the lowermost element is displaced to the position of the topmost element in the right diagonal.
Step 19: To arrange the elements in the character array chararr[][] according to the randomized integer array arr[][]. Initialize i to 1.
Step 20: Store element arr[i][j] in z.
Step 21: Compute the row and column position pointed by the element z which is stored in 'k','l' respectively.
Step 22: Place chararr[k][l] in auxiliary character array chararr2[][] in positions chararr2[i][j].
Step 23: Increment j.
Step 24: If j<=m goto 20
Step 25: Increment i
Step 26: If j<=m goto 20
Step 27: Write the randomized elements in character array chararr2 [i][j] to the intermediate output file.
Step 28:.End.

DECRYPTION PROCESS:

The decryption algorithm follows the reverse process of the four levels of encryption that have been implemented. TTJSA is the first method to be implemented. The three decryption processes employed are Randomization Decryption Method, Columnar Transposition Decryption Method, and Modified Vernam Cipher Decryption with feedback (in the specified order). Again, the algorithm repeatedly performs the decryption by the last three methods in blocks of 900 bytes and the residual bytes of the cipher file (size less than 900 bytes) are processed with the Modified Vernam Decryption Method with feedback. The decryption number is again generated according to the same 64 byte user password

TTJSA Algorithm:

Now here we will describe TTJSA algorithm

A. Algorithm for ENCRYPTION

Step 1	: Start
Step 2	: Initialize the matrix mat[16][16] with numbers 0 to 255 in row major wise.
Step 3	: call keygen() to calculate randomization number(=times), encryption number(=secure)
Step 4	: call randomization() function to generate to make the content of mat[16][16] Randomized.
Step 5	: set times2=times
Step 6	: copy file f1 into file2
Step 7	: set k=1
Step 8	: if k>secure go to Step 15

Step 9 : p=k%6
Step 10 : if p=0
call vernamenc(file2,outf1)
set times=times2
call njjsaa(outf1,outf2)
call msa_encryption(outf2,file1)
else if p=1
call vernamenc(file2,outf1)
set times=times2
call msa_encryption(outf1,file1)
call file_rev(file1,outf1)
call njjsaa(outf1,file2)
call msa_encryption(file2,outf1)
call vernamenc(outf1,file1)
set times=times2
else if p=2
call msa_encryption(file2,outf1)
call vernamenc(outf1,outf2)
set times=times2
call njjsaa(outf2,file1)
else if p=3
call msa_encryption(file2,outf1)
call njjsaa(outf1,outf2)
call vernamenc(outf2,file1)
set times=times2
else if p=4
call njjsaa(file2,outf1)
call vernamenc(outf1,outf2)
set times=times2
call msa_encryption(outf2,file1)
else if p=5
call njjsaa(file2,outf1)
call msa_encryption(outf1,outf2)
call vernamenc(outf2,file1)
set times=times2
Step 11 : call function file_rev(file1,outf1)
Step 12 : copy file outf1 into file2
Step 13 : k=k+1
Step 14 : goto Step 8
Step 15 :End

1) Algorithm of vernamenc(f1,f2)

Step 1 : Start vernamenc() function
Step 2 : Initialize matrix mat[16][16] is initialized with numbers 0-255 in row major wise
Step 3 : call function randomization() to make the content of mat[16][16] random
Step 4 : Copy the elements of random matrix mat[16][16] into key[256] (row major wise)
Step 5 : set pass=1 , times3=1 , ch1=0
Step 6 : Read a block from the input file f1 where number of characters in the block≤256
characters
Step 7 : If block size < 256 then goto Step 15
Step 8 : copy all characters of the block iinto an array str[256]
Step 9 : call function encryption() where str[] is passed as parameter along with the size of the current block
Step 10 : if pass=1
set times=(times+times3*11)%64
set pass=pass+1
else if pass=2
set times=(times+times3*3)%64
set pass=pass+1
else if pass=3
set times=(times+times3*7)%64
set pass=pass+1
else if pass=4
set times=(times+times3*13)%64
set pass=pass+1
else if pass=5
set times=(times+times3*times3)%64
set pass=pass+1
else if pass=6
set
times=(times+times3*times3*times3)%6
4
set pass=1
Step 11 : call function randomization() with current value of times
Step 12 : copy the elements of mat[16][16] into key[256]
Step 13 : read the next block
Step 14 : goto Step 7
Step 15 : copy the last block (residual characters , if any) into str[]
Step 16 : call function encryption() using str[] and the no. of residual characters
Step 17 : Return

2) Algorithm of function encryption(str[],n)

Step 1 : Start encryption() function
Step 2 : set ch1=0
: calculate ch=(str[0]+key[0]+ch1)%256
Step 3 : write ch into output file
Step 4 : set ch1=ch
Step 5 : set i=1
Step 6 : if i≥n then goto Step 13
Step 7 : ch=(str[i]+key[i]+ch1)%256
Step 8 : write ch into the output file
Step 9 : ch1=ch
Step 10 : i=i+1

Step 11 : goto Step 7
Step 12 : Return

B. *Algorithm for DECRYPTION*

Step 1 : Start
Step 2 : initialize mat[16][16] with 0-255 in row major wise
Step 3 : call function keygen() to generate times and secure
Step 4 : call function randomization()
Step 5 : set times2=times
Step 6 : call file_rev(f1,outf1)
Step 7 : set k=secure
Step 8 : if k<1 go to Step 15
Step 9 : call function file_rev(outf1,file2)
Step 10 : set p=k%6
Step 11 : if p=0
call msa_decryption(file2,outf1)
call njjsaa(outf1,outf2)
call vernamdec(outf2,file2)
set times=times2
else if p=1
call function vernamdec(file2,outf1)
set times=times2
call function msa_decryption(outf1,outf2)
call fumction njjsaa(outf2,file2)
call function file_rev(file2,outf2)
call function msa_decryption(outf2,outf1)
call function vernamdec(outf1,file2)
set times=times2
else if p=2
call njjsaa(file2,outf1)
call vernamdec(outf1,outf2)
set times=times2
call msa_decryption(outf2,file2)
else if p=3
call vernamdec(file2,outf1)
set times=times2
call njjsaa(outf1,outf2)
call msa_decryption(outf2,file2)
else if p=4
call msa_decryption(file2,outf1)
call vernamdec(outf1,outf2)
set times=times2
call njjsaa(outf2,file2)
else if p=5
call vernamdec(file2,outf1)
set times=times2
call msa_decryption(outf1,outf2)
call njjsaa(outf2,file2)

Step 12 : copy the content of file2 to outf1
Step 13 : set k=k-1
Step 14 : Goto Step 8
Step 15 : End

1) *Algorithm of function vernamdec(f1,f2)*

The algorithm of vernamdec() function is same as vernamenc() function. Here the only difference is that decryption() function is called instead of encryption() function.

2) *Algorithm of decryption(str[],n)*

Step 1 : Start
Step 2 : ch1=0
Step 3 : ch=(256+str[0]-key[0]-ch1)%256
Step 4 : write ch into the output file
Step 5 : i=1
Step 6 : if i≥n then goto Step 12
: ch=(256+str[i]-key[i]-str[i-1]) %256
Step 7 : write ch into the output file
Step 8 : i=i+1
Step 9 : goto Step 6
Step 10 : ch1=str[n-1]
Step 11 : Return

C. *Algorithm of function file_rev(f1,f2) :*

Step 1 : Start
Step 2 : open the file f1 in input mode
Step 3 : open the file f2 in output mode
Step 4 : calculate n=sizeof(file f1)
Step 5 : move file pointer to n
Step 6 : read one byte
Step 7 :write the byte on f2
Step 8 : n=n-1
Step 9 : if n>=1 then goto step-6
Step 10 :close file f1,f2
Step 11 :return

Now we will describe how we calculate randomization number(=times) and encryption number(=secure). The present method is fully dependent on the text-key which is any string of maximum length 16 characters long. From the text-key we calculate two important parameters (i) Randomization number and (ii) Encryption number. To calculate this two parameters we use the method developed by Nath et al(1).

NJJSAA Algorithm:

Nath et al.[2] proposed a method which is basically a bit manipulation method to encrypt or to decrypt any file.Step-1 : Read 32 bytes at a time from the input file.
Step-2 : Convert 32 bytes into 256 bits and store in some 1-dimensional array.
Step-3: Choose the first bit from the bit stream and also the corresponding number(n) from the key matrix. Interchange the 1st bit and the n-th bit of the bit stream.
Step-4: Repeat step-3 for 2nd bit,3rd bit,…256-th bit of the bit stream
Step-5: Perform right shift by one bit.
Step-6: Perform bit(1) XOR bit(2), bit(3) XOR bit(4),….bit(255) XOR bit(256)
Step-7: Repeat step-5 with 2 bit right, 3 bit right,….n bit right shift followed by step-6 after each completion of right bit shift.

MSA (Meheboob, Saima, Asoke) Encryption and Decryption algorithm:

Nath et al.(1) proposed a symmetric key method where they have used a random key generator for generating the initial key and that key is used for encrypting the given source file. MSA method is basically a substitution method where we take 2 characters from any input file and then search the corresponding characters from the random key matrix and store the encrypted data in another file. MSA method provide us multiple encryption and multiple decryption. The key matrix (16x16) is formed from all characters (ASCII code 0 to 255) in a random order.

The randomization of key matrix is done using the following function calls:
Step-1: call Function cycling()
Step-2: call Function upshift()
Step-3: call Function downshift()
Step-4: call Function leftshift()
Step-5: call Function rightshift()

For detail randomization methods we refer to the done by Nath et al(1).Now we will describe how we perform the encryption process using MSA algorithm (1): We choose a 4X4 simple key matrix:

TABLE-3: KEY MATRIX(4X4)

A	B	C	D
E	F	G	H
I	J	K	L
M	N	O	P

Case-I: Suppose we want to encrypt FF then it will take as GG which is just one character after F in the same row.
Case –II: Suppose we want to encrypt FK where F and K appears in two different rows and two different columns. FK will be encrypted to KH (FK→GJ→HK→KH).
Case-III: Suppose we want to encrypt EF where EF occurs in the same row. Here EF will be converted to HG.
After encrypting 2 bytes we write the encrypted bytes on a new output file. The entire encryption method we apply multiple times and the encryption number will be determined by the process we have described in table-1.

Decryption Method: The decryption method will be the just the reverse process of encryption method as mentioned above.

III. FIG-1: Block Diagram of Ultra Encryption Standard Version-II

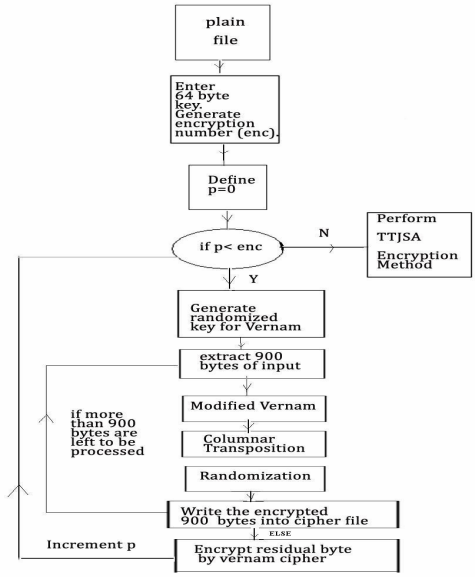

IV. TEST RESULTS:

In the present paper we have used multiple cryptography algorithms. We have applied our method on some known text where the same character repeats for a number of times and we have found that after encryption there is no repetition of pattern in the output file. We have made series of experiments on various known text files and have found the result is satisfactory. In Vernam cipher method we have used the feedback to ensure the same pattern should not be repeated in the encrypted text. The sequence of columns in the columnar method is also derived from the password.

The TTJSA module has been incorporated to strengthen the encryption process even further. The merit of this method is

that it is almost impossible to break the encryption algorithm without knowing the exact key.

Plain Text	Cipher Text
he is good	õµ¿£'†©▯ wÂ
se is good	T|–ßü¢'•_`kPù
ie is great	_+b¶_V¨¦Œ›
The Indian Higher education System has established itself as one of the largest in the world in terms of the number and diversity of institutions and student enrolment. However the nature of demand for higher education in the 21st century is undoubtedly influenced by macro-economic trends like the changing composition and preferences of students, an increasing willingness to spend more on quality education, a greater demand for global education, employability linked education, rapid privatization and globalization.	,~'AVžÈPqÃõ▯ å»æ4œwÝ_–]e+nTd5@«_…Ë[•æsÆÁÈp! ÀmÌW;2I«f›€ŽÜ%¯Y,cÖTÂ rwø^y_Úéòûµ N▯ T³_^há▯ {Fl ¯_àHeùzè_Þ▯ €‰ãñ▯ @ûËõß é8_&ü)"u"ô™|©,6▯ †(ý_ÈÓý ^Úm_13ñN▯ ‰ò²*¶[ÚH_taU ▯ "!²þÄW _Ì{_4_âSQ2¥éýŽ_› _à;ÀaqUÃ2…ƒ_öZ1²LB'aÌ= „X€o_Õ¡juW\$R¦GØf/Ì(@©(_È;ºÙ_›,_17"ªí´çøx,^ˆÑtPr<¦ï #/àÿCjk_ºä}/_¬HrJº__uø_X_ %|Zq*:6F¹ºõr0w/72"@:u¡¾á' çQ¯Ÿ+O7è¿këe¤¤üZ¿/ÝÓÉ ®¯ÝÙMÐp³é£â}/¶ Ì_.AmR| Œ__†e'õ▯ Ç(‡4_▯ `3K$V▯ ÿ _&)˜P:Î▯ 9€¡KŒ }kÏýŽzø¸X &Ný_ó_6_®îþ«Ë_J6▯ ¦¼Ìž¸3 s×•ß‹Sg´úÎ/Yj†}º_G4·1ua/µz/ î9D_ÜÜ.[ËAJ\ÏE1ØÏSû_¼ð UÙ";Cé°ÊrjË§*¢ý£cº_C'▯ _ë þa_Ó™éB¹f_]Ã▯ K•
AAA	A-ÿœ
ABA	º,$
A	½P
B	zº

ACKNOWLEDGEMENT

We are very much grateful to Department of Computer Science to give us opportunity to work on symmetric key Cryptography. One of the authors (AN) sincerely expresses his gratitude to Fr. Dr. Felix Raj and Fr. Jimmy Keepuram for giving constant inspiration to carry out research work. AN is grateful to the University Grants Commission for giving financial assistance through Minor Research Project. JN expresses her gratitude to A.K.School of IT for allowing us to work in research project at St. Xavier's College. SR, NM, TC, SA and AN are also thankful to all 3rd year Computer Science Hons. Students (2011-2012 batch) for their constant encouragement to finish this work.

REFERENCES

[1] Symmetric Key Cryptography using Random Key generator: Asoke Nath, Saima Ghosh, Meheboob Alam Mallik: "Proceedings of International conference on security and management(SAM'10" held at Las Vegas, USA Jull 12-15, 2010), P-Vol-2, 239-244(2010).

[2] A new Symmetric key Cryptography Algorithm using extended MSA method :DJSA symmetric key algorithm, Dripto Chatterjee, Joyshree Nath, Suvadeep Dasgupta and Asoke Nath : Proceedings of IEEE CSNT-2011 held at SMVDU(Jammu) 3-5 June,2011, Page-89-94.

[3] New Symmetric key Cryptographic algorithm using combined bit manipulation and MSA encryption algorithm: NJJSAA symmetric key algorithm: Neeraj Khanna,Joel James,Joyshree Nath, Sayantan Chakraborty, Amlan Chakrabarti and Asoke Nath : Proceedings of IEEE CSNT-2011 held at SMVDU(Jammu) 03-06 June 2011, Page 125-130.

[4] Advanced Symmetric key Cryptography using extended MSA method: DJSSA symmetric key algorithm: Dripto Chatterjee, Joyshree Nath, Soumitra Mondal, Suvadeep Dasgupta and Asoke Nath, Jounal of Computing, Vol3, issue-2, Page 66-71,Feb(2011).

[5] Advanced Steganography Algorithm using encrypted secret message : Joyshree Nath and Asoke Nath, International Journal of Advanced Computer Science and Applications, Vol-2, No-3, Page-19-24, March(2011).

[6] Symmetric key Cryptography using modified DJSSA symmetric key algorithm, Dripto Chatterjee, Joyshree Nath, Sankar Das, Shalabh Agarwal and Asoke nath, Proceedings of International conference Worldcomp 2011 held at Las Vegas, USA, July 18-21, Page 312-318, Vol-I(2011).

[7] Cryptography and Network, Willian Stallings, Prentice Hall of India.

[8] Ultra Encryption Standard(UES) Version-I : Symmetric Key Cryptosystem using generalized modified Vernam Cipher method, Permutation method and Columnar Transposition method, Satyaki Roy, Navajit Maitra, Shalabh Agarwal and Asoke Nath, Proceedings of RACCCT 2012, held at Surat , Mar 29-30, Page-81-88(2012)

[9] An Integrated symmetric key cryptography algorithm using generalized vernam cipher method and DJSA method: DJMNA symmetric key algorithm, Debanjan Das, Joyshree Nath, Megholova Mukherjee, Neha Chaudhury and Asoke Nath, Proceedings of IEEE conference WICT-2011 held at Mumbai University Dec 11-14,2011

[10] Symmetric key cryptosystem using combined cryptographic algorithms-generalized modified vernam cipher method, MSA method and NJJSAA method: TTJSA algorithm, Trisha Chatterjee, Tamodeep Das, Joyshree Nath, Shyan dey and asoke Nath, Proceedings of IEEE conference WICT-2011 held at Mumbai University Dec 11-14,2011.

A case of study for learning to design SPMD applications efficiently on multicore cluster*

Ronal Muresano, Dolores Rexachs and Emilio Luque
Computer Architecture and Operating System Department (CAOS)
Universitat Autònoma de Barcelona, Barcelona, SPAIN
rmuresano@caos.uab.es, dolores.rexachs@uab.es, emilio.luque@uab.es

Abstract— *The current trend in high performance computing (HPC) is to find clusters composed of multicore nodes. These nodes use a hierarchical communication architecture, which has to be handled carefully by students when they want to improve the parallel performance metrics. For this reason, we have proposed a teaching methodology for students in computational sciences with the aim of developing their SPMD (Single Program Multiple Data) parallel applications efficiently based on theoretical and practical sections. This novel methodology for teaching parallel programming is centered on improving parallel applications written by students through their experiences obtained during classes. Students achieved these improvements in their applications through applying novel strategies in order to manage the imbalances issues generated by the hierarchical communication architecture of multicore clusters. Also, this methodology allows students to discover how to improve their applications using characterization, mapping and scheduling strategies. Finally, the SPMD applications are selected because they can present imbalance issues due to the different communication links included on multicore clusters and these issues may create an interesting challenges for students when they wish to enhance the performance metrics. In conclusion, applying our teaching methodology, students obtained a significant learning skill designing their SPMD parallel applications.*

Keywords: Performance Metrics, Multicore, Teaching Models, Methodology for efficient execution, SPMD.

1. Introduccion

The inclusion of parallel processing in undergraduate degree has been widely justified and it has been integrated into the curriculum when it has become much easier to use and much more widely available the parallel resources [1][2]. Currently the trend in high performance computing (HPC) is to find clusters composed of multicore node, and the learning process has to be updated to use this new trends. Also, the multicore nodes add heterogeneity levels inside parallel environments and these heterogeneities have to be handled by students carefully when they wish to improve the performance metrics. Such computation and communication heterogeneities in the nodes generate interesting challenges that students of parallel programming courses must be prepared to deal with, when they want to enhance the application performance.

Also, the integration of multicore nodes in High Performance Computing (HPC) has allowed the inclusion of more parallelism within nodes. However, this parallelism must deal with some troubles present in multicore environments [3]. Problems such as: number of cores per chip, data locality, shared cache, bus interconnection, memory bandwidth, etc., are becoming more important in order to manage the parallel execution efficiently. The increasing use of multicore in HPC can be evidenced in the top500 [1] list in which most of the today cluster are set up with multicore nodes. For this reason, students have to learn new parallel programming strategies with the aim of enhancing the performance metrics in these environments. Indeed, the need for students to learn parallel application topics and tools is growing [4]. In fact, parallel application development has been included in different areas such as: biology, physics, engineering, etc [5] . and these inclusions have created the needs to incorporate this important topic in computer science curriculum. Including the efficient management of multicore environment topic into the parallel programming course content is very important because the current trend in computational science is to use parallel computing.

However to achieve an efficient execution, the instructor has to manage some issues that student can present when they design their parallel applications [6] [7]. One of the difficulties for students is to change their previous programming knowledge, which is focused on designing sequential applications. This focus is totally different when parallel applications are programmed and even more when these applications have to be designed for a multicore cluster. In these order, tasks divisions between cores and the hierarchical communication architecture included on multicore clusters are topics that students have to consider when

* This research has been supported by the MEC-MICINN Spain under contract TIN2007-64974.

*Contact Autor: R. Muresano, rmuresano@caos.uab.es

†This paper is addressed to the FECS conference.

[1]TOP500 is a list which provides a rank of the parallel machines used for high performance computing www.top500.org

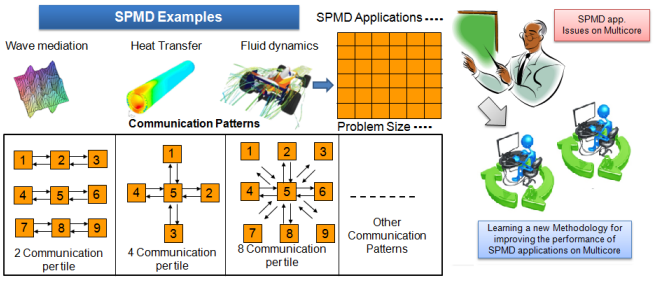

Fig. 1: SPMD and communications patterns.

they want to design their applications efficiently. Another issues presented by students are related to mapping and scheduling strategies, which have to be included in order to develop suitable strategies with the aim of managing the inefficiencies generated by communication heterogeneities.

Given the above, parallel programming courses have to incorporate teaching strategies that allow students to solve their programming issues on multicore environments applying real parallel processing experiences. These strategies have to be focused on executing parallel application efficiently. The main goal of our methodology is to obtain a constructivism learning process of parallel computing, where students can design their applications considering performance metrics such as: execution time, speedup and efficiency. Also, our methodology includes the consideration of how students can improve their application with the aim of executing their applications on multicore clusters efficiently. For this reason, this work is focused on creating a significant learning process for student of parallel programming with the objective of adapting them to the new technologies of multicore and also with the aim of developing a learning environments that permit students to improve the performance on multicore clusters.

To design our teaching methodology, our course was mainly focused on one of the most widely used parallel paradigm in computational science SPMD (Single Program Multiple Data) [8]. This paradigm has been selected due its behavior, which is to execute the same program in all processes but with a different set of tiles [9]. The tiles of this parallel paradigm have to exchange their information between iterations and these exchanging can become in a huge issue when the communication is performed by different communication links with different speeds and latencies. In this sense, students have to work with different communication behaviors and they have to consider these behaviors when they wish to achieve an improvement in parallel performance metrics (Fig. 1). As is shown in figure 1, the communication pattern can vary according to the objective of the application and these patterns are defined in the beginning of the SPMD application.

Taking advantage of the problems presented by students related to: designing parallel applications, programming the communication pattern of SPMD applications and managing of the hierarchical communication architecture of multicore clusters. Our methodology includes strategies, which allow them to design their applications using an active learning process. This process enables students a constant class participation, in which parallel application issues are discussed and improved with the instructor. Our teaching method has been designed to change the traditional lecture method applied in computational classes. We mainly take into consideration the student interactions and their parallel designed contributions. Our methodology is integrated by four phases: an application and multicore architecture analysis, an application performance evaluation, a methodology for improving efficiency and speedup of SPMD applications on multicore clusters and finally a parallel application improvements. These phases allow student to design their SPMD applications on multicore clusters efficiently.

The objective of the first phase is to permit students to create different point of views of the SPMD parallel applications and its communication pattern behavior. Also, this phase describes how to study the multicore architecture (different cache levels, interconnections network on chip (NOC), etc.) and which are the main factors that can affect the performance metrics in parallel applications. This phase allow students to design a first version of their SPMD applications and they can analyze the behavior on these multicore environments.

The application performance analysis phase is focused on determining the issues of students designing their applications. In this phase, students have to consider the efficiency, speedup and execution time as performance evaluation metrics. Next, students analyze their results obtained and they propose the performance improvement which will be applied in the last version together with proposes changes that instructor will give them in next phase.

The following phase is the application by students of a strategy for improving the efficiency and speedup of SPMD applications on multicore clusters [10]. This strategy is organized in four phases: characterization (the application and the environment), tiles distribution (maximum number of tile that each core has to execute), mapping strategy (distribution of the SPMD application tile over the cores), and scheduling policy (execution order of the assigned tile). These phases simultaneously with the student considerations obtained allow students to design their SPMD application efficiently.

The last phase of our teaching methodology is the parallel application improvement. This phase enables students to apply their proposed enhances, and then, they have to expose their final results. Also, this phase includes solutions, which permit them to solve and improve their last parallel applications version. Students make a final comparison in which the first and the last versions are evaluated in order to determine if the new proposed changes have improved the parallel execution.

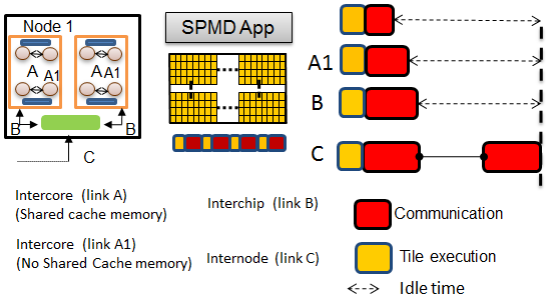

Fig. 2: SPMD applications and multicore cluster

The main approach of this teaching methodology is to allow students to create new parallel applications focusing on the new computational architectures. This methodology is based on creating a significant learning process in which students can identify new point of view and learn how to apply new strategies for improving performance metrics that can be applied with other parallel technologies such as, grid computing, multicluster, cloud etc. Finally, this methodology has been applied in the 2010-2011 period in computer engineering classes to students of the Autonomous University of Barcelona.

This paper is structured as follows: the issues of SPMD applications on multicore clusters is described in section 2, Then, section 3 presents the teaching methodology. Section 4 explains how the methodology has been included into the computer sciences curriculum and gives details about the experiences obtained. Finally, the conclusion are given in section 5.

2. SPMD applications and multicore clusters

The hierarchical communication architecture present on multicore clusters can create imbalance issues between processes and these issues have to be considered by students when they design their parallel applications. These issues can increase when a pure MPI (Message Passing Interface) applications with high communication volume as an SPMD application wants to communicate through different communication links. The figure 2 shows an example of executing an SPMD application over a multicore cluster where tiles are computed in a similar time due the homogeneity of the core but the communications are performed by different links. Each link can include up to one and a half order of magnitude of difference in latency for the same communication volume. These differences are translated into inefficiency and they may decrease the application performance. For this reason, students have to apply strategies using mapping and scheduling policies with the aim of improving the performance metrics in their applications.

The SPMD paradigm shows more frequent design problems related to the communications imbalance factors due to the great communications number between neighbors and

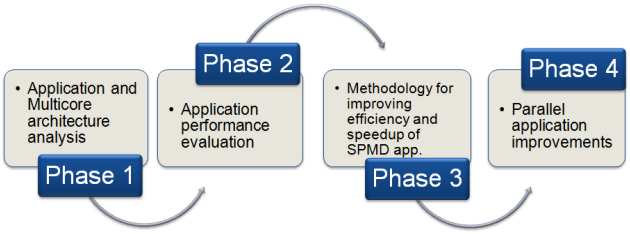

Fig. 3: Teaching methodology phases

the students have to manage when a heterogeneous communication environments as multicore are used. The diversities of these parallel paradigms make their issues and advantages more interesting and challenging when these paradigms are taught to students. For this reason, students have to be focused on learning how to improve the performance metrics in these environments.

From the above, the main objective of our teaching methodology is to allow students through their own experiences (active learning process) to apply techniques, which allow them to solve their computational challenges focusing on optimizing the computational resources. The students have to understand that parallel programming is acquiring an ever increasing acceptance and it is applied to solve high computational performance scientific problems in diverse fields. The trend of using parallel programming is thanks to its achieving more accurate results, highest performance, lowest cost, and lowest execution time and these concept have to be correctly applied by students.

3. Teaching Methodology

The objective of this methodology is that students can learn how to distribute or design their SPMD applications. The issues presented on multicore environments could generate confusion in students when they wish to enhance the performance metrics. However, our methodology is focused on creating a transformation in students through their experiences acquired in the classroom. To achieve these experiences, we have included in our teaching process an strategy for improving SPMD applications on multicore clusters [10]. This strategy is based on creating a balance between the workload tile distribution and the latency of the different communication links. Also, this method is focused on obtaining the maximum speedup of parallel application while the efficiency is defined over a threshold. This kind of strategy has been interesting to include in the teaching process for student because it allows us to explain students how to improve the performance metrics of SPMD applications on multicore clusters.

The phases of our teaching methodology are shown in figure 3 and are divided as follow: an application and multicore architecture analysis phase, an application performance evaluation, a methodology for improving efficiency and speedup of SPMD applications on multicore clusters and finally a parallel application improvements. These phases

are the focus of our methodology and these allow students through active learning to design their parallel applications with the concepts taught in theoretical classes. The teaching methodology can be considered successful, when students propose and apply the strategies, which allow them to enhance the performance metrics. The evaluation process is made through programming assignments, which students have to present at the end of the course. Hence, these phases allow us to have an active interactions with students, which permit them to develop different point of views and create some criteria about how to apply strategies for improving performance and how students can use their own experiences obtained during the classes in their applications.

3.1 Applications and multicore architecture analysis phase

This phase permits students to learn what can be the problematic issues of their parallel applications into a hierarchical communication environment and how they could apply strategies in order to enhance the performance metric. The applications and multicore architecture analysis phase is divided in two directions. The first one is focused on finding the application factors that can affect the performance. In this sense, students have to identify the application communication patterns, the communication volumes, the computational complexity, etc. Next, these factors have to be analyzed using the computational architecture with the objective of obtaining the weak point of the application.

Once students have analyzed the applications, the instructor has to explain the following topics that can have influences in the performance: the effects of the different communication links presented on multicore clusters, the cache size and level, the interconnections between cores (communication busses), etc. The considerations have to be handled carefully by students when they wish to improve the performance metrics.

Using the instructor considerations, students have to design their SPMD applications using the consideration learned in this phase. To develop these applications, students have to apply the concepts learned in theoretical classes. After that, students and instructor have interactions with students, where the issues obtained are discussed and instructor propose some modifications with the aim of improving the performance.

3.2 Application performance evaluation

This evaluation is performed with the aim of checking the hypothesis established in last phase about the effects of different communication links on multicore. The performance evaluation allows students to discover their own error and how these can affect the efficiency and speedup.

In this phase are performed different analyses for the SPMD applications. One of them is focused on the efficiency, in which students have to identify the time that

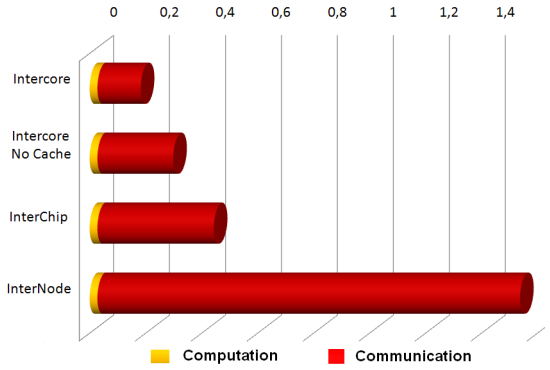

Fig. 4: Application analysis

communications are carried out for the total execution. Also, they have to determine if there are imbalance elements due to the effects of the different communications latencies and speeds and how these elements may affect the efficiency. The next analysis is based on the computational of each tiles and students have to determine the relationship between computational and communication of a tile in SPMD application. After these analyses, students have to discover if they can propose some suitable alternatives in order to improve the performance. The figure 4 illustrates a characterization example of the performance evaluation, where tile communication has different order of magnitude in latency according to the link used to perform the communication. This issues can compromise the parallel application performance and the students have to identify these design problems.

Finally, the instructor and students have interactions in which the performance metrics are discussed and analyzed by them. Thus, in this phase students have to explain their applications and their errors. The first presentations are centered on evaluating the issues of all students and the instructor can determine if the problems for example are related to mapping, load balancing, imbalanced communications, etc. This active learning process permits students to be connected with the parallel programming topics and also creates a learning environment where students opinions are very important for their learning development.

3.3 Methodology for improving the performance of SPMD applications on multicore.

Once the students have understood which are the problems that affect the efficiency and speedup of SPMD applications on multicore environments. They have to apply strategies with the aim of improving the performance metrics. In this sense, we have included one method that allow to design SPMD applications with the objective of reaching the maximum speedup while the efficiency is maintained over a defined threshold by the programmer. The main objective of this mehtod is to find the maximum number of cores that permits us to maintain a relationship between both efficiency and speedup with a specific problem size [10].

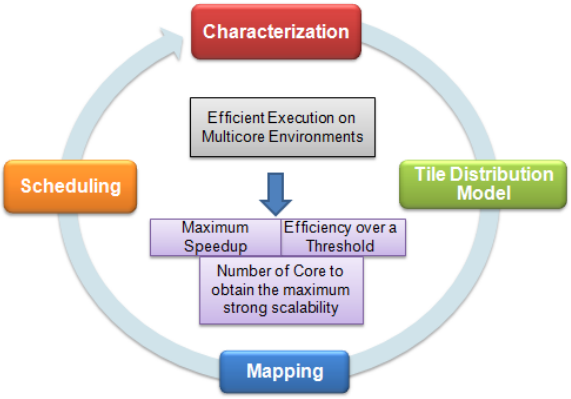

Fig. 5: Method for efficient execution of SPMD applications on multicore Clusters

This method allows students to apply the knowledge learned during the two last phases, in which the computational and communication patterns have been identified and the issues which affect the performance of SPMD applications are discovered. Then, we established a question about how can this performance method be integrated with our teaching methodology in order to obtain a significant learning process?. The answer is focused on creating a learning environment, where the stages of this method are included in our teaching program progressively verifying the learning success of this integration.

The first stage is the characterization process. This stage is responsible for gathering the necessary parameters of SPMD applications and environment in order to calculate the tile distribution model. Students have to run this characterization process in a controlled and monitored manner with the objective of extracting the parameters according to the tile distribution model needs. The characterization parameters are classified in three groups: the application parameters, parallel environment characteristics and the defined efficiency. This characterization enables students to determine the number of communication links, communication volumen of a tile, computation time, etc. In this point, the instructor can reinforce the parameters learned about the multicore architecture and these allow students to create and understand the weak point of SPMD applications.

The second stage (tile distribution model) is based on calculating the ideal number of tiles that must be assigned to each core and the number of core needs with the aim of obtaining the maximum speedup while the efficiency is over a defined threshold. To calculate this model, students have to use the parameters obtained in characterization phase and they have to use an analytical model which was defined in [10]. The objective of this model is to create a set of tiles called Supertile (ST) where a ST is divided in two types internal and edge tiles. The aim of this division is to allow the application executing first the edge tiles and then, to overlap the edge communications with the internal tiles execution.

The following stage is to make use of the mapping strategy. This mapping purpose is to allocate the ST among the cores with the aim of maintaining the desired efficiency. These assignations are made applying a core affinity to assign the set of tiles according to the policy of minimizing the communications latencies. Another element included in the mapping module is the logical distribution of the processes. This distribution process is done through a cartesian topology of the processes. This is a logical process in which students can identify through MPI commands the location of each process. Then with this topology, each process has two coordinates, which enables us to identify the communications neighbors. Also, these two coordinates identify the cores and where it has to be allocated.

Finally, students have to apply the scheduling stage. The objective is to coordinate the execution order of each tile within the core. The scheduling is divided into two main parts: the first one is to develop an execution priority which determines how tiles will be executed inside the core and the second part which is focused on applying an overlapping strategy between internal computation and edge communication tiles. Each tile has an execution priority where the highest priorities are established for tiles, which have communications through slower paths.

The integration of this method to our teaching methodology has allowed us to create interactive classes, where students can apply their learning with the aim of obtaining an efficient parallel execution. Also, students can propose new suitable strategies for improving the SPMD applications. This performance method has been applied during all the semester and students have included this method to design their new versions and compare the result obtained.

3.4 Parallel application improvements

The objective of this phase is to analyze the improvements applied to each SPMD applications by students. These improvements are achieved through the union of the instructor and students considerations, and the application of the performance method explained before. The applications are tuned using the characteristics of the clusters and employing mapping and scheduling strategies.

The students have to perform a new performance evaluation with the aim of evaluating the improvements achieved. This evaluation permits students to analyze the relevance of the performance method and the influences of the multicore architecture into the SPMD applications. In addition, students have to evaluate if they in fact have achieved an improvement in the parallel application metrics and how this improvements have been reached. Students have to evaluate if the concept learned in theoretical classes and the practical method used in labs have allowed them to obtain better efficiency and speedup levels. The interactions between instructor and students allow us to have a feedback

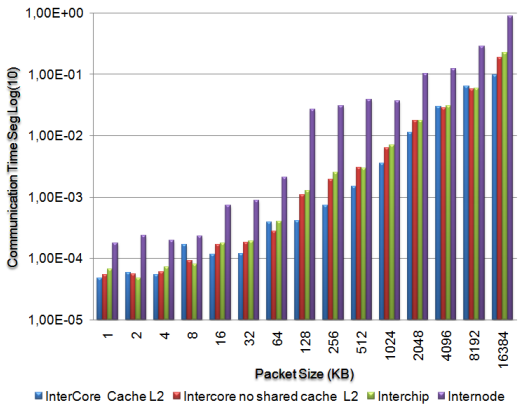

Fig. 6: Latencies of different communication links

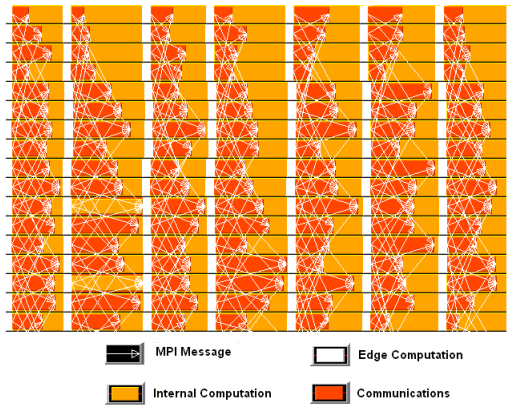

Fig. 8: Execution Trace of Heat Transfer App.

with student, these important iteration have been done in the final assignment, where students have to expose their works.

Finally, our teaching methodology gives students strategies to solve their parallel problem efficiently. An important key of our teaching methodology is that it allows students to learn through their own mistakes and experiences and learn how to solve them efficiently.

4. Methodology results and experiences obtained

Our teaching methodology tries to create innovative learning sceneries, where students can construct new points of views when they design parallel applications. This new teaching methodology has been applied in the period 2010-2011 in the parallel programming course of computer engineering and the modelling and simulation of the master in computer science at the Autonoma of Barcelona University. We applied our teaching methodology to 38 students. These students evaluated a set of scientific SPMD applications according to the communication patterns. The applications analyzed were the heat transfer applications, wave equation and the Nbody, each of these applications have their own communication pattern that could be considered as an interesting challenge for students. Also, the students experiments were conducted on a DELL multicore cluster with 8 nodes, each node has 2 Quadcore Intel Xeon E5430 of 2.66 Ghz processors, and 6 MB of cache L2 shared by each two core and RAM memory of 12 GB by blade.

Under this interesting scenario, we have assigned students the applications mentioned before, where they design their first parallel applications. This process was carried out using our teaching methodology, in which instructor and students interact with the first phase (application and multicore architecture analysis) of our methodology. The most important result of this phase can be observed in figure 6, where were identified the different communication levels on multicore clusters. Also, this process of analysis allowed the instructor to establish the necessaries conditions to answer the multiple numbers of questions of students that arising from the problems visualization of this phase. These interesting exchanges of knowledge between instructor and students permitted the class to be a learning space, where the fundamental key was to create a significant learning process.

Once students have obtained their first draft of their applications, they have to evaluate the performance. The figure 7 shows an example of the first draft, where is evaluated the application efficiency. These applications were designed in groups formed by 3 students and the performance results

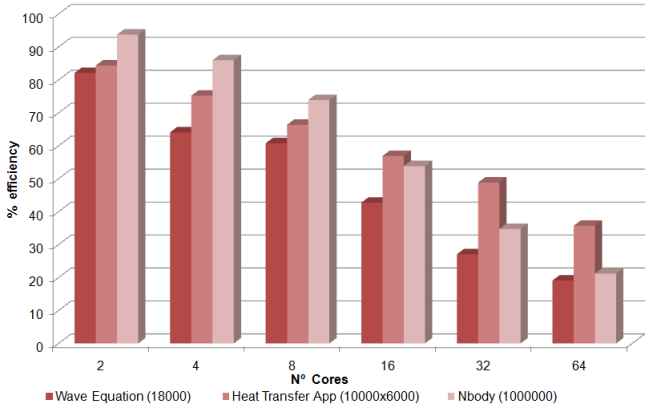

Fig. 7: First draft efficiency average obtained by students

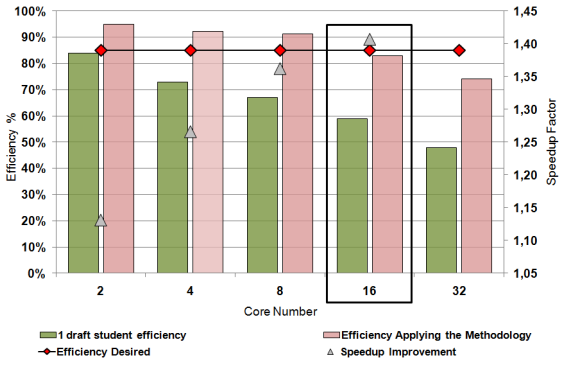

Fig. 9: Heat transfer application efficiency improvements

were acquired by students. Then, they analyzed the effect that can affect the performance on multicore. After this, the instructor reinforces the theoretical concepts and gave examples that student can associate with the issues founded in their parallel versions. In this phase, the most common problems observed were related to workload division, locality, tiles division, few overlap strategies, wrong mapping and scheduling strategy etc. These errors were detected through the interactions between instructor and students.

The next step is to teach the student a strategy for improving the performance metrics. As mentioned before, we used a methodology defined for SPMD applications, where the main objective is to find the number of tiles necessaries in order to achieve the maximum speedup while the efficiency is maintained over a defined threshold. In this order, students applied the stages of this method and they observed the influences that hierarchical communication architecture can have over SPMD applications. The instructor can explain the stage of the method and students applied to their code with the aim of improving efficiency and speedup.

The figure 8 shows an example of student execution trace of heat transfer application, where we can observe how the edge tiles was executed first and then is observed the overlapping process between internal computation tile and edge communication tiles. This strategy has allowed students to improve their SPMD applications because the inefficiency factors have been controlled.

The integration of this performance method with our teaching methodology permit students to develop new skills that allows them to apply their work in the parallel computing field. Finally, the last evaluation is about the effectiveness of this integration. Students have to redesign their application with the consideration and the performance method strategies. In this sense, students can apply the knowledge obtained during the semester into their applications. Finally, students have to design a second version of their application. An example of one student is shown in figure 9, where we can observe the improvements obtained in efficiency and speedup which is around 40% between the firts and the second draft.

The most important element that we have observed during this teaching period was related to students' skills in designing SPMD applications. The experiences and the new concepts developed by students through this learning process have allowed that this teaching methodology can be applied with other parallel paradigm. Only, we have to change the performance method that allows us to execute and to evaluate efficiently the parallel paradigm. Finally, the main key of a significant learning process is to consider the students point of views as a helpful and powerful learning tool.

5. Conclusion and futures works

This article has presented a teaching methodology that allows student through an active learning process to design their parallel applications efficiently on multicore cluster. To obtain this, we have included in the teaching process an efficient method for efficient execution of SPMD applications on multicore clusters using a load balancing, mapping strategy and a scheduling policy. The most important result obtained with our teaching methodology was the reflected motivation found in students when they design their parallel applications efficiently. Students have shown a considerable improvement in their parallel application design skills. These students skills have been improved due to the combination of a teaching methodology with a performance strategy and both elements have created a learning environment where the discussion about how to improve the applications performance has been the most powerful learning strategy.

Also, our teaching methodology allowed students to solve the issues of their parallel applications and students demonstrated how they can apply a methodology for improving SPMD applications on multicore clusters. The results obtained of the students' applications have been successfully, where the best cases they obtained an improvement around 40% over the first draft. This methodology has been taught in the period of 2010-2011 for computer engeniering and computer science master students at University Autonoma of Barcelona. Future works are focused on including other parallel paradigms such as Marter/Worker, pipeline, etc. All these paradigms will be included in our teaching methodology using multicore clusters under the focus of creating an active learning process in students.

References

[1] C. Nevison, "Parallel computing in the undergraduate curriculum," *IEEE Computer*, vol. 28 issue 12, pp. 51–56, 1995.

[2] J. Adam, C. Nevison, and N. Schaller, "Parallel computing to start the millennium," *Thirty first ACM Technical Symposium on Computer Science Education*, pp. 65–69, 2000.

[3] I. M. B. Nielsen and C. L. Janssen, "Multicore challenges and benefits for high performance scientific computing," *Sci. Program.*, vol. 16, pp. 277–285, December 2008.

[4] L. R. S. A. Clark and B. Bagheri, "Education and research challenges in parallel computing:," *International Conference on Computational Science ICCS 2005*, pp. 44–51, 2005.

[5] R. Guha and J. Hartman, "Teaching parallel processing: Where architecture and language meet," *Frontiers in Education, 1992. Proceedings. Twenty-Second Annual conference*, pp. 475–479, 1992.

[6] T. Chen, Q. Shi, J. Wang, and N. Bao, "Multicore challenge in pervasive computing education," pp. 310 –315, 2008.

[7] R. Muresano, D. Rexachs, and E. Luque, "Learning parallel programming: a challenge for university students," *Procedia Computer Science, 10 International Conference on Computational Science 2010*, vol. 1, no. 1, pp. 875 – 883, 2010.

[8] R. Buyya, *High Performance Cluster Computing: Architectures and Systems*, P. Hall, Ed. Prentice Hall PTR Upper Saddle River, NJ, USA, 1999.

[9] F. Darema, "The spmd model: Past, present and future," *Proceedings of the 8th European PVM/MPI*, p. 1, 2001.

[10] R. Muresano, D. Rexachs, and E. Luque., "Methodology for efficient execution of spmd applications on multicore clusters," *10th IEEE/ACM International Conference on Cluster, Cloud and Grid Computing (CCGRID), IEEE Computer Society*, pp. 185–195, (2010).

Modified Caesar Cipher method applied on Generalized Modified Vernam Cipher method with feedback, MSA method and NJJSA method: STJA Algorithm

A. Somdip Dey[1], B. Joyshree Nath[2] and C. Asoke Nath[3]
[1,3]Department of Computer Science
St. Xavier's College [Autonomous]
Kolkata, India.
[2]A.K.Chaudhuri School of IT, Calcutta University, Kolkata, India
Email: [1]somdip007@hotmail.com, [3]joyshreenath@gmail.com [4]asokejoy1@gmail.com

Abstract – *In this paper the authors present a new combined symmetric-key cryptographic method, named STJA, which is basically based on modified Caesar Cipher, generalized modified Vernam Cipher, MSA and NJJSA. The cryptanalysis shows that TTJSA and TTSJA are free from standard cryptographic attacks such as differential attack, plain text attack or any brute force attack. In the present method the authors have used generalized modified Caesar Cipher method, where the authors have modified the standard Caesar Cipher method and then they applied TTJSA method to make the entire crypto system very hard to break. TTJSA is also a combined symmetric key cryptographic method. In modern world keeping the data safe online is most important and of highest concern. For this reason, this combined cryptographic method, STJA is used, so that it is almost difficult for cryptographic hackers to break the cryptography method. This method has been tested on different plain text, consisting of different ASCII values (even with ASCII value 1,2,3 and so on) and the spectral analysis of the plain text and the encrypted is also been shown. The spectral analysis shows that the present cryptography method, STJA can not be broken with any kind of standard cryptography attack.*

Keywords: Caesar Cipher; TTJSA; MSA; NJJSA; UES; DJMNA; Cryptography;

1. Introduction

In modern world, security is a big issue and securing important data is very essential, so that the data can not be intercepted or misused for illegal purposes. For example we can assume the situation where a bank manager is instructing his subordinates to credit an account, but in the mean while a hacker interpret the message and he uses the information to debit the account instead of crediting it. Or we can assume the situation where a military commander is instructing his fellow comrades about an attack and the strategies used for the attack, but while the instructions are sent to the destination, the instructions get intercepted by enemy soldiers and they use the information for a counter-attack. This can be highly fatal and can cause too much destruction. So, different cryptographic methods are used by different organizations and government institutions to protect their data online. But, cryptography hackers are always trying to break the cryptographic methods or retrieve keys by different means. For this reason cryptographers are always trying to invent different new cryptographic method to keep the data safe as far as possible.

The modern day cryptographic methods are of two types: (i) symmetric key cryptography, where the same key is used for encryption and for decryption purpose. (ii) Public key cryptography, where we use one key for encryption and one key for decryption purpose.

Symmetric key algorithms are well accepted in the modern communication network. The main advantage of symmetric key cryptography is that the key management is very simple. Only one key is used for both encryption as well as for decryption purpose. There are many methods of implementing symmetric key. In case of symmetric key method, the key should never be revealed / disclosed to the outside world or to other user and should be kept secure. The key should be known to sender and the receiver only and no one else.

Our present work, STJA is also symmetric key cryptographic method, which is basically based on generalized modified Caesar Cipher method [1] and TTJSA [2], which itself is based on generalized modified Vernam Cipher [2], MSA [3] and NJJSA [4]. Depending on the key entered by the user the functions of generalized modified Caesar Cipher and TTJSA are called randomly and then executed. The present method uses multiple times encryption to encrypt the plain text data.

2. Method Used In The Present Work:

In this method the authors apply a modified form of advanced Caesar Cipher [1] cryptographic method. In cryptography, a Caesar cipher, also known as a Caesar's cipher or the shift cipher or Caesar's code or Caesar shift, is one of the simplest and basic known encryption techniques. It is a type of replacement cipher in which each letter in the plaintext is replaced by a letter with a

fixed position separated by a numerical value used as a "key". But, in this method, STJA, any character (ASCII value 0-255) are not separated by a fixed numerical value, in fact it is a variable numerical value, which is dependent on a non-linear polynomial function.

This present method is achieved by executing following two methods in random:

(i) Encrypt the data using generalized modified Caesar Cipher method
(ii) Encrypt data using TTJSA method

In this present method, STJA, the user enters a secret key called as password and from that key we generate unique codes, which are successively used to encrypt the message. For decryption purpose we use just reverse process to get back the original plain text. During decryption the user has to enter the same secret key otherwise the decryption will not be successful. Now we will describe in detail the encryption procedure.

2.1.Encryption of data using modified Caesar Cipher:

2.1.1 Generation of Code and power_ex from the Secret Key

The key is provided by the user in a string format and let the string be 'pwd[]'. From the given key we generate two numbers:
'code' and 'power_ex', which will be used for encrypting the message. First we generate the 'code' from the pass key.
Generation of code is as follows:

To generate the code, the ASCII value of each character of the key is multiplied with the string-length of the key and with 2^i, where 'i' is the position of the character in the key, starting from position '0' as the starting position. Then we sum up the resultant values of each character, which we got from multiplying, and then each digit of the resultant sum are added to form the 'pseudo_code'. Then we generate the code from the pseudo_code by doing modular operation of pseudo_code by 16, i.e.

code = Mod(pseudo_code, 16).
If code=0, then we set code =pseudo_code

The Algorithm for this is as follows:
Let us assume, pwd[] = key inserted by user

$pp= 2^i$, i=0,1,2,……..n; n ∈ N.

Note: i can be treated as the position of each character of the key.
Step-1 : p[] = pwd[]
Step-2 : $pp = 2^i$
Step-3 : i=0
Step-4 : p[i] = pwd[i];
Step-5 : p[i] = p[i] * strlen(pwd) * pp;
Step-6: csum = csum + p[i];
Step-7: i=i+1
Step-8: if i < length(pwd) then go to step-4
Step-9: if csum ≠ 0 then go to Step-10 otherwise go to Step-14
Step-10: c = Mod(csum , 10)
Step-11: pseudo_code=pseudo_code +c;
Step-12: csum = Int(csum / 10)
Step-13: Go to step-9
Step-14: code =Mod (pseudo_code, 16)
Step-15: End
Note: length(pwd)= number of characters of the secret key pwd[].

The 'power_ex' is calculated as follows:
We generate power_ex from the pseudo_code generated from the above method. We add all the digits of the pseudo_code and assign it as temporary_power_ex. Then we do modular operation on temporary_power_ex with code and save the resultant as power_ex.
i.e.

power_ex =Mod (temporary_power_ex, code)

If power_ex = 0 OR power_ex = 1, then we set power_ex = code.

For example, if we choose the password, i.e. the key to be 'hello world'. Then,
Length of pwd = 11
code = 10
power_ex = 4

Thus, we generate code and power_ex from the key provided by the user.

2.1.2 Encrypting the Message using code and power_ex

Now we use the code and power_ex, generated from the key, to encrypt the main text (message). We extract the ASCII value of each character of the text (message to be encrypted) and add the code with the ASCII value of each character. Then with the resultant value of each character we add the (power_ex)^i, where i is the position of each character in the string, starting from '0' as the starting position and goes up to n, where n=position of end character of the message to be encrypted, and if position = 0, then (power_ex)^i = 0.

It can be given by the formula:

$$\mathbf{text[i] = text[i] + code + (power\_ex)^i}$$

If text[i] > 255 then text[i] = Mod(text[i],256) : 'i' is the position of each character in the text and text[] is the message to be encrypted, where text[i] denotes each character of the text[] at position 'i'.

For example, if the text to be encrypted is 'aaaa' and key=hello world, i.e. text[]=aaaa and pwd=hello world, then

a^0 ->97+10+0 =107->k

a^1 ->97+10+4 =111->o

a^2 ->97+10+16=123->{

a^3 ->97+10+64=171->«

where 0-3 are the positions of 'a' in text[](as per formula given above). The text 'aaaa' becomes 'ko{«' after execution of the above method.

Since, the value of $(power\_ex)^i$ increases with the increasing number of character (byte) i.e. with the increasing number of string length, so we have applied the method of **Modular Reduction** [11][12] to reduce the large integral value to a smaller integral value.

To apply Modular Reduction we apply the following algorithm:

Step 1: n = power_ex * code * 10 ;generate a random number 'n' from code and power_ex
Step 2: calculate n^{th} prime number
Step 3:i=0
Step 4: $(power\_ex)^i$ = Mod($(power\_ex)^i$,(n^{th} prime number))
Step 5: i=i+1
Step 6: if i<length(text) then go to step-4
Step-7: End
Following the above step, we can reduce the value of $(power\_ex)^i$ to a significantly smaller usable number.

2.1.3 Algorithm for Decryption (Modified Caesar Cipher)

For this step we basically reverse the process of encryption technique used in the modified Caesar Cipher. And use the following formula:

$$text[i] = text[i] - code - (power\_ex)^i$$

Note: If, ASCII value of text[i] < 0, then set text[i] =Mod (text[i], 256); 'i' is the position of each character in the text and text[] is the message to be encrypted, where text[i] denotes each character of the text[] at position 'i'.

2.2 Encrypt the data using TTJSA:

TTJSA method is a combination of 3 distinct cryptographic methods, namely, (i) Generalized Modified Vernam Cipher Method, (ii) MSA method and (iii) NJJSA method. To begin the method a user has to enter a text-key, which may be at most 16 characters in length. From the text-key the randomization number and the encryption number is calculated using a method proposed by Nath et al. A minor change in the text-key will change the randomization number and the encryption number quite a lot. The method have also been tested on various types of known text files and have been found that, even if there is repetition in the input file, the encrypted file contains no repetition of patterns.

2.2.1 Algorithm of TTJSA (Encryption)

Step 1: Start
Step 2: Initialize the matrix mat[16][16] with numbers 0 to 255 in row major wise.
Step 3: call keygen() to calculate randomization number (=times), encryption number (=secure)
Step 4: call randomization() function to randomize the contents of mat[16][16].
Step 5: times2=times
Step 6: copy file f1 into file2
Step 7: k=1
Step 8: if k>secure go to Step 15
Step 9: p=k%6
Step 10: if p=0 then
call vernamenc(file2,outf1)
times=times2
call njjsaa(outf1,outf2)
call msa_encryption(outf2,file1)
else if p=1 then
call vernamenc(file2,outf1)
times=times2
call msa_encryption(outf1,file1)
call file_rev(file1,outf1)
call njjsaa(outf1,file2)
call msa_encryption(file2,outf1)
call vernamenc(outf1,file1)
times=times2
else if p=2 then
call msa_encryption(file2,outf1)
call vernamenc(outf1,outf2)
set times=times2
call njjsaa(outf2,file1)
else if p=3 then
call msa_encryption(file2,outf1)
call njjsaa(outf1,outf2)
call vernamenc(outf2,file1)
times=times2
else if p=4 then
call njjsaa(file2,outf1)
call vernamenc(outf1,outf2)
times=times2
call msa_encryption(outf2,file1)
else if p=5 then
call njjsaa(file2,outf1)
call msa_encryption(outf1,outf2)
call vernamenc(outf2,file1)
times=times2
Step 11: call function file_rev(file1,outf1)
Step 12: copy file outf1 into file2
Step 13: k=k+1
Step 14: goto Step 8
Step 15: End

2.2.2 Algorithm of vernamenc(f1,f2)

Step 1: Start vernamenc() function
Step 2: The matrix mat[16][16] is initialized with numbers 0-255 in row major wise order
Step 3: call function randomization() to randomize the contents of mat[16][16].
Step 4: Copy the elements of random matrix mat[16][16] into key[256] (row major wise)

Step 5: pass=1, times3=1, ch1=0
Step 6: Read a block from the input file f1 where number of characters in the block 256 characters
Step 7: If block size < 256 then goto Step 15
Step 8: copy all the characters of the block into an array str[256]
Step 9: call function encryption where str[] is passed as parameter along with the size of the current block
Step 10: if pass=1 then
times=(times+times3*11)%64
pass=pass+1
else if pass=2 then
times=(times+times3*3)%64
pass=pass+1
else if pass=3 then
times=(times+times3*7)%64
pass=pass+1
else if pass=4 then
times=(times+times3*13)%64
pass=pass+1
else if pass=5 then
times=(times+times3*times3)%64
pass=pass+1
else if pass=6 then
times=(times+times3*times3*times3)%64
pass=1
Step 11: call function randomization() with current value of times
Step 12: copy the elements of mat[16][16] into key[256]
Step 13: read the next block
Step 14: goto Step 7
Step 15: copy the last block (residual characters, if any) into str[]
Step 16: call function encryption() using str[] and the no. of residual characters
Step 17: Return

2.2.3 Algorithm of function encryption(str[],n)
Step 1: Start encryption() function
Step2: ch1=0
Step 3: calculate ch=(str[0]+key[0]+ch1)%256
Step 4: write ch into output file
Step 5: ch1=ch
Step 6: i=1
Step 7: if in then goto Step 13
Step 8: ch=(str[i]+key[i]+ch1)%256
Step 9: write ch into the output file
Step 10: ch1=ch
Step 11: i=i+1
Step 12: goto Step 7
Step 13: Return

2.2.4 Algorithm for Decryption
Step 1: Start
Step 2: initialize mat[16][16] with 0-255 in row major wise
Step 3: call function keygen() to generate times and secure
Step 4: call function randomization()
Step 5: set times2=times
Step 6: call file_rev(f1,outf1)
Step 7: set k=secure
Step 8: if k<1 go to Step 15
Step 9: call function file_rev(outf1,file2)
Step 10: set p=k%6
Step 11: if p=0 then
call msa_decryption(file2,outf1)
call njjsaa(outf1,outf2)
call vernamdec(outf2,file2)
times=times2
else if p=1 then
call function vernamdec(file2,outf1)
set times=times2
call function msa_decryption(outf1,outf2)
call fumction njjsaa(outf2,file2)
call function file_rev(file2,outf2)
call function msa_decryption(outf2,outf1)
call function vernamdec(outf1,file2)
times=times2
else if p=2 then
call njjsaa(file2,outf1)
call vernamdec(outf1,outf2)
times=times2
call msa_decryption(outf2,file2)
else if p=3 then
call vernamdec(file2,outf1)
times=times2
call njjsaa(outf1,outf2)
call msa_decryption(outf2,file2)
else if p=4 then
call msa_decryption(file2,outf1)
call vernamdec(outf1,outf2)
times=times2
call njjsaa(outf2,file2)
else if p=5 then
call vernamdec(file2,outf1)
times=times2
call msa_decryption(outf1,outf2)
call njjsaa(outf2,file2)
Step 12: copy the content of file2 to outf1
Step 13: set k=k-1
Step 14: Goto Step 8
Step 15: End

2.2.5 Algorithm of function vernamdec(f1,f2)
The algorithm of vernamdec() function is same as vernamenc() function. Here the only difference is that decryption() function is called instead of encryption() function.

2.2.6 Algorithm of decryption(str[],n)
Step 1: Start
Step 2: ch1=0
Step 3: ch=(256+str[0]-key[0]-ch1)%256
Step 4: write ch into the output file
Step 5: i=1
Step 6: if in then goto Step 12
Step 7: ch=(256+str[i]-key[i]-str[i-1]) %256
Step 8: write ch into the output file
Step 9: i=i+1
Step 10: goto Step 6

Step 11: ch1=str[n-1]
Step 12: Return

2.2.7 Algorithm of function file_rev(f1,f2)

Step 1: Start
Step 2: open the file f1 in input mode
Step 3: open the file f2 in output mode
Step 4: calculate n=sizeof(file f1)
Step 5: move file pointer to n
Step 6: read one byte
Step 7: write the byte on f2
Step 8: n=n-1
Step 9: if n>=1 then goto step-6
Step 10: close file f1, f2
Step 11: Return

2.3 NJJSAA ALGORITHM

Nath et al. [2] proposed a method which is basically a bit manipulation method to encrypt or to decrypt any file.

The encryption number (=secure) and randomization number (=times) is calculated according to the method mentioned in MSA algorithm [1].
Step 1: Read 32 bytes at a time from the input file.
Step 2: Convert 32 bytes into 256 bits and store in some 1- dimensional array.
Step 3: Choose the first bit from the bit stream and also the corresponding number(n) from the key matrix. Interchange the 1st bit and the n-th bit of the bit stream.
Step 4: Repeat step-3 for 2nd bit, 3rd bit...256-th bit of the bit stream
Step 5: Perform right shift by one bit.
Step 6: Perform bit(1) XOR bit(2), bit(3) XOR bit(4),...,bit(255) XOR bit(256)
Step 7: Repeat Step 5 with 2 bit right, 3 bit right,...,n bit right shift followed by Step 6 after each completion of right bit shift.

2.4 MSA (MEHEBOOB, SAIMA, ASOKE) ENCRYPTION AND DECRYPTION ALGORITHM

Nath et al. (1) proposed a symmetric key method where they have used a random key generator for generating the initial key and that key is used for encrypting the given source file. MSA method is basically a substitution method where we take 2 characters from any input file and then search the corresponding characters from the random key matrix and store the encrypted data in another file. MSA method provides us multiple encryptions and multiple decryptions. The key matrix (16x16) is formed from all characters (ASCII code 0 to 255) in a random order.

The randomization of key matrix is done using the following function calls:

Step-1: call Function cycling()
Step-2: call Function upshift()
Step-3: call Function downshift()
Step-4: call Function leftshift()
Step-5: call Function rightshift()

N.B: Cycling, upshift, downshift, leftshift, rightshift are matrix operations performed (applied) on the matrix, formed from the key.

3. Results And Discussions

This method, STJA is used to encrypt different types of data and few results are given below:

Message	Encrypted Message
aaaaaaaaaaaaaaaaaaaa aaaaaaaaaaaaaaaaaaab bbbbbbbbbbbbbbbbb bbbbbbbbbbbbbbbccc cccccccccccccccccccc cccccccccccccccccccc ccdddddddddddddddd dddddddddddddddddd ddd abababababababababab abababababababababab abababababababababab ababababababababacdc dcdcdcdcdcdcdcdcdcdc dcdcdcdcdcdcdcdcdcdc dcd	H‹Gë .¢±7èªS£X]Ó□,ˆ□!aoïà,²d ææ□Næ¼ÜâWŸAéƒ"•Ñ¡ □³: ™¬‰,Â+ŒvSÓx(Ó¡‰Ü □Ø8ã□□yÞyJFµ,qLdL@, S•éô£□FDäâ÷ð;«°b□ãâmJ]nÕ- =¶S”[¯R ÆlœePÕ%RqÔr È³•÷^N—□— Ç□Ì^O˜□VÉ¿{ƒÆÞ¬Uç*‘ □x>Ì($O¨r□E1¯ê{ë^óUq> ; oÜw 8Ø~Æãâ“2œk¢YTµ ZØ?é□MŸk`=Ó£ÚÞ□P›2 e›b«□0R21§CA+\vnF}³□Í ï×□□ò¢æXDß□Ê“Z‹ãÜ²Î ¿À
aaaaaaaaaaaaaaaaaaaaaa aaaaaaaaaaaaaaaaaaaaaa	□‹□v»´“ø¹Ô`† ¿>cÔ¸□Ôë#}ãÞÉ:□„ Ï\Ù”l-Äb›ªaÅ¤ÊÊò²ê_Åt:g ÷H□7Bƒ‰“F□õ□1W□# □à□ÈÚ«‘+óÞš ìÇV10•|□è□‹÷ãS:±□! ’ ¨□û,35Á,J0H□ÝªÄ’i?L/v ^Û O]ß¤ìr Gj3š□□DìáŒÄ□Y □šŸºP‡ ö›_□»¡š□°>□Ô,□ç/ÃŸíà U□ñºW?B□Lq×‘6Z□ŠqG ]í¨□~&¤pœ¹□{ïÅB□ôÎl¢ ÝX7êG□`K-æ<™fº]- T{,™¦³ZLÛì»… □½Õ□: ÊŒjï_□S□Ò•“□ □?ŠH'□éhÑ}ÁTÕµ¶sÕXI $æÝ^0□’□w:q□- ^ª6àW□Ö©Í;à□Ô5vâÚ¥” □Ñ›H□] Üq□À□T— □Ÿ]□ □? ŠH'□éhÑ}ÁTÕµ¶sÕXI$æ Ý^0□’□æw:q□- ^ª6àW□Ö©Í;à□Ô5vâÚ¥” □Ñ›H□] Üq□À□T— □Ÿ]□ Ä’i?L/v^Û O]ß¤ìr Gj3š□□DìáŒÄ□Y □šŸºP‡ ö›_□»¡š□°>□Ô,□ç/ÃŸíà

aaaaaaaaaaaaaaaaaaaa aaaaaaaaaaaaaaaaaaaa aaaaaaaaaaaaaaaaaaaa aaaaaaaaaaaaaaaaaaaa aaaaaaaaaaaaaaaaaaaa aaaaaaaaaaaaaaaaaaaa aaaaaaaaaaaaaaaaaaaa aaaaaaaaaaaaaaaaaaaa aaaaaaaaaaaaaaaaaaaa aaaaaaaaaaaaaaaaaaaa aaaaaaaaaaaaaaaaaaaa aaaaaaaaaaaaaaaaaaaa aaaaaaaaaaaaaaaaaaaa aaaaaaaaaaaaaaaaaaaa aaaaaaaaaaaaaaaaaaaa aaaaaaaaaaaaaaaaaaaa a (1024 a)	U□ñºW?B□Lq×'6Z□ŠqG]í¨□~&¤pœ¹□{ïÅB□ôÎl¢ ÝX7êG□`K-æ<™fº]- T{,™¦³ZLÛì»⋯ Ä'i?L/v^O]ß¤ìr Gj3š□□D ìáŒ□Y□šŸºP‡ ö›_□»¡š□°>□Ô,□ç/ÃŸíà U□ñºW?B□Lq×'6Z□ŠqG ]í¨□~&¤pœ¹□{ïÅB□ôÎl¢ ÝX7êG□`K-æ<™fº]- T{,™¦³ZLÛì»⋯ <Âß□"&□ OÎ□ú□;UíÝ61ùnÛÃï□òŠ `ð□œY□ÿAÇ"Óþ±S□Ñ□ S†I"□Ö¢□ <Â□"&□ OÎ□ú□;UíÝ61ùnÛÃï□òŠ `ð□œY□ÿ¥AöâÇ"Óþ±S□ Ñ□S†I"□Ö¢□
The Xaverian vision education encompasses a sensitive understanding of the realities defining our existence. It is our committed mission to incorporate in the minds of our students an awareness of this social vision so that they can be better equipped to take up the larger responsibilities in every sphere of life.	n□a4ýÍqýè□□□5Z□«□aú ïørJ ^z¯rë□„□}{«z:w□t□ „□ ‰ð*onmk~syx oxmywzk}}o}k}o x}s~s□oxno|}~xnsxq*yp* ~ro*|okvs~ so^&noy|o□,s } Smyws~ ~onws } ~o *sx~r owsxn}ypy|}~ š□□nox~}* kx*kk|oxo}}yp~ rs}}ym š□□skv*s}syx*}y~rk~~ ro*f*m kx*lš□□o*lo~~o|*o{szzo n~y*~ kuoz~ro*vk|qo| |o}zyx}sl svs~so}*sxoo|*f*}zro|š□□o *yp*vspo8

data. Fig 1.1 shows the spectral analysis of frequency of characters of 1024 ASCII value (1) and Fig 1.2 shows the spectral analysis of frequency of characters of the encrypted data.

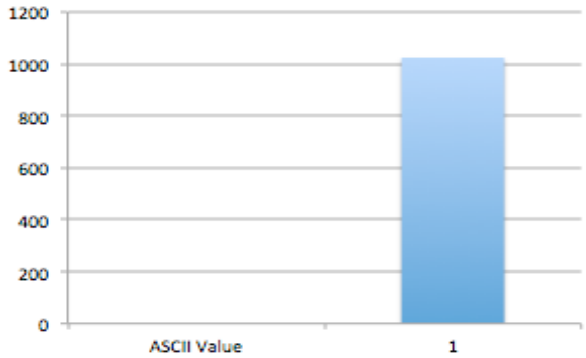

Fig 1.1: Spectral Analysis of Frequency of Characters of 1024 ASCII Value(1)

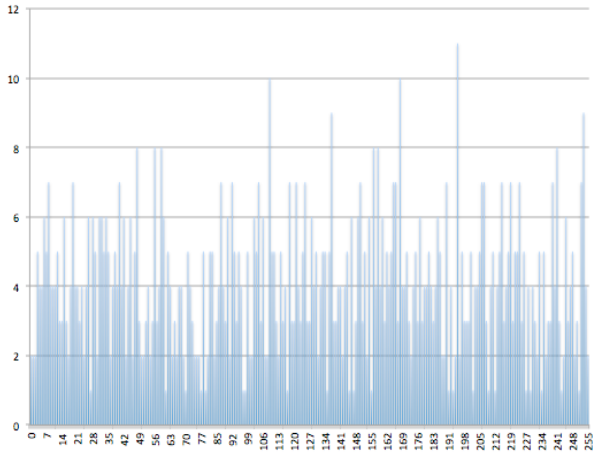

Fig 1.2: Spectral Analysis of Frequency of Characters of Encrypted data of 1024 ASCII value (1)

As 2nd Test case we chose a random text file. The spectral analysis of the frequency of characters of the text file is shown in Fig 2.1 and Fig 2.2 shows the spectral analysis of frequency of characters of encrypted text.

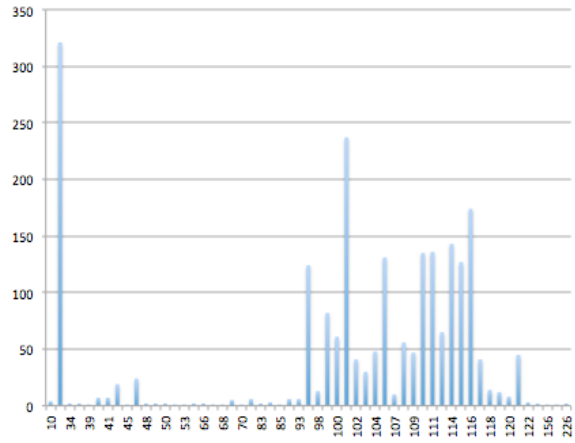

Fig 2.1: Spectral Analysis of frequency of characters of an ordinary text file

4. Spectral Analysis And Cryptanalysis

One of the classical cryptanalysis method used is by detecting the frequency of characters in the encrypted text (message). So to test the effectiveness of STJA method, spectral analysis of the frequency of characters are closely observed. Using this method, STJA, we ran many analysis and tested different strings as input and used various methods of cryptanalysis. To show the usefulness and integrity of this cryptographic module, we used spectral analysis of the frequency of characters.

First, as a test case we chose, a file which contained 1024 ASCII value (1) and used this method to encrypt the

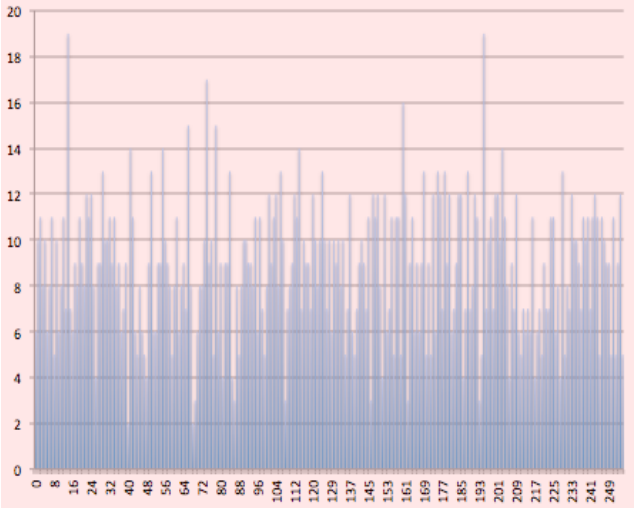

Fig 2.2: Spectral Analysis of frequency of characters of the encrypted text file

Thus from the above spectral analysis it is evident that the method, STJA, used here is very effective and there is no trace of any pattern in the encryption technique.

Since this cryptographic technique uses multiple bit and byte level encryption multiple times, for this reason, the method used here is unique and almost unbreakable because there is no trace of any pattern. And this method is also effective against both Differential Cryptanalysis (Differential Attack) and Brute-Force Attack.

5. Conclusion and Future Scope

In the present work we use three different algorithms to make the encryption process unbreakable from standard cryptographic attack. That is evident from our results. We have applied our method on some known text where the same character repeats for a number of times and we have found that after encryption there is no repetition of pattern in the output file. We have tested this feature closely and have found satisfactory result in almost all cases. This has been possible as we have used modified Caesar Cipher method with polynomial function, modified Vernam Cipher method with feedback mechanism and also NJJSAA and MSA methods, where we use mainly the bit manipulation. We propose that this encryption method can be applied for data encryption and decryption in banks, defense, mobile networks, ATM networks, government sectors, etc. for sending confidential data. The above method, STJA, may be further strengthened using additional bit manipulation method and we have already started to work on it.

6. Acknowledgment

Somdip Dey (SD) expresses his gratitude to all his fellow students and faculty members of the Computer Science Department of St. Xavier's College [Autonomous], Kolkata, India, for their support and enthusiasm. AN is grateful to Dr. Fr. Felix Raj, Principal St. Xavier's College, Kolkata for giving opportunity to work in the field of data hiding and retrieval.

7. References

[1] http://www.purdue.edu/discoverypark/gk12 / downloads/Cryptography.pdf

[2] Symmetric key cryptosystem using combined cryptographic algorithms - Generalized modified Vernam Cipher method, MSA method and NJJSAA method: TTJSA algorithm " Proceedings of Information and Communication Technologies (WICT), 2011 " held at Mumbai, 11th – 14th Dec, 2011, Pages:1175-1180

[3] Symmetric Key Cryptography using Random Key generator: Asoke Nath, Saima Ghosh, Meheboob Alam Mallik: "Proceedings of International conference on security and management(SAM'10" held at Las Vegas, USA Jull 12-15, 2010), P-Vol-2, 239-244(2010).

[4] New Symmetric key Cryptographic algorithm using combined bit manipulation and MSA encryption algorithm: NJJSAA symmetric key algorithm: Neeraj Khanna,Joel James,Joyshree Nath, Sayantan Chakraborty, Amlan Chakrabarti and Asoke Nath : Proceedings of IEEE CSNT-2011 held at SMVDU(Jammu) 03-06 June 2011, Page 125-130.

[5] Advanced Symmetric key Cryptography using extended MSA method: DJSSA symmetric key algorithm: Dripto Chatterjee, Joyshree Nath, Soumitra Mondal, Suvadeep Dasgupta and Asoke Nath, Jounal of Computing, Vol3, issue-2, Page 66-71,Feb(2011)

[6] A new Symmetric key Cryptography Algorithm using extended MSA method :DJSA symmetric key algorithm, Dripto Chatterjee, Joyshree Nath, Suvadeep Dasgupta and Asoke Nath : Proceedings of IEEE CSNT-2011 held at SMVDU(Jammu) 3-5 June,2011, Page-89-94(2011).

.

[7] Symmetric key Cryptography using modified DJSSA symmetric key algorithm, Dripto Chatterjee, Joyshree Nath, Sankar Das, Shalabh Agarwal and Asoke Nath, Proceedings of International conference Worldcomp 2011 held at LasVegas 18-21 July 2011, Page-306-311, Vol-1(2011).

[8] An Integrated symmetric key cryptography algorithm using generalized vernam cipher method and DJSA method: DJMNA symmetric key algorithm : Debanjan Das, Joyshree Nath, Megholova Mukherjee, Neha Chaudhury and Asoke Nath: Proceedings of IEEE International conference : World Congress WICT-2011 to be held at Mumbai University 11-14 Dec, 2011, Page No.1203-1208(2011). .

[9] Symmetric key Cryptography using two-way updated – Generalized Vernam Cipher method: TTSJA algorithm, Trisha Chatterjee, Tamodeep Das, Shayan dey, Joyshree Nath, Asoke Nath , International Journal

of Computer Applications(IJCA, USA), Vol 42, No.1, March, Pg: 34 -39(2012).

[10] Ultra Encryption Standard(UES) Version-I: Symmetric Key Cryptosystem using generalized modified Vernam Cipher method, Permutation method and Columnar Transposition method,
Satyaki Roy, Navajit Maitra, Joyshree Nath,Shalabh Agarwal and Asoke Nath, Proceedings of IEEE sponsored National Conference on Recent Advances in Communication, Control and Computing Technology-RACCCT 2012, 29-30 March held at Surat, Page 81-88(2012).

[11] Peter Montgomery, "Modular Multiplication Without Trial Division," Math. Computation, Vol. 44, pp. 519–521, 1985.

[12] W. Hasenplaugh, G. Gaubatz, and V. Gopal, "Fast Integer Reduction," 18th IEEE Symposium on Computer Arithmetic (ARITH '07), pp. 225– 229, 2007.

Computer Power Management Awareness – An Insight from Youngsters in Mauritius

G.Bekaroo[†], S.Akhal[†], D.L.Padaruth[†], C.Bokhoree[†] & C.Pattinson[‡]

[†] School of Sustainable Development and Tourism,
University of Technology, Mauritius

[‡]Faculty of Arts, Environment & Technology,
Leeds Metropolitan University
Leeds, UK

ABSTRACT

Down the past years, the number of computer and Internet users has been constantly increasing in several countries and today, more and more youngsters are starting to use computers at an earlier age be it at home or in educational institutions. In many countries around the world, computer literacy among youngsters is being promoted since a very young age where computer studies are being taught in schools. However, this increase in the computer usage has led to an increase in power consumption which adversely affects the environment mainly due to the non-renewable power production techniques currently being employed.

Computer Power Management (CPM) interacts with every part of the computer system including the operating system, software, Central Processing Unit, peripheral devices, etc, and is present in most modern operating systems. Different techniques are available today to save power while using computers. Since computers are now being used at an earlier age and are intensively being used by youngsters, an understanding on how the different power saving techniques being employed is very important.

This paper attempts to provide an insight on CPM from youngsters, following a survey carried out where 300 youngsters aged between 19 and 24 were interviewed. The study aimed to find out whether youngsters today are aware of the different CPM strategies, the motivation behind using these strategies and the application of these strategies by youngsters today. This paper also discusses on the method and results of the study conducted, to give an insight on CPM from youngsters and also make recommendations on how CPM techniques can be better promoted to be adopted by youngsters of tomorrow.

KEYWORDS

Computer Power Management, Green IT, Sustainability, Energy Efficiency, Youngsters

INTRODUCTION

Computers were first used for military purposes but since their commercialization, computers have been ever-growing and are invading human life. An increasing number of people are using the computer today because of the various benefits and facilities it provides. But as it grew famous, and as the activities and facilities it provides kept on increasing, the age at which people started using the personal computer has decreased proportionally. Studies have shown that the use of computers and the Internet by youngsters has been rapidly increasing in recent years (US DoC, 2002; ONS, 2010) and that computer and Internet use is more widespread among youngsters aged between 19 and 24 than among adults (DeBell and Chapman, 2003).

Today, youngsters are dominating the Internet population (Canadian News, 2010) and statistics (ONS, 2010) are showing that people are starting to use computers at an earlier age. Kids between the ages of 2 and 12 years old spend more than a quarter of their leisure time on the computer and in that amount of time, 3 to 7 minutes is spent on watching online video (Nielsen Company, 2009). In terms of computer usage, usually boys spend most of this time playing game while girls check their mails, chat or spend time on social networks. The increase in computer and Internet usage by youngsters is due to the fact that computers and Internet are easily accessible at home, in schools and even in public places.

However, studies have shown that personal computers are not being actively used during most of the time they are switched on (Miller, 2008). At home, much power is consumed when computers are left on especially during computer downloading from the Internet which is mostly practiced by youngsters. Even in the working environment, it is estimated that in a normal working day at the office, computers are in use for around 4 hours and idle for another 5.5 hours in average (Miller, 2008). This massively growing use of computer today also has its adverse economical, environmental and social impacts (Hirsch, 2004).

Unsustainable Computer Power Usage

Unsustainable computer power consumption has a direct impact on the environment as well as the global economy, triggering a snowball effect affecting the society and different cultures. It has been estimated that global carbon emissions from information and communication technologies are roughly equal to that of the airline industry (Laing & Scheid, 2010) and this is mainly because of the massive amount of electricity needed in order to operate computers and associated peripheral devices. Similarly, a desktop computer normally has a 200-watt power supply and if 100 million of these machines are turned on at once worldwide, together they would use approximately 20,000 megawatts of electricity which is the total output of 20 average-sized nuclear power plants (Tanenbaum, 2001). On top of that, it is a fact that computers tend to heat-up the environment in its surroundings though it might not be apparent to the user.

As a major negative impact on the environment, high rates of carbon dioxide are released in the air due to increased production of electricity, leading to an increase in the atmosphere's temperature thus accelerating the effects of global warming (International Socialist Group, 2006). Consequently, extreme weather events such as category five cyclones, droughts, rising sea levels and decreased snow cover are already being faced almost everywhere around the world (IPCC, 2007) which drastically affect the lifestyle of species living in these regions while also endangering the fauna. Reducing energy consumption not only makes sense from the environmental perspective but it is also an increasingly economical concern. Energy prices are constantly rising similar to government-imposed levies on carbon production which has an impact on the cost of doing business, thus making many current business practices economically unsustainable. At home, the rising energy costs translate into higher energy bills which in turn affect the lifestyle of people in a society.

Taking cognizance of the environmental and economical impacts caused by the massively growing use of computers today, it is becoming more and more important for home computer users and businesses to act in an environmentally responsible manner. Different measures are already being taken by businesses and also researchers in order to promote greenness. Businesses are applying existing best practices for promoting greenness during their day to day operations and are also providing training to their staffs so that they are aware of the current problems being faced by the environment along with how they can help in improving the situation. Researchers, in turn are focusing on different ways which can be employed in order to improve energy efficiency during all aspects of computer usage. As such, one of the areas of focus by researchers has been Computer Power Management (CPM) techniques which has been constantly evolving down the years and are now available on all latest operating systems (Nordman et al, 1997).

Computer Power Management (CPM)

The computer power management technology was introduced in order to reduce energy consumption for computers that are not in active use. Power management interacts with every part of the computer including the operating system, software, CPU, peripheral devices, etc. This technology is beneficial to the environment in the way that a reduction in power consumption mainly means a reduction in the overall need for the amount of power harnessed and if non-renewable sources are being used to generate electricity, this implies lesser pollution and also lesser adverse impacts on the environment and climate.

Power-management does not reduce the performance of a computer, but simply adds features to reduce their power consumption when not in use (Nordman et al, 2007). Most power management savings come from reducing power when the machine is not fully active by adding low-power or "sleep" modes that kick in when idle. But there are many more techniques that can be used to save energy consumption from computers. Some of the common practices adopted today in order to reduce power consumption from computer usage include:

- *Using built-in power saving features*

  Most operating systems today come with power saving features that turn hardware including hard drives or the computer monitor into sleep mode when inactive for a particular period of time set by the user. Under this mode, power consumption can be reduced by 20 to 50 times (Maurya, 2010).

- *Turning off computer while not in use*

  Completely turning off computers while not in use saves a good amount of electricity since standby or 'phantom' power load can range from a few watts to as much as 20 or even 40 watts depending on equipment (EnergyStar, 2009).

- *Purchasing energy efficient products*

  Using energy efficient products is considered as a good way to save energy and customers may look for logos like the Energy Star (EnergyStar, 2009) to buy computer hardware that offers good energy efficiency. Also, experts estimate that using such products can save around 30 to 40 percent on utility bills (Utility Bill Assistance, 2010).

- *Disable devices that are not in use*

  Desktop computers and laptops come with different devices that a user might not need and if connected, it means power is being consumed. For example, a laptop user who is using a built-in network adapter and a cable to connect to the Internet would probably not need Wi-

Fi, the built-in modem, Bluetooth or infrared and disabling these devices would save power.

- *Reducing screen brightness*

A good amount of power can be saved in the long run of computer usage by reducing brightness of computer monitors.

- *Share hardware where appropriate*

Hardware like printers and scanners that are connected to a computer system is also using power can be saved by sharing these devices.

- *Using efficient power supply units*

The power supply unit basically distributes the power to the various computer components by converting AC power from electric utilities into DC power. Now, the 80 Plus initiative (Plug Load Solutions, 2011) certifies power supply units with an energy efficiency of 80% or more and a true power factor of 0.9 and more, meaning that power supply units need less energy to supply the computer system with the same power.

- *Upgrading screen and peripheral devices*

Power consumption can be reduced by upgrading to more efficient devices. For example, when upgrading CRT monitors to flat panel LCD monitors of the same size, power consumption can be reduced to 1/3 (UCLA Ergonomics, 2009).

Though different techniques to reduce power consumption from computer usage are already available today, the big question that arises is that whether computer users are aware of these techniques. If yes, which of the techniques are they adopting and what are their motivations behind using/not using currently available CPM techniques. This paper presents a study made to answer these different questions in the area of CPM by targeting youngsters in Mauritius aged between 19 and 24, who dominate the Internet users and also represent the future.

RELATED WORK

Different studies in CPM and awareness have been conducted in the past to reduce power consumption in personal computers and servers where most concentrated on improving battery life in portable computers. Today, due to visible climate variability in the world, researchers are focusing more and more on how to reduce energy consumption in all aspect of computer usage.

In the area of household power management, Dillahunt et al (2009) studied to elicit viewpoints and practices surrounding household energy management where 26 low income households from two very different locations were considered. Through photo-elicitation and directed interviews, the relationship between energy saving behaviours, external factors and users' intrinsic values and beliefs were explored. The study showed that most of the participants were saving energy because they wished to save money. The other reasons why the household owners were saving energy were because some wanted to comply with a moral and spiritual aversion to waste and the rest were environmentally motivated. Similarly, Chetty et al (2009) studied 20 households about how people use power management strategies on their home computers. With the help of a logging software installed on the computers, the power state (on, off, standby, etc) as well as basic computer usage, e.g. frequently used applications and their duration of use, were tracked. The results of the experiment after 14 days of study showed that 47% of the total computers had no power management settings turned on. However, the major constraint of this research was that most of the household were in a medium or high income bracket where only 3 among the 20 participants were earning below $.50K annually. As such, most people would not be motivated to reduce power consumption bearing in mind the different reasons why power management strategies are not used.

Also, different power meters and home energy monitoring kits are now available on the market which better help to measure and monitor energy consumed in households. The best way to reduce power consumption in a house is by adopting a two-pronged approach (PowerMeterStore, 2011) which involves firstly to measure and monitor the total power consumption in the house and secondly, to measure and monitor power consumption of individual electronics (including computers and associated peripheral devices) and electric appliances. Common devices for power measurement and monitoring power of individual electronics include Kill A Watt (P3 International Corporation, 2008) and Watts Up Pro (Watts-Up, 2011) and these devices can tell users how much energy is being used for a particular instant or period of time by appliances and electronics plugged to the device. For measuring and monitoring total power consumption, common home energy monitoring kits including Cent-a-Meter (Cent-a-meter, 2011) and Power Cost Monitor (PowerCostMonitor.com, 2011) are now increasingly being used.

Much power is being consumed when computers are left switched on at night by youngsters for downloading online materials. As a solution, Agarwal et al (2008) developed an architecture named Somniloquy that aims to augment network interfaces to allow computers in sleep mode to be responsive to network traffic. As part of the experiment, a small USB connected hardware and software plug-in system was built which allows a PC to remain in sleep mode while continuing to maintain network presence and run well-defined application functions (e.g. VoIP, web downloads, file sharing, etc). By using this implementation, a great amount of power could be saved.

Increasing people awareness is one of the key steps towards promoting Green IT and increasing utilisation of CPM

techniques. Youngsters need to understand the impacts of the growing IT industry on the climate and environment today, and also what techniques are current available that they can adopt in order to reduce power consumption during their normal computer usage. To promote awareness in going green, many training institutions are now providing courses on promoting sustainable development in different areas thus making the participants 'Green Literate'. Even in universities, courses on climate change are available as well as modules related to sustainable development are being integrated in different programmes (Talebi, 2009) so that new graduates from the university can apply their academic skills in the area in their working life and promote greenness.

METHOD

This study builds on the previous studies conducted in Green IT and CPM awareness but focuses on youngsters between 19 and 24 years. In order to understand on whether youngsters today are acquainted with computer power management, their motivations behind computer power management and what are the different techniques they are currently employing, a group of youngsters aged between 19 and 24 were interviewed.

For the case study, students enrolled in tertiary institutions for undergraduate/postgraduate studies were considered and the study started with a national search for the number of students enrolled in the different tertiary institutions in Mauritius. According to the Tertiary Education Commission (2011), around 30,000 students were found taking courses between this age range. From a statistical perspective, considering a confidence level of 95% and a marginal level of 5.5%, 300 students were interviewed at different tertiary institutions in Mauritius. As such, students with different profiles took part of the study with varying family income, years of computer usage and field of study.

During the interview, youngsters were asked different questions and a survey form was filled. Questions asked were related to climate change issues, CPM awareness, motivations behind using CPM, reasons for not using CPM techniques, and interest in sustainability issues.

Respondents Profile

Among the 300 interviewees, there were 176 males and 124 females; and all were computer literate. The respondents were from different fields and levels of undergraduate/postgraduate study, where 96.3% of the respondents were using computer on a daily basis and the remaining 3.7% on a weekly basis. The age distribution of the respondents is shown in Figure 1.

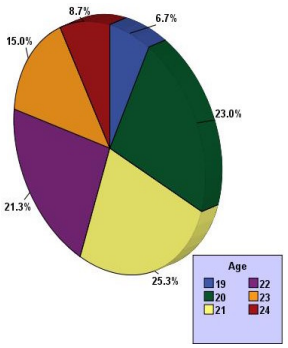

Figure 1- Respondents Age

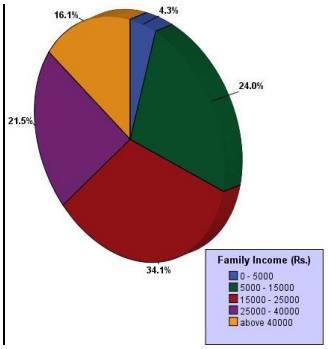

Figure 2- Respondents Family Income

In terms of computer usage experience distribution, 80% of the respondents have been using computers for more than 5 years, 16.3% between 1 and 5 years and 3.7% for less than a year. Also, for the survey, the students had a varying family background where most of them were from medium monthly income between Rs.15,000 and 25,000. Figure 2 shows the percentage of the respondents and their family income.

RESULTS & DISCUSSION

From the general questions asked regarding climate change, results showed that 89.3% of the interviewed youngsters highly agree that the nature is fragile and that people should be careful about not to harm or disrupt it. The same group of respondents also agree that several countries around the world, including Mauritius, are currently facing the effects of climate change and say that it is very important to preserve the environment for future generations. Among the remaining 32 youngsters (representing 10.7%) who disagree that the nature is fragile, 62.2% of the interviewees were students of Human Resources or Management courses. These students are however following non-environmentally linked programmes at the university and are less conscious of environmental threats and their causes. Also, the results showed that 6.7% of the total 300 students coming from the high family (above Rs. 40,000 as monthly salary) disagree to the same fact as compared to 3.0% of participants ranging from low family income.

However, regarding the climate change problems being faced throughout the world, only 40.3% of the youngsters say that they have been paying close attention to the problems. In this group of youngsters, only 16.2% come from high income family, that is, a monthly salary of above Rs 40,000. Also, among all the youngsters, only 22.7 % of youngsters claimed that they are making some efforts to contribute to a greener environment by using common techniques including recycling, power saving and waste reduction. The rest who claim to make no contribution to a greener environment include 30 females (24.2%) as compared to 61 males (35.4%), thus implying that female youngsters are more environment conscious than males as discussed by Hampel et al (1996).

In terms of computer usage, 21 interviewees claim to rarely (weekly or monthly basis) or never switch off computers and the most common reasons for not doing so are as follows:

1. *Computer is always in use (66.8%)*
   The computers of this small group of youngsters are always in use because of the main reasons including downloading files from the internet, gaming, video streaming or spending time on social networks.

2. *Long booting-up times (25.4%)*
   This group of youngsters prefer to leave computers in stand-by mode or screen-saver mode because their computers take quite long to boot-up.

3. *Computer will get damaged (7.8%)*
   A few youngsters still think that their computers will get damaged while constantly switching on and off their computers and prefer to use stand-by or hibernate mode if they will not be using their computers for long hours.

Power monitoring at home, which is one of the practices towards saving electricity is still not practiced by a group of youngsters. Around 60.7% of youngsters monitor electricity usage at home though only 19% are familiar to commercial devices such as Kill a Watt or Power Monitor. During the interviews, youngsters were also asked on their different motivations behind using CPM techniques. The results are shown in Figure 3 where the count and percentage of youngsters opting for the different motivations (out of 300) are labelled on the different bars.

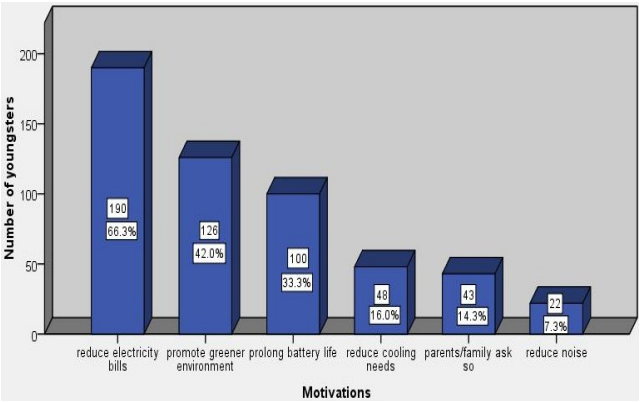

Figure 3 - Motivations behind using CPM techniques

From Figure 3, reduction of electricity bills is found to be the main motivation behind using CPM techniques irrespective of age, sex and family income. However, it has been observed that as the family income rises, reduction of electricity bills becomes less of a motivation to the youngsters. For youngsters hailing from medium to high family income, prolonging battery life is the second main motivation behind using CPM techniques followed by promoting a greener environment. Also, a small percentage of the interviewees say that their parents ask to employ techniques to better save power/energy via computer usage. This group of youngsters hail mostly from low to medium family income earners, similar to the study by Dillahunt's et al (2009), and again this reason becomes less as a motivation again as family income increases.

A big part of the survey was to find out on the different techniques being employed by youngsters in order to save power/energy while using computers. The results obtained are shown in Table 1 arranged in descending order on youngsters count.

No	CPM Technique	Count	Percentage
1.	turn off monitor instead of using screen saver	161	54.60%
2.	turn off computer instead of using standby mode	160	54.20%
3.	built-in power saving features on computer	142	48.10%
4.	turn down screen brightness	124	42.00%
5.	disable devices not in use	84	28.50%
6.	using laptop instead of desktop computers	75	25.40%
7.	using more efficient computer parts	62	21.00%
8.	power saving for USB devices	61	20.70%
9.	upgrade devices	53	18.00%
10.	share hardware where appropriate	39	13.20%

Table 1 – CPM Techniques adopted by youngsters

From the results obtained, techniques involving turning off the devices that is not being used (including monitor, printers, among others), are the most popular techniques. Using energy efficient materials, which is a good technique to save energy, is not much adopted since it involves the cost of upgrading/changing the appropriate devices, where many youngsters are quite reluctant for initial investment. Similarly, the reason for using laptops instead of desktop computers hasn't been for cost saving among many youngsters, but rather because of portability reasons. Also, the power saving feature for USB devices is not that familiar where a big percentage of the interviewees did not know on how to activate this feature on their computers. Another observation is that hardware sharing is very less used, and is even the last on the list in Table 1, though a big amount of energy can be saved while adopting this technique. The main reason behind this is at home, many students do not have a small Personal Area Network or Local Area Network, where they can share devices being used (most commonly the printer or multifunctional devices).

In terms of barriers of CPM usage, the youngsters think that the main barrier is that CPM techniques haven't been much promoted and that nobody really talks about it. Awareness in application of CPM techniques is another barrier where techniques like power saving for USB devices or hardware sharing are not very common. One of the common reasons for the awareness problem is that in many courses, sustainability issues are not given much importance. Among

the interviewed youngsters, only 23.3% remember of having done lectures/modules related to sustainability issues. However, 85.7% of the interviewees claim to be interested if sustainability or energy efficiency based modules are integrated in their course.

RECOMMENDATIONS

During the survey, youngsters have also been proposing different recommendations in order to increase awareness and promote CPM techniques. These are as follows:

1. *Early awareness on CPM techniques*
   One of the first steps towards increasing CPM techniques utilisation is to increase user awareness in the area. Since today more and more people are starting to use computers at an earlier age, improving awareness in the subject area at an earlier age would make CPM techniques utilisation a habit to computer users, including youngsters.

2. *Regular campaigns*
   Promoting CPM and Green ICT techniques by using different means of advertisement and at a regular basis would better promote the subjects to youngsters while at the same time targeting a wider range of computer users. Youngsters should better understand the current climate change problems being faced around the world and what the different solutions are to this problem.

3. *Default CPM techniques set by vendors*
   Computer vendors should set default power saving options on new computers and laptops if they are not already practising this. A big amount of energy can be saved from computers being utilised by youngsters who are not familiar to CPM and Green ICT techniques.

4. *Sustainability courses at all levels*
   So as computer users to be aware of the evolving CPM and Green ICT techniques, courses in the same subject areas should be promoted at all levels of education, namely in schools, colleges and universities.

5. *Supporting research and innovation in green technologies*
   Promoting research and innovation in the green technologies can help in attracting more youngsters into this area, in the common forms of scholarships and prizes through competitions. Research and innovation would also be beneficial in the way that innovative and optimised CPM techniques can be developed to better save energy while computer and associated peripherals usage.

CONCLUSION

This paper presented an insight from youngsters in the area of computer power management. As part of the study, 300 youngsters aged between 19 and 24 were interviewed so as to understand which CPM techniques they are aware of, their motivations behind using these techniques and the barriers behind adoption of CPM techniques. Turning off or disabling devices while not in use is still the most common techniques to save power while using computers and youngsters think that the main barrier to CPM usage is that CPM techniques haven't been much promoted. A set of recommendations to promote and increase awareness on CPM techniques have also been discussed including early awareness on CPM techniques, regular campaigns and supporting research and innovation in green technologies.

REFERENCES

AGARWAL, Y., HODGES, S., SCOTT, J., CHANDRA, R., BAHL, V.; GUPTA, R. (2008), *Somniloquy: Maintaining network connectivity while your computer sleeps* [online]. Microsoft Research. Accessed on: 01 Nov 2009, Available at: http://research.microsoft.com/research/pubs/view.aspx?type=Technical%20Report&id=1458

Canadian News (2010), *Youths rule Internet, but elderly making gains: study* [online], Accessed on: 12 Dec 2010, Available at: http://www.canada.com/topics/technology/story.html?id=1231474

Cent-a-meter (2011), *Think Green* [online], Accessed on: 21 Jan 2011, Available at: http://www.centameter.com.au/

CHETTY, M.; BRUSH, B.A.J., MEYERS, B.R., JOHNS, P. (2009), *It's Not Easy Being Green: Understanding Home Computer Power Management*, Conference on Human Factors in Computing Systems archive, Proceedings of the 27th international conference on Human factors in computing systems, ISBN: 978-1-60558-246-7

DeBell, M.; Chapman, C. (2003), *Computer and Internet Use by Children and Adolescents in the United States*, National Center for Education Statistics

DILLAHUNT, T.; MANKOFF, J.; PAULOS, E.; FUSSELL, S. (2009), *It's Not All About "Green": Energy Use in Low-Income Communities*. Proceedings of the 11th international conference on Ubiquitous computing, p.255-264, ISBN: 978-1-60558-431-7

Energy Star (2009), *How the rating system works* [online], Accessed on: 10 Jan 2011, Available at: http://www.energystar.gov/index.cfm?c=evaluate_performance.pt_neprs_learn

HAMPEL, B; BOLDERO, J.; HOLDSWORTH, R. (1996), Gender patterns in environmental consciousness among adolescents, Journal of Sociology March 1996, vol. 32 (no. 1), p.59

HIRSCH, T. (2004), *Computers 'must be greener'* [online], BBC News, Accessed on: 10 Feb 2012, Available at: http://news.bbc.co.uk/2/hi/technology/3541623.stm

International Socialist Group (2006), *Climate Change- The biggest challenge facing humanity* [online], Accessed on: 02 Oct 09, Available at: http://www.isg-fi.org.uk/spip.php?article303
IUCN; UNEP; WWF (1991), *Caring for the Earth*, IUCN Gland, Switzerland.

IPCC (2007), *Climate Change 2007: Working Group I: The Physical Science Basis* [online], IPCC Fourth Assessment Report: Climate Change 2007, Intergovernmental Panel on Climate Change, Accessed on: 22 Feb 2011, Available at: http://www.ipcc.ch/publications_and_data/ar4/wg1/en/spmsspm-direct-observations.html

KORN, D.; HUANG, R.; BOLIOLI, T.; WALKER, M. (2006), *Computer Power Management for Enterprises- A Practical Guide for Saving up to $100 per Seat Annually in Electricity*, Proceedings of the 2006 IEEE International Symposium on Electronics and the Environment, p. 161-166, ISSN: 1095-2020

LAING, F.; SCHEID, J. (2010), An *Introduction to Green Computing and Sustainable Development* [online], Accessed on: 12 Jan 2011, Available at: http://www.brighthub.com/environment/green-computing/articles/74469.aspx

LENHART, A; HITLIN, P.; MADDEN, M. (2005), *Teens and Technology - Youth are the leading the transition to a fully wired and mobile nation*, PEW Internet & Americal Life Project, Washington, D.C.

MAURYA, R.R. (2010),*Tips to Save PC Energy* [online], Global Review Channel, Accessed on: 19 Feb 2011, Available at: http://www.globalreviewchannel.com/resources/2576-Tips-Save-PC-Energy.aspx

MILLER (2008), *Computer power management* [online], Information Technology, MILLER School of Medicine University of Miami, Accessed on: 5 Jan 2010, Available at: http://it.med.miami.edu/x1159.xml

Nielsen Company (2009), *How Teens Use Media* [online], Accessed on: 22 Feb 2011, Available at: http://blog.nielsen.com/nielsenwire/reports/nielsen_howteensusemedia_june09.pdf

NORDMAN, B.; PIETTE, M.A.; KINNEY K.; WEBBER, C. (1997), *User Guide to Power Management for PCs and Monitors*, Environmental Energy Technologies Division, Lawrence Berkeley National Laboratory

ONS (2010), *Internet Access 60% of adults access Internet every day in 2010*, Office of National Statistics, Accessed on: 22 Feb 2011, Available at: http://www.statistics.gov.uk/cci/nugget.asp?id=8

P3 International Corporation (2008), *Kill A Watt* [online], Accessed on: 04 Dec 2010, Available at: http://www.p3international.com/products/special/P4400/P4400-CE.html

Plug Load Solutions (2011), *80 PLUS Certified Power Supplies and Manufacturers* [online], Accessed on: 17 Feb 2011, Available at: http://www.plugloadsolutions.com/80PlusPowerSupplies.aspx
PowerMeterStore (2011), *Home Energy Monitor Kits* [online], Optimum Energy Products Ltd, Accessed on: 20 Jan 2011, Available at: http://www.powermeterstore.com/c628/home_energy_monitor_kits.php

PowerCostMonitor.com (2011), *PowerCost Monitor Home Energy Meter* [online], Accessed on: 21 Jan 2011, Available at: http://www.powercostmonitor.com/

TANENBAUM, A.S. (2001), *Modern Operating Systems*, 2nd Edition, Published by: Prentice Hall, ISBN: 0130313580

Tertiary Education Commission, *Review of the Tertiary Education Sector 2009/2010* [online], Accessed on: 20 Feb 2011, Available at: http://tec.intnet.mu/tesm_rvw.php

UCLA Ergonomics (2009), *Choosing a computer screen; LCD or CRT*? [online], Accessed on: 18 Feb 2011, Available at: http://www.ergonomics.ucla.edu/articles/LCDvCRT.pdf

US DoC (2002), A Nation Online: *How Americans Are Expanding Their Use of the Internet*, U.S. Department of Commerce, Washington, DC.

Utility Bill Assistance (2010), *Use Energy Efficient Appliances to Help Reduce your Utility Bills* [online], Accessed on: 17 Jan 2011, Available at: http://www.utilitybillassistance.com/html/energy_efficient_appliances_sa.html

Adding a one-to-one and hash function - is the result a one-to-one function?

Elena Braynova[1] and Michael Simmarano[1]
[1] Department of Computer Science, Worcester State University Worcester, MA 01602, USA

Abstract - *Various mathematical concepts and models are used as foundations for different Computer Science areas. One of them is a concept of function. There is almost no a Computer Science problem where we do not use a concept of function and some of its properties. In this paper we focus on one of these fundamental properties, one-to-one property. We study a sum of a one-to-one function and hash function and explore possible cases for the result function to be one-to-one.*

Keywords: function, one-to-one property, sum combination, hash function, *mod* function.

1. Introduction

Functions are one of the fundamental concepts in Mathematics and Computer Science. We hardly can take a few steps in science fields without running into one. The concept of function was developed over a period of several centuries. Various definitions were given. In an ordinary language by "function" we usually mean a relationship between two sets of objects. One of the formal definitions frequently used by mathematicians as well as by computer scientists was first formulated for sets of numbers by the German mathematician Lejeune Dirichlet in 1837.

Definition 1.1: A function F from a set X to a set Y, denoted $F : X \rightarrow Y$, is a relation from X, the domain, to Y, the co-domain, that satisfies two properties:

1. every element in X is related to some element in Y
2. no element in X is related to more than one element in Y. [1]

In this paper we focus on one of the important properties that functions may satisfy: the property of being one- to- one. One-to-one property is one of two requirements for a function for being a one- to- one correspondence and having an inverse function. We may consider a one- to- one correspondence between two sets of objects as a perfect mapping of these two sets, domain and co-domain.
A mapping represents an operation on the domain objects with the operation result in the co-domain. The existence of an inverse function corresponds to the existence of "undo" operation for the given one. In a variety of applications we need the existence not only of a particular mapping, operation, but we would like to be able to have a way to go back and undo the first one. The formal definition of one-to-one property is given by the following definition:

Definition 1.2: Let F be a function from a set X to a set Y. F is one- to- one if, and only if, for all elements x_1 and x_2 in X, if $F(x_1) = F(x_2)$, then $x_1 = x_2$, or, equivalently, if $x_1 \neq x_2$, then $F(x_1) \neq F(x_2)$. [1]

In this paper we study a combination of a one-to-one and not one-to-one function. We focus on a sum of two functions and explore its one-to-one property. We ask the question: *What do we know about the one-to-one property even for a sum of a simplest one-to-one and a hash function?* Hash functions are very well known examples of not one-to-one functions used in a variety of computer science applications.

Definition 1.3: A function F from a set X to a set Y, where the size of X is larger than the size of Y and size of Y is a fixed number, is called a hash function. [1]

In the rest of our discussion we focus on the function $F(n) = n \bmod d + n$, where n is a positive integer, d is a fixed positive integer and *mod* function is defined as
$n \bmod d$ = the remainder when n is divided by d.
mod function is probably one of the most frequently used hash functions in a variety of computer science areas such as databases, data structures, conflict resolution protocols, computer security methods and many other applications [2], [3], [4].

2. Basic Results

In this section we prove a few properties for a sum of the identity function, $f(n) = n$, and a *mod* function. The identity function is known to be one-to-one. We consider $F(n) = n \bmod d + n$, where d is a fixed positive integer. In our proofs we use basic facts from the Number Theory such as the divisibility concept, divisibility properties, and The Quotient-Remainder Theorem.

Definition 2.1: If n and d are integers and $d \neq 0$ then n is divisible by d if, and only if, n equals d times some integer ($n = dk$, $k \in Z$). [1]

The Quotient-Remainder Theorem: Given any integer n and positive integer d, there exist unique integers q and r such that $n = dq + r$ and $0 \leq r \leq d - 1$. [1]

Exploring $F(n) = n \bmod d + n$ for having one-to-one property we have proven the following two properties.

Property 2.1: For every even positive integer d function $F(n) = n \bmod d + n$ is not one-to-one.

Proof: Let n_1 and n_2 be positive integers, such that

$$F(n_1) = F(n_2). \quad (1)$$

This gives us:

$$n_1 + n_1 \bmod d = n_2 + n_2 \bmod d \quad (2)$$

Using The Quotient-Remainder Theorem we have

$$n_1 = q_1 d + r_1 \text{ and } n_2 = q_2 d + r_2,$$

where q_1, q_2 are the quotients, r_1, r_2 are the remainders, when n_1 and n_2 are divided by d respectively.

So, (2) can be written as

$$q_1 d + r_1 + r_1 = q_2 d + r_2 + r_2 \Leftrightarrow$$
$$q_1 d + 2r_1 = q_2 d + 2r_2 \Leftrightarrow$$
$$d(q_1 - q_2) = 2(r_2 - r_1) \quad (3)$$

From (3) we have

$$(q_1 - q_2) = 2(r_2 - r_1)/d$$

or

$$(q_1 - q_2) = (r_2 - r_1)/k, \quad (4)$$

where $d = 2k$, k is a positive integer, $q_1 - q_2$ and $r_2 - r_1$ are integers and $-(2k - 1) \le r_2 - r_1 \le 2k - 1$.

To prove $F(n)$ is not one-to-one we have to find at least one solution for the equation (4) that has $q_1 \ne q_2$, $r_1 \ne r_2$. It is not difficult to see that all (q_1, q_2, r_1, r_2) which satisfy conditions

$$r_2 - r_1 = k = d/2 \quad \text{and} \quad q_1 - q_2 = 1 \quad (5)$$

are solutions of (4). So, we have shown that for any n_1 and n_2, such that $n_1 = q_1 d + r_1$, $n_2 = q_2 d + r_2$ and q_1, q_2, r_1, r_2, that satisfy conditions (5), we have that $n_1 \ne n_2$, but $F(n_1) = F(n_2)$. Hence, $F(n)$ is not one-to-one.

The next statement describes the case of an odd d.

Property 2.2: For every odd positive integer d function $F(n) = n \bmod d + n$ is one-to-one.

Proof: We are going to prove the statement by contradiction using the same reasoning as in Property 2.1. Let us assume that there are two positive integers n_1 and n_2, such that $n_1 \ne n_2$ and $F(n_1) = F(n_2)$. In the same way as in Property 2.1 we get

$$n_1 + n_1 \bmod d = n_2 + n_2 \bmod d \quad (2)$$

Using The Quotient-Remainder Theorem n_1 and n_2 can be written as $n_1 = q_1 d + r_1$ and $n_2 = q_2 d + r_2$, where q_1, q_2 are the quotients, r_1, r_2 are the remainders, when n_1 and n_2 are divided by d respectively. (2) is equivalent to the equation

$$d(q_1 - q_2) = 2(r_2 - r_1) \quad (3)$$

That means that both sides of equation (3) are integers divisible by the same integer divisors. d is odd, so $q_1 - q_2$ must be divisible by 2. This implies that $A = (q_2 - q_1)/2$ is an integer and we can write (3) as

$$dA = r_2 - r_1 \quad (6)$$

where $0 \le |r_2 - r_1| \le d - 1$ and $|A| \ge 1$. That is a contradiction, since $|dA| > |r_2 - r_1|$. Hence, the initial assumption is false and we have proven that $F(n)$ is one-to-one.

3. Conclusion and future work

In this paper, we explore one-to-one property of a sum of the identity function and a *mod* function. We consider two possible cases for a *mod* function and prove or disprove the one-to-one property for each of the cases. A *mod* function is one of the most frequently used hash functions in Computer Science. Sum of two functions is one of the simplest combinations. Similar questions could be asked exploring other type combinations of two functions as well as including broader classes of one-to-one and hash functions.

4. References

[1] S. Susanna, "Discrete Mathematics with Applications", Thomson Course Technology, 4-rd edition.

[2] Bakhtiari, S.; Safavi-Naini, R.; and Pieprzyk, J. "Cryptographic Hash Functions: A Survey". Technical Report 95-09, Department of Computer Science, University of Wollongong, July 1995.

[3] Russell, A. "Necessary and Sufficient Conditions for Collision-Free Hashing", in Abstracts of Crypto 92, 1992.

[4] Press, W. H.; Flannery, B. P.; Teukolsky, S. A.; and Vetterling, W. T. "Cyclic Redundancy and Other Checksums, in Numerical Recipes in FORTRAN: The Art of Scientific Computing", Cambridge University Press, 1992.

An Integrated Measurement Framework for Monitoring IP Networks

Nasreddin B. El-Zoghbi nzoghobi@yahoo.com

Shahid Shamsudeen kbsshan@gmail.com

FACULTY OF INFORMATION TECHNOLOGY
TRIPOLI UNIVERSITY, Tripoli, Libya.

Abstract

Measurements for network monitoring and IP traffic analysis is a complex research field whose results can be exploited for several purposes such as usage based Billing, Quality of Service, Traffic Engineering, Service Level Management, Security etc. In this paper, we propose a measurement framework for monitoring IP networks that includes both active and passive measurement methodologies. Our proposed framework integrates the mechanisms to do an end-to-end measurement using active probes and also explicitly describe complex traffic mixes using traffic meters. It uses the active measurement components to study various properties of the network while the passive measurement components measure the user traffic, and finally to correlate the findings to derive a global picture of the measured network. This paper also describes various traffic metrics that can be measured using this framework. Our system will provide valuable insights regarding the performance, quality, and traffic dynamics of the network under study.

Keywords: *Network Measurements, Passive Monitoring, Active Monitoring, IP Traffic Analysis, Flow Monitoring*

I. Introduction

The measurement and monitoring of IP networks has become essential and challenging due to the rapidly growing requirements from various levels of technology, applications, and user
requirements. A contemporary IP network has three significant characteristics: (1) they provide real-time services, (2) they have become mission critical, and (3) their operating environments are very dynamic[16]. Measuring the networks and understanding data traffic is essential for ensuring the reliable operation and smooth growth of computer networks.

At the most basic level, an IP network could be represented conceptually as a dynamical system consisting of (1) a set of interconnected resources which provide transport

services for IP traffic subject to certain constraints, (2) a demand system representing the offered load to be transported through the network, and (3) a response system consisting of network processes, protocols, and related mechanisms which facilitate the movement of traffic through the network [16]. This paper is focused at (1) and (2), to measure and monitor IP networks at traffic and resource levels. Traffic oriented measurements include delay, delay variation, packet loss, and throughput. While Resource level monitoring addresses the availability, reliability, and optimal utilization of internet work resources.

Traffic measurement is not driven by a single concrete goal. There are large numbers of systems that perform traffic measurement to answer a wide variety of questions. These measurement initiatives implement one of the two measurement methodologies via active measurement techniques or passive measurement techniques. The active measurement techniques send out probe packets and measure how they reply, and/or traverse the network [1] [2] [3]. These techniques typically measure the end-to-end properties of the network. Unlike active measurement, passive measurement measures the production traffic [4] [5]. They capture the packets with their corresponding timestamps and give detailed flow level information. Some passive techniques like SNMP gives device level information of the intermediary networking devices. It should be noted that each measurement methodologies have inherent limitations and drawbacks. In this paper we propose a framework which will eliminate the limitations of the above mentioned measurement techniques. This proposal is novel and loaded with wide scope of application in future as our framework helps in analyzing the network to ensure that the performance characteristics that are pertinent to a specified service class is guaranteed. It also analyses the network in terms of spatial aspect (eg: flow aggregation by src, dst IP address or AS number) which shows the traffic flow pattern relative to network topology, temporal aspect which shows the stochastic behavior of traffic flow (eg: Packet or byte per hour, day, week, month) and composition aspects which describes breakdown of traffic according to the contents, application, packet length and flow duration.

We also discuss here about the metrics expected to be derived from this measurement framework. The measurement provides raw data concerning state parameters and metrics of monitored network and network elements. These raw data have to be evaluated effectively to make inferences regarding the monitored system.

The remainder of this paper is organized as follows:
Section II brings some of the related works in the same domain. Section III details the architecture of the proposed framework. Section IV discusses the general considerations on implementing the proposed framework. Section V describes the traffic metrics measured using this framework. Finally, in Section VI we provide a conclusive summary and suggest future directions.

II. Related Work

There are a wide range of initiatives for network measurement and monitoring. One important architecture for flow based monitoring has been developed by the IETF RTFM working group (Real Time Traffic Flow Measurement) [7]. The architecture of this group

is composed of the 3 modules: manager, meter and meter reader. Another interesting architecture proposed by IETF working group is IPFIX (IP Flow Information export) [8]. Its goal is to define a common architecture and protocol to let different monitoring applications communicate to each other. The proposed architecture of this group consists of two modules: the IPFIX device and the collector. The IETF IP Performance Metrics (IPPM) working group has been developing a set of standard metrics that can be used to monitor the quality, performance, and reliability of Internet services [9]. Some other relevant related works in this field are: RIPE NCC Test Traffic Measurements [10], NIMI [11], Surveyor [12], Flow Scan [13], and Net Flow [14].

III. Proposed Framework for Measurement

The proposed framework is shown in Figure.1 below. The components and the sub divisions of this measurement framework are detailed below:

1. Active Data Measurement Components (ADMC)

This Component implements active measurement procedures to inject measurement probes into the network. It sends out probe packets and measures how they, and/or their replies traverse the network. Active measurement is typically used to measure properties of the network viz, packet delays, packet loss rates, jitter, bandwidth, symmetry, stability, and topology. This Component includes the following daemons:

a) ICMP Probe Daemon
The ICMP probe daemon sends ICMP packets (probes) to a designated host and wait for the host to respond back to the sender to collect end-to-end measurements of the network.

b) TCP/UDP Probe Daemon
The TCP/UDP probe daemon sends TCP and UDP packets (probes) into the network to collect end-to-end performance metrics of the network.

c) Application specific Probe Daemon
The Application specific probe daemon emulates application specific traffic to measure the perceived application-quality over the network. These include real-time applications like multimedia applications and peer to peer applications.

2. Passive Data Measurement Components (PDMC)

Passive measurement is a means of tracking the performance and behavior of packet streams by monitoring the traffic without creating or modifying it. Passive measurement can be implemented by incorporating some additional intelligence into network devices to enable them to identify and record the characteristics and quantity of the packets that flow through them. Packet statistics can then be collected without the addition of any new traffic. The techniques used are SNMP, RMON and Net flow. This component also includes the flow analysis of the raw packets captured through packet sniffers or splitters. The quantum of information collected depends on the network metrics of interest, how

the metrics are being processed and the volume of traffic passing through the monitor device.

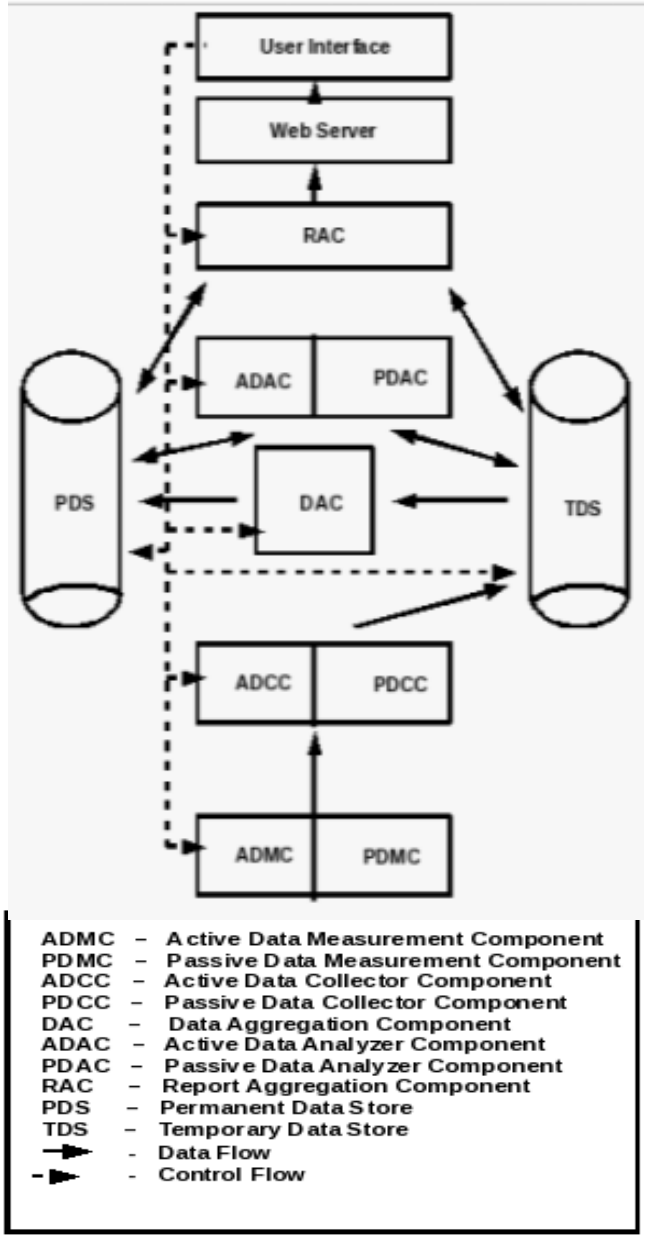

Figure 1. Measurement Framework

The types of information obtained include Bit or packet rates, Packet timing / inter-arrival timing, Queue levels in buffers (which can be used as indicators of packet loss and delay), Traffic/protocol mixes.

a) SNMP/RMON Agents

The SNMP/RMON agents have to be enabled in the intermediary devices (managed entity) for which this framework acts as the management station. These agents gather

traffic and device statistics from the Managed Devices. There are many approaches for reconstructing the traffic matrix based on SNMP counters and network topology and they are collectively known as network tomography. One disadvantage of these methods is that they can only give approximate traffic matrices.

b) Flow Data Probes

Flow level measurement provides traffic information in more detail. Flows define a communication between two endpoints and are identified by certain values for 5 specific fields in the headers of the packets that make up the flow. The five fields are: source IP address, destination IP address, protocol number, source port and destination port. The last three fields indicate which application generated the flow (web, email, etc.). Besides these fields, a flow record contains counters for the number of packets and bytes in the flow, timestamps for when the first and last packets were received, information about protocol flags and a few other details. The flow has to be enabled at transit network on the device that supports Netflow/sFlow and using packet capture mechanisms at edge networks depending on the measurement required.

3. Active Data Collector Component (ADCC)

This component collects the data generated by each active probing mechanisms specified in (2).

These data are categorically stored in the temporary data store (TDC). This collector component can be tuned as per the requirement and interest, from the user interface.

4. Passive Data Collector Component (PDCC)

This component collects the raw data sent from various passive agents deployed in the network. The data are categorically stored in the temporary data store (TDC). This collector component can be (re)defined as per the granularity needed, from the user interface.

5. Active Data Analyzer Component (ADAC)

This component analyses the data collected and stored through active measurement techniques.

It retrieves data from temporary data store (TDS) and permanent data store (PDS). This analyzer component can be configured from the user interface. It gives the result from the perspective in evaluating the end-to-end performance of a network path.

6. Passive Data Analyzer Component (PDAC)

This component analyses the passive data collected and stored through passive measurement techniques. It retrieves data from the temporary data store (TDS) and permanent data store (PDS) based on the analysis to be done. This component can be configured from the user interface. This analysis component gives device level information and also deep insight into IP traffic characteristics and traffic behavior.

7. Data Aggregation Component (DAC)

This component is very crucial as the amount of the expected data is enormous.
This component applies conditional filters and policy based aggregations on the data stored temporarily in TDS. The consolidated data is permanently stored in PDS for further and future evaluations.

8. Report Aggregation Component (RAC)

This component pays attention to the usefulness of the information provided by this framework. This module generates structured and user configurable custom reports based on the analysis records generated by the active and passive analyzer components.

9. Data Store (permanent/temporary)

This is an essential component from the perspective of this system, as a huge amount of data are expected to be handled. The Data Store can be broadly classified into two: 1. Temporary Data Store (TDS) and 2. Permanent Data Store (PDS). As the name explains (1) acts as an intermediary store for the real time-series data which can be used for real time analysis and reporting, while (2) stores the consolidated data for further analysis and long term use. As the expected quantity of data is very high, following storage considerations are to be made for storage optimization.
(a) The aggregated data could be made available using the Mean, Max, or Min entries and saved for historical purposes. (b) Use a time-based algorithm that aggregates data over a specific period of time within a component data, thus requiring fewer entries, to reduce storage space requirements. (c)Periodically delete historical data in accordance with an administrative policy. These considerations are to be made later on operational concern.

10. Web-based User Interface

A web-based user interface is an essential component for such a complex system so that it could be accessed from anywhere using HTTP protocol. It provides a brief/detailed view of the real time and long term data analysis. The self explanatory graphs will aid as a quick and easy reference to entire traffic monitoring.

IV. General Considerations

Following are the general considerations made on this measurement framework:
Active measurement based: (a) intrusiveness must be minimized (b) selective probing schedules; random, periodic, bursty (c) active probes should be indistinguishable from ordinary traffic (d) authorization to restrict the active probing traffic.
Passive measurement based: (a) calibration of memory and processor requirements (b) minimizing the bandwidth consumed (c) ensuring secure transactions
Storage based: device proper policy for data consolidation.

V. Derived Health Metrics of the Network

The following are the metrics collected and analyzed by this framework:
a) Route Changes: This is one of the important metric and an anomaly observed in the production network. Route changes happen due to "route flapping", which are caused by the abnormal routing protocol behavior, network infrastructure failures, reconfiguration of the networks or load balancing strategies used for network performance improvement.

b) Delay: This metric includes the one-way or two-way delay of a packet transmission between a pair of measurement end points. One-way packet delay is the time elapsed from the start of transmission of the first bit of the packet by a source node until the reception of the last bit of that packet by the destination node. Two-way packet delay is the time elapsed from the start of transmission of the first bit of the packet by a source node until the reception of the last bit of the loop-backed packet by the same source node, when the loop back is performed at the packet's destination node.

c) Bandwidth: This metric shows the capacity of the channel by reflecting the congestion levels caused by the network dynamics in the path. The bandwidth characteristics of the path significantly influence the other performance metrics.

d) Jitter: This metric represents the variation in the network delay. This metric also reflects the network dynamics along the measured path.

e) Loss: This metric measures the packet loss ratio between a pair of measurement end points. Packet loss ratio is the ratio of the user-plane packets not delivered to the total number of user-plane packets transmitted during a defined time interval. The number of user-plane packets not delivered is the difference between the number of user-plane packets transmitted by the source node and the number of user-plane packets received at the destination node.

f) Stability: This metric reflects the operational state in which a network does not oscillate in a disruptive manner from one mode to another mode. This metric could be a derived from other measured metrics based on the context specific requirements.

g) Availability: This metric reflects the uptime or downtime of a network device or a service. It excludes the scheduled outages which may be to device or service shutdown for maintenance purposes.

h) Discards and Errors: The discard metric indicates the number of packets discarded on a particular network interface, while error metric indicates the number of corrupted packets received on a network interface. These metrics are indicators of excessive network congestion experienced on the link at that point of time.

I) Utilization: This metric will be measured on the edge network(s) or/and on the link(s) along the network path. It compares the amount of inbound and outbound traffic versus

the bandwidth provisioned on the network segment or/and on the network link in a network path.

j) Flow Information: This includes a series of metrics measured on the basis of flow definition made as per the requirement. This includes various categories including flow size, flow duration, packet and size distribution, flash flows, volume pattern, flow occurrence period, port number and protocol based distribution. It mainly depicts the characterization of IP traffic over time.

VI. Conclusions and Future Work

Our proposed measurement framework for network monitoring and IP traffic analysis integrates the advantages and eliminates the limitations of traditional active and passive measurement methodologies. Passive measurements are accurate, scalable and have low overheads but it needs access to the network under study. On the other hand, active measurements do not require owning the network, but they are intrusive in nature by actively injecting packets which may adversely affect the production traffic on the network. But we observe that both measurements are essential to define and maintain the state of the network. The strategy that we adopted in this proposed framework is aimed at unifying the tasks involved in active and passive measurement methodologies.

Finally, we believe that our approach will lead to a solution for an important issue of extending the measurements to higher protocol layers, as well as a combination of edge-to-edge network measurements and end-to-end application measurements for next generation high speed networks. The generic structure of this framework will help to focus the network under study at its horizontal and vertical levels. In future, we plan to carry forward with prototyping this framework for further experiments, evidences and advancement.

References

[1] S. Shalunov, B. Teittelbaum, "One-way Active Measurement Protocol (OWAMP)", IETF RFC 3763, 2004
[2] NLANR Iperf - http://dast.nlanr.net/Projects/Iperf
[3] Pathchar - http://www.caida.org/tools/utilities/others/pathchar
[4] tcpdump/libpcap,. 2001, http://www.tcpdump.org/.
[5] J. Case, M. Fedor, M. Schoffstall, and J. Davin. A simple network management protocol (SNMP). IETF RFC 1157, 1990.
[6] S. Waldbusser, R. Cole, C. Kalbfleisch, D. Romascanu, " Introduction to the Remote Monitoring (RMON) Family of MIB " IETF RFC 3577, 2003
[7] N. Brownlee, C. Mills, G. Ruth, "Traffic Flow Measurement: Architecture" IETF RFC 2722, 1999
[8] B. Claise, Ed."Specification of the IP Flow Information Export (IPFIX) Protocol for the Exchange of IP Traffic Flow Information" IETF RFC 5101, 2008
[9] E. Stephan, " IP Performance Metrics (IPPM) Metrics Registry " IETF RFC 4148, 2005
[10] http://www.ripe.net/pam2001/Abstracts/talk_06.html
[11] Paxson V., Adams A.K., Mathis M.: "Experiences with NIMI", Proceedings of Passive and Active Measurements (PAM) 2000, Hamilton, New Zealand, 2000.
[12] Kalidindi S., Zekauskas M.: "Surveyor: An Infrastructure for Internet Performance Measurements", INET'99, San Jose, June 1999.

[13] Dave Plonka , "FlowScan: A Network Traffic Flow Reporting adn Visualization Tool", University of Wisconsin-Madison, 2000 LISA XIV, New Orleans, LA
[14] http://www.cisco.com/warp/public/732/Tech/netflow/netflow_techdoc.shtml
[15] http://www.netperf.org/netperf/NetperfPage.html
[16] D. Awduche, A. Chiu, A. Elwalid, I. Widjaja, X. Xiao: "Overview and Principles of Internet Traffic Engineering" IETF RFC 3272, 2002
[17] Abilene. http://abilene.internet2.edu, 2009
[18] Georgatos F., Gruber F., Karrenberg D., Santcroos D., Susanj A., Uijterwaal H., Wilhelm R.: "Providing Active Measurements as a Regular Service for ISP's", Proceedings of Passive and Active Measurements (PAM) 2001, Amsterdam, 23-24 April, 2001.
[19] Nordén P.: "Monitoring of Performance Parameters in IP Networks",Degree project, KTH, 2001.
[20] J. Bolot. End-to-end packet delay and loss behavior in the Internet. In Proceedings of ACM SIGCOMM '93, San Francisco, 1993.
[21] Nistnet home page: http://www.antd.nist.gov/itg/nistnet/.
[22] NeTraMet home page: http://www2.auckland.ac.nz/net/NeTraMet/
[23] http://www.slac.stanford.edu/comp/net/wan-mon/iepm-cf.html
[24] Micheel J., Donnelly S., Graham I.: "Precision Timestamping of Network Packets", ACM SIGCOMM Internet Measurement Workshop, San Francisco, USA, 2001.

SESSION

QUANTUM COMPUTING AND PROTOCOLS

Chair(s)

TBA

Application of a Process Calculus to Security Proofs of Quantum Protocols

Takahiro Kubota[1], **Yoshihiko Kakutani**[1], **Go Kato**[2], **Yasuhito Kawano**[2], **and Hideki Sakurada**[2]
[1]Department of Computer Science, Graduate School of Information Science and Technology,
the University of Tokyo, 7-3-1, Hongo, Bunkyo-ku, Tokyo, Japan
[2]NTT Communication Science Laboratories, NTT Corporation,
3-1, Morinosato, Wakamiya, Atsugi-shi, Kanagawa, Japan

Abstract— *We apply a quantum process calculus to an equivalence proof of quantum key distribution protocols. Whether in classical or quantum cryptography, it is recognized that security proofs tend to be complex and difficult to verify. The use of formal methods is a way to tame such complexity. Quantum process calculi have already been used to model quite simple quantum protocols but not applied to security proofs of practical ones. In this paper, we study a security proof of BB84 in a quantum process calculus qCCS. Shor and Preskill have shown that BB84 can be transformed to an equivalent EDP-based protocol and the latter is secure. We formalize this equivalence of the protocols as the bisimulation of processes. For the formalization, we present a general technique to describe quantum measurements in qCCS. Congruence of bisimulation is useful to show that the two protocols are bisimilar even if they run in parallel.*

Keywords: quantum protocols, BB84, process calculi, bisimulation, formal methods

1. Introduction

Security proofs of cryptographic protocols tend to be complex and difficult to verify. This fact has been recognized in the classical cryptography. Security proofs are also complex in the quantum cryptography, where we must consider attacks using entanglements. The first security proof of BB84 quantum key distribution (QKD) protocol by Mayers [1] is about 50 pages long. After that paper, researchers have been seeking simpler proofs [2], [3].

Since by-hand proofs are prone to human error and time consumption, the efforts have been put into automating the proofs and verification in the classical cryptography [4]. For instance, 11 security properties of Kerberos [5], a commercial authentication protocol, is guaranteed by a mechanized proof [6] in CryptoVerif [4], a software tool based on a process calculus.

To automate a proof, a target system must be formalized in a certain formal framework that a tool supports. Formalization itself is useful besides automation; we write targets in a formal language and deduce security properties using some rules that the framework provides. These make description of targets precise and all deduction steps explicit.

There are several formal frameworks for quantum systems such as quantum process algebra (QPAlg) [7], communicating quantum processes (CQP) [8] and quantum CCS (qCCS) [9]. In CQP, quantum teleportation protocol and a quantum error correcting code are formally verified [10] using bisimulation. In process calculi, bisimulation relation is a key notion denoting behavioural equivalence of processes. An important property of bisimulation is congruence, that is, the relation is closed by parallel composition. Bisimulation has been used for specification and verification of protocols. We write protocols as processes and prove them bisimilar. Weak bisimulation relation is defined in qCCS. Weakly bisimilar processes can perform identical transitions up to actions which are invisible from the outside. As applications of qCCS [9], quantum teleportation and superdense coding protocols are formally verified. Specification of BB84 has been also verified [11] but it is not a security proof.

Quantum process calculi are used for verification of various systems but they have not yet applied to security proofs. In this paper, we apply qCCS to Shor and Preskill's security proof of BB84. In Shor and Preskill's security proof, security of BB84 is proven to be equivalent to that of another protocol based on an entanglement distillation protocol (EDP), and then the latter is proven to be secure.

Our contributions are mainly two. First, we present a general technique to describe quantum measurements. There are two different ways to formalize quantum measurements in qCCS. Quantum measurements provided in the syntax evoke probabilistic branches in the transition system. On the other hand, we can formalize quantum measurement as a quantum operation, which does not cause branches. In fact, the processes with different formalization of a measurement are generally not bisimilar. In Our investigation, the two kinds of processes behave differently from the view of an adversary. The former is observed by an adversary and the latter is not. To make sense, a measurement should be formalized in the former way if the result of the measurement can be recognized by an adversary. Otherwise, it should be formalized in the latter way. Shor and Preskill's security proof is a typical case to apply our formalization technique for quantum measurements.

The second contribution is that we have formalized the

equivalence of BB84 and the EDP-based protocol as the bisimulation. Thanks to congruence property of bisimulation, it is naturally proved that multiple instances of BB84 running in parallel are bisimilar to multiple instances of the EDP-based protocol.

The remainder of this paper is organized as follows. In the next section, we introduce BB84 and the EDP-based protocol that we formalize in this paper. In Section 3, we introduce qCCS framework, namely, the definition of syntax, the operational semantics and bisimulation. In Section 4, we discuss techniques for formalization and formalize the two protocols introduced in Section 2. In Section 5, we prove bisimulation between the two protocols. In Section 6, we draw a brief comparison with related works and conclude the paper.

2. QKD protocols

The word BB84 does not mean one unique protocol, because there are choices to error correction and privacy amplification steps. In this paper, since our target is Shor and Preskill's proof, the implementation of BB84 follows [2]. It employs two classical linear codes C_1, C_2 that satisfy $\{\vec{0}\} \subset C_2 \subset C_1 \subset \{0,1\}^n$, where n is the length of codewords in C_1 and C_2. In this paper, the protocol is slightly modified for simplicity: Alice only generates $2n$ qubits. This modification causes Bob to store qubits in his side, but does not affect the security at all.

2.1 BB84 (slightly modified)

1) Alice generates two random $2n$-bit strings $d_{A,1}, ..., d_{A,2n}$ and $b_{A,1}, ..., b_{A,2n}$.
2) Alice creates a $2n$-qubit string $q_{B,1}, ..., q_{B,2n}$ according to the randomness: for each $q_{B,i} (1 \leq i \leq 2n)$, Alice generates $|0\rangle$ if $d_{A,i} = 0, b_{A,i} = 0$, $|1\rangle$ if $d_{A,i} = 1, b_{A,i} = 0$, $|+\rangle$ if $d_{A,i} = 0, b_{A,i} = 1$, $|-\rangle$ if $d_{A,i} = 1, b_{A,i} = 1$.
3) Alice sends $q_{B,i}$'s to Bob via the quantum channel.
4) Bob receives q_{B_i}'s and announces Alice that fact.
5) Alice announces $b_{A,i}$'s via the classical channel.
6) Bob measures q_{B_i}'s in $\{|0\rangle, |1\rangle\}$ basis if $b_{A,i} = 0$ or in $\{|+\rangle, |-\rangle\}$ basis if $b_{A,i} = 1$. Alice randomly chooses n bits from them as check bits and then tells Bob which are check bits.
7) Alice and Bob announce the values of their check bits to each other. If the error rate is higher than the threshold, they abort the protocol.
8) Alice chooses a codeword $\vec{u}_A \in C_1$ randomly, and announces $\vec{u}_A + \vec{x}_A$, where $\vec{x}_A$ is the remaining non-check bits.
9) (Error correction) Bob calculates $\vec{u}'_B$ from announced $\vec{u}_A + \vec{x}_A$ and his own non-check bits $\vec{x}_B$. Because $\vec{x}_B$ may include some errors, Bob obtains $\vec{u}_B$ by correction of the errors. If this error correction works well, $\vec{u}_B$ is almost equal to $\vec{u}_A$.
10) (Privacy amplification) Alice and Bob determine secret keys $\vec{k}_A, \vec{k}_B$ from the cosets of $\vec{u}_A + C_2, \vec{u}_B + C_2$.

BB84 is transformed into the following EDP-based protocol, which is a modification of the protocol in [3]. This protocol employs a CSS quantum error correcting code [12] that is constructed from two linear codes C_1, C_2 satisfying $\{\vec{0}\} \subset C_2 \subset C_1 \subset \{0,1\}^n$. A CSS code can take bit and phase parameters $u, v \in \{0,1\}^n$.

2.2 the EDP-based protocol

1) Alice generates $2n$ EPR pairs $\vec{q} = (\frac{|00\rangle + |11\rangle}{\sqrt{2}})^{\otimes 2n}$ and $2n$-bit string $b_{A,1}, ..., b_{A,2n}$.
2) According to $b_{A,i}$'s, Alice executes Hadamard transformations on halves of $\vec{q}$ sent to Bob in the next step.
3) Alice sends the halves of $\vec{q}$ to Bob via the quantum channel.
4) Bob receives his halves, and announces it to Alice.
5) Alice announces $b_{A,i}$'s via the classical channel and Bob executes Hadamard transformations according to $b_{A,i}$'s.
6) Alice and Bob measure their halves of the check bits by the $\{|0\rangle, |1\rangle\}$ basis, and share the results. If the error rate is higher than the threshold, they abort the protocol.
7) Alice calculates the parameters of the related CSS code and sends them to Bob. Bob then calculates the syndrome and corrects errors using the parameters. Alice and Bob next decode their qubit strings as the CSS code.
8) Alice and Bob measure their qubits in $\{|0\rangle, |1\rangle\}$ basis to obtain shared secret keys $\vec{k}_A, \vec{k}_B$.

3. Formal framework

In this section, the syntax, semantics and the definition of bisimulation of qCCS [9] are introduced. We only present main rules and definitions here (See [9] for complete ones). We use a sublanguage of qCCS for our formal verification.

3.1 Syntax

Definition 1: the syntax of qCCS process is given as follows.

$$\begin{aligned} Proc \ni P ::= \ & \mathbf{nil} \mid c?x.P \mid c!e.P \mid \mathbf{c}?q.P \mid \mathbf{c}!q.P \\ & \mid \texttt{if } b \texttt{ then } P \mid op[\tilde{q}].P \mid M[\tilde{q};x].P \mid P||P \mid P\backslash L \end{aligned}$$

where $c, x, e, \mathbf{c}, q$ are a classical channel name, a classical variable, a real expression, a quantum channel name and a quantum variable respectively. b, op, $\tilde{q}$, M, L are a condition, a symbol of a super-operator (we may say quantum operator), a sequence of quantum variable, an Hermitian operator and a set of channel names respectively.

Let $cVar, qVar, cChan$ and $qChan$ be the set of all classical variables, the set of all quantum variables, the set of all classical channel names and the set of all quantum

$$\frac{}{\langle \mathbf{c}?q.P,\rho\rangle \xrightarrow{\mathbf{c}?r} \langle P\{r/q\},\rho\rangle} \qquad \frac{}{\langle \mathbf{c}!q.P,\rho\rangle \xrightarrow{\mathbf{c}!q} \langle P,\rho\rangle}$$

$$\frac{\langle P_1,\rho\rangle \xrightarrow{\mathbf{c}?r} \langle P_1',\rho\rangle \; \langle P_2,\rho\rangle \xrightarrow{\mathbf{c}!r} \langle P_2',\rho\rangle}{\langle P_1||P_2,\rho\rangle \xrightarrow{\tau} \langle P_1'||P_2',\rho\rangle} \qquad \frac{\langle P_1,\rho\rangle \xrightarrow{\alpha} \mu \;\; [\![b]\!]=\text{true}}{\langle \texttt{if } b \texttt{ then } P,\rho\rangle \xrightarrow{\alpha} \mu}$$

$$\frac{}{\langle op[\tilde{r}].P,\rho\rangle \xrightarrow{\tau} \langle P,\mathcal{E}^{op}_{\tilde{r}}(\rho)\rangle} \qquad \frac{\langle P_1,\rho\rangle \xrightarrow{\mathbf{c}?r} \langle P_1',\rho\rangle \; r\notin \mathrm{qv}(P_2)}{\langle P_1||P_2,\rho\rangle \xrightarrow{\mathbf{c}?r} \langle P_1'||P_2,\rho\rangle}$$

$$\frac{}{\langle M[\tilde{r};x].P,\rho\rangle \xrightarrow{\tau} \sum_i p_i\langle P\{\lambda_i/x\}, E^i_{\tilde{r}}\rho E^i_{\tilde{r}}/p_i\rangle}$$

where M has the spectrum decomposition

$$M=\sum_i \lambda_i E^i, \text{ and } p_i=\mathrm{tr}(E^i_{\tilde{r}}\rho)/\mathrm{tr}(\rho)$$

Fig. 1: Labelled Transition Rule

channel names. The set of quantum variables occurring in a process P is denoted by $\mathrm{qv}(P)\subseteq qVar$. $P||Q\in Proc$ if and only if $\mathrm{qv}(P)\cap\mathrm{qv}(Q)=\emptyset$ and $\mathbf{c}!q.P\in Proc$ if and only if $q\notin\mathrm{qv}(P)$.

3.2 Labelled Transition System

We assume the supports of probabilistic distributions are finite. The support of a probabilistic distribution μ is denoted by $\mathrm{supp}(\mu)$. With a family of distributions $\{\mu_i\}_{i\in I}$, the joint distribution $\sum_{i\in I} p_i\mu_i$ is defined as $(\sum_{i\in I} p_i\mu_i)(\mathcal{C})=\sum_{i\in I} p_i(\mu_i(\mathcal{C}))$ for all $\mathcal{C}$, where $p_i's$ are probability. If $\mathrm{supp}(\mu)=\{\mathcal{C}\}$, μ is simply written $\mathcal{C}$.

For each $q\in qVar$, there is a corresponding two dimensional Hilbert space $\mathcal{H}_q$ that denotes the state space of q. Let $\mathcal{H}=\bigotimes_{q\in qVar}\mathcal{H}_q$ and let $\mathcal{D}(\mathcal{H})$, ranged over by ρ, be the set of all density operators on $\mathcal{H}$. A configuration is an element of $Proc\times\mathcal{D}(\mathcal{H})$. The set of all configurations, ranged over by $\mathcal{C},\mathcal{D},...$, is denoted Con. The set of all finite support probabilistic distribution on Con is denoted $D(Con)$. Act is the set of actions, namely,

$$\begin{aligned}Act=&\{\tau\}\cup\{c!x,c?v\mid c\in cChan,x\in cVar,v\in\mathsf{Real}\}\\&\cup\{\mathbf{c}!q,\mathbf{c}?q\mid \mathbf{c}\in qChan,q\in qVar\}.\end{aligned}$$

A labelled transition relation is a relation on $Con\times Act\times D(Con)$. $[\![b]\!]$ denotes evaluation of condition b. Labelled transition rules in qCCS are presented in figure 1. A transition relation is lift to that on $D(Con)\times Act\times D(Con)$. Let $\mu,\nu\in D(Con)$. $\mu\xrightarrow{\alpha}\nu$ if and only if $\mathcal{C}_i\xrightarrow{\alpha}\nu_i$ for all $\mathcal{C}_i\in\mathrm{supp}(\mu)$, there exists ν_i such that $\nu=\sum_i\mu(\mathcal{C}_i)\nu_i$.

3.3 Bisimulation

In non-probabilistic process calculus, silent actions are reflexive and transitive closure of $\xrightarrow{\tau}$. They are lifted to those in distributions and denoted by $\Rightarrow$. Relations on Con are also lifted to those on $D(Con)$. The weak bisimulation relation is behavioural equivalence up to silent actions.

Definition 2: A relation $\mathcal{R}\subseteq Con\times Con$ is a bisimulation if $\langle P,\rho\rangle\mathcal{R}\langle Q,\sigma\rangle$ implies $\mathrm{qv}(P)=\mathrm{qv}(Q)$, $\mathrm{tr}_{\mathrm{qv}(P)}(\rho)=\mathrm{tr}_{\mathrm{qv}(Q)}(\sigma)$ and

1) whenever $\langle P,\rho\rangle\xrightarrow{\tau}\mu$ there exists ν such that $\langle Q,\sigma\rangle\Rightarrow\nu$ and $\mu\mathcal{R}\nu$,
2) whenever $\langle P,\rho\rangle\xrightarrow{\mathbf{c}?q}\mu$ there exists ν such that $\langle Q,\sigma\rangle\Rightarrow\xrightarrow{\mathbf{c}?q}\nu$ and $\mathcal{E}(\mu)\mathcal{R}\mathcal{E}(\nu)$ for all quantum operator $\mathcal{E}$ acting on $\mathcal{H}_{\overline{\mathrm{qv}(\mu)-\{q\}}}$,
3) whenever $\langle P,\rho\rangle\xrightarrow{\alpha}\mu$ and α is neither a quantum input nor τ, there exists ν such that $\langle Q,\sigma\rangle\Rightarrow\xrightarrow{\alpha}\Rightarrow\nu$ and $\mu\mathcal{R}\nu$,

and their symmetric conditions named 4), 5), 6) are satisfied. The relation $\approx$ is defined as $\bigcup_{\mathcal{R}:\mathrm{bisimulation}}\mathcal{R}$.
The followings are useful proof techniques.

Proposition 3: $\approx$ is an equivalence relation.

Theorem 4: $\langle P,\rho\rangle\approx\langle Q,\sigma\rangle$ if and only if $\mathrm{qv}(P)=\mathrm{qv}(Q)$, $\mathrm{tr}_{\mathrm{qv}(P)}(\rho)=\mathrm{tr}_{\mathrm{qv}(Q)}(\sigma)$ and

1) whenever $\langle P,\rho\rangle\xrightarrow{\tau}\mu$ there exists ν such that $\langle Q,\sigma\rangle\Rightarrow\nu$ and $\mu\approx\nu$,
2) whenever $\langle P,\rho\rangle\xrightarrow{\mathbf{c}?q}\mu$ there exists ν such that $\langle Q,\sigma\rangle\Rightarrow\xrightarrow{\mathbf{c}?q}\nu$ and $\mathcal{E}(\mu)\approx\mathcal{E}(\nu)$ for all quantum operator $\mathcal{E}$ acting on $\mathcal{H}_{\overline{\mathrm{qv}(\mu)-\{q\}}}$,
3) whenever $\langle P,\rho\rangle\xrightarrow{\alpha}\mu$ and α is neither a quantum input nor τ, there exists ν such that $\langle Q,\sigma\rangle\Rightarrow\xrightarrow{\alpha}\Rightarrow\nu$ and $\mu\approx\nu$,

and their symmetric conditions named 4), 5), 6) are satisfied. To prove $\langle P,\rho\rangle\approx\langle Q,\sigma\rangle$, we do not construct a certain bisimulation relation $\mathcal{R}$. Instead, we check the conditions of theorem 4. We recursively check the conditions of the sets of quantum variables and partial traces, and correspondence of transitions up to silent ones. We then construct a weight function. The theorem below is useful to show bisimulation between protocols in parallel execution.

Theorem 5 (Congruence): If $\langle P,\rho\rangle\approx\langle Q,\sigma\rangle$ and $(\mathrm{qv}(P)\cup\mathrm{qv}(Q))\cap\mathrm{qv}(R)=\emptyset$, then $\langle P||R,\rho\rangle\approx\langle Q||R,\sigma\rangle$.

4. Formalization in qCCS

4.1 On Measurement

qCCS has the syntax of quantum operators $op[\tilde{q}]$ as well as measurements $M[\tilde{q},x]$. Since quantum operator includes quantum measurements, there are two ways to formalize quantum measurements. As a simple example, projective measurement of state $|+\rangle\langle+|$ in $\{|0\rangle,|1\rangle\}$ basis is formalized in the following two ways and the transitions are different.

$$\langle M[q;x].\mathbf{nil},|+\rangle\langle+|_q\rangle\xrightarrow{\tau}\sum_{i\in\{0,1\}}1/2\langle\mathbf{nil},|i\rangle\langle i|_q\rangle$$

$$\langle\texttt{measure}[q].\mathbf{nil},|+\rangle\langle+|_q\rangle\xrightarrow{\tau}\langle\mathbf{nil},1/2(|0\rangle\langle0|+|1\rangle\langle1|)_q\rangle,$$

where M has the spectrum decomposition $M = 0|0\rangle\langle 0| + 1|1\rangle\langle 1|$ and the quantum operator $\mathcal{E}_q^{\mathtt{measure}}(\rho)$ that corresponds to $\mathtt{measure}[q]$ is defined $|0\rangle\langle 0|\rho|0\rangle\langle 0|+|1\rangle\langle 1|\rho|1\rangle\langle 1|$. It is easy to check they are not bisimilar though the two processes apparently denote the same thing. Indeed, the way to formalize quantum measurement is significant in the security proof.

In Shor and Preskill's proof, the EDP-based protocol is transformed to the next protocol based on the fact that nobody outside cannot distinguish the following two processes:

1) Alice measures a half of an EPR pair and then sends the other half.
2) Alice sends a half of an EPR pair and then measures the other half.

There are two possible formalizations. The first is as follows, where measurement is formalized with the constructor $M[\tilde{q}; x]$ that provided by the syntax.

1) $\langle \mathbf{c}!q^B.M[q^A; x].\mathbf{nil}, EPR_{q^A,q^B} \otimes \rho^E\rangle$
2) $\langle M[q^A; x].\mathbf{c}!q^B.\mathbf{nil}, EPR_{q^A,q^B} \otimes \rho^E\rangle$

where $EPR = 1/2(|00\rangle\langle 00|+|11\rangle\langle 00|+|00\rangle\langle 11|+|11\rangle\langle 11|)$, ρ^E is an arbitrary density operator representing adversary's state. The two processes above are not bisimilar.

On the other hand, measurement can be formalized as an instance of quantum operation $op[\tilde{q}]$. We use a quantum operator $\mathcal{E}_{q^A}^{\mathtt{measure}}$ denoting measurement of q^A. For all $\rho \in \mathcal{D}(\mathcal{H}_{q^A} \otimes \mathcal{H}_{q^B})$, let

$$\mathcal{E}_{q^A}^{\mathtt{measure}}(\rho) := (|0\rangle\langle 0|\otimes\mathbb{I})\rho(|0\rangle\langle 0|\otimes\mathbb{I})+(|1\rangle\langle 1|\otimes\mathbb{I})\rho(|1\rangle\langle 1|\otimes\mathbb{I}).$$

The two processes are then formalized as follows and they are bisimilar.

1) $\langle \mathbf{c}!q^B.\mathtt{measure}[q^A].\mathbf{nil}, EPR_{q^A,q^B} \otimes \rho^E\rangle$
2) $\langle \mathtt{measure}[q^A].\mathbf{c}!q^B.\mathbf{nil}, EPR_{q^A,q^B} \otimes \rho^E\rangle$

In this formalization, q^A is treated as a classical bit after the measurement and the resulting state is $1/2(|00\rangle\langle 00| + |11\rangle\langle 11|)_{q^A,q^B}$. Similarly, when the result of measurement of a qubit q is 0 with probability p and 1 with $1-p$ for some $p \in [0,1]$, the resulting state is $(p|0\rangle\langle 0| + (1-p)|1\rangle\langle 1|)_q$.

The two different formalization of a measurement are different from the view of an adversary. Branches evoked by $M[\tilde{q}; x]$ are distinguished in bisimilarity meaning. Therefore, $M[\tilde{q}; x]$ should be used when a transition with a different visible label occurs after the measurement. Otherwise, measurement should be formalized with quantum operator $\mathtt{measure}[\tilde{q}]$. Therefore, we conclude the second formalization is feasible to denote the above case. In fact, all of measurements in the target protocols should be formulated in the second way except the error-rate checking phase.

4.2 On Channels

We do not implement some classical communication as classical channels in qCCS because the classical data prevent a process from dealing with superposition of mixed states correctly. A classical channel is formalized as a quantum channel through which only restricted data are transferred. This situation has essentially the same reason as a physical measurement is represented by not a syntactic measurement but a quantum operation.

In general QKD protocols, three kinds of channels are used: public quantum channels, private classical channels and public no-interpolate classical channels. Since the syntax has channel restriction, formalization of private channels is straightforward. Public no-interpolate channels are realized by copying the data. If classical data v is sent via a public no-interpolate channel c, this is formalized as $...c!v.d!v...\backslash\{..., c, ...\}$. If quantum variable q representing classical bit (i.e. the state of q is $p|0\rangle\langle 0| + (1-p)|1\rangle\langle 1|$ for some $p \in [0,1]$) is sent via a public no-interpolate channel $\mathbf{c}$, it is formalized as $...\mathtt{copy}(q, Q).\mathbf{c}!q.\mathbf{d}!Q...\backslash\{..., \mathbf{c}, ...\}$. The body of the quantum operator copy is easily implemented using cnot.

4.3 Formalization of the EDP-based protocol

Figure 2 is the definition of the configuration $EDPbased^{n,e}_{C_1,C_2}$ denoting the EDP-based protocol. It depends on parameters n and e which determine the length of secret keys and error-threshold. It employs the CSS code constructed from appropriate two linear codes C_1 and C_2. A and B are Alice's and Bob's processes and the protocol is formalized as the parallel composition of them. As they use private channels $\{c_1, c_2, \mathbf{c_2}, ..., \mathbf{c_6}\}$, they are restricted by $'\backslash'$. Density operators ρ^A, ρ^B and ρ^E denote states of qubits that Alice, Bob and Eve have respectively. ρ^A and ρ^B are given concretely but ρ^E is an arbitrary density operator. We may omit scalar multiplication if it is trivial.

For readability, quantum variables in Alice's and Bob's processes are superscribed by A and B. The length of each bit/qubit is fixed by given n, and we may simply write x instead of $x_1, ..., x_m$ for bit/qubit sequences where m is the length of the sequence x. We also write $\mathbf{c}!x$ for $\mathbf{c_1}!x_1...\mathbf{c_m}!x_m$.

We faithfully formalized the protocol introduced in Section 2. The process $EDPbased^{n,e}_{C_1,C_2}$ goes as follows. Alice initially has $2n$ EPR pairs. $q_1^A, ..., q_{2n}^A$ are Alice's halves and $q_1'^A, ..., q_{2n}'^A$ are supposed to be sent to Bob. First n pairs are for check qubits and the last n pairs are for secret keys. Alice randomly performs Hadamard transformation $\mathtt{hadamards}[q'^A, r^A]$ to q'^A according to the randomness r^A with length $2n$. Here, r^A is represented as quantum data in state $(|0\rangle\langle 0| + |1\rangle\langle 1|)^{\otimes 2n}$, that is, they are in the uniform distribution. Alice then shuffles q'^A according to the randomness s^A with sufficient length N by $\mathtt{shuffle}[q'^A, s^A]$. Alice next sends q'^A to Bob via a quantum public channel $\mathbf{c_1}$, and then tells r^A, s^A via a public no-interpolate channel realized with $\mathbf{c_2}, \mathbf{c_3}, \mathbf{d_1}$ and $\mathbf{d_2}$. Bob receives q'^A, r^A and s^A into the quantum variables q^B, r^B and s^B respectively. By this communication, Alice tells Bob which qubits Alice has performed Hadamards and which qubits are for error-rate

check. Bob then recovers the initial order of qubits. using $\texttt{unshuffle}[q^B, s^B]$. He also inverses Hadamards transformations by $\texttt{hadamards}[q^B, r^B]$.

Alice and Bob next measure her and his check qubits by $\texttt{measure}[q_1^A, ..., q_n^A]$ and $\texttt{measure}[q_1^B, ..., q_n^B]$. Bob sends Alice his measurement results $q_1^B, ..., q_n^B$ via a public no-interpolate channel. After receiving Bob's result into the quantum variable t^A, Alice calculates the error rate and determines whether to abort the protocol by the operator $\texttt{abort\_alice}[q_1^A, ..., q_n^A, t^A, b^A]$. This operator depends on the given error threshold e and the quantum variable b^A receives the result. The resulting state of b^A will be of the form $p|0\rangle\langle 0| + (1-p)|1\rangle\langle 1|$ if the abort probability is p. b^A is then measured by $M[b^A; y^A]$, causing probabilistic branch. They abort the protocol if and only if y^A is equal to 0.

If the protocol does not abort, Alice and Bob goes to the error correction and privacy amplification steps. The quantum operator $\texttt{css\_projection}[q_{n+1}^A, ..., q_{2n}^A, u^A, v^A]$ maps Alice's halves $q_{n+1}^A, ..., q_{2n}^A$ to a random CSS codeword. The projection results, which are the bit and phase parameters of CSS code, are stored in u^A and v^A. Alice then decodes her codeword and completes her secret key by $\texttt{css\_decode}[q_{n+1}^A, ..., q_{2n}^A, u^A, v^A]$. Alice then tells Bob the CSS parameters u^A and v^A via public no-interpolate and private classical channels. After receiving, Bob calculates the error syndrome of $q_{n+1}^B, ..., q_{2n}^B$ by `css_syndrome`, corrects errors by `css_correct`, decodes CSS codeword by `css_decode` and finally completes his secret key. Note that the bodies of the quantum operators related to CSS code are given just as they realize the algorithms of CSS code [12]. The processes A and B end with A_2 and B_2, which are Alice's and Bob's processes after sharing the secret key. They may communicate using the shared secret key. To show bisimilarity, A_2 and B_2 are assumed to behave the same with an identical secret key and to keep quantum variables that have not been sent to the outside.

4.4 Formalization of BB84

Figure 3 is the definition of the configuration ${BB84}^{n,e}_{C_1,C_2}$. In BB84, instead of EPR pairs, Alice initially prepares a random $|0\rangle, |1\rangle$ qubit-string with length $2n$, memorizes the bit pattern, and sends the string to Bob after the random Hadamard transformation. Since a density operator represents probabilistic distribution, the initial state is represented with Alice's and Bob's data q^A and q'^A in state $(|00\rangle\langle 00| + |11\rangle\langle 11|)^{\otimes 2n}_{q^A,q'^A}$. Alice then performs Hadamard transformation to q'^A according to the randomness r^A, and then shuffles q^A according to the randomness s^A.

After error-rate checking phase, Alice prepares a random codeword u^A in C_1. The state of u^A is denoted $\sum_{u\in C_1} |u\rangle\langle u|$. Alice then performs `cnot` to u^A with control qubits $q_{n+1}^A, ..., q_{2n}^A$ and sends it to Bob via a public no-interpolate channel realized with $\mathbf{c_5}$ and $\mathbf{d_3}$. Alice then performs `cnot` and `copy`. The bitstring $q_{n+1}^A, ..., q_{2n}^A$ is

$$
\begin{aligned}
EDPbased \equiv\ & \langle A||B\backslash\{c_1, c_2, \mathbf{c_2}, \mathbf{c_3}, \mathbf{c_4}, \mathbf{c_5}, \mathbf{c_6}\},\ \rho^A \otimes \rho^B \otimes \rho^E\rangle \\
A \equiv\ & \texttt{hadamards}[q'^A, r^A].\texttt{shuffle}[q'^A, s^A]. \\
& \mathbf{c_1}!q'^A.c_1?x^A.\texttt{copy}[r^A, R^A].\mathbf{c_2}!r^A.\mathbf{d_1}!R^A. \\
& \texttt{copy}[s^A, S^A].\mathbf{c_3}!s^A.\mathbf{d_2}!S^A.\texttt{measure}[q_1^A, ..., q_n^A]. \\
& \mathbf{c_4}?t^A.\texttt{abort\_alice}[q_1^A, ..., q_n^A, t^A, b^A] \\
& M[b^A; y^A].c_2!y^A.d_1!y^A.\texttt{if } y^A = 0 \texttt{ then} \\
& \ \texttt{css\_projection}[q_{n+1}^A, ..., q_{2n}^A, u^A, v^A]. \\
& \ \texttt{css\_decode}[q_{n+1}^A, ..., q_{2n}^A, u^A, v^A]. \\
& \ \texttt{copy}[u^A, U^A].\mathbf{c_5}!u^A.\mathbf{d_3}!U^A.\texttt{copy}[v^A, V^A].\mathbf{c_6}!v^A.A_2 \\
\rho^A \equiv\ & (|00\rangle\langle 00| + |00\rangle\langle 11| + |11\rangle\langle 00| + |11\rangle\langle 11|)^{\otimes 2n}_{q^A,q'^A} \otimes \\
& (|0\rangle\langle 0| + |1\rangle\langle 1|)^{\otimes 2n}_{r^A} \otimes (|0\rangle\langle 0| + |1\rangle\langle 1|)^{\otimes N}_{s^A} \otimes \\
& (|0\rangle\langle 0|)^{\otimes 2n}_{R^A} \otimes (|0\rangle\langle 0|)^{\otimes N}_{S^A} \otimes |0\rangle\langle 0|_{b^A} \otimes \\
& (|0\rangle\langle 0|)^{\otimes n}_{u^A} \otimes (|0\rangle\langle 0|)^{\otimes n}_{v^A} \otimes (|0\rangle\langle 0|)^{\otimes n}_{U^A} \otimes (|0\rangle\langle 0|)^{\otimes n}_{V^A} \\
B \equiv\ & \mathbf{c_1}?q_1^B, ..., q_{2n}^B.c_1!0.d_2!0. \\
& \mathbf{c_2}?r^B.\texttt{unshuffle}[q^B, r^B].\mathbf{c_3}?s^B.\texttt{hadamards}[q^B, s^B]. \\
& \texttt{measure}[q_1^B, ..., q_n^B].\texttt{copy}[q_1^B, ..., q_n^B, Q_1^B, ..., Q_n^B] \\
& \mathbf{c_4}!q_1^B, ..., q_n^B.\mathbf{d_5}!Q_1^B, ..., Q_n^B. \\
& c_2?y^B.\texttt{if } y^B = 0 \texttt{ then } \mathbf{c_5}?u^B.\mathbf{c_6}?v^B. \\
& \ \texttt{css\_syndrome}[q_{n+1}^B, ..., q_{2n}^B, u^B, v^B, sx^B, sz^B]. \\
& \ \texttt{css\_correct}[q_{n+1}^B, ..., q_{2n}^B, sx^B, sz^B]. \\
& \ \texttt{css\_decode}[q_{n+1}^B, ..., q_{2n}^B, u^B, v^B].B_2 \\
\rho^B \equiv\ & (|0\rangle\langle 0|)^{\otimes n}_{Q^B} \otimes (|0\rangle\langle 0|)^{\otimes n}_{sx^B} \otimes (|0\rangle\langle 0|)^{\otimes n}_{sz^B}
\end{aligned}
$$

Fig. 2: the EDP-based protocol

uniformly random in C_1. Alice finally calculates the coset of $q_{n+1}^A, ..., q_{2n}^A$ in C_2 by $\texttt{key}[q_{n+1}^A, ..., q_{2n}^A]$ and obtains her secret key.

After Bob performs `cnot` and `copy`, the bitstring $q_{n+1}^B, ..., q_{2n}^B$ is same as u^A. As it may contain some errors (it depends on how Eve has interfered), Bob calculates the syndrome and corrects the errors in code C_1 by $\texttt{syndrome}[q_{n+1}^B, ..., q_{2n}^B, sx^B]$ and $\texttt{correct}[q_{n+1}^B, ..., q_{2n}^B, sx^B]$ where sx^B is stored the value of the syndrome. Bob finally calculates the coset of $q_{n+1}^B, ..., q_{2n}^B$ in C_2 by $\texttt{key}[q_{n+1}^B, ..., q_{2n}^B]$ and obtains his secret key.

5. Proof of Bisimulation

5.1 On equivalence of the EDP-based protocol and BB84

Theorem 6: For any classical linear codes C_1, C_2 that satisfy the condition of CSS code, there exist quantum operators corresponding quantum operator symbols in processes, and for any $e \in [0, 1]$, ${EDPbased}^{n,e}_{C_1,C_2} \approx {BB84}^{n,e}_{C_1,C_2}$.

Proof 7: The both protocols end up with the process $A_2||B_2$ after the execution. If the two states σ_{EDP}

$$
\begin{aligned}
BB84 \equiv\ & \langle A||B\backslash\{c_1, c_2, \mathbf{c_2}, \mathbf{c_3}, \mathbf{c_4}, \mathbf{c_5}\},\ \rho^A \otimes \rho^B \otimes \rho^E\rangle \\
A \equiv\ & \texttt{hadamards}[q'^A, r^A].\texttt{shuffle}[q'^A, r^A]. \\
& \mathbf{c_1}!q'^A.c_1?x^A.\texttt{copy}[r^A, R^A].\mathbf{c_2}!r^A.\mathbf{d_1}!R^A. \\
& \texttt{copy}[s^A, S^A].\mathbf{c_3}!s^A.\mathbf{d_2}!S^A. \\
& \mathbf{c_4}?t^A.\texttt{abort\_alice}[q_1^A, ..., q_n^A, t^A, b^A]. \\
& M[b^A; y^A].c_2!y^A.d_1!y^A.\texttt{if } y^A = 0 \texttt{ then} \\
& \ \texttt{cnot}[u^A, q_{n+1}^A, ..., q_{2n}^A].\texttt{copy}[u^A, U^A].\mathbf{c_5}!u^A.\mathbf{d_3}!U^A. \\
& \ \texttt{cnot}[u^A, q_{n+1}^A, ..., q_{2n}^A].\texttt{copy}[u^A, q_{n+1}^A, ..., q_{2n}^A]. \\
& \ \texttt{key}[q_{n+1}^A, ..., q_{2n}^A].A_2 \\
\rho^A \equiv\ & (|00\rangle\langle 00| + |11\rangle\langle 11|)^{\otimes 2n}_{q^A, q'^A} \otimes (|0\rangle\langle 0| + |1\rangle\langle 1|)^{\otimes 2n}_{r^A} \otimes \\
& (|0\rangle\langle 0| + |1\rangle\langle 1|)^{\otimes N}_{s^A} \otimes (|0\rangle\langle 0|)^{\otimes 2n}_{R^A} \otimes (|0\rangle\langle 0|)^{\otimes N}_{S^A} \otimes \\
& |0\rangle\langle 0|_{b^A} \otimes (\sum_{u \in C_1} |u\rangle\langle u|)_{u^A} \otimes \otimes (|0\rangle\langle 0|)^{\otimes n}_{v^A} \otimes \\
& (|0\rangle\langle 0|)^{\otimes n}_{U^A} \otimes (|0\rangle\langle 0|)^{\otimes n}_{V^A} \\
B \equiv\ & \mathbf{c_1}?q_1^B, ..., q_{2n}^B.c_1!0.d_2!0. \\
& \mathbf{c_2}?r^B.\texttt{unshuffle}[q^B, r^B].\mathbf{c_3}?s^B.\texttt{hadamards}[q^B, s^B]. \\
& \texttt{measure}[q_1^B, ..., q_n^B].\texttt{copy}[q_1^B, ..., q_n^B, Q_1^B, ..., Q_n^B]. \\
& \mathbf{c_4}!q_1^B, ..., q_n^B.\mathbf{d_5}!Q_1^B, ..., Q_n^B. \\
& c_2?y^B.\texttt{if } y^B = 0 \texttt{ then } \mathbf{c_5}?u^B. \\
& \ \texttt{cnot}[u^B, q_{n+1}^B, ..., q_{2n}^B].\texttt{copy}[u^B, q_{n+1}^B, ..., q_{2n}^B]. \\
& \ \texttt{syndrome}[q_{n+1}^B, ..., q_{2n}^B, sx^B]. \\
& \ \texttt{correct}[q_{n+1}^B, ..., q_{2n}^B, sx^B].\texttt{key}[q_{n+1}^B, ..., q_{2n}^B].B_2 \\
\rho^B \equiv\ & (|0\rangle\langle 0|)^{\otimes n}_{Q^B} \otimes (|0\rangle\langle 0|)^{\otimes n}_{sx^B} \otimes (|0\rangle\langle 0|)^{\otimes n}_{sz^B}
\end{aligned}
$$

Fig. 3: BB84 (slightly modified)

and σ_{BB84} have the same secret key and partial trace in Eve's view, the configurations $\langle A_2||B_2, \sigma_{EDP}\rangle$ and $\langle A_2||B_2, \sigma_{BB84}\rangle$ are trivially bisimilar. By Theorem 4, we can find the bisimilar configurations which reach $A_2||B_2$ by a single transition in execution paths. Repeating such calculation by going back transition paths, we have $EDPbased^{n,e}_{C_1,C_2} \approx BB84^{n,e}_{C_1,C_2}$ at the starting point. This is the outline of the proof.

Since for τ-transitions by operators, `if` and communication in restricted channels, a configuration before a transition is bisimilar to the configuration after the transition, it is enough to consider other cases.

If a transition of input or output other than $\mathbf{c_1}$ exists in a execution path from $EDPbased^{n,e}_{C_1,C_2}$ to a configuration, we can find the same transition in a path from $BB84^{n,e}_{C_1,C_2}$ to a bisimilar configuration, and vice versa. We can choose pairs of configurations before a transition so that their states of the output variable coincide. For such pair of configurations, it is easy to see that the conditions on variables for Theorem 4 hold automatically. Since the concerned transition is parallel to other transitions, we can see the two configurations are bisimilar by Theorem 4.

The case of a transition of measurement is similar to the above case, but we have to calculate the partial trace condition carefully. Because the transition does not preserve partial traces, a pair of bisimilar configurations before the transition satisfies a stronger condition than the usual trace condition.

The last step is about transitions with the channel $\mathbf{c_1}$. In this case, we have to consider the nondeterministic branching of transitions. Theorem 4 can be applied to the internal communication case after Theorem 4 is applied to the input and output cases.

The proof is completed by showing that $EDPbased^{n,e}_{C_1,C_2}$ and $BB84^{n,e}_{C_1,C_2}$ satisfy the above calculated relation. Though Alice and Bob's starting states in the two protocols are different, we can see that they have the same partial trace. For other conditions, in fact, we can prove by calculation of states in every execution. Especially, the value of the secret key, the traced values of output variables and the probability of the measurement are important.

The value of the secret key is identical because operations in the both protocols related to error correcting codes work equivalently.

The initial states of q^A and q'^A are different but Alice sends only q'^A via $\mathbf{c_1}$. Even if $q_j'^A$ is sent to the outside, the following calculation shows that the partial trace is the same: $\mathrm{tr}_{\{q_j^A\}}(1/2|00\rangle\langle 00| + 1/2|00\rangle\langle 11| + 1/2|11\rangle\langle 00| + 1/2|11\rangle\langle 11|) = \mathrm{tr}_{\{q_j'^A\}}(1/2|00\rangle\langle 00| + 1/2|11\rangle\langle 11|) = 1/2|0\rangle\langle 0| + 1/2|1\rangle\langle 1|$. As for other quantum variables, the conditions are checked by examining the related operators.

When $\texttt{abort\_alice}[q_1^A, ..., q_n^A, s^A, b^A]$ is operated, the states of the inputs correspond. This follows the resulting state of b^A, and then the weight of the probability branch and partial traces after the measurement $M[b^A; y^A]$ correspond.

5.2 On multiple session

From theorem 5, the fact is immediately obtained that the EDP-based protocol and BB84 cannot be distinguished from the outside even if they run in parallel. We first introduce the following lemma.

Lemma 8: If $\langle P_1, \rho_1 \otimes \rho_1^E\rangle \approx \langle Q_1, \sigma_1 \otimes \rho_1^E\rangle$, $\langle P_2, \rho_2 \otimes \rho_2^E\rangle \approx \langle Q_2, \sigma_2 \otimes \rho_2^E\rangle$ and $\mathrm{qv}(P_1) \cap \mathrm{qv}(P_2) = \mathrm{qv}(P_1) \cap \mathrm{qv}(Q_2) = \mathrm{qv}(Q_1) \cap \mathrm{qv}(P_2) = \mathrm{qv}(Q_1) \cap \mathrm{qv}(Q_2) = \emptyset$ hold for all ρ_1^E, ρ_2^E, then $\langle P_1||P_2, \rho_1 \otimes \rho_2 \otimes \rho^E\rangle \approx \langle Q_1||Q_2, \sigma_1 \otimes \sigma_2 \otimes \rho^E\rangle$ holds for all ρ^E.

Proof 9: From the premise, we have $\langle P_1, \rho_1 \otimes \rho_2 \otimes \rho^E\rangle \approx \langle Q_1, \sigma_1 \otimes \rho_2 \otimes \rho^E\rangle$. From theorem 5, we next have $\langle P_1||P_2, \rho_1 \otimes \rho_2 \otimes \rho^E\rangle \approx \langle Q_1||P_2, \sigma_1 \otimes \rho_2 \otimes \rho^E\rangle$. Similarly, we have $\langle Q_1||P_2, \sigma_1 \otimes \rho_2 \otimes \rho^E\rangle \approx \langle Q_1||Q_2, \sigma_1 \otimes \sigma_2 \otimes \rho^E\rangle$. By the transitivity of $\approx$, we obtain the conclusion.

Let s be a natural number and let $A_{EDP,1}, ..., A_{EDP,s}$ be Alice's process executing the EDP-based protocol that are obtained replacing channel names so that they can appropriately communicate, and replacing quantum variables in $A_{EDP,i}$ so that $\mathrm{qv}(A_{EDP,1}) \cap ... \cap \mathrm{qv}(A_{EDP,s}) = \emptyset$.

Let $L_1, ..., L_s$ be the sets of channels that are restricted in each session and let the corresponding density operators be $\rho^A_{EDP,1}, ..., \rho^A_{EDP,s}$. Let Bob's process in the EDP-based protocol, the corresponding states and BB84's counterparts be defined in the same way. We define s session execution of the EDP-based protocol $EDPbased^{n,e}_{C_1,C_2}(s)$ and of BB84 $BB84^{n,e}_{C_1,C_2}(s)$ as follows.

$$
\begin{aligned}
&EDPbased^{n,e}_{C_1,C_2}(s)\\
&\equiv \langle (A_{EDP,1}||B_{EDP,1}\backslash L_1)||...||(A_{EDP,s}||B_{EDP,s}\backslash L_s),\\
&\quad \rho^A_{EDP,1} \otimes \rho^B_{EDP,1} \otimes ... \otimes \rho^A_{EDP,s} \otimes \rho^B_{EDP,s} \otimes \rho^E \rangle\\
&BB84^{n,e}_{C_1,C_2}(s)\\
&\equiv \langle (A_{BB84,1}||B_{BB84,1}\backslash L_1)||...||(A_{BB84,s}||B_{BB84,s}\backslash L_s),\\
&\quad \rho^A_{BB84,1} \otimes \rho^B_{BB84,1} \otimes ... \otimes \rho^A_{BB84,s} \otimes \rho^B_{BB84,s} \otimes \rho^E \rangle
\end{aligned}
$$

Corollary 10: For all natural number s, sufficiently large natural number n and classical linear codes C_1, C_2 that satisfy the condition of CSS code, there exists quantum operators corresponding quantum operator symbols in processes, for any $e \in [0,1]$, $EDPbased^{n,e}_{C_1,C_2}(s) \approx BB84^{n,e}_{C_1,C_2}(s)$.

Proof 11: By Theorem 5, we have $\langle A_{EDP,i}||B_{EDP,i}\backslash L_i, \rho^A_{EDP,i} \otimes \rho^B_{EDP,i} \otimes \rho^{E,i} \rangle \approx \langle A_{EDP,i}||B_{EDP,i}\backslash L_i, \rho^A_{BB84,i} \otimes \rho^B_{BB84,i} \otimes \rho^{E,i} \rangle$ for all i and $\rho^{E,i}$. Next, by induction of the number of the sessions s, we apply Lemma 8.

6. Conclusion

In this paper, we applied a quantum process calculus qCCS [9] to a security proof of BB84 QKD protocol presented by Shor end Preskill [2]. We presented a general technique to describe quantum measurements. A probabilistic branch in the transition system evoked by a quantum measurement $M[\tilde{q}; x]$ is visible from an adversary. It should be used if the process performs different visible actions (e.g. to abort or to continue a protocol) from outside according to the measurement results. Otherwise, quantum measurement should be formalized as a quantum operator $\texttt{measure}[\tilde{q}]$. We formalized BB84 and the EDP-based protocol as qCCS processes and then proved they are bisimilar, which means the two protocols behave same from an adversary. The security equivalence of BB84 and the EDP-based protocol under concurrent execution is immediately obtained from the congruence property of bisimulation.

The result of this paper directly shows the feasibility of process calculi for analyses of security equivalence of QKD protocols. Since cryptographic proofs often discuss equivalence of protocols [2], [13], bisimulation will be versatile way for formal verification of the proofs. Quantum process calculi have been used for analyses of quantum protocols. Davidson et al. formally verified a quantum error correcting code [10] using CQP's bisimulation. As case studies, qCCS developers have applied it to specification and verification of quantum teleportation and superdense coding protocols [9]. It has also been applied to specification of simplified BB84 [11] but this is not a security proof. Since adversary's view is important in cryptography, treatment of branches evoked by quantum measurements is significant for proving security equivalence of protocols.

Future work In this paper, we proposed a technique to formalize quantum measurement. We expect the existence of an algorithm to determine which formulation of a measurement should be used.

If two processes are bisimilar in qCCS's sense, an adversary observes the same behavior with the identical probability up to invisible actions. However, cryptographic proofs often discuss indistinguishability up to some negligible probability. The notion of *probabilistic* bisimulation is useful for such arguments. It will enable us to realize full formalization of security proofs.

Bisimulation is feasible for automatic verification [14]. As for qCCS's bisimulation, theorem 4 suggests that bisimulation is checked by exhausting the non-deterministic execution paths if each path is finite. If we mainly target cryptographic protocols, it is possibly the case. For example, the processes in this paper do not have an infinite path. Automation would truly help formal verification.

References

[1] D. Mayers. Unconditional security in quantum cryptography. *J. ACM*, 48:351–406, May 2001.

[2] P. W. Shor and J. Preskill. Simple proof of security of the bb84 quantum key distribution protocol. *Phys. Rev. Lett.*, 85(2):441–444, Jul 2000.

[3] H.-K. Lo and H. F. Chau. Unconditional security of quantum key distribution over arbitrarily long distances. *Phys. Rev. Lett.*, 283(5410):2050–2056, Mar 1999.

[4] B. Blanchet. A computationally sound automatic prover for cryptographic protocols. In *Workshop on the link between formal and computational models*, Paris, France, June 2005.

[5] C. Neuman, T. Yu, S. Hatman, and K. Raeburn. The kerberos network authentication service (v5). http://www.ietf.org/rfc/rfc4120, Jul 2005.

[6] B. Blanchet, A. D. Jaggard, A. Scedrov, and J.-K. Tsay. Computationally sound mechanized proofs for basic and public-key kerberos. In *Proceedings of the 2008 ACM symposium on Information, computer and communications security*, ASIACCS '08, pages 87–99, New York, NY, USA, 2008. ACM.

[7] P. Jorrand and M. Lalire. From quantum physics to programming languages: A process algebraic approach. In *Unconventional Programming Paradigms*, Lecture Notes in Computer Science.

[8] S. J. Gay and R. Nagarajan. Communicating quantum processes. *SIGPLAN Not.*, 40:145–157, January 2005.

[9] Y. Feng, R. Duan, and M. Ying. Bisimulation for quantum processes. *SIGPLAN Not.*, 46(1):523–534, January 2011.

[10] R.Nagarajan I.V. Puthoor T.A.S. Davidson, S.J.Gay. Analysis of a quantum error correcting code using quantum process calculus. Quantum Physics and Logics, 2011.

[11] Y. Feng Y. Deng. Open bisimulation for quantum processes. arXiv:1201.0416v1, 2012.

[12] A. R. Calderbank and P. W. Shor. Good quantum error-correcting codes exist. *Phys. Rev. A*, 54(2):1098–1105, Aug 1996.

[13] K. Tamaki, M. Koashi, and N. Imoto. Unconditionally secure key distribution based on two nonorthogonal states. *Phys. Rev. Lett.*, 90(16):167904, Apr 2003.

[14] A. Tiu and J. Dawson. Automating open bisimulation checking for the spi calculus. In *Computer Security Foundations Symposium (CSF), 2010 23rd IEEE*, pages 307 –321, july 2010.

An Automated Deduction of the Equivalence of Symmetry of Commutativity and the Orthomodular Law in Quantum Logic

Jack K. Horner
P. O. Box 266
Los Alamos, New Mexico 87544 USA
email: jhorner@cybermesa.com

Abstract

The optimization of quantum computing circuitry and compilers at some level must be expressed in terms of quantum-mechanical behaviors and operations. In much the same way that the structure of conventional propositional (Boolean) logic (BL) is the logic of the description of the behavior of classical physical systems and is isomorphic to a Boolean algebra (BA), so also the algebra, C(H), of closed linear subspaces of (equivalently, the system of linear operators on (observables in)) a Hilbert space is a logic of the descriptions of the behavior of quantum mechanical systems and is a model of an ortholattice (OL). An OL can thus be thought of as a kind of "quantum logic" (QL). C(H) is also a model of an orthomodular lattice, which is an OL conjoined with the orthomodularity axiom (OMA). The rationalization of the OMA as a claim proper to physics has proven problematic, motivating the question of whether the OMA and its equivalents are required in an adequate characterization of QL. Because the propositions of a QL are not in general commutative, quantum logicians have paid much attention to "quasi"-commutative theorems, one of the better known of which is the symmetry of commutativity theorem (SoCT), which states that commutativity is symmetric in an orthomodular lattice. Here I provide automated deductions showing that the SoCT and the OMA, in the context of a QL, are equivalent. The proofs appear to be novel.

Keywords: automated deduction, quantum computing, orthomodular lattice, commutativity, Hilbert space

1.0 Introduction

The optimization of quantum computing circuitry and compilers at some level must be expressed in terms of the description of quantum-mechanical behaviors ([1], [17], [18], [20]). In much the same way that conventional propositional (Boolean) logic (BL,[12]) is the logical structure of description of the behavior of classical physical systems (e.g. "the measurements of the position and momentum of particle P are commutative") and is isomorphic to a Boolean lattice ([10], [11], [19]), so also the algebra, *C(H)*, of the closed linear subspaces of (equivalently, the system of linear operators on (observables in)) a Hilbert space *H* ([1], [4], [6], [9], [13]) is *a* logic of the descriptions of the behavior of quantum mechanical systems (e.g., "the measurements of the position and momentum of particle P are *not* commutative") and is a model ([10]) of an ortholattice (OL; [8]). An OL can thus be thought of as a kind of "quantum logic" (QL; [19]). *C(H)* is also a model of (i.e., isomorphic to a set of sentences which hold in) an orthomodular lattice (OML; [7], [8]), which is an OL conjoined with the orthomodularity axiom (OMA; see Figure 1). The rationalization of the OMA as a

claim proper to physics has proven problematic ([13], Section 5-6),

Lattice axioms

```
      x = c(c(x))                        (AxLat1)
      x v y = y v x                      (AxLat2)
      (x v y) v z = x v (y v z)          (AxLat3)
      (x ^ y) ^ z = x ^ (y ^ z)          (AxLat4)
      x v (x ^ y) = x                    (AxLat5)
      x ^ (x v y) = x                    (AxLat6)
```

Ortholattice axioms

```
      c(x) ^ x = 0                       (AxOL1)
      c(x) v x = 1                       (AxOL2)
      x ^ y = c(c(x) v c(y))             (AxOL3)
```

Orthomodularity axiom (aka Orthomodularity Law)

```
      y v (c(y) ^ (x v y)) = x v y       (OMA)
```

```
where
      x, y are variables ranging over lattice nodes
      ^ is lattice meet
      v is lattice join
      c(x) is the orthocomplement of x
      =  is equivalence ([12])
      1 is the maximum lattice element (= x v c(x))
      0 is the minimum lattice element (= c(1))
```

Figure 1. Lattice, ortholattice, and orthomodularity axioms.

Because of the fundamental role that non-commutativity plays in QL, quantum logicians have paid much attention to "quasi"-commutative theorems, which help to ground a large class of equivalence representations in quantum logic, and are thus of potential interest in optimizing quantum compiler and circuit design. Among the better known of the quasi-commutative theorems is the symmetry of commutativity theorem (SoCT; [7],[8]) shown is in Figure 2

```
   If x and y are elements of an orthomodular lattice,

           xCy  <->  yCx

    where xCy means "x commutes with y", defined as
```

```
xCy <-> (x = ((x ^ y) v (x ^ c(y)))), and

<-> means "if and only if"
```

Figure 2. The SoCT ([7],[8]).

Informally stated, the SoCT says that commutativity is symmetric in an orthomodular lattice. It turns out, as subsequent sections of this paper show, that the SoCT is equivalent to the OMA, in the sense that the axioms of an ortholattice, together with the SoCT, imply the OMA, and the axioms of an orthomodular lattice imply the SoCT.

2.0 Method

The OML and OL axiomatizations of Megill, Pavičić, and Horner ([5], [14], [15], [16], [21], [22]) were implemented in a *prover9* ([2]) scripts ([3]) configured to derive the equivalence of the SoCT and the OMA, then executed in that framework on a Dell Inspiron 545 with an Intel Core2 Quad CPU Q8200 (clocked @ 2.33 GHz) and 8.00 GB RAM, running under the *Windows Vista Home Premium (SP2)/Cygwin* operating environment.

3.0 Results

To prove the equivalence of the symmetry of commutativity with the Orthomodular Law, it suffices to prove the propositions shown in Sections 3.1, 3.2, and 3.3.

3.1 Proof of 'xCy → yCx' in an orthomodular lattice

Figure 3.1.1 shows the proof of proposition 'xCy → yCx' produced by [3] on the platform described in Section 2.0.

```
============================== PROOF =================================

% Proof 1 at 65.32 (+ 1.47) seconds: "Commutativity is symmetric in an orthomodular
lattice".
% Length of proof is 87.
% Level of proof is 23.

2 C(x,y) <-> x = (x ^ y) v (x ^ c(y)) # label("Df: commutes") # label(non_clause).
[assumption].
3 C(x,y) -> C(y,x) # label("Commutativity is symmetric in an orthomodular lattice") #
label(non_clause) # label(goal).  [goal].
6 x = c(c(x)) # label("AxL1").  [assumption].
7 c(c(x)) = x.  [copy(6),flip(a)].
8 x v y = y v x # label("AxL2").  [assumption].
9 (x v y) v z = x v (y v z) # label("AxL3").  [assumption].
11 x v (x ^ y) = x # label("AxL5").  [assumption].
12 x ^ (x v y) = x # label("AxL6").  [assumption].
13 c(x) ^ x = 0 # label("AxOL1").  [assumption].
14 c(x) v x = 1 # label("AxOL2").  [assumption].
15 x v c(x) = 1.  [copy(14),rewrite([8(2)])].
16 x ^ y = c(c(x) v c(y)) # label("AxOL3").  [assumption].
17 x v (c(x) ^ (y v x)) = y v x # label("OMA").  [assumption].
18 x v c(x v c(y v x)) = y v x.  [copy(17),rewrite([16(3),7(2)])].
30 -C(x,y) | (x ^ y) v (x ^ c(y)) = x # label("Df: commutes").  [clausify(2)].
```

```
31 -C(x,y) | c(c(x) v y) v c(c(x) v c(y)) = x.
[copy(30),rewrite([16(2),16(7),7(8),8(9)])].
32 C(x,y) | (x ^ y) v (x ^ c(y)) != x # label("Df: commutes").  [clausify(2)].
33 C(x,y) | c(c(x) v y) v c(c(x) v c(y)) != x.
[copy(32),rewrite([16(2),16(7),7(8),8(9)])].
34 C(c1,c2) # label("Commutativity is symmetric in an orthomodular lattice").  [deny(3)].
35 -C(c2,c1) # label("Commutativity is symmetric in an orthomodular lattice") #
answer("Commutativity is symmetric in an orthomodular lattice").  [deny(3)].
36 c(1) = 0.  [back_rewrite(13),rewrite([16(2),7(2),15(2)])].
37 c(c(x) v c(x v y)) = x.  [back_rewrite(12),rewrite([16(2)])].
38 x v c(c(x) v c(y)) = x.  [back_rewrite(11),rewrite([16(1)])].
40 x v (y v z) = y v (x v z).  [para(8(a,1),9(a,1,1)),rewrite([9(2)])].
42 x v (c(x) v y) = 1 v y.  [para(15(a,1),9(a,1,1)),flip(a)].
43 x v (y v c(x v y)) = 1.  [para(15(a,1),9(a,1)),flip(a)].
44 x v c(x v c(x v y)) = y v x.  [para(8(a,1),18(a,1,2,1,2,1))].
45 x v (c(x v c(y v x)) v z) = y v (x v z).
[para(18(a,1),9(a,1,1)),rewrite([9(2)]),flip(a)].
47 x v c(x v c(y v (z v x))) = y v (z v x).
[para(9(a,1),18(a,1,2,1,2,1)),rewrite([9(8)])].
50 C(c(x),y) | c(x v y) v c(x v c(y)) != c(x).
[para(7(a,1),33(b,1,1,1,1)),rewrite([7(6)])].
53 C(x,y) | c(c(x) v y) v c(c(y) v c(x)) != x.  [para(8(a,1),33(b,1,2,1))].
58 c(c2 v c(c1)) v c(c(c1) v c(c2)) = c1.  [hyper(31,a,34,a),rewrite([8(4)])].
59 c(c1 v c(c2)) v c(c(c1) v c(c2)) != c2 # answer("Commutativity is symmetric in an
orthomodular lattice").  [ur(33,a,35,a),rewrite([8(4),8(10)])].
63 C(x,1) | c(0 v c(x)) v c(1 v c(x)) != x.
[para(36(a,1),33(b,1,2,1,2)),rewrite([8(5),8(9),8(11)])].
64 c(x) v c(x v y) = c(x).  [para(37(a,1),7(a,1,1)),flip(a)].
68 c(0 v c(x)) = x.  [para(15(a,1),37(a,1,1,2,1)),rewrite([36(3),8(3)])].
69 c(x v y) v c(x v c(x v y)) = c(x).
[para(37(a,1),18(a,1,2,1,2)),rewrite([8(5),64(11)])].
71 C(x,x v y) | c(1 v y) v x != x.  [para(37(a,1),33(b,1,2)),rewrite([40(5),42(5)])].
72 1 v x = 1.  [para(36(a,1),37(a,1,1,1)),rewrite([68(6)])].
74 C(x,1) | x v 0 != x.  [back_rewrite(63),rewrite([68(6),72(5),36(4)])].
76 C(x,x v y) | 0 v x != x.  [back_rewrite(71),rewrite([72(4),36(4)])].
81 x v c(c(x) v y) = x.  [para(7(a,1),38(a,1,2,1,2))].
85 x v 0 = x.  [para(15(a,1),38(a,1,2,1)),rewrite([36(2)])].
86 x v c(y v c(x)) = x.  [para(18(a,1),38(a,1,2,1))].
88 x v x = x.  [para(36(a,1),38(a,1,2,1,2)),rewrite([8(3),68(4)])].
90 C(x,1).  [back_rewrite(74),rewrite([85(4)]),xx(b)].
93 x v (y v c(x v c(z v x))) = y v (z v x).  [para(18(a,1),40(a,1,2)),flip(a)].
95 0 v x = x.  [hyper(31,a,90,a),rewrite([8(3),72(3),36(2),36(4),8(4),68(5)])].
98 C(x,x v y).  [back_rewrite(76),rewrite([95(4)]),xx(b)].
112 x v (x v y) = x v y.  [para(88(a,1),9(a,1,1)),flip(a)].
114 x v (y v x) = y v x.  [para(88(a,1),9(a,2,2)),rewrite([8(2)])].
125 C(x v y,x v (y v z)).  [para(9(a,1),98(a,2))].
219 x v (c(c(x) v y) v z) = x v z.  [para(81(a,1),9(a,1,1)),flip(a)].
298 c(x) v c(y v x) = c(x).  [para(7(a,1),86(a,1,2,1,2))].
317 C(c(x),x v y).  [para(112(a,1),50(b,1,1,1)),rewrite([69(10)]),xx(b)].
328 C(c(x),y v x).  [para(8(a,1),317(a,2))].
337 c(x v y) v c(y v c(x v y)) = c(y).  [hyper(31,a,328,a),rewrite([7(2),114(2),7(4)])].
364 C(x v y,y).
[para(86(a,1),53(b,1,2,1)),rewrite([7(2),7(4),8(5),7(8),8(7),18(7),7(5)]),xx(b)].
368 C(x v (y v z),x v z).  [para(40(a,1),364(a,1))].
392 c(c(c1) v c(c2)) v (x v c(c2 v c(c1))) = x v c1.
[para(58(a,1),45(a,2,2)),rewrite([8(26),93(27)])].
406 c(x) v (c(x v y) v z) = c(x) v z.  [para(64(a,1),9(a,1,1)),flip(a)].
414 c(x v y) v c(c(x v y) v c(z v c(x))) = z v c(x).
[para(64(a,1),47(a,1,2,1,2,1,2)),rewrite([64(14)])].
617 C(x v y,y v (x v z)).  [para(8(a,1),125(a,1))].
618 C(x v y,y v (z v x)).  [para(8(a,1),125(a,2)),rewrite([9(3)])].
733 C(x v (y v z),z v x).  [para(8(a,1),368(a,2))].
855 C(c(x v y) v z,z v c(x)).  [para(69(a,1),617(a,2,2))].
1079 C(x v c(y),c(y v z) v x).  [para(64(a,1),733(a,1,2))].
1859 C(c(x v y) v z,z v c(y)).  [para(298(a,1),618(a,2,2))].
1862 C(x v c(y),c(z v y) v x).  [para(298(a,1),733(a,1,2))].
7402 C(c1,c(c2) v c(c(c1) v c(c2))).  [para(58(a,1),855(a,1)),rewrite([8(10)])].
8031 C(c(c2) v c(c(c1) v c(c2)),c1).  [para(58(a,1),1079(a,2)),rewrite([8(9)])].
10398 c(c(c1) v c(c(c2) v c(c(c1) v c(c2)))) = c1.
[hyper(31,a,7402,a),rewrite([43(12),36(2),95(16)])].
```

```
11360 c1 v c(c1 v c(c(c2) v c(c(c1) v c(c2)))) = c(c2) v c(c(c1) v c(c2)).
[hyper(31,a,8031,a),rewrite([8(12),8(26),10398(27),8(15)])].
19020 x v c(y v c(c(x) v y)) = x v c(y).  [para(337(a,1),219(a,1,2)),flip(a)].
19087 c(c2) v c(c(c1) v c(c2)) = c1 v c(c1 v c2).
[back_rewrite(11360),rewrite([19020(13),7(5)]),flip(a)].
21129 c1 v c(c1 v c2) = c1 v c(c2).
[para(64(a,1),392(a,1,2)),rewrite([8(9),19087(9),8(10)])].
21175 c(c2) v c(c(c1) v c(c2)) = c1 v c(c2).  [back_rewrite(19087),rewrite([21129(15)])].
21178 c1 v c(c1 v c(c2)) = c1 v c2.  [para(21129(a,1),44(a,1,2,1)),rewrite([8(10)])].
21180 c(c1 v c2) v c(c1 v c(c2)) = c(c1).
[para(21129(a,1),69(a,1,1,1)),rewrite([21129(12),21178(12),8(10)])].
21882 c(x) v c(y v c(x v y)) = c(x) v c(y).  [para(337(a,1),406(a,1,2)),flip(a)].
22893 c(c1) v c(c2 v c(c1)) = c(c1) v c(c2).
[para(58(a,1),414(a,1,2,1)),rewrite([8(8)])].
35649 C(c(c1),c(c2) v c(c1 v c(c2))).  [para(21180(a,1),1859(a,1)),rewrite([8(10)])].
35650 C(c(c2) v c(c1 v c(c2)),c(c1)).  [para(21180(a,1),1862(a,2)),rewrite([8(8)])].
35718 c(c1 v c(c(c2) v c(c1 v c(c2)))) = c(c1).
[hyper(31,a,35649,a),rewrite([7(3),43(10),36(2),7(4),95(14)])].
35719 c(c2) v c(c1 v c(c2)) = c(c1) v c(c2).
[hyper(31,a,35650,a),rewrite([8(12),21882(12),7(5),8(4),7(17),8(16),35718(17),8(8),22893(
8)]),flip(a)].
70001 c(c1 v c(c2)) v c(c(c1) v c(c2)) = c2.
[para(21175(a,1),69(a,1,1,1)),rewrite([21175(16),35719(13),7(15)])].
70002 $F # answer("Commutativity is symmetric in an orthomodular lattice").
[resolve(70001,a,59,a)].

============================== end of proof ==========================
```

Figure 3.1.1. Summary of a *prover9* ([2]) proof of the proposition 'xCy → yCx' ([7]) in an orthomodular lattice. The proof assumes the inference rules of *prover9*. The general form of a line in this proof is "*line_number conclusion [derivation]*", where *line_number* is a unique identifier of a line in the proof, and *conclusion* is the result of applying the *prover9* inference rules (such as *para*modulation, *copy*ing, and *rewrit*ing), noted in square brackets (denoting the *derivation*), to the lines cited in those brackets. Note that some of "logical" proof lines in the above have been transformed to two text lines, with the *derivation* appearing on a text line following a text line containing the first part of that logical line. The detailed syntax and semantics of these notations can be found in [2]. All *prover9* proofs are by default proofs by contradiction.

3.2 Proof of 'yCx → xCy' in an orthomodular lattice

Substitute x for y and y for x in Figure 3.1.1.

3.3 Proof of '(xCy ↔ yCx) → Orthomodular Law (OMA)' in an ortholattice

---

```
============================== PROOF =================================

% Proof 1 at 0.01 (+ 0.03) seconds: "Symmetry of commutativity implies OMA".
% Length of proof is 39.
% Level of proof is 11.

2 C(x,y) <-> x = (x ^ y) v (x ^ c(y)) # label("Df: commutes") # label(non_clause).
[assumption].
```

```
3 C(y,x) <-> C(x,y) # label("Commutativity is symmetric") # label(non_clause).
[assumption].
4 y v (c(y) ^ (x v y)) = x v y # label("Symmetry of commutativity implies OMA") #
label(non_clause) # label(goal).  [goal].
7 x = c(c(x)) # label("AxL1").  [assumption].
8 c(c(x)) = x.  [copy(7),flip(a)].
9 x v y = y v x # label("AxL2").  [assumption].
10 (x v y) v z = x v (y v z) # label("AxL3").  [assumption].
12 x v (x ^ y) = x # label("AxL5").  [assumption].
13 x ^ (x v y) = x # label("AxL6").  [assumption].
14 c(x) ^ x = 0 # label("AxOL1").  [assumption].
15 c(x) v x = 1 # label("AxOL2").  [assumption].
16 x v c(x) = 1.  [copy(15),rewrite([9(2)])].
17 x ^ y = c(c(x) v c(y)) # label("AxOL3").  [assumption].
29 -C(x,y) | (x ^ y) v (x ^ c(y)) = x # label("Df: commutes").  [clausify(2)].
30 -C(x,y) | c(c(x) v y) v c(c(x) v c(y)) = x.
[copy(29),rewrite([17(2),17(7),8(8),9(9)])].
31 C(x,y) | (x ^ y) v (x ^ c(y)) != x # label("Df: commutes").  [clausify(2)].
32 C(x,y) | c(c(x) v y) v c(c(x) v c(y)) != x.
[copy(31),rewrite([17(2),17(7),8(8),9(9)])].
33 -C(x,y) | C(y,x) # label("Commutativity is symmetric").  [clausify(3)].
34 c1 v (c(c1) ^ (c2 v c1)) != c2 v c1 # label("Symmetry of commutativity implies OMA") #
answer("Symmetry of commutatativity implies OMA").  [deny(4)].
35 c1 v c(c1 v c(c1 v c2)) != c1 v c2 # answer("Symmetry of commutativity implies OMA").
[copy(34),rewrite([9(6),17(7),8(4),9(12)])].
36 c(1) = 0.  [back_rewrite(14),rewrite([17(2),8(2),16(2)])].
37 c(c(x) v c(x v y)) = x.  [back_rewrite(13),rewrite([17(2)])].
38 x v c(c(x) v c(y)) = x.  [back_rewrite(12),rewrite([17(1)])].
40 x v (y v z) = y v (x v z).  [para(9(a,1),10(a,1,1)),rewrite([10(2)])].
42 x v (c(x) v y) = 1 v y.  [para(16(a,1),10(a,1,1)),flip(a)].
53 C(x,1) | c(0 v c(x)) v c(1 v c(x)) != x.
[para(36(a,1),32(b,1,2,1,2)),rewrite([9(5),9(9),9(11)])].
54 c(x) v c(x v y) = c(x).  [para(37(a,1),8(a,1,1)),flip(a)].
58 c(0 v c(x)) = x.  [para(16(a,1),37(a,1,1,2,1)),rewrite([36(3),9(3)])].
60 C(x,x v y) | c(1 v y) v x != x.  [para(37(a,1),32(b,1,2)),rewrite([40(5),42(5)])].
61 1 v x = 1.  [para(36(a,1),37(a,1,1,1)),rewrite([58(6)])].
63 C(x,1) | x v 0 != x.  [back_rewrite(53),rewrite([58(6),61(5),36(4)])].
65 C(x,x v y) | 0 v x != x.  [back_rewrite(60),rewrite([61(4),36(4)])].
74 x v 0 = x.  [para(16(a,1),38(a,1,2,1)),rewrite([36(2)])].
78 C(x,1).  [back_rewrite(63),rewrite([74(4)]),xx(b)].
82 0 v x = x.  [hyper(30,a,78,a),rewrite([9(3),61(3),36(2),36(4),9(4),58(5)])].
85 C(x,x v y).  [back_rewrite(65),rewrite([82(4)]),xx(b)].
107 C(x v y,x).  [hyper(33,a,85,a)].
111 x v c(x v c(x v y)) = x v y.
[hyper(30,a,107,a),rewrite([9(3),9(8),54(8),8(6),9(5)])].
112 $F # answer("Symmetry of commutativity implies OMA").  [resolve(111,a,35,a)].

============================== end of proof ==========================
```

Figure 3.3.1. Summary of a *prover9* ([2]) proof of the proposition '(xCy ↔ yCx) → OMA in an ortholattice.

4.0 Conclusions and discussion

The results in Section 3 motivate several observations:

1. The combination of the proofs in Sections 3.1 and 3.2 constitutes a proof of the SoCT in an orthomodular lattice.

2. The proof in Section 3.3 shows that symmetry of commutativity in an ortholattice implies the OMA.

3. Sections 3.1, 3.2, and 3.3 collectively show that the axioms of an ortholattice, together with the SoCT, implies the OMA, and the axioms of an

orthomodular lattice imply the SoCT. This result is equivalent to one of the two principal propositions of the Foulis-Holland Theorem ([7], [8]). In this sense, the SoCT is equivalent to the OMA.

4. The proofs in Section 3 appear to be novel.

5.0 Acknowledgements

This work benefited from discussions with Tom Oberdan, Frank Pecchioni, Tony Pawlicki, and the late John K. Prentice, whose passion for foundations of physics inspired those of us privileged to have known him. For any infelicities that remain, I am solely responsible.

6.0 References

[1] von Neumann J. *Mathematical Foundations of Quantum Mechanics*. 1936. Translated by R. T. Beyer. Princeton. 1983.
[2] McCune WW. *prover9 and mace4.* URL http://www.cs.unm.edu/~mccune/prover9/. 2009.
[3] Horner JK. SoCT *prover9* scripts. 2011. Available from the author on request.
[4] Dalla Chiara ML and Giuntini R. *Quantum Logics*. URL http://xxx.lanl.gov/abs/quant-ph/0101028. 2004.
[5] Megill ND and Pavičić M. Orthomodular lattices and quantum algebra. *International Journal of Theoretical Physics* 40 (2001), pp. 1387-1410.
[6] Akhiezer NI and Glazman IM. *Theory of Linear Operators in Hilbert Space. Volume I*. Translated by M. Nestell. Frederick Ungar. 1961.
[7] Holland, Jr. SS Orthomodularity in infinite dimensions: a theorem of M. Solèr. *Bulletin of the American Mathematical Society* 32 (1995), pp. 205-234.
[8] Foulis DJ. A note on orthomodular lattices. *Portugaliae Mathematica* 21(1962), 65-72.
[9] Knuth DE and Bendix PB. Simple word problems in universal algebras. In J. Leech, ed. *Computational Problems in Abstract Algebra.* Pergamon Press. 1970. pp. 263-297.
[10] Chang CC and Keisler HJ. *Model Theory*. North-Holland. 1990. pp. 38-39.
[11] Birkhoff G. *Lattice Theory*. Third Edition. American Mathematical Society. 1967.
[12] Church A. *Introduction to Mathematical Logic. Volume I.* Princeton. 1956.
[13] Jauch J. *Foundations of Quantum Mechanics.* Addison-Wesley. 1968.
[14] Megill ND. *Metamath.* URL http://us.metamath.org/qlegif/mmql.html#unify. 2004.
[15] Horner JK. An automated deduction system for orthomodular lattice theory. *Proceedings of the 2005 International Conference on Artificial Intelligence*. CSREA Press. 2005. pp. 260-265.
[16] Horner JK. An automated equational logic deduction of join elimination in orthomodular lattice theory. *Proceedings of the 2007 International Conference on Artificial Intelligence*. CSREA Press. 2007. pp. 481-488.
[17] Messiah A. *Quantum Mechanics*. Dover. 1958.
[18] Horner JK. Using automated theorem-provers to aid the design of efficient compilers for quantum computing. *Los Alamos National Laboratory Quantum Institute Workshop*. December 9–10, 2002. URL http://www.lanl.gov/science/centers/quantum/qls_pdfs/horner.pdf.
[19] Birkhoff G and von Neumann J. The logic of quantum mechanics. *Annals of Mathematics* 37 (1936), 823-243.
[20] Nielsen MA and Chuang L . *Quantum Computation and Quantum Information*. Cambridge. 2000.
[21] Pavičić M and Megill N. Quantum and classical implicational algebras with primitive implication. *International Journal of Theoretical Physics* 37 (1998), 2091-2098. ftp://m3k.grad.hr/pavicic/quantum-logic/1998-int-j-theor-phys-2.ps.gz.
[22] Horner JK. An automated deduction of the relative strength of orthomodular and weakly orthomodular lattice theory. *Proceedings of the 2009 International Conference on Artificial Intelligence*. CSREA Press. 2009. pp. 525-530.

The Lattice-Order Strength of Relevance Implication in Quantum Logic: Part 1

Jack K. Horner
P. O. Box 266
Los Alamos, New Mexico 87544 USA
email: jhorner@cybermesa.com

Abstract

The optimization of quantum computing circuitry and compilers at some level must be expressed in terms of quantum-mechanical behaviors and operations. In much the same way that the structure of conventional propositional (Boolean) logic (BL) is the logic of the description of the behavior of classical physical systems and is isomorphic to a Boolean algebra (BA), so also the algebra, C(H), of closed linear subspaces of (equivalently, the system of linear operators on (observables in)) a Hilbert space is a logic of the descriptions of the behavior of quantum mechanical systems and is a model of an ortholattice (OL). An OL can thus be thought of as a kind of "quantum logic" (QL) In BL, there is only one implication connection; in QL, there are five, none of which are identical to implication in a BL. Here I present automated deductions showing that relevance implication is equal to less than (in the sense of the lattice partial ordering) Sasaki and Dishkant implication in a QL. The proofs may be novel, and both proofs, surprisingly, use the definition of implication in a BL.

Keywords: automated deduction, quantum computing, orthomodular lattice, Hilbert space

1.0 Introduction

The optimization of quantum computing circuitry and compilers at some level must be expressed in terms of the description of quantum-mechanical behaviors ([1], [17], [18], [20]). In much the same way that conventional propositional (Boolean) logic (BL,[12]) is the logical structure of description of the behavior of classical physical systems (e.g. "the measurements of the position and momentum of particle P are commutative", i.e., can be measured in either order, yielding the same results) and is isomorphic to a Boolean lattice ([10], [11], [19]), so also the algebra, *C(H)*, of the closed linear subspaces of (equivalently, the system of linear operators on (observables in)) a Hilbert space *H* ([1], [4], [6], [9], [13]) is *a* logic of the descriptions of the behavior of quantum mechanical systems (e.g., "the measurements of the position and momentum of particle P are *not* commutative") and is a model ([10]) of an ortholattice (OL; [4]). An OL can thus be thought of as a kind of "quantum logic" (QL; [19]). *C(H)* is also a model of (i.e., isomorphic to a set of sentences which hold in) an orthomodular lattice (OML; [4], [7]), which is an OL conjoined with the orthomodularity axiom (OMA). These axioms, and various definitions, are shown in Figure 1.

```
% Miscellaneous definitions
   1 = x v c(x)                                  # label("df-t").
   0 = c(1)                                      # label("df-f").
   (x ^ y) = c( c(x) v c(y))                     # label("df-a").
   le(x,y) <-> ( (x v y) = y )                   # label("df: x less than y").
   id(x,y) = (c(c(x) v c(y)) v c(x v y))    # label("df-b").
   C(x,y) <-> ( x = (  (x ^ y) v ( x ^ c(y))  ) )
                                                 # label("x commutes with y").


% Definitions of implications
   i0(x,y) = (c(x) v y)                          # label("df-i0 Boolean").

   i1(x,y) = ( c(x) v (x ^ y)  )                 # label("df-i1 Sasaki").

   i2(x,y) = ( y v (c(x) ^ c(y))  )              # label("df-i2 Dishkant").

   i3(x,y) = (((c(x) ^ y) v (c(x) ^ c(y))) v (x ^ (c(x) v y)))
                                                 # label("df-i3 Kalmbach").

   i4(x,y) =  (((x ^ y) v (c(x) ^ y)) v ((c(x) v y) ^ c(y)))
                                                 # label("df-i4 non-tollens").

   i5(x,y) = (((x ^ y) v (c(x) ^ y)) v (c(x) ^ c(y)))
                                                 # label("df-i5 relevance").


% Ortholattice axioms
x = c(c(x))                                      # label("ax-a1").
(x v y) = (y v x)                                # label("ax-a2").
((x v y) v z) = (x v (y v z))                    # label("ax-a3").
(x v (y v c(y))) = (y v c(y))                    # label("ax-a4").
(x v c((c(x) v y))) = x                          # label("ax-a5").
(x = y) -> (y = x)                               # label("ax-r1").
((x = y) & (y = z)) -> (x = z)                   # label("ax-r2").
(x = y) -> (c(x) = c(y))                         # label("ax-r4").
(x = y) -> ((x v z) = (y v z))                   # label("ax-r5").

% Orthomodular axiom
(  (z v c(z)) = (c(c(x) v c(y)) v c(x v y) )  )   -> (x = y)
                                                 # label("ax-r3").


where
   x, y, z are variables ranging over lattice nodes
   ^ is lattice meet
   v is lattice join
   c(x) is the orthocomplement of x
   le(x,y) means x ≤ y
   id(x,y) means x is quantum-logic identical to y
   <-> means if and only if
   =  is equivalence ([12])
   1 is the maximum lattice element (= x v c(x))
   0 is the minimum lattice element (= c(1))
```

Figure 1. Lattice, ortholattice, orthomodularity axioms, and some definitions.

The six implications shown in Figure 1 each satisfy the Birkhoff-von Neuman condition

$$((x \rightarrow_i y) = 1) \leftrightarrow \quad le(x,y) \qquad \text{(CBvN)}$$

```
where i = 0,1,2,3,4,5.
```

CBvN can be regarded a generalization of the BL definition of implication, sometimes denoted $\rightarrow_0$. CBvN maps implication onto the lattice partial-order.

2.0 Method

The QL axiomatizations of Megill, Pavičić, and Horner ([5], [14], [15], [16], [21], [22]) were implemented in a *prover9* ([2]) script ([3]) configured to show that relevance implication is less than or equal to (in the sense of the lattice partial ordering; [11], p.4) Sasaki ([8]) and Dishkant ([9]) implication, then executed in that framework on a Dell Inspiron 545 with an Intel Core2 Quad CPU Q8200 (clocked @ 2.33 GHz) and 8.00 GB RAM, running under the *Windows Vista Home Premium /Cygwin* operating environment.

3.0 Results

Figure 2 shows the proofs, generated by [3] on the platform described in Section 2.0, that relevance implication is equal to or less than Sasaki and Dishkant implication.

```
============================== PROOF =================================

% Proof 1 at 0.05 (+ 0.03) seconds: "i5lei1: Relevance implication l.e. Sasaki
implication".
% Length of proof is 24.
% Level of proof is 5.
% Maximum clause weight is 30.
% Given clauses 25.

1 le(x,y) <-> x v y = y # label("df: x less than y") # label(non_clause).  [assumption].
5 x = y & y = z -> x = z # label("ax-r2") # label(non_clause).  [assumption].
9 le(i5(x,y),i1(x,y)) # label("i5lei1: Relevance implication l.e. Sasaki implication") #
label(non_clause) # label(goal).  [goal].
16 x ^ y = c(c(x) v c(y)) # label("df-a").  [assumption].
18 le(x,y) | x v y != y # label("df: x less than y").  [clausify(1)].
20 i0(x,y) = c(x) v y # label("df-i0 Boolean").  [assumption].
21 i1(x,y) = c(x) v (x ^ y) # label("df-i1 Sasaki").  [assumption].
22 i1(x,y) = c(x) v c(c(x) v c(y)).  [copy(21),rewrite([16(3)])].
29 i5(x,y) = ((x ^ y) v (c(x) ^ y)) v (c(x) ^ c(y)) # label("df-i5 relevance").
[assumption].
30 i5(x,y) = (c(c(x) v c(y)) v c(c(c(x)) v c(y))) v c(c(c(x)) v c(c(y))).
[copy(29),rewrite([16(2),16(7),16(14)])].
31 x = c(c(x)) # label("ax-a1").  [assumption].
32 c(c(x)) = x.  [copy(31),flip(a)].
33 x v y = y v x # label("ax-a2").  [assumption].
34 (x v y) v z = x v (y v z) # label("ax-a3").  [assumption].
37 x v c(c(x) v y) = x # label("ax-a5").  [assumption].
38 x != y | z != x | z = y # label("ax-r2").  [clausify(5)].
43 -le(i5(c1,c2),i1(c1,c2)) # label("i5lei1: Relevance implication l.e. Sasaki
implication") # answer("i5lei1: Relevance implication l.e. Sasaki implication").
[deny(9)].
44 -le(c(c1 v c2) v (c(c1 v c(c2)) v c(c(c1) v c(c2))),c(c1) v c(c(c1) v c(c2))) #
answer("i5lei1: Relevance implication l.e. Sasaki implication").
[copy(43),rewrite([30(3),32(9),33(12),32(15),32(16),33(17),22(20)])].
58 x v (y v z) = y v (x v z).  [para(33(a,1),34(a,1,1)),rewrite([34(2)])].
66 c(x) v c(x v y) = c(x).  [para(37(a,1),20(a,2)),rewrite([32(2),20(3)])].
70 x v x = x.  [para(37(a,1),37(a,1,2,1)),rewrite([32(2)])].
81 c(c1) v (c(c1 v c2) v (c(c1 v c(c2)) v c(c(c1) v c(c2)))) != c(c1) v c(c(c1) v c(c2))
# answer("i5lei1: Relevance implication l.e. Sasaki implication").
[ur(18,a,44,a),rewrite([33(27),58(27),58(26),33(25),58(25),70(24),58(19),58(20)])].
```

```
85 c(c1) v (c(c1 v c(c2)) v c(c(c1) v c(c2))) != c(c1) v c(c(c1) v c(c2)) #
answer("i5lei1: Relevance implication l.e. Sasaki implication").
[ur(38,b,34,a(flip),c,81,a),rewrite([66(7)])].
87 $F # answer("i5lei1: Relevance implication l.e. Sasaki implication").
[ur(38,b,34,a(flip),c,85,a),rewrite([66(8)]),xx(a)].

============================== end of proof ==========================


============================== PROOF =================================

% Proof 1 at 0.08 (+ 0.05) seconds: "i5lei2: Relevance implication l.e. Dishkant
implication".
% Length of proof is 34.
% Level of proof is 7.
% Maximum clause weight is 69.
% Given clauses 65.

1 le(x,y) <-> x v y = y # label("df: x less than y") # label(non_clause).  [assumption].
8 z v c(z) = c(c(x) v c(y)) v c(x v y) -> x = y # label("ax-r3") # label(non_clause).
[assumption].
9 le(i5(x,y),i2(x,y)) # label("i5lei2: Relevance implication l.e. Dishkant implication")
# label(non_clause) # label(goal).  [goal].
12 1 = x v c(x) # label("df-t").  [assumption].
13 x v c(x) = 1.  [copy(12),flip(a)].
16 x ^ y = c(c(x) v c(y)) # label("df-a").  [assumption].
18 le(x,y) | x v y != y # label("df: x less than y").  [clausify(1)].
20 i0(x,y) = c(x) v y # label("df-i0 Boolean").  [assumption].
23 i2(x,y) = y v (c(x) ^ c(y)) # label("df-i2 Dishkant").  [assumption].
24 i2(x,y) = y v c(c(c(x)) v c(c(y))).  [copy(23),rewrite([16(4)])].
29 i5(x,y) = ((x ^ y) v (c(x) ^ y)) v (c(x) ^ c(y)) # label("df-i5 relevance").
[assumption].
30 i5(x,y) = (c(c(x) v c(y)) v c(c(c(x)) v c(y))) v c(c(c(x)) v c(c(y))).
[copy(29),rewrite([16(2),16(7),16(14)])].
31 x = c(c(x)) # label("ax-a1").  [assumption].
32 c(c(x)) = x.  [copy(31),flip(a)].
33 x v y = y v x # label("ax-a2").  [assumption].
34 (x v y) v z = x v (y v z) # label("ax-a3").  [assumption].
37 x v c(c(x) v y) = x # label("ax-a5").  [assumption].
41 c(c(x) v c(y)) v c(x v y) != z v c(z) | y = x # label("ax-r3").  [clausify(8)].
42 c(x v y) v c(c(x) v c(y)) != 1 | y = x.  [copy(41),rewrite([33(7),13(9)])].
43 -le(i5(c1,c2),i2(c1,c2)) # label("i5lei2: Relevance implication l.e. Dishkant
implication") # answer("i5lei2: Relevance implication l.e. Dishkant implication").
[deny(9)].
44 -le(c(c1 v c2) v (c(c1 v c(c2)) v c(c(c1) v c(c2))),c2 v c(c1 v c2)) # answer("i5lei2:
Relevance implication l.e. Dishkant implication").
[copy(43),rewrite([30(3),32(9),33(12),32(15),32(16),33(17),24(20),32(21),32(22)])].
54 x v (y v c(x v y)) = 1.  [para(34(a,1),13(a,1))].
58 x v (y v z) = y v (x v z).  [para(33(a,1),34(a,1,1)),rewrite([34(2)])].
66 c(x) v c(x v y) = c(x).  [para(37(a,1),20(a,2)),rewrite([32(2),20(3)])].
67 x v c(y v c(x)) = x.  [para(33(a,1),37(a,1,2,1))].
70 x v x = x.  [para(37(a,1),37(a,1,2,1)),rewrite([32(2)])].
81 c2 v (c(c1 v c2) v (c(c1 v c2) v (c(c1 v c(c2)) v c(c(c1) v c(c2))))) != c2 v c(c1 v
c2) # answer("i5lei2: Relevance implication l.e. Dishkant implication").
[ur(18,a,44,a),rewrite([33(24),58(24),34(23),58(24)])].
84 c(c2 v (c2 v (c(c1 v c2) v (c(c1 v c2) v (c(c1 v c2) v (c(c1 v c(c2)) v c(c(c1) v
c(c2)))))))) v c(c(c2 v c(c1 v c2)) v c(c2 v (c(c1 v c2) v (c(c1 v c2) v (c(c1 v c(c2)) v
c(c(c1) v c(c2))))))) != 1 # answer("i5lei2: Relevance implication l.e. Dishkant
implication").  [ur(42,b,81,a),rewrite([58(31),58(30),58(29),34(28),58(29),58(30)])].
111 x v (x v y) = x v y.  [para(70(a,1),34(a,1,1)),flip(a)].
113 c(c2 v (c(c1 v c2) v (c(c1 v c(c2)) v c(c(c1) v c(c2))))) v c(c(c2 v c(c1 v c2)) v
c(c2 v (c(c1 v c2) v (c(c1 v c(c2)) v c(c(c1) v c(c2)))))) != 1 # answer("i5lei2:
Relevance implication l.e. Dishkant implication").
[back_rewrite(84),rewrite([111(28),111(24),111(21),111(50)])].
197 x v (y v c(z v c(x))) = y v x.  [para(67(a,1),58(a,1,2)),flip(a)].
202 c(x v y) v c(x v (y v z)) = c(x v y).  [para(34(a,1),66(a,1,2,1))].
208 c2 v (c(c1 v c2) v c(c2 v (c(c1 v c2) v (c(c1 v c(c2)) v c(c(c1) v c(c2)))))) != 1 #
answer("i5lei2: Relevance implication l.e. Dishkant implication").
[back_rewrite(113),rewrite([202(48),32(28),33(27),34(27)])].
209 $F # answer("i5lei2: Relevance implication l.e. Dishkant implication").
[para(58(a,1),208(a,1,2,2,1)),rewrite([197(23),33(16),67(16),33(11),54(14)]),xx(a)].
```

```
============================== end of proof ==========================
```

Figure 2. Summary of a *prover9* ([2]) proofs showing that relevance implication is less than or equal to Sasaki and Dishkant implication. The proofs assume the default inference rules of *prover9*. The general form of a line in this proof is "*line_number conclusion [derivation]*", where *line_number* is a unique identifier of a line in the proof, and *conclusion* is the result of applying the *prover9* inference rules (such as *para*modulation, *copy*ing, and *rewrit*ing), noted in square brackets (denoting the *derivation*), to the lines cited in those brackets. Note that some of "logical" proof lines in the above have been transformed to two text lines, with the *derivation* appearing on a text line following a text line containing the first part of that logical line. The detailed syntax and semantics of these notations can be found in [2]. All *prover9* proofs are by default proofs by contradiction.

The total time to produce the proofs in Figure 2 on the platform described in Section 2.0 was approximately 0.2 seconds.

4.0 Discussion

The results of Section 3.0 motivate at least two observations:

1. Relevance implication is less than or equal to (in the sense of the lattice partial order) Sasaki and Dishkant implication.

2. Surprisingly, both the "Sasaki-, and Dishkant-, implication" proofs use the definition of implication in a Boolean logic.

3. The proofs do not use the orthomodularity axiom ("ax-r3" in Figure 1), demonstrating that the strength ordering shown in Figure 2 also holds in an ortholattice.

5.0 Acknowledgements

This work benefited from discussions with Tom Oberdan, Frank Pecchioni, Tony Pawlicki, and the late John K. Prentice, whose passion for foundations of physics inspired those of us privileged to have known him. For any infelicities that remain, I am solely responsible.

6.0 References

[1] von Neumann J. *Mathematical Foundations of Quantum Mechanics*. 1936. Translated by R. T. Beyer. Princeton. 1983.

[2] McCune WW. *prover9 and mace4.* URL http://www.cs.unm.edu/~mccune/prover9/. 2009.

[3] Horner JK. *prover9* scripts for deriving the strength of relevance implication. 2011. Available from the author on request.

[4] Dalla Chiara ML and Giuntini R. *Quantum Logics*. URL http://xxx.lanl.gov/abs/quant-ph/0101028. 2004.

[5] Megill ND and Pavičić M. Orthomodular lattices and quantum algebra. *International Journal of Theoretical Physics* 40 (2001), pp. 1387-1410.

[6] Akhiezer NI and Glazman IM. *Theory of Linear Operators in Hilbert Space. Volume I.* Translated by M. Nestell. Frederick Ungar. 1961.

[7] Holland, Jr. SS Orthomodularity in infinite dimensions: a theorem of M. Solèr. *Bulletin of the American Mathematical Society* 32 (1995), pp. 205-234.

[8] Dishkant H. The first order predicate calculus based on the minimal logic of quantum mechanics. *Rep. Math. Logic* 3 (1974), 9–18.

[9] Mittelstaedt P. *Quantum Logic*. Synthese Library; Vol. 18. Reidel, London. 1978.

[10] Chang CC and Keisler HJ. *Model Theory*. North-Holland. 1990. pp. 38-39.

[11] Birkhoff G. *Lattice Theory*. Third Edition. American Mathematical Society. 1967.

[12] Church A. *Introduction to Mathematical Logic. Volume I.* Princeton. 1956.

[13] Jauch J. *Foundations of Quantum Mechanics.* Addison-Wesley. 1968.

[14] Megill ND. *Metamath.* URL http://us.metamath.org/qlegif/mmql.html#unify. 2004.

[15] Horner JK. An automated deduction system for orthomodular lattice theory. *Proceedings of the 2005 International Conference on Artificial Intelligence.* CSREA Press. 2005. pp. 260-265.

[16] Horner JK. An automated equational logic deduction of join elimination in orthomodular lattice theory. *Proceedings of the 2007 International Conference on Artificial Intelligence.* CSREA Press. 2007. pp. 481-488.

[17] Messiah A. *Quantum Mechanics*. Dover. 1958.

[18] Horner JK. Using automated theorem-provers to aid the design of efficient compilers for quantum computing. *Los Alamos National Laboratory Quantum Institute Workshop.* December 9–10, 2002. URL http://www.lanl.gov/science/centers/quantum/qls_pdfs/horner.pdf.

[19] Birkhoff G and von Neumann J. The logic of quantum mechanics. *Annals of Mathematics* 37 (1936), 823-243.

[20] Nielsen MA and Chuang L . *Quantum Computation and Quantum Information*. Cambridge. 2000.

[21] Pavičić M and Megill N. Quantum and classical implicational algebras with primitive implication. *International Journal of Theoretical Physics* 37 (1998), 2091-2098. ftp://m3k.grad.hr/pavicic/quantum-logic/1998-int-j-theor-phys-2.ps.gz.

[22] Horner JK. An automated deduction of the relative strength of orthomodular and weakly orthomodular lattice theory. *Proceedings of the 2009 International Conference on Artificial Intelligence*. CSREA Press. 2009. pp. 525-530.

The Lattice-Order Strength of Relevance Implication in Quantum Logic: Part 2

Jack K. Horner
P. O. Box 266
Los Alamos, New Mexico 87544 USA
email: jhorner@cybermesa.com

Abstract

The optimization of quantum computing circuitry and compilers at some level must be expressed in terms of quantum-mechanical behaviors and operations. In much the same way that the structure of conventional propositional (Boolean) logic (BL) is the logic of the description of the behavior of classical physical systems and is isomorphic to a Boolean algebra (BA), so also the algebra, C(H), of closed linear subspaces of (equivalently, the system of linear operators on (observables in)) a Hilbert space is a logic of the descriptions of the behavior of quantum mechanical systems and is a model of an ortholattice (OL). An OL can thus be thought of as a kind of "quantum logic" (QL) In BL, there is only one implication connection; in QL, there are five, none of which are identical to implication in a BL. Here I present automated deductions showing that relevance implication is equal to less than (in the sense of the lattice partial order) Kalmbach and non-tollens implication in a QL. The proofs may be novel, and one of the proofs, surprisingly, uses the definition of implication in a BL.

Keywords: automated deduction, quantum computing, orthomodular lattice, Hilbert space

1.0 Introduction

The optimization of quantum computing circuitry and compilers at some level must be expressed in terms of the description of quantum-mechanical behaviors ([1], [17], [18], [20]). In much the same way that conventional propositional (Boolean) logic (BL,[12]) is the logical structure of description of the behavior of classical physical systems (e.g. "the measurements of the position and momentum of particle P are commutative", i.e., can be measured in either order, yielding the same results) and is isomorphic to a Boolean lattice ([10], [11], [19]), so also the algebra, *C(H)*, of the closed linear subspaces of (equivalently, the system of linear operators on (observables in)) a Hilbert space *H* ([1], [4], [6], [9], [13]) is *a* logic of the descriptions of the behavior of quantum mechanical systems (e.g., "the measurements of the position and momentum of particle P are *not* commutative") and is a model ([10]) of an ortholattice (OL; [4]). An OL can thus be thought of as a kind of "quantum logic" (QL; [19]). *C(H)* is also a model of (i.e., isomorphic to a set of sentences which hold in) an orthomodular lattice (OML; [4], [7]), which is an OL conjoined with the orthomodularity axiom (OMA). These axioms, and various definitions, are shown in Figure 1.

```
% Miscellaneous definitions
   1 = x v c(x)                                # label("df-t").
   0 = c(1)                                    # label("df-f").
   (x ^ y) = c( c(x) v c(y))                   # label("df-a").
   le(x,y) <-> ( (x v y) = y )                 # label("df: x less than y").
   id(x,y) = (c(c(x) v c(y)) v c(x v y))    # label("df-b").
   C(x,y) <-> ( x = (  (x ^ y) v ( x ^ c(y))  ) )
                                               # label("x commutes with y").


% Definitions of implications
   i0(x,y) = (c(x) v y)                        # label("df-i0 Boolean").

   i1(x,y) = ( c(x) v (x ^ y)  )               # label("df-i1 Sasaki").

   i2(x,y) = ( y v (c(x) ^ c(y))  )            # label("df-i2 Dishkant").

   i3(x,y) = (((c(x) ^ y) v (c(x) ^ c(y))) v (x ^ (c(x) v y)))
                                               # label("df-i3 Kalmbach").

   i4(x,y) =  (((x ^ y) v (c(x) ^ y)) v ((c(x) v y) ^ c(y)))
                                               # label("df-i4 non-tollens").

   i5(x,y) = (((x ^ y) v (c(x) ^ y)) v (c(x) ^ c(y)))
                                               # label("df-i5 relevance").


% Ortholattice axioms
x = c(c(x))                                    # label("ax-a1").
(x v y) = (y v x)                              # label("ax-a2").
((x v y) v z) = (x v (y v z))                  # label("ax-a3").
(x v (y v c(y))) = (y v c(y))                  # label("ax-a4").
(x v c((c(x) v y))) = x                        # label("ax-a5").
(x = y) -> (y = x)                             # label("ax-r1").
((x = y) & (y = z)) -> (x = z)                 # label("ax-r2").
(x = y) -> (c(x) = c(y))                       # label("ax-r4").
(x = y) -> ((x v z) = (y v z))                 # label("ax-r5").

% Orthomodular axiom
(  (z v c(z)) = (c(c(x) v c(y)) v c(x v y) )  )   -> (x = y)
                                               # label("ax-r3").


where
   x, y, z are variables ranging over lattice nodes
   ^ is lattice meet
   v is lattice join
   c(x) is the orthocomplement of x
   le(x,y) means x ≤ y
   id(x,y) means x is quantum-logic identical to y
   <-> means if and only if
   =  is equivalence ([12])
   1 is the maximum lattice element (= x v c(x))
   0 is the minimum lattice element (= c(1))
```

Figure 1. Lattice, ortholattice, orthomodularity axioms, and some definitions.

The six implications shown in Figure 1 each satisfy the Birkhoff-von Neumann condition

$$((x \rightarrow_i y) = 1) \quad <-> \quad le(x,y) \qquad \text{(CBvN)}$$

where i = 0,1,2,3,4,5.

CBvN is a generalization of the BL definition of implication, sometimes denoted $\rightarrow_0$. CBvN maps implication onto the lattice partial ordering.

2.0 Method

The QL axiomatizations of Megill, Pavičić, and Horner ([5], [14], [15], [16], [21], [22]) were implemented in a *prover9* ([2]) script ([3]) configured to show that relevance implication is less than or equal to (in the sense of the lattice partial ordering; [11]. p. 4) Kalmbach ([8]) and non-tollens ([9], p. 3) implication, then executed in that framework on a Dell Inspiron 545 with an Intel Core2 Quad CPU Q8200 (clocked @ 2.33 GHz) and 8.00 GB RAM, running under the *Windows Vista Home Premium /Cygwin* operating environment.

3.0 Results

Figure 2 shows the proofs, generated by [3] on the platform described in Section 2.0, that relevance implication is equal to or less than Kalmbach and non-tollens implication.

```
============================== PROOF =================================

% Proof 1 at 5.74 (+ 0.09) seconds: "i5lei3: Relevance implication l.e. Kalmbach
implication".
% Length of proof is 40.

1 le(x,y) <-> x v y = y # label("df: x less than y") # label(non_clause).  [assumption].
5 x = y & y = z -> x = z # label("ax-r2") # label(non_clause).  [assumption].
9 le(i5(x,y),i3(x,y)) # label("i5lei3: Relevance implication l.e. Kalmbach implication")
# label(non_clause) # label(goal).  [goal].
16 x ^ y = c(c(x) v c(y)) # label("df-a").  [assumption].
17 -le(x,y) | x v y = y # label("df: x less than y").  [clausify(1)].
18 le(x,y) | x v y != y # label("df: x less than y").  [clausify(1)].
20 i0(x,y) = c(x) v y # label("df-i0 Boolean").  [assumption].
25 i3(x,y) = ((c(x) ^ y) v (c(x) ^ c(y))) v (x ^ (c(x) v y)) # label("df-i3 Kalmbach").
[assumption].
26 i3(x,y) = (c(c(c(x)) v c(y)) v c(c(c(x)) v c(c(y)))) v c(c(x) v c(c(x) v y)).
[copy(25),rewrite([16(3),16(9),16(16)])].
29 i5(x,y) = ((x ^ y) v (c(x) ^ y)) v (c(x) ^ c(y)) # label("df-i5 relevance").
[assumption].
30 i5(x,y) = (c(c(x) v c(y)) v c(c(c(x)) v c(y))) v c(c(c(x)) v c(c(y))).
[copy(29),rewrite([16(2),16(7),16(14)])].
31 x = c(c(x)) # label("ax-a1").  [assumption].
32 c(c(x)) = x.  [copy(31),flip(a)].
33 x v y = y v x # label("ax-a2").  [assumption].
34 (x v y) v z = x v (y v z) # label("ax-a3").  [assumption].
37 x v c(c(x) v y) = x # label("ax-a5").  [assumption].
38 x != y | z != x | z = y # label("ax-r2").  [clausify(5)].
43 -le(i5(c1,c2),i3(c1,c2)) # label("i5lei3: Relevance implication l.e. Kalmbach
implication") # answer("i5lei3: Relevance implication l.e. Kalmbach implication").
[deny(9)].
44 -le(c(c1 v c2) v (c(c1 v c(c2)) v c(c(c1) v c(c2))),c(c1 v c2) v (c(c1 v c(c2)) v
c(c(c1) v c(c2 v c(c1))))) # answer("i5lei3: Relevance implication l.e. Kalmbach
implication").
[copy(43),rewrite([30(3),32(9),33(12),32(15),32(16),33(17),26(20),32(20),32(25),32(26),33
(27),33(33),34(37)])].
53 le(x,y) | y v x != y.  [para(33(a,1),18(b,1))].
58 x v (y v z) = y v (x v z).  [para(33(a,1),34(a,1,1)),rewrite([34(2)])].
66 c(x) v c(x v y) = c(x).  [para(37(a,1),20(a,2)),rewrite([32(2),20(3)])].
```

```
68 x v (c(c(x) v y) v z) = x v z.  [para(37(a,1),34(a,1,1)),flip(a)].
70 x v x = x.  [para(37(a,1),37(a,1,2,1)),rewrite([32(2)])].
81 c(c1 v c2) v (c(c1 v c2) v (c(c1 v c(c2)) v (c(c1 v c(c2)) v (c(c(c1) v c(c2)) v
c(c(c1) v c(c2 v c(c1)))))) != c(c1 v c2) v (c(c1 v c(c2)) v c(c(c1) v c(c2 v c(c1)))) #
answer("i5lei3: Relevance implication l.e. Kalmbach implication").
[ur(18,a,44,a),rewrite([58(38),58(37),34(36),34(35),58(37)])].
84 c(c1 v c2) v (c(c1 v c(c2)) v (c(c1 v c(c2)) v (c(c(c1) v c(c2)) v c(c(c1) v c(c2 v
c(c1)))))) != c(c1 v c2) v (c(c1 v c(c2)) v c(c(c1) v c(c2 v c(c1)))) # answer("i5lei3:
Relevance implication l.e. Kalmbach implication").
[ur(38,b,34,a(flip),c,81,a),rewrite([70(9)])].
103 le(c(c(x) v y),x).  [hyper(53,b,37,a)].
108 x v (x v y) = x v y.  [para(70(a,1),34(a,1,1)),flip(a)].
110 c(c1 v c2) v (c(c1 v c(c2)) v (c(c(c1) v c(c2)) v c(c(c1) v c(c2 v c(c1))))) != c(c1
v c2) v (c(c1 v c(c2)) v c(c(c1) v c(c2 v c(c1)))) # answer("i5lei3: Relevance
implication l.e. Kalmbach implication").  [back_rewrite(84),rewrite([108(32)])].
129 le(c(x v y),c(x)).  [para(32(a,1),103(a,1,1,1))].
131 le(c(x v y),c(y)).  [para(33(a,1),129(a,1,1))].
146 c(x) v c(y v x) = c(x).  [hyper(17,a,131,a),rewrite([33(4)])].
202 c(x) v (y v c(x v z)) = y v c(x).  [para(66(a,1),58(a,1,2)),flip(a)].
220 c(c1 v c2) v (c(c1 v c(c2)) v (c(c(c1) v c(c2)) v c(c(c1) v c(c2 v c(c1))))) != c(c1
v c2) v (c(c1 v (c2 v x)) v (c(c1 v c(c2)) v c(c(c1) v c(c2 v c(c1))))) # answer("i5lei3:
Relevance implication l.e. Kalmbach implication").
[ur(38,a,68,a,c,110,a),rewrite([32(36),34(35)])].
236 c(c1 v c2) v (c(c1 v c(c2)) v (c(c(c1) v c(c2)) v c(c(c1) v c(c2 v c(c1))))) != c(c1
v c2) v (c(c1 v (x v c2)) v (c(c1 v c(c2)) v c(c(c1) v c(c2 v c(c1))))) # answer("i5lei3:
Relevance implication l.e. Kalmbach implication").  [para(33(a,1),220(a,2,2,1,1,2))].
247 c(c1 v c2) v (c(c1 v c(c2)) v (c(c(c1) v c(c2 v c(c1))) v c(c1 v (x v c2)))) != c(c1
v c2) v (c(c1 v c(c2)) v (c(c(c1) v c(c2)) v c(c(c1) v c(c2 v c(c1))))) # answer("i5lei3:
Relevance implication l.e. Kalmbach implication").
[para(33(a,1),236(a,2,2)),rewrite([34(52)]),flip(a)].
360 c(c1 v c2) v (c(c1 v c(c2)) v (c(c(c1) v c(c2 v c(c1))) v c(x v (c1 v c2)))) != c(c1
v c2) v (c(c1 v c(c2)) v (c(c(c1) v c(c2)) v c(c(c1) v c(c2 v c(c1))))) # answer("i5lei3:
Relevance implication l.e. Kalmbach implication").  [para(58(a,1),247(a,1,2,2,2,1))].
423 c(c1 v c2) v (c(c1 v c(c2)) v (c(c(c1) v c(c2 v c(c1))) v c(x v (y v (c1 v c2))))) !=
c(c1 v c2) v (c(c1 v c(c2)) v (c(c(c1) v c(c2)) v c(c(c1) v c(c2 v c(c1))))) #
answer("i5lei3: Relevance implication l.e. Kalmbach implication").
[para(34(a,1),360(a,1,2,2,2,1))].
3874 c(x v c(y)) v c(x v c(y v z)) = c(x v c(y v z)).
[para(202(a,1),146(a,1,2,1)),rewrite([33(8)])].
3877 $F # answer("i5lei3: Relevance implication l.e. Kalmbach implication").
[para(202(a,1),423(a,1,2)),rewrite([33(19),3874(45)]),xx(a)].

============================== end of proof ==========================


============================== PROOF =================================

% Proof 1 at 14.10 (+ 0.11) seconds: "i5lei4: Relevance implication l.e. non-tollens
implication".
% Length of proof is 51.

1 le(x,y) <-> x v y = y # label("df: x less than y") # label(non_clause).  [assumption].
5 x = y & y = z -> x = z # label("ax-r2") # label(non_clause).  [assumption].
9 le(i5(x,y),i4(x,y)) # label("i5lei4: Relevance implication l.e. non-tollens
implication") # label(non_clause) # label(goal).  [goal].
12 1 = x v c(x) # label("df-t").  [assumption].
13 x v c(x) = 1.  [copy(12),flip(a)].
14 0 = c(1) # label("df-f").  [assumption].
15 c(1) = 0.  [copy(14),flip(a)].
16 x ^ y = c(c(x) v c(y)) # label("df-a").  [assumption].
17 -le(x,y) | x v y = y # label("df: x less than y").  [clausify(1)].
18 le(x,y) | x v y != y # label("df: x less than y").  [clausify(1)].
27 i4(x,y) = ((x ^ y) v (c(x) ^ y)) v ((c(x) v y) ^ c(y)) # label("df-i4 non-tollens").
[assumption].
28 i4(x,y) = (c(c(x) v c(y)) v c(c(c(x)) v c(y))) v c(c(c(x) v y) v c(c(y))).
[copy(27),rewrite([16(2),16(7),16(15)])].
29 i5(x,y) = ((x ^ y) v (c(x) ^ y)) v (c(x) ^ c(y)) # label("df-i5 relevance").
[assumption].
30 i5(x,y) = (c(c(x) v c(y)) v c(c(c(x)) v c(y))) v c(c(c(x)) v c(c(y))).
[copy(29),rewrite([16(2),16(7),16(14)])].
31 x = c(c(x)) # label("ax-a1").  [assumption].
```

```
32 c(c(x)) = x.  [copy(31),flip(a)].
33 x v y = y v x # label("ax-a2").  [assumption].
34 (x v y) v z = x v (y v z) # label("ax-a3").  [assumption].
35 x v (y v c(y)) = y v c(y) # label("ax-a4").  [assumption].
36 x v 1 = 1.  [copy(35),rewrite([13(2),13(4)])].
37 x v c(c(x) v y) = x # label("ax-a5").  [assumption].
38 x != y | z != x | z = y # label("ax-r2").  [clausify(5)].
43 -le(i5(c1,c2),i4(c1,c2)) # label("i5lei4: Relevance implication l.e. non-tollens
implication") # answer("i5lei4: Relevance implication l.e. non-tollens implication").
[deny(9)].
44 -le(c(c1 v c2) v (c(c1 v c(c2)) v c(c(c1) v c(c2))),c(c1 v c(c2)) v (c(c(c1) v c(c2))
v c(c2 v c(c2 v c(c1))))) # answer("i5lei4: Relevance implication l.e. non-tollens
implication").
[copy(43),rewrite([30(3),32(9),33(12),32(15),32(16),33(17),28(20),32(26),33(29),33(33),32
(37),33(36),34(38)])].
53 le(x,y) | y v x != y.  [para(33(a,1),18(b,1))].
58 x v (y v z) = y v (x v z).  [para(33(a,1),34(a,1,1)),rewrite([34(2)])].
61 1 v x = 1.  [para(36(a,1),33(a,1)),flip(a)].
63 x v 0 = x.  [para(13(a,1),37(a,1,2,1)),rewrite([15(2)])].
67 x v c(y v c(x)) = x.  [para(33(a,1),37(a,1,2,1))].
68 x v (c(c(x) v y) v z) = x v z.  [para(37(a,1),34(a,1,1)),flip(a)].
69 x v (y v c(c(x v y) v z)) = x v y.  [para(37(a,1),34(a,1)),flip(a)].
70 x v x = x.  [para(37(a,1),37(a,1,2,1)),rewrite([32(2)])].
81 c(c1 v c2) v (c(c1 v c(c2)) v (c(c1 v c(c2)) v (c(c(c1) v c(c2)) v (c(c(c1) v c(c2)) v
c(c2 v c(c2 v c(c1)))))) != c(c1 v c(c2)) v (c(c(c1) v c(c2)) v c(c2 v c(c2 v c(c1)))) #
answer("i5lei4: Relevance implication l.e. non-tollens implication").
[ur(18,a,44,a),rewrite([58(39),58(38),34(37),34(36),58(38),58(37),58(39)])].
97 0 v x = x.  [hyper(38,a,63,a,b,33,a)].
102 le(c(c(x) v y),x).  [hyper(53,b,37,a)].
107 x v (x v y) = x v y.  [para(70(a,1),34(a,1,1)),flip(a)].
109 c(c1 v c2) v (c(c1 v c(c2)) v (c(c(c1) v c(c2)) v c(c2 v c(c2 v c(c1))))) != c(c1 v
c(c2)) v (c(c(c1) v c(c2)) v c(c2 v c(c2 v c(c1)))) # answer("i5lei4: Relevance
implication l.e. non-tollens implication").
[back_rewrite(81),rewrite([107(36),107(31)])].
129 le(c(x v y),c(x)).  [para(32(a,1),102(a,1,1,1))].
131 le(c(x v y),c(y)).  [para(33(a,1),129(a,1,1))].
148 le(c(x v (y v z)),c(x v z)).  [para(58(a,1),131(a,1,1))].
190 x v (c(y v c(x)) v z) = x v z.  [para(67(a,1),34(a,1,1)),flip(a)].
223 c(c1 v c2) v (c(c1 v (c2 v x)) v (c(c1 v c(c2)) v (c(c(c1) v c(c2)) v c(c2 v c(c2 v
c(c1)))))) != c(c1 v c(c2)) v (c(c(c1) v c(c2)) v c(c2 v c(c2 v c(c1)))) #
answer("i5lei4: Relevance implication l.e. non-tollens implication").
[ur(38,a,68,a,c,109,a(flip)),rewrite([32(30),34(29)]),flip(a)].
239 c(c1 v c2) v (c(c1 v (x v c2)) v (c(c1 v c(c2)) v (c(c(c1) v c(c2)) v c(c2 v c(c2 v
c(c1)))))) != c(c1 v c(c2)) v (c(c(c1) v c(c2)) v c(c2 v c(c2 v c(c1)))) #
answer("i5lei4: Relevance implication l.e. non-tollens implication").
[para(33(a,1),223(a,1,2,1,1,2))].
246 c(c1 v c2) v (c(c1 v c(c2)) v (c(c(c1) v c(c2)) v (c(c2 v c(c2 v c(c1))) v c(c1 v (x
v c2))))) != c(c1 v c(c2)) v (c(c(c1) v c(c2)) v c(c2 v c(c2 v c(c1)))) # answer("i5lei4:
Relevance implication l.e. non-tollens implication").
[para(33(a,1),239(a,1,2)),rewrite([34(31),34(30)])].
274 x v (y v (z v c(c(x v (y v z)) v u))) = y v (x v z).
[hyper(38,a,58,a,b,69,a),rewrite([34(7)])].
295 c(c1 v c2) v (c(c1 v c(c2)) v (c(c(c1) v c(c2)) v (c(c2 v c(c2 v c(c1))) v (c(c1 v (x
v c2)) v c(c(c(c1 v c2) v (c(c1 v c(c2)) v (c(c(c1) v c(c2)) v (c(c2 v c(c2 v c(c1))) v
c(c1 v (x v c2)))))) v y))))) != c(c1 v c(c2)) v (c(c(c1) v c(c2)) v c(c2 v c(c2 v
c(c1)))) # answer("i5lei4: Relevance implication l.e. non-tollens implication").
[ur(38,b,69,a(flip),c,246,a),rewrite([34(67),34(66),34(65)])].
799 le(c(x v (y v z)),c(z v y)).  [para(33(a,1),148(a,1,1)),rewrite([34(2)])].
2406 le(c(x v y),c(y v c(z v c(x)))).  [para(190(a,1),799(a,1,1))].
6267 x v (y v (z v (u v c(c(x v (y v (z v u))) v w)))) = y v (z v (x v u)).
[hyper(38,a,34,a,b,274,a),rewrite([34(3),34(9)])].
9918 c(x v y) v c(y v c(z v c(x))) = c(y v c(z v c(x))).  [hyper(17,a,2406,a)].
9952 $F # answer("i5lei4: Relevance implication l.e. non-tollens implication").
[para(61(a,1),295(a,1,2,2,2,2,1,1,2)),rewrite([33(26),61(26),15(25),61(51),33(50),61(50),
15(49),33(49),97(49),97(54),6267(56),9918(24)]),xx(a)].

============================== end of proof ==========================
```

Figure 2. Summary of a *prover9* ([2]) proofs showing that relevance implication is less than or equal to Kalmbach and non-tollens implication. The proofs assume the default inference rules of *prover9*. The general form of a line in this proof is "*line_number conclusion [derivation]*", where *line_number* is a unique identifier of a line in the proof, and *conclusion* is the result of applying the *prover9* inference rules (such as *para*modulation, *copy*ing, and *rewrit*ing), noted in square brackets (denoting the *derivation*), to the lines cited in those brackets. Note that some of "logical" proof lines in the above have been transformed to two text lines, with the *derivation* appearing on a text line following a text line containing the first part of that logical line. The detailed syntax and semantics of these notations can be found in [2]. All *prover9* proofs are by default proofs by contradiction.

The total time to produce the proofs in Figure 2 on the platform described in Section 2.0 was approximately 6 seconds.

4.0 Discussion

The results of Section 3.0 motivate at least three observations:

1. Relevance implication is equal to or less than (in the sense of the lattice partial order) Kalmbach and non-tollens implication.

2. Somewhat unexpectedly, the "Kalmbach-implication" proof uses the definition of implication in a Boolean logic.

3. The proofs do not use the orthomodularity axiom ("ax-r3" in Figure 1), demonstrating that the implicational strength relations shown in Figure 2 also hold in an ortholattice.

5.0 Acknowledgements

This work benefited from discussions with Tom Oberdan, Frank Pecchioni, Tony Pawlicki, and the late John K. Prentice, whose passion for foundations of physics inspired those of us privileged to have known him. For any infelicities that remain, I am solely responsible.

6.0 References

[1] von Neumann J. *Mathematical Foundations of Quantum Mechanics*. 1936. Translated by R. T. Beyer. Princeton. 1983.
[2] McCune WW. *prover9 and mace4.* URL http://www.cs.unm.edu/~mccune/prover9/. 2009.
[3] Horner JK. *prover9* scripts for deriving the strength of relevance implication. 2011. Available from the author on request.
[4] Dalla Chiara ML and Giuntini R. *Quantum Logics*. URL http://xxx.lanl.gov/abs/quant-ph/0101028. 2004.
[5] Megill ND and Pavičić M. Orthomodular lattices and quantum algebra. *International Journal of Theoretical Physics* 40 (2001), pp. 1387-1410.
[6] Akhiezer NI and Glazman IM. *Theory of Linear Operators in Hilbert Space. Volume I.* Translated by M. Nestell. Frederick Ungar. 1961.
[7] Holland, Jr. SS Orthomodularity in infinite dimensions: a theorem of M. Solèr. *Bulletin of the American Mathematical Society* 32 (1995), pp. 205-234.
[8] Kalmbach K. *Orthomodular Lattices*. Academic Press, London. 1983.
[9] Pavičić M and Megill N. Is quantum logic a logic? 2008. http://arxiv.org/abs/0812.2698.
[10] Chang CC and Keisler HJ. *Model Theory*. North-Holland. 1990. pp. 38-39.

[11] Birkhoff G. *Lattice Theory*. Third Edition. American Mathematical Society. 1967.
[12] Church A. *Introduction to Mathematical Logic. Volume I.* Princeton. 1956.
[13] Jauch J. *Foundations of Quantum Mechanics.* Addison-Wesley. 1968.
[14] Megill ND. *Metamath.* URL http://us.metamath.org/qlegif/mmql.html#unify. 2004.
[15] Horner JK. An automated deduction system for orthomodular lattice theory. *Proceedings of the 2005 International Conference on Artificial Intelligence.* CSREA Press. 2005. pp. 260-265.
[16] Horner JK. An automated equational logic deduction of join elimination in orthomodular lattice theory. *Proceedings of the 2007 International Conference on Artificial Intelligence.* CSREA Press. 2007. pp. 481-488.
[17] Messiah A. *Quantum Mechanics*. Dover. 1958.
[18] Horner JK. Using automated theorem-provers to aid the design of efficient compilers for quantum computing. *Los Alamos National Laboratory Quantum Institute Workshop.* December 9–10, 2002. URL http://www.lanl.gov/science/centers/quantum/qls_pdfs/horner.pdf.
[19] Birkhoff G and von Neumann J. The logic of quantum mechanics. *Annals of Mathematics* 37 (1936), 823-243.
[20] Nielsen MA and Chuang L . *Quantum Computation and Quantum Information*. Cambridge. 2000.
[21] Pavičić M and Megill N. Quantum and classical implicational algebras with primitive implication. *International Journal of Theoretical Physics* 37 (1998), 2091-2098. ftp://m3k.grad.hr/pavicic/quantum-logic/1998-int-j-theor-phys-2.ps.gz.
[22] Horner JK. An automated deduction of the relative strength of orthomodular and weakly orthomodular lattice theory. *Proceedings of the 2009 International Conference on Artificial Intelligence*. CSREA Press. 2009. pp. 525-530.

Quantum-Implication-Based Equivalents of the Orthomodularity Law in Quantum Logic: Part 1

Jack K. Horner
P. O. Box 266
Los Alamos, New Mexico 87544 USA
email: jhorner@cybermesa.com

Abstract

The optimization of quantum computing circuitry and compilers at some level must be expressed in terms of quantum-mechanical behaviors and operations. In much the same way that the structure of conventional propositional (Boolean) logic (BL) is the logic of the description of the behavior of classical physical systems and is isomorphic to a Boolean algebra (BA), so also the algebra, C(H), of closed linear subspaces of (equivalently, the system of linear operators on (observables in)) a Hilbert space is a logic of the descriptions of the behavior of quantum mechanical systems and is a model of an ortholattice (OL). An OL can thus be thought of as a kind of "quantum logic" (QL). C(H) is also a model of an orthomodular lattice, which is an OL conjoined with the orthomodularity axiom (OMA). The rationalization of the OMA as a claim proper to physics has proven problematic, motivating the question of whether the OMA and its equivalents are required in an adequate characterization of QL. Here I provide automated deductions of the OMA from three quantum-implication-based equivalents of the OMA. The proofs may be novel.

Keywords: automated deduction, quantum computing, orthomodular lattice, Hilbert space

1.0 Introduction

The optimization of quantum computing circuitry and compilers at some level must be expressed in terms of the description of quantum-mechanical behaviors ([1], [17], [18], [20]). In much the same way that conventional propositional (Boolean) logic (BL,[12]) is the logical structure of description of the behavior of classical physical systems (e.g. "the measurements of the position and momentum of particle P are commutative", i.e., can be measured in either order, yielding the same results) and is isomorphic to a Boolean lattice ([10], [11], [19]), so also the algebra, *C(H)*, of the closed linear subspaces of (equivalently, the system of linear operators on (observables in)) a Hilbert space *H* ([1], [4], [6], [9], [13]) is *a* logic of the descriptions of the behavior of quantum mechanical systems (e.g., "the measurements of the position and momentum of particle P are *not* commutative") and is a model ([10]) of an ortholattice (OL; [4]). An OL can thus be thought of as a kind of "quantum logic" (QL; [19]). *C(H)* is also a model of (i.e., isomorphic to a set of sentences which hold in) an orthomodular lattice (OML; [4], [7]), which is an OL conjoined with the orthomodularity axiom (OMA; see Figure 1). The rationalization of the OMA as a claim proper to physics has proven problematic ([13], Section 5-6), motivating the question of whether the OMA is required in an adequate characterization of QL. Thus formulated, the question suggests that the OMA and its equivalents are specific to an OML, and that as a consequence, banning the OMA from QL yields a "truer" quantum logic. The OMA, it turns out, has strong

connections to implication in QL, as demonstrated in the following.

Lattice axioms

```
      x = c(c(x))                       (AxLat1)
      x v y = y v x                     (AxLat2)
      (x v y) v z = x v (y v z)          (AxLat3)
      (x ^ y) ^ z = x ^ (y ^ z)          (AxLat4)
      x v (x ^ y) = x                   (AxLat5)
      x ^ (x v y) = x                   (AxLat6)
```

Ortholattice axioms

```
      c(x) ^ x = 0                      (AxOL1)
      c(x) v x = 1                      (AxOL2)
      x ^ y = c(c(x) v c(y))            (AxOL3)
```

Orthomodularity axiom

```
      y v (c(y) ^ (x v y)) = x v y      (OMA)
```

Definitions of implications and partial order

```
   i1(x,y) = c(x) v (x ^ y).
   i2(x,y) = i1(c(y), c(x).
   i3(x,y) = (c(x) ^ y) v (c(x) ^ c(y)) v i1(x,y).
   i4(x,y) = i3(c(y), c(x)).
   i5(x,y) = (x ^ y) v (c(x) ^ y) v (c(x) ^ c(y)).
   le(x,y) = (x = (x ^ y)).
```

where
- x, y are variables ranging over lattice nodes
- ^ is lattice meet
- v is lattice join
- c(x) is the orthocomplement of x
- $i1(x,y)$ means $x \rightarrow_1 y$ (Sasaki implication)
- $i2(x,y)$ means $x \rightarrow_2 y$ (Dishkant implication)
- $i3(x,y)$ means $x \rightarrow_3 y$ (Kalmbach implication)
- $i4(x,y)$ means $x \rightarrow_4 y$ (non-tollens implication)
- $i5(x,y)$ means $x \rightarrow_5 y$ (relevance implication)
- le(x,y) means $x \leq y$
- <-> means if and only if
- = is equivalence ([12])
- 1 is the maximum lattice element (= x v c(x))
- 0 is the minimum lattice element (= c(1))

Figure 1. Lattice, ortholattice, orthomodularity axioms, and some definitions.

Consider the proposition shown in Figure 2.

$$((x \rightarrow_i y) = 1) \quad <-> \quad le(x,y)$$

where $i = 1,2,3,4,5$.

Figure 2. Proposition 2.10

Note that there are five QL implications. Proposition 2.10 is a generalization of the BL definition of implication, sometimes denoted $\rightarrow_0$.

2.0 Method

The OML axiomatizations of Megill, Pavičić, and Horner ([5], [14], [15], [16], [21], [22]) were implemented in a *prover9* ([2]) script ([3]) configured to derive OMA from Proposition 2.10i, for each of i = 1, 2, 3 together with ortholattice theory (orthomodular lattice theory, without the OMA), then executed in that framework on a Dell Inspiron 545 with an Intel Core2 Quad CPU Q8200 (clocked @ 2.33 GHz) and 8.00 GB RAM, running under the *Windows Vista Home Premium /Cygwin* operating environment.

3.0 Results

Figure 3 shows the proofs, generated by [3] on the platform described in Section 2.0, that Proposition 2.10i (for each of i = 1,2, 3), together with ortholattice theory, imply the OMA.

```
============================== PROOF =================================

% Proof 1 at 32.98 (+ 0.64) seconds: "OMA".
% Length of proof is 34.
% Level of proof is 10.

1 le(x,y) <-> x = x ^ y # label("Df: less than") # label(non_clause).  [assumption].
3 i1(x,y) = 1 <-> le(x,y) # label("Hypothesis for Proposition 2.10i1") #
label(non_clause).  [assumption].
4 y v (c(y) ^ (x v y)) = x v y # label("OMA") # label(non_clause) # label(goal).  [goal].
6 -le(x,y) | x ^ y = x # label("Df: less than").  [clausify(1)].
7 i1(x,y) != 1 | le(x,y) # label("Hypothesis for Proposition 2.10i1").  [clausify(3)].
11 x = c(c(x)) # label("AxL1").  [assumption].
12 c(c(x)) = x.  [copy(11),flip(a)].
13 x v y = y v x # label("AxL2").  [assumption].
14 (x v y) v z = x v (y v z) # label("AxL3").  [assumption].
16 x v (x ^ y) = x # label("AxL5").  [assumption].
19 c(x) v x = 1 # label("AxOL2").  [assumption].
20 x v c(x) = 1.  [copy(19),rewrite([13(2)])].
21 x ^ y = c(c(x) v c(y)) # label("AxOL3").  [assumption].
23 i1(x,y) = c(x) v (x ^ y) # label("Df: i1").  [assumption].
24 i1(x,y) = c(x) v c(c(x) v c(y)).  [copy(23),rewrite([21(3)])].
33 c1 v (c(c1) ^ (c2 v c1)) != c2 v c1 # label("OMA") # answer("OMA").  [deny(4)].
34 c1 v c(c1 v c(c1 v c2)) != c1 v c2 # answer("OMA").
[copy(33),rewrite([13(6),21(7),12(4),13(12)])].
35 i1(x,y) != 1 | x ^ y = x.  [resolve(7,b,6,a)].
36 c(x) v c(c(x) v c(y)) != 1 | c(c(x) v c(y)) = x.  [copy(35),rewrite([24(1),21(9)])].
41 x v c(c(x) v c(y)) = x.  [back_rewrite(16),rewrite([21(1)])].
43 x v (y v z) = y v (x v z).  [para(13(a,1),14(a,1,1)),rewrite([14(2)])].
46 x v (y v c(x v y)) = 1.  [para(20(a,1),14(a,1)),flip(a)].
48 c(x) v c(c(x) v y) != 1 | c(c(x) v y) = x.
[para(12(a,1),36(a,1,2,1,2)),rewrite([12(10)])].
65 x v c(c(x) v y) = x.  [para(12(a,1),41(a,1,2,1,2))].
81 x v (y v c(y v x)) = 1.  [para(13(a,1),46(a,1,2,2,1))].
96 x v c(y v c(x)) = x.  [para(13(a,1),65(a,1,2,1))].
98 x v (y v c(c(x v y) v z)) = x v y.  [para(65(a,1),14(a,1)),flip(a)].
105 c(x) v c(y v x) = c(x).  [para(12(a,1),96(a,1,2,1,2))].
110 c(x) v c(y v c(x)) != 1 | c(c(x) v y) = x.  [para(13(a,1),48(a,1,2,1))].
400 x v c(y v x) != 1 | y v x = x.
[para(105(a,1),110(a,1,2,1)),rewrite([12(4),13(3),13(9),105(9),12(7)]),flip(b)].
417 x v (c(y v x) v c(c(y v x) v z)) != 1 | x v c(c(y v x) v z) = y v x.
[para(98(a,1),400(a,1,2,1)),rewrite([13(8),43(8),98(16)]),flip(b)].
18101 x v c(x v c(y v x)) = y v x.  [hyper(417,a,81,a),rewrite([13(3)])].
18102 x v c(x v c(x v y)) = y v x.  [para(13(a,1),18101(a,1,2,1,2,1))].
```

```
18181 $F # answer("OMA").  [back_rewrite(34),rewrite([18102(9),13(3)]),xx(a)].

============================== end of proof ==========================


============================== PROOF =================================

% Proof 1 at 148.81 (+ 2.84) seconds: "OMA".
% Length of proof is 51.
% Level of proof is 14.

1 le(x,y) <-> x = x ^ y # label("Df: less than") # label(non_clause).  [assumption].
3 i2(x,y) = 1 <-> le(x,y) # label("Hypothesis for Proposition 2.10i2") #
label(non_clause).  [assumption].
4 y v (c(y) ^ (x v y)) = x v y # label("OMA") # label(non_clause) # label(goal).  [goal].
6 -le(x,y) | x ^ y = x # label("Df: less than").  [clausify(1)].
7 i2(x,y) != 1 | le(x,y) # label("Hypothesis for Proposition 2.10i2").  [clausify(3)].
11 x = c(c(x)) # label("AxL1").  [assumption].
12 c(c(x)) = x.  [copy(11),flip(a)].
13 x v y = y v x # label("AxL2").  [assumption].
14 (x v y) v z = x v (y v z) # label("AxL3").  [assumption].
16 x v (x ^ y) = x # label("AxL5").  [assumption].
17 x ^ (x v y) = x # label("AxL6").  [assumption].
18 c(x) ^ x = 0 # label("AxOL1").  [assumption].
19 c(x) v x = 1 # label("AxOL2").  [assumption].
20 x v c(x) = 1.  [copy(19),rewrite([13(2)])].
21 x ^ y = c(c(x) v c(y)) # label("AxOL3").  [assumption].
25 i2(x,y) = c(c(y)) v (c(y) ^ c(x)) # label("Df: i2").  [assumption].
26 i2(x,y) = y v c(y v x).  [copy(25),rewrite([12(3),21(4),12(3),12(3)])].
33 c1 v (c(c1) ^ (c2 v c1)) != c2 v c1 # label("OMA") # answer("OMA").  [deny(4)].
34 c1 v c(c1 v c(c1 v c2)) != c1 v c2 # answer("OMA").
[copy(33),rewrite([13(6),21(7),12(4),13(12)])].
35 i2(x,y) != 1 | x ^ y = x.  [resolve(7,b,6,a)].
36 x v c(x v y) != 1 | c(c(y) v c(x)) = y.  [copy(35),rewrite([26(1),21(6)])].
39 c(1) = 0.  [back_rewrite(18),rewrite([21(2),12(2),20(2)])].
40 c(c(x) v c(x v y)) = x.  [back_rewrite(17),rewrite([21(2)])].
41 x v c(c(x) v c(y)) = x.  [back_rewrite(16),rewrite([21(1)])].
43 x v (y v z) = y v (x v z).  [para(13(a,1),14(a,1,1)),rewrite([14(2)])].
46 x v (y v c(x v y)) = 1.  [para(20(a,1),14(a,1)),flip(a)].
59 c(x) v c(x v y) = c(x).  [para(40(a,1),12(a,1,1)),flip(a)].
63 c(0 v c(x)) = x.  [para(20(a,1),40(a,1,1,2,1)),rewrite([39(3),13(3)])].
65 1 v x = 1.  [para(39(a,1),40(a,1,1,1)),rewrite([63(6)])].
69 x v c(c(x) v y) = x.  [para(12(a,1),41(a,1,2,1,2))].
74 x v x = x.  [para(39(a,1),41(a,1,2,1,2)),rewrite([13(3),63(4)])].
77 x v c(y v (x v z)) != 1 | c(c(y v z) v c(x)) = y v z.  [para(43(a,1),36(a,1,2,1))].
79 x v 1 = 1.  [para(65(a,1),13(a,1)),flip(a)].
83 x v (x v y) = x v y.  [para(74(a,1),14(a,1,1)),flip(a)].
110 x v c(y v c(x)) = x.  [para(13(a,1),69(a,1,2,1))].
113 x v (y v c(c(x) v z)) = y v x.  [para(69(a,1),43(a,1,2)),flip(a)].
122 c(x) v c(y v x) = c(x).  [para(12(a,1),110(a,1,2,1,2))].
123 x v (c(y v c(x)) v z) = x v z.  [para(110(a,1),14(a,1,1)),flip(a)].
144 c(x) v (y v c(x v z)) = y v c(x).  [para(59(a,1),43(a,1,2)),flip(a)].
185 c(x) v (c(y v x) v z) = c(x) v z.  [para(122(a,1),14(a,1,1)),flip(a)].
431 c(x v y) v c(x v c(c(y) v z)) = c(x v c(c(y) v z)).
[para(113(a,1),122(a,1,2,1)),rewrite([13(8)])].
471 x v (y v c(c(z v c(x)) v y)) = 1.
[para(46(a,1),123(a,1,2)),rewrite([79(2)]),flip(a)].
693 x v c(x v c(y)) != 1 | c(y v c(x)) = c(y).
[para(144(a,1),77(a,1,2,1)),rewrite([59(10),12(8),59(13)])].
1959 c(x) v c(c(y v x) v c(z v x)) = 1.
[para(471(a,1),185(a,1)),rewrite([12(4)]),flip(a)].
3444 x v (y v c(x v c(z v c(x v y)))) = 1.
[para(59(a,1),1959(a,1,2,1,1,1)),rewrite([12(3),12(3),14(8)])].
21441 x v c(x v c(c(y) v c(x v c(x v y)))) = 1.  [para(431(a,1),3444(a,1,2))].
30946 c(c(x) v c(y v c(y v x))) = c(c(x) v c(y)).
[hyper(693,a,21441,a),rewrite([13(8),144(8)]),flip(a)].
31457 c(c(x v y) v c(x v c(x v y))) = x.
[para(83(a,1),30946(a,1,1,2,1,2,1)),rewrite([13(12),59(12),12(10)])].
31474 c(x v y) v c(x v c(x v y)) = c(x).  [para(31457(a,1),12(a,1,1)),flip(a)].
```

```
31586 x v c(x v c(x v y)) = x v y.
[para(31474(a,1),31474(a,1,1,1)),rewrite([12(2),31474(9),12(4),13(3),12(8)])].
31587 $F # answer("OMA").  [resolve(31586,a,34,a)].

============================== end of proof ==========================


============================== PROOF =================================

% Proof 1 at 25.35 (+ 0.36) seconds: "OMA".
% Length of proof is 45.
% Level of proof is 10.

1 le(x,y) <-> x = x ^ y # label("Df: less than") # label(non_clause).  [assumption].
3 i3(x,y) = 1 <-> le(x,y) # label("Hypothesis for Proposition 2.10i3") #
label(non_clause).  [assumption].
4 y v (c(y) ^ (x v y)) = x v y # label("OMA") # label(non_clause) # label(goal).  [goal].
6 -le(x,y) | x ^ y = x # label("Df: less than").  [clausify(1)].
7 i3(x,y) != 1 | le(x,y) # label("Hypothesis for Proposition 2.10i3").  [clausify(3)].
11 x = c(c(x)) # label("AxL1").  [assumption].
12 c(c(x)) = x.  [copy(11),flip(a)].
13 x v y = y v x # label("AxL2").  [assumption].
14 (x v y) v z = x v (y v z) # label("AxL3").  [assumption].
16 x v (x ^ y) = x # label("AxL5").  [assumption].
17 x ^ (x v y) = x # label("AxL6").  [assumption].
18 c(x) ^ x = 0 # label("AxOL1").  [assumption].
19 c(x) v x = 1 # label("AxOL2").  [assumption].
20 x v c(x) = 1.  [copy(19),rewrite([13(2)])].
21 x ^ y = c(c(x) v c(y)) # label("AxOL3").  [assumption].
27 i3(x,y) = ((c(x) ^ y) v (c(x) ^ c(y))) v (c(x) v (x ^ y)) # label("Df: i3").
[assumption].
28 i3(x,y) = c(x v y) v (c(x v c(y)) v (c(x) v c(c(x) v c(y)))).
[copy(27),rewrite([21(3),12(3),21(7),12(6),12(6),13(7),21(9),14(14)])].
33 c1 v (c(c1) ^ (c2 v c1)) != c2 v c1 # label("OMA") # answer("OMA").  [deny(4)].
34 c1 v c(c1 v c(c1 v c2)) != c1 v c2 # answer("OMA").
[copy(33),rewrite([13(6),21(7),12(4),13(12)])].
35 i3(x,y) != 1 | x ^ y = x.  [resolve(7,b,6,a)].
36 c(x v y) v (c(x v c(y)) v (c(x) v c(c(x) v c(y)))) != 1 | c(c(x) v c(y)) = x.
[copy(35),rewrite([28(1),21(16)])].
39 c(1) = 0.  [back_rewrite(18),rewrite([21(2),12(2),20(2)])].
40 c(c(x) v c(x v y)) = x.  [back_rewrite(17),rewrite([21(2)])].
41 x v c(c(x) v c(y)) = x.  [back_rewrite(16),rewrite([21(1)])].
43 x v (y v z) = y v (x v z).  [para(13(a,1),14(a,1,1)),rewrite([14(2)])].
45 c(x) v (c(x v y) v (c(x v c(y)) v c(c(x) v c(y)))) != 1 | c(c(x) v c(y)) = x.
[back_rewrite(36),rewrite([43(12),43(13)])].
48 x v (y v c(x v y)) = 1.  [para(20(a,1),14(a,1)),flip(a)].
55 c(0 v c(x)) = x.  [para(20(a,1),40(a,1,1,2,1)),rewrite([39(3),13(3)])].
56 1 v x = 1.  [para(39(a,1),40(a,1,1,1)),rewrite([55(6)])].
59 x v c(c(x) v y) = x.  [para(12(a,1),41(a,1,2,1,2))].
63 x v 0 = x.  [para(20(a,1),41(a,1,2,1)),rewrite([39(2)])].
64 x v x = x.  [para(39(a,1),41(a,1,2,1,2)),rewrite([13(3),55(4)])].
66 x v 1 = 1.  [para(56(a,1),13(a,1)),flip(a)].
68 0 v x = x.  [para(63(a,1),13(a,1)),flip(a)].
71 x v (y v x) = y v x.  [para(64(a,1),14(a,2,2)),rewrite([13(2)])].
83 c(x v y) v (c(x v (y v z)) v (c(x v (y v c(z))) v c(c(x v y) v c(z)))) != 1 | c(c(x v
y) v c(z)) = x v y.  [para(14(a,1),45(a,1,2,1,1)),rewrite([14(8)])].
96 x v c(y v c(x)) = x.  [para(13(a,1),59(a,1,2,1))].
98 x v (y v c(c(x v y) v z)) = x v y.  [para(59(a,1),14(a,1)),flip(a)].
108 c(x) v c(y v x) = c(x).  [para(12(a,1),96(a,1,2,1,2))].
114 x v (y v c(y v x)) = 1.  [para(13(a,1),48(a,1,2,2,1))].
162 x v c(y v x) != 1 | y v x = x.
[para(20(a,1),83(a,1,2,2,1,1,2)),rewrite([64(3),66(6),39(6),13(9),108(9),12(7),68(6),13(5
),71(6),13(9),108(9),12(7)]),flip(b)].
420 x v (c(y v x) v c(c(y v x) v z)) != 1 | x v c(c(y v x) v z) = y v x.
[para(98(a,1),162(a,1,2,1)),rewrite([13(8),43(8),98(16)]),flip(b)].
18945 x v c(x v c(y v x)) = y v x.  [hyper(420,a,114,a),rewrite([13(3)])].
18946 x v c(x v c(x v y)) = y v x.  [para(13(a,1),18945(a,1,2,1,2,1))].
19025 $F # answer("OMA").  [back_rewrite(34),rewrite([18946(9),13(3)]),xx(a)].

============================== end of proof ==========================
```

Figure 3. Summary of a *prover9* ([2]) proof of Proposition 2.10, for each of i = 1,2,3. The proofs assume the default inference rules of *prover9*. The general form of a line in this proof is "*line_number conclusion [derivation]*", where *line_number* is a unique identifier of a line in the proof, and *conclusion* is the result of applying the *prover9* inference rules (such as *para*modulation, *copy*ing, and *rewrit*ing), noted in square brackets (denoting the *derivation*), to the lines cited in those brackets. Note that some of "logical" proof lines in the above have been transformed to two text lines, with the *derivation* appearing on a text line following a text line containing the first part of that logical line. The detailed syntax and semantics of these notations can be found in [2]. All *prover9* proofs are by default proofs by contradiction.

The total time to produce the proofs in Figure 3 on the platform described in Section 2.0 was approximately 200 seconds.

4.0 Discussion

The results of Section 3.0 motivate several observations:

1. The proofs in Figure 3 have distinct derivational dependencies. In particular, the proof for i = 1 uses axioms L1, L2, L3, L5, OL2, and OL3. The proof for i =2 uses L1, L2, L5, L6, OL1, OL2, and OL3. The proof for i = 3 uses L1, L2, L3, L5, L6, OL1, OL2, and OL3. These results suggest (but do not prove) that distinct types of quantum implication have their "roots" in distinct axiomatic bases. Future work will explore this hypothesis.

2. The proofs in Section 3.0 may be novel.

3. Companion papers provide proofs for i = 4, 5, and for the proposition that orthomodular lattice theory implies Propositions 2.10i, i = 1,2,3,4,5 ([23]).

5.0 Acknowledgements

This work benefited from discussions with Tom Oberdan, Frank Pecchioni, Tony Pawlicki, and the late John K. Prentice, whose passion for foundations of physics inspired those of us privileged to have known him. For any infelicities that remain, I am solely responsible.

6.0 References

[1] von Neumann J. *Mathematical Foundations of Quantum Mechanics*. 1936. Translated by R. T. Beyer. Princeton. 1983.
[2] McCune WW. *prover9 and mace4.* URL http://www.cs.unm.edu/~mccune/prover9/. 2009.
[3] Horner JK. *prover9* scripts for Proposition 2.10. 2011. Available from the author on request.
[4] Dalla Chiara ML and Giuntini R. *Quantum Logics*. URL http://xxx.lanl.gov/abs/quant-ph/0101028. 2004.
[5] Megill ND and Pavičić M. Orthomodular lattices and quantum algebra. *International Journal of Theoretical Physics* 40 (2001), pp. 1387-1410.
[6] Akhiezer NI and Glazman IM. *Theory of Linear Operators in Hilbert Space*. *Volume I*. Translated by M. Nestell. Frederick Ungar. 1961.
[7] Holland, Jr. SS Orthomodularity in infinite dimensions: a theorem of M. Solèr. *Bulletin of the American Mathematical Society* 32 (1995), pp. 205-234.

[8] Marsden EL and Herman LM. *A condition for distribution in orthomodular lattices.* Kansas State University Technical Report #40. 1974.
[9] Knuth DE and Bendix PB. Simple word problems in universal algebras. In J. Leech, ed. *Computational Problems in Abstract Algebra.* Pergamon Press. 1970. pp. 263-297.
[10] Chang CC and Keisler HJ. *Model Theory.* North-Holland. 1990. pp. 38-39.
[11] Birkhoff G. *Lattice Theory.* Third Edition. American Mathematical Society. 1967.
[12] Church A. *Introduction to Mathematical Logic. Volume I.* Princeton. 1956.
[13] Jauch J. *Foundations of Quantum Mechanics.* Addison-Wesley. 1968.
[14] Megill ND. *Metamath.* URL http://us.metamath.org/qlegif/mmql.html#unify. 2004.
[15] Horner JK. An automated deduction system for orthomodular lattice theory. *Proceedings of the 2005 International Conference on Artificial Intelligence.* CSREA Press. 2005. pp. 260-265.
[16] Horner JK. An automated equational logic deduction of join elimination in orthomodular lattice theory. *Proceedings of the 2007 International Conference on Artificial Intelligence.* CSREA Press. 2007. pp. 481-488.
[17] Messiah A. *Quantum Mechanics*. Dover. 1958.
[18] Horner JK. Using automated theorem-provers to aid the design of efficient compilers for quantum computing. *Los Alamos National Laboratory Quantum Institute Workshop.* December 9–10, 2002. URL http://www.lanl.gov/science/centers/quantum/qls_pdfs/horner.pdf.
[19] Birkhoff G and von Neumann J. The logic of quantum mechanics. *Annals of Mathematics* 37 (1936), 823-243.
[20] Nielsen MA and Chuang L . *Quantum Computation and Quantum Information*. Cambridge. 2000.
[21] Pavičić M and Megill N. Quantum and classical implicational algebras with primitive implication. *International Journal of Theoretical Physics* 37 (1998), 2091-2098. ftp://m3k.grad.hr/pavicic/quantum-logic/1998-int-j-theor-phys-2.ps.gz.
[22] Horner JK. An automated deduction of the relative strength of orthomodular and weakly orthomodular lattice theory. *Proceedings of the 2009 International Conference on Artificial Intelligence*. CSREA Press. 2009. pp. 525-530.
[23] Horner JK. Quantum-implication-based equivalents of the Orthomodularity Law in quantum logic: Parts 2-4. Submitted to the *2012 International Conference on Foundations of Computer Science*.

Quantum-Implication-Based Equivalents of the Orthomodularity Law in Quantum Logic: Part 2

Jack K. Horner
P. O. Box 266
Los Alamos, New Mexico 87544 USA
email: jhorner@cybermesa.com

Abstract

The optimization of quantum computing circuitry and compilers at some level must be expressed in terms of quantum-mechanical behaviors and operations. In much the same way that the structure of conventional propositional (Boolean) logic (BL) is the logic of the description of the behavior of classical physical systems and is isomorphic to a Boolean algebra (BA), so also the algebra, C(H), of closed linear subspaces of (equivalently, the system of linear operators on (observables in)) a Hilbert space is a logic of the descriptions of the behavior of quantum mechanical systems and is a model of an ortholattice (OL). An OL can thus be thought of as a kind of "quantum logic" (QL). C(H) is also a model of an orthomodular lattice, which is an OL conjoined with the orthomodularity axiom (OMA). The rationalization of the OMA as a claim proper to physics has proven problematic, motivating the question of whether the OMA and its equivalents are required in an adequate characterization of QL. The OMA, it turns out, has strong connections to implication in QL. Here I provide automated deductions of the OMA from two quantum-implication-based equivalents of the OMA. The proofs may be novel.

Keywords: automated deduction, quantum computing, orthomodular lattice, Hilbert space

1.0 Introduction

The optimization of quantum computing circuitry and compilers at some level must be expressed in terms of the description of quantum-mechanical behaviors ([1], [17], [18], [20]). In much the same way that conventional propositional (Boolean) logic (BL,[12]) is the logical structure of description of the behavior of classical physical systems (e.g. "the measurements of the position and momentum of particle P are commutative", i.e., can be measured in either order, yielding the same results) and is isomorphic to a Boolean lattice ([10], [11], [19]), so also the algebra, *C(H)*, of the closed linear subspaces of (equivalently, the system of linear operators on (observables in)) a Hilbert space *H* ([1], [4], [6], [9], [13]) is *a* logic of the descriptions of the behavior of quantum mechanical systems (e.g., "the measurements of the position and momentum of particle P are *not* commutative") and is a model ([10]) of an ortholattice (OL; [4]). An OL can thus be thought of as a kind of "quantum logic" (QL; [19]). *C(H)* is also a model of (i.e., isomorphic to a set of sentences which hold in) an orthomodular lattice (OML; [4], [7]), which is an OL conjoined with the orthomodularity axiom (OMA; see Figure 1). The rationalization of the OMA as a claim proper to physics has proven problematic ([13], Section 5-6), motivating the question of whether the OMA is required in an adequate characterization of QL. Thus formulated, the question suggests that the OMA and its equivalents are specific to an OML, and that as a consequence, banning the OMA from QL yields a "truer" quantum

logic. The OMA, it turns out, has strong connections to implication in QL, as demonstrated in the following.

Lattice axioms

```
      x = c(c(x))                        (AxLat1)
      x v y = y v x                      (AxLat2)
      (x v y) v z = x v (y v z)          (AxLat3)
      (x ^ y) ^ z = x ^ (y ^ z)          (AxLat4)
      x v (x ^ y) = x                    (AxLat5)
      x ^ (x v y) = x                    (AxLat6)
```

Ortholattice axioms

```
      c(x) ^ x = 0                       (AxOL1)
      c(x) v x = 1                       (AxOL2)
      x ^ y = c(c(x) v c(y))             (AxOL3)
```

Orthomodularity axiom

```
      y v (c(y) ^ (x v y)) = x v y       (OMA)
```

Definitions of implications and partial order

```
   i1(x,y) = c(x) v (x ^ y).
   i2(x,y) = i1(c(y), c(x).
   i3(x,y) = (c(x) ^ y) v (c(x) ^ c(y)) v i1(x,y).
   i4(x,y) = i3(c(y), c(x)).
   i5(x,y) = (x ^ y) v (c(x) ^ y) v (c(x) ^ c(y)).
   le(x,y) = (x = (x ^ y)).

where
   x, y are variables ranging over lattice nodes
   ^ is lattice meet
   v is lattice join
   c(x) is the orthocomplement of x
   i1(x,y) means x →1 y (Sasaki implication)
   i2(x,y) means x →2 y (Dishkant implication)
   i3(x,y) means x →3 y (Kalmbach implication)
   i4(x,y) means x →4 y (non-tollens implication)
   i5(x,y) means x →5 y (relevance implication)
   le(x,y) means x ≤ y
   <-> means if and only if
   =  is equivalence ([12])
   1 is the maximum lattice element (= x v c(x))
   0 is the minimum lattice element (= c(1))
```

Figure 1. Lattice, ortholattice, orthomodularity axioms, and some definitions.

Consider the proposition shown in Figure 2.

```
      ((x →i y) = 1)      <->    le(x,y)

where i = 1,2,3,4,5.
```

Figure 2. Proposition 2.10

Note that there are five implications in QL (BL has only one). Proposition 2.10 is a generalization of the BL definition of implication, sometimes denoted $\rightarrow_0$.

2.0 Method

The OML axiomatizations of Megill, Pavičić, and Horner ([5], [14], [15], [16], [21], [22]) were implemented in a *prover9* ([2]) script ([3]) configured to derive OMA from Proposition 2.10i, for each of i = 4,5 together with ortholattice theory (orthomodular lattice theory, without the OMA), then executed in that framework on a Dell Inspiron 545 with an Intel Core2 Quad CPU Q8200 (clocked @ 2.33 GHz) and 8.00 GB RAM, running under the *Windows Vista Home Premium /Cygwin* operating environment.

3.0 Results

Figure 3 shows the proofs, generated by [3] on the platform described in Section 2.0, that Proposition 2.10i (for each of i = 4,5), together with ortholattice theory, imply the OMA.

```
============================== PROOF =================================

% Proof 1 at 164.91 (+ 2.98) seconds: "OMA".
% Length of proof is 57.
% Level of proof is 13.

1 le(x,y) <-> x = x ^ y # label("Df: less than") # label(non_clause).  [assumption].
3 i4(x,y) = 1 <-> le(x,y) # label("Hypothesis for formula 2.10i4") # label(non_clause).
[assumption].
4 y v (c(y) ^ (x v y)) = x v y # label("OMA") # label(non_clause) # label(goal).  [goal].
5 le(x,y) | x ^ y != x # label("Df: less than").  [clausify(1)].
6 -le(x,y) | x ^ y = x # label("Df: less than").  [clausify(1)].
7 i4(x,y) != 1 | le(x,y) # label("Hypothesis for formula 2.10i4").  [clausify(3)].
8 i4(x,y) = 1 | -le(x,y) # label("Hypothesis for formula 2.10i4").  [clausify(3)].
11 x = c(c(x)) # label("AxL1").  [assumption].
12 c(c(x)) = x.  [copy(11),flip(a)].
13 x v y = y v x # label("AxL2").  [assumption].
14 (x v y) v z = x v (y v z) # label("AxL3").  [assumption].
16 x v (x ^ y) = x # label("AxL5").  [assumption].
17 x ^ (x v y) = x # label("AxL6").  [assumption].
18 c(x) ^ x = 0 # label("AxOL1").  [assumption].
19 c(x) v x = 1 # label("AxOL2").  [assumption].
20 x v c(x) = 1.  [copy(19),rewrite([13(2)])].
21 x ^ y = c(c(x) v c(y)) # label("AxOL3").  [assumption].
29 i4(x,y) = ((c(c(y)) ^ c(x)) v (c(c(y)) ^ c(c(x)))) v (c(c(y)) v (c(y) ^ c(x))) #
label("Df: i4").  [assumption].
30 i4(x,y) = y v (c(y v x) v (c(c(y) v x) v c(c(y) v c(x)))).
[copy(29),rewrite([12(3),21(3),12(4),12(6),12(6),21(5),12(11),21(12),12(11),12(11),13(13)
,14(13)])].
33 c1 v (c(c1) ^ (c2 v c1)) != c2 v c1 # label("OMA") # answer("OMA").  [deny(4)].
34 c1 v c(c1 v c(c1 v c2)) != c1 v c2 # answer("OMA").
[copy(33),rewrite([13(6),21(7),12(4),13(12)])].
35 i4(x,y) != 1 | x ^ y = x.  [resolve(7,b,6,a)].
36 x v (c(x v y) v (c(c(x) v y) v c(c(x) v c(y)))) != 1 | c(c(y) v c(x)) = y.
[copy(35),rewrite([30(1),21(15)])].
37 i4(x,y) = 1 | x ^ y != x.  [resolve(8,b,5,a)].
38 x v (c(x v y) v (c(c(x) v y) v c(c(x) v c(y)))) = 1 | c(c(y) v c(x)) != y.
[copy(37),rewrite([30(1),21(15)])].
39 c(1) = 0.  [back_rewrite(18),rewrite([21(2),12(2),20(2)])].
40 c(c(x) v c(x v y)) = x.  [back_rewrite(17),rewrite([21(2)])].
41 x v c(c(x) v c(y)) = x.  [back_rewrite(16),rewrite([21(1)])].
43 x v (y v z) = y v (x v z).  [para(13(a,1),14(a,1,1)),rewrite([14(2)])].
46 x v (y v c(x v y)) = 1.  [para(20(a,1),14(a,1)),flip(a)].
```

```
48 x v (c(x v c(y)) v (c(c(x) v y) v c(c(x) v c(y)))) != 1 | c(y v c(x)) = c(y).
[para(12(a,1),36(a,1,2,2,2,1,2)),rewrite([13(11),12(17)])].
59 c(0) = 1.  [para(39(a,1),12(a,1,1))].
66 c(x) v c(x v y) = c(x).  [para(40(a,1),12(a,1,1)),flip(a)].
70 c(0 v c(x)) = x.  [para(20(a,1),40(a,1,1,2,1)),rewrite([39(3),13(3)])].
74 1 v x = 1.  [para(39(a,1),40(a,1,1,1)),rewrite([70(6)])].
86 x v c(c(x) v y) = x.  [para(12(a,1),41(a,1,2,1,2))].
90 x v 0 = x.  [para(20(a,1),41(a,1,2,1)),rewrite([39(2)])].
92 x v x = x.  [para(39(a,1),41(a,1,2,1,2)),rewrite([13(3),70(4)])].
100 x v 1 = 1.
[para(59(a,1),38(b,1,1,1)),rewrite([90(2),13(4),70(5),59(4),13(4),74(4),39(3),90(3),13(2)
,20(2),74(7),39(6)]),xx(b)].
112 x v (x v y) = x v y.  [para(92(a,1),14(a,1,1)),flip(a)].
148 x v c(y v c(x)) = x.  [para(13(a,1),86(a,1,2,1))].
149 x v (c(c(x) v y) v z) = x v z.  [para(86(a,1),14(a,1,1)),flip(a)].
151 x v (y v c(c(x) v z)) = y v x.  [para(86(a,1),43(a,1,2)),flip(a)].
162 c(x) v c(y v x) = c(x).  [para(12(a,1),148(a,1,2,1,2))].
163 x v (c(y v c(x)) v z) = x v z.  [para(148(a,1),14(a,1,1)),flip(a)].
175 c(x) v (c(x v y) v z) = c(x) v z.  [para(66(a,1),14(a,1,1)),flip(a)].
234 c(x) v (c(y v x) v z) = c(x) v z.  [para(162(a,1),14(a,1,1)),flip(a)].
525 x v c(x v c(c(x v y) v z)) != 1 | c(c(x v y) v z) = c(c(x) v z).
[para(149(a,1),48(a,1,2,2,1,1)),rewrite([12(2),12(12),43(18),149(19),151(15),13(7),12(11)
,13(14),175(14),12(14)]),flip(b)].
621 c(x v y) v c(x v c(c(y) v z)) = c(x v c(c(y) v z)).
[para(151(a,1),162(a,1,2,1)),rewrite([13(8)])].
675 x v (y v c(c(z v c(x)) v y)) = 1.
[para(46(a,1),163(a,1,2)),rewrite([100(2)]),flip(a)].
1924 c(x) v c(c(y v x) v c(z v x)) = 1.
[para(675(a,1),234(a,1)),rewrite([12(4)]),flip(a)].
2974 x v (y v c(x v c(z v c(x v y)))) = 1.
[para(66(a,1),1924(a,1,2,1,1,1)),rewrite([12(3),12(3),14(8)])].
23541 x v c(x v c(c(y) v c(x v c(x v y)))) = 1.  [para(621(a,1),2974(a,1,2))].
35630 c(c(x v y) v c(x v c(x v y))) = x.
[hyper(525,a,23541,a),rewrite([112(4),112(11),66(14),12(10)])].
35641 c(x v y) v c(x v c(x v y)) = c(x).  [para(35630(a,1),12(a,1,1)),flip(a)].
35817 x v c(x v c(x v y)) = x v y.
[para(35641(a,1),35641(a,1,1,1)),rewrite([12(2),35641(9),12(4),13(3),12(8)])].
35818 $F # answer("OMA").  [resolve(35817,a,34,a)].

============================== end of proof ==========================


============================== PROOF =================================

% Proof 1 at 215.39 (+ 3.15) seconds: "OMA".
% Length of proof is 61.
% Level of proof is 13.

1 le(x,y) <-> x = x ^ y # label("Df: less than") # label(non_clause).  [assumption].
3 i5(x,y) = 1 <-> le(x,y) # label("Hypothesis for formula 2.10i5") # label(non_clause).
[assumption].
4 y v (c(y) ^ (x v y)) = x v y # label("OMA") # label(non_clause) # label(goal).  [goal].
6 -le(x,y) | x ^ y = x # label("Df: less than").  [clausify(1)].
7 i5(x,y) != 1 | le(x,y) # label("Hypothesis for formula 2.10i5").  [clausify(3)].
11 x = c(c(x)) # label("AxL1").  [assumption].
12 c(c(x)) = x.  [copy(11),flip(a)].
13 x v y = y v x # label("AxL2").  [assumption].
14 (x v y) v z = x v (y v z) # label("AxL3").  [assumption].
16 x v (x ^ y) = x # label("AxL5").  [assumption].
17 x ^ (x v y) = x # label("AxL6").  [assumption].
18 c(x) ^ x = 0 # label("AxOL1").  [assumption].
19 c(x) v x = 1 # label("AxOL2").  [assumption].
20 x v c(x) = 1.  [copy(19),rewrite([13(2)])].
21 x ^ y = c(c(x) v c(y)) # label("AxOL3").  [assumption].
31 i5(x,y) = ((x ^ y) v (c(x) ^ y)) v (c(x) ^ c(y)) # label("Df: i5").  [assumption].
32 i5(x,y) = c(x v y) v (c(x v c(y)) v c(c(x) v c(y))).
[copy(31),rewrite([21(2),21(7),12(7),13(9),21(12),12(11),12(11),13(12)])].
33 c1 v (c(c1) ^ (c2 v c1)) != c2 v c1 # label("OMA") # answer("OMA").  [deny(4)].
34 c1 v c(c1 v c(c1 v c2)) != c1 v c2 # answer("OMA").
[copy(33),rewrite([13(6),21(7),12(4),13(12)])].
35 i5(x,y) != 1 | x ^ y = x.  [resolve(7,b,6,a)].
```

```
36 c(x v y) v (c(x v c(y)) v c(c(x) v c(y))) != 1 | c(c(x) v c(y)) = x.
[copy(35),rewrite([32(1),21(14)])].
39 c(1) = 0.  [back_rewrite(18),rewrite([21(2),12(2),20(2)])].
40 c(c(x) v c(x v y)) = x.  [back_rewrite(17),rewrite([21(2)])].
41 x v c(c(x) v c(y)) = x.  [back_rewrite(16),rewrite([21(1)])].
43 x v (y v z) = y v (x v z).  [para(13(a,1),14(a,1,1)),rewrite([14(2)])].
46 x v (y v c(x v y)) = 1.  [para(20(a,1),14(a,1)),flip(a)].
49 c(x v y) v (c(y v c(x)) v c(c(y) v c(x))) != 1 | c(c(y) v c(x)) = y.
[para(13(a,1),36(a,1,1,1))].
52 c(x v (y v z)) v (c(x v (y v c(z))) v c(c(x v y) v c(z))) != 1 | c(c(x v y) v c(z)) =
x v y.  [para(14(a,1),36(a,1,1,1)),rewrite([14(6)])].
66 c(x) v c(x v y) = c(x).  [para(40(a,1),12(a,1,1)),flip(a)].
70 c(0 v c(x)) = x.  [para(20(a,1),40(a,1,1,2,1)),rewrite([39(3),13(3)])].
73 1 v x = 1.  [para(39(a,1),40(a,1,1,1)),rewrite([70(6)])].
83 x v c(c(x) v y) = x.  [para(12(a,1),41(a,1,2,1,2))].
87 x v 0 = x.  [para(20(a,1),41(a,1,2,1)),rewrite([39(2)])].
90 x v x = x.  [para(39(a,1),41(a,1,2,1,2)),rewrite([13(3),70(4)])].
96 x v 1 = 1.  [para(73(a,1),13(a,1)),flip(a)].
98 0 v x = x.  [para(87(a,1),13(a,1)),flip(a)].
105 x v (x v y) = x v y.  [para(90(a,1),14(a,1,1)),flip(a)].
107 x v (y v x) = y v x.  [para(90(a,1),14(a,2,2)),rewrite([13(2)])].
111 x v (y v c(y v x)) = 1.  [para(13(a,1),46(a,1,2,2,1))].
140 x v c(y v c(x)) = x.  [para(13(a,1),83(a,1,2,1))].
143 x v (y v c(c(x) v z)) = y v x.  [para(83(a,1),43(a,1,2)),flip(a)].
148 x v (y v (x v z)) = y v (x v z).  [para(105(a,1),14(a,2,2)),rewrite([43(3),14(2)])].
151 c(x) v c(y v x) = c(x).  [para(12(a,1),140(a,1,2,1,2))].
152 x v (c(y v c(x)) v z) = x v z.  [para(140(a,1),14(a,1,1)),flip(a)].
153 x v (y v c(z v c(x v y))) = x v y.  [para(140(a,1),14(a,1)),flip(a)].
197 x v c(y v x) != 1 | y v x = x.
[para(107(a,1),49(a,1,1,1)),rewrite([14(5),20(4),96(4),39(4),13(7),151(7),12(5),98(4),13(
3),13(9),151(9),12(7)]),flip(b)].
205 c(x) v (c(y v x) v z) = c(x) v z.  [para(151(a,1),14(a,1,1)),flip(a)].
208 c(x v y) v c(x v (z v y)) = c(x v y).  [para(43(a,1),151(a,1,2,1))].
483 c(x v y) v c(x v c(c(y) v z)) = c(x v c(c(y) v z)).
[para(143(a,1),151(a,1,2,1)),rewrite([13(8)])].
502 c(x v (y v z)) v (c(y v (x v c(y v z))) v c(c(y v x) v c(y v z))) != 1 | c(c(y v x) v
c(y v z)) = y v x.  [para(148(a,1),52(a,1,1,1))].
528 x v (y v c(c(z v c(x)) v y)) = 1.
[para(46(a,1),152(a,1,2)),rewrite([96(2)]),flip(a)].
620 x v c(x v y) != 1 | y v x = x.  [para(13(a,1),197(a,1,2,1))].
2363 c(x) v c(c(y v x) v c(z v x)) = 1.
[para(528(a,1),205(a,1)),rewrite([12(4)]),flip(a)].
2583 x v (y v c(z v c(y v x))) = x v y.  [para(13(a,1),153(a,1,2,2,1,2,1))].
3525 x v (y v c(x v c(z v c(x v y)))) = 1.
[para(66(a,1),2363(a,1,2,1,1,1)),rewrite([12(3),12(3),14(8)])].
3984 c(x v y) v c(x v c(z v c(x v y))) = c(x v c(z v c(x v y))).
[para(153(a,1),208(a,1,2,1)),rewrite([13(9)])].
24616 x v c(x v c(c(y) v c(x v c(x v y)))) = 1.  [para(483(a,1),3525(a,1,2))].
35661 x v c(c(y) v c(x v c(x v y))) = x.  [hyper(620,a,24616,a),rewrite([13(8)])].
35666 x v c(y v c(x v c(x v c(y)))) = x.  [para(12(a,1),35661(a,1,2,1,1))].
35725 x v c(x v c(x v y)) = x v y.
[para(35666(a,1),502(a,1,2,2,1)),rewrite([13(6),66(6),12(4),13(3),2583(6),13(8),66(8),12(
6),13(5),3525(10),39(4),12(6),98(5),13(4),14(4),111(4),13(11),66(11),12(9),13(8),3984(12)
,12(10)]),xx(a)].
35726 $F # answer("OMA").  [resolve(35725,a,34,a)].

============================== end of proof ==========================
```

Figure 3. Summary of a *prover9* ([2]) proof of the OMA from Proposition 2.10, for each of i = 4,5. The proofs assume the default inference rules of *prover9*. The general form of a line in this proof is "*line_number conclusion [derivation]*", where *line_number* is a unique identifier of a line in the proof, and *conclusion* is the result of applying the *prover9* inference rules (such as *para*modulation, *copy*ing, and *rewrit*ing), noted in square brackets (denoting the *derivation*), to the lines cited in those brackets. Note that some of "logical" proof lines in the above have been transformed to two text lines, with the *derivation* appearing on a text line following a text line containing the first part of that logical line.

The detailed syntax and semantics of these notations can be found in [2]. All *prover9* proofs are by default proofs by contradiction.

The total time to produce the proofs in Figure 3 on the platform described in Section 2.0 was approximately 380 seconds.

4.0 Discussion

The results of Section 3.0 motivate several observations:

1. The proofs in Figure 3 are symmetric in their dependencies on the axioms of QL. This suggests (but does not prove) that the implications determined by i = 4, 5 have common "roots" in the axioms. Future work will explore this hypothesis.

2. The proofs in Section 3.0 may be novel.

3. Companion papers provide proofs for i = 1,2,3, and for orthomodular lattice theory implies Propositions 2.10i, i = 1,2,3,4,5 ([23]).

5.0 Acknowledgements

This work benefited from discussions with Tom Oberdan, Frank Pecchioni, Tony Pawlicki, and the late John K. Prentice, whose passion for foundations of physics inspired those of us privileged to have known him. For any infelicities that remain, I am solely responsible.

6.0 References

[1] von Neumann J. *Mathematical Foundations of Quantum Mechanics*. 1936. Translated by R. T. Beyer. Princeton. 1983.

[2] McCune WW. *prover9 and mace4.* URL http://www.cs.unm.edu/~mccune/prover9/. 2009.

[3] Horner JK. *prover9* scripts for Proposition 2.10. 2011. Available from the author on request.

[4] Dalla Chiara ML and Giuntini R. *Quantum Logics*. URL http://xxx.lanl.gov/abs/quant-ph/0101028. 2004.

[5] Megill ND and Pavičić M. Orthomodular lattices and quantum algebra. *International Journal of Theoretical Physics* 40 (2001), pp. 1387-1410.

[6] Akhiezer NI and Glazman IM. *Theory of Linear Operators in Hilbert Space. Volume I.* Translated by M. Nestell. Frederick Ungar. 1961.

[7] Holland, Jr. SS Orthomodularity in infinite dimensions: a theorem of M. Solèr. *Bulletin of the American Mathematical Society* 32 (1995), pp. 205-234.

[8] Marsden EL and Herman LM. *A condition for distribution in orthomodular lattices.* Kansas State University Technical Report #40. 1974.

[9] Knuth DE and Bendix PB. Simple word problems in universal algebras. In J. Leech, ed. *Computational Problems in Abstract Algebra.* Pergamon Press. 1970. pp. 263-297.

[10] Chang CC and Keisler HJ. *Model Theory*. North-Holland. 1990. pp. 38-39.

[11] Birkhoff G. *Lattice Theory.* Third Edition. American Mathematical Society. 1967.

[12] Church A. *Introduction to Mathematical Logic. Volume I.* Princeton. 1956.

[13] Jauch J. *Foundations of Quantum Mechanics.* Addison-Wesley. 1968.

[14] Megill ND. *Metamath.* URL http://us.metamath.org/qlegif/mmql.html#unify. 2004.
[15] Horner JK. An automated deduction system for orthomodular lattice theory. *Proceedings of the 2005 International Conference on Artificial Intelligence.* CSREA Press. 2005. pp. 260-265.
[16] Horner JK. An automated equational logic deduction of join elimination in orthomodular lattice theory. *Proceedings of the 2007 International Conference on Artificial Intelligence.* CSREA Press. 2007. pp. 481-488.
[17] Messiah A. *Quantum Mechanics*. Dover. 1958.
[18] Horner JK. Using automated theorem-provers to aid the design of efficient compilers for quantum computing. *Los Alamos National Laboratory Quantum Institute Workshop.* December 9–10, 2002. URL http://www.lanl.gov/science/centers/quantum/qls_pdfs/horner.pdf.
[19] Birkhoff G and von Neumann J. The logic of quantum mechanics. *Annals of Mathematics* 37 (1936), 823-243.
[20] Nielsen MA and Chuang L . *Quantum Computation and Quantum Information*. Cambridge. 2000.
[21] Pavičić M and Megill N. Quantum and classical implicational algebras with primitive implication. *International Journal of Theoretical Physics* 37 (1998), 2091-2098. ftp://m3k.grad.hr/pavicic/quantum-logic/1998-int-j-theor-phys-2.ps.gz.
[22] Horner JK. An automated deduction of the relative strength of orthomodular and weakly orthomodular lattice theory. *Proceedings of the 2009 International Conference on Artificial Intelligence*. CSREA Press. 2009. pp. 525-530.
[23] Horner JK. Quantum-implication-based equivalents of the Orthomodularity Law in quantum Logic: Parts 1, 3,4. Submitted to the *2012 International Conference on Foundations of Computer Science*.

Quantum-Implication-Based Equivalents of the Orthomodularity Law in Quantum Logic: Part 3

Jack K. Horner
P. O. Box 266
Los Alamos, New Mexico 87544 USA
email: jhorner@cybermesa.com

Abstract

The optimization of quantum computing circuitry and compilers at some level must be expressed in terms of quantum-mechanical behaviors and operations. In much the same way that the structure of conventional propositional (Boolean) logic (BL) is the logic of the description of the behavior of classical physical systems and is isomorphic to a Boolean algebra (BA), so also the algebra, C(H), of closed linear subspaces of (equivalently, the system of linear operators on (observables in)) a Hilbert space is a logic of the descriptions of the behavior of quantum mechanical systems and is a model of an ortholattice (OL). An OL can thus be thought of as a kind of "quantum logic" (QL). C(H) is also a model of an orthomodular lattice, which is an OL conjoined with the orthomodularity axiom (OMA). The rationalization of the OMA as a claim proper to physics has proven problematic, motivating the question of whether the OMA and its equivalents are required in an adequate characterization of QL. The OMA, it turns out, has strong connections to implication in QL. Here I provide an automated deduction of three implication-based equivalents of the OMA from orthomodular lattice theory. The proofs may be novel.

Keywords: automated deduction, quantum computing, orthomodular lattice, Hilbert space

1.0 Introduction

The optimization of quantum computing circuitry and compilers at some level must be expressed in terms of the description of quantum-mechanical behaviors ([1], [17], [18], [20]). In much the same way that conventional propositional (Boolean) logic (BL,[12]) is the logical structure of description of the behavior of classical physical systems (e.g. "the measurements of the position and momentum of particle P are commutative", i.e., can be measured in either order, yielding the same results) and is isomorphic to a Boolean lattice ([10], [11], [19]), so also the algebra, *C(H)*, of the closed linear subspaces of (equivalently, the system of linear operators on (observables in)) a Hilbert space *H* ([1], [4], [6], [9], [13]) is *a* logic of the descriptions of the behavior of quantum mechanical systems (e.g., "the measurements of the position and momentum of particle P are *not* commutative") and is a model ([10]) of an ortholattice (OL; [4]). An OL can thus be thought of as a kind of "quantum logic" (QL; [19]). *C(H)* is also a model of (i.e., isomorphic to a set of sentences which hold in) an orthomodular lattice (OML; [4], [7]), which is an OL conjoined with the orthomodularity axiom (OMA; see Figure 1). The rationalization of the OMA as a claim proper to physics has proven problematic ([13], Section 5-6), motivating the question of whether the OMA is required in an adequate characterization of QL. Thus formulated, the question suggests that the OMA and its equivalents are specific to an OML, and that as a consequence, banning the OMA from QL yields a "truer" quantum logic. The OMA, it turns out, has strong

connections to implication in QL, as demonstrated in the following.

Lattice axioms

```
      x = c(c(x))                       (AxLat1)
      x v y = y v x                     (AxLat2)
      (x v y) v z = x v (y v z)         (AxLat3)
      (x ^ y) ^ z = x ^ (y ^ z)         (AxLat4)
      x v (x ^ y) = x                   (AxLat5)
      x ^ (x v y) = x                   (AxLat6)
```

Ortholattice axioms

```
      c(x) ^ x = 0                      (AxOL1)
      c(x) v x = 1                      (AxOL2)
      x ^ y = c(c(x) v c(y))            (AxOL3)
```

Orthomodularity axiom

```
      y v (c(y) ^ (x v y)) = x v y      (OMA)
```

Definitions of implications and partial order

```
   i1(x,y) = c(x) v (x ^ y).
   i2(x,y) = i1(c(y), c(x).
   i3(x,y) = (c(x) ^ y) v (c(x) ^ c(y)) v i1(x,y).
   i4(x,y) = i3(c(y), c(x)).
   i5(x,y) = (x ^ y) v (c(x) ^ y) v (c(x) ^ c(y)).
   le(x,y) = (x = (x ^ y)).
```

where
   x, y are variables ranging over lattice nodes
   ^ is lattice meet
   v is lattice join
   c(x) is the orthocomplement of x
   i1(x,y) means $x \rightarrow_1 y$ (Sasaki implication)
   i2(x,y) means $x \rightarrow_2 y$ (Dishkant implication)
   i3(x,y) means $x \rightarrow_3 y$ (Kalmbach implication)
   i4(x,y) means $x \rightarrow_4 y$ (non-tollens implication)
   i5(x,y) means $x \rightarrow_5 y$ (relevance implication)
   le(x,y) means $x \leq y$
   <-> means if and only if
   = is equivalence ([12])
   1 is the maximum lattice element (= x v c(x))
   0 is the minimum lattice element (= c(1))

Figure 1. Lattice, ortholattice, orthomodularity axioms, and some definitions.

Consider the following proposition.

$$((x \rightarrow_i y) = 1) \quad <-> \quad le(x,y)$$

where i = 1,2,3,4,5.

Figure 2. Proposition 2.10

Note that there are five implications in QL (BL has only one). Proposition 2.10 is a generalization of the BL definition of implication, sometimes denoted $\rightarrow_0$.

2.0 Method

The OML axiomatizations of Megill, Pavičić, and Horner ([5], [14], [15], [16], [21], [22]) were implemented in a *prover9* ([2]) script ([3]) configured to derive Proposition 2.10i, for each of i = 1, 2, 3 from orthomodular lattice theory, then executed in that framework on a Dell Inspiron 545 with an Intel Core2 Quad CPU Q8200 (clocked @ 2.33 GHz) and 8.00 GB RAM, running under the *Windows Vista Home Premium /Cygwin* operating environment.

3.0 Results

Figure 3 shows the proofs, generated by [3] on the platform described in Section 2.0, that orthomodular lattice theory implies Proposition 2.10i, for each of i=1,2,3.

```
============================== PROOF =================================

% Proof 1 at 0.08 (+ 0.03) seconds.
% Length of proof is 44.
% Level of proof is 8.

1 le(x,y) <-> x = x ^ y # label("Df: less than") # label(non_clause).  [assumption].
3 i1(x,y) = 1 <-> le(x,y) # label("Proposition 2.10i1") # label(non_clause) #
label(goal).  [goal].
6 x = c(c(x)) # label("AxL1").  [assumption].
7 c(c(x)) = x.  [copy(6),flip(a)].
8 x v y = y v x # label("AxL2").  [assumption].
9 (x v y) v z = x v (y v z) # label("AxL3").  [assumption].
11 x v (x ^ y) = x # label("AxL5").  [assumption].
12 x ^ (x v y) = x # label("AxL6").  [assumption].
13 c(x) ^ x = 0 # label("AxOL1").  [assumption].
14 c(x) v x = 1 # label("AxOL2").  [assumption].
15 x v c(x) = 1.  [copy(14),rewrite([8(2)])].
16 x ^ y = c(c(x) v c(y)) # label("AxOL3").  [assumption].
17 x v (c(x) ^ (y v x)) = y v x # label("OMA").  [assumption].
18 x v c(x v c(y v x)) = y v x.  [copy(17),rewrite([16(3),7(2)])].
20 i1(x,y) = c(x) v (x ^ y) # label("Df: i1").  [assumption].
21 i1(x,y) = c(x) v c(c(x) v c(y)).  [copy(20),rewrite([16(3)])].
28 i5(x,y) = ((x ^ y) v (c(x) ^ y)) v (c(x) ^ c(y)) # label("Df: i5").  [assumption].
29 i5(x,y) = c(x v y) v (c(x v c(y)) v c(c(x) v c(y))).
[copy(28),rewrite([16(2),16(7),7(7),8(9),16(12),7(11),7(11),8(12)])].
30 -le(x,y) | x ^ y = x # label("Df: less than").  [clausify(1)].
31 -le(x,y) | c(c(x) v c(y)) = x.  [copy(30),rewrite([16(2)])].
32 le(x,y) | x ^ y != x # label("Df: less than").  [clausify(1)].
33 le(x,y) | c(c(x) v c(y)) != x.  [copy(32),rewrite([16(2)])].
34 i1(c1,c2) = 1 | le(c1,c2) # label("Proposition 2.10i1").  [deny(3)].
35 c(c1) v c(c(c1) v c(c2)) = 1 | le(c1,c2).  [copy(34),rewrite([21(3)])].
36 i1(c1,c2) != 1 | -le(c1,c2) # label("Proposition 2.101").  [deny(3)].
37 c(c1) v c(c(c1) v c(c2)) != 1 | -le(c1,c2).  [copy(36),rewrite([21(3)])].
38 c(1) = 0.  [back_rewrite(13),rewrite([16(2),7(2),15(2)])].
39 c(c(x) v c(x v y)) = x.  [back_rewrite(12),rewrite([16(2)])].
40 x v c(c(x) v c(y)) = x.  [back_rewrite(11),rewrite([16(1)])].
44 x v (c(x) v y) = 1 v y.  [para(15(a,1),9(a,1,1)),flip(a)].
54 le(x,y) | c(c(y) v c(x)) != x.  [para(8(a,1),33(b,1,1))].
57 c(c1) v c(c(c1) v c(c2)) = 1 | c(c(c1) v c(c2)) = c1.  [resolve(35,b,31,a)].
63 c(x) v c(x v y) = c(x).  [para(39(a,1),7(a,1,1)),flip(a)].
67 c(0 v c(x)) = x.  [para(15(a,1),39(a,1,1,2,1)),rewrite([38(3),8(3)])].
68 c(x v y) v c(x v c(x v y)) = c(x).
[para(39(a,1),18(a,1,2,1,2)),rewrite([8(5),63(11)])].
69 1 v x = 1.  [para(38(a,1),39(a,1,1,1)),rewrite([67(6)])].
```

```
73 x v (c(x) v y) = 1.  [back_rewrite(44),rewrite([69(5)])].
78 x v 0 = x.  [para(15(a,1),40(a,1,2,1)),rewrite([38(2)])].
80 x v x = x.  [para(38(a,1),40(a,1,2,1,2)),rewrite([8(3),67(4)])].
91 0 v x = x.  [para(78(a,1),8(a,1)),flip(a)].
93 x v (x v y) = x v y.  [para(80(a,1),9(a,1,1)),flip(a)].
338 c(c(c1) v c(c2)) = c1.
[para(57(a,1),29(a,2,1,1)),rewrite([29(17),7(27),93(26),7(27),7(32),73(31),38(26),8(26),9
1(26),8(25),68(25),7(11),38(11),7(19),93(18),7(19),7(24),73(23),38(18),8(18),91(18),91(17
)]),flip(b),merge(b)].
339 -le(c1,c2).  [back_rewrite(37),rewrite([338(8),8(4),15(4)]),xx(a)].
340 $F.  [ur(54,a,339,a),rewrite([8(5),338(6)]),xx(a)].

============================== end of proof ==========================


============================== PROOF =================================

% Proof 1 at 2.32 (+ 0.08) seconds.
% Length of proof is 35.
% Level of proof is 8.

1 le(x,y) <-> x = x ^ y # label("Df: less than") # label(non_clause).  [assumption].
3 i2(x,y) = 1 <-> le(x,y) # label("Proposition 2.10i2") # label(non_clause) #
label(goal).  [goal].
6 x = c(c(x)) # label("AxL1").  [assumption].
7 c(c(x)) = x.  [copy(6),flip(a)].
8 x v y = y v x # label("AxL2").  [assumption].
11 x v (x ^ y) = x # label("AxL5").  [assumption].
12 x ^ (x v y) = x # label("AxL6").  [assumption].
13 c(x) ^ x = 0 # label("AxOL1").  [assumption].
14 c(x) v x = 1 # label("AxOL2").  [assumption].
15 x v c(x) = 1.  [copy(14),rewrite([8(2)])].
16 x ^ y = c(c(x) v c(y)) # label("AxOL3").  [assumption].
17 x v (c(x) ^ (y v x)) = y v x # label("OMA").  [assumption].
18 x v c(x v c(y v x)) = y v x.  [copy(17),rewrite([16(3),7(2)])].
22 i2(x,y) = c(c(y)) v (c(y) ^ c(x)) # label("Df: i2").  [assumption].
23 i2(x,y) = y v c(y v x).  [copy(22),rewrite([7(3),16(4),7(3),7(3)])].
30 -le(x,y) | x ^ y = x # label("Df: less than").  [clausify(1)].
31 -le(x,y) | c(c(x) v c(y)) = x.  [copy(30),rewrite([16(2)])].
32 le(x,y) | x ^ y != x # label("Df: less than").  [clausify(1)].
33 le(x,y) | c(c(x) v c(y)) != x.  [copy(32),rewrite([16(2)])].
34 i2(c1,c2) = 1 | le(c1,c2) # label("Proposition 2.10i2").  [deny(3)].
35 c2 v c(c1 v c2) = 1 | le(c1,c2).  [copy(34),rewrite([23(3),8(4)])].
36 i2(c1,c2) != 1 | -le(c1,c2) # label("Proposition 2.10i2").  [deny(3)].
37 c2 v c(c1 v c2) != 1 | -le(c1,c2).  [copy(36),rewrite([23(3),8(4)])].
38 c(1) = 0.  [back_rewrite(13),rewrite([16(2),7(2),15(2)])].
39 c(c(x) v c(x v y)) = x.  [back_rewrite(12),rewrite([16(2)])].
40 x v c(c(x) v c(y)) = x.  [back_rewrite(11),rewrite([16(1)])].
57 c2 v c(c1 v c2) = 1 | c(c(c1) v c(c2)) = c1.  [resolve(35,b,31,a)].
62 le(x,x v y).  [resolve(39,a,33,b)].
78 x v 0 = x.  [para(15(a,1),40(a,1,2,1)),rewrite([38(2)])].
79 x v c(y v c(x)) = x.  [para(18(a,1),40(a,1,2,1))].
91 0 v x = x.  [para(78(a,1),8(a,1)),flip(a)].
362 c2 v c(c1 v c2) = 1 | c1 v c2 = c2.  [para(57(b,1),79(a,1,2)),rewrite([8(11)])].
6823 c1 v c2 = c2.
[para(362(a,1),18(a,1,2,1)),rewrite([38(8),8(8),91(8)]),flip(b),merge(b)].
6824 -le(c1,c2).  [back_rewrite(37),rewrite([6823(4),15(4)]),xx(a)].
6828 $F.  [para(6823(a,1),62(a,2)),unit_del(a,6824)].

============================== end of proof ==========================


============================== PROOF =================================

% Proof 1 at 8.81 (+ 0.12) seconds.
% Length of proof is 50.
% Level of proof is 9.

1 le(x,y) <-> x = x ^ y # label("Df: less than") # label(non_clause).  [assumption].
3 i3(x,y) = 1 <-> le(x,y) # label("Proposition 2.10i3") # label(non_clause) #
label(goal).  [goal].
```

```
6 x = c(c(x)) # label("AxL1").  [assumption].
7 c(c(x)) = x.  [copy(6),flip(a)].
8 x v y = y v x # label("AxL2").  [assumption].
9 (x v y) v z = x v (y v z) # label("AxL3").  [assumption].
11 x v (x ^ y) = x # label("AxL5").  [assumption].
12 x ^ (x v y) = x # label("AxL6").  [assumption].
13 c(x) ^ x = 0 # label("AxOL1").  [assumption].
14 c(x) v x = 1 # label("AxOL2").  [assumption].
15 x v c(x) = 1.  [copy(14),rewrite([8(2)])].
16 x ^ y = c(c(x) v c(y)) # label("AxOL3").  [assumption].
17 x v (c(x) ^ (y v x)) = y v x # label("OMA").  [assumption].
18 x v c(x v c(y v x)) = y v x.  [copy(17),rewrite([16(3),7(2)])].
24 i3(x,y) = ((c(x) ^ y) v (c(x) ^ c(y))) v (c(x) v (x ^ y)) # label("Df: i3").
[assumption].
25 i3(x,y) = c(x v y) v (c(x v c(y)) v (c(x) v c(c(x) v c(y)))).
[copy(24),rewrite([16(3),7(3),16(7),7(6),7(6),8(7),16(9),9(14)])].
28 i5(x,y) = ((x ^ y) v (c(x) ^ y)) v (c(x) ^ c(y)) # label("Df: i5").  [assumption].
29 i5(x,y) = c(x v y) v (c(x v c(y)) v c(c(x) v c(y))).
[copy(28),rewrite([16(2),16(7),7(7),8(9),16(12),7(11),7(11),8(12)])].
30 -le(x,y) | x ^ y = x # label("Df: less than").  [clausify(1)].
31 -le(x,y) | c(c(x) v c(y)) = x.  [copy(30),rewrite([16(2)])].
32 le(x,y) | x ^ y != x # label("Df: less than").  [clausify(1)].
33 le(x,y) | c(c(x) v c(y)) != x.  [copy(32),rewrite([16(2)])].
34 i3(c1,c2) = 1 | le(c1,c2) # label("Proposition 2.10i3").  [deny(3)].
35 c(c1 v c2) v (c(c1 v c(c2)) v (c(c1) v c(c(c1) v c(c2)))) = 1 | le(c1,c2).
[copy(34),rewrite([25(3)])].
36 i3(c1,c2) != 1 | -le(c1,c2) # label("Proposition 2.10i3").  [deny(3)].
37 c(c1 v c2) v (c(c1 v c(c2)) v (c(c1) v c(c(c1) v c(c2)))) != 1 | -le(c1,c2).
[copy(36),rewrite([25(3)])].
38 c(1) = 0.  [back_rewrite(13),rewrite([16(2),7(2),15(2)])].
39 c(c(x) v c(x v y)) = x.  [back_rewrite(12),rewrite([16(2)])].
40 x v c(c(x) v c(y)) = x.  [back_rewrite(11),rewrite([16(1)])].
42 x v (y v z) = y v (x v z).  [para(8(a,1),9(a,1,1)),rewrite([9(2)])].
43 c(c1) v (c(c1 v c2) v (c(c1 v c(c2)) v c(c(c1) v c(c2)))) != 1 | -le(c1,c2).
[back_rewrite(37),rewrite([42(19),42(20)])].
44 c(c1) v (c(c1 v c2) v (c(c1 v c(c2)) v c(c(c1) v c(c2)))) = 1 | le(c1,c2).
[back_rewrite(35),rewrite([42(19),42(20)])].
46 x v (c(x) v y) = 1 v y.  [para(15(a,1),9(a,1,1)),flip(a)].
56 le(x,y) | c(c(y) v c(x)) != x.  [para(8(a,1),33(b,1,1))].
64 c(x) v c(x v y) = c(x).  [para(39(a,1),7(a,1,1)),flip(a)].
68 c(0 v c(x)) = x.  [para(15(a,1),39(a,1,1,2,1)),rewrite([38(3),8(3)])].
69 c(x v y) v c(x v c(x v y)) = c(x).
[para(39(a,1),18(a,1,2,1,2)),rewrite([8(5),64(11)])].
70 1 v x = 1.  [para(38(a,1),39(a,1,1,1)),rewrite([68(6)])].
74 x v (c(x) v y) = 1.  [back_rewrite(46),rewrite([70(5)])].
79 x v 0 = x.  [para(15(a,1),40(a,1,2,1)),rewrite([38(2)])].
81 x v x = x.  [para(38(a,1),40(a,1,2,1,2)),rewrite([8(3),68(4)])].
90 c(c1) v (c(c1 v c2) v (c(c1 v c(c2)) v c(c(c1) v c(c2)))) = 1 | c(c(c1) v c(c2)) = c1.
[resolve(44,b,31,a)].
93 0 v x = x.  [para(79(a,1),8(a,1)),flip(a)].
95 x v (x v y) = x v y.  [para(81(a,1),9(a,1,1)),flip(a)].
336 c(x) v (c(x v y) v z) = c(x) v z.  [para(64(a,1),9(a,1,1)),flip(a)].
347 c(c1) v c(c(c1) v c(c2)) = 1 | c(c(c1) v c(c2)) = c1.
[back_rewrite(90),rewrite([336(20),336(15)])].
350 c(c1) v c(c(c1) v c(c2)) != 1 | -le(c1,c2).
[back_rewrite(43),rewrite([336(20),336(15)])].
20075 c(c(c1) v c(c2)) = c1.
[para(347(a,1),29(a,2,1,1)),rewrite([29(17),7(27),95(26),7(27),7(32),74(31),38(26),8(26),
93(26),8(25),69(25),7(11),38(11),7(19),95(18),7(19),7(24),74(23),38(18),8(18),93(18),93(1
7)]),flip(b),merge(b)].
20076 -le(c1,c2).  [back_rewrite(350),rewrite([20075(8),8(4),15(4)]),xx(a)].
20077 $F.  [ur(56,a,20076,a),rewrite([8(5),20075(6)]),xx(a)].

============================== end of proof ==========================
```

Figure 3. Summary of a *prover9* ([2]) proof of Proposition 2.10i, for each of i = 1,2,3 from orthomodular lattice theory. The proofs assume the default inference rules of *prover9*. The general

form of a line in this proof is "*line_number conclusion [derivation]*", where *line_number* is a unique identifier of a line in the proof, and *conclusion* is the result of applying the *prover9* inference rules (such as *para*modulation, *copy*ing, and *rewrit*ing), noted in square brackets (denoting the *derivation*), to the lines cited in those brackets. Note that some of "logical" proof lines in the above have been transformed to two text lines, with the *derivation* appearing on a text line following a text line containing the first part of that logical line. The detailed syntax and semantics of these notations can be found in [2]. All *prover9* proofs are by default proofs by contradiction.

The total time to produce the proofs in Figure 3 on the platform described in Section 2.0 was approximately 11 seconds.

4.0 Discussion

The results of Section 3.0 motivate several observations:

1. The proofs in Figure 3 for i=1 and i=3 use L1, L2, L3, L5, L6, OL1, OL2, and OL3. In contrast, the proof for i=2 uses L1, L2, L5, L6, OL1, OL2, and OL3. This suggests (but does not prove) that Proposition 2.10, for i = 1,2, may have axiomatic bases that are more closely related to each other than they are to the axiomatic basis for i = 3. Future work will explore this hypothesis.

2. The proofs in Section 3.0 may be novel.

3. Companion papers provide proofs for i = 4, 5, and for Propositions 2.10i, i = 1,2,3,4,5, imply the OMA ([23]).

5.0 Acknowledgements

This work benefited from discussions with Tom Oberdan, Frank Pecchioni, Tony Pawlicki, and the late John K. Prentice, whose passion for foundations of physics inspired those of us privileged to have known him. For any infelicities that remain, I am solely responsible.

6.0 References

[1] von Neumann J. *Mathematical Foundations of Quantum Mechanics*. 1936. Translated by R. T. Beyer. Princeton. 1983.

[2] McCune WW. *prover9 and mace4.* URL http://www.cs.unm.edu/~mccune/prover9/. 2009.

[3] Horner JK. *prover9* scripts for Proposition 2.10. 2011. Available from the author on request.

[4] Dalla Chiara ML and Giuntini R. *Quantum Logics*. URL http://xxx.lanl.gov/abs/quant-ph/0101028. 2004.

[5] Megill ND and Pavičić M. Orthomodular lattices and quantum algebra. *International Journal of Theoretical Physics* 40 (2001), pp. 1387-1410.

[6] Akhiezer NI and Glazman IM. *Theory of Linear Operators in Hilbert Space. Volume I.* Translated by M. Nestell. Frederick Ungar. 1961.

[7] Holland, Jr. SS Orthomodularity in infinite dimensions: a theorem of M. Solèr. *Bulletin of the American Mathematical Society* 32 (1995), pp. 205-234.

[8] Marsden EL and Herman LM. *A condition for distribution in orthomodular lattices.* Kansas State University Technical Report #40. 1974.

[9] Knuth DE and Bendix PB. Simple word problems in universal algebras. In J. Leech, ed. *Computational Problems in Abstract Algebra.* Pergamon Press. 1970. pp. 263-297.

[10] Chang CC and Keisler HJ. *Model Theory.* North-Holland. 1990. pp. 38-39.

[11] Birkhoff G. *Lattice Theory*. Third Edition. American Mathematical Society. 1967.

[12] Church A. *Introduction to Mathematical Logic. Volume I.* Princeton. 1956.

[13] Jauch J. *Foundations of Quantum Mechanics.* Addison-Wesley. 1968.

[14] Megill ND. *Metamath.* URL http://us.metamath.org/qlegif/mmql.html#unify. 2004.

[15] Horner JK. An automated deduction system for orthomodular lattice theory. *Proceedings of the 2005 International Conference on Artificial Intelligence.* CSREA Press. 2005. pp. 260-265.

[16] Horner JK. An automated equational logic deduction of join elimination in orthomodular lattice theory. *Proceedings of the 2007 International Conference on Artificial Intelligence.* CSREA Press. 2007. pp. 481-488.

[17] Messiah A. *Quantum Mechanics*. Dover. 1958.

[18] Horner JK. Using automated theorem-provers to aid the design of efficient compilers for quantum computing. *Los Alamos National Laboratory Quantum Institute Workshop.* December 9–10, 2002. URL http://www.lanl.gov/science/centers/quantum/qls_pdfs/horner.pdf.

[19] Birkhoff G and von Neumann J. The logic of quantum mechanics. *Annals of Mathematics* 37 (1936), 823-243.

[20] Nielsen MA and Chuang L . *Quantum Computation and Quantum Information*. Cambridge. 2000.

[21] Pavičić M and Megill N. Quantum and classical implicational algebras with primitive implication. *International Journal of Theoretical Physics* 37 (1998), 2091-2098. ftp://m3k.grad.hr/pavicic/quantum-logic/1998-int-j-theor-phys-2.ps.gz.

[22] Horner JK. An automated deduction of the relative strength of orthomodular and weakly orthomodular lattice theory. *Proceedings of the 2009 International Conference on Artificial Intelligence*. CSREA Press. 2009. pp. 525-530.

[23] Horner JK. Quantum-implication-based equivalents of the Orthomodularity Law in quantum logic: Parts 1,2,4. Submitted to the *2012 International Conference on Foundations of Computer Science.*

Quantum-Implication-Based Equivalents of the Orthomodularity Law in Quantum Logic: Part 4

Jack K. Horner
P. O. Box 266
Los Alamos, New Mexico 87544 USA
email: jhorner@cybermesa.com

Abstract

The optimization of quantum computing circuitry and compilers at some level must be expressed in terms of quantum-mechanical behaviors and operations. In much the same way that the structure of conventional propositional (Boolean) logic (BL) is the logic of the description of the behavior of classical physical systems and is isomorphic to a Boolean algebra (BA), so also the algebra, C(H), of closed linear subspaces of (equivalently, the system of linear operators on (observables in)) a Hilbert space is a logic of the descriptions of the behavior of quantum mechanical systems and is a model of an ortholattice (OL). An OL can thus be thought of as a kind of "quantum logic" (QL). C(H) is also a model of an orthomodular lattice, which is an OL conjoined with the orthomodularity axiom (OMA). The rationalization of the OMA as a claim proper to physics has proven problematic, motivating the question of whether the OMA and its equivalents are required in an adequate characterization of QL. The OMA, it turns out, has strong connections to implication in QL. Here I provide automated deductions of two quantum-implication-based equivalents of the OMA from orthomodular lattice theory. The proofs may be novel.

Keywords: automated deduction, quantum computing, orthomodular lattice, Hilbert space

1.0 Introduction

The optimization of quantum computing circuitry and compilers at some level must be expressed in terms of the description of quantum-mechanical behaviors ([1], [17], [18], [20]). In much the same way that conventional propositional (Boolean) logic (BL,[12]) is the logical structure of description of the behavior of classical physical systems (e.g. "the measurements of the position and momentum of particle P are commutative", i.e., can be measured in either order, yielding the same results) and is isomorphic to a Boolean lattice ([10], [11], [19]), so also the algebra, *C(H)*, of the closed linear subspaces of (equivalently, the system of linear operators on (observables in)) a Hilbert space *H* ([1], [4], [6], [9], [13]) is *a* logic of the descriptions of the behavior of quantum mechanical systems (e.g., "the measurements of the position and momentum of particle P are *not* commutative") and is a model ([10]) of an ortholattice (OL; [4]). An OL can thus be thought of as a kind of "quantum logic" (QL; [19]). *C(H)* is also a model of (i.e., isomorphic to a set of sentences which hold in) an orthomodular lattice (OML; [4], [7]), which is an OL conjoined with the orthomodularity axiom (OMA; see Figure 1). The rationalization of the OMA as a claim proper to physics has proven problematic ([13], Section 5-6), motivating the question of whether the OMA is required in an adequate characterization of QL. Thus formulated, the question suggests that the OMA and its equivalents are specific to an OML, and that as a consequence, banning the OMA from QL yields a "truer" quantum logic. The OMA, it turns out, has strong

connections to implication in QL, as demonstrated in the following.

Lattice axioms

```
      x = c(c(x))                       (AxLat1)
      x v y = y v x                     (AxLat2)
      (x v y) v z = x v (y v z)          (AxLat3)
      (x ^ y) ^ z = x ^ (y ^ z)          (AxLat4)
      x v (x ^ y) = x                   (AxLat5)
      x ^ (x v y) = x                   (AxLat6)
```

Ortholattice axioms

```
      c(x) ^ x = 0                      (AxOL1)
      c(x) v x = 1                      (AxOL2)
      x ^ y = c(c(x) v c(y))            (AxOL3)
```

Orthomodularity axiom

```
      y v (c(y) ^ (x v y)) = x v y      (OMA)
```

Definitions of implications and partial order

```
   i1(x,y) = c(x) v (x ^ y).
   i2(x,y) = i1(c(y), c(x).
   i3(x,y) = (c(x) ^ y) v (c(x) ^ c(y)) v i1(x,y).
   i4(x,y) = i3(c(y), c(x)).
   i5(x,y) = (x ^ y) v (c(x) ^ y) v (c(x) ^ c(y)).
   le(x,y) = (x = (x ^ y)).
```

where
   x, y are variables ranging over lattice nodes
   ^ is lattice meet
   v is lattice join
   c(x) is the orthocomplement of x
   i1(x,y) means $x \rightarrow_1 y$ (Sasaki implication)
   i2(x,y) means $x \rightarrow_2 y$ (Dishkant implication)
   i3(x,y) means $x \rightarrow_3 y$ (Kalmbach implication)
   i4(x,y) means $x \rightarrow_4 y$ (non-tollens implication)
   i5(x,y) means $x \rightarrow_5 y$ (relevance implication)
   le(x,y) means $x \leq y$
   <-> means if and only if
   = is equivalence ([12])
   1 is the maximum lattice element (= x v c(x))
   0 is the minimum lattice element (= c(1))

Figure 1. Lattice, ortholattice, orthomodularity axioms, and some definitions.

Consider the proposition shown in Figure 2:

$$((x \rightarrow_i y) = 1) \quad <-> \quad le(x,y)$$

where $i = 1,2,3,4,5$.

Figure 2. Proposition 2.10

Note that there are five implications in QL (there is only one in BL). Proposition 2.10 can be regarded as a generalization of the BL definition of implication, sometimes denoted $\rightarrow_0$.

2.0 Method

The OML axiomatizations of Megill, Pavičić, and Horner ([5], [14], [15], [16], [21], [22]) were implemented in a *prover9* ([2]) script ([3]) configured to derive Proposition 2.10i, for each of i = 4,5 from orthomodular lattice theory ,then executed in that framework on a Dell Inspiron 545 with an Intel Core2 Quad CPU Q8200 (clocked @ 2.33 GHz) and 8.00 GB RAM, running under the *Windows Vista Home Premium /Cygwin* operating environment.

3.0 Results

Figure 3 shows the proofs, generated by [3] on the platform described in Section 2.0, that orthomodular lattice theory implies Proposition 2.10i, for each of i=4,5.

```
============================== PROOF =================================

% Proof 1 at 6.52 (+ 0.22) seconds.
% Length of proof is 43.
% Level of proof is 9.

1 le(x,y) <-> x = x ^ y # label("Df: less than") # label(non_clause).
[assumption].
3 i4(x,y) = 1 <-> le(x,y) # label("Proposition 2.10i4") # label(non_clause) #
label(goal).  [goal].
6 x = c(c(x)) # label("AxL1").  [assumption].
7 c(c(x)) = x.  [copy(6),flip(a)].
8 x v y = y v x # label("AxL2").  [assumption].
9 (x v y) v z = x v (y v z) # label("AxL3").  [assumption].
11 x v (x ^ y) = x # label("AxL5").  [assumption].
12 x ^ (x v y) = x # label("AxL6").  [assumption].
13 c(x) ^ x = 0 # label("AxOL1").  [assumption].
14 c(x) v x = 1 # label("AxOL2").  [assumption].
15 x v c(x) = 1.  [copy(14),rewrite([8(2)])].
16 x ^ y = c(c(x) v c(y)) # label("AxOL3").  [assumption].
17 x v (c(x) ^ (y v x)) = y v x # label("OMA").  [assumption].
18 x v c(x v c(y v x)) = y v x.  [copy(17),rewrite([16(3),7(2)])].
22 i2(x,y) = c(c(y)) v (c(y) ^ c(x)) # label("Df: i2").  [assumption].
23 i2(x,y) = y v c(y v x).  [copy(22),rewrite([7(3),16(4),7(3),7(3)])].
26 i4(x,y) = ((c(c(y)) ^ c(x)) v (c(c(y)) ^ c(c(x)))) v (c(c(y)) v (c(y) ^
c(x))) # label("Df: i4").  [assumption].
27 i4(x,y) = y v (c(y v x) v (c(c(y) v x) v c(c(y) v c(x)))).
[copy(26),rewrite([7(3),16(3),7(4),7(6),7(6),16(5),7(11),16(12),7(11),7(11),8(1
3),9(13)])].
30 -le(x,y) | x ^ y = x # label("Df: less than").  [clausify(1)].
31 -le(x,y) | c(c(x) v c(y)) = x.  [copy(30),rewrite([16(2)])].
32 le(x,y) | x ^ y != x # label("Df: less than").  [clausify(1)].
33 le(x,y) | c(c(x) v c(y)) != x.  [copy(32),rewrite([16(2)])].
34 i4(c1,c2) = 1 | le(c1,c2) # label("Proposition 2.10i4").  [deny(3)].
35 c2 v (c(c1 v c2) v (c(c1 v c(c2)) v c(c(c1) v c(c2)))) = 1 | le(c1,c2).
[copy(34),rewrite([27(3),8(4),8(9),8(15)])].
36 i4(c1,c2) != 1 | -le(c1,c2) # label("Proposition 2.10i4").  [deny(3)].
37 c2 v (c(c1 v c2) v (c(c1 v c(c2)) v c(c(c1) v c(c2)))) != 1 | -le(c1,c2).
[copy(36),rewrite([27(3),8(4),8(9),8(15)])].
38 c(1) = 0.  [back_rewrite(13),rewrite([16(2),7(2),15(2)])].
39 c(c(x) v c(x v y)) = x.  [back_rewrite(12),rewrite([16(2)])].
40 x v c(c(x) v c(y)) = x.  [back_rewrite(11),rewrite([16(1)])].
42 x v (y v z) = y v (x v z).  [para(8(a,1),9(a,1,1)),rewrite([9(2)])].
```

```
57 c2 v (c(c1 v c2) v (c(c1 v c(c2)) v c(c(c1) v c(c2)))) = 1 | c(c(c1) v
c(c2)) = c1.  [resolve(35,b,31,a)].
62 le(x,x v y).  [resolve(39,a,33,b)].
78 x v 0 = x.  [para(15(a,1),40(a,1,2,1)),rewrite([38(2)])].
79 x v c(y v c(x)) = x.  [para(18(a,1),40(a,1,2,1))].
91 0 v x = x.  [para(78(a,1),8(a,1)),flip(a)].
196 x v (c(y v c(x)) v z) = x v z.  [para(79(a,1),9(a,1,1)),flip(a)].
336 c(c(c1) v c(c2)) = c1 | c2 v c(c2 v (c(c1 v c2) v (c(c1 v c(c2)) v c(c(c1)
v c(c2))))) = c2.
[para(57(a,1),23(a,2,2,1)),rewrite([23(27),38(33),8(33),91(33)])].
4403 x v (y v (c(z v c(x)) v u)) = y v (x v u).
[para(196(a,1),42(a,1,2)),flip(a)].
4550 c(c(c1) v c(c2)) = c1 | c1 v c2 = c2.
[back_rewrite(336),rewrite([4403(28),79(21),8(15),18(17)])].
4552 c2 v c(c1 v c2) != 1 | -le(c1,c2).
[back_rewrite(37),rewrite([4403(19),79(12),8(6)])].
16868 c1 v c2 = c2.  [para(4550(a,1),79(a,1,2)),rewrite([8(8)]),merge(b)].
16869 -le(c1,c2).  [back_rewrite(4552),rewrite([16868(4),15(4)]),xx(a)].
16876 $F.  [para(16868(a,1),62(a,2)),unit_del(a,16869)].

============================== end of proof ==========================



============================== PROOF =================================

% Proof 1 at 95.86 (+ 1.70) seconds.
% Length of proof is 50.
% Level of proof is 10.

1 le(x,y) <-> x = x ^ y # label("Df: less than") # label(non_clause).
[assumption].
3 i5(x,y) = 1 <-> le(x,y) # label("Proposition 2.10i5") # label(non_clause) #
label(goal).  [goal].
6 x = c(c(x)) # label("AxL1").  [assumption].
7 c(c(x)) = x.  [copy(6),flip(a)].
8 x v y = y v x # label("AxL2").  [assumption].
9 (x v y) v z = x v (y v z) # label("AxL3").  [assumption].
11 x v (x ^ y) = x # label("AxL5").  [assumption].
12 x ^ (x v y) = x # label("AxL6").  [assumption].
13 c(x) ^ x = 0 # label("AxOL1").  [assumption].
14 c(x) v x = 1 # label("AxOL2").  [assumption].
15 x v c(x) = 1.  [copy(14),rewrite([8(2)])].
16 x ^ y = c(c(x) v c(y)) # label("AxOL3").  [assumption].
17 x v (c(x) ^ (y v x)) = y v x # label("OMA").  [assumption].
18 x v c(x v c(y v x)) = y v x.  [copy(17),rewrite([16(3),7(2)])].
28 i5(x,y) = ((x ^ y) v (c(x) ^ y)) v (c(x) ^ c(y)) # label("Df: i5").
[assumption].
29 i5(x,y) = c(x v y) v (c(x v c(y)) v c(c(x) v c(y))).
[copy(28),rewrite([16(2),16(7),7(7),8(9),16(12),7(11),7(11),8(12)])].
30 -le(x,y) | x ^ y = x # label("Df: less than").  [clausify(1)].
31 -le(x,y) | c(c(x) v c(y)) = x.  [copy(30),rewrite([16(2)])].
32 le(x,y) | x ^ y != x # label("Df: less than").  [clausify(1)].
33 le(x,y) | c(c(x) v c(y)) != x.  [copy(32),rewrite([16(2)])].
34 i5(c1,c2) = 1 | le(c1,c2) # label("Proposition 2.10i5").  [deny(3)].
35 c(c1 v c2) v (c(c1 v c(c2)) v c(c(c1) v c(c2))) = 1 | le(c1,c2).
[copy(34),rewrite([29(3)])].
36 i5(c1,c2) != 1 | -le(c1,c2) # label("Proposition 2.10i5").  [deny(3)].
37 c(c1 v c2) v (c(c1 v c(c2)) v c(c(c1) v c(c2))) != 1 | -le(c1,c2).
[copy(36),rewrite([29(3)])].
38 c(1) = 0.  [back_rewrite(13),rewrite([16(2),7(2),15(2)])].
39 c(c(x) v c(x v y)) = x.  [back_rewrite(12),rewrite([16(2)])].
40 x v c(c(x) v c(y)) = x.  [back_rewrite(11),rewrite([16(1)])].
```

```
42 x v (y v z) = y v (x v z).  [para(8(a,1),9(a,1,1)),rewrite([9(2)])].
46 x v c(x v c(x v y)) = y v x.  [para(8(a,1),18(a,1,2,1,2,1))].
48 x v (y v c(x v (y v c(z v (x v y))))) = z v (x v y).
[para(18(a,1),9(a,1)),rewrite([9(7)]),flip(a)].
57 c(c1 v c2) v (c(c1 v c(c2)) v c(c(c1) v c(c2))) = 1 | c(c(c1) v c(c2)) = c1.
[resolve(35,b,31,a)].
62 le(x,x v y).  [resolve(39,a,33,b)].
63 c(x) v c(x v y) = c(x).  [para(39(a,1),7(a,1,1)),flip(a)].
67 c(0 v c(x)) = x.  [para(15(a,1),39(a,1,1,2,1)),rewrite([38(3),8(3)])].
69 1 v x = 1.  [para(38(a,1),39(a,1,1,1)),rewrite([67(6)])].
78 x v 0 = x.  [para(15(a,1),40(a,1,2,1)),rewrite([38(2)])].
79 x v c(y v c(x)) = x.  [para(18(a,1),40(a,1,2,1))].
83 x v (y v c(x v c(z v x))) = y v (z v x).  [para(18(a,1),42(a,1,2)),flip(a)].
91 0 v x = x.  [para(78(a,1),8(a,1)),flip(a)].
196 x v (c(y v c(x)) v z) = x v z.  [para(79(a,1),9(a,1,1)),flip(a)].
204 c(x v c(y)) v (z v y) = z v y.
[para(79(a,1),48(a,1,2,2,1,2,2,1,2)),rewrite([196(10),83(9),79(9)])].
334 c(c(c1) v c(c2)) = c1 | c(c1 v c2) v (c(c1 v c(c2)) v (c(c(c1) v c(c2)) v
x)) = 1.  [para(57(a,1),9(a,1,1)),rewrite([69(10),9(26)]),flip(b)].
18704 c(c(c1) v c(c2)) = c1 | c2 v c(c1 v c2) = 1.
[para(204(a,1),334(b,1,2)),rewrite([8(20),79(20),8(14)])].
75845 c2 v c(c1 v c2) = 1 | c1 v c2 = c2.
[para(18704(a,1),79(a,1,2)),rewrite([8(11)])].
76052 c1 v c2 = c2.
[para(75845(a,1),18(a,1,2,1)),rewrite([38(8),8(8),91(8)]),flip(b),merge(b)].
76053 c(c2) v (c(c1 v c(c2)) v c(c(c1) v c(c2))) != 1 | -le(c1,c2).
[back_rewrite(37),rewrite([76052(3)])].
76058 le(c1,c2).  [para(76052(a,1),62(a,2))].
76059 c1 v c(c1 v c(c2)) = c2.
[para(76052(a,1),46(a,1,2,1,2,1)),rewrite([8(10),76052(10)])].
76068 c(c1) v c(c2) = c(c1).  [para(76052(a,1),63(a,1,2,1))].
76662 $F.
[back_unit_del(76053),rewrite([76068(12),7(10),8(9),76059(9),8(4),15(4)]),xx(a)
,unit_del(a,76058)].

============================== end of proof ==========================
```

Figure 3. Summary of a *prover9* ([2]) derivations of Proposition 2.10i for each i = 4,5, from orthomodular lattice theory. The proofs assume the default inference rules of *prover9*. The general form of a line in this proof is "*line_number conclusion [derivation]*", where *line_number* is a unique identifier of a line in the proof, and *conclusion* is the result of applying the *prover9* inference rules (such as *para*modulation, *copy*ing, and *rewrit*ing), noted in square brackets (denoting the *derivation*), to the lines cited in those brackets. Note that some of "logical" proof lines in the above have been transformed to two text lines, with the *derivation* appearing on a text line following a text line containing the first part of that logical line. The detailed syntax and semantics of these notations can be found in [2]. All *prover9* proofs are by default proofs by contradiction.

The total time to produce the proofs in Figure 3 on the platform described in Section 2.0 was approximately 110 seconds.

4.0 Discussion

The results of Section 3.0 motivate several observations:

1. Both proofs in Figure 3 use L1, L2, L3, L5, L6, OL1, OL2, and OL3. This suggests (but does not prove) that the implications defined by i = 4, 5 share an

axiomatic basis. Future work will investigate this suggestion.

2. The proofs in Section 3.0 may be novel.

3. Companion papers provide proofs for i = 1,2,3, and for the claim that "Propositions 2.10i, i = 1,2,3,4,5, imply the OMA" ([23]).

5.0 Acknowledgements

This work benefited from discussions with Tom Oberdan, Frank Pecchioni, Tony Pawlicki, and the late John K. Prentice, whose passion for foundations of physics inspired those of us privileged to have known him. For any infelicities that remain, I am solely responsible.

6.0 References

[1] von Neumann J. *Mathematical Foundations of Quantum Mechanics*. 1936. Translated by R. T. Beyer. Princeton. 1983.

[2] McCune WW. *prover9 and mace4.* URL http://www.cs.unm.edu/~mccune/prover9/. 2009.

[3] Horner JK. *prover9* scripts for Proposition 2.10. 2011. Available from the author on request.

[4] Dalla Chiara ML and Giuntini R. *Quantum Logics*. URL http://xxx.lanl.gov/abs/quant-ph/0101028. 2004.

[5] Megill ND and Pavičić M. Orthomodular lattices and quantum algebra. *International Journal of Theoretical Physics* 40 (2001), pp. 1387-1410.

[6] Akhiezer NI and Glazman IM. *Theory of Linear Operators in Hilbert Space. Volume I.* Translated by M. Nestell. Frederick Ungar. 1961.

[7] Holland, Jr. SS Orthomodularity in infinite dimensions: a theorem of M. Solèr. *Bulletin of the American Mathematical Society* 32 (1995), pp. 205-234.

[8] Marsden EL and Herman LM. *A condition for distribution in orthomodular lattices.* Kansas State University Technical Report #40. 1974.

[9] Knuth DE and Bendix PB. Simple word problems in universal algebras. In J. Leech, ed. *Computational Problems in Abstract Algebra.* Pergamon Press. 1970. pp. 263-297.

[10] Chang CC and Keisler HJ. *Model Theory.* North-Holland. 1990. pp. 38-39.

[11] Birkhoff G. *Lattice Theory.* Third Edition. American Mathematical Society. 1967.

[12] Church A. *Introduction to Mathematical Logic. Volume I.* Princeton. 1956.

[13] Jauch J. *Foundations of Quantum Mechanics.* Addison-Wesley. 1968.

[14] Megill ND. *Metamath.* URL http://us.metamath.org/qlegif/mmql.html#unify. 2004.

[15] Horner JK. An automated deduction system for orthomodular lattice theory. *Proceedings of the 2005 International Conference on Artificial Intelligence.* CSREA Press. 2005. pp. 260-265.

[16] Horner JK. An automated equational logic deduction of join elimination in orthomodular lattice theory. *Proceedings of the 2007 International Conference on Artificial Intelligence.* CSREA Press. 2007. pp. 481-488.

[17] Messiah A. *Quantum Mechanics*. Dover. 1958.

[18] Horner JK. Using automated theorem-provers to aid the design of efficient compilers for quantum computing. *Los Alamos National Laboratory Quantum Institute Workshop.* December 9–10, 2002. URL http://www.lanl.gov/science/centers/quantum/qls_pdfs/horner.pdf.

[19] Birkhoff G and von Neumann J. The logic of quantum mechanics. *Annals of Mathematics* 37 (1936), 823-243.

[20] Nielsen MA and Chuang L . *Quantum Computation and Quantum Information*. Cambridge. 2000.

[21] Pavičić M and Megill N. Quantum and classical implicational algebras with primitive implication. *International Journal of Theoretical Physics* 37 (1998), 2091-2098. ftp://m3k.grad.hr/pavicic/quantum-logic/1998-int-j-theor-phys-2.ps.gz.

[22] Horner JK. An automated deduction of the relative strength of orthomodular and weakly orthomodular lattice theory. *Proceedings of the 2009 International Conference on Artificial Intelligence*. CSREA Press. 2009. pp. 525-530.

[23] Horner JK. Quantum-implication-based equivalents of the Orthomodularity Law in quantum logic: Parts 1, 2, 3. Submitted to the 2*012 International Conference on Foundations of Computer Science*.

SESSION

NOVEL SYSTEMS, LANGUAGES, QUANTUM SECRET SHARING

Chair(s)

Prof. Hamid R. Arabnia

A static type system for the Language of Effective Definitions (LED)

Jarred Blount and J. Nelson Rushton
Department of Computer Science, Texas Tech University

Abstract - *This paper augments the Language of Effective Definitions (LED) with a static type system, supporting prenex polymorphism, but not user-defined types. The semantics of LED are recast in the framework of small-step reduction rule semantics to facilitate the type safety argument. The main theorem of this paper is type safety for the augmented system.*

Keywords: Static Type System, Functional Programming Language

1 Introduction

The Language of Effective Definitions (LED) was introduced in [1], as a formal language for defining computable functions and predicates. The objectives of the language are (1) that it be definable in just a few pages, (2) that it have precise formal semantics, and (3) that its definitions resemble informal mathematical definitions as closely as possible.

A type system has been introduced for LED which permits function overloading, together with and an algorithm for certifying that overloading does not introduce ambiguities [2]. We conjectured that the algorithm is *sound* in the sense it never certifies a program in which ambiguities actually occur, and *complete* in the sense that if the algorithm fails then ambiguities do exist in the program; but we have only proven the algorithm to be sound.

In this paper we present a type system for LED that is *safe*, meaning that well typed programs cannot encounter type errors during execution. In order to use the standard method for establishing this, known as *the syntactic approach*[3], the semantics of LED are recast here in the form of a small-step reduction system. The reduction rules may be applied nondeterministically, and so the same safety theorem already applies when using a variety of optimized algorithms for evaluation (optimized, in particular, by making clever choices of how to resolve the nondeterminism). The paper is organized as follows: Section 2 defines syntax, Section 3 gives semantics, Section 4 gives the type system, section 5 is the type safety argument.

2 Abstract Syntax

A *symbol* is a string of non-white-space characters not beginning with a digit and not containing parentheses or single quotes (').

A *reserved symbol* is any of the following identifiers: `def lambda branch if set tuple error.`

A *built-in function symbol* is any of the following: `^ * / mod + - = < > <= >= in and intersect or union \ card`.

A *digit string* is a string of one or more digits.

A *numeral* is either a digit string or a digit string preceded by a minus sign (−).

An *atom* is an arbitrary sequence of printable characters enclosed by double quotes (").

A *constant* is a built-in function symbol, a numeral, or an atom.

The *expressions* of LED have the following (abstract) syntax:

e ::= c
| a
| (e_1 … e_n)
| (`set` e … e)
| (`tuple` e … e)
| (`lambda` (a… a) e)
| (`branch` (`if` e e) … (`if` e e))
| `error`

where c and a are non-terminals representing arbitrary constants, and symbols respectively.

A *lambda abstraction* is an expression of the form (`lambda` (x_1 … x_n) e), where x_1 … x_n are symbols, and e is an expression. The symbols x_1 … x_n are the *parameters* of (`lambda` (x_1 … x_n) e), and are bound in (`lambda` (x_1 … x_n) e). A symbol that is not bound is *free*. $FV(e)$ is the set of symbols that occur free in expression e. An expression with no free variables is *closed*. The abstraction (`lambda` (x_1 … x_n) e) is *well-formed* if the symbols $x_1 \ldots x_n$ are pairwise

distinct. We restrict our attention to expression containing only well-formed lambda abstractions.

A *function definition* is an expression of the form, (`def` (f $x_1 \ldots x_n$) e) where $n \geq 0$, f is a symbol, $x_1 \ldots x_n$ are symbols, and e is an expression. The symbol f is the *defined function symbol* of the function definition, and e is called the *body* of the function definition. The symbols $x_1 \ldots x_n$ are its *parameters* and bound within the function definition. A *symbol definition* is an expression of the form, (`def` g e) where $n \geq 0$, g is a symbol, $x_1 \ldots x_n$ are symbols, and e is an expression. The symbol g is the *defined symbol* of the symbol definition. The expression e is called the *body* of the symbol definition. A *program* is a set of definitions, and a definition which is an element of program P is called a *definition of P*. The defined function symbols of P and the defined symbols of P may be called, collectively, the *defined symbols of P*. Given a program P, an expression e is *P-closed* if FV(e) contains only defined symbols of P. A program is *well-formed* if no defined symbol of P occurs as a parameter in P, and every body of every definition is P-closed.

3 Semantics

Before the reduction rules are detailed, some preliminary definitions must be given. A *set literal* is an expression of the form (`set` $v_1 \ldots v_n$) where $v_1 \ldots v_n$ are values. A *tuple literal* takes the form (`tuple` $v_1 \ldots v_n$) where n>1 and $v_1 \ldots v_n$ are values. A *value* is a constant, symbol, set literal, tuple literal, or lambda abstraction. An *answer* is either a value or the reserved symbol `error`. Given a program P, a *P-value* is a value or defined function symbol of P. For the remainder of this paper let P be a fixed program. The meta-variables e,e_1,e_2,… will vary over expressions; v,v_1,v_2,... will vary over values; x,x_1,... will vary over symbols; n,n_1,n_2,… will vary over numerals; s,s_1,s_2,… will vary over set literals, and *Op* will vary over built-in function symbols.

A *substitution* is a finite set of pairs (x, e) where x is a variable symbol and e is an expression, such that no variable occurs as the first coordinate of more than one such pair. If e is an expression and S is a substitution, then $e[S]$ denotes the expression obtained from e by replacing all free occurrences of x with g whenever $(x,g) \in S$. The substitution of e for x in p is *safe* if no free occurrence of a variable in e becomes bound when it is substituted for x in p. All substitutions described in the semantics are presumed to be safe, by renaming variables whenever necessary. The capture avoiding substitution of P-closed expression e_1 for P-closed expression e_2 in expression e is written $e[e_1:=e_2]$ is defined similar to the 'regular' substitution used to replace free variables with values.

The semantics below are based upon an operational formulation of the language's semantics by term rewriting,. The *reduction* relation is a binary relation over closed expressions e_1 and e_2, written $e_1 \Rightarrow e_2$. We say "e_1 *reduces* to e_2" if $e_1 \Rightarrow e_2$ is the conclusion of a deduction constructed according to the inference rules below. Let $\Rightarrow^*$ be the reflexive and transitive closure of $\Rightarrow$. For each program P, the partial function $eval_P$ is defined from closed expressions to values so that the following holds:

(eval) $eval_P(e) = v$ iff $e \Rightarrow^* v$

The relationship between the semantics given in the section and the semantics given in [1] described by the following conjecture.

Soundness: Given well-formed program P,
if $eval_P(e)=v$ then e denotes v under P.

Where the precise meaning of "denotes under P" is given in [1]. It is straightforward to see the definition of value given earlier in the section corresponds to the definition of datum in [1], ie. each builtin function symbol, numeral, atom, set literal, and tuple literal corresponds to a datum.

As in [1], builtin function symbols are only meaningful if applied to appropriate arguments, ie. (/ 1 0) is application of '/' to erroneous arguments. The denotation rules in [1], place these restrictions in each semantic rule. Here we specify the relation *Defined*((*Op* $v_1 \ldots v_n$)), which essentially collects all of the conditions under which an application of a built-in function symbol to values $v_1,\ldots,v_n$ is meaningful.

Defined((*Op* n_1 n_2)) if *Op* ∈ {+,-,*+, -, *, ^, < >, <=, >=}
Defined((^ n_1 n_2)) if n_1 is zero implies n_2 is nonnegative
Defined((*Op* n_1 n_2)) if *Op* in {/,mod} and n is not 0
Defined((*Op* v_1 v_2)) if *Op* in {and, or} and v_1,v_2 in {true, false}
Defined((not v_1)) if v_1 in {true,false}
Defined((in v_1 s_2))
Defined((*Op* s_1 s_2)) if *Op* in {union, intersect, setminus},
Defined((card s_1))
Defined((= v v_2))

A *built-in redex* is an application of a built-in function symbol to a sequence of values, eg. (+ 1 2), and (not false), and (union (set 1 2) (set 3)). The partial function δ from built-in redexes to values, and *Defined* must satisfy the following correctness condition:

If *Defined*((*Op* $v_1 \ldots v_n$)) then there is some value v such that δ((*Op* $v_1 \ldots v_n$)) = v and "(*Op* v_1 ..v_n) denotes v"

Reduction rules

[Delta]
($Op\ v_1 \ldots v_n$) ⇒ δ($Op\ v_1 \ldots v_n$) if *Defined*(Op, $v_1, \ldots, v_n$)
($Op\ v_1 \ldots v_n$) ⇒ `error` otherwise

Data Structures
[set] (set $e_1 \ldots e_n$) ⇒ (set $e_1 \ldots e_n$)[e_i:=e] (for expressions $e\ e_1 \ldots e_n$ where some $1 \le i \le n$ $e_i \Rightarrow e$)

[tuple] (tuple $e_1 \ldots e_n$) ⇒ (tuple $e_1 \ldots e_n$)[e_i:=e] (for expressions $e\ e_1 \ldots e_n$ where some $1 \le i \le n$ $e_i \Rightarrow e$)

Application

[app] ($e_1 \ldots e_n$) ⇒ ($e_1 \ldots e_n$) [e_i:=e] if $e_i \Rightarrow e$ (for expressions $e_1 \ldots e_n$ where some $1 \le i \le n$ $e_i \Rightarrow e$)

Beta reduction

[β] ((lambda ($x_1 \ldots x_n$) e) $v_1 \ldots v_n$) ⇒ e[{(x_1,v_1),…, (x_n,v_n)}] (for symbols $x_1 \ldots x_n$, and expressions e, values $v_1 \ldots v_n$)

Defined function

[deffun] ($a\ v_2 \ldots v_n$) ⇒ e[{(x_2,v_2),…,(x_n,v_n)}] (for (def ($a\ x_2 \ldots x_n$) e) in P and values $v_2 \ldots v_n$)

[defsym] $a \Rightarrow e$ (for (def $a\ e$) in P)

Branch

[branchT] (branch (if $v_1\ e_1$)…(if $v_n\ e_n$)) ⇒ e_i (for values $v_1 \ldots v_n$, expression $e_1 \ldots e_n$ such that some $1 \le i \le n$ g_i=true)

[branchF] (branch (if false e_1)…(if false e_n)) ⇒ error (for expressions $e_1 \ldots e_n$)

[branchG] (branch (if $g_1\ e_1$)…(if $g_n\ e_n$)) ⇒ (branch (if $g_1\ e_1$)…(if $g_n\ e_n$))[g_i:=g] (for expressions $g_1 \ldots g_n$ and $e_1 \ldots e_n$ where some $1 \le i \le n$ $g_i \Rightarrow g$)

Error propagation

($a_1 \ldots a_n$) ⇒ error (for answers $a_1 \ldots a_n$ where some $1 \le i \le n$ a_i=error)

(branch (if $g_1\ e_1$)…(if $g_n\ e_n$)) ⇒ error (for expressions $g_1 \ldots g_n$ and $e_1 \ldots e_n$ where some $1 \le i \le n$ g_i=error)

(tuple $e_1 \ldots e_n$) ⇒ error (for expressions $e_1 \ldots e_n$ where some $1 \le i \le n$ e_i=error)

(set $e_1 \ldots e_n$) ⇒ error (for expressions $e_1 \ldots e_n$ where some $1 \le i \le n$ e_i=error)

4 Type System

Before introducing the inference system that assigns an expression a particular type, we must define the type language. Each sort of value has a different type, so the type language has *simple* types as well as *compound* types. For example, the type of the successor function (`lambda (x).x+1`) is `int→int`. In the same way the identity function (`lambda (x).x`) for integers has type `int→int`, but for booleans it has type `bool→bool`. It is clear that the identity function may be defined without taking into account the type of its parameter. To express this abstraction of the type of the parameter, the type variable α, is bound by a quantifier, so the type of the polymorphic identity function is `all` α.α→α. Similarly, the types of (`set 1 2`) and (`tuple 1 2`) are {`int`} and `int×int`, respectively.

The type language contains two syntactic categories, *types* and *type schemas*.

Types: a *type* τ is either
1. one of the *scalar types*: `int`, `bool`, `atom`,
2. a type variable α,
3. a *function type*, $\tau_1 \rightarrow \tau_2$, where τ_1 and τ_2 are types,
4. a *tuple type*, $\tau_1 \times \ldots \times \tau_n$, where $n>1$ and each τ_i is a type,
5. a set type, {τ}, where τ is a type.

Type schemas: a *type scheme* σ is either
1. a type τ,
2. a polymorphic type σ = `all` $\alpha_1 \ldots \alpha_n.\tau$ where τ is a type, and $\alpha_1 \ldots \alpha_n$ are distinct type variables.

Type variables $\alpha_1 \ldots \alpha_n$ are *bound* in (`all` $\alpha_1 \ldots \alpha_n.\tau$), variables that are not bound are *free*. We will write *FTV(σ)* and *BTV(σ)* for the sets of free and bound variables of a type scheme σ. A type schema σ_1 is called an *instance* of a type scheme σ_2, if there exists a substitution S of types for free type variables such that $\sigma_1 = \sigma_2[S]$. Instantiation acts on *free* variables: if *S* is written $[\alpha_i \mapsto \tau_i]$ with $\alpha_i \in$ FTV(σ) then σ[S] is obtained by replacing every free occurrence of α_i with τ_i (renaming the bound variable in σ if necessary). The domain of *S* is written *domain(S)*.

The type scheme σ_1 has a *generic instance* σ_2, written $\sigma_1 \succ \sigma_2$, if there exists substitution *S* such that $\tau_2 = \tau_1[S]$ where *domain*(*S*) ⊆ {$\alpha_1,\ldots,\alpha_n$}, and {$\beta_1,\ldots,\beta_m$ } ∩ FTV(σ_1) = ∅ when σ_1= (all α1...αn.τ1) , and σ_2= (`all` $\beta_1 \ldots \beta_m.\tau_2$), and $\tau_1 = \tau_2$ when σ_1 and σ_2 are types instead of polymorphic types.

Examples of generic instance.
α ≻ α

`int×bool` ≻ `int×bool`
`all` α.α→α ≻ `int→int`
`all` $\alpha_1\,\alpha_2.\alpha_1\to\alpha_2$ ≻ `int→bool`
`all` α.α→α ≻ $\alpha_1\to\alpha_1$
`all` $\alpha_1\,\alpha_2.\alpha_1\to\alpha_2$ ≻ `all` β.β→α

Intuitively, the type of an expression containing symbols, either defined or variable, depends on context in which the expression appears. This contextual information is represented in the type environment, Γ. A *type environment* is a finite mapping from symbols to type schemes, written $\{x_1\mapsto\sigma_1,\ldots,x_n\mapsto\sigma_n\}$. Given symbol *x* type scheme *σ* and type environment Γ, the *update of Γ with* $x\mapsto\sigma$, written $x\mapsto\sigma\cdot\Gamma$, is a type environment gotten by updating Γ to now associate *x* with *σ*, so that $\Gamma(x)=\sigma$. The free type variables, written FTV(Γ), of a type environment Γ are the free type variables of the type schemas in its range.

To make the presentation of the type rules more clear, the types of constants are represented by the definition of the *TypeOf* function. *TypeOf* is a total function from constants to type schemas, defined below.

TypeOf (*n*) = `int` (for numeral *n*)
TypeOf(*a*) = `atom` (for atom *a*)
TypeOf (`true`)=`bool`
TypeOf (`false`)=`bool`
TypeOf (*c*) = `int×int→int` (for c in {+,−,*,/,^,`mod`})
TypeOf (*c*) = `int×int→bool` (for c in {<,>,<=,>=})
TypeOf (*c*) = `all` α .({α},{α})→{α} (for *c* in {`union`, `intersect`, `setminus`})
TypeOf (*card*) = `all` α .{α}→`int`
TypeOf (*c*) = `bool×bool→bool` (for *c* in {`and`, `or`})
TypeOf (`not`) = `bool→bool`
TypeOf (`in`) = `all` α .α×{α}→`bool`
TypeOf (=) = `all` α .α×α→`bool`
TypeOf (`(set)`) = {α} (for type variable α)

Type rules

Constants
(Tconst) $\Gamma\vdash c:\tau$ (for constant *c* and type τ such that TypeOf(*c*) ≻ τ)

(Terror) $\Gamma\vdash$ `error`$:\tau$ (for any type τ)

Application
(Tabs) $\Gamma\vdash$ (`lambda` $(x_1\ldots x_n)\ e):\tau_1\times\ldots\times\tau_n\to\tau_2$ if $x_1\mapsto\tau_1\cdot\ldots\cdot x_n\mapsto\tau_n\cdot\Gamma\vdash e:\tau_2$

(Tapp) $\Gamma\vdash(e_1\ e_2\ldots e_n):\tau_2$ if $\Gamma\vdash e_2:\tau_2$ and … and $\Gamma\vdash e_n:\tau_n$ and $\Gamma\vdash e_1:\tau_2\times\ldots\times\tau_n\to\tau$

Data
(Ttuple) $\Gamma\vdash$ (`tuple` $e_1\ldots e_n):\tau_1\times\ldots\times\tau_n$ if $\Gamma\vdash e_1:\tau_1$ and … and $\Gamma\vdash e_n:\tau_n$

(Tset) $\Gamma\vdash$ (`set` $e_1\ldots e_n):\{\tau\}$ if $\Gamma\vdash e_1:\tau$ and $\Gamma\vdash$ (`set` $e_2\ldots e_n):\{\tau\}$

(Tsym) $\Gamma\vdash a:\tau$ (for symbol *a* and type τ such that $\Gamma(x)\succ\tau$)

Conditional
(Tbranch) $\Gamma\vdash$ (`branch` (`if` $g_1\ e_1)\ldots$ (`if` $g_n\ e_n)):\tau$ if for every $1\le i\le n$ $\Gamma\vdash g_i:$`bool` and $\Gamma\vdash e_i:\tau$

The *expression e has type τ under type environment Γ*, $\Gamma\vdash e:\tau$, is a *type judgment*, if it a conclusion of a deduction constructed according to the type rules. An expression is *well-typed* if for some type τ and type environment Γ, $\Gamma\vdash e:\tau$ is a type judgment.

A definition (`def` ($a\ x_1\ldots x_n$) e) is *well-typed* by Γ if
- $\Gamma(a)\succ\tau_1\times\ldots\times\tau_n\to\tau$, and
- $a\mapsto(\tau_1\times\ldots\times\tau_n\to\tau_2)\cdot x_1\mapsto\tau_1\cdot\ldots\cdot x_n\mapsto\tau_n\cdot\Gamma\vdash e:\tau$, and
- $\Gamma(a)=$ Close$(\tau_1\times\ldots\times\tau_n\to\tau,\Gamma)$. where Close$(\tau,\Gamma)$ = `all` $\alpha_1\ldots\alpha_n\ .\ \tau'$ where $\{\alpha_1\ldots\alpha_n\}=$ FTV(τ)\FTV(Γ)

A definition (`def` a e) is *well-typed* by Γ if
- $\Gamma(a)=\tau$ and $\Gamma\vdash e:\tau$.

A well-formed program is *well-typed* by type environment Γ if every definition is well typed by Γ.

5 Type Safety

A static type system attempts to prevent the occurrence of type errors during execution. Intuitively, a *type error* is the application of a function to erroneous arguments, or the attempted application of a non-function. A static type system is *safe* if well-typed programs and expressions cannot cause type error. Below, we utilize a variation of syntactic approach[3] due to Harper[4], which proves safety by proving *Progress* and *Preservation* lemmas. The progress lemma ensures that well-typed expressions are either values or can be further reduced. The preservation lemma says that reduction preserve typing. Before we move onto the lemmas, note that the following condition is true of the builtins. It's proof is obvious upon examination of the reduction rules, and the definition of TypeOf, while paying special attention to the [divZero] reduction rule, and (Terror) type rule.

Lemma [δ-typability]
For every constant values $v_2,\ldots,v_n$,

(δ–typability) if $TypeOf(c) \succ (\tau_2 \times \ldots \times \tau_n \rightarrow \tau)$ and $\vdash v_2:\tau_2$ and $\ldots \vdash v_n:\tau_n$ then $\delta(c,v_2,\ldots,v_n)$ is defined and $\delta(c,v_2,\ldots,v_n): \tau$

Theorem:[Progress]
For program *P*, well-typed by Γ, and P-Closed expression *e*,:
if $\Gamma \vdash e:\tau$ then one of the following must be true
1. *e* is a *P*-value
2. *e* is `error`
3. there is some *e'* such that $e \Rightarrow e'$

Sketch of proof by rule induction over $\Gamma \vdash e:\tau$. Each case, one for each type rule, generally takes the following form. First, the Inversion lemma, discussed below, is applied to the last step in the type judgment of $\Gamma \vdash e:\tau$, yielding the type judgments of the immediate subexpressions of *e*. Next, the induction hypothesis is applied to these subderivations. Lastly by applying the Canonical Forms lemma, or by appealing the reduction rules an expression *e'* is constructed such that $e \Rightarrow e'$.

Lemma:[Preservation]
For program P, well-typed by Γ, and P-Closed expression *e*,
if $\Gamma \vdash e: \tau$ and $e \Rightarrow e'$ then $\Gamma \vdash e': \tau$

Proof by rule induction over e⇒e' relation. Each case, one for each reduction rule, generally takes the following form. First, the reduction rule is examined to determine the relationship between subexpressions of *e* and the subexpressions of *e'*. Next, the inversion lemma is applied to the last step in the type judgment of $\Gamma \vdash e:\tau$, yielding the type judgments of the immediate subexpressions of *e*. Then, the induction hypothesis is applied to these subexpressions, yielding type judgments for the subexpressions of *e*. Lastly, the Substitution lemma, and/or the type rules are used to construct the type judgment $\Gamma \vdash e': \tau$.

Lemma [Inversion]:
Given type program P, well-typed by environment Γ, type τ, P-closed expression *e*,

(Tconst) if $\Gamma \vdash c:\tau$ then $TypeOf(c) \succ \tau$

(Tsym) if $\Gamma \vdash a:\tau$ then $\Gamma(a) \succ \tau$

(Tabs) if $\Gamma \vdash$ (`lambda` $(x_1 \ldots x_n)$ e): $\tau_1 \times \ldots \times \tau_n \rightarrow \tau$, then $x_1 \mapsto \tau_1 \cdot \ldots \cdot x_n \mapsto \tau_n \cdot \Gamma \vdash e:\tau$

(Tapp) if $\Gamma \vdash (e_1\ e_2 \ldots e_n):\tau$, then $\Gamma \vdash e_2:\tau_2$ and … and $\Gamma \vdash e_n:\tau_n$ and $\Gamma \vdash e_1: \tau_2 \times \ldots \times \tau_n \rightarrow \tau$

(Ttuple) if $\Gamma \vdash$ (`tuple` $e_1 \ldots e_n$)$:\tau_1 \times \ldots \times \tau_n$, then $\Gamma \vdash e_1:\tau_1$ and … and $\Gamma \vdash e_n:\tau_n$

(Tset) if $\Gamma \vdash$ (`set` $e_1 \ldots e_n$) : $\{\tau\}$, then $\Gamma \vdash e_1:\tau$ and … and $\Gamma \vdash e_n:\tau$

(Tbranch) if $\Gamma \vdash$ (`branch` (if g_1 e_2)… (if g_n e_n)):τ, then $\Gamma \vdash g_1$: `bool` and … and $\Gamma \vdash g_n$:`bool` and $\Gamma \vdash e_1: \tau$ and … and $\Gamma \vdash e_n: \tau$

Proof: is straightforward upon examination of type rules, and definition of type judgment.

Lemma [Canonical Forms]:
Suppose P is a program well-typed by Γ,
(int) if *v* is a value of type `int`, then *v* is a numeral.

(bool) if *v* is a value of type `bool`, then *v* is either `true` or `false`.

(tuple) if *v* is a value of type $(\tau_1,\ldots,\tau_n)$, then *v* is of the form (`tuple` $v_1 \ldots v_n$) and $v_1:\tau_1$ and ... and $v_n:\tau_n$.

(set) if *v* is a value of type $\{\tau\}$, then *v* is of the form (`set` $v_1 \ldots v_n$) and $v_1:\tau$ and … and $v_n:\tau$.

(abs) if *v* is a value of type $\tau_1 \times \ldots \times \tau_n \rightarrow \tau$, then v is fo the form (`lambda` $(x_1 \ldots x_n)$ e) and $x_1 \mapsto \tau_1 \cdot \ldots \cdot x_n \mapsto \tau_n \cdot \Gamma \vdash e:\tau$, or *v* is defined function symbol of P

Lemma:[Substitution]
For program P, well-typed by Γ, and P-Closed expressions *e*,*e'*, variable *x*, and types *τ*, *τ'*
if $\{x \mapsto \tau\} \cdot \Gamma \vdash e':\tau'$ and $\Gamma \vdash e: \tau$ then $\Gamma \vdash e'[\{(x,e)\}]: \tau'$

Proof: by rule induction over $\{x \mapsto \tau\} \cdot \Gamma \vdash e':\tau'$

6 References

[1] Rushton, J., Blount, J. The Language of Effective Definitions. *International Conference on Frontiers in Education: Computer Science and Computer Engineering 2011*.

[2] Blount, J., Rushton, J. *Type Disjointness in the Language of Effective Definitions*. *International Conference on Foundations of Computer Science*, 2011

[3] Wright, A.,Felleisen, M. A Syntactic Approach to Type Soundness. *Information and Computation*, 115(1):38-94, 1994

[4] Pierce, B. Types and Programming Languages, MIT Press, 2002

Implementation of a Software IP Router using Ant Net Algorithm

A. Jusrut, A. Khedan , and V. Ramnarain-Seetohul
Computer Science and Engineering Department, University Of Mauritius, Reduit, Mauritius
Computer Science and Engineering Department, University Of Mauritius, Reduit, Mauritius

Abstract - *Nowadays, routing standards are governed by the Internet, and the state-of-the-art is link-state routing. These types of algorithms adapt well to network topology changes, but respond poorly in high-traffic environment, where the network load changes dynamically. Very often the shortcomings of these algorithms are not apparent, because their poor performance is compensated for by powerful routers and high-bandwidth links. In this paper, Ant Net, a novel routing approach based on research done mostly in reinforcement learning and swarm intelligence was explored. A Software router using Ant Net algorithm to route IP packets between Ethernet networks was implemented. CNET, a network simulator was used to test the routing algorithm. The simulations done were used create network environment so as to test all aspects of the routing algorithm. Besides these simulations, the software router was tested on a test-router, constructed using a Pentium-4 PC, equipped with 3 PCI Ethernet Network Interface Cards, and running a Linux distribution. Using this test-router, the forwarding mechanisms of the algorithm were tested on real Ethernet hardware.*

Keywords: Ant Net, Algorithms, CNET, Ethernet, topology, router

1 Introduction

Today, computer networks are the core of modern communication. For a computer to send data to another computer found in its own LAN, communication is straightforward (e.g., broadcasting on Ethernets). But when it comes to inter-connecting different networks together, a whole new layer of protocols needs to be introduced. A router is a device dedicated to the task of routing data from one network to another and every router maintains a routing table. A hardware router has several ports to connect to different network and also has processing power and memory. Routers are generally expensive devices and their maintenance and reparation costs in case of failure are also very high. Moreover, modern routing algorithms implemented by hardware routers have some shortcomings that make them unsuitable in certain situations. Hence a software router with same capabilities as a hardware router can be a way to reduce cost and efficiently route packets. The paper consists of designing and implementing a software router that will help network administrators in experimenting with routing, without actually requiring a specialized hardware router. The router will run as a software application on a computer. It will provide the routing functionality of a real (physical) router efficiently, so that it can be used as a viable alternative by network designers. The paper focuses mainly on routers for connectionless networks; more specifically, the focus is on IPv4 routers. Since the objective is to find a useful, efficient and inexpensive solution to routing, only the routing and forwarding functionalities of a router are considered, while specialized hardware routers may provide a variety of other functions, aside from routing, such as NAT, firewall, DHCP among others. Static routing is not implemented in the software router, as the aim is to design a software router to work in dynamic environment.

2 Swarm Intelligence in networking

Swarm intelligence is the collective constructive behaviour that is observed when many individuals work independently, and coordinates by interacting amongst each other or with their direct environment [1].

2.1 Ant Net Algorithm

Ant Net [2,3] is a new type of routing algorithm, inspired from work done in the fields of ant colony optimization, where the natural characteristics of biological swarms (e.g., ants) are studied to solve optimization problems. Ant Net has been implemented and tested on simulation networks and real networks. The results and conclusions from Di Caro and Dorigo's[4] original paper show that the algorithm is superior to all its competitors that were also subjected to the same tests. The competing algorithms included OSPF. Ant Net makes use of mobile agents, known as agents or ants. The agents are data units, generated, received and processed by the routers. The purpose of the agents is to explore the network and to exchange collected information. The marked difference here between Ant Net and other protocols, like OSPF, is that the agents communicate indirectly [4]. In OSPF, each router explicitly sends protocol packets to other routers, but in Ant Net, the agents just travel around the network, modifying routing tables

of routers accordingly. This type of communication that happens through the environment and not directly between agents is called stigmergy; a concept inspired from social insects [5]. Ant Net uses two types of mobile agents: forward ants and backward ants [4]. Forward ants are launched at intervals by each router. The forward ant moves step-by-step towards the destination, and at each intermediate node it collects information as to how much time it took for the trip. On reaching the destination, the forward ant becomes a backward ant, with all the collected information [6]. The backward ant visits the same nodes as the forward ant, but in reverse, and updates routing data structures at each node. Each router keeps two data structures [4]: Fig. 1 shows the data structures required by Ant Net.

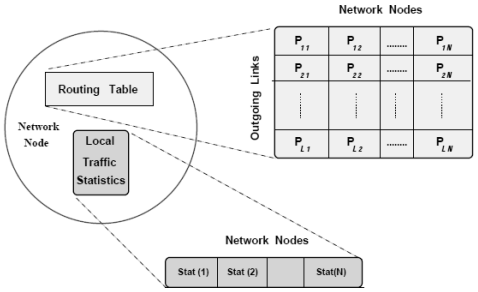

Fig. 1: data structures required by Ant Net[4]

The Ant Net algorithm is robust, scalable with respect to network growth, highly traffic adaptive and provides inherent load balancing [7]. However, if topology is large, routing protocol traffic increases with ant stack size [8].

2.2 Modified Ant Net algorithm

A simplified version of the Ant Net algorithm will be implemented. The changes made to the algorithm, and the rationale behind will be discussed. The main change that will be done is that a constant reinforcement factor will be used to update routing table probabilities. Normally, in the original algorithm, the rfactor is calculated from the trip times of ants [4]. There is a practical difficulty in calculating packet trip times, since the clocks of all routers must be synchronized. Using a constant rfactor eliminates the need to use trip times and thus there is also no need for the statistical models: only the routing table is required. The probability values are then affected only by the arrival rates of ants [2]. *Newly generated* forward ants are forwarded on all router-router links. The changes mentioned will desirably have the following effects: Much lower protocol traffic, since ant stacks no longer contain trip times and considerable reduction of router processing loads. Calculation of the reinforcement factor repeatedly, and working with trip times, in the original algorithm, required lots of floating-point operations.

3 Proposed System

The software router will be used in packet-switched networks and will run on a computer that will need some additional hardware configuration. The machine to be used for routing will need to have more than one network interface card, else it will have the capacity to act only as a standalone host. The software will support only Ethernet NICs. The number of NICs installed will effectively determine the number of links that the router will have, and directly affect the number of networks that can be connected to it. Hosts on connected networks will not require any special configurations; they are configured normally for IP communication. A router may connect to another router, to a single host, or to a LAN. LANs may connect to the router via a switch, as in switched Ethernet. Fig. 2 illustrates the possible connections.

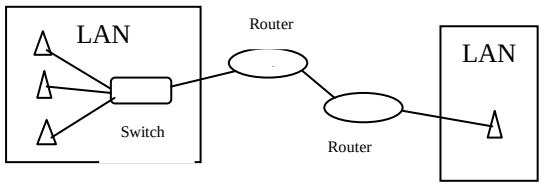

Fig. 2: Topology of proposed system

The sets of all the routers will form the backbone. Some routers in the backbone may not connect to any network, but only provide routing. These may be used on sites where data traffic between networks is very high, and will effectively tend to improve performance as they provide additional routes for packets to travel. The software router will implement the modified Ant Net algorithm as its adaptive routing algorithm. A router distinguishes between two types of packets: data packets and routing protocol packets. Any other packet not forming part of the routing protocol will be treated as plain data, and forwarded using information from the routing table. The routing packets will be packets generated, decoded and processed by the routers to construct the routing table. The router will work directly at layer 3 of the TCP/IP stack; routing protocol packets will have the IPv4 header as the last encapsulation. The router will not use any transport mechanism to ensure routing packets get delivered. This is also applied to data packets. As Ant Net protocol is designed for best-effort packet-switched networks, the routers will not be responsible for any data loss. For reliability, hosts will need to implement TCP. If the routers have to be configured for dynamic routing, then some configurations will be needed initially. Each router should know all reachable networks and its neighbors. This information will be available in configuration files.

4 System Architecture

4.1 Design

The software router will be implemented and tested on a network simulator first, and then if the algorithm works, the code will be tested on a Linux machine. Due to peculiarities with how network simulators work, there will be architectural differences in the implementations of the two versions. The core router architecture should be independent of platform specific details. The core architecture comprises of the routing and forwarding mechanisms, and platform refers to the environment in which the router will be implemented and tested; that is, on the network simulator or on a real physical setup. This prevents tying the core design with the intricacies of the simulation tool. It will also be easier to change the software later to use the libpcap API [9]. The performance of router should also be considered. A router is a complex real-time processing system, with hard deadlines. If it is poorly design, this will result in an excessive loss of packets.

4.2 Architectural Design

Most networking software is written with a layered design. The interfaces of the router need to be managed at a very low level; network traffic should be handled as soon as they enter an interface. This will allow link statistics to be maintained, and most importantly, allow the flexibility to queue up packets based on their incoming/outgoing interface. Thus, a proper architecture operating at the link layer needs to be designed. The way the Ant Net algorithm is defined requires a lot of book-keeping at the link level [5]. Hence it is important to decide when to process inbound and outbound packets. One possibility with inbound packets is to start processing them immediately as soon as they have been stored by the interface hardware (i.e., Ethernet card). Similarly, outbound packets are sent to the hardware for transmission as soon as they have been processed. However, this scheme has inherent problems:

- Inefficient processing/scheduling. The operating system will have a limited buffer for incoming packets. Processing packets one by one as soon as they come will mean that the OS buffer will tend to fill up, resulting in loss of packets.
- It is difficult to build up data-structures (queues) that are required for statistical data collection.

The solution that was chosen is to defer the processing of incoming packets. Packets are stored for later processing or transmission. As soon as a packet comes, it is buffered in a queue. Each interface on the router has a corresponding queue to store incoming packets. Packets are then dequeued from the queues and processed. Similarly, when packets have been processed, they are queued in the outgoing queue for the appropriate link. Later on, the queues will be emptied and the packets will be transmitted on the network card. Fig. 3 depicts this architecture.

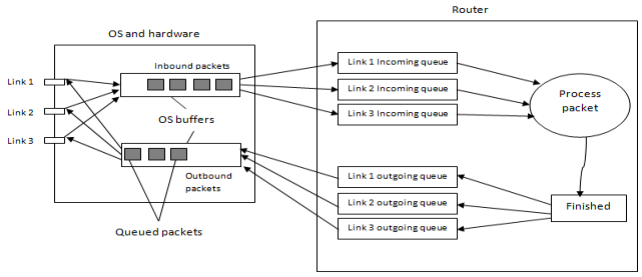

Fig 3: Efficient queuing and processing of incoming packets: The link queues will actually hold Ethernet *frames.*

At the network layer, the modified Ant Net algorithm is used. This layer determines how to process packets received from the link layer, and after processing, packets are sent again to the link layer, to be queued. A suitable format for an ant packet will be designed. This layer is best described by means of the data-structures and algorithms. The link layer and network layer have to exchange messages. One possibility is to copy the protocol data units from layer-to-layer. But, there will be too much processor time wasted in copying data around. Instead, a different design is used, but it blurs to some extent the separating line between both layers. When a frame comes in, the link layer allocates memory needed to store it in the queue. When the network layer requests a packet, instead of copying the packet in the frame, the memory reference of the frame itself is passed. All processing will happen on this memory, and it is this memory itself that will be queued on an outgoing link queue. Hence, only memory addresses, and not whole memory buffers will be passed back and forth. Fig. 4 illustrates this concept.

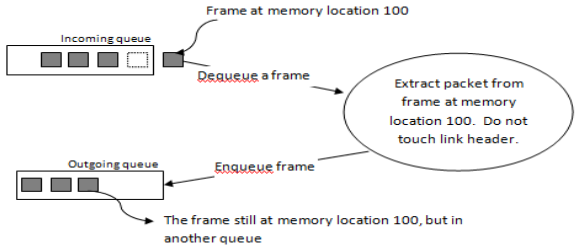

Fig 4: Communication between network and link layers

A radically different approach will be used for the link queues: the length of a queue will have no limit. Dedicated hardware routers have limited memory; hence they use fixed-length queues and perform load-shedding if there is no more room. The software router will run on a Linux PC, and Linux provides a virtual address space of 4 GB, irrespective of physical RAM installed. When a new frame comes in, the Operating System will be requested for memory to store the frame. If the request is unsuccessful, only then the frame is discarded. Queues will be serviced in a round-robin manner. The design of the router is inherently multi-threaded. The multi-threading API of Linux will be used. All the threads will have simultaneous access to shared data segments, like the

routing table. Mutexes will be used to provide mutual exclusion between threads, for variables that can change values during program execution. Locks will be applied whenever shared memory needs to be read or written.
The frame queues will be constructed using linked lists. Frame queues are lists of *ether_frame* structures, logically maintained as FIFO data-structures (queues). Each link on the router will have its own incoming and outgoing queue. Moreover, there is a priority queue for holding backward ant packets, since these have to be processed very fast. All the queues are implemented in the same way; a queue is accessed using a global variable, which is an array of pointers to the queue heads. The queue heads are *ether_frames.*

4.3 Simulation Plan

The simulations will be carried out on topologies that consist only of routers and LANs. A LAN will have a network id and a subnet mask. A LAN will be represented by a single host workstation with an IP address. The LANs in the simulation are hereafter referred to as hosts. Different simulation topologies consisting of different numbers of routers and hosts will be created, and the routing algorithm will be tested on them. Fig.5 illustrates a simple topology.

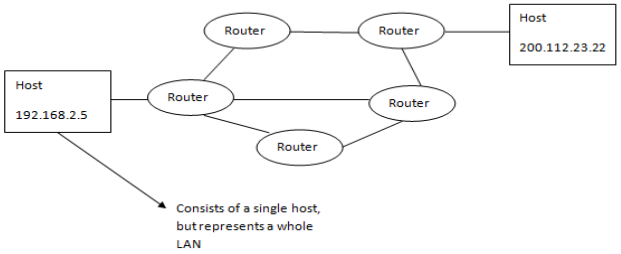

Fig 5: Sample simulation topology

Each node in the simulation, router or host, will have a log file to which it will dump information about its operations. These log files will provide the basis for the simulation analysis. Modification made to the routing tables can be verified by analysing these files.

5 Implementation and testing

The software router was first simulated using the CNET simulator. Fig. 6 shows a simulation window, with the network shown graphically. The simulation consists of five hosts each on a different network and six routers to route data on the network.

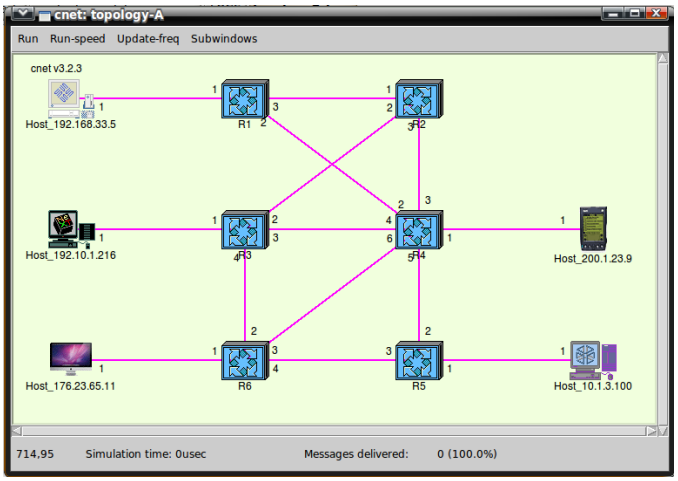

Fig 6: CNET Simulation shown graphically

5.1 Testing

Using simulator CNet, performance testing was done. The variables that were tested were packet delay, packet size packet loss, data rate.

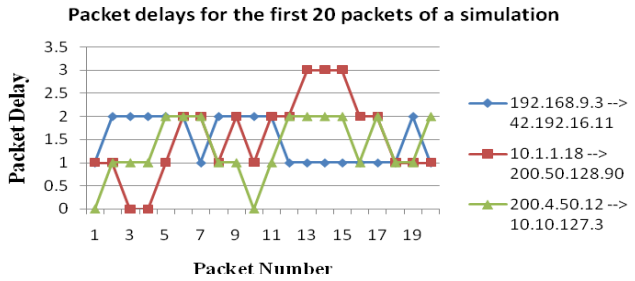

Fig 7: graph for delays for packets in 3 specific flows

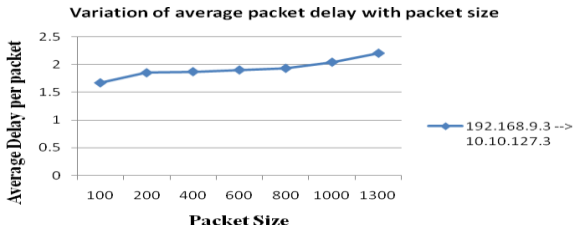

.

Fig 8:graph for packet delay variation with packet size.

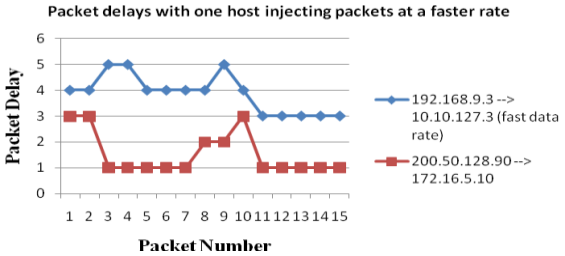

Fig 9: Graph for packet delay variation with time, given one particular flow is made to generate data at a fast rate.

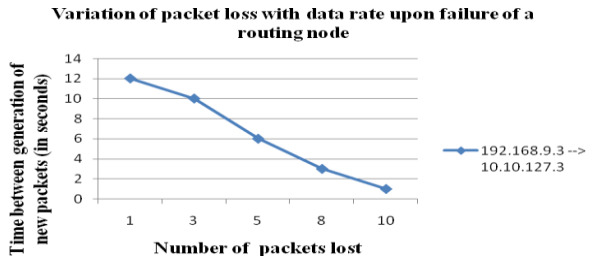

Fig 10: Variation of the number of packets lost with data rate along a particular flow, when a router in the best path along that flow fails.

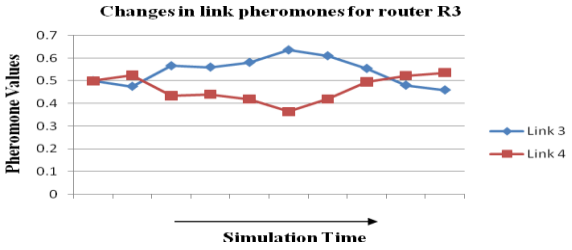

Fig 11: the variation pheromone values of a router

According to results obtained it can be deduced that on average the packet delay does not increase considerably as number of packets increases. As packet size increases, there is a slight increase in the packet delay. If a given flow is made to generate data at a faster rate, it can be observed that the packet delay increases considerably at first but it then stabilises as number of packets increases. If a particular routing node has failed then according to its data rate, variation of the packet loss was measured and results concluded that as number of packets lost increases, the time between generations of new packets decreases. Finally the variation pheromone values of a router were tested. This test helps to analyze the changes in routing table during load-balancing. Result shows that the best path is through link 4 in Fig. 11, and is used initially. But soon, due to a fast data rate towards a host, this best path suffers some delays. Hence, an alternate path, through link 3 is then chosen. However after some time, the performance of the alternate path starts degrading due to congestion and gradually, the router starts switching packets on link 4 again.

To fully test its operations, the software router has to be tested in real life situation but the main limitation was the unavailability of a real network to perform the testing. Hence, to counterbalance this limitation, the software router has been tested on a PC with three LAN cards to verify if it is operating correctly. It was observed that the software router was indeed forwarding data to the hosts. However to create a topology for testing, several PCs with more NICs were required.

6 Conclusion

The software router understands only IP at the internetwork layer of TCP/IP. There is no support for additional protocols like ICMP, IGMP, IP multicasting, IPsec. Support for these protocols can be added by extending the router code base to distinguish special IP packets from normal data packets. Furthermore, the software router also understands only IPv4. To support IPv6, a redesign of the routing table and other major data structures will be needed. At the link layer, the router simply broadcasts packets on destination LANs, and the network layer on hosts' filters them based on IP address. This can be avoided by implementing ARP and maintaining an ARP cache on the router. Also, the router can be made to detect neighbors and networks by implementing hello and flooding mechanisms similar to OSPF. The flooding will only aid in discovering new networks being added, and the hello packets will query neighbors. However, these mechanisms will be done less frequently than in OSPF, since here they do not form integral part of the routing algorithm.

7 References

[1] Kassabalidis, I., El-Sharkawi, M. A., Marks II, R. J., Arabshahi, P. and Gray, A. A. (2001). Swarm intelligence for routing in communication networks, *IEEE Globecom*

[2] G. Di Caro and M. Dorigo, "An adaptive multi-agent routing algorithm inspired by ants behavior", *Proc. PART98 - Fifth Annual Australasian Conference on Parallel and Real-Time Systems*, Adelaide, Australia, 28-29,Sept. 1998.

[3] G. Di Caro and M. Dorigo, "Ant colonies for adaptive routing in packetswitched communications networks", *Proc. PPSN V – Fifth International Conference on Parallel Problem Solving from Nature*, Amsterdam, Holland, 27-30,Sept. 1998.

[4] G. Di Caro and M. Dorigo, "AntNet: distributed stigmergetic control for communications networks", *Journal of Artificial Intelligence Research*, vol. 9, pp. 317-365, 1998.

[5] M. Dorigo, E. Bonabeau, G. Theraulaz, Ant algorithms and stigmergy, Future Generation Computer Systems vol 16 No 8, 2000 pp. 851–871.

[6] Kwang Mong Sim and Weng Hong Sun, "Ant Colony Optimization for Routing and Load-Balancing: Survey and New Directions ",*IEEE transactions on systems and humans*,Vol.33,No.5 Sept 2003.

[7] J. Chen, P. Druschel, and D. Subramanian, A new approach to routing with dynamic metrics. In *Proceedings of IEEE INFOCOM '99*, pp 661–670, New York, NY, March 1999.

[8] M. Dorigo, V. Maniezzo, and A. Colorni. The ant system: Optimization by a colony of cooperating agents. *IEEE Transactions on Systems, Man, and Cybernetics-Part B*, Vol. 26, No 1:pp. 29– 41, 1996.

[9] Sly technologies jNetPcap 2012 [online] Available at: http://jnetpcap.com/node/60

Quantum secret sharing with noisy channels

[1]Aziz Mouzali, [2]Fatiha Merazka, [3]Damian Markham
[1]Department of physics, ENP, Algiers, Algeria.
[2]Electronic & Computer Science Faculty, USTHB, Algeria.
[3]Laboratoire Traitement et Communication de l'Information.
CNRS - Télécom ParisTech, France.

Abstract- *This paper is devoted to quantum error correction for secret sharing with a five qubits graph state through five noisy channels. The correction procedure is described for the five, seven and nine qubits codes. These three codes are similar if one among the sent qubits is infected by an error in the transmission channel. However, If two qubits are infected, then the correction result changes from one code to another. The three codes are compared in this work by computing the average fidelity which is the distance between the sent secret and that measured by the receivers. To reduce the complexity of the problem, we will treat the case where, at most, two qubits are disturbed in each depolarizing channels.*

Keywords: Quantum Correction, Quantum communication, Graph State, Quantum Secret Sharing, Feynman Program.

1 Introduction

The graph state can be very useful for several quantum protocols as secret sharing, measurement-based computation, error correction, teleportation and quantum communications. Then, it would be in the future a good way to unify these topics in one formalism. The quantum secret sharing with graph state is very well described in [1], particularly the five qubits graph state. In this work, we investigate the effects of the five, seven and nine qubits codes used to protect a five qubits graph state containing a secret and sent by a dealer to five players. Some of the results have been obtained using a simulator called "Feynman Program", witch is a set of procedures supporting the definition and manipulation of an n-qubits system and the unitary gates acting on them. This program is described in details in [2][3][4][5] and obtainable from [6].

2 Quantum secret Sharing

Quantum secret sharing (QSS) is a quantum cryptographic protocol wherein a dealer shares private or public quantum channels with each player, while the players share private quantum or classical channels between each other. The dealer prepares an encoded version of the secret using a qubits string which he transmits to n players, only a subset k of them can collaborates to reconstruct the secret. We call a (k,n) threshold secret sharing a protocol where each player receives one equal share of the encoded secret and a threshold of any k players can access the secret. This scheme is a primitive protocol by which any other secret sharing is achieved. In this work, we treated the case (k,n)=(3,5) where the dealer sends through five depolarizing channels, a quantum secret encoded in a five qubits graph state [1].

3.1 Five qubits graph state

Graph states are a an efficient tool for multipartite quantum information processing task like secret sharing. Also, they have a graphical representation witch offers an intuitive picture of information flow. The graph state $|\Psi_G\rangle$ given by equation (2) and containing the quantum secret $|\Psi_s\rangle = \alpha|0\rangle + \beta|1\rangle = cos(\theta/2)|0\rangle + e^{i\phi}sin(\theta/2)|1\rangle$, should be transmitted by a dealer to five players through five different channels. First, he constructs the state $|G\rangle$ from an initial five qubits state $|\Psi_0\rangle = |00000\rangle$, then applies the Hadamard gate H on each qubit and the controlled-Z gate CZ on qubits $[1,2],[2,3],[3,4],[4,5],[5,1]$:

$$|G\rangle = \prod_{1\leq i\leq 4} CZ_{[i,i+1]} |+\rangle^{\otimes 5} \quad (1)$$

The dealer intricates an additional qubit called D with each of the five qubits and add to the obtained system the secret qubit S in the state $|\Psi_s\rangle = \alpha|0\rangle + \beta|1\rangle$. Then, he performs a Bell measurement on qubits D and S and obtains finally [1] :

$$|\Psi_G\rangle = \alpha|G\rangle + \beta[\prod_{1\leq i\leq 5} Z_i]|G\rangle \quad (2)$$

3.2 Perfect channel

We describe below the procedure allowing players to access the secret. The secret should be accessible only for player 1, 2 and 3, players 4 and 5 being considered as eavesdroppers. Players 1 and 3 measure their qubits in the Bell basis and transmit the result to player 2 which

applies on its qubit the suitable recovering gate R_G given in table 1 to access the secret state [1].

The graph state $|\Psi_G\rangle$ can be decomposed in terms of Bell states $|B_{ij}\rangle_{13}$ and $|B_{ij}\rangle_{45}$ [1] :

$$|\Psi_G\rangle = (\tfrac{1}{2})\{ |B_{00}\rangle_{13} [\alpha|+\rangle + \beta|-\rangle]_2 |B_{01}\rangle_{45} + |B_{01}\rangle_{13} [\alpha|+\rangle - \beta|-\rangle]_2 |B_{10}\rangle_{45} + |B_{10}\rangle_{13} [\alpha|-\rangle - \beta|+\rangle]_2 |B_{00}\rangle_{45} + |B_{11}\rangle_{13} [\alpha|-\rangle + \beta|+\rangle]_2 |B_{11}\rangle_{45})\} \quad (3)$$

Equation (3) can be written :

$$|\Psi_G\rangle = |B_{00}\rangle_{13} (|\Psi\rangle_a)_{245} + |B_{01}\rangle_{13} (|\Psi\rangle_b)_{245} + |B_{10}\rangle_{13} (|\Psi\rangle_c)_{245} + |B_{11}\rangle_{13} (|\Psi\rangle_d)_{245} \quad (4)$$

Measurement in the Bell base $\{|B_{ij}\rangle_{13}\}$ gives only one term in (4), then the density matrix :

$$\rho_{_{1..5}} = (\tfrac{1}{4})(\rho_{_{ij}})_{13}(\rho_x)_{245} \quad (\ x = a, b, c \text{ or } d) \quad (5)$$

The partial trace over qubits $(4, 5)$ gives the density matrix of qubit 2 :

$$\rho_{_2}^{'} = \left|\Psi_2^{'}\right\rangle \left\langle\Psi_2^{'}\right| = P_{tr}[(\rho_x)_{245}]_{4,5} \quad (6)$$

Then the secret state :

$$\rho_{_2} = R_g^* \rho_{_2}^{'} R_g \quad \text{or} \quad |\Psi_2\rangle = R_g \left|\Psi_2^{'}\right\rangle \quad (7)$$

$\|B_{ij}\rangle_{13}$	B_{00}	B_{01}	B_{10}	B_{11}
R_g	H	ZH	ZXH	XH

Table 1 : Secret recovering gate R_g used by player 2 versus the Bell state $|B_{ij}\rangle_{13}$ measured by players 1 and 3.

3.3 Fidelity

The sent qubits can be affected by error X, Z or Y represented respectively by the Pauli matrix $X = \begin{pmatrix} 0 & 1 \\ 1 & 0 \end{pmatrix}$, $Z = \begin{pmatrix} 1 & 0 \\ 0 & -1 \end{pmatrix}$ and $Y = -iXZ = i \begin{pmatrix} 0 & -1 \\ 1 & 0 \end{pmatrix}$ corresponding to rotation π around ox or oz or both in the block sphere. The fidelity is one of the mathematical quantities which permits to know how close are two quantum states represented by the density matrix σ and ρ by measuring a distance between them [7] :

$$F(\sigma, \rho) = \left| Tr(\sqrt{\sqrt{\sigma}\rho\sqrt{\sigma}}) \right|^2 \quad (8)$$

In the case of a pure state $\sigma = |\Psi\rangle\langle\Psi|$ and an arbitrary state ρ, the fidelity is the overlap of the two states [7] :

$$F(|\Psi\rangle, \rho) = \langle\Psi| \rho |\Psi\rangle \quad (9)$$

In this work we measure the overlap between the correct secret state $\sigma_s = |\Psi_s\rangle\langle\Psi_s|$ and the qubit state $\rho_2 = |\Psi_2\rangle\langle\Psi_2|$ measured by player 2 to access the secret. Then, the fidelity is function of the angles (θ, ϕ) in the Block sphere and the average fidelity is :

$$F_a = (1/4\pi) \int_0^{\pi} \int_0^{2\pi} F(\theta, \phi) sin(\theta) d\theta d\phi \quad (10)$$

We will describe below the procedure giving the fidelity. If any Pauli errors affects the state $|\Psi_G\rangle$ then equation (4) becomes :

$$\left|\Psi_G^E\right\rangle = (\tfrac{1}{2})\{|B_{00}\rangle_{13} \left|\Psi_a^E\right\rangle_{245} + |B_{01}\rangle_{13} \left|\Psi_b^E\right\rangle_{245} + |B_{10}\rangle_{13} \left|\Psi_c^E\right\rangle_{245} + |B_{11}\rangle_{13} \left|\Psi_d^E\right\rangle_{245}\} \quad (11)$$

$\left|\Psi_{a,b,c,d}^E\right\rangle_{245}$ are the states of qubits $(2, 4, 5)$ modified by the channel errors.

After measuring on the Bell states of qubits $(1, 3)$ only one term will remain in (11) :

$$\left|\Psi_G^E\right\rangle^{'} = (\tfrac{1}{2}) |B_{ij}\rangle_{13} \left|\Psi_x^E\right\rangle_{245} \quad (12)$$

The corresponding affected density matrix is :

$$\rho_{_{1..5}}^E = (\tfrac{1}{4})(\rho_{_{ij}})_{13}(\rho_x^E\ )_{245} \quad (13)$$

The partial trace over qubits $(4, 5)$ gives the measured density matrix of qubit 2 :

$$\rho_2^{\prime E} = \left|\Psi_2^{\prime E}\right\rangle \left\langle\Psi_2^{\prime E}\right| = P_{tr}[(\rho_x^E\ )_{245}]_{4,5} \quad (14)$$

Then the affected secret state measured by player two :

$$\rho_2^E = R_G^* \rho_2^{\prime E} R_G = \left|\Psi_2^E\right\rangle \left\langle\Psi_2^E\right| \quad (15)$$

We multiply by the secret state $|\Psi_s\rangle = \alpha|0\rangle + \beta|1\rangle$ to obtain the fidelity :

$$F(\theta, \phi) = \langle\Psi_s| \rho_2^E |\Psi_s\rangle \quad (16)$$

Table 2 gives the fidelity $F(\theta, \phi)$ calculated for all errors on qubits $i = 1, 2$ or 3.

$Error$	$\|\Psi\rangle_2$	$F(\theta, \phi)$	F_a
ε_a	$\alpha\|1\rangle - \beta\|0\rangle$	$\|sin(\theta)sin\phi\|^2$	1/3
ε_b	$\alpha\|0\rangle - \beta\|1\rangle$	$cos^2(\theta)$	1/3
ε_c	$\alpha\|1\rangle + \beta\|0\rangle$	$\|sin(\theta)cos\phi\|^2$	1/3
ε_d	$\alpha\|0\rangle + \beta\|1\rangle$	1	1

Table 2 : Fidelity and measured state $|\Psi_2\rangle$ versus different errors groups ε_x on qubits $i = 1, 2, 3$.

3.4 Depolarizing channel

The depolarizing channel is a particular model for the noise on quantum systems. In this process, the global density matrix ρ is replaced by a mixed one $\rho(P)$ function of the probability P that a Pauli error $E_{ij} = (\sigma_{1j} = \sigma_{xj}$, $\sigma_{2j} = \sigma_{yj}$ or $\sigma_{3j} = \sigma_{zj})$ affects any qubit "j" in the n-qubits system. The matrix density is given by $(17a)$ for one-qubit system[2] and can be generalized by $(17b)$ for the n-qubits system :

$$\rho_1(P) = (1-P)\rho + \tfrac{P}{3}[X\rho X + Y\rho Y + Z\rho Z] \quad (17a)$$

$$\rho_n(P) = (1-P)^n\rho + .. + \tfrac{P^k}{3^k}(1-P)^{n-k}[\sum_{1\le i\le 3}^{1\le j_l\le n}(\Pi_{1\le l\le k}\sigma^*_{ij_l})] \rho(\Pi_{1\le l\le k}\sigma_{ij_l}) + ... + \tfrac{P^n}{3^n}[\sum_{1\le i\le 3}^{1\le j_l\le n}(\Pi_{1\le l\le n}\sigma^*_{ij_l})]\rho(\Pi_{1\le l\le n}\sigma_{ij_l}) \quad (17b)$$

Consider now the case where the five qubits are sent by the dealer through five depolarizing channels. Suppose the probability P that any single error occurs on any qubit is the same in the five channels. Then we can use equation (19) as if the dealer send the five qubits through only one depolarized channel. We describe below the procedure to obtain the average fidelity $F_a(P)$, considering all the possible errors in the five transmitting noisy channels. We begin by writing the affected density matrix $\rho^E_{1..5}(P)$ received by the five players :

$$\rho^E_{1..5}(P) = (1-P)^5\rho_{1..5} + \tfrac{P}{3}(1-P)^4[\rho^{E_1}_{1..5} + \rho^{E_2}_{1..5} + \rho^{E_3}_{1..5} + \rho^{E_4}_{1..5} + \rho^{E_5}_{1..5}] + \tfrac{P^2}{9}(1-P)^3[\rho^{E_1E_2}_{1..5} + \rho^{E_1E_3}_{1..5} + \rho^{E_1E_4}_{1..5} + \rho^{E_1E_5}_{1..5} + \rho^{E_2E_3}_{1..5} + \rho^{E_2E_4}_{1..5} + \rho^{E_2E_5}_{1..5} + \rho^{E_3E_4}_{1..5} + \rho^{E_3E_5}_{1..5} + \rho^{E_4E_5}_{1..5}] + \tfrac{P^3}{27}(1-P)^2[\rho^{E_1E_2E_3}_{1..5} + \rho^{E_1E_2E_4}_{1..5} + \rho^{E_1E_2E_5}_{1..5} + \rho^{E_1E_3E_4}_{1..5} + \rho^{E_1E_3E_5}_{1..5} + \rho^{E_1E_4E_5}_{1..5} + \rho^{E_2E_3E_4}_{1..5} + \rho^{E_2E_3E_5}_{1..5} + \rho^{E_2E_4E_5}_{1..5} + \rho^{E_3E_4E_5}_{1..5}] + \tfrac{P^4}{81}(1-P)[\rho^{E_1E_2E_3E_4}_{1..5} + \rho^{E_1E_2E_3E_5}_{1..5} + \rho^{E_1E_2E_4E_5}_{2} + \rho^{E_1E_3E_4E_5}_{1..5} + \rho^{E_2E_3E_4E_5}_{1..5}] + \tfrac{P^5}{243}\rho^{E_1E_2E_3E_4E_5}_{1..5} \quad (18)$$

With $\rho^{E_i}_{1..5}$ the density matrix affected by errors on qubit "i" :

$$\rho^{E_i}_{1..5} = X_i\rho_{1..5}X_i + Y_i\rho_{1..5}Y_i + Z_i\rho_{1..5}Z_i \quad (19)$$

The density matrix $\rho^{E_iE_j}_{1..5}$, $\rho^{E_iE_jE_k}_{1..5}, \rho^{E_iE_jE_kE_l}_{1..5}$ and $\rho^{E_iE_jE_kE_lE_m}_{1..5}$ are summation of respectively 9, 27, 81 and 243 terms and represent the density matrix affected by error on two, three, four and five qubits.

After measuring on the Bell states of qubits $(1,3)$, tracing over qubits $(4,5)$,multiplying by the recovering gate R_g, we multiply by the secret state and integrate over (θ,ϕ) to obtain the average fidelity :

$$\langle\Psi_s|\rho^E_2|\Psi_s\rangle = (1-P)^5 + \tfrac{P}{3}(1-P)^4[F^{E_1}_a + F^{E_2}_a + F^{E_3}_a + F^{E_4}_a + F^{E_5}_a] + \tfrac{P^2}{9}(1-P)^3[F^{E_1E_2}_a + F^{E_1E_3}_a + F^{E_1E_4}_a + F^{E_1E_5}_a + F^{E_2E_3}_a + F^{E_2E_4}_a + F^{E_2E_5}_a + F^{E_3E_4}_a + F^{E_3E_5}_a + F^{E_4E_5}_a] + \tfrac{P^3}{27}(1-P)^2[F^{E_1E_2E_3}_a + F^{E_1E_2E_4}_a + F^{E_1E_2E_5}_a + F^{E_1E_3E_4}_a + F^{E_1E_3E_5}_a + F^{E_1E_4E_5}_a + F^{E_2E_3E_4}_a + F^{E_2E_3E_5}_a + F^{E_2E_4E_5}_a + F^{E_3E_4E_5}_a] + \tfrac{P^4}{81}(1-P)[F^{E_1E_2E_3E_4}_a + F^{E_1E_2E_3E_5}_a + F^{E_1E_2E_4E_5}_a + F^{E_1E_3E_4E_5}_a + F^{E_2E_3E_4E_5}_a] + \tfrac{P^5}{243}F^{E_1E_3E_4E_5E_5}_a \quad (20)$$

$$\langle\Psi_s|\rho_2|\Psi_s\rangle = 1 \; ; \; F^E_a = \langle\Psi_s|\rho^E_2|\Psi_s\rangle \quad (21)$$

We deduce from tables 2 the values of F^E_a and obtain the average fidelity :

$$F_a(P) = 1 - 2P + \tfrac{8}{3}P^2 - \tfrac{32}{27}P^3 \quad (22)$$

4 The five-qubits code

This code is described in [7][8] and uses five qubits to protect one of them in a superposed state from any error X, Y or Z. The dealer protects each of the three qubits $(1,2,3)$ with four ancillas as showed in figure 4 and send them through three noisy channel which introduce a bit or phase flip or both with probability $P = 1$.

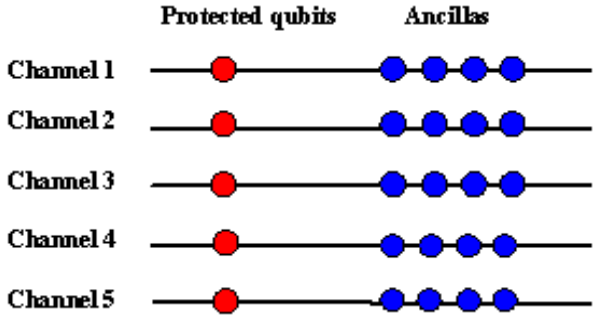

Figure 1 : Transmission of five protected qubits through five channels.

The graph state (3) can be written as follow :

$$|\Psi_G\rangle = (\sqrt{2}/8)\{[\alpha|0\rangle + \beta|1\rangle]_i|\Psi_a\rangle_{jklm} + [\alpha|0\rangle - \beta|1\rangle]_i|\Psi_b\rangle_{jklm} + [\beta|0\rangle + \alpha|1\rangle]_i|\Psi_c\rangle_{jklm} + [\beta|0\rangle - \alpha|1\rangle]_i|\Psi_d\rangle_{jklm}] \quad (23)$$

$$[i = 1,(j,k,l,m) = 2,3,4,5],[i = 2,(j,k,l,m) = 1,3,4,5][i = 3,(j,k,l,m) = 1,2,4,5] \quad (24)$$

After coding , syndrome measurement, correction and decoding, the players suppress the ancillas. If the qubit

"i" is affected by error $E_i = X_i$, Y_i or Z_i then the graph state becomes :

$$\left|\Psi_G^{E_i}\right\rangle = E_i\left|\Psi_G\right\rangle = (\tfrac{\sqrt{2}}{8})\{E_i[\alpha\left|0\right\rangle + \beta\left|1\right\rangle]_i\left|\Psi_a\right\rangle_{jklm} + E_i[\alpha\left|0\right\rangle - \beta\left|1\right\rangle]_i\left|\Psi_b\right\rangle_{jklm} + E_i[\beta\left|0\right\rangle + \alpha\left|1\right\rangle]_i\left|\Psi_c\right\rangle_{jklm} + E_i[\beta\left|0\right\rangle - \alpha\left|1\right\rangle]_i\left|\Psi_d\right\rangle_{jklm}\} \quad (25)$$

Table 3 gives the error E_i affecting the to be protected physical qubit "i" after correcting double input errors as the single error having same syndrome. The ancillas are designed by "a_j" and the to be protected qubit by "i" with $i = 1, 2, 3$ and $j = 1, 2, 3, 4$.

$Error$	E_i
$X_i, (Z_{a_2}Z_{a_3}), (X_{a_3}Z_{a_4}, Z_{a_1}X_{a_2})$	$I_i, (X_i), (Z_i)$
$X_{a_1}, (Z_{a_3}Z_{a_4}), (Z_iX_{a_4}, Z_{a_2}X_{a_3})$	$I_i, (X_i), (Z_i)$
$X_{a_2}, (Z_iZ_{a_4}), (X_iZ_{a_1}, Z_{a_3}X_{a_4})$	$I_i, (X_i), (Z_i)$
$X_{a_3}, (Z_iZ_{a_1}), (X_iZ_{a_4}, X_{a_1}Z_{a_2})$	$I_i, (X_i), (Z_i)$
$X_{a_4}, (Z_{a_1}Z_{a_2}), (X_{a_2}Z_{a_3}, Z_iX_{a_1})$	$I_i, (X_i), (Z_i)$
$Z_i, (X_{a_1}X_{a_4}), (X_{a_2}Z_{a_4}, Z_{a_1}X_{a_3})$	$I_i, (X_i), (Z_i)$
$Z_{a_1}, (X_iX_{a_2}), (Z_iX_{a_3}, Z_{a_2}X_{a_4})$	$I_i, (X_i), (Z_i)$
$Z_{a_2}, (X_{a_1}X_{a_3}), (X_iZ_{a_3}, Z_{a_1}X_{a_4})$	$I_i, (X_i), (Z_i)$
$Z_{a_3}, (X_{a_2}X_{a_4}), (X_iZ_{a_2}, X_{a_1}Z_{a_4})$	$I_i, (X_i), (Z_i)$
$Z_{a_4}, (X_iX_{a_3}), (X_{a_1}Z_{a_3}, Z_iX_{a_2})$	$I_i, (X_i), (Z_i)$
$Y_i, (X_{a_2}X_{a_3}, Z_{a_1}Z_{a_4})$	$I_i, (Y_i)$
$Y_{a_1}, (X_{a_3}X_{a_4}, Z_iZ_{a_2})$	$I_i, (Y_i)$
$Y_{a_2}, (X_iX_{a_4}, Z_{a_1}Z_{a_3})$	$I_i, (Y_i)$
$Y_{a_3}, (X_iX_{a_1}, Z_{a_2}Z_{a_4})$	$I_i, (Y_i)$
$Y_{a_4}, (X_{a_1}X_{a_2}, Z_iZ_{a_3})$	$I_i, (Y_i)$

Table 3 : Error E_i on the physical qubit "i" versus errors on the logical qubit "i".

Consider three double errors E_kE_l, E_mE_n and E_oE_p occurring respectively in depolarizing channels "1", "2" and "3" on any qubits (k,l,m,n,o,p) and corrected as the three single error with similar syndrome. The qubits $(4, 5)$ can be affected by any error X, Y or Z. If the probability that channel error occurs on one qubit is equal to P, then the density matrix received by the five players is :

$$\rho^{E}_{(123a)(45)} = (1-P)^8\rho_{(123a)(45)} + \tfrac{P}{3}(1-P)^7[\textstyle\sum\rho^{E_x}_{(123a)(45)}] + \tfrac{P^2}{3^2}(1-P)^6[\textstyle\sum\rho^{E_xE_y}_{(123a)(45)}] + \tfrac{P^3}{3^3}(1-P)^5[\textstyle\sum\rho^{E_xE_yE_z}_{(123a)(45)}] + \tfrac{P^4}{3^4}(1-P)^4[\textstyle\sum\rho^{E_xE_yE_zE_u}_{(123a)(45)}] + \tfrac{P^5}{3^5}(1-P)^3[\textstyle\sum\rho^{E_xE_yE_zE_uE_v}_{(123a)(45)}] + \tfrac{P^6}{3^6}(1-P)^2[\textstyle\sum\rho^{E_xE_yE_zE_uE_vE_w}_{(123a)(45)}] + \tfrac{P^7}{3^7}(1-P)[\textstyle\sum\rho^{E_x.....E_s}_{(123a)(45)}] + \tfrac{P^8}{3^8}[\textstyle\sum\rho^{E_kE_lE_mE_nE_oE_pE_4E_5}_{(123a)(45)}] \quad (26)$$

The notation (123a) represents the logical qubits 1,2 and 3, each one protected by four ancillas and :

$$\textstyle\sum\rho^{E_x}_{(123a)(45)} = \rho^{E_k}_{(123a)(45)} + \rho^{E_l}_{(123a)(45)} + \rho^{E_m}_{(123a)(45)} + \rho^{E_n}_{(123a)(45)} + \rho^{E_o}_{(123a)(45)} + \rho^{E_p}_{(123a)(45)} + \rho^{E_4}_{(123a)(45)} + \rho^{E_5}_{(123a)(45)}$$

is the error E_i affecting after decoding the to be protected physical qubit "i". $(27a)$

$$\rho^{E_k}_{(123a)(45)} = \rho^{X_k}_{(123a)(45)} + \rho^{Y_k}_{(123a)(45)} + \rho^{Z_k}_{(123a)(45)}\ ;\ \rho^{X_k}_{(123a)(45)} = X_k^*\rho_{(123a)(45)}X_k,... \quad (27b)$$

The summations $\sum\rho^{E_x}_{(123a)(45)}$, $\sum\rho^{E_xE_y}_{(123a)(45)}$, $\sum\rho^{E_xE_yE_z}_{(123a)(45)}$, $\sum\rho^{E_xE_yE_zE_u}_{(123a)(45)}$, $\sum\rho^{E_xE_yE_zE_uE_v}_{(123a)(45)}$, $\sum\rho^{E_xE_yE_zE_uE_vE_w}_{(123a)(45)}$ and $\sum\rho^{E_xE_yE_zE_uE_vE_wE_s}_{(123a)(45)}$ contains respectively 8X3, $28X3^2$, $56X3^3$,$70X3^4$, $56X3^5$, $28X3^6$ and $8X3^7$ terms. The expression $\rho^{E_kE_lE_mE_nE_oE_pE_4E_5}_{(123a)(45)}$ is the summation of 3^8 terms. After decoding, measuring on the Bell states of qubits $(1, 3)$, tracing over qubits $(4, 5)$, multiplying by the recovering gate and the secret state and integrating, we obtain the average fidelity :

$$F_a(P) = (1-P)^8 + 8P(1-P)^7 + 26P^2(1-P)^6 + 44P^3(1-P)^5 + \tfrac{128}{3}P^4(1-P)^4 + \tfrac{80}{3}P^5(1-P)^3 + \tfrac{346}{27}P^6(1-P)^2 + \tfrac{116}{27}P^7(1-P) + \tfrac{13}{27}P^8 \quad (28)$$

5 Comparison among the three codes

The Steane and Shor codes described respectively in [9] and [7], use respectively seven and nine qubits to protect one of them in a superposed state from any error X, Y or Z. The procedure giving the average fidelity described in section 4 for the five qubit code is the same for the seven and nine qubits codes. The difference comes from the number n of double channel errors on logical qubit which let the protected qubit "i" free of error. The simulation with Feynman Program gives for respectively the five, seven and nine qubits codes :

$$\tfrac{n_5}{N_5} = 0;\ \tfrac{n_7}{N_7} = \tfrac{39}{81};\ \ \tfrac{n_9}{N_9} = \tfrac{108}{144} \quad (29)$$

With N_5=40 N_7=81 and N_9=144 the total number of double errors for the three codes. Then we can deduce the average fidelity for the seven and nine qubits codes by changing the value $F_a = \frac{1}{3}$ in table 2 by an average value f_n and obtain for each code :

$$f_5 = \tfrac{1}{3}\quad ;\quad f_7 = \tfrac{(n_7\times 1+(N_7-n_7)\times\frac{1}{3}}{81} = \tfrac{53}{81}\quad ;\quad f_9 = \tfrac{(n_9\times 1+(N_9-n_9)\times\frac{1}{3}}{144} = \tfrac{5}{6} \quad (30)$$

The average fidelity is then for any code :

$$F_a(P) = (1-P)^8 + 8P(1-P)^7 + (3f_n+25)P^2(1-P)^6 + (18f_n+38)P^3(1-P)^5 + (41f_n+29)P^4(1-P)^4 + (44f_n+12)P^5(1-P)^3 + (\frac{205f_n+47}{9})P^6(1-P)^2 + (\frac{50f_n+22}{9})P^7(1-P) + \frac{13}{27}P^8 \quad (31)$$

6 Summary

The results are summarized on table 4 where the symbols C_0 and C_n correspond respectively for no correction and the n-qubits code. The figure 2 compares the variation of average fidelity without and with correction by the three codes. The figure 1 shows logically that the average fidelity is decreasing with P without and with correction by any code. The values of fidelity are always better and the decrease is slower when using codes. The best average fidelity is given by the nine qubits code, followed by the seven qubits code then the five qubits code. The reason is that for the five qubits code all the double input errors let the protected qubits affected, while some of them could be covered when using the two other codes. We considered in this work that triple input errors and more are very unlikely, so that syndrome measurement allows (in seven and nine qubits code) recovering errors. We note that if P=1, then the average fidelity $Fa(P=1) = \frac{13}{27} = 0.4815$ is the same regardless the used code.

Code	$F_a(P)$
C_0	$1-2P+\frac{8}{3}P^2-\frac{32}{27}P^3$
C_n	$(1-P)^8+8P(1-P)^7+(3f_n+25)P^2(1-P)^6+(18f_n+38)P^3(1-P)^5+(41f_n+29)P^4(1-P)^4+(44f_n+12)P^5(1-P)^3+(\frac{205f_n+47}{9})P^6(1-P)^2+(\frac{50f_n+22}{9})P^7(1-P)+\frac{13}{27}P^8$
C_5	$(1-P)^8+8P(1-P)^7+26P^2(1-P)^6+44P^3(1-P)^5+\frac{128}{3}P^4(1-P)^4+\frac{80}{3}P^5(1-P)^3+\frac{346}{27}P^6(1-P)^2+\frac{116}{27}P^7(1-P)+\frac{13}{27}P^8+$
C_7	$(1-P)^8+8P(1-P)^7+\frac{728}{27}P^2(1-P)^6+\frac{448}{9}P^3(1-P)^5+\frac{4522}{81}P^4(1-P)^4+\frac{3304}{81}P^5(1-P)^3+\frac{14672}{729}P^6(1-P)^2+\frac{4432}{729}P^7(1-P)+\frac{13}{27}P^8$
C_9	$(1-P)^8+8P(1-P)^7+\frac{55}{2}P^2(1-P)^6+53P^3(1-P)^5+\frac{379}{6}P^4(1-P)^4+\frac{146}{3}P^5(1-P)^3+\frac{1307}{54}P^6(1-P)^2+\frac{191}{27}P^7(1-P)+\frac{13}{27}P^8$

Table 4 : Expressions of fidelity without and with correction by the five, seven and nine qubits codes.

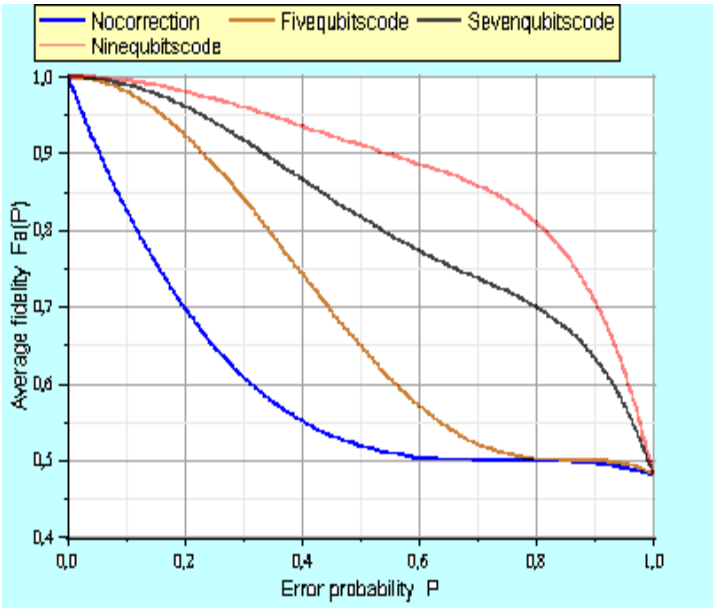

Figure 2 : Fidelity without and with correction.

7 Conclusion

This work was devoted to error correction for quantum secret sharing. The results show that the nine qubits code gives the best fidelity, followed by the seven, then the five qubits code, regardless the depolarizing channel error probability P. This conclusion seems to confirm the simulation work done in [11], where errors were introduced by the correction process itself. We conclude that higher is the ancillas number better is the fidelity. The reason is that the nine qubits code allows the recovering of a higher fraction of double channel input errors. In fact, as only single and double errors have been considered, this code gives a specific syndrome for a higher number of double errors, then allowing their recovery and leading to fidelity equal to one. We have supposed that triple errors and more are very unlikely and then with negligible effect on the obtained results.

Acknowledgement

We would like to thank very much Mrs S.Fritzsch and T.Radtke for providing us with the version 4 (2008) of Feynman Program.

8 References

[1] Graph States for Quantum Secret Sharing, Damian Markham and Barry C. Sanders, Phys. Rev. A 78, 042309 (2008).
[2] T.Radtke, S.Fritzsche: 'Simulation of n-qubits quantum systems', I. Quantum gates and registers, CPC, Volume 173, Issues 1–2, 2005, Pages 91–113.
[3] T.Radtke, S.Fritzsche: 'Simulation of n-qubits quantum systems', II. Separability and entanglement, CPC, Volume 175, Issue 2, 2006, Pages 145–166.
[4] T.Radtke, S.Fritzsche: 'Simulation of n-qubits quantum systems', III. Quantum operations, CPC, Volume 176, Issues 9–10, 2007, Pages 617–633.
[5] T.Radtke, S.Fritzsche: 'Simulation of n-qubits quantum systems',IV. Parametrization of quantum states, CPC, Vol 179, Issue 9, 2008, Pages 647–664.
[6] CPC Prog Lib, Queen's University of Belfast, N.Ireland, Apr 2008.
M.A. Nielsen, I.L Chuang: "Quantum computation and information", Cambridge University Press, UK, 2000.
[8] Raymond Laflamme and co "Perfect Quantum Error Correcting Code", Physic Review Letters, Volume 77, Number 1,198-201, july 1996, .
[9] A. M. Steane. "Multiple particle interference...". Proc. R. Soc. Lond. A, 452:2551–2576, 1996. quant-ph/9601029.
[10] A.G.Fowler, "Constructing arbitrary Steane code single logical qubit fault-tolerant gates", Quantum Information and Computation,11: 867-873 (2011).
[11] Jumpei Niwa, Keiji Matsumoto, Hiroshi Imai, "Simulating the Effects of Quantum Error-correction Schemes", arXiv:quant-ph/0211071v1 13 Nov 2002.